Spatio-temporal organisation of histone variants : from nucleosomes to nuclei

Tina Karagyozova

PSL UNIVERSITÉ PARIS

THÈSE DE DOCTORAT
DE L'UNIVERSITÉ PSL

Préparée à l'Institut Curie

Spatio-temporal organisation of histone variants: from nucleosomes to nuclei

Organisation spatio-temporelle des variants d'histone: du nucléosomes aux noyaux

Soutenue par
Tina KARAGYOZOVA
Le 8 septembre 2023

Ecole doctorale n° 515
Complexité du vivant

Spécialité
Biologie cellulaire et développement

Composition du jury :

Sarah LAMBERT DR, CNRS – Institut Curie, Orsay	*Présidente du jury*
Constance ALABERT Principal investigator, University of Dundee, Dundee	*Rapportrice*
Florian STEINER Associate professor, Université de Genève, Genève	*Rapporteur*
Giacomo CAVALLI DR, CNRS – Institut de Génétique Humaine, Montpellier	*Examinateur*
Geneviève ALMOUZNI DR, CNRS – Institut Curie, Paris	*Directrice de thèse*

UMR 3664
Dynamique du noyau

institutCurie | PSL

На родителите ми,

To my parents.

“The important thing is not to stop questioning.

Curiosity has its own reason for existence.”

- Albert Einstein

Acknowledgements

When embarking on this PhD journey, I expected to be faced with challenges, triumphs, and disappointments, but I never anticipated the excitement, fun and laughter that would come in among them. These years have been a steep learning curve in both the scientific and personal sense, and while there is much left to improve in both aspects, one fact is abundantly clear: I did not get to where I am today on my own. Thus, instead of rushing to the end, as I tend to do, I would like to take some time to express my appreciation for everyone that has been by my side and given their unfaltering support. This work, and the time spent doing it, would not have been a source of pride and joy without you.

First of all, I would like to thank my supervisor, Geneviève Almouzni. It has been a great privilege to learn from you, and I would like to thank you for all the opportunities to grow that you have given me. I greatly admire your scientific rigour, your critical approach, your perspective on 'the big picture' and your imagination. You have challenged me to become a better scientist and have been a model of what it is to be a great one. Your passion, strength and determination have been an inspiration to me, both in the professional and personal sense. I am grateful for your guidance and encouragement along the way, and for the confidence you have had in me when I myself have not.

I would also like to thank my mentor, even if not in an official capacity, Alberto Gatto. I will always be grateful for your support, from near or far, far away in sunny California, throughout all these years. Thank you for your patience with my million questions, for sharing your expertise and for always finding time for me when I needed it. This project would not have become what it is without you.

I express my gratitude to the members of the scientific community who have spent their time following and evaluating my work, for sharing their perspectives and giving their insightful comments. I thank the rapporteurs of my PhD jury, Dr Constance Alabert and Dr Florian Steiner, for their critical reading and evaluation of my thesis. I also thank my examinateurs, Dr Giacomo Cavalli and Dr Sarah Lambert, for kindly taking part in my PhD jury. I am also grateful to the members of my thesis advisory committee, Dr Daan Noordermeer, Dr Joshua Waterfall and Dr Martial Marbouty, as well as the team leaders of the UMR3664, Angela Taddei, Nathalie Dostatni, Ines Drinnenberg and Antoine Coulon. Thank you for the constructive discussions and advice throughout the development of the project. Finally, I would also like to thank Leonid Mirny and Marc Marti-Renom for valuable inputs to my work.

I also wish to thank the entire unit UMR3664 and the Pavillon Pasteur of Institut Curie for their diverse perspectives and all the stimulating discussions we have had. A big thank you to Marie, Caroline and Marion for making everything run smoothly. Un grand merci à Anifa, Prisca et Maureen aussi pour l'aide quotidienne. Thank you to Patricia, Mickael and David at the PICT-IBISA Imagerie Platform for all the help with the microscopes and to Shauna, Ines and Imène at the LABEX-DEEP for the many stimulating courses, events and seminars they helped organise.

Thank you to the doctoral school Complexité du Vivant, Institut Curie, and the Université Paris Sciences et Lettres, for giving me the opportunity to work in such a supportive environment. Special thanks to the H2020 MSCA-ITN ChromDesign program, ran by Dr. Luciano Di Croce and managed by Dr. Jonas Krebs and Dr. David Brena, and to La Ligue Contre le Cancer for the funding to pursue my PhD.

Throughout these years, many people have joined and left the Chromatin Dynamics lab (Frogteam), and I have appreciated knowing and interacting with all of them. From the current team, I would like to thank Christèle, Delphine, Iva, Sébastien and Weitao for their support, as well as Hatem, Magali and Valentyna from our former members. Thanks to Dominique and Jean-Pierre for your reassurance and for your patience in answering all my questions when I would suddenly turn up at the bench after 6 months of data analysis. Special thanks to Audrey for teaching me and helping me with experiments, collaborating and sharing an office with you has been a pleasure. Thanks to Alodie and Emma for all your support on the administrative side and the lab meeting sweets. Thank you to Nicole and Marina for your encouragement of my work and your insistence (and assistance) on taking care of myself, it has really helped me to slow down and enjoy the little things in life. Special thanks to Kamila for your endless positivity, insightful advice, and continuous attempts to reason me out of doing 10h-long, 20-condition experiments, but helping me plan them anyway. Thank you to DJ and Shweta for your kindness when welcoming me into the team. Finally, thanks to Katia for your help in the beginning and for your grounding perspective.

A special word is needed for the rest of the PhD students from the team, who have been a staunch support, a source of knowledge and great fun to spend time with, both in the lab and in the many bars around. Thank you to Charlène, for your endless kindness and patience, help with all things French and for the incredible entertainment of your (and Florian's) practical jokes on Stefano. I admire your diligence and strength, and I have no doubt you will do great! From those who have already defended, thank you first to David. Even if we overlapped briefly, I was happy to be around your laid-back attitude and the ridiculous arguments with Alberto and Stefano at the sacred coffee times, and I am proud to have inherited your lab giraffe. Next, thank you Julia, for your advice, honesty, and kindness. It is a joy be around your positivity and enthusiasm (not to mention your fashion sense), and I am glad I still get to experience it, though in museums and cafés rather than in the lab. You helped me find my feet at the start, and I will always be grateful. Finally, thank you to Stefano for being my little sun all these years. I cannot imagine how this time might have gone without having you by my side, ready to amuse, annoy and confuse me all at the same time. I definitely would have known less about birds and Latin, and likely would have been banned from Italy for ordering anything but espresso. Thank you for listening to me worry about anything and everything over and over, for calming me down, for answering questions at 11pm in August, for playing Dua Lipa in cell culture, for baptising out incubator, for teaching me to drink spritz. Your determination to keep moving forward and your perspective on what really matters have made me reconsider how I think about life. Thank you for being my friend.

Outside of the team, but together anyway (at least every 6-12 months), I would like to thank the students from the ITN “ChromDesign”, Alicia, Antonia, Arun, Blanka, Carla, Gianni, Kourosh, Livia, Mrinmoy, Nathalie and Rodrigo. Special thanks to Pia, my unexpected roommate, for your advice and candour, and to Michael, my Austrian ‘French’ friend, for your positivity and spontaneity. I could not have asked for a better cohort to go through the madness of week-long online courses or to play beach volleyball in February with than you. I would also like to thank our Beer Pressure group, i.e. the rest of the current and former PhD students and the postdocs in the Pavillon Pasteur for making me look forward to spending my time in the building, whether it is for coffee breaks or doing experiments on the weekends. Having your scientific input and personal support has been invaluable and I am grateful to have shared both highs and lows with you. Special thank you to Gonçalo for the parties, to Gertjan for the arguments, to Manuela for the existential discussions, to Kyra for the reassurance. I am also grateful to the rest of my friends in Paris for making it feel like somewhere I belong. To Mariya, for always making time and being a small reminder of home, to Sol, for her positivity and being a link to another home, to Brianna, for her care and perseverance, to Marci and Enci, for their enthusiasm, initiative and understanding. Finally, special thank you to Anouk, my little family in Paris. Your passion motivates me to do better.

I have been away from home for a long time, and Paris was not the first stop, but I have been lucky to keep the friends I made along the way. Thank you to the ‘Glasgow Rangers’ Anastasia, Dalia, Elena, Jakub, Maksim, Marie, Natalia, and to Marc and Suli. Julija, meeting you changed my life. I will always be grateful for the time we spent together, and I hope one day we will end up in the same place again. Magi, thank you for all the advice. Claire, thank you for your faith in me. Going back to my roots, I will finish in Bulgarian. Първо, благодаря на „старите“ си приятели за подкрепата ви през годините от гимназията до сега. Оценявам колко е рядко толкова голяма група хора да останат близки въпреки времето и разстоянието, и съм изключително благодарна за усилията, които полагате, за да се запази това. На Рал, че си неизменно насреща. На Марти, за вярата ти в мен. На Крем и Милица, за съветите и реализма. На Поли, за приключенията. На Стунджи, за бягането. На Добчо, за въпросите. На Геша и Кольо, за философските дискусии. На Вальо, за Боро. И на всички, за диваните.

Накрая, искам да благодаря на семейството си. Без постоянната ви подкрепа, окуражение и увереност в мен, никога не бих могла да постигна това, което съм. Благодаря ви за това, че винаги сте ми давали свобода да следвам целите си и за всичко, което сте жертвали, за да ми помогнете да ги постигна. Майко, благодаря ти, че винаги си на един телефон разстояние, и ме караш да се чувствам все едно все още съм във Варна. Тате, благодаря ти за примера, който си ми давал от малка, да бъда постоянна и да не ме е страх да преследвам това, което искам. Ники, благодаря ти за това, че винаги си вярвал в мен. Бабо, благодаря ти за безкрайната грижа и подкрепа. Дължа ви всичко и се надявам, че се можете да се гордеете с това постижение. То е толкова ваше, колкото и мое.

Preamble

The discovery of the molecular structure of DNA (Franklin and Gosling, 1953; Watson and Crick, 1953) provided essential insights into how it could carry out its function of heritable information storage. This led to the idea that the order of the four bases of the otherwise identical nucleotides acted as a code, and the zipper-like organization into two complementary could provide the means for a semi-conservative replication, as shown later experimentally. Next, the first level of chromatin organization with the packing of DNA around histones into nucleosomes, forming 'beads-on-a-string', and its link with transcriptional output opened up a whole range of additional questions. When considering the arrangement of chromatin at the scale of the nucleus, early observations showed that it is clearly non-random (Rabl, 1885; Boveri, 1888). However, attempts to bridge the gap between the nucleosomal and the nuclear scale have only begun succeeding recently. This has been possible thanks to the combined progress in the development of powerful sequencing techniques, as well as improvements in microscopy and automation. Furthermore, when examining these different scales, the dynamic nature of chromatin organization throughout the life of a cell should be considered. Chromatin undergoes major reorganization during each cell cycle: it is entirely duplicated upon replication in S phase, incorporating new histones; it forms highly condensed chromatids in mitosis to facilitate cell division and then it de-compacts as cells enter G1, allowing RNA polymerases and other proteins to access DNA and prepare for S phase re-entry. In the context of development, chromatin also undergoes major changes in its composition and arrangement. During gametogenesis, this contributes to the formation of highly specialised gametes, while upon fertilization extensive reprogramming occurs to establish the totipotent zygote and subsequently commit to distinct cell lineages in early embryogenesis.

Understanding the relationships between different levels of chromatin organization and the mechanisms that drive them is an exciting and still open question. We do not know to what extent chromatin structure contributes to the regulation of the various processes exerted onto DNA, including replication, repair and transcription, and whether this role is context-specific. Conversely, while there is ample documentation concerning how these activities disrupt nucleosome organisation, the investigation on their impact on the higher-order arrangement of chromatin is still under way.

During my Ph.D., I aimed to address this gap of knowledge by investigating how changing the composition of the nucleosome affects higher-order organization of the genome. I then asked whether this is linked to chromatin function, focusing on DNA replication.

In the following introduction, I will provide an overview of chromatin and its main components. I will describe the key features of its organization in interphase cells and the methodologies used to discover them, before diving into the process and control of DNA replication. I will then present my results on the role of the H3.3-specific chaperone HIRA on chromatin organization. Finally, I will discuss my findings in the context of current literature to open up perspectives beyond this work.

Table of contents

Introduction **11**

1. Chromatin organization: from nucleosomes to nuclei 12

1.1. Foreword 12
1.2. DNA 14
1.3. The nucleosome: the basic unit of chromatin 15

1.3.1. Histone post-translational modifications 17
1.3.2. Histone variants 20

The non-replicative or replacement variant H3.3: balancing dynamics and stability *24*

Importance in normal cell function 25
Importance in development 26
Importance in disease 28

The centromeric variant CenH3: a paradigm for epigenetic definition of chromatin landmarks *29*
Other non-replicative H3 variants *30*

1.3.3. Histone chaperones 30

CAF-1 complex *32*
HIRA complex *33*
DAXX/ATRX complex *35*
HJURP *36*

1.3.4. Chromatin remodellers 37

1.4. Higher order chromatin organization in interphase 38

1.4.1. Where am I? Defining chromatin landmarks and nuclear positioning by fixed cell imaging 38
1.4.2. Who am I? Identifying genomic enrichment of chromatin marks and DNA interaction patterns by sequencing-based methods 41

Mapping beads along the string *43*
Adding dimensions to connect the dots *46*

Chromosome territories 46
Compartments 46

We interrupt your programme with a burning question: How is this happening? *50*

Returning to your scheduled (sequence) identity crisis: TADs and loops 54

Loops and compartments: one of those things is not like the other *55*
Is this real life? Is this just bulk Hi-C? (adapted from Mercury, 1975) *58*

1.4.3. What am I doing? Adding dynamics by live-cell imaging 60

1.5. Chromatin organization during the cell cycle 61
1.6. Structure-function relationship: What is the role of 3D genome organization in regulating genome function? How do genomic processes affect its organization? 63

Chromosome territories: Keep it to yourself *63*
Compartments: I can do it on my own *64*

Are genome function (transcription and replication) and compartments interdependent? 64
Are nuclear repositioning and compartment switching corresponding events? 65

TADs: 'Lean on me' *66*
Looping: 'Should I stay or should I go?' *68*

2. Chromatin replication: disrupting organization every doubling 71
2.1. The mechanics of DNA replication 71
2.2. Chromatin replication: maintain genome integrity and epigenetic states 74
2.2.1. *De novo* histone deposition in S phase 74
2.2.2. Recycling of parental histones during replication 76
2.2.3. Re-establishment of the chromatin landscape 79
2.2.4 Importance of maintenance of the histone landscape for genome and epigenome integrity 81
2.3. Spatiotemporal organization of replication: replication timing (RT) programme 84
2.3.1. RT establishment: definition and selection of origins of replication 84
In the beginning, there was sequence *84*
Strength in numbers *86*
How to define an origin? *87*
The efficient bird gets the worm *89*
RIF1: Show them who's boss? *91*
2.3.2. Organization of RT 93
2.3.3. Impact of replication timing on other processes 95
Question 97
Results 99
General approaches and methodology 100
Manuscript 103
Abstract 103
Introduction 104
Results 107
Discussion 124
Supplementary figures 129
Materials and Methods 145
References 151
Additional results 158
H3 variant pattern and early firing are disrupted at TAD borders without impairing their strength or position 158
Enhancer, but not promoter-associated histone marks are decreased in the absence of HIRA on the kb scale 162
H3 variants redistribute along the mouse genome linearly and with respect to 3D genome features across scales during differentiation 164
Methods 168
Discussion 169
H3 variant organisation across scales: a dynamic balancing act 170
H3 variant re-distribution in 3D chromatin space: functional implications 173
How does the H3 variant balance define early IZs? 175
H3 variants and chromatin organization in differentiation and development 176
H3 variants, replication and chromatin organization in disease 177
Conclusion 179
References 181

Abbreviations

ATRX (α-thalassemia mental retardation syndrome X-linked)
ASF1 (anti-silencing factor)
bp (base pair)
BrdU (5-bromo-2-deoxyuridine)
CABIN1 (calcineurin-binding protein 1)
CTCF (CCCTC-binding factor)
CENP-A (centromeric protein A)
CAF-1 (chromatin assembly factor 1)
3C (chromosome conformation capture)
CT (chromosome territory)
CGI (CpG island)
ChIP-seq (chromatin immunoprecipitation followed by sequencing)
DAXX (Death domain-associated protein)
DNA (deoxyribonucleic acid)
DNMT (DNA methyltransferase)
DSC (DNA synthesis-coupled)
DSI (DNA synthesis-independent)
EdU (5-ethynyl-2-deoxyuridine)
EV (eigenvector)
FISH (fluorescence in situ hybridization)
G4 (G-quadruplex)
H3K27ac (H3 lysine (K) 27 acetylation)
H3K27me3 (H3K27 trimethylation)
H3K4me1/3 (H3K4 mono/tri-methylation)
H3K9me3 (H3K9 trimethylation)
HP1 (heterochromatin protein 1)
Hi-C (high-throughput chromosome conformation capture)
HFD (histone fold domain)
HIRA (histone regulator A)
HJURP (Holliday junction recognition protein)
DHS (DNA hypersensitive site)
IZ (initiation zone)
kDa (kiloDalton)
kb (kilobase)
KD (knock-down)
KO (knock-out)
LLPS (liquid-liquid phase separation)
Mb (megabase)
MNase (micrococcal nuclease)
MCM (minichromosome maintenance)
micro-C (MNase digestion-based Hi-C)
mESCs (mouse embryonic stem cells)
NCP (nucleosome core particle)
NDR (nucleosome-depleted region)
nt (nucleotide)
ORC (origin recognition complex)
PHC (pericentromeric heterochromatin)
PRC (Polycomb repressive complex)
PTM (post-translational modification)
PCNA (proliferating cell nuclear antigen)
RIF1 (RAP1-interacting factor 1)
RD (replication domain)
RT (replication timing)
RNAPII (RNA polymerase II)
TAD (topologically-associating domain)
TF (transcription factor)
TSS (transcription start site)
UBN (ubinuclein)
ZGA (zygotic genome activation)

Introduction

1. Chromatin organization: from nucleosomes to nuclei

1.1. Foreword

The term ‘chromatin’ introduced by Walter Flemming (1882, 1879) described the linear dye-stained structures he observed in the nucleus of mitotic cells (Figure 1A). He suggested that it corresponded to the ‘nuclein’ isolated by Friedrich Miescher (1871) from lymphocyte nuclei, which was the first purification of deoxyribonucleic acid (DNA). Along with the negatively charged nuclein, Miescher isolated positively charged proteins, which he termed ‘protamines’ from salmon sperm. In 1884, Albrecht Kossel biochemically purified histones from avian erythrocytes for the first time, thus defining chromatin as a nucleic acid complexed with proteins. They hypothesized that chromatin was the hereditary material of the cell, a theory proven right and further developed in the early 1900s with the re-discovery of the principles of Mendelian genetics (de Vries, 1900a, 1900b; Sutton, 1900), with the idea of genes as units of heredity (Morgan, 1910) and the discovery of a ‘transforming principle’ (Griffith, 1928). However, it was not until 1944 that DNA was identified as the carrier of genetic information (Avery et al., 1944).

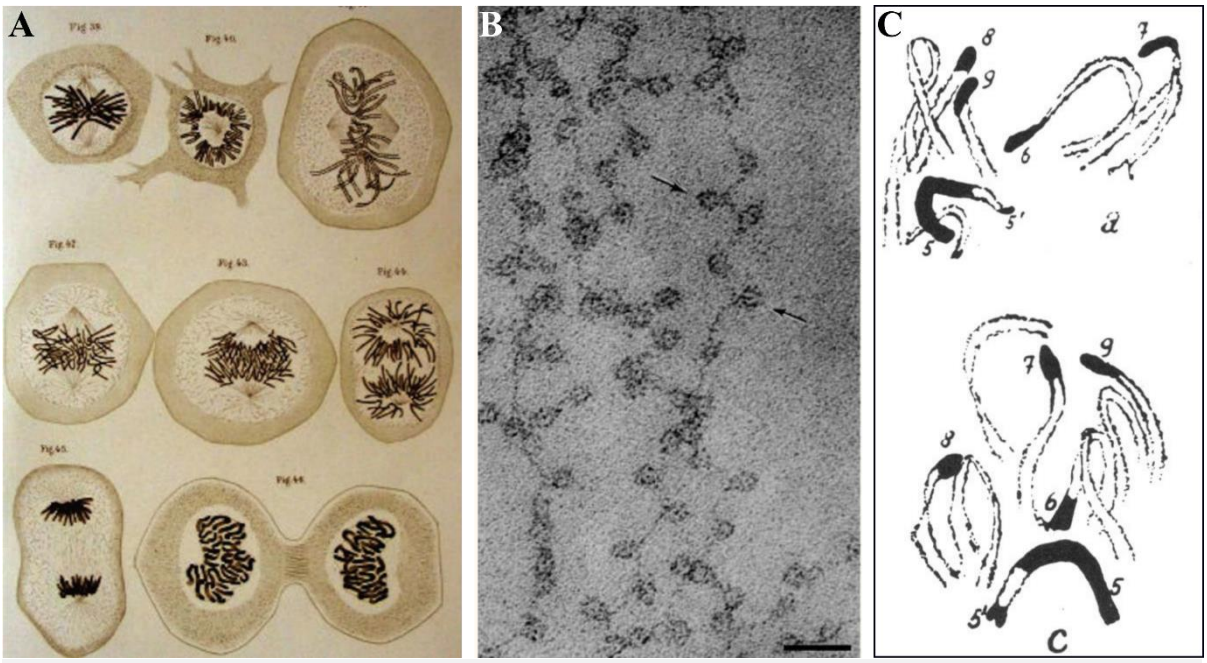

Figure 1. Early visualizations of chromatin

A. Drawings of mitotic chromosomes (chromatin) by Walter Flemming, 1882. **B.** Electron micrographs of ν bodies (nucleosomes) arranged as ‘beads on a string’ from chromatin spreads at low ionic strength, scale bar = 30m (adapted from Olins and Olins, 2003). **C.** Drawings of heterochromatin of the *Pellia epiphylla* by Heitz (1928).

In terms of molecular insight, following the discovery of the structure of the DNA double helix (Franklin and Gosling, 1953; Watson and Crick, 1953; Wilkins et al., 1953), it is the description of its organization with a set of histones to define the basic unit termed ν (‘nu’) body, and their appearance as ‘beads on a string’ that set the stage only 20 years later (Olins and Olins, 1974; Woodcock et al., 1976, Figure 1B).

In the meantime, biochemical (Johns et al., 1960) and structural (D'Anna and Isenberg, 1974; Roark et al., 1974) characterisation of histones proceeded, while work on nuclease-treated chromatin revealed that association with histones protected DNA from digestion (Sahasrabuddhe and Van Holde, 1974). These studies culminated in a model of the nucleosome (Oudet et al., 1975), comprising ~200bp DNA and an octamer of histones (Kornberg, 1974).

However, it had been already established that at a chromosomal level, chromatin structure was not homogenous. Studying moss cells, (Heitz, 1928) observed that several chromosomes contained darkly stained condensed regions persisting after mitotic exit, which he termed 'heterochromatin', as opposed to 'euchromatin', which could not be observed in interphase (Passarge, 1979, Figure 1C). Furthermore, light (euchromatin) bands of *Drosophila melanogaster* salivary gland polytene chromosomes were shown to be gene-rich (Heitz, 1935), transcriptionally active (Pelc and Howard, 1956) and early-replicating (Fujita, 1965; Pelling, 1964), establishing a correlation between chromatin structure and function. Chemical modifications of histones like acetylation and methylation were linked to transcription (Allfrey et al., 1964) and chromatin compaction (Grunstein, 1997). In addition, a role for nucleosome positioning was put forward in the regulation of gene expression (Jiang and Pugh, 2009).

In the 1990s, chromatin research merged with the broader field of 'epigenetics'. The term introduced by the embryologist Conrad Waddington in 1942, derived from the early concept of 'epigenesis' (Aristotle, William Harvey, 1651) whereby complexity emerges progressively during the development of an organism starting from a naïve entity, the egg. According to Waddington (1942), epigenetics established the connection between 'genotype and phenotype', which required the integration of inherited (genetic) information and environmental signals. In this context, he proposed that in development, cell fate determination is a process of canalisation during which a cell will follow a path down an 'epigenetic landscape', shaped by the action of specific genes (Waddington, 1957, Figure 2). Since then, the definition of epigenetics has undergone several changes and is still a matter of debate. In a molecular context, it has been defined as 'the study of mitotically and/or meiotically heritable changes in gene function that cannot be explained by changes in DNA sequence' (Russo et al., 1996). Here, I will consider epigenetics as adaptations of chromatin components (DNA, RNA, and histones) and its higher-order organization, as to register, enforce and maintain changes in activity (Bird, 2007).

In the following section, I will describe how chromatin is organized across multiple scales in the nucleus, from its basic unit, the nucleosome, to its arrangement in the nucleus. I will then detail how this organization is dynamically altered during the cell cycle, in development and in disease, and what is its functional importance in these contexts.

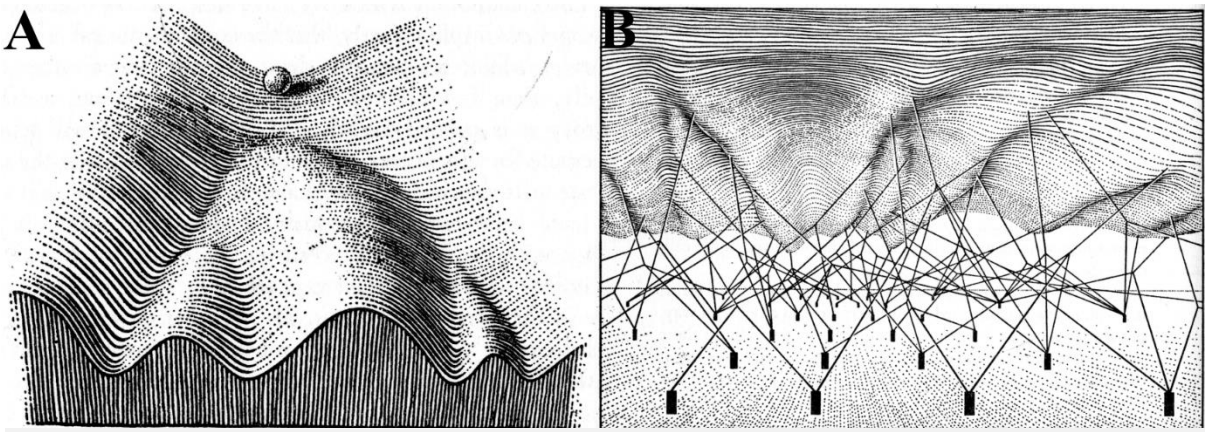

Figure 2. Waddington landscape of epigenetics

A. The cell (represented by the ball) at the top of the diagram can follow different developmental trajectories (paths down the slope), but changing or reverting cell fate requires overcoming a threshold. **B.** The surface of the epigenetic landscape is modelled by the underlying genetic factors (represented by the pegs) interplaying with environmental cues (adapted from Waddington, 1957).

1.2. DNA

DNA is a long nucleic acid polymer which encodes the hereditary genetic information in all living organisms. Its right-handed double helix structure is formed by two strands of nucleotides running anti-parallel to each other (Franklin and Gosling, 1953; Watson and Crick, 1953; Wilkins et al., 1953). Each strand has a sugar-phosphate backbone, and the two are held together by pairing of the complementary bases adenine (A) and thymine (T) or guanine (G) and cytosine (C) (Chargaff, 1950). In eukaryotic nuclei, DNA is organised in several linear molecules, termed chromosomes (Waldeyer, 1888), which are typically present in two copies (homologues) in most cell types, making them diploid.

Like histones, DNA can be chemically modified (Greenberg and Bourc'his, 2019), and the most common modification detected in mammalian cells is 5mC, the addition of a methyl ($-CH_3$) group to a cytosine 5'-carbon (Razin and Cedar, 1977), although others (5hmC, 5-hydroxymethyl-C, 6-mA, N^6-methyl on adenine) have been more recently detected (Liyanage et al., 2014). In early embryonic development, 5mC methylation (DNAme) is established *de novo* by the DNA methyltransferases (DNMT) DNMT3A, DNMT3B and their co-factor DNMT3L (Bourc'his et al., 2001; Okano et al., 1999, 1998), after global erasure of parental DNAme patterns after fertilization (Monk et al., 1987; Sanford et al., 1987). In somatic cells, hemi-methylated DNA is produced because of semi-conservative DNA replication as unmodified nucleotides are incorporated in the daughter strands. In this context, DNAme of the daughter strand is catalysed by DNMT1, which is recruited to hemi-methylated palindromic CG di-nucleotides, also called CpGs (Bird, 1978; Doskočil and Šorm, 1962) by its interactor UHRF1 (Bostick et al., 2007; Nishiyama et al., 2013). For a long time, it was thought that DNAme could only be lost through dilution over cell division in the absence of DNMT1 in a process termed 'passive demethylation', until the discovery of ten-eleven translocation (TET) dioxygenases (He et al., 2011; Ito

et al., 2011, 2010; Tahiliani et al., 2009). TET enzymes can catalyse several consecutive oxidations of 5mC and its products until its conversion to 5caC (5-carboxy-C), which is recognised and exchanged with an unmodified base by base excision repair (BER, Maiti and Drohat, 2011; Weber et al., 2016).

CpGs are sparsely distributed along the mammalian genome, except for CpG islands (CGIs), which are CpG clusters of ~1kb in size, commonly found near gene promoters (McKeon et al., 1982). The majority (70-80%) of non-CGI CpGs are methylated (Bird et al., 1985), contributing to repression of transposable elements. Conversely, CGIs are largely unmodified, except at imprinted, germline-specific or inactive X genes, where their methylation is key for stable repression (Li and Zhang, 2014). DNAme can directly inhibit binding of transcription factors, preventing activation of their target genes, but it often acts in concert with other repressive mechanisms, including histone deacetylation (Razin, 1998) and histone H3 lysine (K) 9 trimethylation (H3K9me3, Hashimshony et al., 2003).

In addition to modulating the state of histone post-translational modifications (PTMs), DNAme has also been reported to change the physical properties of nucleosomes, increasing their rigidity (Choy et al., 2010) and the amount of DNA wrapping around the histone core (Lee and Lee, 2012) *in vitro*. In a recent study, Buitrago et al. (2021) introduced DNMTs in *Saccharomyces cerevisiae*, normally absent in this species, demonstrating that DNAme alone is sufficient to decrease chromatin flexibility. However, data suggesting DNAme can increase nucleosome accessibility has also been reported, although differences may be due to the various techniques and sequences used (Shuxiang Li et al., 2022). Nevertheless, it is important to consider how methylation impacts the physical properties of DNA and consequently, its organisation into chromatin.

1.3. The nucleosome: the basic unit of chromatin

The length of the haploid human genome is ~3 billion base pairs, or about 2m DNA. Its compaction allows it to fit in a nucleus of average size of 10um yet it retains the ability to carry out processes like transcription and replication in a highly regulated manner. This is achieved by organising DNA into chromatin, the basic unit of which is the nucleosome (Figure 3, Olins and Olins, 2003).

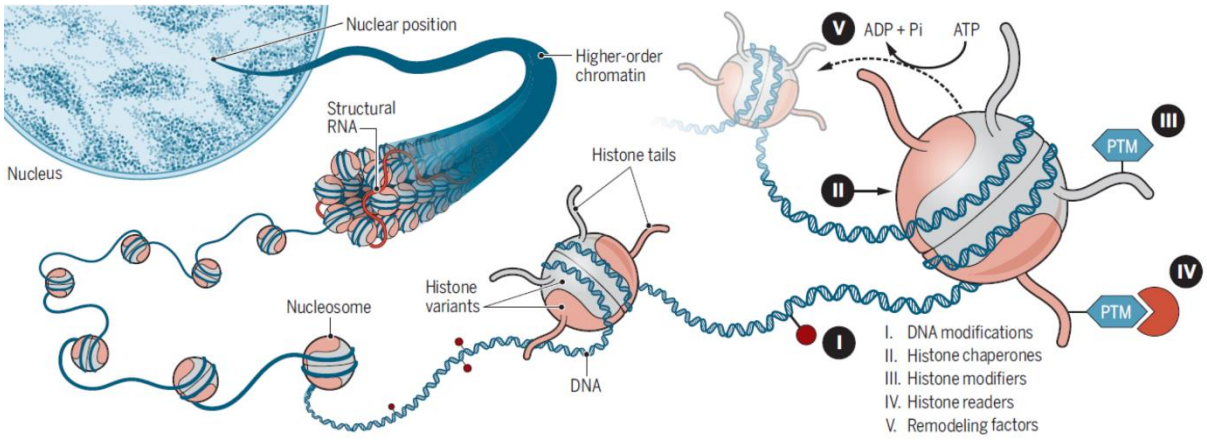

Figure 3. Chromatin folding: from nucleosomes to nuclei

The first level of chromatin organisation is the formation of the basic unit, the nucleosome, followed by the assembly of higher-order structures. This allows the genome to be contained in the nucleus and to fulfil its functions. Nucleosomes themselves are versatile entities whose composition, post-translational modifications and occupancy provide opportunities for regulation of both the structure and the function of chromatin (image from Yadav et al., 2018).

The nucleosome core particle (NCP) consists of an octamer of four histones, H2A, H2B, H3 and H4, with ~146bp DNA wrapped around it ~1.65 times in a left-handed helix (Figure 4A, Luger et al., 1997). Core histones are small (~20KDa), positively charged and among the most highly conserved proteins throughout eukaryotes. Each exhibits a characteristic 'histone fold' motif: 3 alpha helices connected by flexible loops (α1-L1-α2-L2-α3) forming a U-shape, flanked by extending N- and C-terminal tails. H2A-H2B and H3-H4 dimers are formed through the 'handshake' interaction of their histone fold domains (HFDs) in an anti-parallel orientation. The H3-H4 tetramer is established through a bundle of the two α2 and α3 helices of H3, whereas a similar interaction between H4 and H2B enables the formation of the octamer. This results in a histone core with a pseudo-dyad (two-fold) symmetry, whose central axis is at the H3-H3' interface (Luger et al., 1997).

Nucleosomes comprise the NCP and the 20-90bp linker DNA which connects them to one another (Van Holde, 1989). Linker DNA can be bound by histone H1, which is non-nucleosomal and the least conserved of the histones (Figure 4B). It contains a globular domain and positively charged tails (Allan et al., 1980; Ramakrishnan et al., 1993). H1 is thought to associate with DNA at the entry/exit site of the nucleosome, found at the dyad axis (Bednar et al., 2017; Noll and Kornberg, 1977; Simpson, 1978). Thus, H1 binding is proposed to reduce nucleosome mobility, promote compaction and stabilise higher-order chromatin organization (Prendergast and Reinberg, 2021).

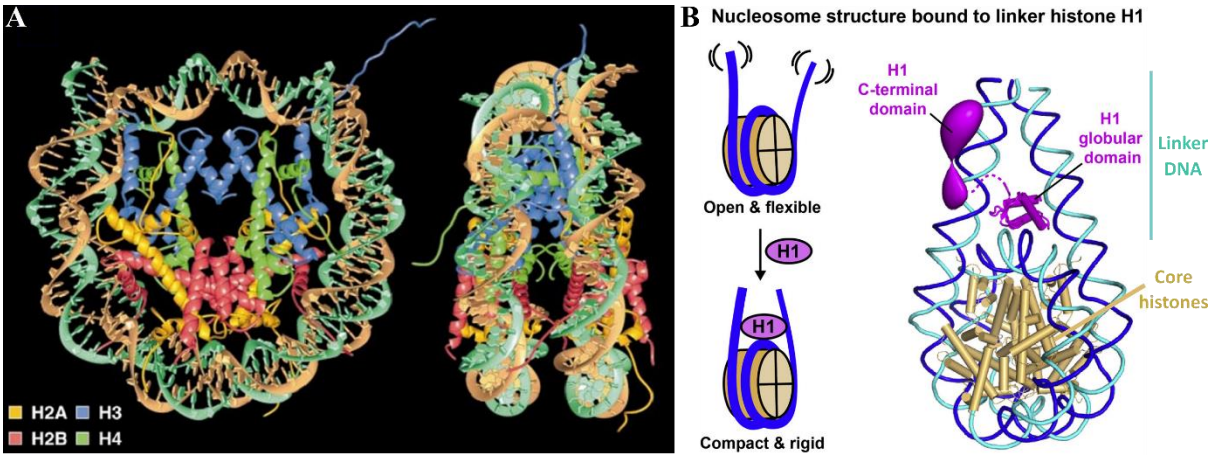

Figure 4. Insights into nucleosome structure

A. Crystal structure of the nucleosome core particle, viewed from the top (left) and the side (right), at 2.8Å resolution (adapted from Luger et al., 1997). **B.** Schematic (left) and crystal structure of the globular domain of *X. laevis* H1.0 at 5.5Å resolution (adapted from Bednar et al., 2017).

Although the entire genome is packaged into nucleosomes, they are not all the same: their positioning and stability can be influenced by the underlying DNA sequence, its methylation status and the variants or modifications of the core histones. This makes nucleosomes a versatile unit which can contribute to the regulation and/or execution of processes using DNA as a template, in addition to the higher-order arrangement of chromatin.

1.3.1. Histone post-translational modifications

Histones, like other proteins, are subject to post-translational modifications (PTMs), which can affect nucleosomal structure and/or function. Many histone marks are specifically deposited, recognised, or removed by dedicated proteins, termed 'writers', 'readers' and 'erasers', respectively. These are often part of large multi-protein complexes and their activity along the genome is controlled via regulation of their expression or interaction with accessory subunits or chromatin-associated factors like histone chaperones, chromatin remodellers, transcription factors and RNA polymerase. The dynamic deposition and removal of histone PTMs, coupled with nucleosome turnover and histone variant exchange, enables the establishment, maintenance, and modification of distinct chromatin states throughout the cell cycle and in response to developmental cues, external stimuli, and stress (Loyola and Almouzni, 2007). Among the most widely studied marks are acetylation, methylation, and phosphorylation, although many more PTMs have been detected (Millán-Zambrano et al., 2022).

Following their synthesis, histones undergo specific modifications prior to their incorporation into chromatin with a few exceptions. Notably, newly translated H4 is acetylated at K5 and K12, which is quickly removed after incorporation into chromatin, providing a proxy to follow histone dynamics. Additionally, the two H3 variants, H3.1 and H3.3 exhibit different modifications on K9 (H3.1K9me1 vs H3.3K9ac), priming them for interactions with distinct readers after nucleosome assembly (Loyola et al., 2006). Once on chromatin, histones can be further modified depending on their surrounding environment or the binding of *trans*-acting factors which recruit writers or erasers. The establishment of chromatin states is mediated by the initial recruitment of histone modifiers by a cell-type specific combination of TF/DNA-binding protein occupancy, genome sequence (e.g. Polycomb responsive elements in *D. melanogaster*) and non-coding transcripts (e.g. Xist from the inactive X or Major satellite RNA from PHC, Allshire and Madhani, 2018).

Once established, PTMs can spread from the site of nucleation and/or be maintained through cell division by coupling of their read/write mechanisms. This has been well-characterised for the heterochromatin marks H3K9me3 and H3K27me3. H3K9me3 is 'read' by HP1a, which recruits its writers SetDB1 and Suv39h1/2 (Allshire and Madhani, 2018). H3K27me3 is recognised by the PRC1 complex, which deposits another mark, H2AK119ub, recognised by the H3K27me3 writer complex PRC2 (Schuettengruber et al., 2017). H3K9me3 and H3K27me3 also allosterically stimulate the activity of their respective writers, thereby promoting their maintenance in the absence of the original trigger

(Escobar et al., 2021). This positive read/write feedback allows the formation of domains bearing H3K9me3 or H3K27me3 covering large regions of the genome and is thought to contribute to their function in stable repression throughout the cell cycle (Allshire and Madhani, 2018, Schuettengruber et al., 2017). It also argues they function as *bona fide* epigenetic marks, unlike other PTMs with high turnover, often associated with activity (Escobar et al., 2021).

Although both H3K9me3 and H3K27me3 are associated with repression, they display distinct genomic distribution (Peters et al., 2003). H3K9me3 is enriched at constitutive heterochromatin like repetitive DNA sequences (pericentromeres, telomeres, retroviral elements) (Mikkelsen et al., 2007; Nicetto and Zaret, 2019; Peters et al., 2001), whereas H3K27me3 decorates developmental genes in facultative heterochromatin like the inactive X in females in mammals (Aranda et al., 2015; Bernstein et al., 2006). Other modifications have been rather associated with activity. For instance, H3K36me3 is found at gene bodies, where it is deposited co-transcriptionally due to the interaction of RNA polymerase II (RNAPII) with the methyltransferase SetDB2 (Edmunds et al., 2008; Yoh et al., 2008). H3K4me1, H3K4me3 and H3K27ac are found at active regulatory elements (Heintzman et al., 2009; Rada-Iglesias et al., 2011) due to the recruitment of their modifiers (MLL3/4, SET1A/B and p300/CBP, respectively) by DNA-bound TFs, also facilitated by the presence of already established active marks (Schuettengruber et al., 2017; Shahbazian and Grunstein, 2007).

Histone modifications have been suggested to exert either direct (by influencing charge-dependent DNA-histone or histone-histone interactions) or indirect (via recruitment of 'readers') effects on chromatin organization and subsequently, genome function. An example of PTMs with a direct effect is acetylation of lysines in the nucleosome core (H3K56, H3K64, H3K122), which result in reduced nucleosome stability and/or increased spontaneous DNA unwrapping ('breathing', Millán-Zambrano et al., 2022). Indeed, histone acetylation was the first type of histone PTM shown to correlate with increased RNAPII activity (Allfrey et al., 1964). Further studies have shown increase transcription rate *in vitro* with these modifications (Protacio et al., 2000; Tropberger et al., 2013). *In vivo*, acetylation at various positions in the histone core (H3K64ac, Di Cerbo et al., 2014) and the N-terminal tail is observed at active promoters (H3K9ac, Wang et al., 2008) and enhancers (H3K27ac, Creyghton et al., 2010; Heintzman et al., 2009). Unlike acetylation, methylation does not change the charge of the residue it is added to, and there is no general relationship between transcription and histone methylation, indicating its potential effects on genome function are more likely indirect. This is also supported by the association of different methylation levels (me1/2/3) with distinct genomic features, and the fact that N-terminal tail PTMs do not impact nucleosome stability (Millán-Zambrano et al., 2022).

Despite the strong correlation between combinations of histone PTMs and specific chromatin states (Figure 5), whether the marks instruct genome function or result from genome activities *in vivo* has remained an ongoing debate. Considering the promoter mark H3K4me3 (Bernstein et al., 2005; Pokholok et al., 2005) functional studies showed that it is dispensable for transcription in many cases

(Henikoff and Shilatifard, 2011), although it may contribute to reinforce expression programmes (Millán-Zambrano et al., 2022). Mechanistically, recent work demonstrated how it may impact RNAPII promoter-proximal pausing and elongation (Wang et al., 2023), yet its writer SET1A/B can also regulate expression independently of its methyltransferase activity (Hughes et al., 2023). Thus, this histone PTMs may simply reflect an epigenetic memory of the binding of their writers, which contribute to genome function through non-catalytic functions (Henikoff and Shilatifard, 2011). On the other hand, the presence of H3K4me3 inhibits *de novo* DNA methylation (Ooi et al., 2007), which takes place in early development: a stage at which H3K4me3 exhibits a broader genome-wide enrichment pattern, thought to prevent from inappropriate DNAme (Zhang et al., 2016). Conversely, DNAme prevents H3K4me3 deposition by MLL2 in oocytes (Hanna et al., 2018), highlighting the fact that histone PTMs can interplay with other mechanisms of epigenetic regulation. This also showcases that a PTM may not necessarily recruit readers to actively stimulate a process like transcription, but rather prevent the binding of inhibitory factors (Millán-Zambrano et al., 2022, Schuettengruber et al., 2017). Finally, the role of a PTM should not be considered in isolation, but in the context of its surrounding chromatin landscape: despite the link of H3K4me3 with expression, it can also co-occur on the same nucleosome with the repressive H3K7me3 mark, forming 'bivalent' chromatin (Bernstein et al., 2006). Bivalency maintains genes in a poised state in early development before lineage commitment, at which point genes become fully expressed or repressed and the bivalent domains are resolved, becoming solely H3K4me3 or H3K27me3-marked, respectively (Vastenhouw and Schier, 2012).

In summary, modifying histones once they are incorporated into chromatin can contribute to the regulation of DNA-templated processes or the establishment of chromatin landmarks. However, the modified nucleosomes are not static: histones turn over and may be exchanged for different variants which may contain unique modifiable residues, providing an additional layer of complexity.

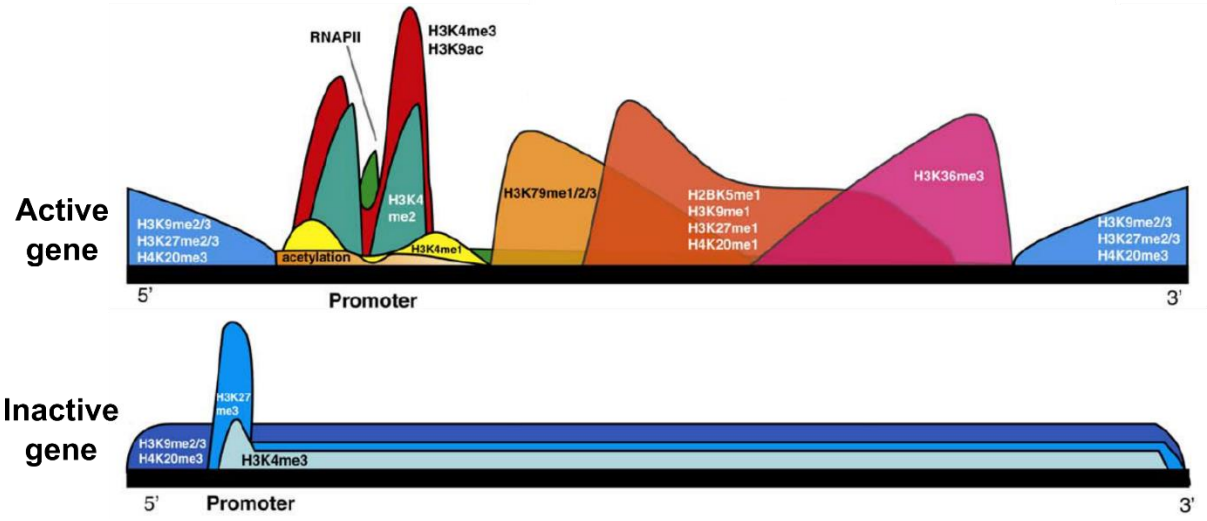

Figure 5. Histone PTM distribution at genes

Profiles of histone PTM enrichment at active (top) and inactive (bottom) genes (adapted from Barth and Imhof, 2010).

1.3.2. Histone variants

All core (Franklin and Zweidler, 1977) and linker H1 (Kinkade and Cole, 1966) histones exist as several non-allelic variants, which can be highly similar in amino acid (AA) sequence, but are subject to different expression regulation, chromatin incorporation and/or eviction and modifications. Due to their basic nature, free histones tend to form cytotoxic aggregates, so throughout their cellular life they are escorted by dedicated chaperones (Gurard-Levin et al., 2014, discussed in detail in Histone chaperones). The incorporation of each histone variant into chromatin plays a key role in establishing distinct epigenetic states, thus contributing to the control of genome organisation, transcriptional activity and cell identity (Mendiratta et al., 2019; Yadav et al., 2018).

Histone variants (Table 1) can be classified in two main groups: replicative and non-replicative (also called replacement for H3.3), based on their expression pattern during the cell cycle and mode of incorporation into chromatin. Replicative variants (often referred to as 'canonical' histones) have a peak of expression in S phase and their deposition is DNA synthesis-coupled (DSC), ensuring the immediate assembly into chromatin of newly replicated DNA (Alabert and Groth, 2012; Corpet and Almouzni, 2009) and protecting it from damage (Ye et al., 2003). The tight coupling between cell cycle progression and replicative histone expression is mediated in part by their unique gene organization. Firstly, in mammals, replicative histone genes show the following characteristics: they have short UTRs, no introns and a conserved stem loop at their 3' end. Their mRNAs are not polyadenylated and are instead processed by specific factors like stem-loop binding protein (SLBP), required for cleavage of their 3' stem loop. Moreover, replicative histone genes are organised in clusters (HIST1, 6p22, HIST2, 1q21 and HIST3, 1q42 in human), which are spatially compartmentalised in the nucleus in foci termed histone locus bodies (HLBs, Liu et al., 2006). HLBs are present throughout S phase and enriched for factors required for the transcription and processing of replicative histone genes (Mendiratta et al., 2019).

Conversely, expression of non-replicative variants does not peak in S phase, and their deposition onto chromatin is DNA synthesis independent (DSI). This is important for the maintenance of chromatin integrity, as nucleosomes can be evicted during transcription or DNA repair outside of S phase, and they need to be re-assembled (Ray-Gallet et al., 2011). Incorporation of non-replicative variants is also key for defining chromatin landmarks: for example, the presence of the centromeric H3 variant CENP-A (CenH3) defines the position of the centromere in mammalian cells. Additionally, CENP-A demonstrates that replacement variant expression and dynamics can also be subject to tight cell cycle control, as its transcription and deposition are restricted to G2/M and G1, respectively (Müller and Almouzni, 2017).

Table 1. Core histone variants in mammals		
Histone	Chaperones (**function**)	Function (**genome distribution**)
H2A		
H2A (replicative)	NAP1 (**import & deposition**) FACT, Nucleolin (**deposition & exchange**) POLA1 (**recycling at replication fork**)	chromatin integrity (**genome-wide**)
H2A.X	FACT (**deposition & exchange**)	DNA damage response, chromatin remodelling (**genome-wide**)
H2A.Z.1	p400/SRCAP (**deposition**) ANP32E/INO80 (**eviction**) POLA1 (**recycling at replication fork**)	binding of regulatory complexes (**regulatory regions (promoters, enhancers), heterochromatin**)
H2A.Z.2.1 H2A.Z.2.2	p400/SRCAP (**deposition**) ANP32E (**eviction**) POLA1 (**recycling at replication fork**)	
macroH2A1.1 macroH2A1.2 macroH2A2	ATRX (**antagonises deposition**) FACT (**eviction**)	gene silencing and higher-order compaction (**heterochromatin**)
H2A.B (H2A.Bbd)	NAP1 (**deposition and removal**)	nucleosome destabilization, transcription and splicing (**euchromatin**), *testis and brain only*
H2A.L	NAP2L4 (**H2A.L2 splice form**)	histone-to-protamine transition, *absent in human, testis-specific*
H2B		
H2B (replicative)	co-chaperoned with H2A as a dimer	chromatin integrity (**genome-wide**)
H2B.W (H2BFWT)	SWI-SNF (**remodelling**)	*testis-specific*
H2B.1 (TH2B)		histone-to-protamine transition, *testis-specific*
H3		
H3.1, H3.2 (replicative)	NAP1 (**import**) NASP1 (**protection from degradation**) ASF1 (**transfer to CAF-1**) CAF-1 (***de novo* deposition at DNA synthesis sites**) Spt2 (**deposition**) FACT (**exchange**) MCM2/POLE3-4/POLA (**replication fork recycling**)	chromatin integrity (**genome-wide**)
H3.3	NAP1 (**import**) NASP1 (**protection from degradation**) ASF1 (**transfer to HIRA**), HIRA (***de novo* deposition & recycling at active sites**) DAXX-ATRX (**deposition at heterochromatin**), DEK (**supply to DAXX-ATRX at PML bodies**), Spt2 (**deposition**) FACT (**exchange**) MCM2/POLE3-4/POLA (**replication fork recycling**)	transcriptional activation (**active genes and regulatory regions**); heterochromatin formation and telomere stabilization (**repetitive elements**)

Table 1. Core histone variants in mammals		
Histone	Chaperones (**function**)	Function (**genome distribution**)
H3		
CENP-A	HJURP (**deposition**) MCM2 (**recycling at replication fork**)	centromere identity and genome stability (**centromeres**)
H3.Y (H3.Y.1)	HIRA (**deposition**)	regulation of cell cycle genes (**euchromatin**), *primate-specific, testis and brain only*
H3.X (H3.Y.2)		*primate-specific, testis and brain only*
H3.4 (H3T, H3.1t)	NAP2 (**deposition at euchromatin**)	histone-to-protamine transition, *testis-specific*
H3.5		
H4		
H4 (replicative)	co-chaperoned with H3 as a dimer	chromatin integrity (**genome-wide**)
H4G	Nucleophosmin/NPM1	upregulation of rDNA transcription
The role of the chaperones is specified in brackets and in bold (column 2), the genome distribution is given in brackets and in bold (column 3). Tissue-specific expression and species specificity is in italics (column 3). Adapted from Martire and Banaszynski, 2020.		

The number and diversity of variants differ substantially between histone families (Table 1). Linker histone H1 has many variants, in addition to the five replicative H1.1-H1.5. Notably, there is considerable sequence variability between its replicative variants, which is conserved among species, suggesting they carry out different functions (Prendergast and Reinberg, 2021). H1 has long been linked with gene repression and chromatin compaction, but disentangling the biological functions of its variants has been challenging due to their different expression levels and distinct enrichment patterns depending on the variant, cell state and stage of the cell cycle. Generally, replicative H1 variants are enriched in heterochromatin, whereas its two somatic replacement variants, H1.0 and H1x tend to be found in more GC-rich, open chromatin regions (Millán-Ariño et al., 2016). H1 also has three testis-specific (H1t, H1T2, HILS1) variants, which are expressed during different stages of spermatogenesis and contribute to progressive chromatin compaction prior to the histone-to-protamine exchange. Finally, the oocyte-specific H1oo which is required for chromatin compaction and development of the female gametes persists until ZGA and is incorporated in the paternal pronucleus at the protamine-to-histone transition (Pérez-Montero et al., 2016).

Concerning H4, only one hominidae-specific H4 variant, H4G, has been identified to date. Localised in the nucleolus, it is thought to promote rDNA transcription through chromatin decompaction, leading to increased proliferation of breast cancer cells (Long et al., 2019; Pang et al., 2020).

In mammals, H2B has few variants: subH2B (H2B.L, in rodents and primates, but not humans), H2B.E (expression restricted to olfactory neurons in mouse, Santoro and Dulac, 2012, and down-regulated in human neoplastic keratinocytes, Rotondo et al., 2015), and H2B.W and H2B.1, both of which are testis-

specific. Functionally, H2B.1 proved important for the histone-to-protamine transition in early spermatocytes, as well as the protamine-to-histone exchange after fertilization (Montellier et al., 2013). Recent phylogenetic studies have also identified H2B.K and H2B.N, specifically expressed in the maternal germline (Raman et al., 2022). These findings emphasise the importance of histone variants in highly specialised post-mitotic cells and in development.

Unlike H2B, H2A has three main variants (H2A.X, H2A.Z and macroH2A) broadly expressed across cell types which contribute to the maintenance of normal genome function at different regions, in addition to a set of testis-specific isoforms (Bönisch and Hake, 2012). Among those, H2A.X, found genome-wide, differs from replicative H2A at few amino acids. Most notably, its C-terminal extension includes a unique Serine (S) at position 139. Phosphorylation at this site, referred to as γH2A.X, occurs at sites of DNA damage and is required for the recruitment of downstream repair proteins (Martire and Banaszynski, 2020; Piquet et al., 2018; Talbert and Henikoff, 2014). MacroH2A has a distinct large C-terminal (macro) domain connected by a short unstructured linker to its HFD and has been associated with repression due to its absence at active genes and link with chromatin condensation. Finally, H2A.Z also differs from replicative H2A at its C-terminal tail sequence, which also varies between its three isoforms (H2A.Z.1, encoded by H2AZ1, and H2A.Z.2.1 and H2A.Z.2.2, splice isoforms of H2AZ2). H2A.Z, enriched at active regulatory regions (promoters and enhancers), can form double-variant H3.3-H2A.Z-containing nucleosomes. They showed less thermodynamic stability than nucleosomes bearing only one or neither of the replacement variants due to steric hindrance of the H2A.Z tail with the H3.3 acidic patch (Jin et al., 2009; Jin and Felsenfeld, 2007). This property has been suggested to promote open chromatin formation at these sites, facilitating their transcription. More recently, H2A.Z has also been linked to licensing and firing of replication origins in early S phase by recruiting the methyltransferase Suv420h1, which deposits H4K20me2, promoting association of the origin recognition complex (ORC) protein ORC1 (Long et al., 2020). Surprisingly, H2A.Z can also be enriched at inactive regions (Hardy et al., 2009; Rangasamy, 2003), where it can promote acquisition of the inactive H3K27me3 mark (Banaszynski et al., 2013), and in turn be ubiquitinylated at K119 (another repressive modification, Draker et al., 2011; Sarcinella et al., 2007). Finally, H2A.Z is also important for normal centromere function, contributing to their silencing and spatial organization (Boyarchuk et al., 2014; Greaves et al., 2007; Rangasamy et al., 2004).

Finally, mammalian H3 exists as at least 6 non-replicative variants: H3.3 and CENP-A, which are expressed across tissues and the most well-studied (Figure 6), H3.4 and H3.5, which are testis-specific, and the recently discovered H3.X and H3.Y present only in primates. There are also two replicative H3 variants: H3.1 and H3.2, which differ from each other at a single AA at position 96 in the α2 helix of its HFD. The presence of a Cysteine (C) in H3.1 instead of a S in H3.2 has been suggested to enable the formation of sulphur bridges in H3.1-containing nucleosomes (Hake and Allis, 2006). In human cells, distinct methylation on K9 and K27 has also been detected between the two using mass spectrometry

(Hake et al., 2006). Due to their extreme similarity, antibodies cannot distinguish between H3.1 and H3.2 but tagged versions have been used to profile their genome-wide occupancy by chromatin immunoprecipitation (ChIP) followed by sequencing (ChIP-seq). This has demonstrated H3.1 is enriched in broad domains corresponding to inactive chromatin (Clément et al., 2018; Deaton et al., 2016; Ray-Gallet et al., 2011) in human and mouse cells. H3.2 showed a similar pattern in mouse embryonic stem cells (mESCs, Deaton et al., 2016; Goldberg et al., 2010), but not in mouse myoblasts (Maehara et al., 2015; Yukawa et al., 2014). They also show distinct incorporation dynamics in early mouse development (Akiyama et al., 2011; Nashun et al., 2011), despite their common deposition pathway involving chromatin assembly factor 1 (CAF-1, **Histone chaperones**). Thus, further studies along with the development of adequate tools will be required to understand their functional differences.

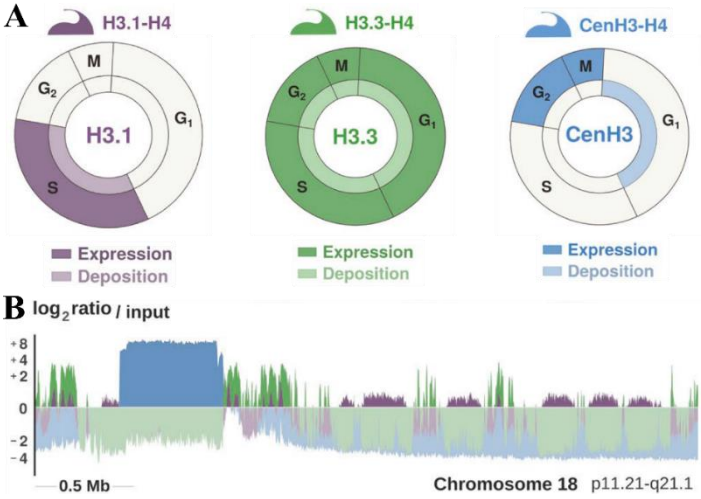

Figure 6. Cell cycle dynamics and genomic distribution of H3 variants
A. Representation of expression and deposition timing of H3.1, H3.3 and CenH3 **B.** Enrichment pattern along chr18: p11.21-q21.1 for H3.1, H3.3 (data from Clément et al., 2018) and CenH3 (data from Lacoste et al., 2014) in HeLa cells, shown as log_2IP/input (adapted from Mendiratta et al., 2019).

The non-replicative or replacement variant H3.3: balancing dynamics and stability

The main non-replicative or replacement H3 variant H3.3 is most similar to the ancestral form and only non-centromeric H3 protein present in *S. cerevisiae* (Baxevanis and Landsman, 1998). In mammals, H3.3 is encoded by two unique multi-exon genes, H3F3A and H3F3B, which produce the same protein (Akhmanova et al., 1995; Albig et al., 1995; Brush et al., 1985). Although both are expressed throughout the cell cycle and in quiescence (Wu et al., 1983; Wu and Bonner, 1982, 1981), they have distinct patterns throughout development and cell differentiation (Mendiratta et al., 2019). In terms of protein sequence, H3.3 differs from the replicative H3.1 only by 5 AA, sufficient to confer its unique function. Four of these fall in the HFD: one is S96, which is identical to H3.2, whereas the other three are A87-I89-G90, instead of the S87-V89-M90 present in H3.1/2. These three residues constitute the 'chaperone recognition' motif of the variants and enable the differential handling by their respective chaperones (Ahmad and Henikoff, 2002; Liu et al., 2012; Ricketts et al., 2015), resulting in their distinct modes of deposition (Tagami et al., 2004, **Histone chaperones**), dynamics and enrichment pattern on chromatin (Goldberg et al., 2010, discussed in detail below). Finally, H3.3 also differs from the replicative variants at position 31 in its N-terminal tail, containing a Serine that can be phosphorylated unlike the Alanine in H3.1/2. This is key for H3.3-specific phosphorylation in mitosis (Hake et al., 2005; Hinchcliffe et al.,

2016; Wong et al., 2009) and proved essential for gastrulation in *Xenopus laevis* development (Sitbon et al., 2020; Szenker et al., 2012).

Importance in normal cell function

The availability of H3.3 throughout the cell cycle, coupled with its DSI mode of incorporation into chromatin (Drané et al., 2010; Tagami et al., 2004), enables nucleosome turnover in cycling cells outside S phase, as well as in quiescent and post-mitotic cells.

H3.3 levels correlate with gene transcription (Ahmad and Henikoff, 2002; Goldberg et al., 2010; Jin et al., 2009; Mito et al., 2005; Ray-Gallet et al., 2011) and turnover at active regulatory elements (Deaton et al., 2016; Ha et al., 2014; Schlesinger et al., 2017), where it is deposited by its chaperone HIRA (Goldberg et al., 2010; Tagami et al., 2004). Despite this association, crystal structure of core particles containing H3.3 did not show different characteristics compared to H3.1 (Tachiwana et al., 2011b). However, under high ionic strength conditions, H3.3 nucleosomes show reduced stability compared to H3.1 (Jin and Felsenfeld, 2007; Thakar et al., 2009). The co-occurrence of H3.3 with H2A.Z is linked with reduced nucleosome stability (Jin et al., 2009), although not on *in vitro* assembled nucleosomes (Thakar et al., 2009), and increased nucleosome unwrapping (Wen et al., 2020). H3.3 can also antagonize H1 association with chromatin, preventing its compaction, in several organisms (Braunschweig et al., 2009; Loppin and Berger, 2020). Thus, whether the presence of H3.3 facilitates nucleosome dynamics or simply reflect this property is still an open question.

On one hand, several studies in mESCs have shown that H3.3 is dispensable for the maintenance of basal transcriptional activity (Banaszynski et al., 2013; Goldberg et al., 2010; Jang et al., 2015; Martire et al., 2019). However, the loss of H3.3 leads to changes in chromatin accessibility of promoters and enhancers (Tafessu et al., 2023; Yang et al., 2021), where phosphorylation of H3.3S31 has recently been shown to promote p300-mediated H3K27ac, contributing to efficient induction of gene expression upon differentiation (Martire et al., 2019) or hormonal stimulation (Morozov et al., 2023). In stimulated macrophages, H3.3S31phos becomes enriched along the bodies of stimulus-responsive genes (Armache et al., 2020). There, it promotes the methyltransferase activity of SETD2, resulting in increased K36me3 (Armache et al., 2020), whose maintenance is dependent on H3.3 recycling (Torné et al., 2020). Higher K36me3 results in increased gene transcription due to eviction of ZMYND11, a protein which recognises the H3.3-specific combination of unmodified S31 and K36me3 and reduces RNAPII elongation rate when bound to chromatin (Wen et al., 2014). This indicates H3.3 can play an important regulatory role for rapid induction of gene transcription upon stimulation both due to its mode of deposition and its unique S31 residue.

H3.3 has also been linked with repression of heterochromatin regions like telomeric or pericentromeric repeats and transposable elements, where the ATRX/DAXX complex ensures this enrichment (Drané et al., 2010; Elsässer et al., 2015; Goldberg et al., 2010; He et al., 2015; Navarro et al., 2020; Udugama et

al., 2015). In mESCs, the presence of H3.3 in these regions is required for their H3K9me3, preventing their expression and recombination (Elsässer et al., 2015; He et al., 2015; Navarro et al., 2020; Udugama et al., 2015)). At telomeres, H3.3S31phos inhibits the demethylase activity of KDM4B, promoting H3K9me3 retention (Udugama et al., 2022). Finally, several studies have reported changes in accessibility of heterochromatin (mESCs, Navarro et al., 2020) and at regulatory elements upon loss of H3.3 (mESC, Yang et al., 2021, Tafessu et al., 2023) or its chaperone HIRA (mESC, Yang et al., 2021, Tafessu et al., 2023, human prostate cancer cells, Morozov et al., 2023), indicating its importance for chromatin organization. However, it remains to be understood if the contribution of H3.3 to accessibility is due to the possibility to be deposited independently of replication, or due to potential PTM interplay with its unique Serine 31.

H3.3 also contributes to several important aspects related to cell cycle progression. In mitosis, H3.3S31phos occurs at peri-centromeres in various differentiated cells (Hake et al., 2005) and at mESC telomeres (Wong et al., 2009), where it contributes to their normal organization. It also plays a key signalling role by marking lagging and mis-segregated chromosomes, triggering p53-mediated cell cycle arrest (Hinchcliffe et al., 2016). In S phase, both H3.1 and H3.3, but not CENP-A, are deposited *de novo* on newly synthesized DNA. In this context, H3.3 has been proposed to serve as a placeholder for CENP-A until its deposition in the following G1 phase (Dunleavy et al., 2011). Finally, there is emerging evidence for a role of H3.3 in replication control. Strobino et al. (2020) showed that in *Caenorhabditis elegans* (*C. elegans)* grown in temperature stress conditions, H3.3 is required for normal replication fork progression and re-start. Recent work from our team (Gatto et al., 2022) in HeLa cells demonstrated that early replication initiation zones are defined by the boundaries of H3.1 and H3.3 established by the dual deposition mode of the variants, but independently of transcription.

Thus, H3.3 is key for several aspects of normal cell function: induction of transcriptional programmes, maintenance of genome and chromatin integrity, and replication initiation and/or progression. These functions depend on either its DSI incorporation, the presence of its unique S31 residue, or both.

Importance in development

In mammals, H3.3 is an essential protein for normal development: deletion of both H3F3A and H3F3B in mice results in embryonic lethality around embryonic day (E) 6.5, considered to be the result of aberrant chromosomal segregation (Jang et al., 2015). Conversely, single H3.3 gene deletions results in a variety of growth and reproductive defect phenotypes in mice, attributed to the different animal strains used, as well as differential regulation of the two H3.3 genes (Bush et al., 2013; Couldrey et al., 1999; Tang et al., 2015, 2013). In *D. melanogaster*, loss of H3.3 leads to infertility with mutant flies remaining viable, although their early development may be supported by the presence of maternally provided histones (Sakai et al., 2009). Thus, replicative H3 can compensate for the absence of H3.3 to some extent from larval stage onwards (Hödl and Basler, 2009; Sakai et al., 2009).

In mammalian spermatogenesis, a small number of nucleosomes bearing H3.3 are retained after the histone-to-protamine transition (Erkek et al., 2013; Hammoud et al., 2009), although their functional importance is unclear. During mouse oogenesis, continuous HIRA-mediated H3.3 incorporation is required to maintain normal nucleosome density, transcriptional activity, DNA methylation and oocyte viability (Nashun et al., 2015). Notably, H3.3 exhibits a 'non-canonical' pattern in oocytes, where H3.3 becomes broadly distributed along the genome, showing weak enrichment in inactive chromatin (Ishiuchi et al., 2020). Somatic cell nuclear transfer (SCNT) experiments have also shown that upon injection, the H3 histones of the donor somatic cell chromatin are exchanged for H3.3 derived from the oocyte, resulting in shift of somatic-to-oocyte expression pattern (Jullien et al., 2012; Nashun et al., 2011).

Upon fertilization, the epigenetic landscape of the two parental gametes undergoes major rearrangement to generate a totipotent zygote able to give rise to all embryonic and extra-embryonic tissues. One of the first steps in this process is the protamine-to-histone transition of the paternal pronucleus, which depends on deposition of maternally stored H3.3 (Akiyama et al., 2011; Jang et al., 2015; Loppin et al., 2005; Smith et al., 2021; Tang et al., 2015; Torres-Padilla et al., 2006). This results in a 'non-canonical' H3.3 enrichment pattern on the paternal genome, similar to the one inherited on maternal chromatin. *De novo* establishment of the 'canonical' H3.3 distribution takes place during S phase of 2-cell-stage embryos in mice and relies on replication-coupled H3.1 deposition, but the significance of these re-organizations is unclear (Ishiuchi et al., 2020). The incorporation of H3.3 during the protamine-to-histone transition is also essential for proper heterochromatin establishment (Liu et al., 2020; Loppin et al., 2005; Santenard et al., 2010) and transcription at the stage of zygotic genome activation (ZGA) of the paternal genome (Kong et al., 2018). Going one step further, Sitbon et al. (2020) used the *X. laevis* early gastrulation as a model system to disentangle the importance of H3.3 variant identity versus mode of incorporation. H3.3 had been previously determined to be essential at this stage of development (Szenker et al., 2012) and Sitbon et al. (2020) revealed that it is the presence of S31, and not the deposition pathway of the variant, which is key for its function. These experiments showcase that either the identity of H3.3, its DSI deposition or both can be important for the establishment of new chromatin states in early development.

In the context of cell fate decisions, H3.3 is required for acquisition of H3K27me3 at developmentally induced genes in mESCs, contributing to their bivalent state and preventing expression of extra-embryonic gene. Thus, H3.3 contributes both to restrict expression of other cell lineages and to maintain the capacity of the cells to differentiate (Banaszynski et al., 2013). In mESCs, H3K27ac at enhancers is promoted by H3.3S31phos (discussed above) and required for efficient cell state conversion upon induction of differentiation (Martire et al., 2019). Notably, (Sankar et al., 2022) recently demonstrated that changes of methylation, rather than acetylation of this residue, are key for restricting or promotog cell fate transitions using panH3K27R mutant mESCs. The role of H3.3 for maintenance of

reprogramming capability is also evidenced by the impairment of mESC differentiation upon H3.3K4A substitution, which decreases nucleosome turnover at regulatory elements (Gehre et al., 2020). Conversely, H3.3K36A mutants showed dysregulation of expression only after differentiation into neurons, indicating a distinct role for H3.3 in the *de novo* establishment of transcriptional programmes after cell fate commitment (Gehre et al., 2020).

The presence of two distinct roles of H3.3: safeguarding vs facilitating transition of cell states, is also supported by following its dynamics during reprogramming in several contexts: generation of induced pluripotent stem cells (iPSCs) or haematopoietic cells (iHPs) from mouse embryonic fibroblasts (MEFs) and mESC differentiation to neurons (Fang et al., 2018). Notably, this study also identified K4 and K36, but not K9 and K27 as key for H3.3 function in their systems (Fang et al, 2018). This is in agreement with an importance of H3.3 to respond to stimuli, including heat shock (Kim et al., 2011) and interferon signalling (Armache et al., 2020; Tamura et al., 2009). Finally, H3.3 accumulates in post-mitotic neurons (Maze et al., 2015; Piña and Suau, 1987) and several studies have shown its critical role for normal differentiation and synaptic excitation, contributing to maintain cognitive function (Maze et al., 2015; Michod et al., 2012; Xia and Jiao, 2017).

In summary, H3.3 plays a dual role in cell reprogramming: its re-distribution is required to change cell fate, whereas its retention at cell type-specific genes safeguards their identity. This underpins its critical role in early development and gametogenesis, when cells undergo major epigenetic reprogramming. It also explains why it is dispensable for normal cell function in fast-cycling mESCs, but not post-mitotic neurons where H3.3 is the only histone available for DSI deposition.

Importance in disease

Given the importance of H3.3 for maintenance of cell state, differentiation and normal development, it the dysregulation of H3.3 expression and/or deposition linked with disease is not surprising. Developmental conditions like DiGeorge syndrome (deletion of 22q11, Lamour et al., 1995) and X-Linked Mental Retardation with α-Thalassemia (ATR-X syndrome, Gibbons et al., 1995) are characterised by deletion of HIRA or mutations in ATRX, respectively. However, the main driver of DiGeorge syndrome is the loss of another gene, Tbx2, and in the case of ATRX it is not clear whether the disease due to the absence of its H3.3 chaperone function or unrelated activities. As mentioned above, H3.3K36me3 deposition in gene bodies regulates ZMYND11 recruitment and plays a role in tumour suppression (Wen et al., 2014). Recently, Gomes et al. (2019) also linked the switch between incorporation of H3.1/2 with H3.3 to increased aggressiveness and metastatic potential due to changes in the chromatin landscape in breast and non-small cell lung cancer.

Finally, a driver role in cancer has been attributed to missense mutations in both H3.1 and H3.3, termed ‘oncohistones’ (Behjati et al., 2013; Schwartzentruber et al., 2012). These substitutions, typically found on the N-terminal histone tail are gain-of-function mutations acting in a dominant negative manner.

They can modulate the activity of histone modifying enzymes (Fang et al., 2016; Jiao and Liu, 2015; Justin et al., 2016; Lu et al., 2016), which can lead to a global re-distribution of PTMs and re-organization of the chromatin landscape. The most well-known example is the genome-wide decrease of H3K27me3 and reciprocal increase in H3K27ac due to reduced PRC2 activity in the presence of the K27M oncohistone (Bender et al., 2013; Chan et al., 2013; Lee et al., 2019; Lewis et al., 2013; Stafford et al., 2018; Venneti et al., 2013). The mode of action of this mutation is mimicked by the small protein EZHIP (EZH inhibitory protein) (Jain et al., 2020, 2019) which normally regulates PRC2 in gametogenesis (Ragazzini et al., 2019). Notably, the effect of the mutation depends not only on its position, but also on the identity of the new residue (Brown et al., 2014; Lewis et al., 2013). Furthermore, the two H3.3 genes have a distinct mutation spectrum and are linked to different tumour subtypes, typically of paediatric brain and bone cancer (Behjati et al., 2013; Schwartzentruber et al., 2012; Yuen and Knoepfler, 2013). H3.1 oncohistones can have the same substitutions as H3.3, but do not lead to the same phenotypes, emphasizing again the significance of the variants' identity and incorporation (Mitchener and Muir, 2022).

The centromeric variant CenH3: a paradigm for epigenetic definition of chromatin landmarks

CenH3 (called CENP-A in mammals, Earnshaw and Rothfield, 1985) is the most divergent H3 variant (Palmer et al., 1987, 1991; Sullivan et al., 1994), sharing only ~50% sequence identity with the replicative H3.1 and with low conservation across species as compared to H3.1 and H3.3 (Malik and Henikoff, 2009). CENP-A is generally assembled in homotypic (2x CENP-A–H4 dimers) nucleosomes, which compact only 121bp DNA (Hasson et al., 2013; Lacoste et al., 2014; Tachiwana et al., 2011a) in a manner which is less stable than H3.1 or H3.3-containing particles (Ali-Ahmad et al., 2019; Arimura et al., 2019; Panchenko et al., 2011; Sekulic et al., 2010; Tachiwana et al., 2011a).

In most eukaryotes, CENP-A is the epigenetic determinant of the centromere (Barnhart et al., 2011; Fachinetti et al., 2013) defining the point of kinetochore assembly during mitosis (Howman et al., 2000; Oegema et al., 2001). Although in normal cells the centromere is specifically enriched in CENP-A, this variant comprises only ~10% of all nucleosomes there and is interspersed with H3.1 and H3.3-containing particles (Dunleavy et al., 2009). Unlike H3.3, CENP-A expression and incorporation are tightly regulated with respect to the cell cycle: it is transcribed from a single gene (Régnier et al., 2003; Sullivan et al., 1994) in late G2/M (Shelby et al., 1997), and it is deposited at centromeres by its chaperone Holliday junction recognition protein (HJURP, Dunleavy et al., 2009; Foltz et al., 2009) in early G1 (Jansen et al., 2007).

CENP-A is required for the recruitment of other core centromeric proteins (Foltz et al., 2006; Westhorpe et al., 2015). This enables the formation of the kinetochore, which connects the chromosomes to the mitotic spindle through microtubule attachment, ensuring their alignment at the metaphase plate (Cleveland et al., 2003). Therefore, CENP-A plays a key role for ensuring normal chromosomal

segregation and maintaining genome stability. This is demonstrated upon its experimental upregulation by the accumulation of mitotic defects (Shrestha et al., 2017) and sensitivity to DNA damage (Lacoste et al., 2014), or when downregulated (Howman et al., 2000; Maehara et al., 2010), leading to chromosome segregation defects.

CENP-A overexpression is observed in many >44% human cancer types (Jeffery et al., 2021; Lacoste et al., 2014) and is associated with aggressiveness and metastasis (Renaud-Pageot et al., 2022). Recent work from the team has shown this can be due to the role of CENP-A overexpression in promoting epithelial-to-mesenchymal (EMT) transition (Jeffery et al., 2021). Thus, CENP-A is key for maintaining chromosome stability, genome integrity and cell state.

Other non-replicative H3 variants

H3 has two testis-specific variants, H3.4 (also known as H3t, Tachiwana et al., 2010; Witt et al., 1996) and H3.5 (hominid-specific, Schenk et al., 2011). Both promote a more open chromatin structure, could contribute to early spermatogenesis, enabling proper histone-to-chromatin transition (Ueda et al., 2017; Urahama et al., 2016). Finally, there are also two primate-specific variants, H3.Y.1 (H3.Y) and H3.Y.2 (H3.X), both of which contain an A87-I89-G90 motif and are expressed in several cell lines and human brain (Wiedemann et al., 2010). Structural studies of H3.Y have revealed it forms either homotypic of heterotypic (H3.Y– H3.3) nucleosomes, which are more susceptible to nuclease digestion compared to homotypic H3.3 and prevent histone H1 binding, impairing chromatin compaction (Kujirai et al., 2016). Additionally, H3.Y is only recognized by HIRA and not DAXX due to a V46L substitution (Zink et al., 2017), also present in H3.X. H3.Y is overexpressed in stress conditions in U2OS cells, and knock-down of H3.Y alone or H3.X and H3.Y resulted in significant decrease in cell growth (Wiedemann et al., 2010). Finally, expression of both was induced by the early embryo transcription factor (TF) DUX4, resulting in their incorporation at DUX4 target genes (Resnick et al., 2019). This enabled their faster re-expression, showing a potential link between their effect on nucleosome packing, mode of incorporation and induction of transcription.

1.3.3. Histone chaperones

As described above, the versatility of histone variant function can be attributed to their gene expression control, amino acid identity, which impacts nucleosome stability and PTMs, but also to their mode of deposition and/or eviction from chromatin. The latter, as already alluded to in the previous section, is mediated by histone chaperones – proteins which escort the histones and mediate their transfer to and from other proteins or DNA ‘without being part of the final product’ (De Koning et al., 2007). *In vitro*, all histone chaperones are defined by their capability to reconstitute nucleosomes on naked DNA, even if this is not necessarily their function in the cell. *In vivo*, histone chaperones also contribute to the maintenance of a reservoir of soluble histones, preventing their aggregation or inappropriate interactions with other proteins, which may arise due to their highly basic nature (Dilworth et al., 1987;

Loyola and Almouzni, 2004). Indeed, the first histone chaperone described by Laskey et al. (1978) was nucleoplasmin. This chaperone is required for the storage of maternal H2A-H2B dimers in *X. laevis* eggs. Histone chaperones can be classified based on several criteria: selectivity (H2A-H2B and/or H3-H4, general or variant-specific, *de novo* synthesised or recycled histones), stage of the life of the histones they manage (nuclear import, storage, transfer to other chaperones or onto DNA, eviction from chromatin) or process they are involved in (replication, transcription, repair). In Figure 7, I present a brief overview of the steps of the supply chain of H3-H4 dimers (Hammond et al., 2017) before describing in more detail the H3 variant-specific chaperones and their functions below.

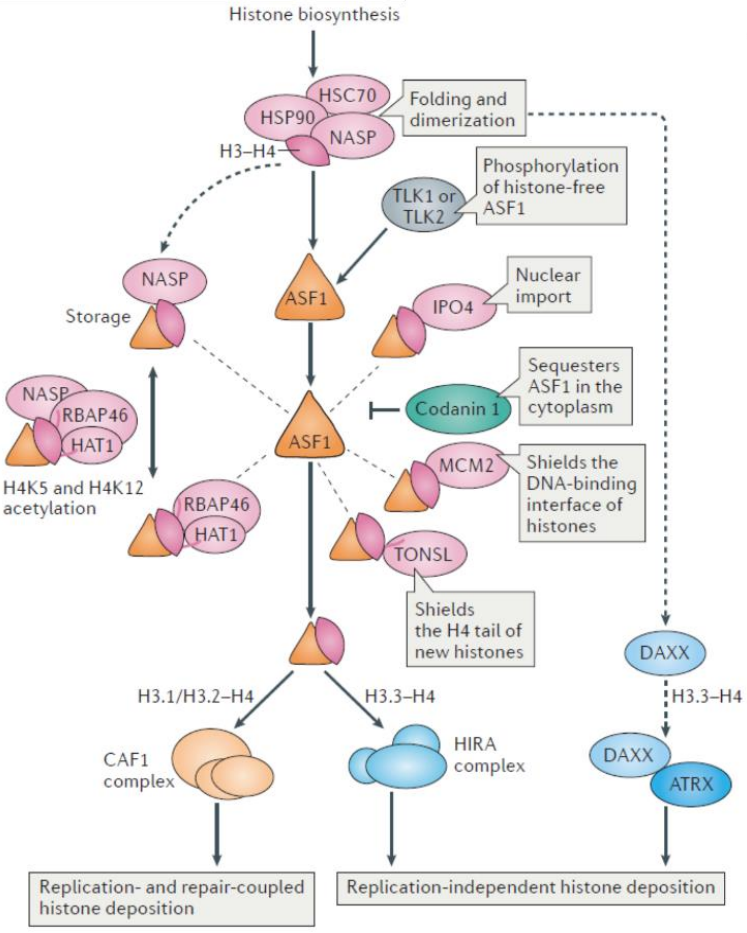

Figure 7. The histone supply chain
After translation, H3 and H4 monomers associate with the heat shock proteins HSC70 and HSP90, followed by dimerization of H3-H4, which form a complex with the somatic nuclear autoantigenic sperm protein (sNASP) chaperone, and acetylation of H4 on K5 and K12, a highly conserved 'new' histone mark. sNASP can store H3-H4 dimers, contributing to the maintenance of a soluble histone pool (Campos et al., 2010; Carraro et al., 2022; Cook et al., 2011) or hand them to another general chaperone, ASF1 (C.-P. Liu et al., 2021; Tyler et al., 1999), which plays a pleiotropic role in regulating the H3-H4 supply (Hammond et al., 2017).

ASF1 in mammals is encoded by two paralogues, ASF1a and ASF1b, which have distinct interaction preferences and expression regulation in different cell types and cell cycle stages but are partially redundant (Abascal et al., 2013; X. Wang et al., 2021). ASF1 can interact with importin 4 (IPO4), which shuttles H3-H4 into the nucleus (Alvarez et al., 2011; Bernardes et al., 2022; Campos et al., 2010; Jasencakova et al., 2010), and with MCM2 (Huang et al., 2015) and TONSL (Saredi et al., 2016), which shield different parts of the histone dimer, preventing improper tetramerization. In the context of *de novo* nucleosome assembly coupled to DNA synthesis, ASF1b transfers H3.1-H4 to CAF-1 and ASF1a hands H3.3-H4 to the HIRA (Grover et al., 2018; Tang et al., 2006) complex. ASF1 is also required for H3-H4 recycling: during DNA replication together with MCM2 (Groth et al., 2007), and during transcription, coordinated by HIRA (Torné et al., 2020). The spatial redistribution of histone variants and PTMs upon ASF1 depletion in S phase highlights the role of histone recycling for the maintenance of chromatin states (Clément et al., 2018).

Finally, recent work from the team revealed that ASF1 also regulates the histone supply by affecting replicative histone RNA processing during S phase, emphasizing the importance of proper histone-chaperone balance (Mendiratta et al., 2022).In the context of DNA replication, several components of the replisome, including MCM2, POLE3-4 and POLA have been recently shown to play a role in H3-H4 recycling, ensuring a symmetrical distribution of 'new' and 'old' histones on the two daughter strands (Stewart-Morgan et al., 2020, discussed in detail in Chromatin replication). During transcription, several factors like FACT (Tsunaka et al., 2016), Spt6 (Bortvin and Winston, 1996; Nourani et al., 2006) and Spt2 (Chen et al., 2015; Osakabe et al., 2013) have also been put forward as general H3-H4 chaperones, enabling the disassembly of nucleosomes ahead of RNAPII and histone recycling after its passage, thought to prevent cryptic transcription (image adapted from in Hammond et al., 2017).

CAF-1 complex

The chromatin assembly factor 1 (CAF-1) complex was discovered for its unique ability to promote chromatin assembly coupled to DNA synthesis in the context of DNA replication (Smith and Stillman, 1989) and repair (Gaillard et al., 1996; Martini et al., 1998). CAF-1 comprises three subunits: p150, p60 and p48 (Smith and Stillman, 1989) which carry out distinct functions. The largest subunit, p150, interacts with the proliferating nuclear antigen (PCNA) component of the replisome, linking *de novo* H3.1-H4 incorporation with replication fork progression (Moggs et al., 2000; Shibahara and Stillman, 1999), whereas the p60 subunit handles the H3.1-H4 dimers (Abascal et al., 2013). The role of the smallest subunit, p48, which is also part of several chromatin remodelling (NuRD, NURF), modifying (HDAC, PRC2) or repressive (DREAM) complexes, remains unclear. Its presence in complex with the replicative H3 enabled to demonstrate that H3.1 is deposited in a DNA synthesis-coupled manner on chromatin (Tagami et al., 2004, Figure 8).

The DSC mechanism of nucleosome deposition by CAF-1 ensures the efficient chromatinization of newly replicated DNA (Almouzni and Méchali, 1988a, 1988b). It plays a key role in supporting S phase progression (Hoek and Stillman, 2003), preventing DNA damage (Ye et al., 2003), and promoting new histone deposition at DNA repair sites (Polo et al., 2006). CAF-1-mediated H3.1 deposition is also required for epigenome integrity and lineage commitment, as knock-down of CAF-1 subunits makes cell state changes easier (Cheloufi et al., 2015, Ishiuchi et al., 2015; Franklin et al., 2022, Nakatani et al., 2022). This may be due to its role in constitutive (H3K9me3) heterochromatin establishment through its interaction with HP1a (Quivy et al., 2004) and SetDB1 (Loyola et al., 2009). Indeed, CAF-1 null embryos arrest at the 16-cell stage due to a defect in heterochromatin maturation (Houlard et al., 2006), and CAF-1 in the female germline contributes to LTR repression by H3K9me3 stages (Ishiuchi et al., 2020; C. Wang et al., 2018). Recent work has also shown CAF-1 promotes the establishment of facultative (H3K27me3) heterochromatin and gene silencing upon induction of mESC differentiation (Cheng et al., 2019). CAF-1-mediated H3 deposition can contribute to transcriptional repression even

in the absence of histone PTMs, as was shown recently in *Schizosaccharomyces pombe* (*S. pombe*, Chen et al., 2023), emphasizing the importance of maintaining nucleosome density.

HIRA complex

Histone regulator A (HIRA, Lamour et al., 1995), discovered as a candidate gene for the DiGeorge syndrome by positional cloning was found to function as a histone chaperone to promote chromatin assembly independently of DNA synthesis (Ray-Gallet et al., 2002). It is found as a complex together with calcineurin-binding protein 1 (CABIN1, Balaji et al., 2009; Rai et al., 2011) and ubinuclein 1or 2 (UBN1/2, (Aho et al., 2000; Banumathy et al., 2009). The discovery of its presence in complex with H3.3 and the specific deposition of H3.3 in a DNA synthesis-independent manner identified it as a key H3.3-specific chaperone (Tagami et al., 2004), The HIRA protein (~112KDa) acts as an assembly scaffold for the rest of the complex (Rai et al., 2011) and is required for the stability of the other components, as its depletion results in a concomitant decrease in CABIN1 and UBN1 protein levels (Ray-Gallet et al., 2011). HIRA also mediates the interaction with other partners like ASF1a, whereas the UBN1 subunit is the one that interacts with H3.3, recognising its A87-I89-G90 motif (Ricketts et al., 2015). HIRA also promotes recruitment of H3.3 at sites of UV damage to enable transcription recovery (Adam et al., 2016). Structural and biochemical work from the lab has shown that *in vitro* HIRA forms a homotrimer, which is required for the binding of two CABIN1 subunits, although this is mediated by a different domain of HIRA (Ray-Gallet et al., 2018). Homotrimerization is required for *de novo* H3.3 deposition (Ray-Gallet et al., 2018), as is binding to UBN1 in the context of transcription (Torné et al., 2020). However, recycling old H3.3 at transcribed regions requires only the interaction of HIRA with ASF1, indicating the HIRA trimer may act as a platform to coordinate the *de novo* deposition and recycling of H3.3 at sites of chromatin disruption (Torné et al., 2020).

HIRA targets H3.3 incorporation to transcriptionally active sites (Golberg et al., 2010, Banaszynski et al., 2013) and regulatory elements (Martire et al., 2019, **The non-replicative or replacement variant H3.3: balancing dynamics and stability**) through its interaction with RNAPII (Ray-Gallet et al., 2011), transcription factors (Pchelintsev et al., 2013; Soni et al., 2014), the insulator CTCF (Pchelintsev et al., 2013; Weth et al., 2014) or RPA (Zhang et al., 2017). As discussed above (Histone variants), HIRA-mediated H3.3 deposition can contribute to transcriptional regulation, as is the case in terminally differentiated mouse neurons, where this turnover is required for normal function (Maze et al., 2015). This is additionally supported by the fact that depleting HIRA in human cells leads to a modest reduction in nascent RNA levels (Torné et al., 2020). Finally, our laboratory found most recently that HIRA is critical for the definition of early initiation replication zones by establishing a balance between H3.3 and H3.1 both at expressed regions and independently of transcription (Gatto et al., 2022).

In *D. melanogaster*, the chromatin remodeller CHD1 also recruits HIRA to chromatin, which is important for normal gene expression (Konev et al., 2007; Schoberleitner et al., 2021). In human cells,

it can instead be recruited by CHD2 at double-strand breaks (DSBs), where it deposits H3.3, promoting DNA repair by non-homologous end-joining (NHEJ, Luijsterburg et al., 2016). HIRA is also important for transcriptional restart after nucleotide excision repair of UV-induced DNA damage, where it deposits H3.3 (Adam et al., 2013). Surprisingly, a follow-up study revealed a role for HIRA in transcriptional re-start after UVC damage genome-wide in a manner independent from its H3.3 chaperone activity, but on the presence of its UBN2 subunit and down-regulation of the transcriptional repressor ATF3 (Bouvier et al., 2021).

All components of the HIRA complex can bind naked DNA *in vitro* individually and the complex is responsible for partially compensating nucleosome assembly in the absence of CAF-1 (Ray-Gallet et al., 2011). These observations, along with the fact that sites of H3.3 visualized by immunofluorescence showed a broad distribution (Ray-Gallet et al, 2011), has led to the hypothesis that HIRA could also function in a 'gap-filling' mechanism. This is also supported by studies showing increased sensitivity to DNaseI digestion upon HIRA knock-down (Ray-Gallet et al., 2011) and increased promoter and enhancer accessibility in the absence of HIRA (mESC, Tafessu et al., 2023; Yang et al., 2021, human prostate cancer cells, Morozov et al., 2023). These data demonstrate the contribution of HIRA to the maintenance of nucleosome density and thus to chromatin integrity, genome protection and transcriptional control.

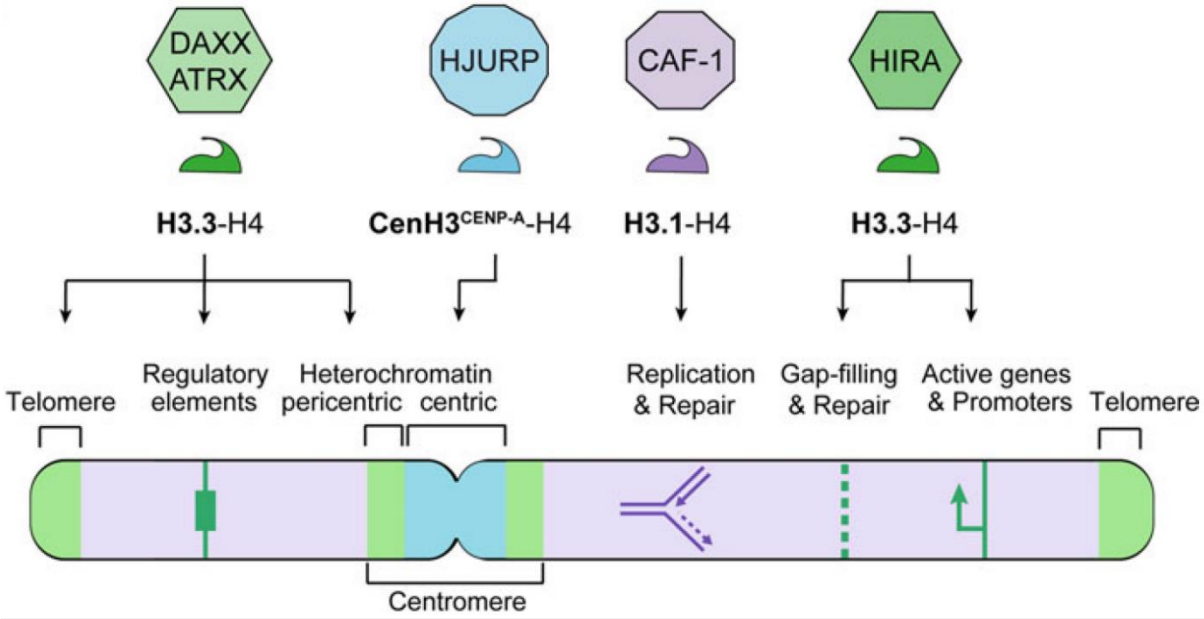

Figure 8. H3 variant-specific chaperones

De novo deposition of H3 variants by their dedicated chaperone in the context of the genomic processes and locations they are associated with. CAF-1 promotes DSC H3.1-H4 incorporation in DNA replication in S phase and in DNA repair. The HIRA complex deposits H3.3-H4 at active genes and regulatory elements, at sites of DNA repair and also performs a gap-filling role throughout the cell cycle. ATRX/DAXX contribute to H3.3 enrichment mainly at pericentric and telomeric regions but may also promote its deposition at regulatory elements. HJURP targets CENP-A incorporation at the centromere in late M/G1(adapted from Ray-Gallet and Almouzni, 2021).

Deletion of HIRA in mice leads to growth retardation and embryonic lethality (Roberts et al., 2002). In the context of cell differentiation, deposition of H3.3 by HIRA largely contributes to its dual role in restricting cell lineage, while also providing an opportunity to change state (**The non-replicative or replacement variant H3.3: balancing dynamics and stability**). In mESC, the alternative association of the HIRA complex with UBN1 or UBN2 acts redundantly to deposit H3.3 at promoters and enhancers (Xiong et al., 2018), with UBN2 more specifically required for retrotransposon silencing through H3K9me3 (Zhang et al., 2022). Furthermore, HIRA interacts with PRC2 (depositing H3K27me3, Banaszynski et al., 2013) and the remodeller SRCAP (depositing H2A.Z, Yang et al., 2021) at mESC promoters, contributing to the control of developmental gene expression. HIRA is also key for the normal function of the nerve cells, which can be related to its H3.3 chaperone function (Maze et al., 2015) or interactions with the SetD1A methyltransferase (depositing H3K4me3 at promoters, Li and Jiao, 2017).

Thus, the HIRA complex is required for normal cell function and development. This is likely relying on its DSI H3.3 chaperone function to promote cell plasticity, but one should also consider other H3.3-independent roles through linkns with other subunits or other interactors.

DAXX/ATRX complex

The second main H3.3-specific chaperone complex in mammals is Death domain-associated protein (DAXX, Yang et al., 1997) / α-thalassemia mental retardation syndrome X-linked (ATRX, Gibbons et al., 1995). DAXX directly interacts with H3.3, depositing it in a DSI manner at pericentric regions (Drané et al., 2010; Elsässer et al., 2015; Goldberg et al., 2010) and at telomeres (Lewis et al., 2010). DAXX is targeted to heterochromatin through interaction with ATRX (Goldberg et al., 2010; Tang et al., 2004; Wong et al., 2010), allowing the incorporation of H3.3 required for heterochromatin maintenance and repression of transcription (Chang et al., 2013; Elsässer et al., 2015; Goldberg et al., 2010), retroelement transposition (Sadic et al., 2015) and telomere recombination (He et al., 2015). Recognition of specific retroelement (Sadic et al., 2015) or repeat-associated G-rich sequences (Clynes et al., 2015) by ATRX directs binding of the complex, preventing G-quadruplex formation and contribute to genome stability (Teng et al., 2021). Additionally, telomeric repression by DAXX/ATRX-mediated H3.3 incorporation also relies on H3.3 phosphorylation of the unique S31 residue which inhibits KDM4A demethylase activity at these sites (Udugama et al., 2022, **Histone variants**).

Heterochromatin maintenance also relies on DAXX/ATRX using the SetDB1 methyltransferase axis to promote H3K9me3 and binding of the transcriptional repressor KAP1 (Elsässer et al., 2015; He et al., 2015; Hoelper et al., 2017; Udugama et al., 2015). Recently, Carraro et al. (2023) showed DAXX bound to H3.3-H4 can interact with SetDB1 and Suv39h1, thereby promoting H3.3K9me3 prior to deposition on chromatin. This is similar to the way H3.1 has been involved in heterochromatin propagation during chromocenter replication, where its chaperone CAF-1 also interacts with SetDB1 to provide H3K9me1

to Suv39h1/2 (Loyola et al., 2009). It is also interesting to note that previous work showed that H3.3 associated with HIRA but not DAXX/ATRX can be acetylated at K9 (Elsaesser and Allis, 2010), thus indicating that the choice of the chaperone can be critical. Overall, these studies emphasize that both the choice of ATRX/DAXX and the nature of H3.3 once incorporated specifically contribute to maintaining heterochromatin and telomere integrity.

Notably, DAXX-mediated H3.3 incorporation has been linked to gene activation upon stimulation of terminally differentiated neurons (Michod et al., 2012), in line with the importance of H3.3 in induction of new transcriptional programmes (discussed above). It also suggests that in addition to their specific functions, different chaperone complexes may have partially redundant roles. Alternatively, it could indicate chaperones can perform cell type-specific functions due to different expression levels or control mechanisms available.

Promyelocytic leukaemia (PML) bodies are marked with both DAXX and ATRX (Nan et al., 2007; Xue et al., 2003), and are suggested to act as a reservoir for *de novo* synthesized H3.3. Accumulation of the variant there depends on DAXX and ASF1a, but not ATRX, indicating the two components of the complex can have distinct chromatin-related functions (Corpet et al., 2014; Delbarre et al., 2013). Conversely, knock-down of DAXX led to the enrichment of HIRA at PML, which in physiological conditions is observed only in senescence, viral infection, and immune signalling bodies (Kleijwegt et al., 2023). The intricate interplay between variant and chaperone levels is further illustrated by the fact that H3.3 is required for DAXX and HIRA, but not ATRX recruitment to chromatin (Banaszynski et al., 2013), and reduced H3.3 levels associate with a decrease in DAXX, but not ATRX or HIRA (Elsässer et al., 2015; Hoelper et al., 2017). Importantly, ATRX also has many other interactors (Aguilera and López-Contreras, 2023) and is a member of the SWI/SNF chromatin remodeller family (**Chromatin remodellers**) which can shift nucleosomes along DNA *in vitro* in complex with DAXX (Lewis et al., 2010) or HP1 in *D. melanogaster* (Emelyanov et al., 2010). It can act independently of DAXX to prevent macroH2A accumulation on chromatin at the α-globin locus (Ratnakumar et al., 2012), whereas in its absence macroH2A1.2 is lost from telomeres upon replication stress, resulting in DSBs and telomere recombination in the context of alternative lengthening of telomeres (ALT) cancers (Kim et al., 2019). Thus, it is important to consider the function of the distinct chaperone complex subunits independently and beyond their capacity to handle a specific variant.

HJURP

Holliday junction recognition protein (HJURP), originally identified in the context of DNA repair (Kato et al., 2007) has been demonstrated to be the CENP-A-specific chaperone (Dunleavey et al., 2009, Foltz et al., 2009). Both *de novo* CENP-A deposition in G1, which ensures the maintenance of centromere identity through mitosis (Jansen et al., 2007), and recycling of parental CENP-A during replication require HJURP (Zasadzińska et al., 2018). HJURP is recruited to centromeres via its interaction with

DNA (Müller et al., 2014) and the MIS18 complex (Wang et al., 2014), allowing the timely deposition of CENP-A-H4 (Müller and Almouzni, 2017). The dimerization of HJURP (Müller et al., 2014) further enables the assembly of homotypic CENP-A nucleosomes (Zasadzińska et al., 2013). While some ectopic CENP-A deposition at active sites along chromosome arms can occur in G1 in normal cells, this CENP-A is removed during S phase, presumably replaced by H3.1 deposited by CAF-1 (Nechemia-Arbely et al., 2019).

CENP-A and HJURP, stand out as a uniquely co-regulated pair both at the mRNA (Chen et al., 2013; Fischer et al., 2016; Wang et al., 2005) and protein level (Bassett et al., 2012; Filipescu et al., 2017). Maintaining their balance is essential for proper targeting of CENP-A to the centromere, as evidenced by overexpression experiments (Filipescu et al., 2017), which leads to aberrant localization along chromosome arms (Athwal et al., 2015; Gascoigne et al., 2011; Jeffery et al., 2021; Lacoste et al., 2014; Shrestha et al., 2021, 2017; Van Hooser et al., 2001). This incorporation is mediated by the H3.3 chaperone DAXX (independently of ATRX) and results in the formation of heterotypic CENP-A–H3.3-containing nucleosomes at sites of H3.3 enrichment (Lacoste et al., 2014), including active gene promoters, regulatory regions (Athwal et al., 2015; Lacoste et al., 2014; Saha et al., 2020), pericentromeric and sub-telomeric regions (Athwal et al., 2015; Nye et al., 2018).

In summary, histone chaperones escort histones from their synthesis to their deposition onto DNA and contribute to the establishment of distinct chromatin states due to their variant selectivity, temporal control during the cell cycle and interaction with different factors.

1.3.4. Chromatin remodellers

Nucleosome repositioning or dissociation (partially or fully) occurs in the context of transcription factor (TF) or other protein binding, RNA and DNA polymerase passage or DNA repair. This process of nucleosome sliding and/or eviction involves chromatin remodellers: multi-protein complexes characterized by the presence of an ATPase domain. They use the ATP hydrolysis to generate tension and break DNA-histone interactions, leading to displacement of nucleosomes along the DNA or their complete expulsion from chromatin (Clapier et al., 2017). There are four main classes of chromatin remodellers: switch/sucrose non-fermentable (SWI/SNF), chromodomain helicase DNA-binding (CHD), imitation switch (ISWI) and inositol requiring 80 (INO80), grouped based on the conservation of their ATPase domain and association with accessory subunits, which can regulate their enzymatic activity or targeting (Hargreaves and Crabtree, 2011).

SWI/SNF remodellers are largely involved in sliding nucleosomes and eviction of histone dimers or whole nucleosome particles. Thus, they allow access to the underlying sequence for other DNA-templated processes, including transcriptional activation and DNA repair (Clapier et al., 2017). As a member of this class, the ability of ATRX to displace nucleosomes has been suggested to contribute to its role in promoting H3.3 accumulation at telomeres (Aguilera and López-Contreras, 2023). CHD

family members can be part of both activating and repressing complexes, owing to their function of repositioning nucleosomes along the DNA (Clapier et al., 2017). HIRA colocalises with SWI/SNF (BRG1, BRM, INI1) subunits at transcription start sites (TSSs, Pchelintsev et al., 2013), and with CHD remodellers in the context of H3.3 exchange in the male pronucleus (*D. melanogaster* CHD1, Konev et al., 2007) and DNA repair (CHD2, Luijstreburg et al., 2016). ISWI remodellers instead use their capacity to mobilize nucleosomes to promote the establishment of evenly spaced arrays, important for TF binding and transcription (Clapier et al., 2017). *In vitro,* CHD1 (CHD family) and ACF (ISWI family) also contribute to space nucleosome regularly post-deposition by the chaperone NAP1, with ACF also promoting linker histone H1 association to the DNA (Lusser et al., 2005; Torigoe et al., 2011). Finally, INO80 members show variant-specific remodelling activities: INO80 promotes H2A.Z-H2B exchange with H2A-H2B, whereas p400 and SRCAP catalyse the opposite process (Clapier et al., 2017; Magaña-Acosta and Valadez-Graham, 2020). p400 also promotes H3.3 occupancy at enhancers in U2OS cells and exchanges H3.1 for H3.3 in an ATP- and chromatin-dependent manner *in vitro* (Pradhan et al., 2016). In mECS, SRCAP can be recruited to target promoters by HIRA (Yang et al., 2021). Thus, the interplay and coordination between chromatin remodeller and histone chaperone activities further contribute to the establishment and maintenance of the chromatin environment (Klein and Hainer, 2020).

1.4. Higher order chromatin organization in interphase

I will now describe the different levels of chromatin organization in the nucleus based on approaches used to study this topic over the years. While early studies on mitotic chromosomes documented them as highly condensed and rigid structures (Flemming, 1882; Heitz, 1928), interphase chromatin showed many differences between cell types and organisms (Cremer and Cremer, 2006a, 2006b). Since cells spend the majority of their life in interphase where they show variable transcription, DNA replication timing and repair profiles, understanding how chromatin varies in nuclear space and in time can provide insights into how cells control DNA-templated processes.

1.4.1. Where am I? Defining chromatin landmarks and nuclear positioning by fixed cell imaging

The use of light microscopy along with chromatin-staining dyes already suggested over a hundred years ago that in interphase individual chromosomes would occupy distinct territories corresponding to their mitotic counterpart (Boveri, 1902). Studying moss cells after mitotic exit, Heitz (1928) could distinguish heterochromatin which remained densely stained. He documented the clustering of heterochromatin from different chromosomes in chromocenters in plants (Heitz, 1929) and linked high gene density with euchromatin in *D. melanogaster* cells (Heitz, 1933), a first connection between chromatin structure and function. Applying electron microscopy (EM) to ultra-thin rat liver cell slices Monneron and Bernhard (1969) characterised the organization of the nucleus, demonstrating the

enrichment of heterochromatin at the nuclear periphery and around the nucleolus, in addition to describing nuclear substructures like coiled (Cajal) bodies (Cajal, 1903). Going from the entire nucleus to individual chromatin fibres, electron microscopy also enabled the discovery of the packing of DNA into nucleosomes as 'beads-on-a-string' (Olins and Olins, 1974), which organised into a higher-order structure ('30nm fibre') when assembled on purified DNA *in vitro* (Finch and Klug, 1976; Rattner and Hamkalo, 1979). At the same time, fluorescence microscopy enabled the visualization of banding patterns on mitotic chromosomes stained with quinacrine mustard, a DNA-intercalating compound which preferentially binds AT-rich regions (Caspersson et al., 1972). As stained regions typically corresponded to heterochromatin (Caspersson et al., 1970), these results provided a first link between DNA sequence and its chromosomal arrangement (Figure 9A). Furthermore, comparing this AT-rich banding on condensed chromosomes to the patterns visualized in mitosis obtained after labelling replicating DNA with a pulse of nucleotide analogue incorporation in S phase further connected genome function (replication timing) and its organisation (Jackson and Pombo, 1998; Zink, 2006).

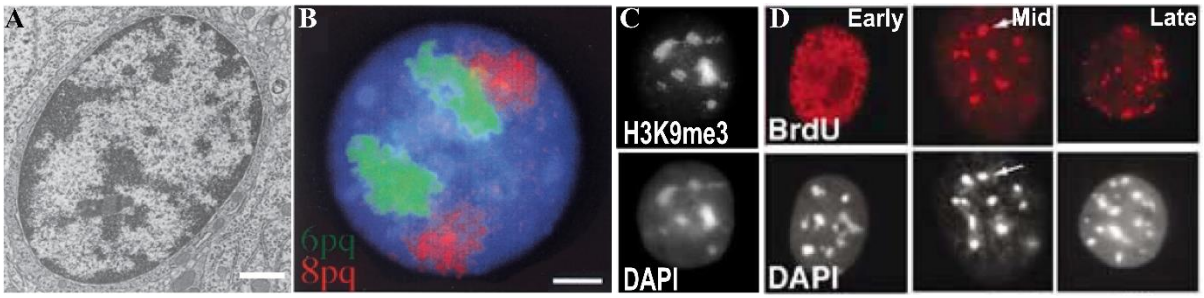

Figure 9. Chromatin landmarks in the nucleus

A. Electron micrograph of a rat glial cell with darkly stained heterochromatin and lightly stained euchromatin (scale bar = 1μm, adapted from Pueschel et al., 2016). **B.** Chromosome territory organization of chr6 and 8 in human lymphoblasts visualizes by FISH (scale bar = 2μm, adapted from Boyle et al., 2001). C. H3K9me3 Ab labelling (top) and DAPI (bottom) in mESCs (adapted from Peters et al., 2003). D. Early (E), mid (M) and late (L) S phase patterns of 10min BrdU incorporation (top) and DAPI (bottom) in mouse 3T3 cells (adapted from Quivy et al., 2004).

However, connecting the sequence identity of chromatin to a particular pattern of organization only became possible with the advent of *in situ* hybridization (ISH) methods (Pardue and Gall, 1969). The combination with probes conjugated to biotin or fluorescent moieties (FISH, Bauman et al., 1980; Langer et al., 1981; van der Ploeg, 2000) enabled the visualization of several regions at a time, from painting entire chromosomes (Bolzer et al., 2005; Lichter et al., 1988) to following individual genes (Lawrence et al., 1990). This confirmed interphase chromosomes were organised in discrete territories (Bolzer et al., 2005, Figure 9B) which intermingled little (up to 20%, Branco and Pombo, 2006) and revealed their stochastic positioning in the nucleus with some radial preferences. In human cells, smaller, gene-rich chromosomes tended to be in the nuclear interior, whereas larger, gene-poor chromosomes were preferentially found near the lamina (Boyle, 2001; Croft et al., 1999). Activation or repression of single genes correlated with their re-location to the nuclear centre or lamina, respectively

(Takizawa et al., 2008) and active genes were typically found at the periphery of chromosome territories (Osborne et al., 2004; Schoenfelder et al., 2010). However, this was not always the case, indicating a somewhat tenuous functional connection between genome activity and spatial organization (Bickmore, 2013).

In parallel, methods using specific antibodies (Abs, Köhler and Milstein, 1975) enabled the development of immunofluorescence methods to visualise non-nucleic acid epitopes and map the distribution of nuclear proteins. This allowed the molecular characterization of many nuclear entities previously observed like Cajal bodies (Cajal, 1903; Pueschel et al., 2016). By detecting histone modifications, it was possible to observe the enrichment of inactive marks like H3K9me3 (Peters et al., 2001; 2003, Figure 9C) at chromocenters in mouse cells, whereas the use of GFP-tagged H3.3 showed its association with active marks in chromatin, distributed broadly throughout the nuclear interior in *D. melanogaster* cells (Ahmad and Henikoff, 2002). When examining replication, by labelling newly synthesized DNA by BrdU pulse, early-replicating regions marked the interior whereas late-replicating were at the periphery of the nucleus (Dimitrova and Berezney, 2002; Fox et al., 1991, Figure 9D), indicating a spatial compartmentalisation of chromatin states and genomic processes.

Even with the advent of FISH, three main limitations to access genome organization from the scale of entire chromosomes to small loci remained: the method of production of the probes (resulting in maximal genomic resolution of 10s of kilobases), the spectral overlap of fluorophores (leading to the inability to distinguish many different regions simultaneously in the same cell) and the diffraction limit of light (resulting in maximal optical resolution ~200-300nm).

These issues have been largely tackled in the past decade due to the development and combination of Oligopaints, microfluidics and super-resolution microscopy (Boettiger and Murphy, 2020). Oligopaints comprise libraries of short (20-50nt) DNA oligos which tile a sequence of interest and are either fluorescently labelled (Beliveau et al., 2012; Schmidt et al., 2015) or have a unique barcode which can be used to label them with a fluorescent complementary oligo in a second hybridization step (Beliveau et al., 2015). This allows the labelling of much smaller targets, improving genomic resolution, and combined with microfluidic devices that control the flow of oligos, enables sequential labelling of the same cells with multiple colours at a time to trace the path of long stretches of chromatin step (Beliveau et al., 2017).

Imaging techniques, such as super-resolution microscopy, resolve individual objects closer than 200nm apart, going beyond the light diffraction limit. These include stochastic optical reconstruction microscopy (STORM, Rust et al., 2006) and structured illumination microscopy (SIM, Schermelleh et al., 2008). Their rationale is based on excitation of different subsets of all the fluorophores in the sample at any one moment, combined with recording the distinct emissions over time and reconstructing a single image, thus avoiding the problem of spatially dense labelling (Boettiger and Murphy, 2020).

The application of STORM coupled to the labelling of histone variants and PTMs evidenced the heterogeneous organisation of nucleosomes in the nucleus, which instead of an ordered 30nm fibre form 'clutches' or 'conglomerates' with varying compaction (Ricci et al., 2015), density and/or volume throughout the cell cycle (Clément et al., 2018) or depending on their nuclear position and chromatin state (Xu et al., 2018, Figure 10). Oligopaints (Wang et al., 2016) have been combined with super-resolution imaging (Bintu et al., 2018; Nir et al., 2018) in methods for chromatin tracing like optical reconstruction of chromatin architecture (ORCA, Mateo et al., 2019), high-throughput multiplexed sequential imaging (Hi-M, Cardozo Gizzi et al., 2019) and fluorescence *in situ* sequencing of barcoded Oligopaint probes (OligoFISSEQ, Nguyen et al., 2020). They not only allowed to probe chromatin folding at different scales and unprecedented resolution, bridging the gap between the nucleosomal and nuclear scale, but have also been instrumental in aiding the interpretation of results from bulk genomic assays, developed in the years prior as an alternative method to interrogate 3D genome organization **(Is this real life? Is this just bulk Hi-C? (adapted from Mercury, 1975)**).

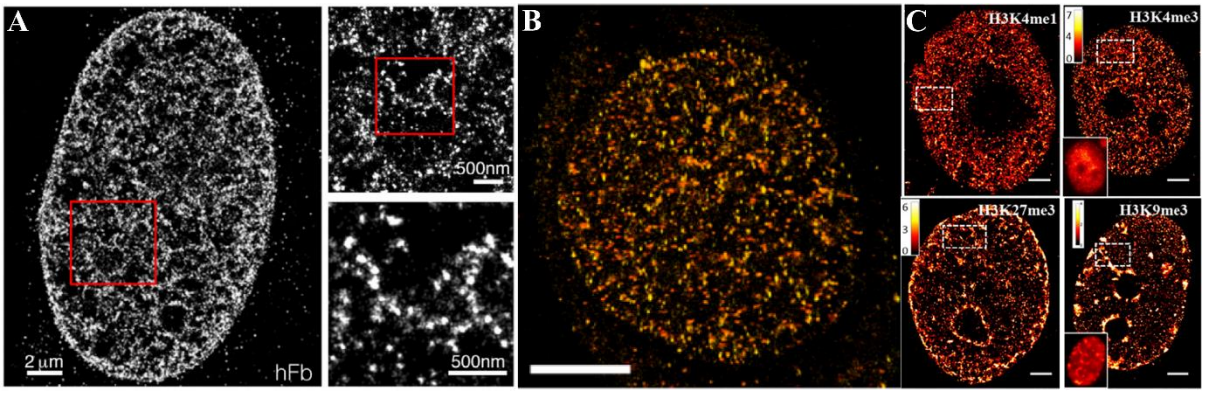

Figure 10. Chromatin organisation at super-resolution

STORM imaging of **A.** H2B Ab labelling in human fibroblasts (Ricci et al., 2015). **B.** H3.1-SNAP labelled with TMR in HeLa cells outside of S phase (scale bar = 5µm, Clément et al., 2018). **C.** Active (H3K4me1, top left, H3K4me3, top right) and inactive (H3K27me3, bottom left, H3K9me3, bottom right) histone PTMs, in MCF-10A cells (scale bars = 2µm, adapted from Xu et al., 2018).

1.4.2. Who am I? Identifying genomic enrichment of chromatin marks and DNA interaction patterns by sequencing-based methods

In parallel with imaging approaches, methods for molecular characterisation of chromatin structure, mapping of chromatin-associated/interacting proteins and DNA-DNA contacts also progressed. The organization of specific sequences isolated by restriction enzyme (RE) digestion and gel electrophoresis was interrogated by digestion with endonucleases like DNase I and micrococcal nuclease (MNase), demonstrating the presence of 'open', nucleosome-free hypersensitive sites (HSs) at the 5' end of genes (corresponding to TATA box/promoter, Wu, 1980) and origins of replication (SV40 minichromsome, Varshavsky et al., 1978). These HSs were shown to be cell-type specific and to change upon stress (e.g. heat shock), linking gene expression control with local chromatin organization (Wu, 1984). Furthermore, experiments inserting *D. melanogaster* heat shock protein (hsp) genes and their flanking

sequence into *S. cerevisiae* showed that they retained their HSs, indicating nucleosome positioning may be sequence-dependent (Costlow and Lis, 1984).

Chromatin immunoprecipitation (ChIP) boosted the study of specific proteins association with DNA (Solomon et al., 1988). In cross-linked (X)-ChIP method, cells cross-linked with formaldehyde prior to chromatin isolation, mechanical or enzymatic shearing, are subjected to immunoprecipitation with target-specific Ab, followed by isolation of associated DNA fragments. Conversely, for proteins associated tightly with chromatin (e.g. nucleosome components), native (N)-ChIP can also be used (Hebbes et al., 1988). There, chromatin obtained from non-fixed cells is digested with a nuclease prior to immunoprecipitation (O'Neill and Turner, 2003). Using the hsp70 gene as a model system, Solomon et al. (1988) demonstrated the presence of histone H4 both at the hsp70 HS and throughout the gene even when transcribed, contrary to previous nuclease digestion studies. These results highlight the importance of using different methods to map nucleosome or protein occupancy on chromatin as they may have distinct technical biases (Simpson, 1999). With the aim of avoiding potential fixation artefacts, van Steensel and Henikoff (2000) established DamID as an alternative approach to monitor protein association with DNA. DamID is based on fusion of a protein of interest with the bacterial DNA adenine methyltransferase Dam (modifies A in GATC motifs, a non-eukaryotic DNA mark), which results in methylation of sequences proximal to the protein of interest that can be recognized by methylated A-specific Abs or digestion with methylation-dependent enzymes (Steensel and Henikoff, 2000).

In addition to protein-DNA, detection of DNA-DNA contacts could provide information about the higher-order structure of chromatin. It could also help to address long-standing questions about the mechanisms of transcriptional regulation by distal regulatory elements and insulators, one model for which was loop formation (Grosveld et al., 1993). The approach devised by Dekker et al. (2002), chromosome conformation capture (3C), relies on cross-linking of intact nuclei with formaldehyde, followed by chromatin isolation, RE digestion and ligation in extremely diluted conditions. This results in preferential ligation between DNA strands within cross-linked fragments, generating chimeric molecules that contained (potentially) linearly distant genomic loci, reflecting their physical proximity in 3D nuclear space (Figure 11, left). This procedure results in a genome-wide library of contacts, from which interactions between specific loci could be evaluated using quantitative polymerase chain reaction (qPCR) with primers that would only generate a product from these chimeric molecules, but not linear DNA as template (Dekker et al., 2002). Used in *S. cerevisiae*, this technology recapitulated known features of its chromosome organization like their Rabl configuration (centromere clustering on one side of the nuclear lamina) and telomere clustering (Dekker et al., 2002). Using the same method in mammals, Tolhius et al. (2002) demonstrated that, the regulatory HSs (enhancers) in the locus control region (LCR) of the β-globin locus come in proximity with the β-globin gene promoter and a distal (~130kb away) 3' HS only when the gene is expressed. This work provided evidence in support of the

looping model where the β-globin LCR, 3' HS and active gene cluster together in space only in expressing cells (Tolhuis et al., 2002).

Even though at the time of their conception, these techniques inherently allowed the detection of all DNA-protein or DNA-DNA interactions, the number of loci analysed was limited by the methods of DNA detection available (Southern blot and (q)PCR) and the scarcity of genome sequence maps and information. However, the development of microarrays (Pease et al., 1994; Schena et al., 1995) and later, short-read/next generation sequencing (NGS, Bentley et al., 2008; Margulies et al., 2005; Rothberg et al., 2011), along with the publication of the human genome (Lander et al., 2001; Venter et al., 2001) increased the throughput of these approaches from (sets of) individual, pre-selected genes to the whole genome from a single sequencing (-seq) experiment. Further modifications on many of these methods have been implemented to improve recovery of material, signal-to-noise ratio, maximal resolution and other parameters (Table 2). Below, I will discuss how they have complemented the imaging studies described above to further document organization of the genome across scales.

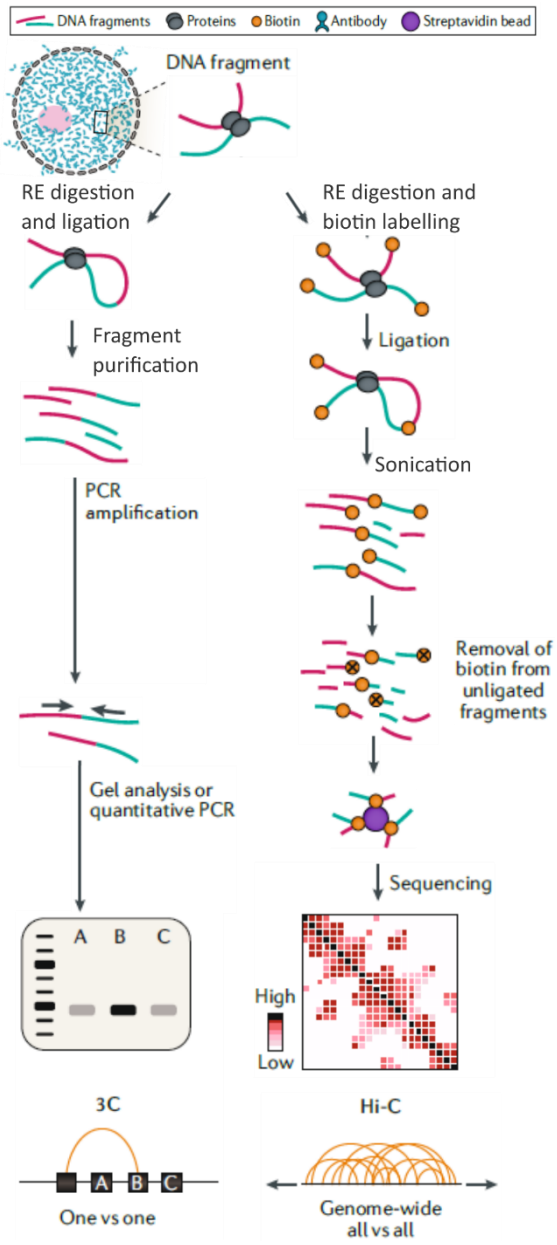

Figure 11. Chromosome conformation capture (3C) and high-throughput adaptation (Hi-C) Schematic representation of 3C (left, Dekker et al., 2002) and Hi-C (right, Lieberman-Aiden et al., 2009) workflows (adapted from Kempfer and Pombo, 2019).

Mapping beads along the string

MNase-seq has been one of the most prevalent methods to study nucleosome occupancy (how often a fragment is protected) and positioning (how specifically localised a nucleosome is in a population of cells), due to the ability of MNase to digest free DNA, resulting in fragments corresponding to mono-, di-, tri- and oligo-nucleosomes, depending on digestion time and enzyme concentration (Clark, 2010). In mammals, while nucleosomes generally show a stochastic positioning along the genome, a dinucleotide periodicity reflects DNA bending around the histone octamer (Voong et al., 2017). While nucleosome positions do not appear to be sequence-driven, they can be affected by the binding of some TFs like CTCF leading to well-positioned flanking nucleosomal arrays (Fu et al., 2008). Histone

variant-specific ChIP-seq further revealed that CTCF-occupied sites are flanked by H3.3-containing nucleosomes (Lacoste et al., 2014).

Table 2. Commonly used methods for mapping protein occupancy on chromatin

Approach	Principle	Advantages	Disadvantages
Chromatin immuno-precipitation followed by sequencing (**ChIP–seq**)	Cross-linked (e.g. with formaldehyde) (X-ChIP) and sonication or micrococcal digestion; or native (N-ChIP) and micrococcal digestion	Single-nucleotide resolution is possible with ultra-low-input material (ULI-NChIP). For many years ChIP–seq was the gold standard: countless reference data sets and many ChIP-grade antibodies are available. X-ChIP is well suited for transient interactions	High background noise; standard protocols require high cellular input and high sequencing depth; in X-ChIP cross-linking can mask epitopes recognized by antibodies; time-intensive protocol
DamID	Expression of a fusion of the bacterial adenine methylase (Dam, targets GATC sequences) with a protein of interest coupled with methylation-sensitive PCR	No cross-linking or DNA digestion Does not require stable interaction of target with chromatin, used to map proximity to lamina and nucleolus Can be used at single-cell level	Requires the design and expression of a fusion protein for each new target
Cleavage under targets and release using nuclease (**CUT&RUN**)	Recombinant MNase fused to protein A and/or protein G binding to specific antibody against PTM of interest	Avoids cross-linking and fragmentation of DNA, reduced background noise, possible with low input, fast protocol, only low sequencing depth required, used for single cells. CUT&RUN ChIP used to assess histone PTM co-occupancy	MNase digestion needs careful optimization. In addition to cleaving DNA next to PTMs, Mnase can also cleave DNA that is far away but close in three dimensions. Often antibodies are only validated for X-ChIP; transient interactions might be missed
Cleavage under targets and tagmentation (**CUT&Tag**)	Recombinant Tn5 transposase fused to protein A and/or protein G binding to specific antibody against PTM of interest	No cross-linking and library preparation step, sensitive, easy workflow, low sequencing depth required, can be performed at single-cell level and used for multiple chromatin targets or PTMs in the same assay (MulTI-Tag), single-cell genome-wide spatial-CUT&Tag possible	Tn5 enzyme biases: Tn5 preferentially tags accessible chromatin; potential background from mitochondrial DNA

References: ChIP-seq (Barski et al., 2007; Brind'Amour et al., 2015; Hebbes et al., 1988); CUT&RUN (Brahma and Henikoff, 2019; Hainer and Fazzio, 2019; Skene and Henikoff, 2017); CUT&TAG (Deng et al., 2022; Gopalan et al., 2021; Kaya-Okur et al., 2019; Meers et al., 2023); DamID (van Steensel and Henikoff, 2000, Guelen et al., 2008); Adapted from Millán-Zambrano et al. (2022).

Transcription start sites (TSSs) of active genes are usually preceded by a nucleosome-depleted region (NDR) with well-positioned -1 and +1 nucleosomes. The downstream array of nucleosomes progressively lose periodicity in the gene body. The occupancy of the NDR by a nucleosome has been linked with lower gene activity, potentially due to occlusion of the TATA box in the core promoter, preventing pre-initiation complex assembly (Schones et al., 2008). However, alternative methods of mapping nucleosome occupancy independent of enzyme digestion have not corroborated these findings, as they were able to detect a nucleosome at the NDR of active genes (Voong et al., 2016). This discrepancy may arise due to the composition of the nucleosomes found in the NDR, which contain H3.3-H2A.Z (Jin et al., 2009), resulting in reduced stability and increased susceptibility to MNase digestion (Voong et al., 2017).

To identify and characterise regions of 'open' vs 'closed' chromatin, DNase-seq and more recently, assay for transposase-accessible chromatin (ATAC)-seq, which relies on a Tn5 transposase directly inserting sequencing adaptors to 'tagment' accessible chromatin, have been extensively used. They have been combined with mapping of histone variants, PTMs and other chromatin-associated proteins by ChIP-seq, CUT&RUN, CUT&TAG and DamID (Table 2). A series of studies showed a general correlation between open chromatin and gene activity/early replication as opposed to closed chromatin, associated with repression and replication in mid/late S-phase. More specifically, sites of high chromatin accessibility tend to be discrete, enriched in active PTMs, H3.3 and H2A.Z, have high histone turnover and often correspond to active promoters (H4K4me3), enhancers (H3K4me1, H3K27ac) or early replication origins. In contrast, inactive chromatin is typically organised in larger domains associated with the nuclear lamina and/or the nucleolus, and broadly classified as either facultative (marked by H3K27me3, bound by PRC1 and/or PRC2 and covering developmental genes) or constitutive (enriched in DNAme, H3K9me3, bound by HP1a, spread over telomeres, centromeres and repetitive elements, Millán-Zambrano et al., 2022, **Histone post-translational modifications**). Importantly, one should bear in mind that these relationships are correlations and not absolute. This was illustrated in a recent study of mESC heterochromatin of intracisternal A-type particle (IAP) repeats, which dynamically incorporate H3.3, enriched in the repressive mark H3K9me3 and inaccessible (Navarro et al., 2020).

The general association between histone PTMs and accessibility, in line with observations about the distribution of chromatin marks by imaging, was corroborated by LaminB1- (Kind and Van Steensel, 2010) and nucleolar-DamID (Bersaglieri et al., 2022), which sequences in proximity to these nuclear landmarks. However, these methods provide only one-dimensional information about protein distribution along the genome but do not assay the 3D organization of chromatin.

Adding dimensions to connect the dots

To address this challenge, a wide variety of increased throughput modifications of 3C have been developed (Table 3). They allow the detection of interactions of: one region ('viewpoint') with the rest of the genome (4C-seq) (Simonis et al., 2006; Zhao et al., 2006), many pre-defined regions with one another (5C-seq) (Dostie et al., 2006) and all genomic regions with each other (Hi-C, Figure 11, right). Hi-C has been the most widely used approach to study genome organization globally, ranging from the scale of whole chromosomes to individual enhancer (E) – promoter (P) contacts (Figure 12). More recently, digestion with MNase instead of REs improved maximal resolution (micro-C) (Hsieh et al., 2020, 2016, 2015), whereas oligo-based pull-down of regions of interest (Capture-HiC) (Mifsud et al., 2015; Schoenfelder et al., 2015b, 2015a) or immunoprecipitation of sequences associated with a protein of interest (ChIA-PET/PLAC-seq) (Fang et al., 2016; Fullwood et al., 2009) allowed to focus on functionally important sites while reducing library size and sequencing costs. Detection of contacts between 3 or more loci has been enabled by improved analysis methods (Tavares-Cadete et al., 2020) and the use of crosslinking-independent approaches like SPRITE (Quinodoz et al., 2018) and GAM (Beagrie et al., 2017), while radial distribution of chromatin in the nucleus has been assayed by GPSeq (Girelli et al., 2020), reviewed in (Jerkovic and Cavalli, 2021; Kempfer and Pombo, 2019).

Chromosome territories

In mammalian cells, Hi-C detects chromosome territories, demonstrated by the higher probability of regions to be in contact when on the same chromosome (in *cis*, even up to 200Mb apart) compared to between chromosomes (in *trans,* Lieberman-Aiden et al., 2009, Figure 12A). Hi-C also detects higher *trans* contacts between small-gene rich chromosomes known by FISH studies to cluster in the nuclear interior (Lieberman-Aiden et al., 2009). Finally, Hi-C can also recapitulate *trans* interaction patterns in species with centromere (*D. melanogaster,* Sexton et al., 2012) or telomere (*S. cerevisiae,* Dekker et al., 2002, Duan et al., 2010) clustering or alignment of the chromosomes on a centromere-to-telomere axis (Hoencamp et al., 2021).

Compartments

On the scale of megabases (Mb), mammalian Hi-C maps exhibit a characteristic plaid or checkerboard appearance, whereby the genome is split in two interspersed sets of large segments, which show interactions within, but not between sets (Lieberman-Aiden et al., 2009, Figure 12B). These sets, termed A (accessible, active, early-replicating) and B (closed, repressed, late-replicating) compartments (Lieberman-Aiden et al., 2009; Pope et al., 2014) broadly correspond to eu- and heterochromatin as identified by imaging (Monneron and Bernhard, 1969). This is also corroborated by the differences in A/B compartment of up to 50% of the genome between various cell types in accordance with changes in epigenetic state and transcriptional activity (Bonev et al., 2017; Dixon et al., 2015; Lieberman-Aiden et al., 2009). However, despite the general correlation between compartments and genome function,

these associations are neither absolute nor necessarily causal: B compartments can contain active genes and conversely, not all genes in compartment A are transcribed (Kempfer and Pombo, 2019; Rowley

Assay	Description	Contacts per experiment	Multiplicity of contacts	Single-cell information
3C-based methods				
3C	Proximity ligation and selection of target regions with primers, detection by quantitative PCR	One vs one	Pairwise	No
4C	Proximity ligation and enrichment for contacts with one bait region by inverse PCR, detection by sequencing	One vs all		
5C	Proximity ligation and enrichment for larger target region with primers, detection by sequencing	Many vs many		
Hi-C	Proximity ligation after RE digestion and enrichment for all ligated contact pairs, detection by sequencing	All vs all		
micro-C	Proximity ligation after MNase digestion and enrichment for all ligated contact pairs, detection by sequencing	All vs all		
ChIA-PET	Proximity ligation and pull- down of specific protein-mediated contacts, detection by sequencing	Many vs many		
Capture-C, cHi-C	Proximity ligation and target enrichment using probes for genomic regions of interest, detection by sequencing	Many vs all		
single-cell Hi-C	Proximity ligation and enrichment for all ligated contact pairs, detection by sequencing	All vs all		Yes
Ligation-free methods				
GAM	Cryosectioning of fixed cells, DNA extraction from nuclear sections and sequencing, inferring spatial distances from co- segregation of genomic regions in nuclear sections	All vs all	Many	Yes
SPRITE	Fixation of cells, identification of crosslinked chromatin fragments by split- pool barcoding and sequencing	All vs all		No
GPSeq	Timecourse of RE digestion followed by ligation of barcodes enabling visualization by FISH and sequncing of radial fractions (from centre to periphery)	N/A, provides radial positioning	N/A	No (only by FISH)

3C, chromosome conformation capture; 4C, circular chromosome conformation capture; 5C, chromosome conformation capture carbon copy; ChIA-PET, chromatin interaction analysis by paired-end tag sequencing; cHiC, capture HiC; GAM, genome architecture mapping; GPSeq, Genomic loci positioning by sequencing; Hi-C, high-throughput chromosome conformation capture; micro-C, MNase-digested Hi-C; SPRITE, split-pool recognition of interactions by tag extension; Adapted from Kempfer and Pombo, 2019.

and Corces, 2018).

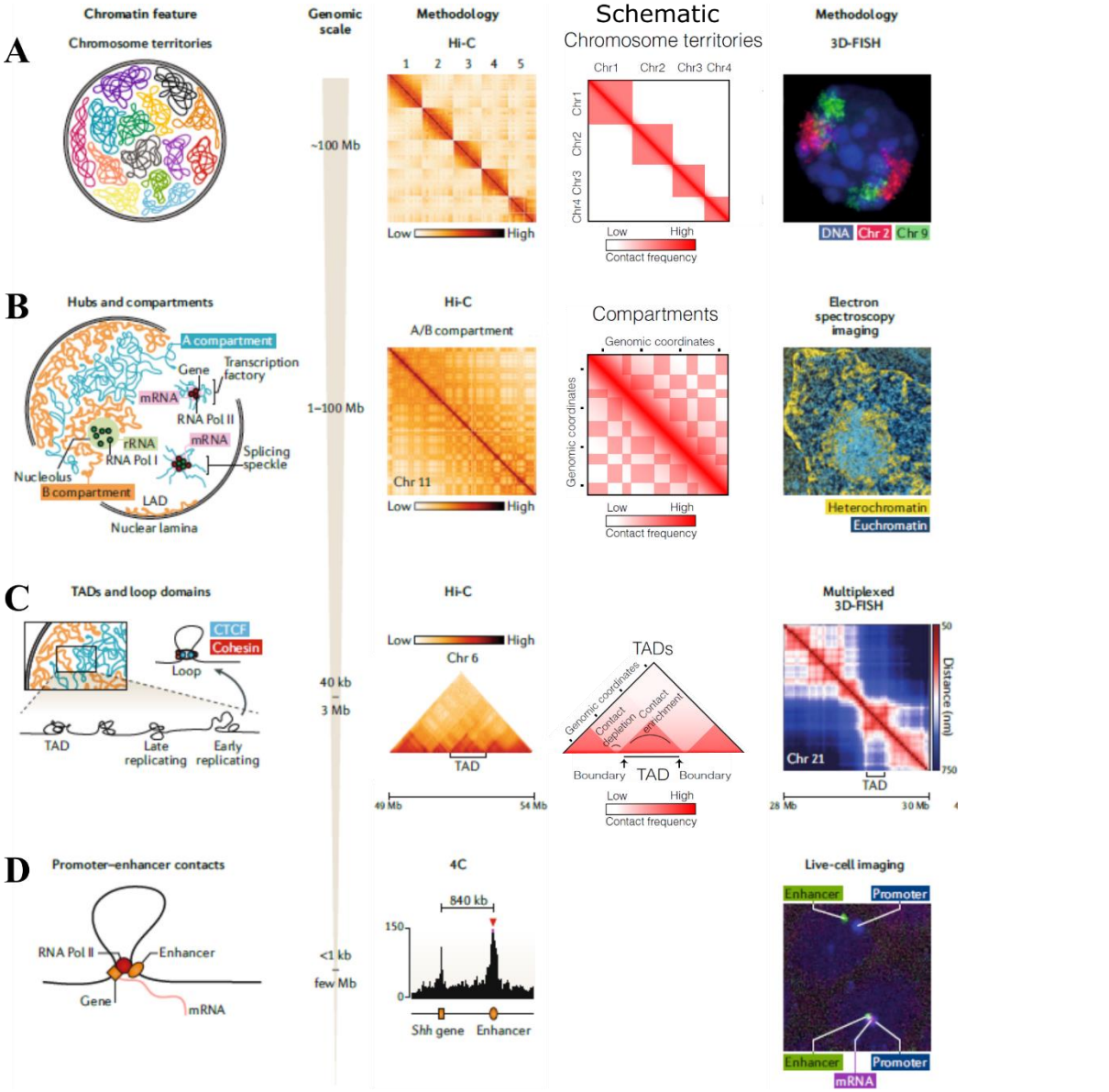

Figure 12. Hi-C reveals interaction patterns across genomic scales

Features of chromatin organisation (1st column) represented on Hi-C maps (actual data, schematic representation, middle) and identified by imaging methods (last column) across genomic scales. **A**. Chromosome territories are visible on Hi-C maps at the 100s Mb scale as enrichment of contacts within chromosomes (in *cis*) and few interactions in *trans*. 3D-FISH of chr2 (red) and chr9 (green) in mESCs show territoriality observed by imaging **B.** Compartments are detectable as a plaid pattern at the Mb scale, reflecting chromatin is spatially segregated in two. A (active) and B (inactive) compartments largely correspond to eu- (blue) and heterochromatin (yellow), respectively, originally identified based on differences in electron density (left). **C.** Topologically-associating domains (TADs) were identified from Hi-C as a sub-Mb scale feature as regions of the genome enriched in contacts within and depleted in interactions with neighbouring regions. Subsequent super-resolution imaging work demonstrated they can exist as physical domains (for example the average distance map of chr21 obtained by multiplexed FISH from single cell, left). However, TADs are highly dynamic and heterogenous over time and between cells.

D. E-P contacts can be detected as dots of enrichment on maps from higher resolution genome-wide methods like micro-C, or by lower-throughput approaches focusing on a single locus like 4C. They can also be detected by imaging, for instance live-cell imaging in *Drosophila* embryos (left, adapted from Kempfer and Pombo, 2019 and Szabo et al., 2019)

To confirm their Hi-C results, Lieberman-Aiden et al., 2009 used 3D FISH of regions which are linearly adjacent but belong to a different compartment to show that their spatial proximity is reflected by their Hi-C contacts rather than genomic arrangement. Furthermore, calculating the frequency of interaction between loci within A and B compartment separated by similar linear distance revealed consistently higher contacts between B compartment regions, indicating they may be more highly compact, in line with what is expected for heterochromatin (Lieberman-Aiden et al., 2009). Thus, at the Mb scale, Hi-C describes characteristics of chromatin organization already detected by imaging. Additionally, it provided sequence information for the interactions within the whole genome, although it did not reflect nuclear positioning with respect to the interior or lamina.

To infer A and B compartment locations, dimensionality reduction approaches like eigenvector (EV) decomposition are applied on a normalised Hi-C matrix. The result of this mathematical operation is that the matrix can be described as a sum of eigenvectors (1D representation of a feature of the matrix) multiplied by their respective eigenvalue (weights, Figure 13). The 1st eigenvector (EV1) summarises the most dominant feature of the matrix, which on the Mb scale for mammalian genomes is usually compartmentalization (Lieberman-Aiden et al., 2009; Open 2C et al., 2022). A cut-off at 0 has been used to separate the genome into two compartments, and additional information (GC content, gene

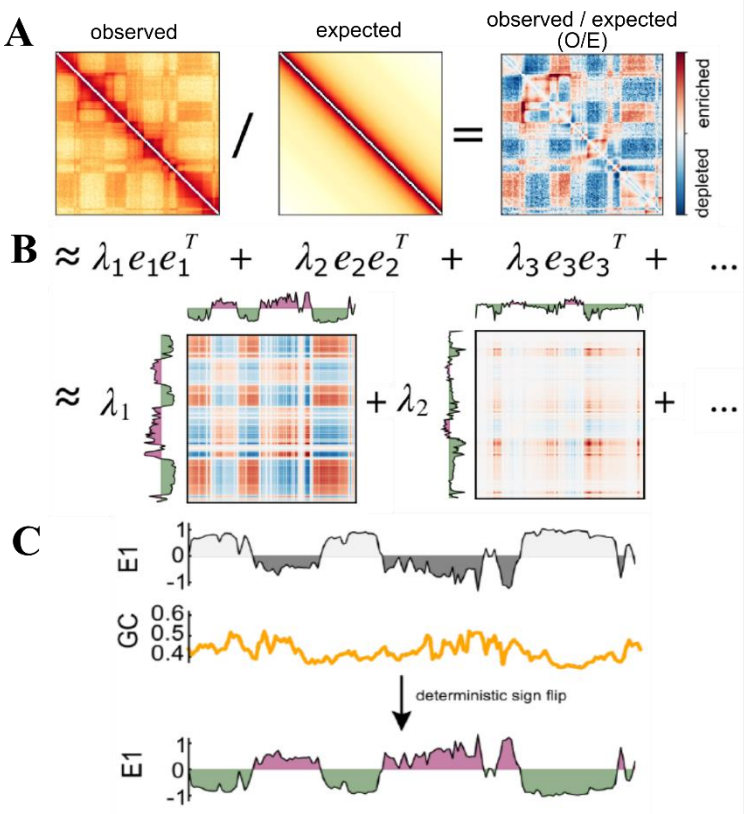

Figure 13. Compartment calling
A. Observed data is divided by expected matrix, computed from the observed assuming equal decay of contacts with distance from the diagonal for each genomic bin. This results in an observed/expected (O/E) normalised matrix used for compartment calling in **B.** Eigenvector decomposition of the O/E matrix). **C.** The 1st eigenvector (EV1) typically represents compartment segregation in mammalian Hi-C. To assign the nature of the compartment (A/B), EV1 track is phased by comparing to any genomic feature correlated with activity, e.g. GC content (adapted from Open2C et al., 2022).

density, PTM ChIP-seq) is required to orient the sign of EV1 and identify which regions are A (active) and B (inactive). With increasing resolution and improved analytical tools, compartments can now be called from up to 0.5k-binned maps, allowing to investigate the organization of smaller features like individual genes, promoters, and enhancers (Harris et al., 2023).

Incorporating information from matrix decomposition beyond EV1 enabled the identification of subcompartments within A and B with distinct interaction preferences associated with different types of chromatin or functional state in several cell types (Liu et al., 2021; Rao et al., 2014; Spracklin et al., 2022). For example, A1 and A2 are both active and gene-dense, but A1 shows earlier replication timing (Rao et al., 2014), an association with nuclear speckles and higher transcriptional activity (Spracklin et al., 2022). The three studies also detect a different number of B subcompartments, but among those, they all identified one enriched in H3K27me3 and one in H3K9me3/HP1, corresponding to facultative and constitutive heterochromatin, respectively (Rao et al., 2014, Liu et al., 2021, Spracklin et al., 2022). Beyond revealing the various ways in which cells can organise their heterochromatin, Hi-C can thus identify different chromatin subtypes based on interaction patterns alone.

We interrupt your programme with a burning question: How is this happening?

A question which remains open in the field is what drives the formation and maintenance of compartments (Hildebrand and Dekker, 2020). One widely discussed hypothesis is that compartmentalization is the consequence of phase separation: the segregation of two entities when mixed due to their physical properties (Figure 14A, Erdel and Rippe, 2018; McSwiggen et al., 2019). In this framework, chromatin is considered as a block copolymer, composed of alternating segments of monomers of different kinds (i.e. regions of the genome with a distinct chromatin state or A/B compartment identity). This idea is consistent with the fact that chromatin subcompartments exhibit distinct epigenetic profiles, including histone variants (e.g. H3.3, H2A.Z) and PTMs (e.g. histone acetylation) which may (i) confer different physical properties to the nucleosomes they form and/or (ii) recruit specific readers which could interact with other chromatin segments or each other.

With respect to the former, *in vitro* assembled chromatin forms liquid droplets when using unacetylated histones, with the extent of compaction depending on linker DNA length and the presence of histone H1 (Gibson et al., 2019). While droplets dissolved if acetylated histones were used, they reform upon addition of BRD4 (transcriptional co-activator with a bromodomain that recognises lysine acetylation), which led to the establishment of a separate phase (Figure 14B, Gibson et al., 2019). In cells, BRD4 and MED1 (subunit of the transcriptional co-activator Mediator) are enriched at super-enhancers (SE, kb-long domains of H3K27ac) and can be observed as puncta by IF. Both proteins contain intrinsically disordered regions (IDRs): unstructured amino acid stretches which have been implicated in the formation of multivalent protein-protein interactions involved in LLPS. Indeed, both BRD4 and MED1 form droplets *in vitro* and treatment with 1,6-hexanediaol (1,6-HD, a compound disrupting LLPS

condensates) results in dissolution of BRD4 and MED1 puncta in cells (Sabari et al., 2018). This is also true for RNAPII, which can form condensates in cells due to its C-terminal domain (CTD, Boehning et al., 2018; Guo et al., 2019), although other work has shown RNAPII can cluster in a manner not driven by LLPS (McSwiggen et al., 2019a). However, inhibition of transcription or depletion of RNAPII components does not disrupt A/B compartmentalization (Barutcu et al., 2019; Hsieh et al., 2020; Jiang et al., 2020; Xie et al., 2022), indicating that active chromatin segregation is not dependent on transcriptional activity or the presence of RNAPII-mediated condensates. On the other hand, depletion of the co-activator BRD2 (Xie et al., 2022) or the nuclear speckle component SRRM2 (Hu et al., 2019) results in weakening of A compartment interactions, although it is unclear whether this is due to disruption of phase separation. Thus, proteins associated with active chromatin can impact the association of A compartments but the mechanism of this remains unclear.

Phase separation has also been proposed to explain segregation of B (sub-)compartments (Figure 14B, Erdel, 2023). Developmental genes in facultative heterochromatin (H3K27me3-marked) can be organised in foci, known as Polycomb bodies, via the establishment of long-range contacts between them when bound by the PRC1 complex (Bantignies et al., 2011; Noordermeer et al., 2011; Ogiyama et al., 2018; Schoenfelder et al., 2015). CBX2, one of its subunits, has been shown to form droplets *in vitro*, whereas mutating it results in loss of Polycomb puncta (Plys et al., 2019; Tatavosian et al., 2019) and reduced nucleosome compaction (Lau et al., 2017) *in vivo*. However, another PRC1 subunit, PHC1 which enables PRC1 oligomerisation through its sterile alpha motif (SAM), is also required for Polycomb clustering and the local insulation, compaction, and long-range interactions of target genes (Kundu et al., 2017; Wani et al., 2016).

Constitutive heterochromatin (H3K9me3-modified) is bound by HP1a, which also contains an IDR and assembles into condensates *in vitro* (Larson et al., 2017; Strom et al., 2017). In human HCT-116 cancer cells, knock-out of DNMT1 and DNMT3b leads to loss of DNAme and strong reduction of H3K9me3 and HP1 binding in heterochromatin in the B_4 subcompartment. This resulted in loss of the preferential homotypic interactions between B_4 domains, accompanied by a shift to a different B subcompartment (Spracklin et al., 2022). Another study using the same cell line also observed decreases strength of B compartment strength (Du et al., 2021), indicating a role for HP1 in promoting self-interactions between regions where it is bound. In agreement with these results, Wijchers et al. (2016) showed that in mESCs, anchoring either WT or mutant Suv39h1 (lacking H3K9me3 recognition and HP1a interaction domains) to a region could induce result in its H3K9me3, but only the WT Suv39h1 could promote its switch from A to B compartment, potentially due to its interaction with HP1a. Conversely, knock-down (KD) of all HP1 isoforms impaired Rabl configuration, decreased B compartment strength and increased compaction along chromosome arms in *cis* in transcriptionally inactive *D. melanogaster* embryos, but not somatic S2 cells, indicating it is important for the establishment, but not maintenance of constitutive heterochromatin organization (Zenk et al., 2021). Indeed, in mouse cells double deletion of Suv39h1/2

abolishes H3K9me3 at pericentromeric heterochromatin (PHC), leading to loss of HP1 binding without disrupting their clustering into chromocenters (Peters et al., 2001). Erdel et al. (2020) have confirmed these findings and shown HP1a does not form droplets on chromatin, suggesting it might instead form bridging interactions through its capacity to oligomerise (Machida et al., 2018).

Another feature of heterochromatin organization is its enrichment at the lamina and/or nucleolus, in what have been termed lamina-/nucleolus-associated domains (LADs (Guelen et al., 2008)/NADs (Németh et al., 2010; van Koningsbruggen et al., 2010), respectively). Indeed, the vast majority of

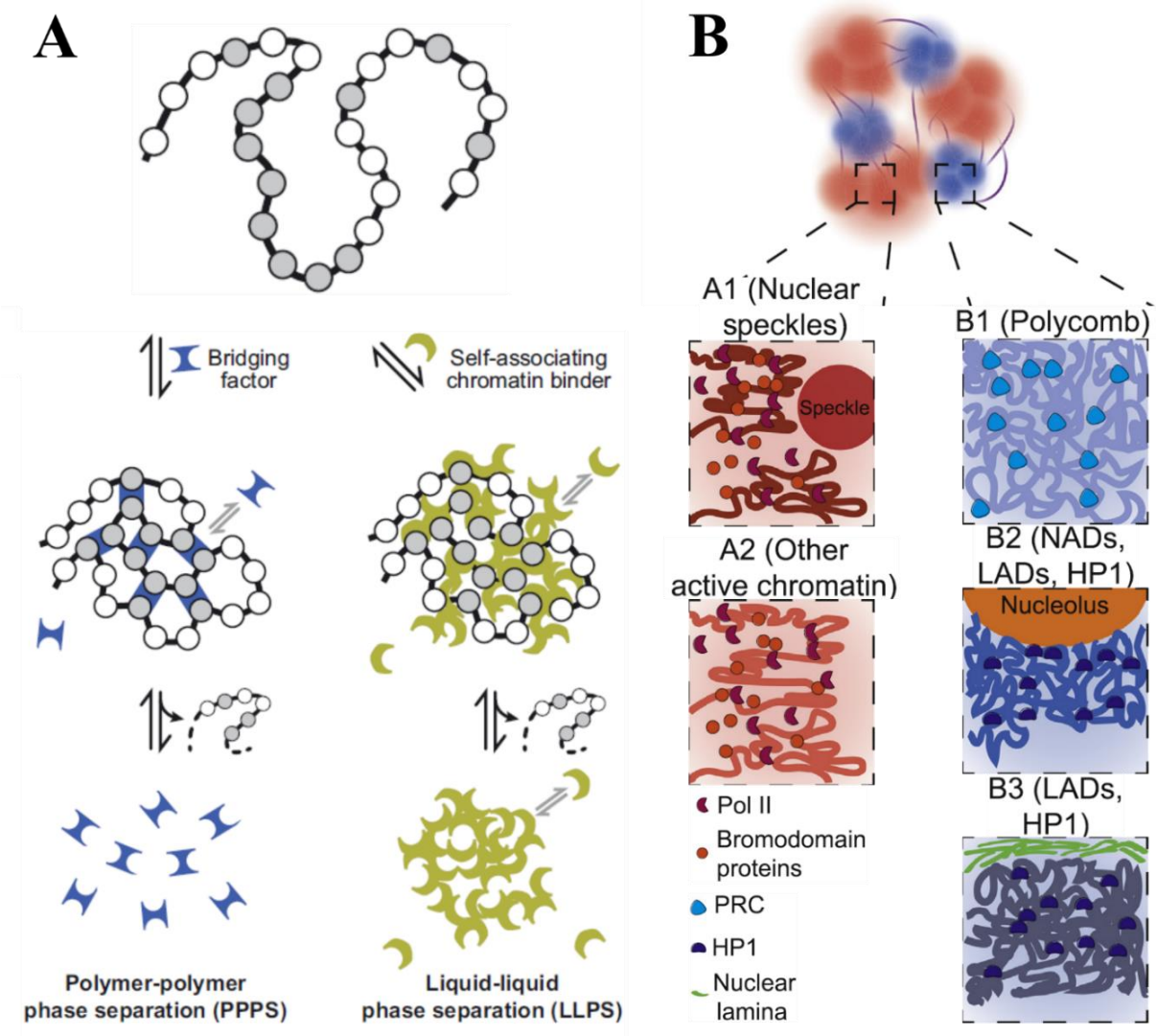

Figure 14. Phase separation as a mechanism for chromatin compartmentalization

A. There are different types of phase separation, but two of the main ones considered in the context of chromatin organization are polymer-polymer and liquid-liquid phase separation (PPPS and LLPS, respectively). PPPS (**left**) could be the result of bridging factors directly binding distant regions of chromatin and bringing them together, whereas LLPS (**right**) would occur if chromatin-associated proteins form unspecific, multi-valent interactions with each other, forming high-concentration liquid-like droplets (adapted from Erdel and Rippe, 2018). B. Formation of subcompartments (detected by Hi-C) by phase separation mediated by distinct chromatin-interacting factors (adapted from Hildebrand and Dekker, 2020).

LADs are found in compartment B in differentiated cells (Luperchio et al., 2018). A large proportion (~50%) of NADs and LADs overlap, although there are also sequences that are found exclusively either at the nucleolus (NAD-only, Vertii et al., 2019) or the lamina (LAD-only, Kind et al., 2013), and the three types of regions have distinct combinations of PTM enrichment (Bersaglieri et al., 2022). While the nucleolus exhibits some droplet-like properties, suggesting it might be phase-separated (Erdel et al., 2020; Frottin et al., 2019; Lafontaine et al., 2021), the sequestration of heterochromatin at the periphery has been suggested to be mediated by specific protein-protein interactions between HP1 with components of the lamina like the lamin B receptor (LBR, Ye et al., 1997). However, it remains unclear how regions can be differentially targeted the nucleolus or the lamina considering their similar enrichment of H3K9me3 (Bersaglieri et al., 2022). Finally, localization to the lamina is not required for the formation of B compartment (Falk et al., 2019), although it can affect its strength (Bertero et al., 2019).

Computational modelling of biological phenomena is a powerful tool to test and generate new hypothesis that could explain the observed data. Based on another dominating feature of Hi-C maps, the decay of contacts with distance from the diagonal, which follows a power law and reflects the fact that linear proximity is also a strong determinant of how often regions will interact, Lieberman-Aiden et al. (2009) suggested chromatin can be modelled as a polymer, organized as a fractal (unentangled) globule. This approach has been extended to understand what drives genome compartmentalization by modelling chromatin as a long co-polymer consisting of several types of monomers (typically two, corresponding to A and B compartment) that alternate linearly along the chain, avoid each other and experience self-attraction (between the same kind, Di Pierro et al., 2017; Jost et al., 2014). The aim is to fit a model, from which *an in silico* Hi-C map can be produced to compare to experimental observations, such that it fits the data best while requiring the least number of parameters (Abdulla et al., 2023; Haddad et al., 2017; Jerkovic and Cavalli, 2021).

Using three states, A (euchromatin), B (heterochromatin) and C (constitutive pericentromeric/telomeric heterochromatin), for modelling chromatin in a confined space, Falk et al. (2019) have demonstrated that attraction between B compartments is sufficient to drive compartmentalization, whereas A compartment interactions are dispensable. Furthermore, they show that interactions between B compartments and lamina are required to 'orient' chromatin organization, but not to segregate compartments (Falk et al., 2019). A similar model has also been employed by Zenk et al. (2021) to distinguish between the role of HP1a enrichment at pericentric regions, where it contributed to the establishment of Rabl configuration of chromosomes and heterochromatin condensation, in contrast to binding along chromosome arms, which could prevent their compaction and promote B-B interactions. However, this model is not able to discern the mechanism by which HP1a performs its function (Zenk et al., 2021). Finally, another type of polymer modelling has been used to predict 3D compartment organization based on tracks of 1D epigenetic information (mainly histone PTMs) with the aim of

uncovering interactions between which sets are the most important for accurate recapitulation of real Hi-C maps from the same cells (rev in Jerkovic and Cavalli, 2021, Abdulla et al., 2023). While some studies have put forward particular marks and/or their interactors as sufficient for compartment definition (Nichols and Corces, 2021), others have concluded that it is the combinatorial information that distinguishes different states and promotes their 3D organization (Esposito et al., 2022).

In conclusion, both experimental evidence and modelling results suggest that chromatin compartmentalization can be driven by its activity and epigenetic state. However, it is likely that this scale of organization is controlled by several mechanisms, which may operate in concert, but also to different extent at distinct regions of the genome.

Returning to your scheduled (sequence) identity crisis: TADs and loops

Increasing sequencing depth allowed analysis of Hi-C maps on the sub-Mb scale (binned at ~40kb, Dixon et al., 2012; Hou et al., 2012; Nora et al., 2012; Sexton et al., 2012). This revealed the presence of contiguous domains which were enriched in interactions within, but depleted of contacts (~33% less, Rao et al., 2014) with their neighbouring sequences, even though they are linearly adjacent (Dixon et al., 2012, Nora et al., 2012). These self-associating regions, termed topologically associating domains (TADs, Figure 12C, 15), are demarcated by boundaries enriched in the insulator protein CTCF (~75% boundaries, mESCs), active promoters and/or house-keeping genes (~35% boundaries, mESCs) and repeat elements in both mammalian (Dixon et al., 2012; Nora et al., 2012) and *D. melanogaster* genomes (Hou et al., 2012; Sexton et al., 2012). Mammalian TADs have a median size of ~880kb (mESCs, Dixon et al., 2012) and their boundaries are shared between cell types (60-90%, Dixon et al., 2012). Furthermore, differences in short-range contacts between cell types are usually within TADs (Dixon et al., 2012) and upon cell differentiation, entire domains switch compartment concordant with gene expression changes (Dixon et al., 2015), whereas few new boundaries are established (Bonev et al., 2017), suggesting TADs may be stable structural and functional units of genome organization (Beagan and Phillips-Cremins, 2020; Szabo et al., 2019).

Improvements of the Hi-C protocol (Rao et al., 2014) enabled the examination of maps at 1kb resolution, revealing that mammalian TADs were nested structures containing smaller subdomains, termed subTADs (Phillips-Cremins et al., 2013). About 50% their boundaries were common between cell lines and their median size was 185kb, much closer to the TADs originally identified in *D. melanogaster* (median length ~100kb, Hou et al., 2012; Sexton et al., 2012). A subset (~40%) of these smaller domains exhibited a ‘corner dot’: a high-frequency focal interaction away from the diagonal, corresponding to contact enrichment specifically between the two boundaries (Figure 15). This was interpreted to reflect the presence of a loop anchored at the two domain boundaries, predominantly (>85%) co-occupied by CTCF in convergent orientation together with the cohesin complex (Rao et al., 2014). Finally, in addition to ‘loop domains’, the authors also described ‘ordinary’ or ‘compartment’

domains, which corresponded to a single epigenetic state, indicating different processes may be responsible for their establishment (Rao et al., 2014).

Notably, loop domains were only 40% out of all loops detected: another ~30% were interactions between CTCF/cohesin-bound sites within domains, and the remaining 30% corresponded instead to enhancer-promoter (E-P) contacts, ~half of which also were enriched for CTCF and cohesin (Rao et al., 2014). Like loop domains, loops are well-conserved (55-75%) between cell lines (Rao et al., 2014) and cell type-specific loops tendentially smaller, within TADs and predominantly between enhancers and promoters in a manner related to differential regulation of gene expression (Grubert et al., 2020; Phillips-Cremins et al., 2013). Thus, loops can be broadly classified as structural, when associated only with CTCF/cohesin co-occupancy, and functional, including E-P, P-P and Polycomb-mediated loops, which are more likely to fall within TADs and be linked with transcriptional control (Hsieh et al., 2020).

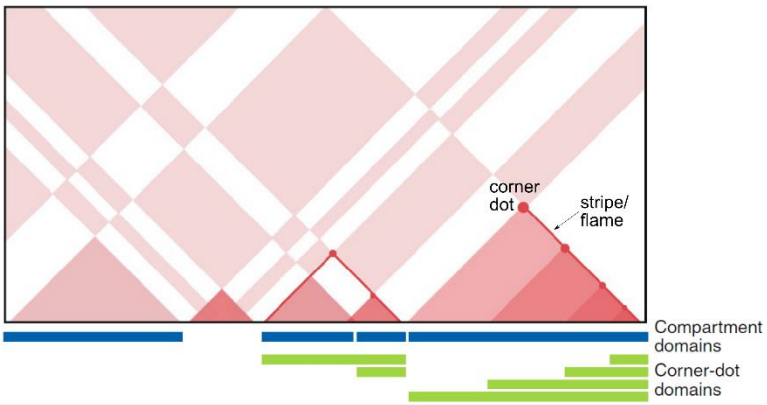

Figure 15. TADs and loops

Schematic representation of distinct classes of TADs. Compartment domains refer to TADs demarcated by compartment shifts. Corner-dot or loop domains refer to regions where the point of interaction between the two boundaries is focally enriched in contacts. Loops are characterised by the presence of corner dots at their base, and by stripes/flames emerging from one or both anchors, which can contain several weaker dots (cohesin pause sites) and may continue beyond the loop anchor (adapted from Beagan and Phillips-Cremins, 2020).

Loops and compartments: one of those things is not like the other

Mechanistic understanding of how loops and loop domains are formed came from the combination of polymer modelling and rapid protein depletion experiments (Beagan and Phillips-Cremins, 2020; Szabo et al., 2019). The idea of loop formation in the context of E-P communication had already been put forward to explain control of expression by distal regulatory elements (Grosveld et al., 1993), and experimental evidence suggested the cohesin complex may interplay with Mediator to promote E-P contacts (Kagey et al., 2010; Phillips-Cremins et al., 2013). Cohesin, identified for its role in maintaining sister chromatid cohesion after replication, is one of the three structural maintenance of chromosomes (SMC) complexes in mammals, together with condensin (I and II) and Smc5/6 (Davidson and Peters, 2021). All SMC complexes have a common ring-like pentameric organisation (Figure 16), which allows them to bind DNA and translocate along it in an ATP-driven manner. Unlike cohesin, condensins are required in mitosis for the formation of tightly compacted, linear chromosomes, which polymer modelling demonstrated could be mediated by the process of extrusion of nested loops

(Goloborodko et al., 2016; Naumova et al., 2013), as hypothesized previously (Alipour and Marko, 2012; Nasmyth, 2001).

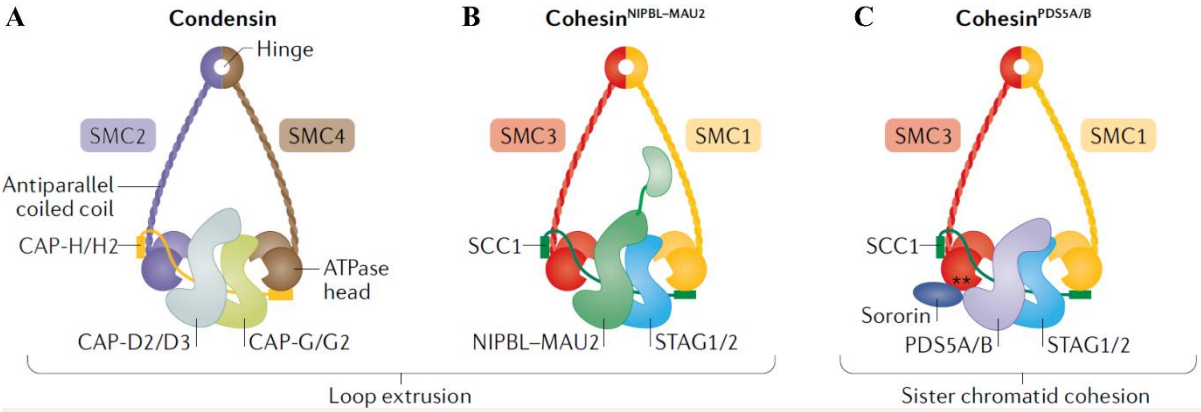

Figure 16. SMC complex structure

All SMC complexes consist of two SMC subunits, comprising ~50nm-long coiled coil with a hinge domain on one end, which enables heterodimerization, and an ATPase head on the other end, which participates in translocation. The two ATPase domain are connected by a kleisin subunit, which completes the formation of the ring. Two additional subunits, termed HEAT repeat proteins associated with kleisins (HAWKs), which can play regulatory roles are part of the final complex. **A.** Condensin I and II share the SMC2/4 proteins but have distinct kleisin (CAP-H/H2, respectively) and HAWK (CAP-D2, CAP-G for condensin I and CAP-D3, CAP-G2 for condensin II) subunits. **B.** Extruding and **C.** cohesive cohesin share SMC1/3 and Rad21 (kleisin). Extruding cohesin associates with the NIPBL-MAU2 complex, required for loading and extrusion, and STAG1 or 2. In cohesive cohesin, NIPBL is replaced by PDS5A or B, making it unable to extrude loops (adapted from Davidson and Peters, 2021).

Thus, an active 'loop extrusion' mechanism in interphase was proposed, where cohesin is loaded onto chromatin and translocates bi-directionally in an ATP-dependent manner, forming a loop, until it reaches a barrier element (CTCF-occupied site in the correct orientation), where it becomes arrested until it is released (Figure 17, Fudenberg et al., 2016, 2017). This model could recapitulate the emergence of TAD and loop-like structures (domains and 'corner dots', respectively) on Hi-C maps at the resolution that had been achieved at the time (Fudenberg et al., 2016), but also predicted the presence of 'stripes' or 'flames', emanating from the boundary on diagonal and proceeding until or even past the other loop anchor, which were only observed later when higher-resolution Hi-C (Fudenberg et al., 2017) and micro-C (Hsieh et al., 2020; Krietenstein et al., 2020) maps were generated. Furthermore, this model made testable predictions on the consequences of loss of CTCF or cohesin, which were experimentally confirmed by multiple studies in the following year (Fudenberg et al., 2017) thanks to the use of near-complete, rapid and reversible protein depletion via the auxin-inducible degron (AID) system.

Depletion of CTCF led to the loss of CTCF/cohesin-dependent loops and strongly reduced the insulation of most (~80%) TADs (mESCs, Nora et al., 2017, Hela, Wutz et al., 2017), in agreement with previous observations that some TADs are not CTCF-dependent (Rao et al., 2014), without affecting compartmentalization. On the other hand, depletion of the cohesin loader NIPBL (mouse hepatocytes,

Schwarzer et al., 2017) – MAU2, which also stimulates cohesin's ATPase activity and is required for extrusion (HAP1 cells, Haarhuis et al., 2017) or its kleisin subunit RAD21 (HeLa, Wutz et al., 2017, HCT-116, Rao et al., 2017) resulted in complete ablation of loops and TADs and was also accompanied by stronger compartmentalization. Conversely, rapid loss of the cohesin release factor WAPL (Haarhuis et al., 2017; Wutz et al., 2017) or PDS5A/B, which may cooperate with it (Wutz et al., 2017) resulted in increased retention of cohesin on chromatin, leading to the formation of highly compacted 'vermicelli' chromosomes, which exhibited weaker compartments, larger TADs and stronger loops.

Higher resolution (micro-C) maps have demonstrated that while CTCF and cohesin are required for many E-P loops (El Khattabi et al., 2019; Grubert et al., 2020; Krietenstein et al., 2020; Thiecke et al., 2020), some E-P, P-P and Polycomb target contacts are retained, while some enhancer interactions are strengthened in their absence (Rao et al., 2017, Thiecke et al., 2020). Developing region capture micro-C (RCMC) to obtain nucleosome-level resolution and ultra-high coverage on a set of regions, Goel et al. (2023) show that many enhancers and promoters form nested microcompartments, largely resistant to either cohesin or transcription loss. These results are in agreement with extremely deeply sequenced Hi-C, where computing compartmentalisation at 500bp resolution shows promoters and enhancers tend to be engaged in precise compartment A interactions even when in generally B (inactive) domains (Harris et al., 2023). This supports the idea that cohesin and CTCF are involved in the formation of larger structural loops, whereas contacts associated with gene expression regulation can take place independently.

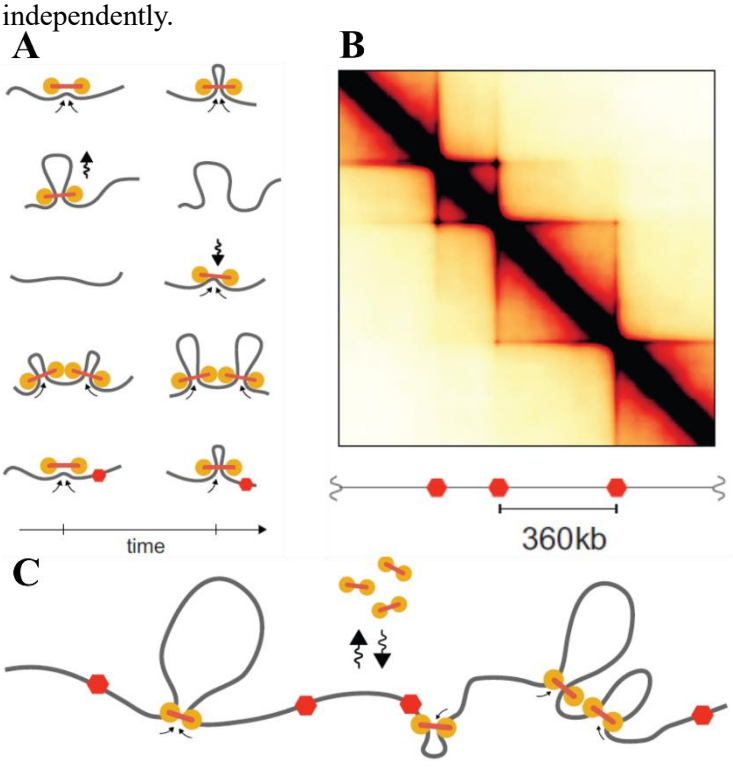

Figure 17. Loop extrusion model

A. Illustrative examples of a loop extruding factor (LEF, in orange), likely cohesin, binding randomly, extruding loops and releasing from chromatin (in grey). Several cohesins can bind along chromatin and potentially interfere with each other's movement. Cohesin may also pause or arrest if it meets a barrier (in red), often corresponding to an occupied CTCF site in the correct orientation. RNAPII and pre-replicative complexes (discussed below) may also function as barriers.

B. Example of a Hi-C map generated based on simulated data including loop extrusion. Key features like TADs, corner dots and stripes are recapitulated. **C.** Schematic of LEFs and barriers along the genome (adapted from Fudenburg et al., 2016).

Despite their different effects on compartmentalization, no PTM spreading was detected upon either CTCF (Nora et al., 2017) or cohesin depletion (Rao et al., 2017), in agreement with the idea that compartments may be driven by PTM distribution while also showing that TAD borders are not key for regulating chromatin state. Loss or increased retention of cohesin on chromatin, unlike changes in CTCF binding, led to a change in chromatin compaction, observable visually on Hi-C maps and detectable as a change in the shape of the power law relationship between contact frequency and genomic distance (P(s), Wutz et al., 2017). This indicated that in the absence of CTCF, cohesin is likely still binding and extruding loops, but without being blocked at particular sites, which could explain the unique role of cohesin in counteracting compartmentalization and the stronger effect its depletion has on TADs and loops compared to the loss of CTCF (Nuebler et al., 2018).

Is this real life? Is this just bulk Hi-C? (adapted from Mercury, 1975)

While the results from these and a number of follow-up studies provide support for the loop extrusion model, they are all based on the detection of TADs and loops from ensemble Hi-C, which provides an average snapshot of the genome organization of millions of cells. Thus, as TADs had not been previously observed by imaging, it was unclear whether they represent actual physical structures or were a technical consequence due to the bulk nature of Hi-C assays (Beagan and Phillips-Cremins, 2020). The first evidence in support of TADs as physical entities came from single-cell Hi-C (scHi-C), which demonstrated that in individual cells, contacts tended to be enriched between regions that were found in the same TAD defined by ensemble Hi-C (Nagano et al., 2013). However, TADs in individual cells could not be called due to the sparsity of the data, and later studies revealed a large cell-to-cell heterogeneity of contacts at the sub-Mb scale (Flyamer et al., 2017; Giorgetti et al., 2014; Stevens et al., 2017). Conversely, A/B compartment interactions were consistent between single cells (Stevens et al., 2017), potentially reflecting the different dynamics of the processes that establish loops and compartments.

While the vast majority of mammalian TADs are CTCF/cohesin-dependent, this is not the case in *D. melanogaster*. High-resolution Hi-C has shown that *D. melanogaster* TADs could be as small as 10s of kbs, corresponding to clusters of transcribed genes forming distinct compartment domains. Indeed, despite the presence of CTCF and other insulator proteins, TAD demarcation in *D. melanogaster* is linked to epigenetic state transitions rather than loop extrusion (Rowley et al., 2017; Ulianov et al., 2016; Q. Wang et al., 2018), which makes it a well-suited model to investigate the organization of self-associating domains. Super-resolution imaging combined with Oligopaints has clearly demonstrated that consecutive TADs in three distinct states (active, inactive, Polycomb) are physically separated and exhibit characteristic levels of compaction associated with their epigenetic profile despite cell-to-cell heterogeneity (Figure 18A, Cardozo Gizzi et al., 2019; Mateo et al., 2019; Szabo et al., 2018). Thus, TADs in *D. melanogaster* are strongly associated with compartmentalization and are organized in

distinct nanodomains (Szabo et al., 2019), indicating TADs can be identifiable structural units of genome organization.

Super-resolution imaging has also been used in to trace TADs in human cells, the results of which can be compared to Hi-C by computing 2D maps where 3D distances between each pair of loci imaged per chromosome is plotted (Bintu et al., 2018; Finn et al., 2019; Nir et al., 2018). Average distance maps (from all cells) showed high similarity to ensemble Hi-C maps, and individual (sub)TADs could be observed as globular structures delimited by CTCF sites in some single cells. Nevertheless, individual chromosomes exhibited a variety of conformations, including many where several TADs were intermingled with each other and loci across a TAD boundary were closer than ones within the same domain (Figure 18B, Bintu et al., 2018). Moreover, upon cohesin depletion structures became undetectable on average, but not single cell distance maps, reflecting the persistence of chromatin folding into domains. While preference for CTCF boundary positions was abolished in cohesin-depleted cells, this was not the case for A/B compartment transition borders, indicating their independent association with domain formation, similar to observations in *Drosohpila* (Bintu et al., 2018).

Subsequent work in mESCs demonstrated that cohesin is important for promoting enrichment of contacts within TADs, whereas CTCF is key for boundary demarcation (Szabo et al., 2020). It also corroborated that mammalian TADs tend to be composed of several globular sub-structures (termed 'chromatin nanodomains' (CNDs) due to their similarity to the ones observed in *D. melanogaster*), which persist in the absence of CTCF and cohesin, but are disrupted upon histone hyperacetylation (Szabo et al., 2020). Curiously, another study in human HCT-116 cells showed that the presence of cohesin also promotes intermingling of loci across TAD boundaries, which is counteracted by CTCF and WAPL (Luppino et al., 2020). This suggests that cohesin can bypass some boundaries, in agreement with micro-C data showing stripes which can contain several dots (sites of pausing) and even extend past them (Hsieh et al., 2020, Krietenstein et al., 2020). Finally, recent imaging work by Hafner et al. (2023) has shown that by

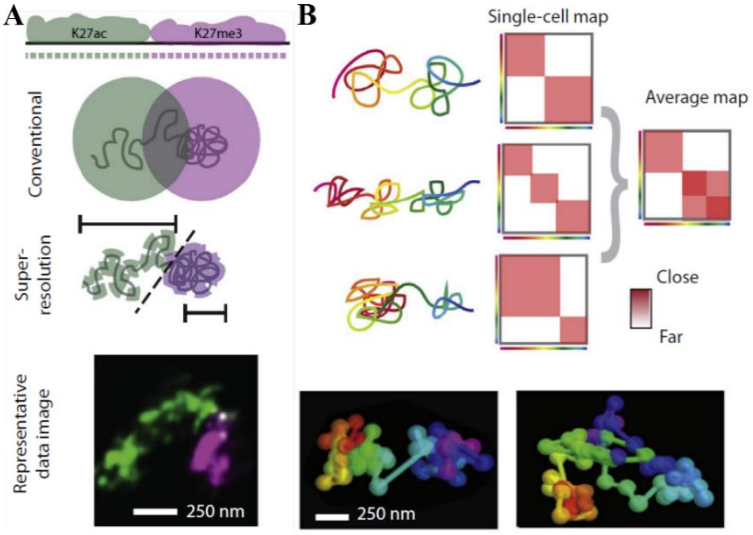

Figure 18. Super-resolution imaging illuminates kb-scale chromatin folding in individual cells

A. Super-resolution imaging of TADs of different chromatin states reveals they are distinct physical entities with packing density linked to their epigenetic marks. **B.** Tracing of individual TADs in 100s-1000s cells with Oligopaints demonstrates TAD boundaries reflect statistically frequent separation between globular domains (from Boettiger and Murphy, 2020).

extruding loops, cohesin promotes interactions at distances <4Mb, resulting in the clustering of CTCF-bound anchors of multiple loops, which extend from this cluster in a 'rosette' arrangement. This results in stronger separation of regions >4Mb apart, providing another potential mechanism for cohesin to antagonise compartmentalization by preventing homotypic A-A or B-B interactions of distant loci (Hafner et al., 2023).

In summary, mammalian TADs are a population-derived feature with highly dynamic and heterogeneous organization in single cells, which is only partially driven by loop extrusion. They can be composed of one or several nanodomains, which also vary between cells and are dependent on nucleosomal interactions rather than CTCF and cohesin, indicating epigenetic mechanisms or phase separation may also be important for this level of chromatin organization.

1.4.3. What am I doing? Adding dynamics by live-cell imaging

One question that cannot be definitively answered by either the imaging or sequencing fixed cell approaches described above is if cohesin can actually extrude loops on chromatin. Work *in vitro* has demonstrated that condensin (Ganji et al., 2018), cohesin (Davidson et al., 2019) and Smc5/6 (Pradhan et al., 2022b) can extrude loops on naked DNA. Condensins can also traverse each other (Kim et al., 2020) and other large roadblocks, similarly to cohesin (Pradhan et al., 2022a), and form loops on supercoiled DNA in vitro (Kim et al., 2022). Davidson et al., (2023) have further demonstrated that CTCF can not only act as a barrier to cohesin-mediated extrusion, but it can also reverse its direction in a manner dependent on DNA tension. Thus, in addition to supporting the loop extrusion model, these experiments have also provided insight into the way SMC complexes can interact with CTCF and DNA, although it remains to be seen how they would translocate along a chromatin substrate.

Conversely, two recent studies have examined CTCF and cohesin dynamics *in vivo* by live-cell imaging of fluorescently labelled pairs of loci in mESCs (Gabriele et al., 2022; Mach et al., 2022). They have shown that cohesin-mediated loops are rare and highly dynamic: 3-6.5% cells for 10-30min for a ~500kb loop (Gabriele et al., 2022), and ~27% cells for 5-15min for a 150kb loop (Mach et al., 2022). Mach et al. (2022) also demonstrate that extrusion by cohesin results in reduced chromatin mobility and that, together with the presence of CTCF sites, also decreases the variability of physical distances between linearly proximal loci. Thus, they suggest that loop extrusion can promote less variable chromatin organization, in line with previous super-resolution studies (Bintu et al., 2018, Szabo et al., 2020, Hafner et al., 2023). Finally, these data suggest that it may be the dynamics of the extrusion process and the 'reproducible' generation of many transient contacts, rather than stable structures, which is functionally important.

1.5. Chromatin organization during the cell cycle

The dynamics of chromatin organization should be considered not only on the minute time scale, but also with respect to the cell cycle, during which the genome goes through several major re-arrangements: (i) the decompaction of mitotic chromosomes at the entry of G1 (Zhang and Blobel, 2023), (ii) the 2-fold dilution of parental histones (Stewart-Morgan et al., 2020) and sister chromatid cohesion (Peters and Nishiyama, 2012) during S phase and (iii) condensation of chromosomes following the G2/M transition (Batty and Gerlich, 2019). While understanding how these processes are regulated and executed are interesting questions in their own right, here I will focus on what they reveal about the relationship between genome organization and function.

After mitosis, chromosomes are decompacted, expanding into their territories, and interphase genome organization is gradually reestablished (Zhang and Blobel, 2023). The length of interphase imposes a limit on the time chromosomes have to diffuse and intermingle, although CTs are readily detected in post-mitotic cells (Burns et al., 1985; Cremer and Cremer, 2006a). Unlike CTs, compartments and TADs are thought to be formed by active processes, dependent on chromatin state and CTCF/cohesin, respectively (as detailed above). Indeed, many histone PTMs are retained on chromatin during mitosis, acting as epigenetic bookmarking factors for transcriptional activity (Gonzalez et al., 2021), and likely contribute to compartment re-establishment. Conversely, the extent of CTCF binding in mitosis varies dramatically between cell types (Chen et al., 2019; Oomen et al., 2019; Owens et al., 2019). However, even when fully evicted from mitotic chromosomes in somatic cells, it is reassociated with chromatin already in ana/telophase, providing TAD boundary demarcation (Oomen et al., 2019) prior to cohesin reloading, which happens at a markedly slower rate (H. Zhang et al., 2021) starting at cytokinesis (Abramo et al., 2019).

Several studies have shown that compartments are reestablished rapidly (in ~30min) upon G1 entry, followed by a progressive increase in their strength over ~4 hours (Abramo et al., 2019; Pelham-Webb et al., 2021; Zhang et al., 2019). Notably, segregation of B compartments appears to precede increase in A-A contacts (Abramo et al., 2019), potentially reflecting different kinetics of binding or propensity to cluster together of the distinct proteins that bind them. Analysing the restoration of heterochromatin organization from the perspective of nuclear positioning revealed that future LADs first cluster together in the interior (Kind et al., 2013, Luperchio et al., 2018) before becoming anchored at the lamina through recognition of H3K9me2 (Poleshko et al., 2019; See et al., 2020), indicating that relocation to the periphery is not required for compartmentalization. Finally, setting up the replication timing (RT) programme in early G1 takes places concomitantly with compartment reemergence, but while G1 chromatin organization is maintained through S phase into G2, RT information is erased, implying that genome architecture is not sufficient to instruct replication (Dileep et al., 2015b).

TADs and CTCF/cohesin loops are also gradually re-formed in a broadly similar timeframe to compartments, although the exact kinetics reported differ between studies, potentially due to variability in the synchronization protocol and/or the cell types used (Zhang et al., 2019, Abramo et al., 2019, Pelham-Webb et al., 2021). Conversely, E-E/E-P/P-P contacts are re-established before CTCF loops (Zhang et al., 2019, Abramo et al., 2019, Pelham-Webb et al., 2021) and can be detected even in the absence of cohesin (H. Zhang et al., 2021), indicating they may be dependent on the binding and/or spatial association of RNAPII or transcriptional activators. However, global genome reactivation takes place already in ana/telophase (Hsiung et al., 2016), prior to loop and TAD emergence, and is not limited to the specific E-P pairs (Zhang et al., 2019, Pelham-Webb et al., 2021). Loss of mitotic H3K27ac (preventing transcriptional re-activation, Pelham-Webb et al., 2021) or inhibition of RNAPII in M/G1 (Zhang et al., 2021) did not impair the restoration of 3D organization, suggesting its relationship with transcription is not necessarily functional. In contrast, Pelham-Webb et al., 2021 also showed that rapid activation of genes after mitosis was associated with E-P looping and expression kinetics corresponded to TAD boundary insulation increase. Furthermore, another study found that long-term (14h) RNAPII depletion in G2-arrested cells prior to mitosis and G1 re-entry globally perturbed the refolding of the genome due to impairment of cohesin re-loading (S. Zhang et al., 2021), suggesting the picture is more complicated.

In summary, reestablishment of genome organization after mitotic exit is gradual and better coordinated with replication timing definition rather than transcriptional re-start. Furthermore, 3D organization is neither required for, nor driven by the restart of gene expression in this context, suggesting it may be independently restored based on epigenetic memory mediated by PTMs and chromatin-binding factors.

No major reorganization of the genome takes place in the progression from G1 to G2 (Gibcus et al., 2018; Nagano et al., 2017; Naumova et al., 2013; Wutz et al., 2017), despite two key events which occur as the genome replicates in S phase: the two-fold dilution of histone variants and their PTMs on nascent chromatin (Stewart-Morgan et al., 2020, **Chromatin replication: maintain genome integrity and epigenetic states**) and sister chromatid cohesion (Peters and Nishiyama, 2012). Nevertheless, Nagano et al. (2017) showed, using scHi-C, that compartments get stronger from G1 to G2, whereas insulation of TAD boundaries gets weaker as they are replicated. Developing sister chromatid-sensitive (scs)Hi-C to differentiate between the conformation of the two sister chromatids, Mitter et al. (2020) later demonstrated that while the sister chromatids were overall aligned, they could have regions of local separation of up to 3Mb in G2. TAD boundaries were typically enriched in contacts between the sisters, whereas pairing between sister TADs varied, with H3K27me3-marked domains showing the highest levels. The authors show that this enrichment of *trans*-sister contacts at boundaries and their depletion within TADs is driven by extruding cohesin (Mitter et al., 2020). This indicates that loop extrusion in G2 by non-cohesive cohesin can contribute to partial separation of the two sisters prior to entry in mitosis, which has been recently shown (Batty et al., 2023).

It would be interesting to investigate the strength of TAD boundaries from *cis*-sister data only (Mitter et al., 2020) in order to understand if the weaker insulation detected in previous work with S phase progression (Nagano et al., 2017) reflects the pairing between the sister chromatids. Another unanswered question is whether the contribution of sister chromatid contacts can be the reason for the increase in compartment segregation detected in G2 (Nagano et al., 2017). This observation is somewhat counterintuitive, considering the dilution and slow restoration kinetics of inactive PTMs (Stewart-Morgan et al., 2020), which are important for B-B compartment interactions, thought to be key for A/B segregation (Falk et al., 2019).

Finally, interphase chromatin organization is rapidly dismantled (5-10min) upon entry in mitosis, when chromosomes are re-organised into rod-like shapes due to the concerted activity of condensin I and II, resulting in the formation of nested loops (Gibcus et al., 2018, Batty and Gerlich, 2019). One of the proteins required for this process is WAPL, which enables the release of extruding cohesin from chromosomes (Gandhi et al., 2006; Kueng et al., 2006). Notably, condensins are not required for the compaction of mitotic chromosomes, which is dependent on histone PTMs (Schmitz et al., 2020). H3S10phos interferes with HP1a binding to H3K9me3 (Fischle et al., 2005; Hirota et al., 2005), whereas global deacetylation promotes general chromatin compaction (Wilkins et al., 2014; Zhiteneva et al., 2017). This process demonstrates that how quickly and synchronously genome structure can be disassembled, compared to the much longer process of restoration after mitosis, emphasizing the complex interplay that takes place during its restoration in G1.

1.6. Structure-function relationship: What is the role of 3D genome organization in regulating genome function? How do genomic processes affect its organization?

Following the reshaping of chromatin architecture over the cell cycle already suggests that while it may be functionally linked to transcription and replication, this relationship is not straightforward. To disentangle the interplay between genome structure and activity, I will provide an overview of the roles suggested for chromatin organization at different scales, their proposed role in development and differentiation and the impact of their perturbation.

Chromosome territories: Keep it to yourself

Localisation of genes at the periphery of or beyond their CT (Mahy et al., 2002; Volpi et al., 2000; Williams et al., 2002) and clustering in space (Osborne et al., 2004) of genes from the same or different chromosomes (i.e. intermingling, Branco and Pombo, 2006; Maharana et al., 2016) has been associated with expression. Indeed, transcriptional inhibition changes CT intermingling patterns without disrupting overall chromosome organization, indicating transcription may play instructive role in the positioning of sequences within CTs and their spatial overlap (Branco and Pombo, 2006). However, this effect may

depend on the genes in question, as other work has shown transcriptional activation can take place without gene relocation (Bickmore, 2013; Morey et al., 2007). Intermingling also correlates with translocation patterns between chromosomes in normal (Engreitz et al., 2012) and cancer cells (Branco and Pombo, 2006; Roix et al., 2003), indicating CT organization can have an impact on genome stability. Indeed, a recent study in *D. melanogaster* showed that the extent of chromosome intermingling (controlled by the levels of condensin II in this system) corresponded to the capacity to generate inter-chromosomal translocations following DNA damage (Rosin et al., 2019). Thus, CTs are a structural rather than functional feature of genome organization but can impact the outcome of processes like recombination/repair.

Compartments: I can do it on my own

Compartments are already present at 1-cell stage zygotes on the paternal pronucleus (Flyamer et al., 2017) and gradually emerge on the maternally-inherited chromatin, increasing in strength on both genomes until they equalize around the 8-cell stage (Gassler et al., 2017), after which they become similar to the ones in mESCs (Du et al., 2017; Ke et al., 2017). Then, with ESC differentiation, B compartments consolidate into larger domains (Dixon et al., 2015) and interact more strongly with each other (Bonev et al., 2017; Miura et al., 2019). This corresponds to the reduced dynamics (Meshorer et al., 2006), increased compaction (Ricci et al., 2015) and stronger repression (Wen et al., 2009) of chromatin and loss of ESC-characteristic 'promiscuous transcription' (Efroni et al., 2008) that accompany the exit from pluripotency (Lim and Meshorer, 2020; Schlesinger and Meshorer, 2019). In addition to changes in strength, ~36% genome shifts A-to-B/B-to-A compartment in a manner associated with decreased/increased expression of the contained genes, respectively (Dixon et al., 2015; Miura et al., 2019). While compartment switches can occur prior to transcription (Stadhouders et al., 2018) or RT (Dileep et al., 2019; Miura et al., 2019) changes, they can themselves be preceded by gain or loss of histone PTMs (Stadhouders et al., 2018) or nuclear repositioning (Miura et al., 2019), making it difficult to assess the significance of the compartment shift. Furthermore, as the majority of imaging studies so far have investigated relocation with respect to nuclear landmarks or looping in and out of CTs, it is still difficult to compare results as it is unclear to what extent these events correspond to compartment switching. Thus, there are two distinct relationships to be considered: (i) compartments and genome function (transcription/replication) and (ii) compartment switching and nuclear repositioning.

Are genome function (transcription and replication) and compartments interdependent?

The establishment of compartments in the early mouse embryo takes place prior to zygotic genome activation (ZGA, Du et al., 2017; Flyamer et al., 2017; Gassler et al., 2017) and is not affected by transcriptional inhibition at this stage, although it may require going through replication (Ke et al., 2017). Transcriptional inhibition in mESCs and more differentiated cells also does not disrupt

compartmentalization (Barutcu et al., 2019; Hsieh et al., 2020; Jiang et al., 2020; Xie et al., 2022)implying expression is not required for A/B compartment establishment or maintenance. On the other hand, depletion of RIF1, a protein thought to be key in organising the RT programme (**RIF1: Show them who's boss?**) results in changes in short/long-range contacts in mESCs (Foti et al., 2016) and leads to A/B switching and weaker A-A interactions (Klein et al., 2021), indicating that the coordination of replication may be important for genome organization.

Considering the effect of compartmentalization on transcription, in 2- to 8-cell stage mouse embryos, compartments correlate worse with transcription than LADs, suggesting they are not important for transcription at least at this stage (Borsos et al., 2019). In mouse embryonic fibroblasts, pericentromeric heterochromatin repression by HP1a can occur without formation of physical domains (Erdel et al., 2020). Conversely, tethering Suv39h1 to a lacO array results in deposition of H3K9me3 and switching to B compartment of the array and its flanking sequence but does not reduce expression of genes in the region that switches in mESCs (Wijchers et al., 2016). Finally, knock-down of all HP1 isoforms in transcriptionally silent *D. melanogaster* embryos strongly perturbs genome organization and B-B compartment strength but does not affect gene expression before or after ZGA (Zenk et al., 2021). Thus, the segregation of genome compartments is not required for normal transcription.

Are nuclear repositioning and compartment switching corresponding events?

Using early mouse embryogenesis as a model, Borsos et al. (2019) have shown that compartment and LAD establishment proceed at the same time, but between 2- and 8-cell stage, many LADs are not in B compartment, indicating a disconnect between repressive chromatin and peripheral positioning. During differentiation of mouse eye rod cells, and 'inverted' nuclear organization emerges, with heterochromatin clustered in the nuclear interior, flanked by euchromatin positioned near the nuclear lamina (Solovei et al., 2013, 2009). Polymer modelling based on Hi-C data from these cells indicates that B-B compartment interactions are what drives compartmentalization independently of contacts with the lamina (Falk et al., 2019). Indeed, reduction of lamin A/C in cardiac cells leads to stronger, rather than weaker compartment segregation and upon differentiation, these cells experience A/B compartment switches which do not necessarily become repositioned with respect to the periphery (Bertero et al., 2019).

As we still do not understand the mechanisms that drive compartmentalization, it is difficult to disrupt it directly and investigate how that affects cellular processes. However, it has become clear that despite the general correlation with transcription, compartmentalisation is not driven by it and, conversely, weaker segregation of compartments and A/B switches do not necessarily result in changes in expression. Furthermore, despite the good correspondence between B compartments and LADs, association with the lamina is not required for B compartment segregation and A/B compartment switching does not necessarily correspond to relocation to the nuclear periphery.

TADs: 'Lean on me'

When initially characterized, TADs were found to have conserved boundaries across many cell types (Bonev et al., 2017; Dixon et al., 2012, 2015; Rao et al., 2014) and to often contain clusters of co-regulated genes (Shen et al., 2012; Symmons et al., 2014), hinting they may be stable regulatory units. This was further supported by observations that the majority of E-P contacts take place within TADs (Bonev et al., 2017; Dowen et al., 2014; Hsieh et al., 2020; Ji et al., 2016; Lupiáñez et al., 2015; Noordermeer et al., 2008; Ramírez et al., 2018) and that entire domains switch between A/B compartment in differentiation concordantly with changes in gene expression (Dixon et al., 2015, Bonev et al., 2017). However, as the understanding of what TADs are and how they are established has developed, the question now is how can they function as regulatory units if they do not have a stable structure?

Elegant work from Zuin et al. (2022) has revealed that E-P contact frequency within a TAD translates non-linearly to transcriptional output, providing a potential explanation for why E-P proximity does not necessarily correlate with transcription in single cells (**Looping: 'Should I stay or should I go?'**). It also showed that the presence of CTCF between the enhancer and promoter can strongly reduce expression without a major effect on E-P contact probabilities (at least within a TAD), suggesting CTCF-mediated insulation is not simply dependent on modulating physical interactions (Zuin et al., 2022). In agreement with this, stripes on micro-C data evidence that loop extrusion by cohesin can bypass boundaries, generating inter-TAD contacts (Hsieh et al., 2020, Krietenstein et al., 2020). This has also been confirmed by super-resolution imaging in Luppino et al. (2020), which also demonstrate boundary-proximal genes are among the ones most strongly affected by cohesin loss due to reduction in transcriptional bursting. Thus, the accumulation of CTCF and cohesin at TAD boundaries may have a functional impact on gene expression beyond their role in genome organization.

In development, TAD boundaries play a key role in preventing ectopic enhancer-promoter contacts at particular loci with precise developmental timing (Franke et al., 2016; Hnisz et al., 2016; Lupiáñez et al., 2015; Spielmann et al., 2018). Conversely, cancer cells exhibit disruption of CTCF association with the genome due to binding site methylation (Flavahan et al., 2016) or mutations (Katainen et al., 2015), mutations of CTCF itself (Debaugny and Skok, 2020), as well as structural variants (deletions, inversions, translocations) resulting in improper E-P communication and proto-oncogene activation (Beroukhim et al., 2017; Gröschel et al., 2014; Hnisz et al., 2016). In contrast, a study in *D. melanogaster* carrying highly re-arranged balancer chromosomes showed that the gross re-organization of short- and long-range E-P contacts did not predict the expression differences detected from the affected alleles (Ghavi-Helm et al., 2019). In agreement with this, in mammalian cells depletion of CTCF (Nora et al., 2017) or cohesin (Schwartzer et al., 2017; Wutz et al., 2017) does not result in global gene expression dysregulation, indicating this level of organization is not required to maintain transcriptional programmes. Conversely, the absence of cohesin impairs the activation of ~40% LPS-

induced genes in macrophages (Cuartero et al., 2018). Thus, TADs may provide a dynamic scaffold required not for maintenance, but efficient induction of changes of the transcriptional state (Karpinska and Oudelaar, 2023).

Activation of developmental genes could lead to the establishment of new TAD boundaries and increased transcription of boundary-proximal genes increases insulation (Bonev et al., 2017; Stadhouders et al., 2018), indicating transcription could play a role in TAD organization. These effects are suggested to be mediated by the binding of and/or progression of RNAPII, which can act as a moving barrier (Brandão et al., 2019; Valton et al., 2022; Zhang et al., 2023) and/or also push cohesin (Banigan et al., 2023; Busslinger et al., 2017; Davidson et al., 2016). However, ectopic induction of transcription alone is not sufficient to generate a TAD boundary, indicating there are other factors at play (Bonev et al., 2017). Indeed, in early mouse embryogenesis, TADs are not (Du et al., 2017; Flyamer et al., 2017; Ke et al., 2017) or barely (Collombet et al., 2020) detectable in zygotes and emerge gradually, while ZGA is a single event at the 2-cell stage, suggesting they are somewhat independent. Furthermore, TADs can partially consolidate even if ZGA is blocked, de-coupling them partially from transcription (Du et al., 2017; Ke et al., 2017).

From the point of view of replication, TAD boundaries have also found to be enriched in early replication origins (Akerman et al., 2020; Giles et al., 2022; Petryk et al., 2016) whose extent of 3D connectivity has been shown to correlate with their efficiency (Jodkowska et al., 2022). TADs also show a good correspondence with replication domains (RDs): regions of the genome that replicate at the same time (Vouzas and Gilbert, 2021, **Organization of RT**). Some mechanistic understanding of these observations can be provided by investigations of the interplay between cohesin and the minichromosome maintenance (MCM) complex, part of the replicative helicase loaded at replication origins (**The mechanics of DNA replication**). About 10-100x more origins are licensed in G1 than the one that fire in S phase, when MCM is converted to its active helicase conformation (Hu and Stillman, 2023). Dequeker et al. (2022) demonstrated that MCM can pause extrusion by cohesin by directly interacting with it in G1 HCT-116 cells and mouse oocytes. In the same human cell line, Emerson et al. (2022) showed that the presence of cohesin in G1 improves the precise position of early initiation zones (IZs, clusters of origins) at TAD boundaries, and that deletion or insertion of CTCF sites can lead to the disappearance or emergence, respectively, of an early IZ, accompanied by changes in insulation. Thus, they propose that cohesin can either reposition MCM complexes to TAD boundaries by pushing them when extruding, or that it could somehow promote the activation of origins specifically positioned there (Emerson et al., 2022). However, similar boundary deletion experiments in mESCs do not result in loss of early replication at these sites (Sima et al., 2019), and global CTCF (Sima et al., 2019) or cohesin (Cremer et al., 2020) depletions do not affect RT. Thus, the relationship between CTCF/cohesin-mediated chromatin organization and replication may vary between species or cells of different potential.

Finally, TAD boundaries have also been found to restrict the spread of the signalling PTM gH2A.X in DNA double-strand break repair (Arnould et al., 2021). However, depletion of CTCF (Nora et al., 2017) or cohesin (Rao et al., 2017) does not result in PTM spreading, in line with the absence of gene expression changes. In HAP1 cell, WAPL KO led to a reduction of K9me3 at heterochromatin domains, potentially due to the accumulation of loops preventing phase separation and inhibiting spreading of the mark rather than a defect of TAD boundaries (Haarhuis et al., 2022).

In light of the recent evidence demonstrating the transient and dynamic nature of TADs in mammals and the lack of strong impairment of transcriptional regulation upon global disruption of boundary insulation, the organization of the genome in TADs is not required for maintaining expression, replication or chromatin modification patterns. However, TADs may provide a flexible framework for gene induction upon stimuli and throughout development as an additional regulatory layer.

Looping: 'Should I stay or should I go?'

Cohesin-mediated loop extrusion and (temporary) blockade at CTCF sites have been suggested to promote more 'reproducible' contacts between distal elements in the genome (Mach et al., 2022), thereby limiting expression heterogeneity (Hafner et al., 2023). It has also been proposed to act as a mechanism to facilitate E-P searches, although how much CTCF and cohesin promote or antagonise contacts between regulatory elements or Polycomb targets is still an open question (Karpinska and Oudelaar, 2023, **Loops and compartments: one of those things is not like the other**). However, considering the lack of transcriptional dysregulation upon loss of CTCF or cohesin, this raises the question of whether E-P loops are necessary for transcriptional regulation.

Several studies have demonstrated the importance of E-P proximity in driving expression in *D. melanogaster* (Chen et al., 2018) and mouse (Kragesteen et al., 2018) development. However, there is also evidence that (i) the presence of a loop does not indicate the gene is expressed (Ghavi-Helm et al., 2014; Jin et al., 2013; Montavon et al., 2011; Paliou et al., 2019) and that (ii) promoters and enhancers can actually increase physical distance (Alexander et al., 2019; Benabdallah et al., 2019) and, counterintuitively, contact frequency (Gómez Acuña et al., 2023) upon induction of expression. This emphasizes the bias that may be introduced by the cross-linking step in C-based methods and cautions against direct translation of interaction frequencies into physical distances (Gómez Acuña et al., 2023).

Long-range contacts can also be associated with silencing, as is the case with Polycomb bodies (Schuettengruber et al., 2017). In this setting, the physical interaction between target loci is functionally important for repression by PRC1 in *D. melanogaster*, although loop formation in this case is likely the consequence of PRC1 phase separation rather than extrusion by cohesin (Ogiyama et al., 2018). Recent work in mouse oocytes (Du et al., 2020) and early embryo (Collombet et al., 2020) has demonstrated the presence of H3K27me3-rich Polycomb-associating domains (PADs), which self-associate at short-ranges (unlike typical Polycomb-mediated interactions, which can span Mbs). They become weaker

until becoming undetectable at ~8-cell stage, although their genes remain repressed (Collombet et al., 2020). However, it is unclear whether this means their structure is not important or if its loss is compensated for by compartmentalization and LAD emergence at the same time (Du et al., 2017; Flyamer et al., 2017; Gassler et al., 2017; Ke et al., 2017). The loss of PRC2 in early oogenesis does not lead to loss of PADs in mature oocytes, where ~10-20% H3K27me3 levels are maintained in the same genome-wide pattern. Conversely, loss of PRC1 leads to de-repression of target genes and loss of long-range PAD interactions, as well as reduced insulation of their boundaries (Du et al., 2020). Thus, it remains unclear whether PRC1 binding or bridging of long-range contacts is important for silencing in this context.

In conclusion, the process of loop extrusion can be a mechanism to bring together distal elements from the genome, facilitating searches between enhancers and target promoters and either promoting or opposing PRC1-mediated clustering. However, the functional importance of this remains an open question, and its answer may depend on the cellular and developmental context.

2. Chromatin replication: disrupting organization every doubling

Every cell cycle, to ensure that the two daughter cells inherit equivalent genetic information, the genome has to be fully and accurately duplicated in S phase. The fidelity of DNA polymerases is key to faithfully copy the genomic sequence along with a proper replication machinery. However, the maintenance of distinct epigenomic states needed to preserve cell identity and its normal function during multiple division in a cell lineage requires other components.

2.1. The mechanics of DNA replication

DNA must be replicated once and only once per cell cycle. For this, DNA replication uses specific initiations sites in S phase, termed origins of replication (Attali et al., 2021; Costa and Diffley, 2022; Hu and Stillman, 2023). These sites are already occupied by the multi-subunit pre-replicative complex (pre-RC) assembled in late M/G1 but firing occurs later. In yeast both genetics (Hartwell, 1976; Hereford and Hartwell, 1974; Maine et al., 1984) and biochemical work (Bell and Stillman, 1992) advanced the field. In parallel, the biochemical power of extract derived from eggs of *X. laevis* (Harland and Laskey, 1980) provided a lot of important information. Together this allowed the identification of the key components (Hartwell, 1976; Hereford and Hartwell, 1974; Maine et al., 1984), mechanism (Bell and Stillman, 1992) and regulation (Harland and Laskey, 1980) of this process in eukaryotes. Homologous factors identified in mammals enabled to explore conservation of these processes (Vashee et al., 2001). However, despite the evolutionary conservation of the components of the initiation machinery, there are considerable differences in the mechanisms employed in *S. cerevisiae* compared to other complex eukaryotes. The most striking difference lies in how origins of replication are defined.

Licensing: The first step of the initiation process is origin licensing (Fragkos et al., 2015, Figure 19A) in which the origin recognition complex 1 (ORC1) binds to all potential origins (**RT establishment: definition and selection of origins of replication**) at the M/G1 transition (Okuno, 2001). Then, the remaining subunits of the complex (ORC2-6, Kara et al., 2015) become associated, followed by cell division cycle 6 (CDC6) and CDC10-dependent transcript 1 (CDT1, Takisawa et al., 2000). This in turn allows the recruitment of the replicative helicase minichromosome maintenance (MCM2-7), loaded as a hexamer in an 'open' conformation that encircles the dsDNA (Evrin et al., 2009). Then, a series of ATP hydrolysis reactions and conformational changes lead to ejection of CDC6 and CDT1 while ORC remains bound. Structural studies with *S. cerevisiae* complexes could show how the entire process (from ORC1 binding or CDC6 recruitment onwards) is repeated, resulting in the formation of a head-to-head oriented MCM 2-7 double hexamer (DH). This is the final step of assembly of the pre-RC, comprising ORC and MCM2-7 DH (Attali et al., 2021; Costa and Diffley, 2022). Notably, this MCM2-7 double hexamer, while inactive as a helicase at this stage, diffuses along the DNA non-directionally *in vitro* (Evrin et al., 2009). *In vivo* molecular motors like RNAPII can push it without compromising its ability to promote initiation (Foss et al., 2019; Gros et al., 2015; Scherr et al., 2022). Cohesin potentially does

the same thing (Emerson et al., 2022). Thus, the final locations of replication initiation may not exactly correspond to the ones of pre-RC assembly.

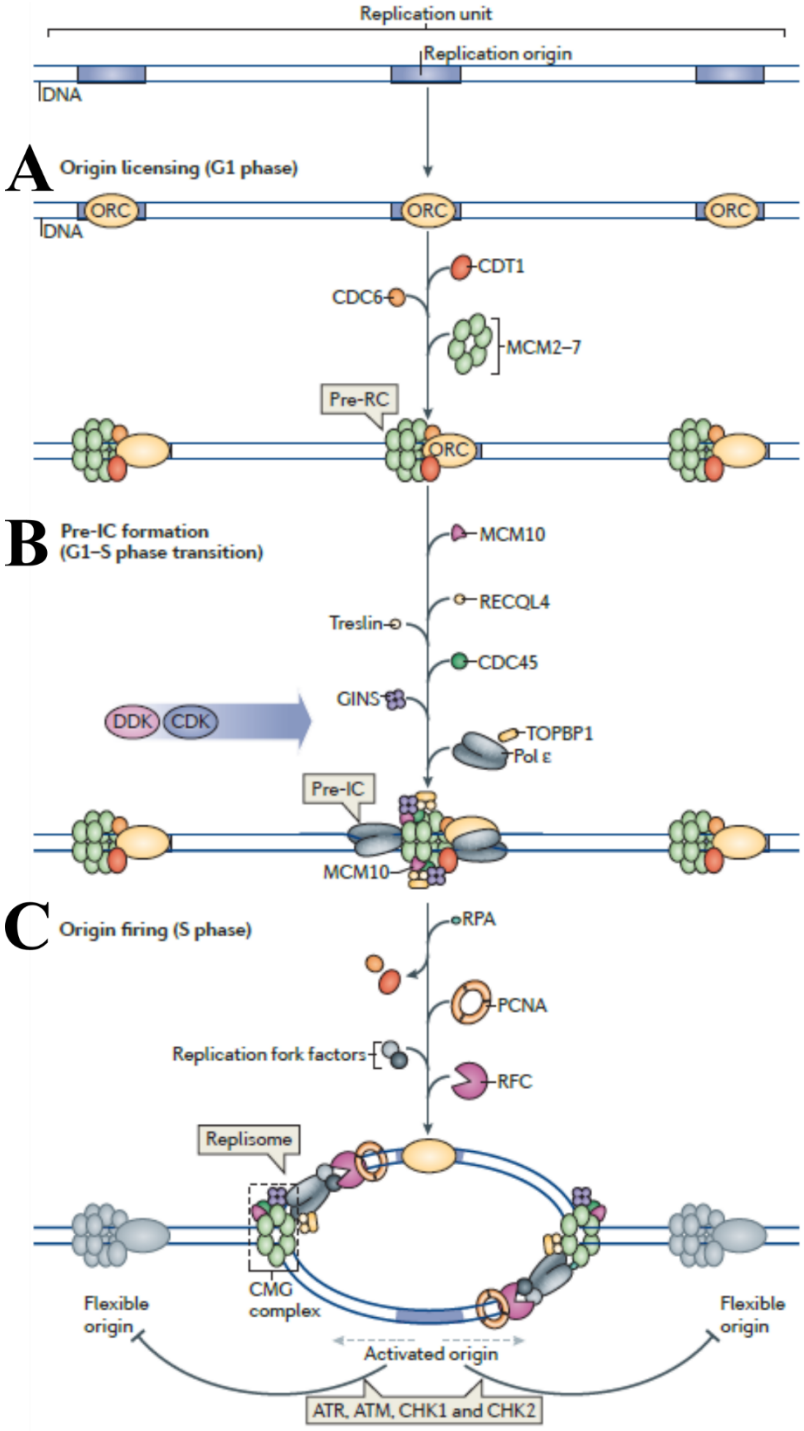

Figure 19. DNA replication initiation

A. Origin licensing (pre-RC formation) is restricted to G1 phase and comprises the sequential association of ORC, CDC6, CDT1 and MCM2-7 with origins of replication. The outcome of this process is the loading of MCM2-7 DH in large excess (x10-100), providing licensed origins capable of being activated in S phase. **B., C. Origin firing** comprises pre-IC conversion (**B.**) and initiation (**C.**). Firing can only take place upon entry into S phase, as it is dependent on the activity of S-CDK and DDK, which phosphorylate several proteins, enabling pre-IC conversion, splitting of the MCM2-7 DH and assembly of two active CMG helicases. This is followed by the binding of other initiation factors (MCM10) and replisome components (PCNA, CTF4). C. Upon initiation, two active replisomes start progressing bi-directionally from the origin. This inhibits the activation of nearby origins in a process termed negative interference (adapted from Fragkos et al., 2015).

Pre-initiation: After the G1/S transition, the conversion of the pre-RC into to a pre-initiation complex (pre-IC) is part of the origin firing process (Figure 19B). Phosphorylation of the helicase MCM2-7 DH and binding of other factors like Treslin/TICCR (Sld3 in yeast) and the leading strand polymerase Pol ε facilitate the recruitment of Cdc45 and go-ichi-ni-san (GINS) complex (Yeeles et al., 2015), respectively. This results in the separation of the MCM2-7 DH into individual hexamers, each participating in the formation of an S-phase helicase CDC45-MCM2-7-GINS (CMG) complex. The two CMG helicases, oriented tail-to-tail, unwind 6-7bp DNA concomitantly with their formation. The final step in origin firing requires the binding of MCM10 and ATP hydrolysis to complete CMG activation. This results in the displacement of one (the lagging) strand of DNA from the helicase channel (Costa and Diffley, 2022). Several additional factors are also recruited, among them replication protein A (RPA), which coats the lagging single stranded DNA (ssDNA) and replication factor C (RFC), which promotes the binding of proliferating cell nuclear antigen (PCNA) and CTF4 (chromosome transmission fidelity 4, also called AND-1 in human). This enables the formation of the replisome, the multi-subunit machine that ensures all aspects of DNA replication, where both proteins act as coordination hubs. While PCNA is important for the tethering and processivity of the leading and lagging strand polymerases on the DNA template, CTF4 orchestrates the activity of the priming polymerase Pol α on the two strands (Attali et al., 2021).

Tight cell cycle control exerted over this process ensures that all DNA is replicated completely and exactly once. The key players in this regulation are the E3 ubiquiting ligase Anaphase-promoting complex/cyclosome (APC/C), cyclin-dependent kinases (CDKs) and Dbf4-dependent kinase (DDK). Their concerted action ensures the association of firing factors with the pre-RC only after the G1/S transition until the end of S phase and inhibits the licensing of new origins in S/G2, preventing re-replication (Siddiqui et al., 2013).

Replication initiation: In S-phase, the final step of this process is replication initiation (Figure 19C). It starts from the pre-IC, with the bi-directional progression of the two replisomes, forming two replication forks. At each fork, replication on both strands is initiated by the generation of a short RNA primer by Pol α and proceeds in 5'-3' direction. This results in processive *de novo* DNA synthesis on the leading strand by Pol ε, and the discontinuous synthesis of Okazaki fragments on the lagging strand by Pol δ. The CMG helicase precedes both leading and lagging strand polymerases until replication of the region is completed (Burgers and Kunkel, 2017). As Cdc45 is present in limiting amounts and needs to be recycled to a different origin after replication termination, this can contribute to the spatiotemporal control of origin firing (Tanaka et al., 2011, **The efficient bird gets the worm, RIF1: Show them who's boss?**).

2.2. Chromatin replication: maintain genome integrity and epigenetic states

Cells replicate not only their DNA, but also duplicate their chromatin, and restoring features associated with the pre-existing chromatin state is important to maintain genomic and epigenomic integrity in a given cell lineage. This is accomplished by the concerted recycling of parental (old) histones and the deposition of *de novo* synthesised (new) histones (Ray-Gallet and Almouzni, 2021, Figure 20), supported by the peak of replicative histone expression in S phase to maintain nucleosome density. This enables the restoration of full nucleosome occupancy, protecting DNA from damage, but also results in a two-fold dilution of the parental histone variants and PTMs. Thus, the time of replication provides a challenge to the maintenance of the epigenomic state and a window of opportunity for cellular reprogramming (Stewart-Morgan et al., 2020).

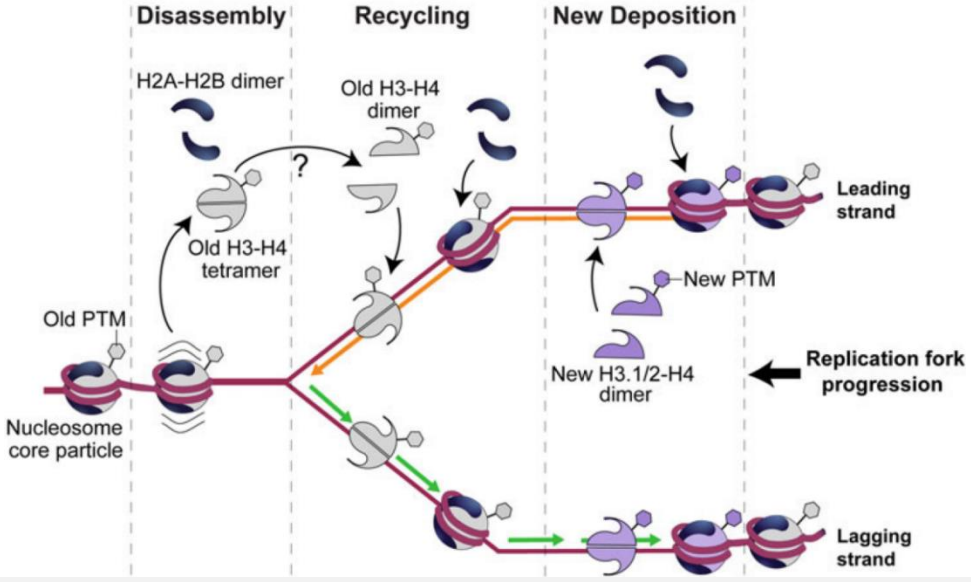

Figure 20. Histone H3 dynamics at the replication fork

Nucleosomes ahead of the replisome are disassembled due to a combination of torsional stress and the activity of histone chaperones like FACT. H2A-H2B dimers dissociate first, followed by the H3-H4 tetramer, which is recycled intact or after splitting into dimers randomly on the two strands. New H3-H4 dimers are deposited in a DSC manner to ensure a full complement of nucleosomes on nascent chromatin (adapted from Ray-Gallet and Almouzni, 2021).

2.2.1. *De novo* histone deposition in S phase

In vitro experiments indicated early on that H3-H4 dimers are assembled onto chromatin almost immediately after replication, followed by H2A-H2B (Almouzni et al., 1990; Worcel et al., 1978). Further work demonstrated that unlike new H3-H4, new H2A-H2B did not exhibit preferential association with replicated DNA (Jackson and Chalkley, 1981, 1981), reflecting their higher levels of replication-independent exchange (Jackson, 1990; Kimura and Cook, 2001). Thus, H3-H4 have been considered as the main carrier of epigenetic memory and most of the work discussed below will focus on them.

Newly synthesized histones prior to incorporation show distinct PTMs compared to their incorporated forms. These PTMs have been involved in their processing, nuclear import and differential recognition by histone chaperones, directing their assembly pathway on chromatin (Annunziato, 2015; Burgess and Zhang, 2013, **Histone post-translational modifications**). Work in yeast (Ejlassi-Lassallette et al., 2011) and human (Alvarez et al., 2011; Campos et al., 2010) has shown that new H4K5acK12ac modified by HAT1 promotes efficient nuclear import (Annunziato, 2012). Furthermore, HAT1-mediated acetylation of both new H3 (K9, K18) and H4 is required for DSC incorporation and genome stability in mouse embryonic fibroblasts (Nagarajan et al., 2013). Following deposition on chromatin, H4 is deacetylated within 20-30min (Cousens and Alberts, 1982; Jackson et al., 1976; Ruiz-Carrillo et al., 1975). This is accompanied by a concomitant gain of monomethylation at H4K20 by PR-Set7 (Scharf et al., 2009). Prior to this maturation, unmodified H4K20 is recognized by DNA repair factors like TONSL-MMS22L (Saredi et al., 2016) and BRCA1-BARD (Nakamura et al., 2019), but not 53BP1 (Pellegrino et al., 2017). Thus, this distinct marking promotes repair by homologous recombination of post-replicative chromatin. PTMs on new histones may also have variant-specific effects: the enrichment of H3K9me1 on H3.1 (Loyola et al., 2006) compared to H3K14acK8ac on H3.3 (Alvarez et al., 2011) may bias the subsequent establishment of inactive (Loyola et al., 2009)/active chromatin, respectively. Finally, Kang et al. (2011) have proposed that the non-nucleosomal H4S47phos mark promotes H3.3-H4 interactions with HIRA and prevents H3.1-H4 association with CAF-1 to regulate the assembly of particular chromatin states.

DNA synthesis-coupled assembly is promoted by CAF-1 (Smith and Stillman, 1989), which deposits the new replicative H3.1/2-H4 (Tagami et al., 2004, Figure 21). This coordination involves the direct interaction of the CAF-1 subunit p150 with the replisome component PCNA (Moggs et al., 2000; Shibahara and Stillman, 1999, **CAF-1 complex**). The capacity of p150 to dimerise has been proposed to promote H3.1-H4 tetramer formation on chromatin (Quivy, 2001) following the transfer of individual H3.1-H4 dimers from ASF1 to the p60 subunit (Abascal et al., 2013) in mammalian cells. In yeast, CAF-1 preferentially interacts with new H3K56ac histones (Li et al., 2008), a mark that is rare

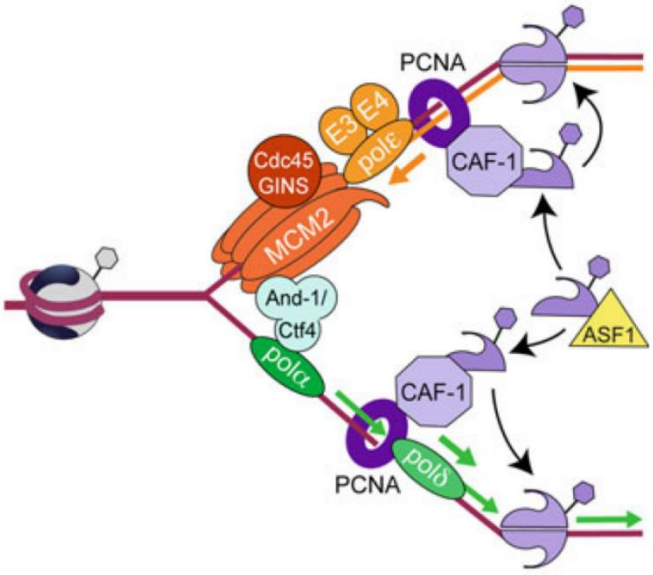

Figure 21. *De novo* histone deposition at the replication fork

Deposition of newly synthesized histones onto nascent DNA is mediated by the CAF-1 complex, which receives new H3.1-H4 dimers from ASF1. This process is coupled to fork progression through the interaction of CAF-1 with PCNA (adapted from Ray-Gallet and Almouzni, 2021).

(<1%) in mammals (Jasencakova et al., 2010; M. Xu et al., 2010). Thus, how CAF-1 in mammals may favour *de novo* synthesized rather than recycled histones handed from ASF1 remains unclear, although it may simply be mass action. Recent work has shown that CAF-1 recruitment to PCNA requires its interaction with DNA and histones in fission yeast (Ouasti et al., 2023) and metazoans (Rouillon et al., 2023). Curiously, Rouillon et al. (2023) also show that CAF-1 and Polε compete for PCNA binding without impairing *de novo* DSC assembly. Thus they may bind one at a time enabling enough DNA to be synthsized before CAF-1 can deposit histones.

In addition to replication-coupled, although largely underappreciated, DSI assembly of nucleosomes using newly synthesized H3.3-H4 mediated by HIRA also takes place in S phase (Gatto et al., 2022). In normal conditions, HIRA continuously targets H3.3 to its pre-existing sites of enrichment (Gatto et al., 2022). Additionally, HIRA may perform a 'gap-filling' function, depositing new H3.3 to maintain nucleosome density (Ray-Gallet et al., 2011). This may be important when CAF-1 can be limiting.

2.2.2. Recycling of parental histones during replication

As mentioned above, once incorporated into chromatin, histones rapidly lose the marks indicating they were newly synthesized. During this process of chromatin maturation, histones can also accumulate distinct sets of PTMs dependent on the region they are placed in. After eviction from chromatin, histones retain their PTMs, preserving a memory of the local epigenetic state and providing an opportunity to maintain it. In the context of replication, this can be accomplished if (i) old histones are recycled on both daughter strands and (ii) close to their original location, and (iii) PTMs can be used as a seed for read-write mechanisms, so they would be propagated on nearby *de novo* assembled nucleosomes (Escobar et al., 2021; Probst et al., 2009; Stewart-Morgan et al., 2020).

Early *in vitro* experiments indicated that during replication, chromatin-bound histones are randomly recycled to the two daughter strands (Jackson and Chalkley, 1985; Russev and Hancock, 1982). During nucleosome assembly, H3-H4 tetramers contain either two new or recycled dimers but could 'mix' with newly synthesized H2A-H2B (Jackson, 1988; Yamasu and Senshu, 1990). Subsequent work confirmed this for H3.1-H4 tetramers but revealed that a small fraction ~10% H3.3-H4 split in a manner associated with replication over the course of one cell cycle (M. Xu et al., 2010). Overall, the passage of the fork leads to a two-fold dilution of histone variants and their PTMs, as confirmed by assessing their levels on nascent chromatin using stable isotope labelling in culture (SILAC, Alabert et al., 2015).

More recently, two methods to genomically map histone deposition in a strand-specific manner have been developed: sister chromatids after replication by DNA sequencing (SCAR-seq) in mESCs (Petryk et al., 2018) and enrichment and sequencing of protein-associated nascent DNA (eSPAN) in yeast (Yu et al., 2018). Both rely on combining nascent DNA labelling and Ab pull-down of new/old PTMs (H4K5ac/H4K20me2, Petryk et al., 2018, H3K56ac/H3K4me3, Yu et al., 2018) followed by strand-specific sequencing. Integrating the obtained histone segregation information with initiation zone

(Petryk et al., 2018) / origin (Yu et al., 2018) locations enabled genome-wide investigation of histone deposition with respect to the path of the replication fork. These studies confirmed that genome-wide, new and old histones are largely randomly and symmetrically deposited on the leading and lagging strand at the replication fork (Gan et al., 2018; Petryk et al., 2018; Yu et al., 2018).

Whether recycling of parental histones is performed locally has important implications about the maintenance of distinct epigenetic states along the genome. Work in yeast using a tag-swapping strategy of H3 combined with ChIP-seq at different timepoints revealed the recycling of parental histones within 400bp of their original location (Radman-Livaja et al., 2011). This was later corroborated by profiling strand-specific H3K4me3 occupancy (as a mark of parental histones) on nascent DNA genome-wide (Yu et al., 2018) and by biotinylating histones in a locus-specific manner pre-replication and tracking their fate (Schlissel and Rine, 2019). Local histone recycling has also been demonstrated by *in vitro* chromatin replication assays in *X. laevis* egg extracts (Gruszka et al., 2020; Madamba et al., 2017). Finally, the combination of the SNAP tag and a pulse-chase strategy to label parental H3.1/H3.3-SNAP in HeLa cells revealed their distribution with respect to nascent DNA by super-resolution imaging (Clément et al., 2018).

To examine the local recycling in mammalian cells, Reverón-Gómez et al. (2018) developed chromatin occupancy after replication (ChOR-seq) by using a short EdU pulse to label newly synthesized DNA, followed by ChIP for the PTM of interest and the by pull-down of nascent DNA fragments associated with it. This approach showed that the levels of both active (H3K4me3) and repressive (H3K27me3) chromatin-associated PTMs undergo a two-fold dilution post-replication, while their occupancy profiles are maintained genome-wide in HeLa cells (Reverón-Gómez et al., 2018). In contrast, Escobar et al. (2019) engineered a mESC line which allowed them to specifically biotinylate H3.1/2 at target loci in G1 and follow their behaviour post-replication. This revealed ~2-fold dilution at repressed genes, compared to an almost 90% reduction in levels at active regions 12h post-release in S, even when transcription was inhibited (Escobar et al., 2019). This led the authors to conclude that H3.1/2 is faithfully recycled only at repressed, but not active domains, and explain the maintenance of active mark profiles observed by Reverón-Gómez et al. (2018) with rapid re-establishment due to transcriptional re-start rather than local recycling. However, Escobar et al. (2019) did not follow the fate of parental H3.3 which may be part of a large proportion of nucleosomes at active sites and may be continuously re-targeted there even in the absence of transcription (Gatto et al., 2022). Furthermore, the higher mobility of core histones in ESCs compared to differentiated cells (Meshorer et al., 2006), may also explain this discrepancy. Thus, whether distinct recycling strategies are employed depending on the chromatin domain or the time of its replication remains unclear.

The first histone recycling factor identified, ASF1 (Figure 22), found in complex with an H3-H4 dimer, can form a bridge with the MCM2 subunit of the replicative helicase from both nuclear and cytosolic extracts (Groth et al., 2007). Notably, the chromatin-associated H3K9me3 and H4K16ac marks detected

on the H3-H4 handled by ASF1, indicated an interaction with parental histones. Disrupting the balance between histone supply and ASF1 levels (either by ASF1 knock-down or overexpression of H3.1 and H4) impaired DNA unwinding, highlighting the importance of coordination between DNA replication and histone dynamics at the fork (Groth et al., 2007). In agreement with these findings, Clément et al. (2018) later demonstrated that ASF1 depletion led to a reduced retention of parental histones at sites of DNA synthesis. Additionally, this led to recycling of parental H3.3 at a distance from the nascent DNA only in mid/late, but not early S phase, whereas the recycling of H3.1 was shifted distally in all cases (Clément et al., 2018). This implies that another chaperone contributes to the local recycling of H3.3 in early S. Since more recent work from the team has shown the *de novo* deposition activity of HIRA in early-replicating regions (Gatto et al., 2022), it is tempting to speculate that HIRA represents a strong candidate for this faithful recycling. However, recycling of H3.3 in the context of transcription requires interaction with ASF1 (Torné et al., 2020), and it is unclear how and if this may be equally required at the replication fork.

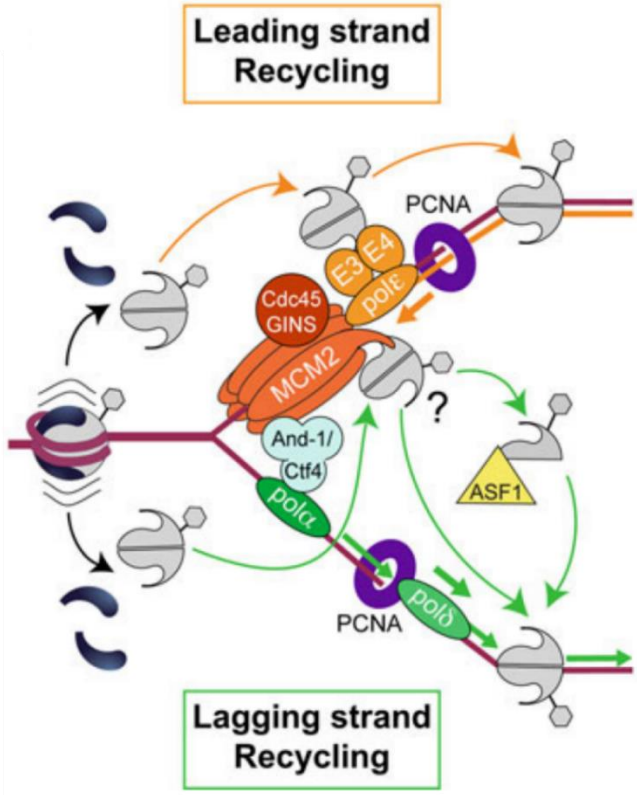

Figure 22. Histone recycling at the replication fork

Parental H3-H4 histones displaced from nucleosomes ahead of the replication fork are efficiently and largely symmetrically recycled onto nascent DNA on the leading and lagging strands through several replisome components. Leading strand recycling is mediated by the POLE3-4 subunits of the leading strand Pol ε. On the lagging strand MCM2 and Pol α, coordinated through CTF4, ensure reincorporation of old histones, potentially supported by the interaction of MCM2 with ASF1 (adapted from Ray-Gallet and Almouzni, 2021).

Importantly, the seminal work by Groth et al. (2007) also suggested that parental H3-H4 tetramers must be split transiently during recycling, in agreement with earlier studies showing mammalian ASF1 binding to H3-H4 dimers is mutually exclusive with tetramer formation (English et al., 2006; Mousson et al., 2005; Natsume et al., 2007). This presented a challenge to the idea that parental H3-H4 are re-incorporated without splitting, which remains unclear although potential mechanisms to avoid mixing of old and new dimers have been proposed (Clément and Almouzni, 2015). Further insights were brought by structural work characterising the complexes of ASF1 and MCM2 with histones (Huang et al., 2015; Richet et al., 2015). This revealed that MCM2 can bind an H3-H4 tetramer by disrupting its

contacts with DNA and H2A-H2B, potentially facilitating nucleosome disassembly ahead of the fork (Huang et al., 2015; Richet et al., 2015). This may also be enabled by interaction with the general chaperone FACT, which associates with chromatin-bound MCM2-7 and promotes DNA unwinding at initiation in human cells (Tan et al., 2006).

Notably, Huang et al. (2015) also showed that full-length MCM2 exhibits chaperone activity *in vitro*, in agreement with previous work (Ishimi et al., 2001), indicating a potential pathway for recycling of intact tetramers. Addition of ASF1 to the MCM2-tetramer complex destabilises the H3-H4 dimer-dimer interactions, resulting in a heterotetrameric complex of MCM2-H3-H4-ASF1 at 1:1:1:1 stoichiometry (Huang et al., 2015; Richet et al., 2015), consistent with the data from Groth et al. (2007). MCM2, likely in its soluble form, can also chaperone new dimers together with ASF1, contributing to histone supply maintenance, but as Huang et al. (2015) showed it is not required for CAF-1-mediated *de novo* nucleosome assembly. Finally, Huang et al. (2015) demonstrated that MCM2 can bind all H3 variants, including replicative H3.1/2, non-replicative H3.3 (corroborated by Xu et al., 2022) and the centromeric CENP-A, together with its dedicated chaperone HJURP (corroborated by Zasadzińska et al., 2018). Thus, the chromatin-associated MCM2-$(H3\text{-}H4)_2$ complex provides a mechanism to couple histone recycling to replication progression genome-wide, whereas the soluble MCM2-H3-H4-ASF1 complex may contribute to both recycling of old dimers and buffering the storage of old and new histones.

Subsequent functional studies interrogated whether MCM2 fulfils its chaperone function on both DNA strands using SCAR-seq (Petryk et al., 2018) and eSPAN (Gan et al., 2018; Li et al., 2020) in cells encoding an MCM2 histone binding mutant. This work revealed that MCM2 favours recycling of parental histones on the lagging strand (Petryk et al., 2018), in a complex with Ctf4 and Polα (Gan et al., 2018; Li et al., 2020). Notably, Polα can also bind H2A-H2B dimers (Evrin et al., 2018) and recycle parental H2A-H2B on the lagging strand (Flury et al., 2023). Around the same time, Bellelli et al. (2018a) discovered two subunits of the leading strand Polε, POLE3-4 can handle H3-H4 tetramers in human cells, while Yu et al. (2018) used eSPAN in POLE3-4 mutant yeast cells to demonstrate that they help recycling parental H3-H4 on the leading strand. Work in yeast has also documented a role for RPA (Liu et al., 2017) and FACT (P. Wang et al., 2021) in parental histone recycling, although such observations have not been made yet in mammalian cells.

Thus, the local and symmetric re-incorporation of parental histones is coupled to fork passage through the interaction of histone chaperones (ASF1, FACT) with the replicative helicase subunit MCM2, and the chaperone activities of key replisome components.

2.2.3. Re-establishment of the chromatin landscape

Following replication, restoration of the nascent chromatin landscape to re-establish its pre-replication state before the next S phase is needed to maintain epigenetic information throughout cell generations.

This re-establishment involves several aspects, including the re-association of chromatin-bound proteins, restoration of nucleosome positioning, variant occupancy and PTM levels.

Work in yeast (Gutiérrez et al., 2019; Vasseur et al., 2016) and *D. melanogaster* (Ramachandran and Henikoff, 2016) demonstrated that nucleosomes are deposited over NDRs, promoters and enhancers post-replication and ordered nucleosome arrays within gene bodies are lost. The restoration of these features correlated with RNAPII and chromatin remodeller binding and exhibited locus-specific dynamics (Gutiérrez et al., 2019; Ramachandran and Henikoff, 2016). For example, recovery of cell type-specific enhancers was barely evident 1h post-replication, unlike general enhancers and promoters where it was readily detectable, but incomplete (Ramachandran and Henikoff, 2016), supporting the idea that replication provides an opportunity to re-wire the epigenetic state. Notably, hir1 (yeast HIRA orthologue) but not the remodellers CHD1 or ISWI1a is required during chromatin maturation to increase nucleosome packing (Vasseur et al., 2016), which may rely on its capacity to deposit H3 in a DSI manner.

Stewart-Morgan et al. (2019) investigated this question in mESCs using repli-ATAC-seq, which allowed them to profile nascent (10min EdU pluse) or mature chromatin accessibility and follow maturation dynamics. They demonstrated that recovery of chromatin accessibility is concomitant with transcriptional restart and detected faster a recovery of super- and house-keeping gene enhancers compared to ones specific for mESCs (Stewart-Morgan et al., 2019), in agreement with Ramachandran and Henikoff (2016). Furthermore, inhibition of transcription initiation and elongation confirmed that RNAPII binding alone can promote chromatin maturation, but elongation is required for complete re-establishment of the pre-replicative state (Stewart-Morgan et al., 2019). Quantitative proteomics of factors associated with nascent and maturing chromatin over the cell cycle revealed that 50% proteins re-bind chromatin within 15min post-replication, while 15% are incompletely restored until the following G1 (Alvarez et al., 2023). Strikingly, restoration of protein binding at heterochromatin proceeded faster than euchromatin, likely driven by efficient read-write repressive mechanisms (Alvarez et al., 2023), consistent with the faster heterochromatin maturation observed in yeast (Gutiérrez et al., 2019).

Among proteins with delayed re-association with chromatin, Alvarez et al. (2023) identified some histone variants and modifiers, reflecting earlier studies that demonstrated that the kinetics of PTM recovery after 2-fold dilution following replication vary between marks (Alabert et al., 2015; Barth and Imhof, 2010; Scharf et al., 2009; Xu et al., 2012). More specifically, H3.3 and H2A.X, but not H2A.Z are similarly enriched on nascent and total chromatin, likely reflecting not only efficient recycling, but also *de novo* deposition (Alabert et al., 2015). This is in line with the HIRA-mediated *de novo* H3.3 incorporation in S phase that we detected (Gatto et al., 2022). Furthermore, Alabert et al. (2015) show that most methylation marks examined (including mono- and di-methylation on H3 K9, K27, K36, K79 and H4K20) are restored within 2-24h, mainly through modification of new histones. In contrast, tri-

methylation of H3 K9 and K27 on new histones alone is not sufficient to reach mature chromatin levels within 24h and the two residues are also modified on recycled old histones (Alabert et al., 2015).

The different kinetics of PTM restoration post-replication likely reflect the distinct modes for imposing or removing these marks, their genomic distribution, and the processes they are associated with. *Bona fide* repressive PTMs like H3K9me3 and H3K27me3, usually distributed in broad domains with low nucleosome turnover, are thus maintained thanks to their read-write mechanisms. In contrast, modifications linked to transcription like H3K4me3 and H3K36me3, which mark smaller, more dynamic regions, are continuously replenished due to the presence of TFs or RNAPII, respectively (Escobar et al., 2021). Indeed, Reverón-Gómez et al. (2018) show H3K4me3 is restored to mature chromatin levels at 50% sites within 1hr post-replication, with the remaining sites recovering within 6hrs, whereby restoration rate is linked to transcriptional activity. This is in line with the rapid turnover of this mark, recently described by (Wang et al., 2023). Conversely, only ~20% H3K27me3 domains were recovered 10hr post-replication, and these included domains with the highest enrichment of the mark and its writer, EZH2 (Reverón-Gómez et al., 2018). The reestablishment of H3K9me3 and H3K27me3 domains can also be aided by additional features recruiting their writers. The *de novo* assembly complex CAF-1 interacts with the H3K9me3 reader HP1a (Quivy et al., 2004) and the methyltransferase SetDB1 to provide H3K9me1 as substrate for Suv39h1 during replication of pericentric heterochromatin in mouse (Loyola et al., 2009). With regards to H3K27me3, recent work demonstrated that H2A-H2B dimers are locally recycled and provide short-term memory of Polycomb-mediated repression, as PRC2 recognises H2AK119ub (Flury et al., 2023).

In summary, different aspects of chromatin maturation after replication can take from minutes (TF binding, H4K5K12diac removal) up to several hours (H3K4me3, H4K20me2 recovery) and even until the subsequent S phase (H3K9me3, H3K27me3 restoration). The dynamics of this process depend on the genomic context and on the chromatin feature in question. Curiously, binding of chromatin-associated proteins is restored first in inactive regions, despite their slow rate of PTM re-establishment. Thus, replication causes a major disruption to the epigenetic landscape which may provide an opportunity for cell reprogramming, but also result in aberrant phenotypes if the mechanisms involved in histone deposition, recycling or modification fail.

2.2.4 Importance of maintenance of the histone landscape for genome and epigenome integrity

Genome integrity is dependent on efficient *de novo* deposition and recycling of histones. POLE4 deficiency is embryonic lethal in mice, leads to increased replication stress and dormant origin firing and promotes tumorigenesis (Bellelli et al., 2018b). Conversely, in the absence of adequate new histone supply for *de novo* nucleosome assembly due to down-regulation of CAF-1 (Hoek and Stillman, 2003; Ye et al., 2003), ASF1 (Groth et al., 2007, 2005) or histones (Mejlvang et al., 2014; Nelson et al., 2002)

replication forks slow down, DNA damage checkpoints are activated, and S phase progression is impaired. Furthermore, POLE3 or POLE4 deletion and MCM2 histone binding mutants in mESCs lead to increased mitotic defects, with double mutants (POLE3/4 deletion/MCM2 mutants) resulting in exacerbated phenotypes (Xu et al., 2022).

Restoring nucleosome density post-replication is critical for the maintenance of cell state, as evidenced by the enhanced reprogramming upon CAF-1 depletion in mESCs (Ishiuchi et al., 2015), mouse embryonic fibroblasts (Cheloufi et al., 2015) and myeloid progenitors (Franklin et al., 2022). This may rely on the interaction of CAF-1 with HP1a/SetDB1 (Loyola et al., 2009; Quivy et al., 2004) or EZH2 (Cheng et al., 2019) to promote heterochromatin establishment and maintenance. However, in *S. pombe* CAF-1 promotes repression independently of such mechanisms (Chen et al., 2023), indicating that nucleosomal occupancy alone can also contribute to preserve cell state. Indeed, reducing replication fork speed by HU treatment, limiting the dNTP pool, or USP7 knock-down in mESCs promotes 2CLC emergence, which may be a consequence of changes in the dynamics of nucleosome assembly or chromatin maturation (Nakatani et al., 2022). The positioning of nucleosomes may also be important, as Alvarez et al. (2023) detected increased enrichment of chromatin remodellers and a subset of TFs on nascent compared to mature chromatin, supporting the idea that replication can facilitate changes in cell state.

Ensuring symmetric local recycling is also required to maintain the epigenetic landscape. Deletion of POLE3-4 in yeast results in impaired heterochromatin silencing without affecting overall nucleosome occupancy (He et al., 2017; Iida and Araki, 2004; Yu et al., 2018). Polα (Evrin et al., 2018, Gan et al., 2018) and MCM2 (Foltman et al., 2013; Gan et al., 2018; Saxton and Rine, 2019) histone binding mutants alone or in combination (Li et al., 2020) give similar aberrations. Conversely, MCM2 mutants lacking POLE3/4 displayed even stronger heterochromatin re-activation, though curiously not in a manner correlated with the number of nucleosomes inherited (Saxton and Rine, 2019). In mESCs, Polα and MCM2 histone binding mutants lead to de-repression of repetitive elements due to local reduction of H3K9me3 (Li et al., 2020). Furthermore, Polα is required to recover H3K27me3 post-replication due to its H2A-H2B recycling activity (Flury et al., 2023). Finally, ASF1 depletion in human cells resulted in nuclear re-distribution of both H3K9me3 and H3K27me3, whereby their enrichment at the nuclear and nucleolar periphery was lost (Clément et al., 2018). Thus, safeguarding the stability of repressive domains and promoting the maintenance of established transcriptional programmes is mediated by replication-coupled *de novo* histone deposition and faithful recycling of parental histones. This generates a nascent chromatin environment which allows the reestablishment of the histone variant and PTM landscape through the reassociation of TFs, RNAPII and the action of PTM read-write mechanisms.

There are some notable exceptions to symmetric histone recycling, which have been linked to asymmetric cell division producing two daughter cells with different potential (Urban et al., 2022). The

first evidence was observed in male *D. melanogaster* germ stem cells, where upon asymmetric division, parental histones are preferentially retained in the stem daughter, whereas new histones are inherited by the differentiating gonidoblast (Tran et al., 2012). Notably, only replicative H3.1-H4, but not H3.3-H4 (Tran et al., 2012), H2A-H2B or H1 (Wooten et al., 2019) demonstrated asymmetric inheritance patterns, potentially reflecting the different dynamics of the histones. However, no H2A asymmetry was detected on nascent DNA from the sister chromatids, while old H3-H4 were enriched on the leading strand (Wooten et al., 2019), arguing that the difference between H2A-H2B and H3-H4 is not due to different dynamics post-replication. This would be in line with the fact that recycling of both H3-H4 (Gan et al., 2018) and H2A-H2B (Flury et al., 2023) on the lagging strand is executed by Polα, whereas POLE3-4 deposits specifically parental H3-H4 on the leading strand (Bellelli et al., 2018a, Yu et al., 2018).

Strand bias alone cannot ensure asymmetric histone inheritance as forks proceed from origins bidirectionally, but Wooten et al. (2019) showed that unidirectional fork progression was ~3-fold (from 17% to 42%) increased in germline stem cells compared to symmetrically dividing cells. To understand the different behaviour of H3 and H3.3, Chandrasekhara et al. (2023) swapped their unique residue at position 31, which does not impact chaperone recognition, but has important function on chromatin in development (Sitbon et al., 2020), induction of gene expression (Martire et al., 2019) and mitosis (Hinchcliffe et al., 2016). H3A31S mutation disrupted the asymmetric H3 inheritance and become more enriched at promoters, whereas H3.3S31A resulted in increased turnover of parental histones and was more often found at repressed regions. Notably, the two mutations had opposing phenotypes, with H3A31S leading to expansion of the stem cell population and H3.3S31A decreasing it (Chandrasekhara et al., 2023).

Furthermore, Kahney et al. (2021) documented asymmetric histone inheritance in female *D. melanogaster* germ cell divisions only at differentiation and stemness-related genes and for both H3.1 and H3.3. Asymmetric inheritance of the centromeric H3 variant detected in *D. melanogaster* intestinal stem cells showed that parental CENP-A together with the inner kinetochore protein CENP-C segregated into the stem progeny (García Del Arco et al., 2018). Finally, Zion et al., (2020) showed that new and parental H3-H4 distributed asymmetrically between daughter cells of asymmetrically dividing intestinal stem cells, and mutations (H3T3A) disrupting this distribution could lead to uncontrolled proliferation.

In mESCs, asymmetric division of single cells prompted by culture on Wnt3a-coated beads showed that parental H3.1-H4, but not H3.3-H4 or H2A-H2B are preferentially recycled on the leading strand (Ma et al., 2020), in agreement with the findings in *D. melanogaster* discussed above. However, during asymmetric division of mouse muscle stem cells no such bias of H3.1 or H3.3 inheritance occurred (Evano et al., 2020). Thus, asymmetric inheritance of a variant in certain contexts proved critical for normal development and differentiation, yet how this is established remains unclear.

2.3. Spatiotemporal organization of replication: replication timing (RT) programme

Due to the size of mammalian genomes, with an average fork speed of ~2kb/min (Conti et al., 2007), it would take ~3 years for the haploid human genome (~3100Mb) to replicate with a single origin. Instead, the normal S phase duration is about ~6-8 hours (Ciemerych and Sicinski, 2005). This is consistent with replication initiation using many origins (Cairns, 1966; Huberman and Riggs, 1968) in a specific spatiotemporal order. This is termed the replication timing (RT) programme and it is set in early G1 at the timing decision point (TDP) coincident with the re-establishment of nuclear organization (Dimitrova and Gilbert, 1999). Notably, this takes place after MCM loading, but prior to the origin decision point (ODP), when specific initiation sites in early or late-replicating regions are selected to be used as active origins (Wu and Gilbert, 1996). The establishment, regulation and functional role of RT are far from well understood and many open questions remain. Below, I will focus on three of them: (i) how is the RT programme established, (ii) how is it organized with respect to other genome functions and (iii) is it functionally linked to them?

2.3.1. RT establishment: definition and selection of origins of replication

As described above, the initiation of DNA replication begins at origins of replication, but this does not happen simultaneously at all licensed origins at the entry into S phase. Furthermore, it does not occur at all licensed origins. Indeed they are assembled in large excess and only a small fraction (1-10%) of them fire in any one cell in a given S phase, while the rest remain dormant (Cayrou et al., 2011; Friedman et al., 1997; Taylor, 1977). Furthermore, firing patterns are not random: individual sites (in budding yeast, Czajkowsky et al., 2008) or initiation zones comprising several origins (in metazoans, Besnard et al., 2012; Cayrou et al., 2011; Dellino et al., 2013; Petryk et al., 2016; W. Wang et al., 2021) have a characteristic probability to be used across a cell population. This feature is termed firing efficiency and correlates with the timing of replication initiation in S, which has given rise to the idea that genome-wide RT patterns can be explained by a stochastic model of origin firing (Rhind, 2006; Rhind et al., 2010). This model posits that each initiation site/zone has an intrinsic probability to fire which determines its RT. The more efficient a region is, the more likely it will fire in early S phase (Vousaz and Gilbert, 2021).

Thus, two questions have dominated in the field: how are only a fraction of origins selected to initiate and how is the timing of origin firing controlled? To answer them, the first thing to determine is how origins are defined and distributed along the genome.

In the beginning, there was sequence

In budding yeast, specific regions termed autonomous replication sequences (ARSs) were identified as origins of replication when inserted into plasmids (Stinchcomb et al., 1979) and in chromosomes

(Brewer and Fangman, 1987; Huberman et al., 1987). ARSs comprise a repeated 11-nt core sequence (ACS, Palzkill and Newlon, 1988), part of an A element, and three B elements (Marahrens and Stillman, 1992), which are recognised by ORC (Bell and Stillman, 1992). This is mediated by a loop in Orc2 and a helix in Orc4 (Li et al., 2018; Yuan et al., 2017). In many other eukaryotes, including in human the absence of such elements explains the lack of sequence-defined origins (Schaarschmidt et al., 2004; Vashee et al., 2003).

In metazoans, the two main types of approaches used to define origins relied on mapping pre-RC components or nascent DNA, both of which have distinct caveats (Table 4). The potential of the pre-RC to move from its assembly location (**The mechanics of DNA replication**, Emerson et al., 2022;

Table 4. Methods for mapping origins of replication

Method	Description	Data	Ref
2D gel assays and fork direction analysis	uses distinct gel migration patterns to characterize replication intermediates and detect origin firing efficiency	population-based data	Brewer and Fangman, 1987, Huberman et al., 1987
ChIP-seq	identify locations of ORC and MCM binding sites to predict the location of replication origins		Lucas and Raghuraman, 2003, MacAlpine et al., 2004, 2010, Belsky et al., 2015, Long et al., 2020
Initiation site (ini-seq)	label nascent DNA with DNA analogs and either immuno-precipitate the labeled nascent DNA or separate the labeled nascent DNA from unreplicated DNA using density difference		Langley et al., 2016, Guilbaud et al., 2022
Okazaki fragment (OK-seq)	isolate and sequence Okazaki fragments to map replication fork direction in asynchronous population of cells		Petryk et al., 2016
short nascent strand (SNS-seq)	identify nascent RNA-primed DNA synthesized at origins by the primase DNA polymerase a (Pol α)		Cadoret et al., 2008, Cayrou et al., 2011, Besnard et al., 2012, Picard et al., 2014
Repli-seq	label nascent DNA with BrdU; look for the enrichment of BrdU-immunoprecipitated DNA in late S cells compared with early S cells		Zhao et al., 2020
scRepli-seq	uses a commercial whole genome amplification kit (SeqPlex,Sigma) to prepare libraries	single-cell data	Miura et al., 2019, Takahashi et al., 2019
DNA combing	fluorescently label nascent DNA; DNA molecules stretched and aligned along a slide and visualized by fluorescence microscopy	single-molecule data from population of cells	Bensimon et al., 1994, Michalet et al., 1997, Pasero et al., 2002
ORM (optical replication mapping)	fluorescent nucleotide analog pulse-labeled nascent DNA in combination with the optical mapping method (Bionano Genomics) to map long individual DNA molecules		W. Wang et al., 2021

Adapted from Hu and Stillman, 2023.

Scherr et al., 2022) means that its occupancy may not be an accurate reflection of origin positions. Furthermore, there are technical challenges in generating antibodies appropriate for pull-down experiments, so these methods have not been so widely used. Alternatively, techniques based on detection of replication forks or nascent DNA are only able to identify active origins, which are only a small fraction of all licensed sites. Furthermore, most of these approaches are applied on bulk cell populations, which further biases the mapping towards more efficient, early origins, as they will be used in a larger proportion of cells. Thus, it has been challenging to disentangle what is important for origin definition and firing in metazoans (Hu and Stillman, 2023).

Strength in numbers

Early studies in mammalian cells could identify either distinct active origin sites (0.5-2kb in size) or initiation zones (IZs) tens of kbs in length, based on nascent DNA strands (NS) or replication bubble analysis, respectively (DePamphilis, 1999). Higher resolution genome-wide NS studies resolved this discrepancy, showing that individual active origins tend to be clustered in IZs (Besnard et al., 2012; Cadoret et al., 2008; Cayrou et al., 2011). Recent mapping of early initiation events in an *in vitro* reconstituted system (ini-seq2) has indicated the organization of origins in 'ini domains' (median size 205kb) may be hierarchical, with origins near the borders showing higher efficiency (Guilbaud et al., 2022). Origin clustering was also detected in IZs of 20-40kb in size identified by Okazaki fragment sequencing (OK-seq, Petryk et al., 2016, Figure 23). IZs of similar length are also observed by optical replication mapping (ORM, W. Wang et al., 2021). ORM is a single-molecule approach, which reveals that several origins can be fired in one IZ at a time if spaced >15kb apart (W. Wang et al., 2021), an estimate somewhat lower than previous work (>30kb, Lebofsky et al., 2006). This is due to a phenomenon termed origin interference, whereby the presence of two origins too close to one another results in the firing of only one of them and the passive replication of the other (Brewer and Fangman, 1993). Finally, thanks to the increased throughput of their fibre analysis, W. Wang et al. (2021) show that initiation in neighbouring early IZs (median distance of 168kb) is independent, unlike previous work which had suggested nearby IZs fire synchronously (Marheineke and Hyrien, 2004).

With respect to genome features and function, Cadoret et al. (2008) showed active origins were enriched in DHSs and active PTMs (H3K4me, H3ac, H4ac) and overlapped CpG islands (CGIs), promoters, regulatory elements, and binding sites of potent transcriptional activators, in agreement with previous work (Beall et al., 2002; Bosco et al., 2001). Subsequent studies reinforced the colocalization of origins with open chromatin (MacAlpine et al., 2010), promoters (Dellino et al., 2013) and CGIs (Cayrou et al., 2012, 2011, independently of promoters). Despite the link with transcriptional activity, origins could also be found in inactive chromatin, associated with HP1a (MacAlpine et al., 2010). Cadoret et al. (2008) also showed increased clustering of origins with higher GC content, in line with the occurrence of origins at CGIs and/or promoters. Dellino et al. (2013) demonstrated that ORC1-bound sites are enriched in open chromatin, with detectable RNA produced from 82% of them in HeLa cells. Higher

transcription correlated with earlier replication timing, although ~50% origins that replicated in early S had no or low expression. Thus, the authors suggest this may reflect their passive replication in early S instead of being fired (Dellino et al., 2013). This was in agreement with pioneering work in *D. melanogaster* showing ORC1 binding partially overlaps RNAPII binding sites, whereas transcriptional activity and early replication correlated at the scale of broad domains (MacAlpine et al., 2004). A subsequent study profiled the organization of active origins with respect to chromatin features in mESC (Cayrou et al., 2015). This demonstrated that early firing is associated with both active enhancer and promoter marks, but also bivalent chromatin (H3K4me3/H3K27me3, Cayrou et al., 2015). These data suggest that efficient firing/early replication is not necessarily dependent on expression but is more likely affected by the chromatin state (Masai et al., 2010). Indeed, the conflict between transcription and pre-RC assembly (Martin et al., 2011; Nieduszynski, 2005) may explain why highly efficient origins are found at TSSs, whereas origins at the end of transcriptional units are less efficient (Donato et al., 2006).

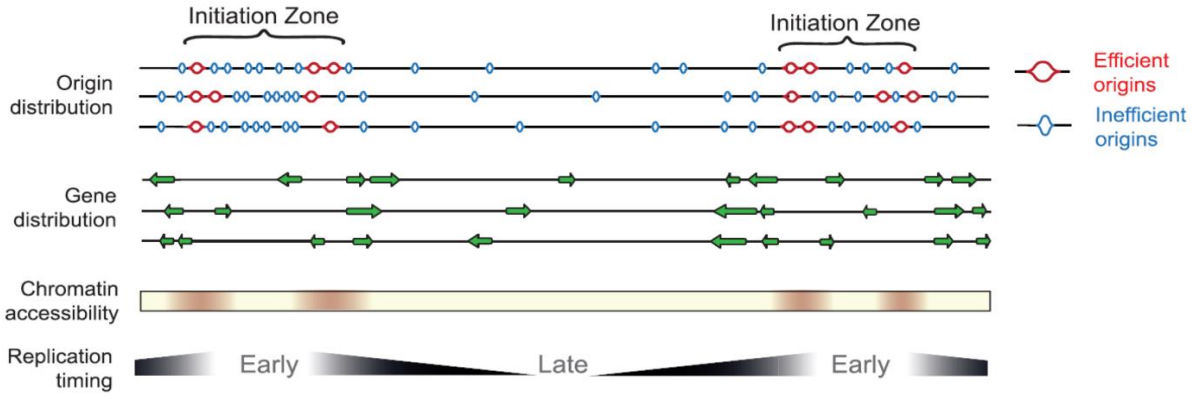

Figure 23. Organisation of origins of replication

Schematic representation of the genomic architecture of replication origins in metazoans and the correspondence with other features (genes, chromatin accessibility, RT). Origins are clustered in initiation zones (IZs, 20-40kb) with more efficient origins found at their borders. They are found in regions of accessible chromatin and upstream of active TSSs, minimising the chance of transcription-replication conflicts. In S phase, one of the origins within an IZ fires stochastically, which results in passive replication of the rest. The more efficient an origin is, the earlier in S it fires. Thus, the clustering of efficient origins results in consistent early firing IZs, whereas less efficient origins dispersed along the genome tend to replicate late (adapted from Guilbaud et al., 2022).

How to define an origin?

Characterization of origin sequences of animal viruses (DePamphillis, 1999) and individual metazoan genes (Altman and Fanning, 2004; Paixão et al., 2004; Wang et al., 2004) shows that they contain distinct DNA features like DNA-unwinding elements (DUEs), AT-rich tracks, matrix attachment regions (MARs, Debatisse et al., 2004; DePamphilis, 1999) or negative supercoiling (Remus et al., 2004), suggesting that origin definition in metazoans may partially rely on sequence or DNA properties.

Genome-wide short NS (SNS) analysis has demonstrated the colocalization of mouse and *D. melanogaster* origins with CpG islands (CGIs), with a particular organization: origins overlap AT-rich sequences that flank GC-rich regions, termed G-rich repeated elements (OGREs, Cayrou et al., 2011, 2012). OGREs were predicted to be either nucleosome-occupied (Cayrou et al., 2012) or to form G-quadruplexes (G4, Cayrou et al., 2011; Prorok et al., 2019), which are 4-stranded loops of ssDNA that may favour protein binding or DNA unwinding (Huppert and Balasubramanian, 2005). In human cells, the same approach revealed only partial overlap between origins and CGIs (Besnard et al., 2012; Cadoret et al., 2008) but showed an enrichment of G4 motifs at origins (Besnard et al., 2012), or up to 1.5kb upstream (Akerman et al., 2020). In avian DT40 cells, deletion of G4 motifs from endogenous origins ablates initiation, whereas their inversion affects origin position in concert with other *cis*-acting elements (Valton et al., 2014). In mESCs, deletion of G4/OGRE also prevents origin firing, whereas insertion of such elements or their stabilization leads to new initiation events (Prorok et al., 2019) 240bp away from the motif (as described in Cayrou et al., 2012). However, there is not a 1:1 correspondence between OGRE/G4 motifs and origins, indicating that factors beyond DNA sequence also contribute to origin determination (Cayrou et al., 2011, 2012).

Mapping components of ORC has shown it binds DNase I-sensitive chromatin decorated with active PTMs and/or H3.3 (MacAlpine et al., 2010) in a sequence-independent manner in *D. melanogaster* (Eaton et al., 2011) and human cells (Dellino et al., 2013; Miotto et al., 2016). This is in agreement with yeast studies, which have shown ARSs are nucleosome-depleted (Lipford and Bell, 2001; Nieduszynski et al., 2006) but flanked by ordered nucleosome arrays (Berbenetz et al., 2010; Eaton et al., 2010). The establishment of these arrays may rely on intrinsic ORC remodelling activity (Sai Li et al., 2022) or interaction with remodellers, and be important for origin function (Chacin et al., 2023). Mapping origins based on MCM, Sugimoto et al. (2018) show MCM7 is also enriched in open chromatin, whereas Li et al., (2023) demonstrate MCM2-7 DH are organised in clusters, flanked by ORC. MCM2-7 clusters are also depleted in RNAPII and nascent RNA, confirming the physical separation of transcription and replication machinery previously shown (Cadoret et al., 2008, Cayrou et al., 2011).

Somewhat unexpectedly, human ORC subunits have been pulled down with histones bearing the repressive H3K9me3, H3K27me3 and H4K20me3 marks (Vermeulen et al., 2010). This association may be mediated through ORCA/LWRD1, which can bind H3K9me3 and recruit ORC1 there (Gómez and Brockdorff, 2004; Shen et al., 2010; Wang et al., 2017). Interestingly, human ORC1 already binds chromosomes in late mitosis, but then exhibits distinct spatial distributions throughout G1 as detected by immunofluorescence. In early G1, ORC1 shows a punctate pattern in the nuclear interior, while in late G1 it appears more enriched in larger foci (Kara et al., 2015; Wu and Nurse, 2009). These are reminiscent of the early and mid/late S-phase patterns of nascent DNA, corresponding to active and inactive chromatin, respectively (Vouzas and Gilbert, 2021, **Organization of RT**).

It is unclear what controls this spatiotemporal aspect of ORC1 binding, but it may be affected by differential chromatin accessibility or levels of inactive marks (fully recovered only in late G1, **Re-establishment of the chromatin landscape**). Similar dynamics of ORC have also been observed in fission yeast (Wu and Nurse, 2009), where the authors suggest that the different kinetics of ORC1 association with the genome at active compared to inactive chromatin result in earlier completion of pre-RC assembly in euchromatin and thus, more efficient origins. In line with this observation, Mei et al. (2022) reported that in human cells, MCM loading occurs at euchromatin in early G1 and heterochromatin in mid G1, which is likely precluded in early G1 by the lack of histone acetylation. In this system MCM loading accelerated with G1 progression at an increasing rate at hetero- compared to euchromatin. This led to a comparable enrichment of MCM at inactive chromatin by the end of G1 (Mei et al., 2022), in a manner promoted by ORCA. However, the authors could not differentiate between loading of single MCM2-7 and DH formation. Thus, their data does not exclude the possibility that by the time pre-RCs are assembled on heterochromatin, cells have reached the G1/S transition and limited pre-IC components like Cdc45 (Wong et al., 2011; Wu and Nurse, 2009) or Treslin/TICCR (Collart et al., 2013; Mantiero et al., 2011; Tanaka et al., 2011) have bound euchromatic pre-RCs.

The efficient bird gets the worm

In addition to playing a role in the definition of origins, chromatin can also impact firing efficiency and subsequently, replication timing. Detailed below are the proposed mechanisms of how some histone PTMs and/or their readers can affect replication initiation, but the potential function of many others has been discussed in Fragkos et al. (2015).

The histone acetylase KAT7 (HBO1 in yeast) promotes origin licensing although it is unclear whether this is due to direct interaction with ORC1 (Iizuka and Stillman, 1999), modification of licensing factors (Miotto and Struhl, 2008), histone substrates (Miotto and Struhl, 2010), or a combination of these activities. Increased histone acetylation alone can increase origin efficiency and thus lead to earlier firing (Pasero et al., 2002) due to increased Cdc45 recruitment in budding yeast (Vogelauer et al., 2002). In *X. laevis*, higher acetylation of a discrete origin increases its efficiency without affecting ORC occupancy (Danis et al., 2004), indicating that an active chromatin state can facilitate firing as well as licensing. In addition to acetylation, the extent of chromatin accessibility is also linked to origin efficiency, as demonstrated by the higher DNase I sensitivity of active compared to dormant origins (Sugimoto et al., 2018, Figure 23). In mESCs, Sima et al. (2019) have identified a set of *cis*-acting early replication control elements (ERCEs), which are highly acetylated, but not origins themselves. ERCEs contact each other in a CTCF-independent manner and are required for the early replication of the domain they are a part of (Sima et al., 2019). Although it is unclear how they fulfil their function, it is possible that they are bound by the acetyl readers BRD2/4, which can interact with Treslin/TICCR (Sansam et al., 2018), promoting origin firing (Vousaz and Gilbert, 2021).

As another example, Kuo et al. (2012) showed that metazoan ORC1 can recognise H4K20me2, which is required for loading of the complex on chromatin and efficient G1/S transition. Increased levels of Pr-SET7, one of the H4K20 methylases, results in re-replication, indicating its importance for origin licensing (Tardat et al., 2010). Recent work by Long et al. (2020) has further elucidated this mechanism, showing that the histone variant H2A.Z **(**linked with active transcription but also found in heterochromatin, **Histone variants**) is bound by SUV420H1, which deposits H4K20me2. They also link H2A.Z with origin firing, showing H2A.Z-H4K20me2-ORC1 co-occupied origins tend to be more efficient and initiate earlier compared to the rest (Long et al., 2020). However, H4K20me2 is one of the most abundant histone PTMs, present on >95% nucleosomes, which makes it difficult to understand how it may direct specific origin assembly or firing (Prioleau and MacAlpine, 2016).

Recent work from the lab has demonstrated that the histone variant H3.3 also plays a role in regulating early replication initiation in mammals (Gatto et al., 2022). This study demonstrated that the different deposition modes of the replicative H3.1 and replacement H3.3 variants (**Histone variants**) lead to the establishment of H3.3-enriched sites, flanked by H3.1. The H3.3/H3.1 boundaries of these regions define early replication IZs, which is mediated by the H3.3-specific chaperone HIRA (Gatto et al., 2022). Notably, in the absence of HIRA two classes of sites can be differentiated, termed blurred and buried. Blurred sites are transcribed and in HIRA KO, they remain relatively H3.3-enriched and early initiation still takes place at their boundaries, but the patterns of both H3.3 and nascent DNA synthesis become fuzzy. Buried sites, on the other hand, have low or no transcriptional activity, and completely lose H3.3 enrichment and stop replicating early in the absence of HIRA (Gatto et al., 2022). Although it remains unclear how the H3.3/H3.1 balance affects initiation, it shows that HIRA is critical for a chromatin-based definition of early IZs in a transcription-independent fashion (Gatto et al., 2022).

Chromatin-associated factors can also play a role in decreasing origin efficiency, thereby promoting late initiation. Upon global disruption of replication timing in the absence of RIF1 (**RIF1: Show them who's boss?**), late replication is maintained specifically at H3K9me3 domains in HCT-116 cancer cells, but not in hESCs, where large regions of H3K9me3 are absent **(**Klein et al., 2021). In *D. melanogaster*, the presence of the H3K9me3 reader HP1a at centromeres is required for their replication in late S phase, but its association with pericentromeric and interspersed repeats promotes initiation there in early S (Schwaiger et al., 2010). This is in concordance with earlier work in fission yeast, where the HP1 homologue Swi6 facilitates Treslin/TICCR recruitment to the pre-IC (Hayashi et al., 2009). Additionally, H3K9me3-independent recruitment of HP1a to *D. melanogaster* promoters is required for their early replication (Figueiredo et al., 2012), potentially due to its interaction with ORC (Hiratani et al., 2008; Pak et al., 1997; Schübeler et al., 2002). Thus, chromatin context may be an important modulator for particular factor to function.

As histone acetylation, open chromatin and H2A.Z/H3.3 enrichment are common features of active promoters and enhancers (Millán-Zambrano et al., 2022, **Histone variants**), KAT7 itself acts as a

transcriptional co-activator (Miotto et al., 2008), and promoters often contain GC-rich elements (**How to define an origin?**), this can underlie the strong correlation between early origin firing in S phase and transcriptionally active chromatin in metazoans (Hiratani et al., 2008; Schübeler et al., 2002, **Organization of RT**). In contrast, the enrichment of H3K9me3/HP1 in heterochromatin links repression with late replication. Importantly, the work discussed above argues that the connection of pre-RC assembly and origin efficiency with transcription is mediated by the state and binding factors present on chromatin.

RIF1: Show them who's boss?

So far, RIF1 is the only protein known for its role in the global orchestration of the RT programme (Blasiak et al., 2021; Cornacchia et al., 2012; Hayano et al., 2012). RIF1 was originally identified in yeast, where its recruitment to telomeres prevents their elongation by telomerase (Hardy et al., 1992; Kanoh and Ishikawa, 2001). In human cells, under normal circumstances RIF1 does not associate with telomeres, but it becomes enriched there upon DNA damage (Xu and Blackburn, 2004) or dysfunction, dependent on the DNA repair factors ATM and 53BP1 (Silverman et al., 2004). Follow-up work demonstrated that RIF1 is specifically important for replication fork re-start upon stalling (Buonomo et al., 2009; D. Xu et al., 2010). In *D. melanogaster* RIF1 neither associates with telomeres, nor participates in the DNA damage response, but instead accumulates at heterochromatin (Sreesankar et al., 2012). Xu and Blackburn (2004**)** reported a similar observation in human cells, where RIF1 shows some accumulation at the lamina and broad nuclear enrichment with some foci.

RIF1 exhibits the same nuclear pattern in mouse embryonic fibroblasts (MEFs) in G1 or G2, whereas it dynamically redistributes in S phase (Cornacchia et al., 2012). RIF1 first becomes enriched in chromocenters prior to their replication, co-localising briefly with MCM3, re-localises to chromocenter interior as their periphery begins replicating, and then completely dissociates from them without co-localising with nascent DNA. Loss of RIF1 resulted in cells with aberrant replication patterns which cannot be clearly classified as early or late as detected by labelling newly synthesized DNA by EdU incorporation. This indicates that RIF1 is involved in RT regulation, complemented by Repli-seq analysis showing both early-to-late and late-to-early transitions (Cornacchia et al., 2012). Similar results were obtained upon loss of human RIF1 (Yamazaki et al., 2012). Work in fission yeast further supported this conclusion with inappropriate activation of dormant origins and reduced firing of normally efficient origins in RIF1 deletion strains (Hayano et al., 2012). Notably, RIF1 deletion in mouse cells also resulted in impairment of G1/S transition and organization of chromocenter, which became less compact, but did not change their PTM enrichment (Cornacchia et al., 2012). This points to the importance of the RT programme not only for normal cell cycle progression, but also chromatin organization.

In mESCs, RIF1 could be immuno-precipitated with H3K9me3 writers and readers, and its knock-down resulted in reduced H3K9me3 at heterochromatin, although the authors did not assess RT (Dan et al., 2014). Conversely, Foti et al. (2016) show that RIF1 ensures the late replication of non-lamina-associated heterochromatin and prevents its interactions with other genomic regions in 3D space independently of histone PTMs. More recently, rapid depletion of RIF1 in hESCs and HCT-116 cells combined with single-cell (sc)Repli-seq showed that RIF1 is required to maintain the global RT programme (Klein et al., 2021). In its absence, rather than discrete shifts in timing, there is a general loss of RT pattern in hESCs, whereas H3K9me3 domains retain late RT in HCT-116, indicating that additional mechanisms ensure late replication of heterochromatin. RT disruption in this context is associated with both histone PTM and genome organization changes in a replication-dependent fashion, suggesting that RT can be important for the maintenance of the epigenetic state.

In addition to RT regulation, another line of research focused on the role of RIF1 in DNA repair (Mattarocci et al., 2016). RIF1 is important for replication fork protection and re-start (Mukherjee et al., 2019) by preventing nascent DNA degradation (Garzón et al., 2019). RIF1 also inhibits resection of double-strand breaks (DSBs), promoting repair by non-homologous end-joining (NHEJ, Isobe et al., 2021). Interestingly, this role requires RIF1 interaction with ASF1a, although the requirement for its chaperone activity is unclear (Feng et al., 2022; Tang et al., 2022). Feng et al. (2022) further show that RIF1-ASF1 handles H3K9me1-H4 dimers and promotes heterochromatin formation and chromatin condensation at DSBs or at discrete loci if exogenously recruited there. This data suggests that RIF1 may exert its function at heterochromatin beyond preventing early firing of origins and that some effects of its depletion may relate to the disrupted interactions with its other partners.

How does RIF1 perform these diverse functions? In fission yeast, RIF1 associates with late-replicating chromatin at M/G1 and prevents firing in early S phase by inhibiting Cdc45 incorporation and pre-IC formation (Hayano et al., 2012). Work in human cells later revealed that RIF can interact with protein phosphatase 1 (PP1), which allows to counteract the modification of both cell cycle and DNA repair-associated kinases. In the context of repair, the PP1 interaction mediates the role of RIF1 in fork protection (Mukherjee et al., 2019, Garzón et al., 2019) and prevention of DSB resection (Isobe et al., 2021). Furthermore, the RIF1-PP1 complex plays a dual role in replication control (Hiraga et al., 2017). In S phase, RIF1-PP1 reduce MCM4 phosphorylation, limiting origin firing (also shown by Alver et al., 2017), whereas in G1, the complex acts on ORC1 and prevents its untimely degradation, promoting origin licensing (Hiraga et al., 2017). Comparing the spatio-temporal organization of ORC1 at late M/G1 to RIF1 and assaying if it is affected in RIF1-depleted cells may give interesting hints as to how RIF1 can control RT. Disrupting the domain of RIF1 responsible for its association with ASF1a may also be of interest, as ASF1a predominantly handles H3.3-H4, which Gatto et al. (2022) have shown to play a role in early IZ definition. This may also be interesting, as Strobino et al. (2020) have

demonstrated that H3.3 is required for efficient fork re-start in *C. elegans* grown at restrictive temperatures.

2.3.2. Organization of RT

The non-random distribution of origins along the genome and their characteristic firing efficiency can be influenced by transcription, chromatin state and other DNA-binding factors, resulting in a cell type-specific spatial and temporal pattern of DNA replication. As described above, efficient early-firing initiation zones are enriched in active chromatin, providing an explanation for the well-established general correlation between early/late RT with active/inactive chromatin, respectively (Fujita, 1965, Zink, 2006, Vousaz and Gilbert, 2021). What does this mean for the spatial organization or RT?

Analysis of stretched DNA fibres isolated from cells following a short pulse of radio-labelled thymidine (Huberman and Riggs, 1968) or an analogue (Jackson and Pombo, 1998) reveals 75kb-150kb regions of newly synthesized DNA replicated from a single location. There were termed replicons (Berezney et al., 2000; Jackson and Pombo, 1998) and may correspond to the more recently defined IZs (described above, Figure 23, Vousaz and Gilbert, 2021). Often, several (2-10) replicons initiate synchronously, clustered (Edenberg and Huberman, 1975; Hand, 1978) in replication domains (RDs) of 400kb-1Mb in size, which have a good correspondence to chromosome bands (White et al., 2004; Zink, 2006). About half of RDs replicate at the same time in S across different cell types, whereas the other half change RT in at least one (Marchal et al., 2019). RT shifts are typically linked to transcriptional reprogramming (Hiratani et al., 2008; Ryba et al., 2010), suggesting they can be a functional unit of RT control (Dileep et al., 2015a; Rivera-Mulia et al., 2015).

Visualizing *de novo* synthesized DNA in intact nuclei demonstrates that RDs are organized in replication foci (Jackson and Pombo, 1998; Nakamura et al., 1986). During S phase, these foci exhibit characteristic patterns: in early S, they are spread throughout the nucleoplasm and were estimated to be up to ~1000 in number (Jackson and Pombo, 1998; Ma et al., 1998), whereas in mid/late S they organize in larger structures around the nuclear periphery and nucleolus (Berezney et al., 2000; Nakayasu and Berezney, 1989). RDs have recently been characterised by super-resolution microscopy, which provided estimates for their radius (150nm) and number of replicons (4), corresponding to ~70kb labelled DNA (Xiang et al., 2018). Notably, an early study in *X. laevis* elucidated that replicon length correlates with the size of nuclear matrix-anchored DNA loops that remain after high salt and detergent extraction to remove nucleoplasmic proteins and histones from DNA (Buongiorno-Nardelli et al., 1982). This was confirmed in the same system (Lemaitre et al., 2005) and in Chinese hamster ovary cells (Courbet et al., 2008), suggesting that chromatin folding was related to RT organization. This was also supported by data in *D. melanogaster* (MacAlpine et al., 2010) and HeLa cells (Guillou et al., 2010) showing that cohesin subunits interact with pre-RC components and are enriched at origins of replication.

More recently, the connection between 3D genome organization and RT has been investigated by integrating analysis of Hi-C and Repli-seq (Pope et al., 2014; Ryba et al., 2010, Figure 24) with increasing temporal resolution (Zhao et al., 2020) or at the single cell level (Dileep and Gilbert, 2018; Miura et al., 2019). Early work demonstrated a strong correlation between A/B compartments and early/late RT across cell types (Ryba et al., 2010, Dileep et al., 2019, Miura et al., 2019), indicating chromatin organization and RT experience coordinated changes during differentiation. On the kb scale, RDs correspond well to TADs identified by Hi-C, although there is not 1:1 correspondence between their borders (Dang et al., 2023; Pope et al., 2014). On the other hand, Petryk et al. (2016) showed that TAD borders are enriched in early origins of replication, in agreement with the previously observed cohesin enrichment there (Guillou et al., 2010; MacAlpine et al., 2010). Furthermore, TAD emergence upon G1 entry takes place in the same timeframe as the set-up of the RT programme (Dileep et al.,

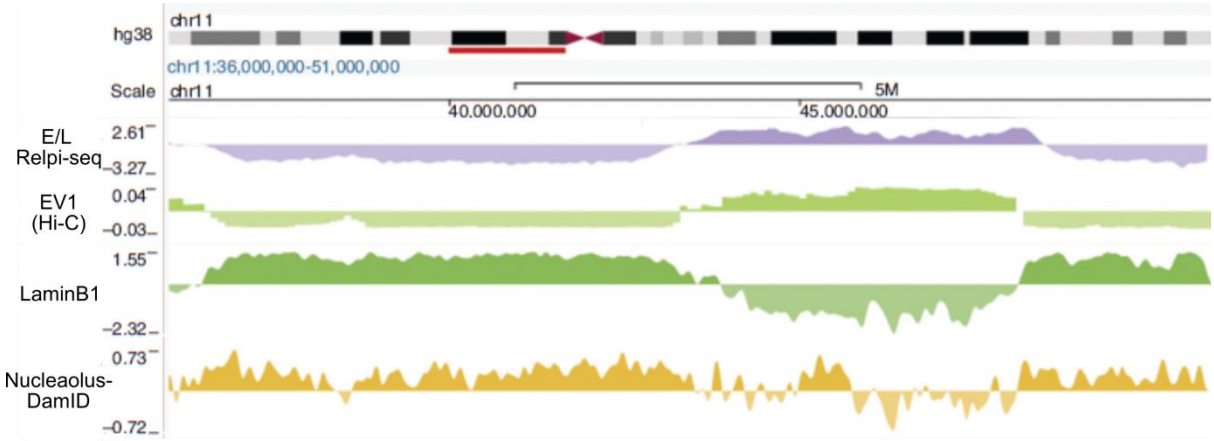

Figure 24. Organisation of RT and correspondence to 3D genome organization features
Replication timing (RT, purple track) is highly correlated with A/B compartments identified from Hi-C (EV1 track, light green). Furthermore, late-replicating regions are enriched in lamina (dark green LaminB1) and nucleolus (DamID, yellow) interactions. Tracks show a representative 15Mb region from K562 cells (adapted from Vouzas and Gilbert, 2021).

2015a), although it is not clear if the two processes are related. Indeed, both TADs and compartments persist in G2, whereas RT control information is absent (Dileep et al., 2015a; Lu et al., 2010), indicating genome structure alone is not sufficient to instruct RT.

From a developmental perspective, after fertilization in early *D. melanogaster* and *X. laevis* embryos most origins fire with high efficiency, enabling extremely rapid cell divisions (4min in *D. melanogaster*, Blumenthal et al., 1974, 30min in *X. laevis*, Callan, 1974; Graham and Morgan, 1966). After zygotic genome activation (ZGA), when embryonic transcription begins, replication initiation re-localises to intergenic regions as spatiotemporal order of firing is established (Hyrien et al., 1995). ZGA is also the time in *D. melanogaster* embryos when genome organization (on the scale of compartments and TADs) is established (Hug et al., 2017, Zenk et al., 2021). Notably, this is independent of transcription, although the TF Zelda is required for the emergence of TAD borders (Hug et al., 2017). In mammals, S phase length in early embryos is similar to differentiated cells (Howlett and Bolton, 1985), and spatiotemporal

RT patterns are observed in 1 cell stage mouse embryos (Ferreira and Carmo-Fonseca, 1997). Thus, the RT programme may already be established pre-ZGA, as is the case in *C. elegans* (Pourkarimi et al., 2016), when compartments and TADs are weakly detectable (Du et al., 2017; Flyamer et al., 2017; Ke et al., 2017). In early mouse (Miura et al., 2019) and human (Dileep et al., 2019) ESC differentiation, B-to-A compartment switches are either followed or preceded by late-to-early RT changes, respectively. Thus, developmental studies indicate that the RT programme and genome architecture are not systematically linked.

This is also confirmed by depletion of CTCF (Sima et al., 2019) and cohesin (Cremer et al., 2020), which disrupt TAD organization without affecting RT. However, ERCE (**The efficient bird gets the worm**) deletion that result in early-to-late shifts of discrete RDs also result in A-to-B compartment switching and disrupt local TAD organization, indicating RT can impact genome organization (Sima et al., 2019). Indeed, RIF1 depletion in mouse (Foti et al., 2016) cells lead to increased inter-domain interactions, whereas in human (Klein et al., 2021) cells, it decreased A-A compartment contacts and was accompanied by PTM re-distribution and compartment switching. Notably, late-replicating regions located at the lamina in mESCs (Foti et al., 2016) or part of large H3K9me3-marked domains in differentiated human cells (Klein et al., 2021) were resistant to RT dysregulation, indicating that their 3D organization may contribute to their replication regulation. Indeed, perturbing B compartments by depleting DNMT1 and DNMT3b in HCT-116 (**We interrupt your programme with a burning question: How is this happening?**) resulted in coordinated A-to-B switching, reduced H3K9me3, increased gene expression and advanced RT as reported by Du et al. (2021), although RT seemed unaffected in Spracklin et al. (2022).

Collectively, these data indicate that the RT programme and genome architecture do not always behave concordantly. Further work is needed to understand what underlies the connection between the two, to disentangle the effects of transcription and chromatin state, and investigate their respective functional importance.

2.3.3. Impact of replication timing on other processes

Does this spatial and temporal segregation of replication impact other DNA-related processes? Data from scRepli-seq has suggested that despite the stochastic nature of origin firing, the RT programme is highly similar on a cell-to-cell basis, indicating possible functional importance (Dileep and Gilbert, 2018; Takahashi et al., 2019).

First, the fact that a large proportion of origins are dormant but can be activated upon replication stress is key mechanism to maintain genome integrity (Blumenfeld et al., 2017; Ge et al., 2007; Ibarra et al., 2008; Lengronne and Schwob, 2002; Shreeram et al., 2002; Tanaka and Diffley, 2002; Woodward et al., 2006). Indeed, one characteristic of sites of frequent chromosome breakage under replication stress, termed common fragile sites (CFSs) is scarcity of origins (Ozeri-Galai et al., 2014). Hence, CFSs are

typically late-replicating and it has been hypothesized that they cannot finish replicating prior to M (Beau et al., 1998). However, a new class of early-replicating CFSs overlapping long expressed genes was identified (Helmrich et al., 2011), where instability is thought to be a consequence of transcription-replication collisions (Barlow et al., 2013). From this perspective, the participation of RIF1 in both origin licensing/firing control and fork stabilization is an interesting coincidence, as the connection between its two roles is unclear (**RIF1: Show them who's boss?**, Alavi et al., 2021).

Differential expression of DNA repair enzymes in S phase, for example downregulation of mismatch repair (MMR) proteins in mid-S, leads to a mutational signature of single base substitutions in late-replicating regions (Supek and Lehner, 2015). Similarly, shifting from DSBR by homologous recombination (HR) in early S to NHEJ in late S results in distinct CNV profiles (Koren et al., 2012). Larger scale re-arrangements like amplifications and translocations tend to occur in early-replicating regions in human cancers, although this may vary depending on cell type and organism (Blumenfeld et al., 2017). Finally, shared RT of loci found on different chromosomes can increase the probability of their translocation and promote tumorigenesis in B cells (Peycheva et al., 2021).

Finally, having spatially and temporally separated replication may facilitate the maintenance of epigenome integrity. As evicted histones are recycled locally, replicating different types of chromatin in distinct foci and S phase stages could limit mixing of parental histones. This would ensure they would be re-incorporated in a similar type of environment, even if they diffuse further from their replication focus in conditions of replication stress (Clément et al., 2018). Finally, Nakatani et al. (2022) showed that slowing down fork speed in mESCs results in increased number of origins that fire and promotes the emergence of totipotent 2 cell embryo-like cells (2CLCs). This was accompanied discrete RT changes, only ~30% of which corresponded to induction of 2CLC-specific transcripts. At one of those, the authors detect increase in H3.3 enrichment, which they interpret because of its earlier RT and increased expression (Nakatani et al., 2022). However, it is also possible that reduced replication rate and increased origin firing affect chromatin maturation after fork passage. This may allow more time for H3.1-H3.3 exchange and establish new boundaries between the variants, which could create an epigenetic memory of initiation changes and/or facilitate expression of regions shifting to earlier RT.

Question

The dynamic organization of chromatin in the nucleus at all scales contributes to the regulation of genome function throughout the cell cycle and during cell fate transitions. To date, disentangling how the multiple scales of chromatin organization affect each other, from packaging into nucleosomes up to the formation of higher-order structures in nuclear space remains a major challenge. Major processes acting on DNA, including transcriptional activation, repression or recombination, repair and replication are in fact exerted on chromatin. Thus, in each case changes in nucleosome composition, histone post-translational modifications (PTMs) and nuclear positioning of chromatin should be considered as they occur concomitantly with the DNA transaction. Furthermore, the pre-existing chromatin state may also influence how the transaction can be exerted.

Thus, in my PhD I aimed at understanding the functional interplay between nucleosome composition, higher-order genome architecture and regulation of chromatin-templated processes with a focus on replication. The choice was motivated by the tight regulation that operates on replication initiation in mammals to ensure a complete genome duplication, especially because no sequence specific sites have been identified to date. Furthermore, recent work from the team revealed the critical importance of the balance between H3 variants in defining early replication initiation zones independently of transcription.

During the course of my PhD, I have tried to address these fundamental questions:

How are histone H3 variants organized in 3D genome space?

How are H3.1 and H3.3 distributed with respect to features of 3D genome architecture across scales?

Do H3 variants become spatially repartitioned if their deposition is impaired?

Is targeted H3.3 deposition important for 3D chromatin architecture?

Is 3D genome organization affected when H3.3 is redistributed along the genome?

Is H3.3 reorganization associated with a change of post-translational modifications patterns?

Is the role of H3 variant balance in defining early replication initiation zones related to an impact on their spatial arrangement?

How are early replication initiation zones organized in space?

Is the spatial organization of initiation zones affected when H3 variant balance is disrupted, impairing their early firing?

Does the balance of H3 variants promote early firing at initiation zones by modulating their 3D arrangement?

Results

During my PhD, I aimed to understand the interplay between the H3 variant composition of chromatin, its multi-scale higher-order organization in space, and their link to the control of early replication initiation. I provide a summary of the general approach and methodology I used below. My results are included in the form of a manuscript ready for submission, titled 'HIRA-mediated H3.3 deposition impact on 3D genome organization and early replication'. Furthermore, I investigated this relationship at additional scales, and in other organisms during differentiation, and I present the outcome of this analysis in the section titled 'Additional results'.

General approaches and methodology

How to map histone H3 variant distribution?

To characterise the occupancy of H3 variants along the genome, I needed an approach that would allow me (i) to distinguish between the highly similar H3.1 and H3.3 and (ii) to profile their enrichment prior to S phase, when their distribution is most clearly reflected. This was particularly important for H3.1, whose enrichment pattern in asynchronous cells would arise as a mix of its steady state occupancy and new deposition coupled to fork progression (Tagami et al., 2004), which can be highly dissimilar (Gatto et al., 2022). Using HeLa cells as a model, I exploited a combination of G1/S synchronization with use of the SNAP-tag system (Jansen et al., 2007; Keppler et al., 2003), which has been well-established in the lab to follow H3.1 and H3.3 by imaging (Clément et al., 2018; Ray-Gallet et al., 2011; Torné et al., 2020) and more recently by sequencing methods (Gatto et al., 2022, Forest et al., in prep). The SNAP is a 20KDa self-labelling enzyme, which binds covalently and irreversibly to its benzylguanine substrate. Fused to a protein of interest, it allows labelling with fluorescently-tagged moieties and visualization by microscopy (Torné et al., 2018), as well as SNAP capture by magnetic beads followed by sequencing of associated DNA (SNAP-seq, Gatto et al., 2022, Forest et al., in prep). Combined with cell synchronization at the G1/S boundary and quench-chase-pulse labelling strategies (Torné et al., 2018), SNAP-seq presents a powerful approach to map the genomic distribution of total and *de novo* synthesized H3 variants during S phase progression, which the lab recently published (Gatto et al., 2022, Figure 25).

Thus, I could integrate previously generated H3 variant-specific information (Gatto et al., 2022) with publicly available Hi-C data (Wutz et al., 2017) to show that H3.1 and H3.3 exhibit distinct enrichment patterns at 3D genome organization features on the Mb (compartments) and sub-Mb (TAD borders) scale in WT cells. I further combined this with analysis of H3 variant profiled from cells where the H3.3-specific chaperone HIRA was knocked out (KO). This revealed a re-distribution of the variants at 3D organization features at both scales. Gatto et al. (2022) had previously established the importance of HIRA for early initiation zone (IZ) definition, while 3D organization, chromatin state and replication have also been linked (Klein et al., 2021; Vouzas and Gilbert, 2021). I thus asked if disrupting H3.3

targeting in HIRA KO impacts genome architecture and if that was linked to the replication defect we observed.

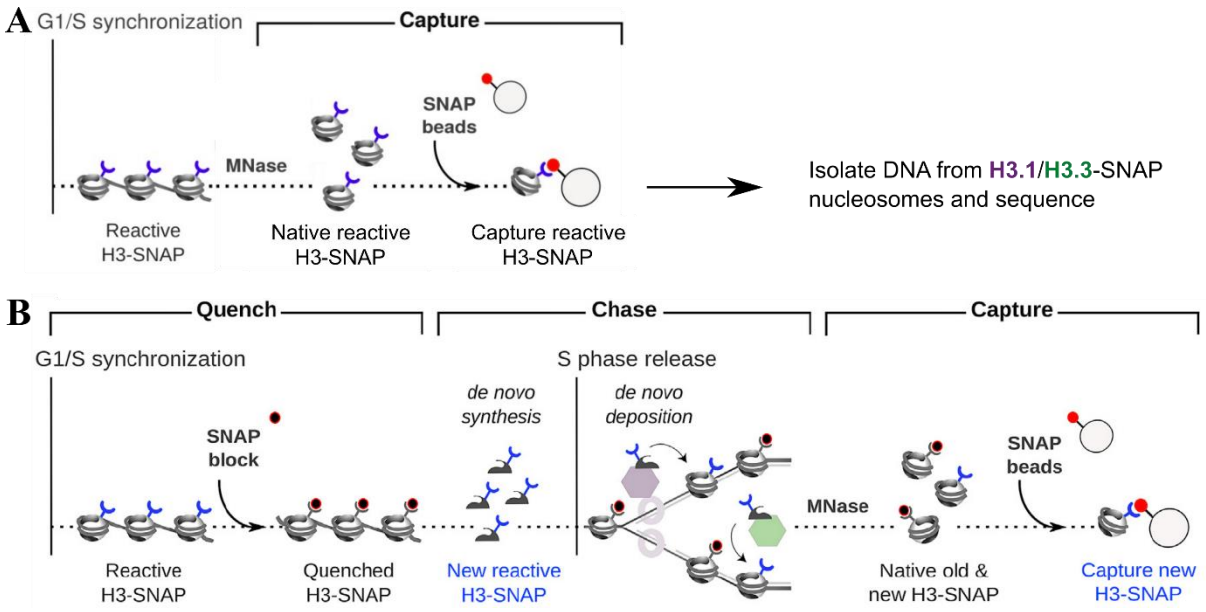

Figure 25. SNAP-seq strategy

HeLa cells constitutively expressing H3.1/H3.3-SNAP are synchronised at the G1/S boundary by a double thymidine block **A.** Capture of total H3-SNAP following MNase digestion of native chromatin by SNAP capture beads. **B.** Quench-chase-pulse strategy to selectively label new H3.1/H3.3. Quench: all reactive H3-SNAP (old histones) is blocked (2h). Chase: SNAP block is removed for 0.5h to allow synthesis of reactive H3-SNAP prior to release in S phase (2h), when new histones are deposited on chromatin. Capture: Native chromatin is MNase-digested to mononucleosomes before pull-down by SNAP capture beads (adapted from Gatto et al, 2022).

Is targeted H3.3 deposition important for 3D chromatin architecture globally and at early IZs?

To understand the impact of HIRA KO on chromatin folding, I performed Hi-C (Figure 11, right) in HIRA WT and KO cells. This allowed me to analyse the impact of HIRA loss both on genome architecture globally and to focus specifically on the organization of HIRA-dependent early IZs. On the Mb scale, I could observe an effect on compartments, whose segregation has been linked to histone marks (Hildebrand and Dekker, 2020). Thus, I also optimised a native ChIP-seq protocol in the lab to map a selection of active (H3K4me1, H3K4me3, H3K27ac) and inactive (H3K9me3, H3K27me3) PTMs in order to further disentangle the effects of H3.3 redistribution on epigenetic states. To deepen the genome-wide Hi-C analysis, I collaborated with Leonid Mirny at MIT, Harvard, while he was at sabbatical at Institut Curie. To focus on the arrangement of early IZs, I collaborated with Marc Marti-Renom at CNAG-CRG, Barcelona, who recently developed an approach to assess the spatial correlation of chromatin-associated proteins called METALoci (Mota-Gómez et al., 2022).

Is the role of H3 variant balance in defining early replication initiation zones related to an impact on their spatial arrangement?

To disentangle whether the importance of HIRA for early replication initiation relates to nucleosome composition, genome folding or both, I performed rescue experiments. Re-supplying HIRA for 48 hours in asynchronous or G1/S-arrested cells, coupled with SNAP-seq, EdU-seq after 2h release in S phase, and Hi-C allowed me to simultaneously assess the impact on H3 variant distribution, early replication and chromatin architecture.

Manuscript

HIRA-mediated H3.3 deposition impact on 3D genome organization and early replication

Authors: T. Karagyozova[1], A. Gatto[1,2], A. Forest[1], J.-P. Quivy[1], M. Marti-Renom[3,4,5], L. Mirny[6] & G. Almouzni[1]

[1] Institut Curie, PSL University, Sorbonne Université, CNRS, Nuclear Dynamics, 75005 Paris, France

[2] Roche Sequencing Solutions, 4300 Hacienda Dr, Pleasanton, CA 94588, US

[3] CNAG-CRG, Centre for Genomic Regulation (CRG), Barcelona Institute of Science and 11 Technology (BIST), Baldiri i Reixac 4, 08028 Barcelona, Spain

[4] CRG, 21 BIST, Dr. Aiguader 88, 08003 Barcelona, Spain

[5] Universitat Pompeu Fabra (UPF), 08002 Barcelona, Spain

[6] Institute for Medical Engineering and Science, and Department of Physics, Massachusetts Institute of Technology, Cambridge, MA 02139, USA

Corresponding author: genevieve.almouzni@curie.fr

Abstract

In each cell, genome replication, chromatin states and 3D architecture are intimately related. Much progress has been made to determine where to initiate replication, where to place histones, how to fold chromatin. However, integrating all three aspects to understand their functional interrelationships remains a puzzle. Here, we aimed to follow simultaneously, early replication, H3 variant distribution and 3D genome organization while manipulating H3 deposition. For this, we combined KO and rescue experiments focusing on the histone chaperone HIRA recently linked to the definition of early-replication initiation zone. Our findings show first that at Mb scale, HIRA promotes, H3.3 incorporation in A compartment and stabilizes interactions within compartments independently of histone marks. Second, on the sub-Mb scale, we focused on early replication initiation zones (IZ) heavily affected upon HIRA KO. We found that A compartment identity was compromised for the disrupted non-transcribed early IZs in HIRA KO. However, rescue experiments with HIRA showed a recovery of early IZ without necessarily restoring A compartment identity. We thus propose that the nature of the variant at a local scale is dominant to control early initiation over the compartmentalization of the genome. We discuss the implication of a hierarchy between various scales in chromatin organization to impact cellular programs such as replication and transcription.

Introduction

The synthesis of new DNA starts at the origins of replication: estimated 30,000-50,000 sites in the mammalian genome, which are recognised by ORC1 and licensed by loading MCM2-7 helicase in G1 before only a small subset are fired stochastically in S phase (Méchali, 2010). While in *S. cerevisiae* initiation sites are sequence-specific (Brewer and Fangman, 1987; Huberman et al., 1987), how origins are defined and selected to fire in metazoans is much less clear. This is partially due to the technical challenges to map them, biased predominantly towards efficient, early-firing origins (Hu and Stillman, 2023). Mammalian origins, usually clustered in initiation zones (IZs) of 20-40kb (Cadoret et al., 2008; Cayrou et al., 2011), do not fire at the same time: IZ containing higher efficiency origins tend to fire early, whereas less efficient IZs are activated later in S phase (Rhind et al., 2010). In mammals, origin definition combines properties of DNA sequences (Cayrou et al., 2011; Dellino et al., 2013) and epigenetic features (Cadoret et al., 2008; MacAlpine et al., 2010; Miotto et al., 2016). Additionally, firing efficiency correlates with transcription (Dellino et al., 2013), active histone PTMs (Cayrou et al., 2015), chromatin accessibility (Sugimoto et al., 2018) and H2A.Z enrichment (Long et al., 2020). Early origins also show a particular organisation in space as measured by Hi-C: they are enriched at the borders of insulated, topologically-associating domains (TADs) (Akerman et al., 2020; Giles et al., 2022; Petryk et al., 2016), and are often close to each other in space (Jodkowska et al., 2022).

The spatiotemporal pattern or origin activation in S phase, termed the replication timing (RT) programme, is cell type-specific and strongly correlates with chromatin state and its three-dimensional (3D) organization (Vouzas and Gilbert, 2021). Typically, early-replicating regions are decorated by active histone marks and correspond to compartment A identified by Hi-C, while late-replicating domains are enriched in heterochromatic PTMs and largely coincide with B compartments (Hansen et al., 2010; Pope et al., 2014; Rivera-Mulia et al., 2015). Given these extensive correlations and the poor understanding of what governs RT (Vouzas and Gilbert, 2021) and genome compartmentalization (Hildebrand and Dekker, 2020), it has been a major challenge to understand the functional connections between RT control, epigenetic state, and 3D chromatin organization. However, emerging evidence indicates that they may be separable in particular contexts, although their functional interdependence remains a puzzle. Indeed, during differentiation of human embryonic stem cells (ECSs) late-to-early RT switches take place without B-to-A compartment changes, although the PTM enrichment at these regions is likely modified (Dileep et al., 2019). Conversely, in mouse ESC differentiation B-to-A switches precede both late-to-early RT shifts and gene activation (Miura et al., 2019). Using HCT-116 cells with a double knock-out (DKO) of maintenance (DNMT1) and *de novo* (DNMT3B) DNA methylases as a model system, (Du et al., 2021) demonstrate that DNA hypomethylation leads to coordinated shifts in RT and compartment identity in a small proportion of the genome (~3% changes RT). However, these regions also experienced PTM re-distribution and gene expression changes, making it difficult to disentangle cause and consequence. In contrast in the same DKO HCT-116 cells,

(Spracklin et al., 2022) showed that changes of interactions between compartment B sub-types are not accompanied by RT switches, although in this case the regions investigated remain in compartment B overall. Thus, the role of compartmentalisation in RT control remains to be further explored. Conversely, disrupting 3D organization on the sub-Mb scale by CTCF (Sima et al., 2019) or cohesin (Cremer et al., 2020) depletion did not impact RT, indicating that TADs are not important for its regulation.

Alternatively, experimentally enforcing changes in RT can reveal if it is important to maintain chromatin state and/or spatial organization. A specific class of *cis*-acting sequences (3-40kb in size), likely corresponding to super-enhancers but distinct from IZs, were found to confer early replication of a 5Mb domain in mouse ESCs (Sima et al., 2019). These regions, termed early replication *cis* elements (ERCEs), also promoted transcriptional activity, A compartment identity and TAD border insulation of the domain (Sima et al., 2019). In this context however, it is difficult to disentangle whether the changes observed on chromatin organisation are a consequence of the RT switch, potential changes in histone marks, which were not evaluated, or the absence of DNA-binding proteins that would normally occupy these ERCEs. In a more global approach, several studies have depleted RIF1, considered to be a key regulator of the RT program, in mouse (Cornacchia et al., 2012; Foti et al., 2016) and human cells (Klein et al., 2021; Yamazaki et al., 2012). This resulted in changes in inter-TAD interactions in G1, followed by RT shifts in S phase in mouse embryonic fibroblasts without impacting histone PTMs (Foti et al., 2016). In human ES or cancer cells, RIF1 loss induced RT disruption, accompanied by compartment switches, weaker A compartment interactions and histone mark re-distribution (Klein et al., 2021). Notably, the impact on both chromatin organization and PTMs in this system required passage through S phase, indicating proper RT may be important for maintenance of chromatin state and genome folding. However, the results from these studies also emphasize the potential of species- or cell type-specificity of the functional relationships between genome folding, chromatin state and RT.

Considering histone variants, we established a first link with RT showing that the enrichment pattern of the histone variants H3.3 and H3.1 followed early versus late RT respectively (Clément et al., 2018). The replicative H3.1 variant, produced at high levels at S phase entry, is deposited in a DNA-synthesis-coupled manner (DSC) mediated by the CAF-1 complex (Tagami et al., 2004). This mechanism ensures deposition over the entire genome (Deaton et al., 2016; Gatto et al., 2022; Goldberg et al., 2010) in S phase. In contrast, the replacement variant H3.3 is incorporated in a DNA-synthesis-independent (DSI) manner throughout the cell cycle (Drane et al., 2010; Tagami et al., 2004). The first identified chaperone involved in this DSI pathway is the HIRA complex (Tagami et al., 2004). Enrichment of H3.3 mapped to active regions (Mito et al., 2005), regulatory elements (Goldberg et al., 2010; Jin et al., 2009) and sites of high turnover (Deaton et al., 2016) depends on HIRA (Goldberg et al., 2010; Ray-Gallet et al., 2011). At other sites, H3.3 can be incorporated via gap-filling (Ray-Gallet et al., 2011) by HIRA. Finally, HIRA proved important for the establishment of bivalent domains at developmental gene

promoters in mouse embryonic stem cells (Banaszynski et al., 2013). In addition, H3.3 can accumulate at telomeres, pericentromeric and repetitive regions, but in this case relying on the activity of ATRX/DAXX (Elsässer et al., 2015; Goldberg et al., 2010).

However, only recently development of the the SNAP-tag technology for the mapping of the *de novo* incorporation of both H3.1 and H3.3 along the genome in S phase allowed to follow their respective deposition during replication (Gatto et al., 2022). These data showed that in S phase, new H3.3 deposition occurred systematically at pre-existing H3.3-enriched sites identified in early G1/S, preserving their genomic distribution. In contrast, new H3.1 deposition followed the replication fork movement, changing as replication proceeds. This dual deposition mechanism resulted in the establishment of H3.3/H3.1 boundaries, corresponding to locations of early replication IZs. Notably, HIRA knock-out (KO) cells disrupted not only these boundaries defined by the variants' distribution but also the corresponding replication initiation zones (Gatto et al., 2022). The next major issue was thus to understand which functional relationships could link H3.3 deposition and early replication. Given the links between RT and high order chromatin organization, we thus aimed to explore in combination all three aspects: H3.3 deposition, early replication, and higher-order chromatin organization. For this, we combined KO and rescue experiments focusing on the histone chaperone HIRA recently linked to the definition of early-replication initiation zones.

We show first that on the Mb scale, HIRA promotes H3.3 incorporation in A compartment, which is important for its interactions independently of PTMs. Second, on the sub-Mb scale, we focused on early replication IZ heavily affected upon HIRA KO. We found that HIRA KO compromised compartment identity of non-transcribed early IZs initially in A compartment as they lost capacity to initiate replication. However, rescue experiments with HIRA showed a recovery of early IZ without necessarily restoring their compartment A identity. We thus propose that the nature of the variant at a local scale is dominant to control early initiation over the compartmentalization of the genome.

Results

H3.3 redistributes in A/B compartments without changing histone PTMs in absence of HIRA

To examine how histone H3 variants distribute in wild-type (WT) cells with respect to 3D genome organization features, we first compared our unique H3.1 and H3.3 SNAP ChIP-seq data (Gatto et al., 2022) with publicly available Hi-C from HeLa cells (Wutz et al., 2017). This enabled us to call A and B compartments at 50kb resolution and to demonstrate that H3.3 was enriched in A and depleted in B compartment regions regardless of their size (Figure 1A, Supplementary Figure 1A). In contrast, H3.1 was weakly depleted in A and showed a clear enrichment only in large (>2Mb) B domains (Supplementary Figure 1B). These results proved consistent with our previous observations showing H3.3 enriched in early-replicating, active regions through targeted deposition by HIRA, whereas the genome-wide H3.1 pattern reflects its DSC incorporation by CAF-1 combined with eviction from active regions (Clément et al., 2018; Gatto et al., 2022). We then explored how the knock-out (KO) of the H3.3-specific chaperone HIRA affected the distribution patterns of each H3 variant. We observed a striking re-distribution of H3.3, which diminished throughout all A compartment domains, while increasing specifically in large B regions (>2Mb, Figure 1A, Supplementary Figure 1A). In contrast, H3.1 showed weaker changes and no significant decrease in large B regions (Supplementary Figure 1B). Given the substantial H3.3 re-distribution detected, we investigated if this resulted in a re-distribution of H3 PTMs. This was relevant to consider given the reports showing that phosphorylation of the H3.3-specific S31 residue can promote H3K27ac deposition by p300 (Armache et al., 2020; Martire et al., 2019) and inhibit H3K9me3 removal by KDM4A (Udugama et al., 2022). To investigate this, we performed native ChIP-seq for a panel of selected active (H3K4me3, promoter and H3K4me1, H3K27ac, enhancer) and inactive (H3K9me3, constitutive and H3K27me3, facultative heterochromatin) H3 marks. Our analysis did not reveal significant corresponding changes in their pattern in A/B compartments (Figure 1B, C, Supplementary Figure 1C). Thus, we can conclude that on the Mb scale, it is the chromatin environment of where a particular histone variant is placed, rather than the identity of the variant, which is dominant to impact post-translational modifications. We conclude that lack of HIRA leads to a general decrease of H3.3 in all A compartments while it increases in large B compartment without affecting enrichment in PTMs.

Figure 1

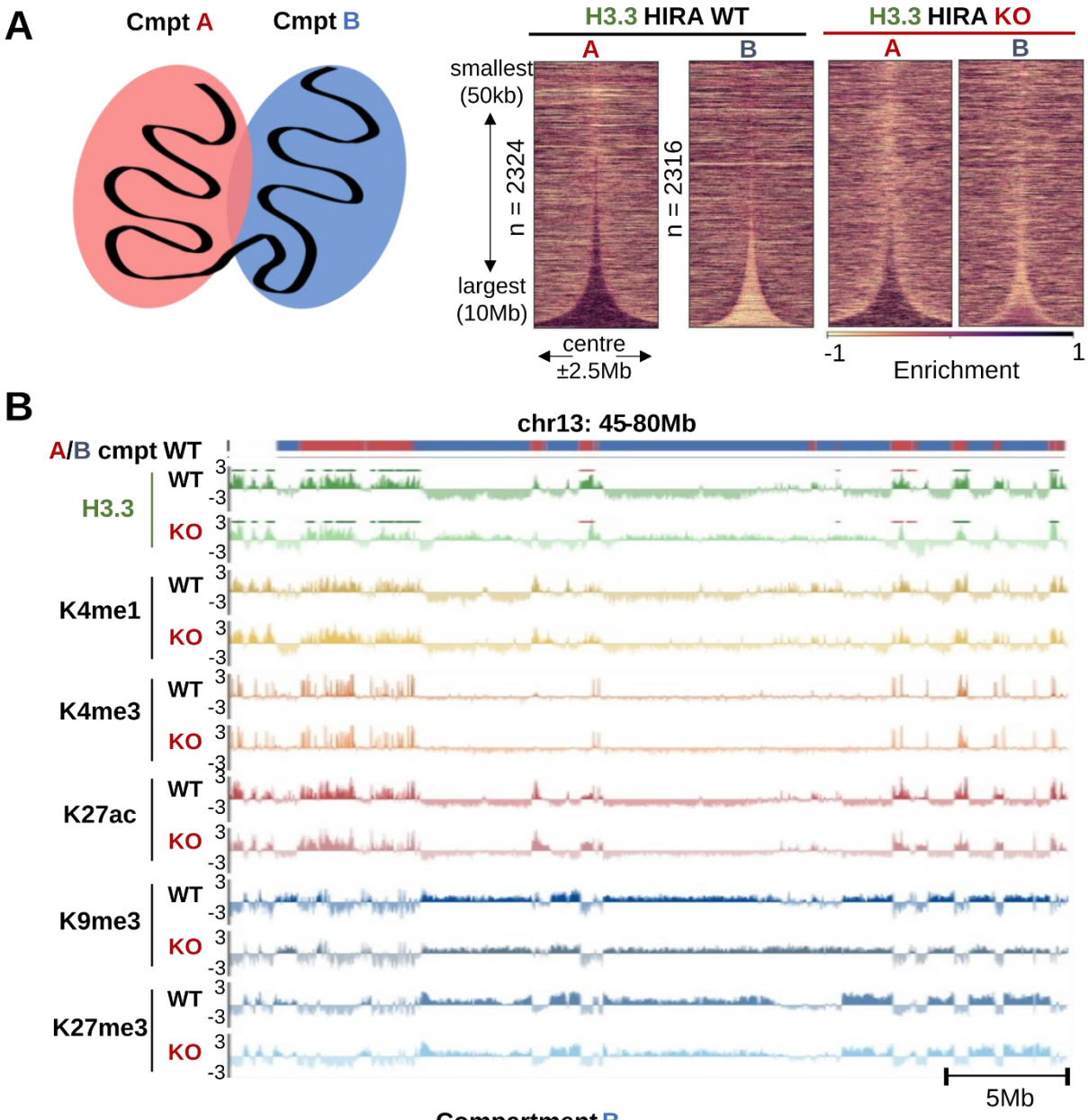
A
Cmpt A
Cmpt B
H3.3 HIRA WT
H3.3 HIRA KO
A
B
A
B
smallest (50kb)
largest (10Mb)
n = 2324
n = 2316
centre ±2.5Mb
-1
1
Enrichment
B
chr13: 45-80Mb
A/B cmpt WT
H3.3
K4me1
K4me3
K27ac
K9me3
K27me3
WT
KO
5Mb
C
Compartment B
K4me1
K4me3
K27ac
K9me3
K27me3
Enrichment
2.5
0
-2.5
***
ns
WT
KO
≤2Mb
>2Mb
Compartment size

Figure 1. Loss of HIRA leads to re-distribution of H3.3 from A to large B compartments without corresponding PTM changes

A. Left: Schematic of A and B compartments. Right: Total H3.3 enrichment (z-score of $\log_2$ IP/input) at 10kb bins from G1/S-arrested cells at A and B compartment domains called from WT HeLa cells (Wutz et al., 2017), sorted by size and centred at their middle ±2.5Mb.

B. Compartment assignment (based on WT HeLa Hi-C, Wutz et al., 2017) and enrichment of H3.3 (G1/S-arrest), active (H3K4me1, H3K4me3, H3K27ac) and repressive (H3K9me3, H3K27me3) PTMs from HIRA WT and KO cells (chr13: 45-80Mb). ChIP-seq (z-score of $\log_2$ IP/input ratio of cpm) is shown at 10kb bins smoothed over 3 non-zero bins.

C. Active (H3K4me1, H3K4me3, H3K27ac) and repressive (H3K9me3, H3K27me3) histone PTM enrichment from HIRA WT and KO cells quantified in A and B compartments per indicated domain sizes. Two-tailed Mann-Whitney U test adjusted for multiple testing by FDR (5% cut-off) was used to determine significance of differences between WT and KO. Significance was noted as: * ($p<=0.05$), ** ($p<=0.01$), *** ($p<=0.001$).

Minor identity switch for A and B compartments in the absence of HIRA but decreased interactions in compartment A domains

To understand if the genome-wide repartitioning of H3.3 in HIRA KO cells affected 3D genome organization, we performed Hi-C in HeLa HIRA WT and KO cells, using two independent lines bearing exogenous H3.1 or H3.3 fused with a SNAP-tag (established and characterized in Ray-Gallet et al. (2018). We first confirmed that Hi-C maps from the H3.1-SNAP and H3.3-SNAP cell lines had high similarity of genome-wide matrices (SCC > 0.98), cis/trans ratios and distribution of short- to long-range interactions (Supplementary Figure 2A-C). Calling A/B compartments at 50kb resolution showed very few compartment changes between the two cell lines (0.7% A-to-B and 0.7% B-to-A, Supplementary Figure 2D). In contrast, Hi-C maps from HIRA WT and KO cells had lower genome-wide correlation than the two cell lines (Supplementary Figure 2A). However, we did not detect obvious changes in the cis/trans ratio, decay of interactions with genomic distance or checkerboard pattern (Supplementary Figure 2B, C, E), indicating that the loss of HIRA did not affect genome architecture in a major way. Indeed, most of the genome (96.9%) remained in the same compartment in HIRA KO cells (Figure 2A). Nevertheless, we could detect a proportion of changes (2.1% A-to-B and 1% B-to-A) that exceeded the background levels of compartment switching between the two cell lines indicating some specific changes only in the cells with the KO of HIRA.

We then questioned if the strength of interactions within compartments could be affected, even if their identity remained largely unaffected. To evaluate this, we computed differential maps at 1Mb resolution (Figure 2B). We found reduced contact frequency between A-A and A-B in parallel with increased interactions between B-B regions in *cis*. Genome-wide analysis by saddle plots confirmed this observation (Figure 2C, D, Supplementary Figure 2F, G). Furthermore, we found that in B domains the increased contact frequency occurred between regions of different compartment strength. Thus, HIRA is important for maintaining (i) compartment identity in a small proportion of the genome (3.1 %), and (ii) strength in compartment interactions without major change in H3 PTMs.

Figure 2

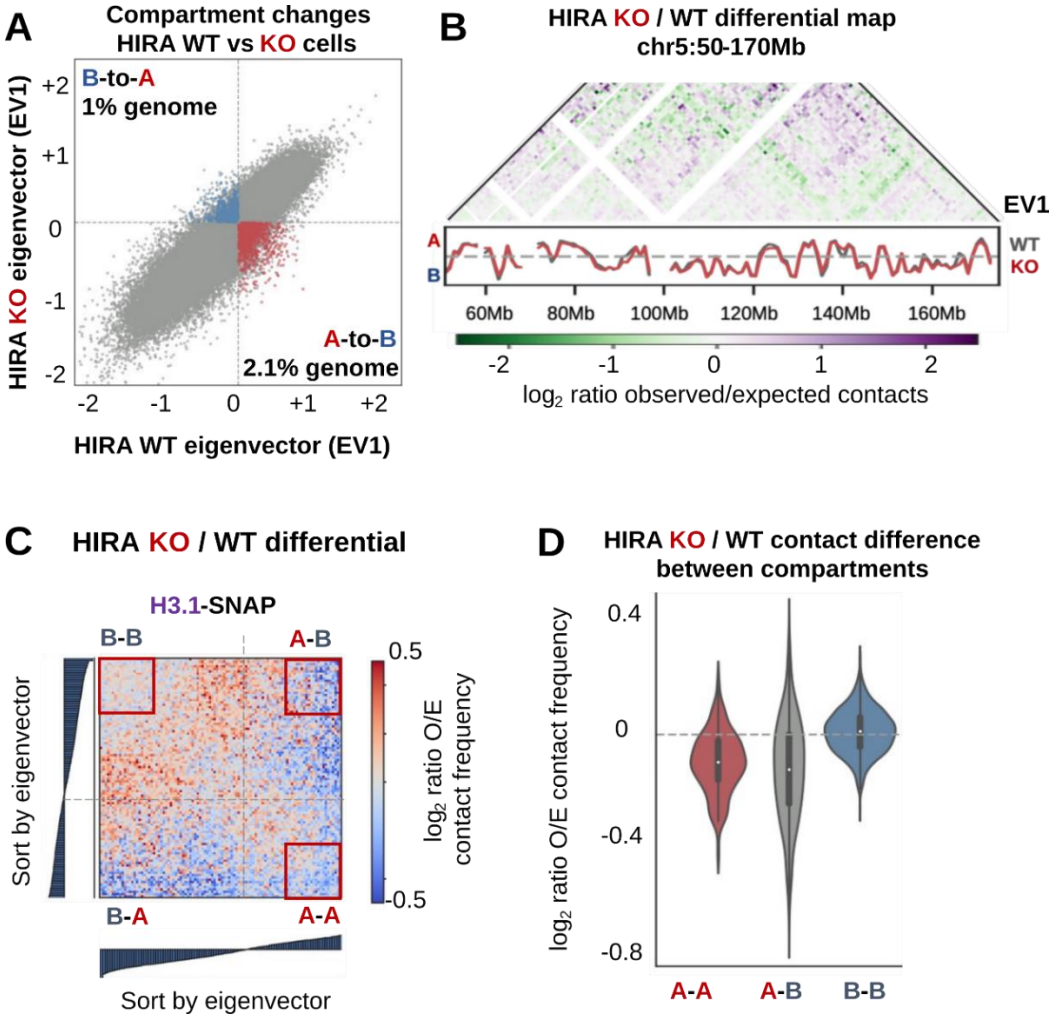

Figure 2. Compartment A domains show a decrease in interactions, but largely maintain their identity in the absence of HIRA

A. EV1 (1st eigenvector, indicating compartment) of 50kb-binned Hi-C matrices from H3.1-SNAP HIRA WT vs KO cells. Bins which change from A-to-B (lower right quadrant) or B-to-A (upper left quadrant) in the same direction in both cell lines are coloured (red and blue, respectively) and quantified.

B. Differential Hi-C observed/expected (O/E) map (log_2 ratio HIRA KO/WT) at 1Mb resolution of chromosome 5:50-170Mb from 0-50Mb away from the diagonal. Tracks below show EV1 (HIRA WT in grey, KO in red).

C. Differential saddle plot (log_2 ratio of O/E contacts) of H3.1-SNAP HIRA KO/WT at 50kb resolution based on EV1 percentiles. Red squares denote the regions used for B-B (top left), A-A (bottom right) and A-B (top right) quantifications (Fig. 1D).

D. Difference (log_2 HIRA KO/WT ratio) of O/E contact frequency between the sets of strongest A/B compartment bins (top/bottom quartile EV1 value, respectively) based on H3.1-SNAP differential saddle-plot (cf. Fig. 1C).

Switching from A-to-B compartment in absence of HIRA affects specifically early replication initiation zones associated with low transcriptional activity

We previously found that disrupting HIRA-mediated deposition leads to loss of precise H3.3 targeting to pre-existing enriched sites in G1, resulting in two scenarios. First, in broadly active regions, which are typically transcribed, we find a blurring of H3.3 pattern (blurred sites) along with a fuzziness of the corresponding early replication IZs at the boundaries of the site. Second, in inactive domains with no/low transcriptional activity, a complete disappearance of singular H3.3 peaks (buried sites, Figure 3A) occurred along with abrogation of replication initiation at the early IZs at their flanks (Gatto et al., 2022). Given the link between early replication and A compartment, we focused on these regions and investigated their compartment identity in HIRA WT cells and how it was affected upon HIRA KO (Figure 3B). Blurred sites corresponded predominantly to compartment A in WT cells and remained largely in A compartment in HIRA KO cells (83% A-to-A, Figure 3C), as expected given their active transcription and early replication in both conditions. As both the control of early replication initiation (Long et al., 2020; Van Rechem et al., 2021) and compartment switching (Klein et al., 2021) have been associated with histone PTMs, we also profiled the enrichment of the marks we tested (Supplementary Figure 3A). However, we did not observe any change in the enrichment pattern of the active (H3K4me1, H3K4me3, H3K27ac) or inactive (H3K9me3, H3K27me3) PTMs that would correspond to the fuzzier H3.3 enrichment at blurred sites in HIRA KO (Supplementary figure 3B).

In contrast, only a small proportion of buried sites were in A compartment and stayed there in HIRA KO despite losing both H3.3 enrichment and early replication initiation at their boundaries (20% A-to-A). In fact, buried sites were mainly in compartment B, where they remained (65% B-to-B) in HIRA KO. Notably, 14% buried sites switched from A-to-B in HIRA KO (Figure 3C, Supplementary Figure 4A). This fraction was significantly above what one would expect for a random switch (Supplementary Figure 4B). As was the case for blurred sites, we did not observe drastic changes in PTM distribution that would echo the loss of H3.3 enrichment at buried sites (Supplementary figure 3A). We then focused specifically on the A-to-B buried sites and quantified the changes in PTM enrichment from HIRA WT to KO cells (Supplementary figure 3B). This analysis demonstrated there was a significant decrease in H3K4me1, accompanied by an increase in both H3K9me3 and H327me3 at A-to-B buried sites upon HIRA KO, whereas A-to-A buried sites gained H3K27ac. However, the extent of these changes was much smaller than the ones for H3.3. From this, we can conclude that the role of HIRA for defining early replication initiation zones is not mediated by the PTMs on H3.3.

Given the association of compartment A with gene expression, we also investigated the relationship between compartment switching and transcription at blurred and buried sites (Figure 3D). Most blurred sites were actively transcribed, and the proportion which switched from A-to-B was not higher than expected by chance. Nevertheless, A-to-B blurred sites had lower RNA-seq signal than the ones that remained in A (A-to-A, Supplementary Figure 4C). Conversely, most buried sites had low or

undetectable levels of transcription, especially A-to-B compared to A-to-A sites (Supplementary Figure 4C). Importantly, there was no significant difference in expression for either type of sites (Supplementary Figure 4C) between HIRA WT and KO. Therefore, our data reveal that HIRA is essential to maintain A compartment identity for non-transcribed buried sites. Conversely, transcription in the absence of H3.3 deposition at A-to-A buried sites cannot solely ensure the maintenance of their compartment identity in HIRA KO cells.

Figure 3

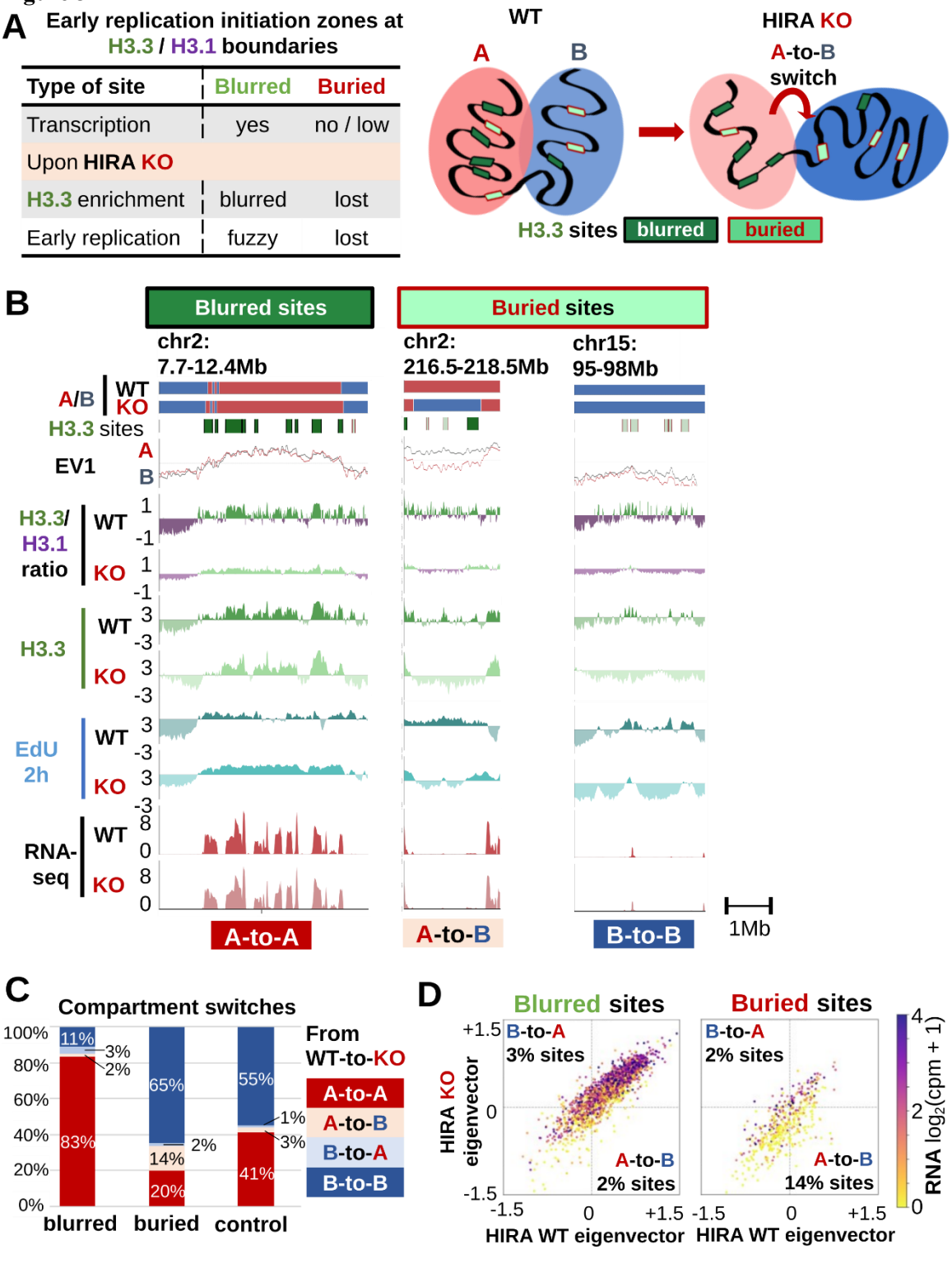

Figure 3. A-to-B compartment switching occurs specifically at early replication initiation zones associated with low transcriptional activity in absence of HIRA

A. Left: Classification of early replication initiation zones defined by H3/3/H3.1 boundaries as defined in Gatto et al., 2022. Right: Schematic representation of the change in compartment interactions in HIRA KO, reflecting the reduced A-A and A-B *cis* interactions.

B. Compartment assignment (HIRA WT, top and KO, bottom), H3.3 site positions (blurred in dark green and black, buried in light green and red), EV1 (WT in grey, KO in red), H3.3/H3.1 ratio, H3.3 enrichment, early-replicating DNA (EdU 2h) and transcription (RNA-seq) at representative regions. Shown are a set of blurred sites in A compartment that remain A in HIRA KO (A-to-A, left), and buried sites that switch from A-to-B (middle) or that were in B and remain there (B-to-B, right). H3.3/H3.1 ratio, H3.3 ChIP-seq and EdU-seq (z-score of $\log_2$ IP/input ratio of cpm) and RNA-seq ($\log_2$(cpm + 1)) are shown at 10kb bins smoothed over 3 non-zero bins.

C. Distribution of blurred and buried sites by A/B compartment shifts from HIRA WT to KO. A set of randomised sites was quantified as control.

D. Mean EV1 value at blurred (left) and buried (right) sites from HIRA WT vs KO cells. Colour represents transcriptional activity ($\log_2$(cpm + 1) RNA-seq) from HIRA WT G1/S-arrested cells. Proportion of sites which change from A-to-B (lower right quadrant) or B-to-A (upper left quadrant) compartment in the same direction in both cell lines are quantified.

Local re-partitioning of H3.3 at early IZ does not associate with changes in local folding

We next wished to visualize the local organisation of early initiation zones considering our classification in blurred and buried sites to determine if this level of organization was affected by the absence of HIRA. To achieve this, we used METALoci (Mota-Gómez et al., 2022), which generated 2D spatial layouts from 10kb-binned data of 2Mb-long segments of chromatin centred on the blurred and buried sites, coloured by their H3.3 enrichment (Figure 4A, left). We could, for each bin, compare its H3.3 enrichment with that of its neighbours in space (Figure 4A, right), and calculate the correlation between the two for the whole region. This analysis showed that in HIRA WT cells, H3.3 partitioned in space in the 2Mb segments flanking blurred and buried sites. In HIRA KO, H3.3 better segregated in space (Figure 4B), in agreement with the blurring or complete loss of individual H3.3 peaks at blurred and buried sites, respectively.

To compare the similarity of H3.3 enrichment at the sites and their surroundings in space from HIRA WT and KO cells, we calculated the distance between the mid-point of each site between HIRA WT and KO conditions from the scatterplots in Figure 4. Thus, buried sites underwent a larger change in their spatial H3.3 organisation compared to blurred sites, which behaved as random control (Figure 4C). Notably, this took place without significant changes to local structure of the 2Mb segments (Supplementary Figure 5A). As an alternative approach, we also computed pile-ups of distance-normalised matrices centred on the starts of the blurred and buried sites, which confirmed they did not change their local interaction pattern with flanking sequences (Supplementary Figure 5B). Indeed, calculating insulation score at 10kb resolution showed similar correlation between the two cell lines and between HIRA WT and KO cells (Supplementary Figure 5C). These results indicate that the local spatial re-partitioning of H3.3 upon the loss of HIRA does not impact genome organisation on the kb scale at the blurred and buried sites or genome-wide.

Figure 4

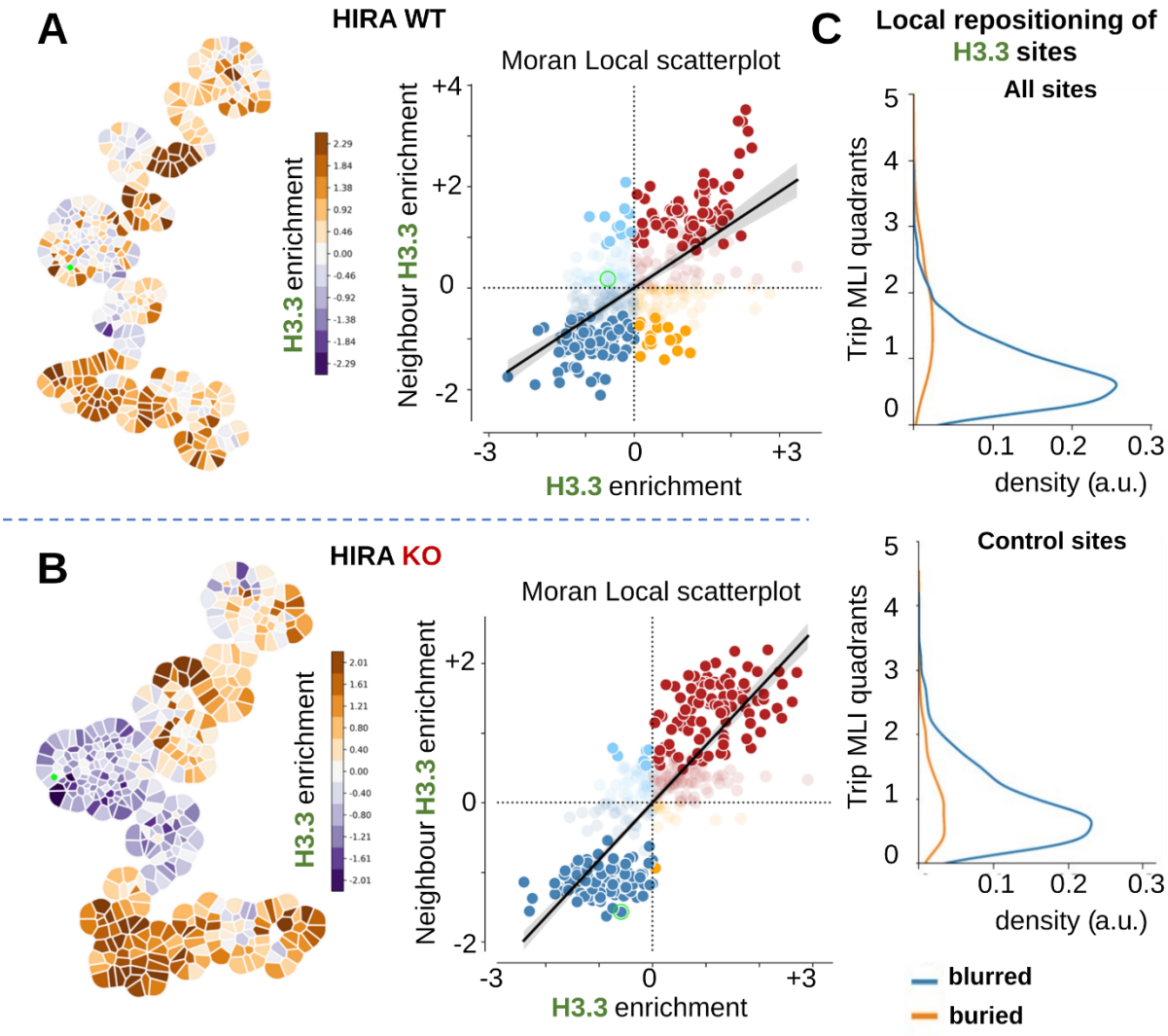

Figure 4. Re-partitioning of H3.3 at blurred and buried sites it not associated with changes in local folding

A. Left: Gaudi plot representing H3.3 enrichment mapped onto a Kamada-Kawaii spatial layout of a 2Mb example region. The centre is the mid-point (green dot) of an A-to-B buried site based on 10kb-binned Hi-C data from HIRA WT cells. ChIP-seq signal is computed as z-score of log2 IP/input ratio of cpm at 10kb bins.

Right: Local Moran Index (LMI) scatterplot of H3.3 enrichment (x axis) vs spatial lag (y axis), representing the H3.3 enrichment of the neighbouring bins in space for each 10kb bin in the 2Mb representative region. Mid-point of the buried site is contoured in green.

B. Same as in **A.** using HIRA KO data (H3.3 enrichment and Hi-C).

C. Distribution of distances between the midpoints of each blurred or buried site (top) or random control (bottom) from scatterplots of HIRA WT and KO, representing the amount of repositioning of the site locally within the spatial layout.

HIRA rescue re-establishes typical H3.3 pattern at early initiation zones and restores timing of EdU incorporation in early S

To disentangle the causal relationship between H3.3 deposition, early replication initiation and genome organization, we then performed rescue experiments. We aimed to test if re-establishing precise H3.3 deposition can restore both timely firing at early replication sites and 3D genome organization. We performed rescue by transient transfection of HIRA (HIRA-YFP) or control (YFP) plasmid for 48h, in H3.1-SNAP and H3.3-SNAP HIRA KO cells followed by G1/S-synchronization (Figure 5A). We first evaluated the restoration of H3.3 and H3.1 enrichment at blurred and buried sites by SNAP-Capture ChIP-seq. Rescue with HIRA, but not control plasmid, restored both the pattern and levels of H3.3 at blurred sites (Figure 5B, C, top, Supplementary Figure 6A). It also re-established the pattern of H3.1 enrichment at their flanks, although without the same extent of depletion within the sites (Supplementary Figure 6A-C). Notably, HIRA add-back was also sufficient to target H3.3 incorporation in buried sites, despite their complete loss of H3.3 upon HIRA KO and low or absent transcriptional activity (Figure 5B, C, bottom). Additionally, although H3.3 enrichment at buried sites was not restored to WT levels, it was accompanied by a significant decrease in H3.1 (Supplementary Figure 6A-C). This resulted in remarkable recovery of the H3.3/H3.1 ratio (Supplementary Figure 7A-C), reflecting both reduced blurring and re-emergence of H3.3 peaks at blurred and buried sites, respectively. Thus, adding back HIRA even if H3.1 is not restored perfectly, enables the re-establishment of H3.3 and at blurred and buried sites.

Next, we examined whether the recovery of the H3 variant pattern was sufficient to drive restoration of firing in early replication zones in S phase. To test this, we released G1/S-arrested HIRA rescue cells for 2h in S phase and performed 30min EdU incorporation pulse to label early-replicating sequences (Figure 5A) as in Gatto et al. (2022). We then assayed EdU incorporation in early S phase by two approaches: imaging and EdU IP followed by sequencing (EdU-seq). Counting the proportion of EdU positive cells showed an increase in the fraction that could enter S phase 2h after release in cells transfected with HIRA, indicating a reversal of the phenotype we observed upon its loss (data not shown). To investigate if this was due to increase in early firing specifically at the blurred and buried sites, we used EdU-seq (Supplementary Figure 7A, bottom tracks). This demonstrated that at blurred sites, the EdU incorporation became restricted to H3.3 sites, although the signal was enriched throughout the sites without peaking at the boundaries as in WT cells. Additionally, at buried sites we detected a significant increase in EdU incorporation (Figure 5D, E, Supplementary Figure 7D). Our data support the view according to which the restoration of early replication firing follows the extent of H3.3/H3.1 balance re-establishment.

Figure 5

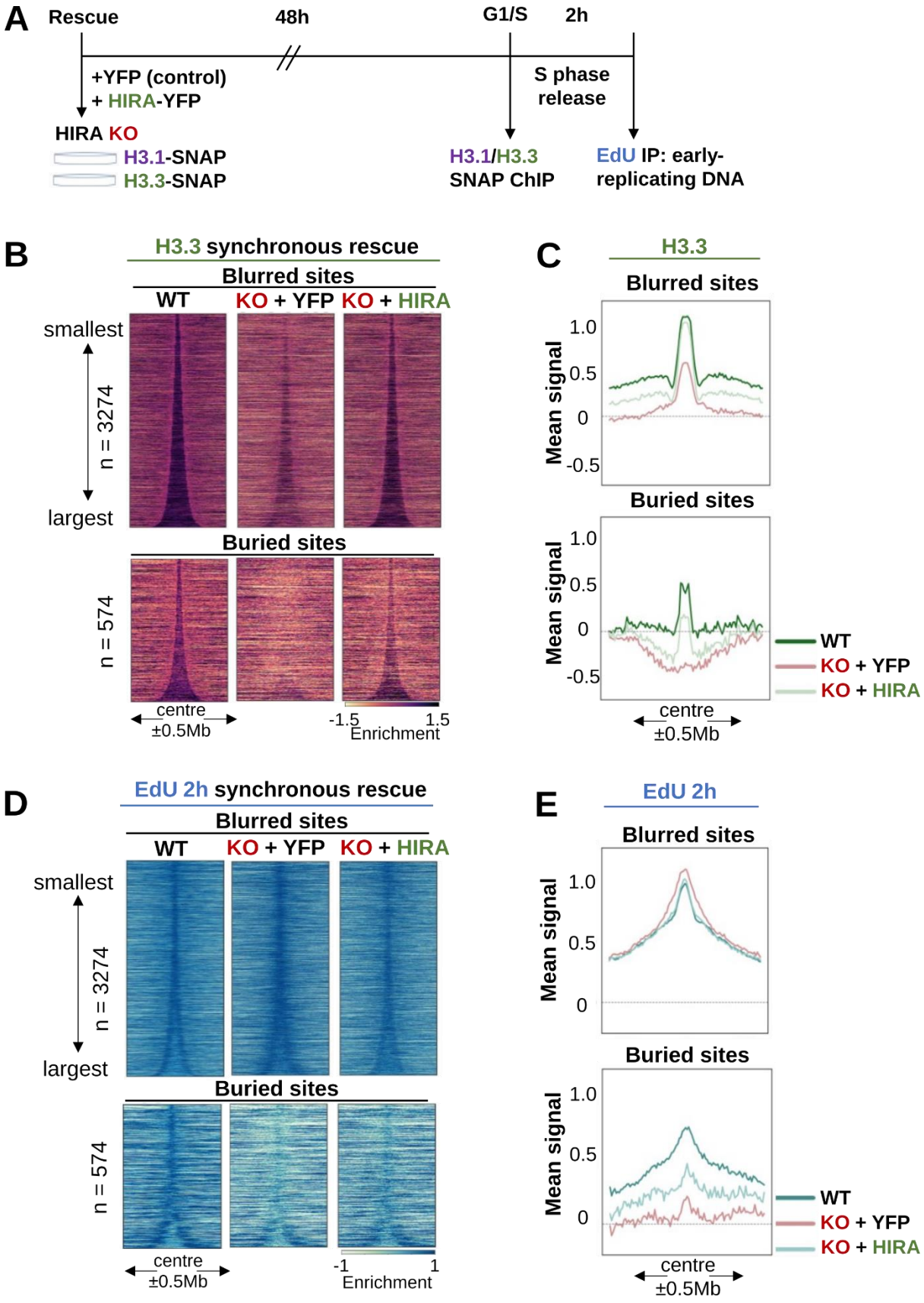
A
Rescue
48h
G1/S
2h
+YFP (control)
+ HIRA-YFP
S phase release
HIRA KO
H3.1-SNAP
H3.3-SNAP
H3.1/H3.3 SNAP ChIP
EdU IP: early-replicating DNA
B
H3.3 synchronous rescue
Blurred sites
WT
KO + YFP
KO + HIRA
smallest
n = 3274
largest
Buried sites
n = 574
centre ±0.5Mb
-1.5
1.5
Enrichment
C
H3.3
Blurred sites
Mean signal
1.0
0.5
0
-0.5
Buried sites
WT
KO + YFP
KO + HIRA
centre ±0.5Mb
D
EdU 2h synchronous rescue
Blurred sites
WT
KO + YFP
KO + HIRA
smallest
n = 3274
largest
Buried sites
n = 574
centre ±0.5Mb
-1
1
Enrichment
E
EdU 2h
Blurred sites
Mean signal
1.0
0.5
0
Buried sites
WT
KO + YFP
KO + HIRA
centre ±0.5Mb

Figure 5. HIRA rescue can re-establish H3.3 pattern and early replication initiation at both blurred and buried sites

A. Scheme of experimental strategy to perform HIRA rescue combined with G1/S synchronization to assay total H3.1/H3.3-SNAP by ChIP-seq and new DNA synthesis in early S phase (2h release). Asynchronous cells constitutively expressing H3.1- or H3.3-SNAP were transfected with YFP (control) or HIRA-YFP plasmid. Cells were then arrested at the G1/S boundary by double thymidine block (starting 6h post-transfection). Total H3.1- and H3.3-SNAP were assayed by SNAP-Capture ChIP-seq of native MNase-digested chromatin, with matching inputs collected. For EdU-seq, cells were released in S phase for 1.5h, followed by 30min EdU pulse and collection at 2h in S phase, followed by EdU IP.

B. H3.3 (G1/S-arrest) and **D.** EdU at 2h in S enrichment profiles from HIRA WT (as reference), and HIRA KO rescue with YFP (control) and HIRA plasmid at blurred sites (top) and buried sites (bottom), centred at their middle ±0.5Mb and sorted by size.

C. H3.3 (G1/S-arrest) and **E.** EdU at 2h in S mean signal at blurred (top) and buried (bottom) sites between 60-160kb in length, centred in their middle ±0.5Mb, is summarized in the bottom panel.

Enrichment relative to input was calculated at 10kb bins as z-score of $\log_2$ IP/input.

HIRA rescue recovers H3.3 distribution within compartments and their interaction patterns, but does not lead to reversal of compartment switches

Next, to assess if changes in genome organization also reverted upon HIRA rescue, we performed Hi-C in asynchronous H3.1-SNAP and H3.3-SNAP HIRA KO cells transfected with HIRA (HIRA-YFP) or control (YFP) plasmid for 48h (Supplementary Figure 8A). First, we validated the re-establishment of H3 variant patterns by SNAP-capture ChIP-seq (Supplementary Figure 8B). This demonstrated H3.3 targeting was effectively re-established to blurred and buried sites, although restoration of the H3.1 pattern was not yet detectable, likely due to the mix of cells in different stages of the cell cycle. We then performed global assessment of 3D genome folding upon HIRA rescue. As before, we observed good concordance between the H3.1-SNAP and H3.3-SNAP cells per condition (Supplementary Figure 9A-D). Notably, HIRA KO + YFP and HIRA rescue Hi-C maps had higher genome-wide similarity than what was observed between the two cells lines, and found a lower proportion of compartment-switching bins (Supplementary Figure 9A, D), indicating that HIRA rescue may not be sufficient to restore 3D genome changes in this timeframe.

Upon HIRA add-back, we detected a significant increase in H3.3 enrichment throughout compartment A regions, at the expense of a decrease in large (>2Mb) B domains (Figure 6A, B), making the HIRA rescue more similar to the situation in HIRA WT cells. We also observed an increase in contacts between A-A and A-B compartments along with a decrease between B-B in *cis* (Figure 6C, D, Supplementary Figure 9E), opposing the effect of HIRA KO. Thus, the simple add back of HIRA could also restore global changes in compartments induced by HIRA loss. Finally, we focused our analysis on the early replication IZ at the blurred and buried sites. As expected, blurred sites maintained their prevalence in compartment A (89% A-to-A), whereas buried sites predominantly remained in compartment B (Figure 7A, B, Supplementary Figure 9F). Indeed, only 2% buried sites switched from B-to-A, despite increasing H3.3 enrichment and EdU incorporation in early S phase in both B-to-A and B-to-B sites to comparable levels (Figure 7C). Thus, these analyses showed that the role of precise H3.3 deposition by HIRA at early replication initiation zones is separable from its effect on 3D genome organization.

Figure 6

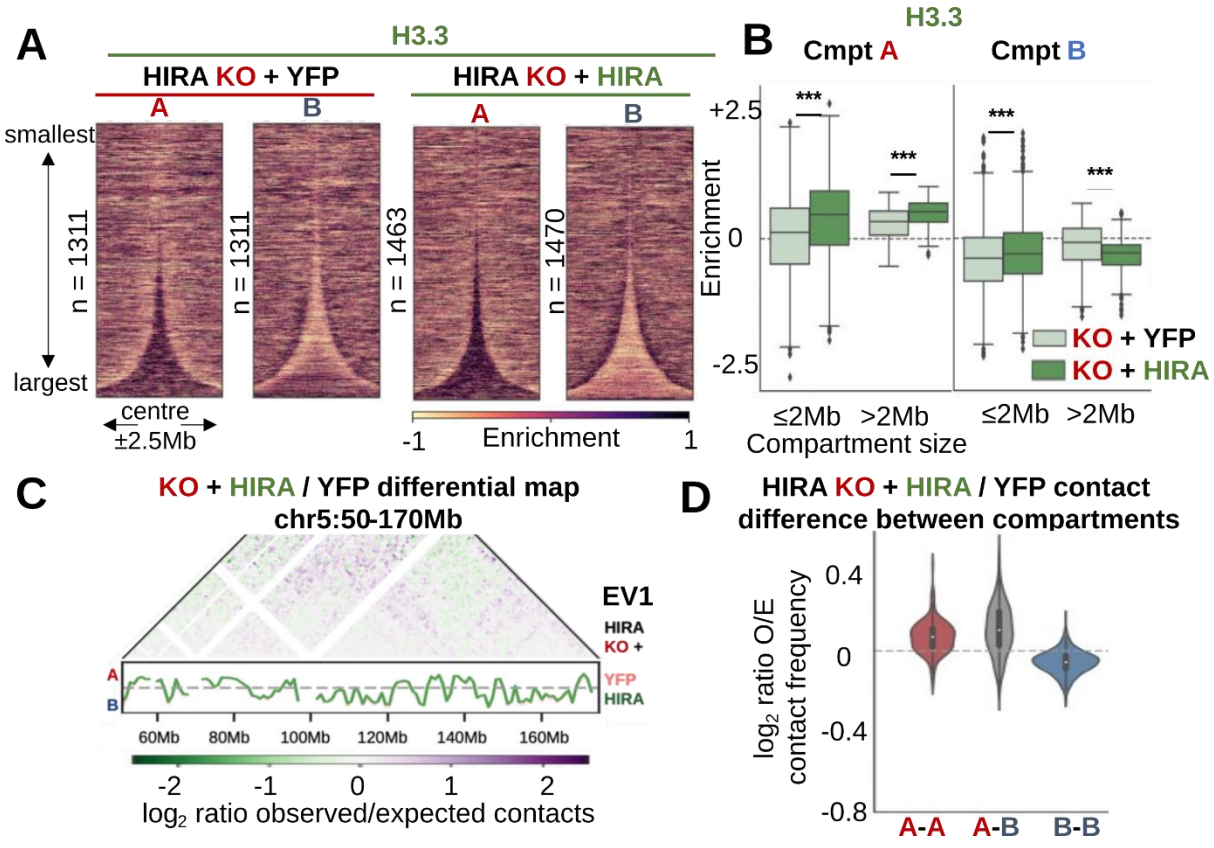

Figure 6. HIRA rescue recovers H3.3 distribution within compartments and their interaction patterns

A. Total H3.3 from G1/S-arrested cells at A and B compartment domains called from HIRA KO + YFP and KO + HIRA rescue cells, sorted by size and centred at their middle ±2.5Mb.

B. H3.3 from G1/S-arrest of HIRA KO + YFP (control) or HIRA quantified in A/B compartments per indicated domain sizes.

C. Differential O/E Hi-C map (log_2 ratio HIRA + HIRA/ + YFP (control)) at 1Mb resolution of chromosome 5:50-170Mb from 0-40Mb away from the diagonal. Tracks below show EV1 (HIRA KO + YFP (control) in pink, HIRA KO + HIRA in light green).

D. Difference (log_2 HIRA KO + HIRA/YFP ratio) of O/E contact frequency between the sets of strongest A/B compartment bins (top/bottom quartile EV1 value, respectively) based on *cis* saddleplots from H3.1-SNAP cells (cf. Suppl. Fig. 9E).

Enrichment relative to input was calculated at 10kb bins as z-score of log_2 IP/input. Two-tailed Mann-Whitney U test corrected for multiple testing by FDR (5% cut-off) was used to determine significance of differences between KO + YFP and KO + HIRA. Significance was noted as: * (p<=0.05), ** (p<=0.01), *** (p<=0.001) for all comparisons.

Figure 7

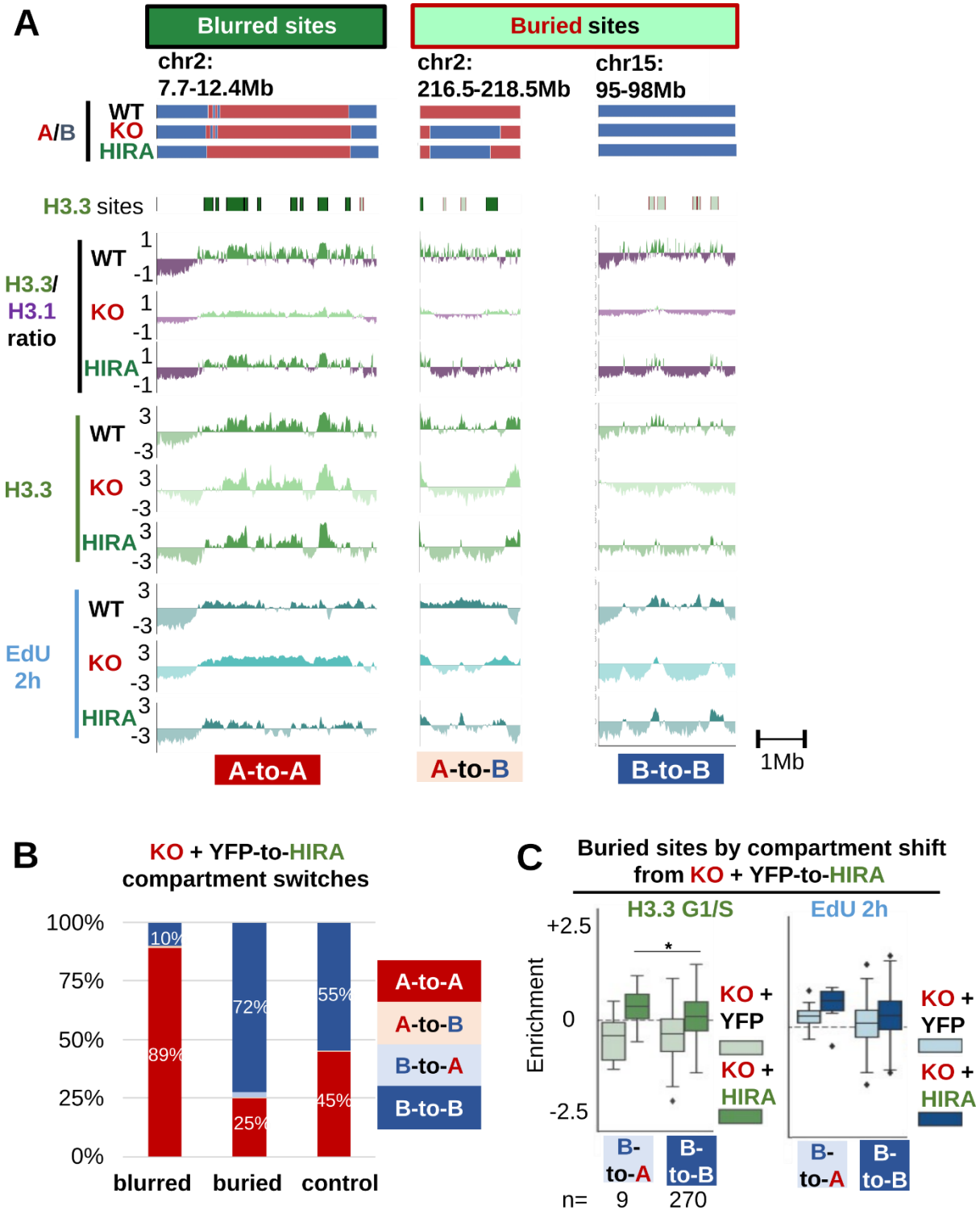
A
Blurred sites
Buried sites
chr2:
7.7-12.4Mb
chr2:
216.5-218.5Mb
chr15:
95-98Mb
A/B
WT
KO
HIRA
H3.3 sites
H3.3/
H3.1
ratio
H3.3
EdU
2h
A-to-A
A-to-B
B-to-B
1Mb
B
KO + YFP-to-HIRA
compartment switches
100%
75%
50%
25%
0%
10%
89%
72%
25%
55%
45%
blurred
buried
control
A-to-A
A-to-B
B-to-A
B-to-B
C
Buried sites by compartment shift
from KO + YFP-to-HIRA
H3.3 G1/S
EdU 2h
+2.5
0
-2.5
Enrichment
*
KO +
YFP
KO +
HIRA
B-
to-A
B-
to-B
n=
9
270

Figure 7. HIRA rescue does not reverse compartment switches of buried sites despite increased H3.3 enrichment and early firing

A. Compartment assignment, H3.3 site positions (blurred in dark green and black, buried in light green and red), H3.3/H3.1 ratio, H3.3 and early-replicating DNA (EdU 2h) enrichment at representative regions from HIRA WT, KO and KO + HIRA rescue. Shown are a set of blurred sites in A compartment that remain A in HIRA KO (A-to-A, left), and buried sites that switch from A-to-B (middle) or that were in B and remain there (B-to-B, right, cf Fig. 3A).

B. Distribution of blurred, buried and random sites by A/B compartment shifts from HIRA KO + YFP to HIRA KO + HIRA rescue cells.

C. H3.3 (G1/S arrest) and EdU 2h in S enrichment from HIRA KO + YFP and KO + HIRA cells at buried sites switching from B-to-A or B-to-B from KO + YFP-to-HIRA rescue. Number of sites per compartment switch category is noted below. Differences between KO + YFP and KO + HIRA are significant (***) for both H3.3 and EdU 2h.

Enrichment relative to input was calculated at 10kb bins as z-score of $\log_2$ IP/input. H3.3/H3.1 ratio, H3.3 ChIP-seq and EdU-seq (z-score of $\log_2$ IP/input ratio of cpm) are shown at 10kb bins smoothed over 3 non-zero bins. Two-tailed Mann-Whitney U test corrected for multiple testing by FDR (5% cut-off) was used to determine significance of differences between KO + YFP and KO + HIRA or between different compartment-switching behaviours in HIRA KO + HIRA. Significance noted: * ($p<=0.05$), ** ($p<=0.01$), *** ($p<=0.001$) for all comparisons.

Discussion

In this study, we examined the organization of histone H3 variants across genomic scales and investigated the role of the H3.3-specific chaperone HIRA on chromatin folding and early replication initiation. First, we observed that H3.3 is enriched in A and depleted in B compartments, whereas H3.1 showed a weak depletion in A and strong enrichment only in large B compartments. In HIRA KO cells, H3.3 redistributed from A to large B regions without a corresponding change in H3.1 or H3 PTMs. With respect to genome organization, we find that the targeted H3.3 deposition by HIRA impacts (i) the Mb scale, where it is important for A compartment interactions in a PTM-independent manner (Figure 8A). On (ii) the sub-Mb scale, HIRA-mediated H3.3 incorporation contributes to maintaining A compartment identity of early IZs in the absence of transcription without impacting their local folding. Importantly, our rescue experiments revealed that the role of HIRA in ensuring proper early replication initiation is separate from its effect on 3D genome organization and does not depend on A-to-B compartment switching (Figure 8B). Below, we discuss the implications of our findings with respect to the role of HIRA in genome compartmentalization and regulation of replication initiation in cellular models and in the context of development.

HIRA-mediated H3.3 incorporation is important for chromatin organization on the Mb scale independently of PTMs

Our experiments demonstrated that in the absence of HIRA, H3.3 redistributed from A to large B compartment domains without a corresponding mis-localisation of H3 PTMs including active (H3K4me1, H3K4me3, H3K27ac) and inactive (H3K9me3, H327me3) marks in the context of higher-order genome organization (Figure 1). This was surprising given that H3.3 with its unique H3.3S31 residue and phosphorylation can impact the activity of several histone modifying enzymes, including p300 (depositing H3K27ac, Martire et al., 2019; Morozov et al., 2023), SETD2 (depositing H3K36me3, Armache et al., 2020) and KDM4B (removing H3K9/K36me3, Udugama et al., 2022), resulting in redistribution of the modifications they impose. However, both Martire et al. (2019) and Armache et al. (2020) examined modifications at promoters and enhancers after induction of new gene expression programmes, while we investigated PTMs at a larger scale at a steady state in the HeLa cell model. Also, we did not examine repetitive regions where there are possible changes. Indeed H3.3S31phos affects the absolute levels of H3K9me3 and KDM4B only at telomeres, which accumulate H3.3 due to the action of another chaperone complex, ATRX/DAXX (Udugama et al., 2022). Nevertheless, we can safely conclude that at the scale of compartments, in unchallenged human cells, the pre-existing chromatin environment and not the choice of H3 variant dictate H3 PTM distribution. This is consistent with previous reports showing that modifications on both H3.1 and H3.3 from oligonucleosomes show the same features and rather relate to the chromatin environment (Loyola et al., 2006).

Figure 8

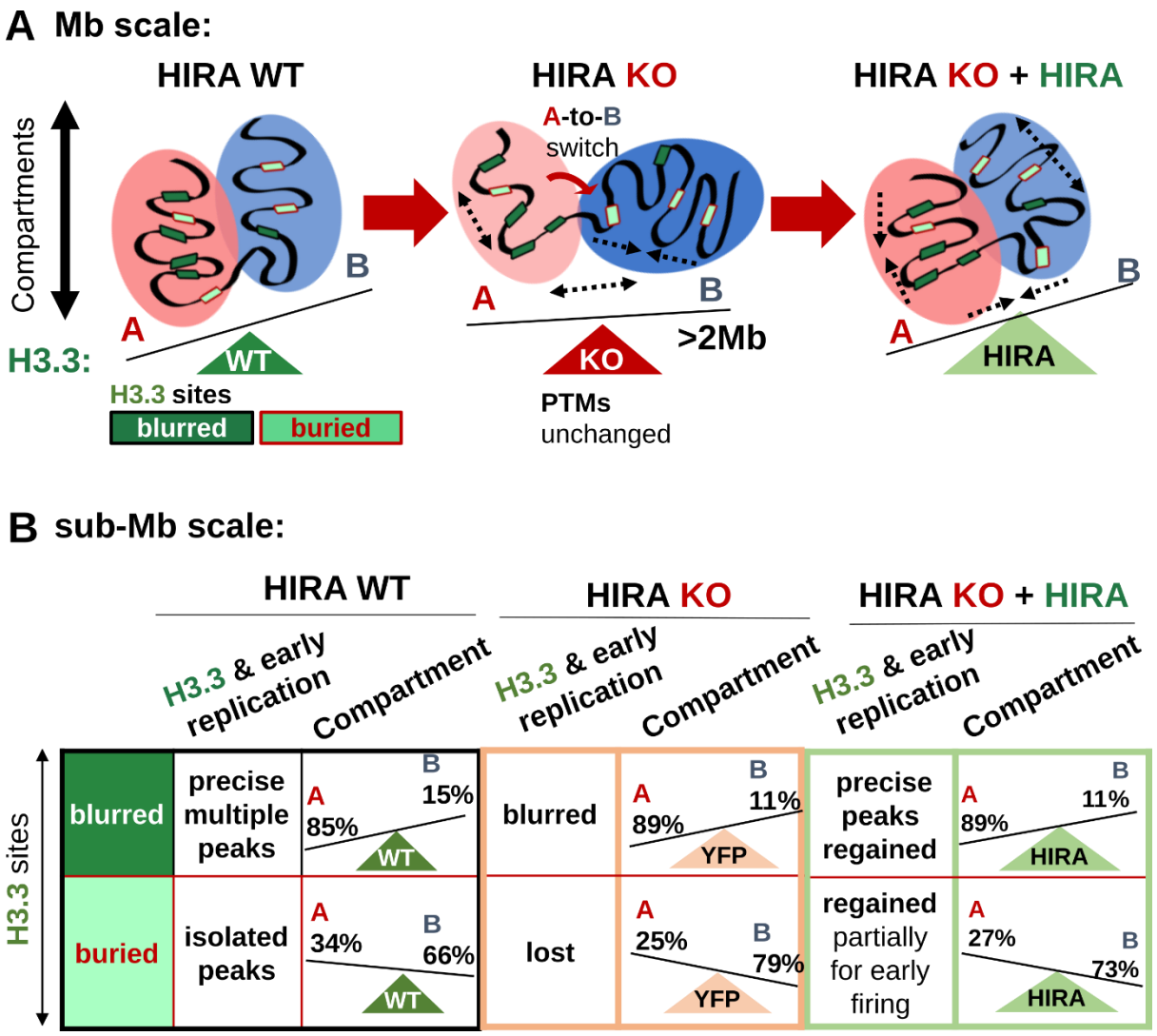

Figure 8. HIRA-mediated H3.3 deposition impacts 3D genome organisation and early replication

A. On the Mb scale, HIRA mediates H3.3 enrichment in A compartments. In the absence of HIRA, H3.3 redistributes from A to large B regions, concomitantly with decrease in A-A and A-B contacts, but without changes in PTM patterns. HIRA rescue restores both H3.3 enrichment and compartment A interaction patterns.

B. On the kb scale, HIRA establishes H3.3/H3.1 boundaries which define early replication initiation zones. Blurred sites, which are transcribed and continue firing early in HIRA KO also maintain their A compartment identity. Buried sites, which lose H3.3 enrichment and early S firing in the absence of HIRA, are predominantly in B compartment. In HIRA KO, compartment A buried sites further switch to B in the absence of transcription. HIRA add-back recovers the H3.3 enrichment and early initiation at buried sites without promoting B-to-A switch, indicating that early initiation is not dependent on compartment identity.

In HIRA KO cells, compartments largely maintained their identity, but we observed a decrease in contacts between A compartments with each other and the rest of the genome (Figure 2). Global alterations of A/B compartment interactions of a similar magnitude have been reported upon depletion of the histone acetylation reader BRD2 in mESCs (Xie et al., 2022) and the H3K9me3 reader HP1a in *Drosophila* embryos, but not cell lines (Zenk et al., 2021). Compartmentalisation was also affected upon DNMT1/DNMT3B KO in HCT-116 cells, where it was accompanied by the redistribution of several PTMs (H3K4me1, H3K4me3, H3K9me3, H3K27me3) (Du et al., 2021). Indeed, polymer modelling could recapitulate the changes in compartment interactions upon loss of PTM reader binding (Xie et al., 2022; Zenk et al., 2021). The absence of PTM re-distribution in compartments upon HIRA KO suggests that either the identity of H3.3 or the process of its deposition by HIRA throughout interphase at A compartments may be what promotes their interactions. HIRA depletion has been shown to result in decreased H3.3 on chromatin (Ray-Gallet et al., 2018, 2011), increased DNase I sensitivity (Ray-Gallet et al., 2011) and changes in enhancer and promoter accessibility (Morozov et al., 2023; Tafessu et al., 2023; Yang et al., 2021). These features may reflect differences in nucleosome occupancy at active regions, impacting contacts between A compartments. Transient downregulation of HIRA has also been shown to result in ~20% global reduction in transcriptional activity (Torné et al., 2020), although this is unlikely to explain the reduced A compartment interactions, as global transcriptional inhibition (Barutcu et al., 2019; Hsieh et al., 2020) and acute RNAPII component depletion (Jiang et al., 2020) do not disrupt compartmentalization. Thus, our work emphasises that nucleosomes are not static entities decorated by a set of PTMs, but dynamic units which can exchange histone dimers throughout the cell cycle. Thus, it will be important to consider these dynamics when trying to understand the processes underpinning the segregation of the genome in compartments in the future.

Reestablishment of H3 variant balance, but not compartment identity is required for the recovery of initiation zone firing in early S phase

Restoration of the H3.3 pattern upon HIRA rescue was accompanied by a partial re-establishment of H3.1 distribution and recovery of the firing at early replication IZs (Figure 5). Strikingly, this restoration took place regardless of the transcriptional status of the IZ although expressed regions showed better recovery. We hypothesize that HIRA may be recruited there more efficiently due to its interaction with RNAPII, while its association with non-transcribed IZs may occur via its ‘gap-filling’ mechanism (Ray-Gallet et al., 2011), if in its absence they have a reduced nucleosome density, as observed in other settings (Ray-Gallet et al., 2011; Yang et al., 2021). In our experimental set-up, HIRA expression varied between cells and lasted only for 48 hours, allowing the completion of one S phase at most. As H3.1 incorporation is coupled to DNA synthesis (Tagami et al., 2004), this would allow only one round of new deposition, which may be insufficient for the full re-establishment of the H3.1 enrichment pattern. Subsequently, the balance between H3.3 and H3.1 would not be fully restored, leading to an incomplete rescue of the early firing in S phase.

RT and compartmentalization are highly correlated across cell types, although changes in the two can be discordant during early mouse (Miura et al., 2019) and human (Dileep et al., 2019) ESC differentiation. Furthermore, in human cells depletion of the RT control factor RIF1 leads to loss of temporal organization of the replication programme, accompanied by reduced active marks at A compartments, weaker A-A interactions and A-to-B switching (Klein et al., 2021). Passage through S phase was required for the reorganization of both PTMs and compartments and independently of gene expression changes (Klein et al., 2021), leading the authors to conclude that proper RT is required for the maintenance of chromatin state and 3D organization. In our system, we have demonstrated that impairing early IZ firing by HIRA KO results in compartment switching only in the absence of transcription (Figure 3). Furthermore, non-transcribing IZs can regain both H3.3 enrichment and firing in early S phase without switching back from B-to-A compartment (Figure 7), despite the global recovery of A compartment interactions (Figure 6) in the timeframe we examined. This demonstrates that early IZ firing is independent of both their transcriptional activity and compartment identity. It also implies that the role in HIRA in defining early IZs is separate from its impact on compartment interactions and independent of histone PTMs, unlike RIF1. It would be interesting to examine the H3.3/H3.1 balance upon RIF1 loss and investigate whether RIF1 may function with HIRA, especially since it has been shown to interact with the general H3-H4 chaperone ASF1 in the context of DNA repair (Feng et al., 2022; Tang et al., 2022). Furthermore, RIF1 showed a preference for the ASF1a paralogue (Feng et al., 2022), which interacts with HIRA (Daganzo et al., 2003; Tagami et al., 2004; Zhang et al., 2005) and preferentially associates with H3.3 (Wang et al., 2021).

On the sub-Mb scale, the absence of HIRA did not disrupt the local organization of early IZs (Figure 4, Supplementary Figure 4), despite the complete loss of firing in the absence of transcription. This is in line with the maintenance of TAD border positions observed upon RIF1 loss, although Klein et al. (2021) reported an increase in border strength in this condition. Early-firing origins have been shown to be enriched at TAD borders (Akerman et al., 2020; Giles et al., 2022; Petryk et al., 2016) and often contacting each other in 3D space (Jodkowska et al., 2022). Thus, our experiments demonstrate that maintaining spatial organization on this scale does not suffice to ensure the timely firing of early IZs.

Insights into the importance of HIRA in development: beyond transcriptional control?

HIRA (Roberts et al., 2002) is essential for normal mammalian development, and while its importance has largely been attributed to its role in transcription, our results indicate it is also important for compartment organization and early replication. In the context of differentiation, H3.3 incorporation (Wen et al., 2014b, 2014a) and CAF-1 down-regulation (resulting in decreased H3.1/2 deposition) (Cheloufi et al., 2015; Ishiuchi et al., 2015; Nakatani et al., 2022) have been shown to promote cell reprogramming, which is often accompanied by RT and compartment changes (Dileep et al., 2019; Miura et al., 2019). Focusing on fertilization and early embryogenesis, Ishiuchi et al. (2020) have demonstrated that mouse MII oocytes display a ‘non-canonical’ pattern of H3.3, found more evenly

distributed along the genome with a slight enrichment in inactive regions, accompanied by absence of compartments in these cells (Du et al., 2017; Flyamer et al., 2017; Gassler et al., 2017). The establishment of the 'canonical' H3.3 pattern at the 2-cell stage required DNA replication and the concomitant H3.1/2 deposition by CAF-1. Once re-established, the H3.3 pattern is maintained (Ishiuchi et al., 2020), while compartments gradually emerge as the embryo continues dividing independently of transcription (Du et al., 2017; Flyamer et al., 2017; Gassler et al., 2017). Nakatani et al. (2022) investigated the opposite process, the emergence of 2-cell-like cells (2CLCs) from ESCs, showing it was promoted by reduced replication fork speed, particularly in early S phase. Slower replication was associated with increased number of firing origins, accompanied by advanced RT and H3.3 enrichment of 2CLC-specific genes (Nakatani et al., 2022). Reduced fork speed would allow more time for chromatin maturation and H3.1-H3.3 exchange at early-replicating regions and may contribute to maintaining their early replication in the subsequent S phases. *In vivo*, replication fork speed progressively increases from 2-cell until blastocyst stage (Nakatani et al., 2022), as 3D organization is also getting established cells (Du et al., 2017; Flyamer et al., 2017; Gassler et al., 2017), and it is possible that setting up a proper H3.3/H3.1 balance may contribute to both. However, it is important to note 2CLCs are not equivalent to 2-cell stage cells, as have much stronger compartments (Kruse et al., 2019), and their H3.3 enrichment has not been profiled.

To separate the roles of HIRA and H3.3 on replication and genome compartments, non-dividing cells may also be considered. Focusing on later developmental stages, Maze et al. (2015) have shown H3.3 accumulates in adult post-mitotic mouse neurons, and its HIRA-mediated turnover is important to maintain basal gene expression and normal cell function. On the other hand, Bonev et al. (2017) showed that in cortical neurons (differentiated *in vitro*) compared to ESCs, B-B compartments interact more strongly at the expense of A-A, and this was accompanied by a reduced correlation of eigenvector values and active PTMs. Thus, it would be interesting to examine if the change in compartment interactions in this system is related to a potential re-distribution or accumulation of H3.3 on chromatin.

In conclusion, our work reveals histone variant composition impacts both replication initiation and higher-order organization of chromatin. We show H3.3 targeting is important for compartment organization independently of PTMs, highlighting the role of histone dynamics in genome architecture. Finally, we demonstrate that the role of H3.3 deposition by HIRA at compartments is independent of its function in early IZ definition, we can use this system to disentangle the mechanisms of replication initiation control from 3D chromatin organization.

Supplementary figures

Supplementary Figure 1

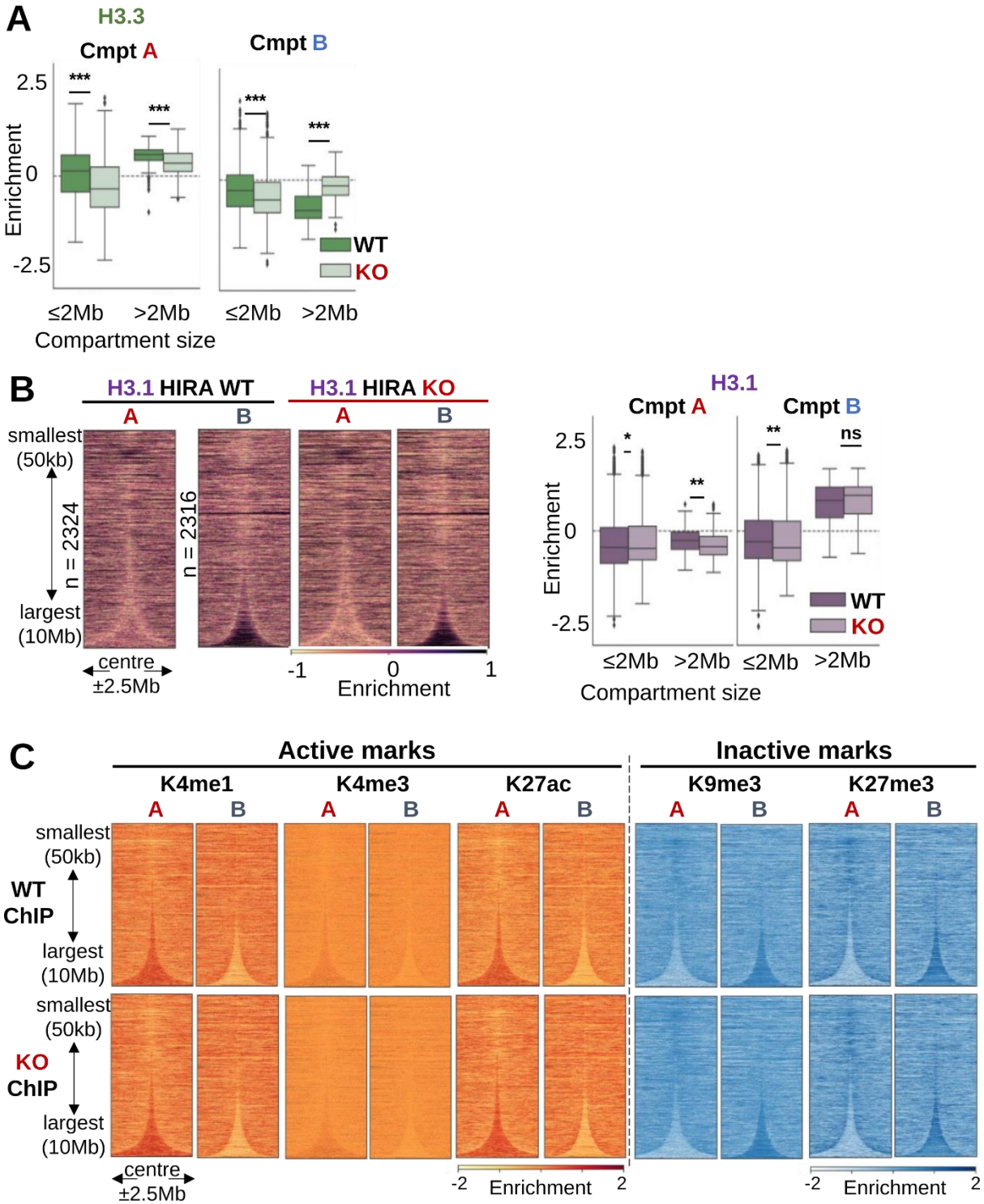

Supplementary Figure 1. Absence of HIRA leads to re-distribution of H3.3 from A to large B compartments without corresponding PTM changes

A. Total H3.3 from G1/S-arrested HIRA WT and KO cells (z-score $\log_2$ IP/input) quantified in A/B compartments per indicated domain sizes. Two-tailed Mann-Whitney U test adjusted for multiple testing by FDR (5% cut-off) was used to determine significance of differences between WT and KO.

B. Left: Total H3.1 enrichment (z-score of $\log_2$ IP/input) at 10kb bins from G1/S-arrested cells at A and B compartment domains called from HIRA WT and KO cells, sorted by size and centred at their middle ±2.5Mb. Right: Quantification of the signal in the heatmaps in A/B compartments per indicated domain sizes. Two-tailed Mann-Whitney U test adjusted for multiple testing by FDR (5% cut-off) was used to determine significance of differences between WT and KO.

C. Enrichment of active (H3K4me1, enhancer, H3K4me3, promoter and H3K27ac, enhancer) and inactive (H3K9me3, constitutive and H3K27me3, facultative heterochromatin) histone PTMs (z-score of $\log_2$ IP/input) at 10kb bins from HIRA WT and KO cells at A and B compartment domains, sorted by size and centred at their middle ±2.5Mb.

Supplementary Figure 2

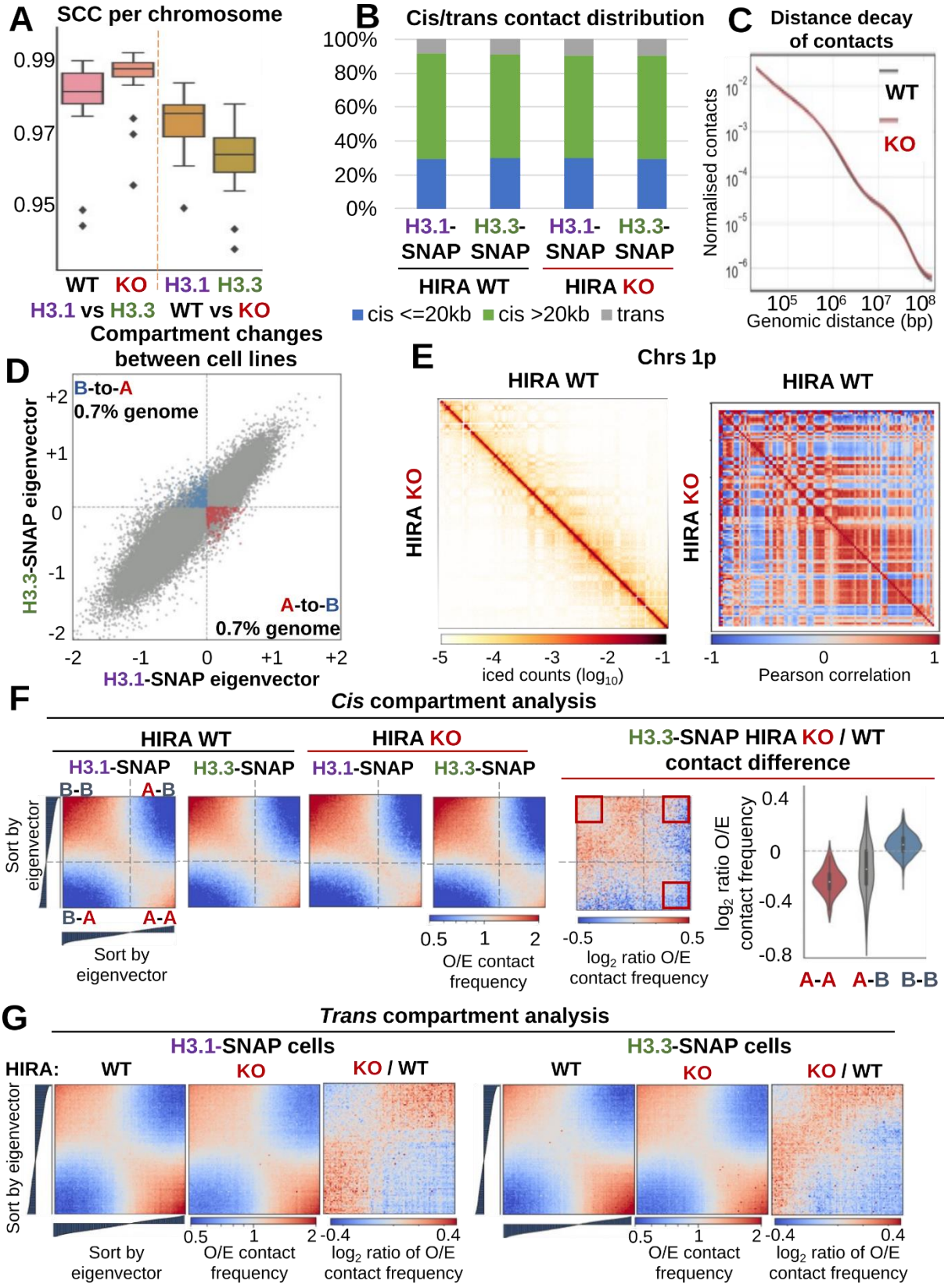

Supplementary Figure 2. Compartment A domains show a decrease in interactions, but largely maintain their identity in the absence of HIRA

A. Matrix similarity between H3.1- and H3.3-SNAP cell lines per HIRA status and between HIRA WT and KO per cell line measured by SCC (stratum-adjusted correlation coefficient) at 1Mb resolution.

B. Proportion of short-range (<=20kb), long-range (>20kb) *cis* and *trans* contacts from Hi-C maps of HIRA WT or KO H3.1- and H3.3-SNAP HeLa cells.

C. Decay of contact frequency with genomic distance (P(s) curves) from HIRA WT (grey) and KO (red) maps, binned at 10kb after masking of blacklisted regions and ICE normalization.

D. EV1 (1st eigenvector, indicating compartment) of 50kb-binned Hi-C matrices from H3.1- vs H3.3-SNAP HIRA WT cells. Bins which change from A-to-B (lower right quadrant) or B-to-A (upper left quadrant) in the same direction in both conditions are coloured (red and blue, respectively) and quantified.

E. Left: Normalised count (log_{10} contact frequency, ICE-normalised after masking of blacklisted regions) and right: Perason correlation maps at 1Mb resolution of chromosome 1p from HIRA WT (top right) and KO (bottom left) H3.1-SNAP HeLa cells.

F. Left: Saddle plots of observed/expected (O/E) interaction frequency at 50kb resolution based on EV1 percentiles from H3.1 and H3.3-SNAP HIRA WT and KO cells. Right: Differential saddle plot (log_2 ratio of O/E contacts) of H3.3-SNAP HIRA KO/WT at 50kb resolution based on EV1 percentiles. Red squares denote the regions used for B-B (top left), A-A (bottom right) and A-B (top right) quantification in violinplot on the right.

G. *Trans* saddle plots of observed/expected (O/E) interaction frequency at 50kb resolution based on EV1 percentiles from H3.1-SNAP (left) and H3.3-SNAP (right) HIRA WT and KO and differential saddle plot (log_2 ratio of O/E contacts) of HIRA KO/WT

Supplementary Figure 3

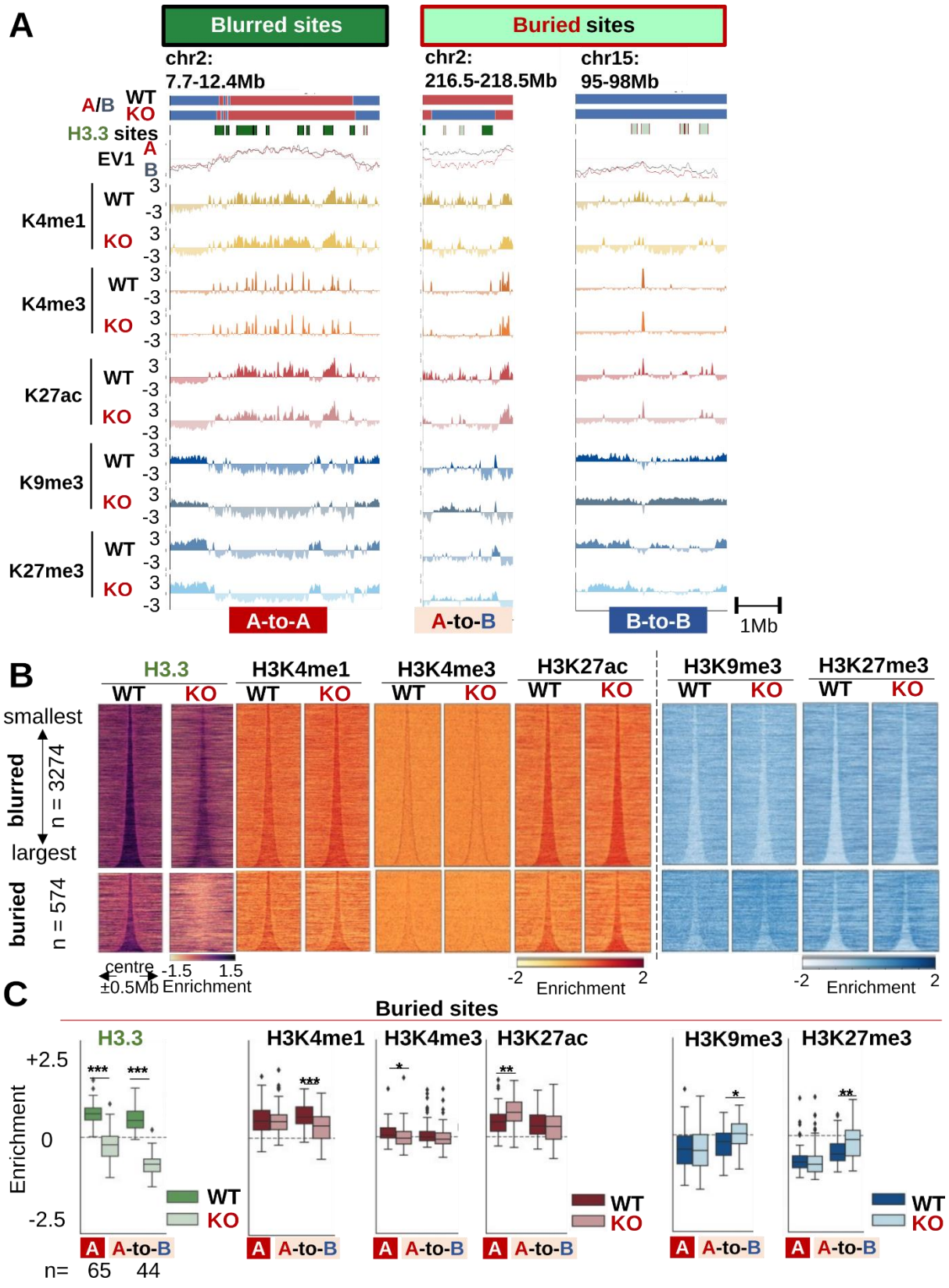

Supplementary Figure 3. Loss of targeted H3.3 incorporation by HIRA and impaired firing at early replication zones is not associated with PTM redistribution

A. Compartment assignment, EV1 (WT in grey, KO in red), active (H3K4me1, H3K4me3, H3K27ac) and repressive (H3K9me3, H3K27me3) histone PTM enrichment from HIRA WT and KO at representative blurred (left) and buried (right) sites (as in Fig. 3A).

B. H3.3, active (H3K4me1, H3K4me3, H3K27ac) and repressive (H3K9me3, H3K27me3) histone PTM enrichment profiles from HIRA WT and KO G1/S-arrested cells at blurred (top) and buried (bottom) sites, centred at their middle ±0.5Mb and sorted by size.

C. H3.3, active (H3K4me1, H3K4me3, H3K27ac) and repressive (H3K9me3, H3K27me3) histone PTMs enrichment from HIRA WT and KO cells at A-to-A and A-to-B buried sites. Number of sites per compartment switch category is noted below. Differences in WT enrichment between A-to-A and A-to-B blurred sites are significant (***) for H3.3 and K27me3.

Enrichment relative to input was calculated at 10kb bins as z-score of $\log_2$ IP/input. Two-tailed Mann-Whitney U test corrected for multiple testing by FDR (5% cut-off) was used to determine significance of differences between WT and KO or between different compartment-switching behaviours in HIRA WT. Significance was noted as: * ($p<=0.05$), ** ($p<=0.01$), *** ($p<=0.001$) for all comparisons.

Supplementary Figure 4

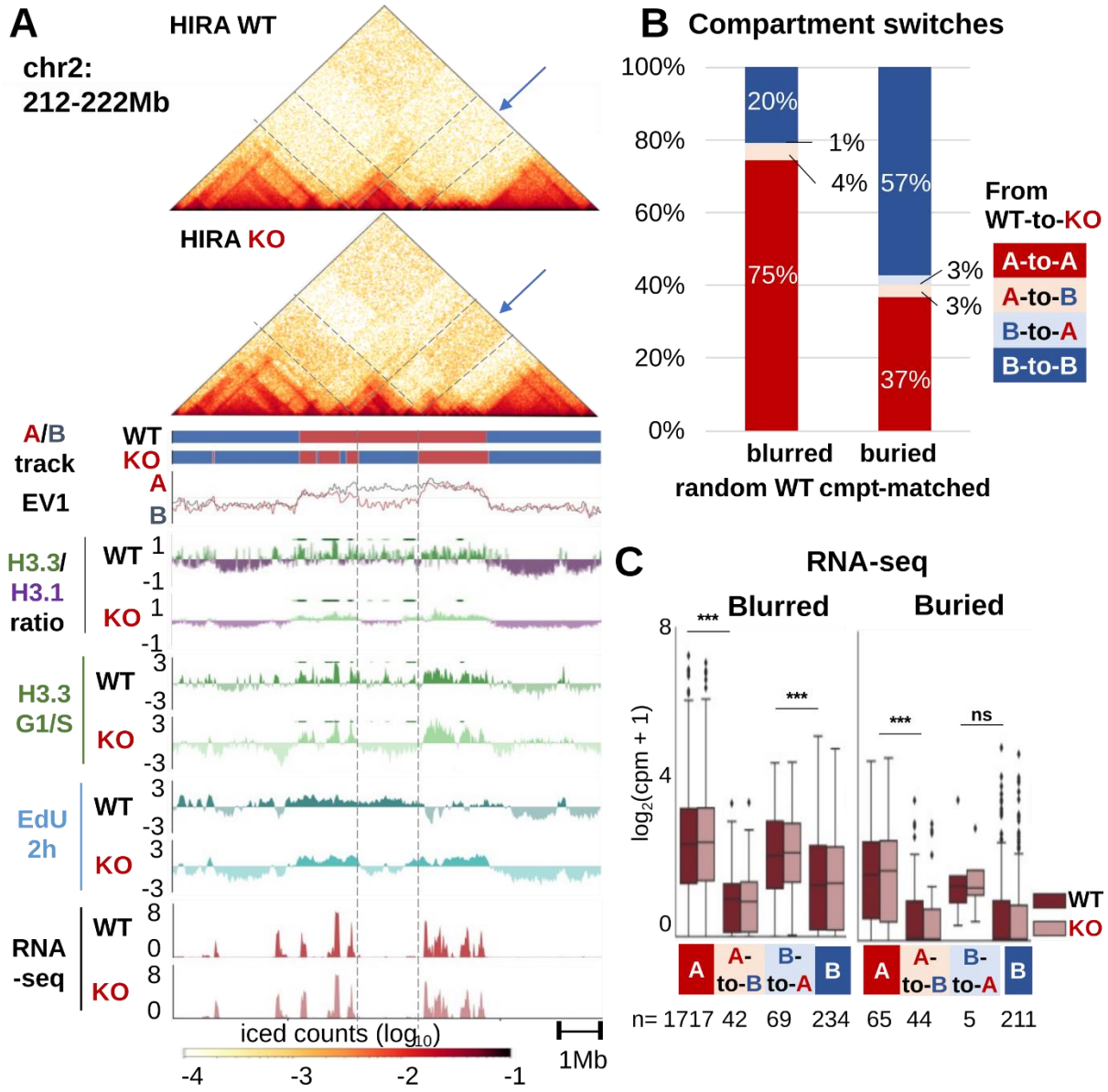

Supplementary Figure 4. A-to-B compartment switching occurs specifically at early replication initiation zones associated with low transcriptional activity in absence of HIRA

A. Hi-C maps, compartment assignment, EV1 (HIRA WT in grey, KO in red), H3.3/H3.1 ratio, H3.3 enrichment, early-replicating DNA (EdU 2h) and transcription (RNA-seq) at a representative region (chr2: 212-222Mb). H3.3/H3.1 ratio, H3.3 ChIP-seq and EdU-seq (z-score of $\log_2$ IP/input ratio of cpm) and RNA-seq ($\log_2$(cpm + 1)) are shown at 10kb bins smoothed over 3 non-zero bins. Blurred and buried site locations are noted as dark and light green lines, respectively, above the H3.3/H3.1 ratio and H3.3 ChIP-seq tracks. Grey vertical lines denote a cluster of buried sites which are not transcribed and switch from A to B compartment concomitantly with losing EdU incorporation at 2h in S phase and H3.3 enrichment in HIRA KO (cf Fig. 6E).

B. Distribution of a size- and WT compartment assignment-matched set of blurred or buried sites according to their compartment shifts from HIRA WT to KO.

C. RNA-seq (log_2(cpm + 1)) from G1/S-arrested cells at blurred and buried sites stratified by compartment change from HIRA WT to KO. Number of sites per compartment switch category is noted below. Two-tailed Mann-Whitney U test corrected for multiple testing by FDR (5% cut-off) was used to determine significance of differences between WT and KO or between different compartment-switching behaviours in HIRA WT. Significance was noted as: * ($p<=0.05$), ** ($p<=0.01$), *** ($p<=0.001$) for all comparisons. Difference between WT and KO was not significant for any of the categories.

Supplementary figure 5

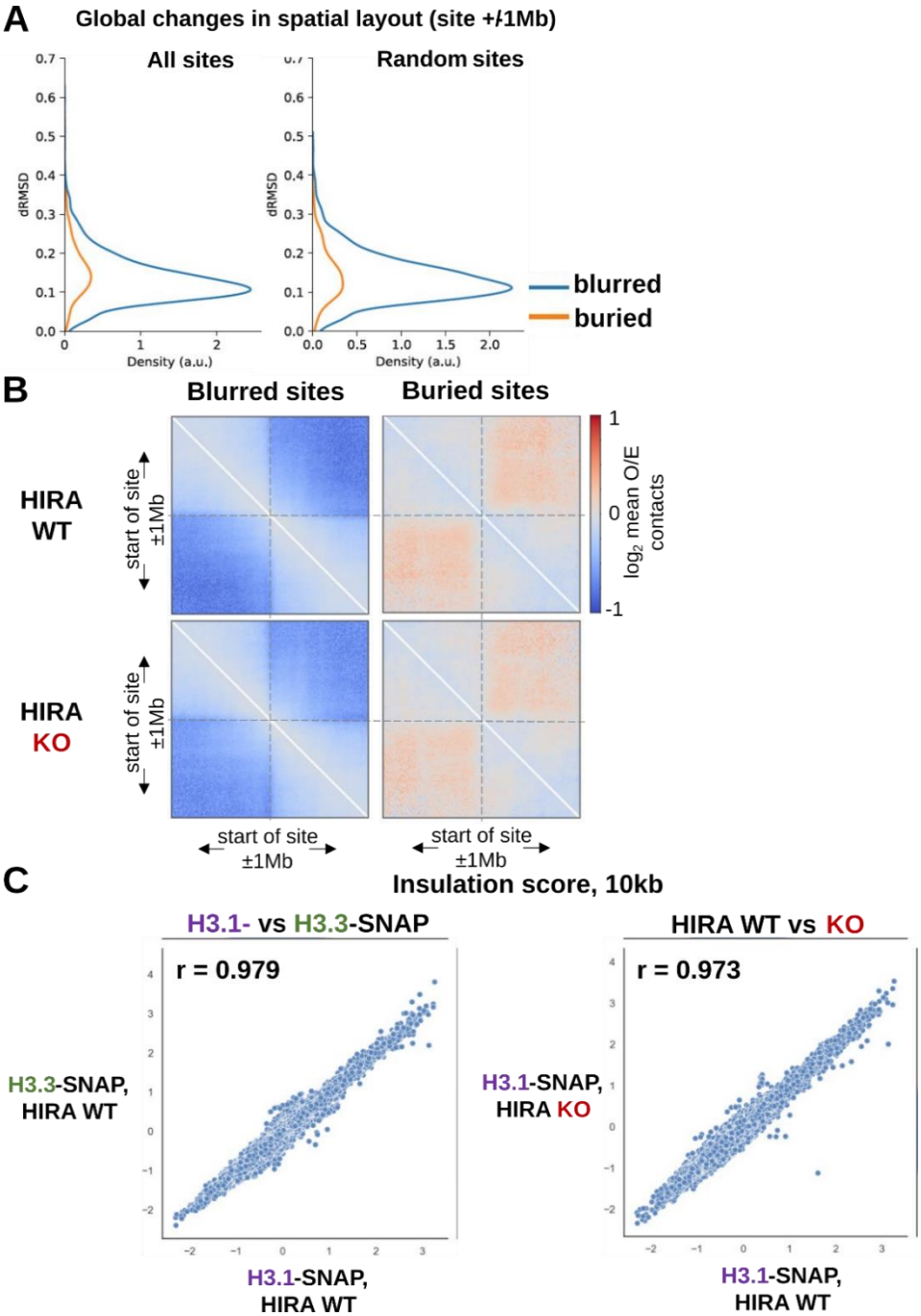

Supplementary figure 5. Re-partitioning of H3.3 at blurred and buried sites it not associated with changes in local folding

A. Difference in root mean square deviation (dRMSD) between all points of HIRA WT vs KO 2Mb spatial layout per blurred and buried site (left) or randomized sites (right).

B. On-diagonal pile-ups of blurred (left) and buried (right) sites from HIRA WT (top) and KO (bottom) cells, centred at the start of each site and taking 1Mb up- and downstream flanking sequence.

C. Insulation score from 10kb-binned Hi-C matrices from H3.1- vs H3.3-SNAP HIRA WT cells (left) or HIRA WT vs KO H3.1-SNAP cells (right). Pearson correlation is noted.

Supplementary Figure 6

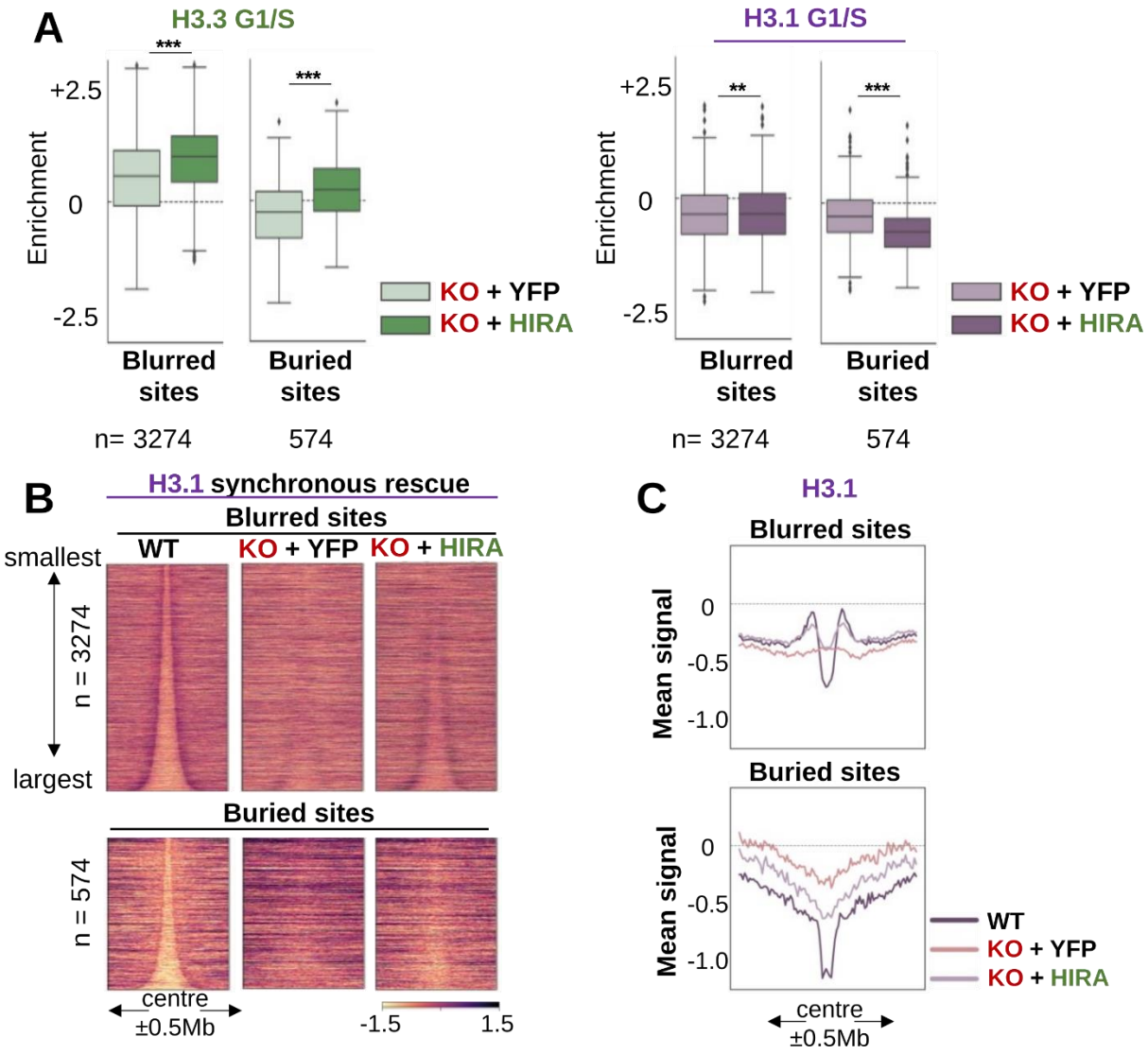

Supplementary Figure 6. HIRA rescue can re-establish H3 variant at blurred and buried sites

A. H3.3 (left) and H3.1 (right) from G1/S-arrested HIRA KO cells transfected with YFP (control) or HIRA plasmid quantified at blurred and buried sites. Two-tailed Mann-Whitney U test adjusted for multiple testing by FDR (5% cut-off) was used to determine significance of differences between HIRA KO + YFP (control) and HIRA KO + HIRA rescue. Significance was noted as: * (p<=0.05), ** (p<=0.01), *** (p<=0.001).

B. H3.1 (G1/S-arrest) from HIRA WT (as reference), and HIRA KO rescue with YFP (control) and HIRA plasmid at blurred sites (top) and buried sites (bottom), centred at their middle ±0.5Mb and sorted by size.

C. H3.1 mean signal at blurred (top) and buried (bottom) sites between 60-160kb in length, centred in their middle ±0.5Mb, is summarized in the bottom panel.

Enrichment relative to input was calculated at 10kb bins as z-score of $\log_2$ IP/input.

Supplementary Figure 7

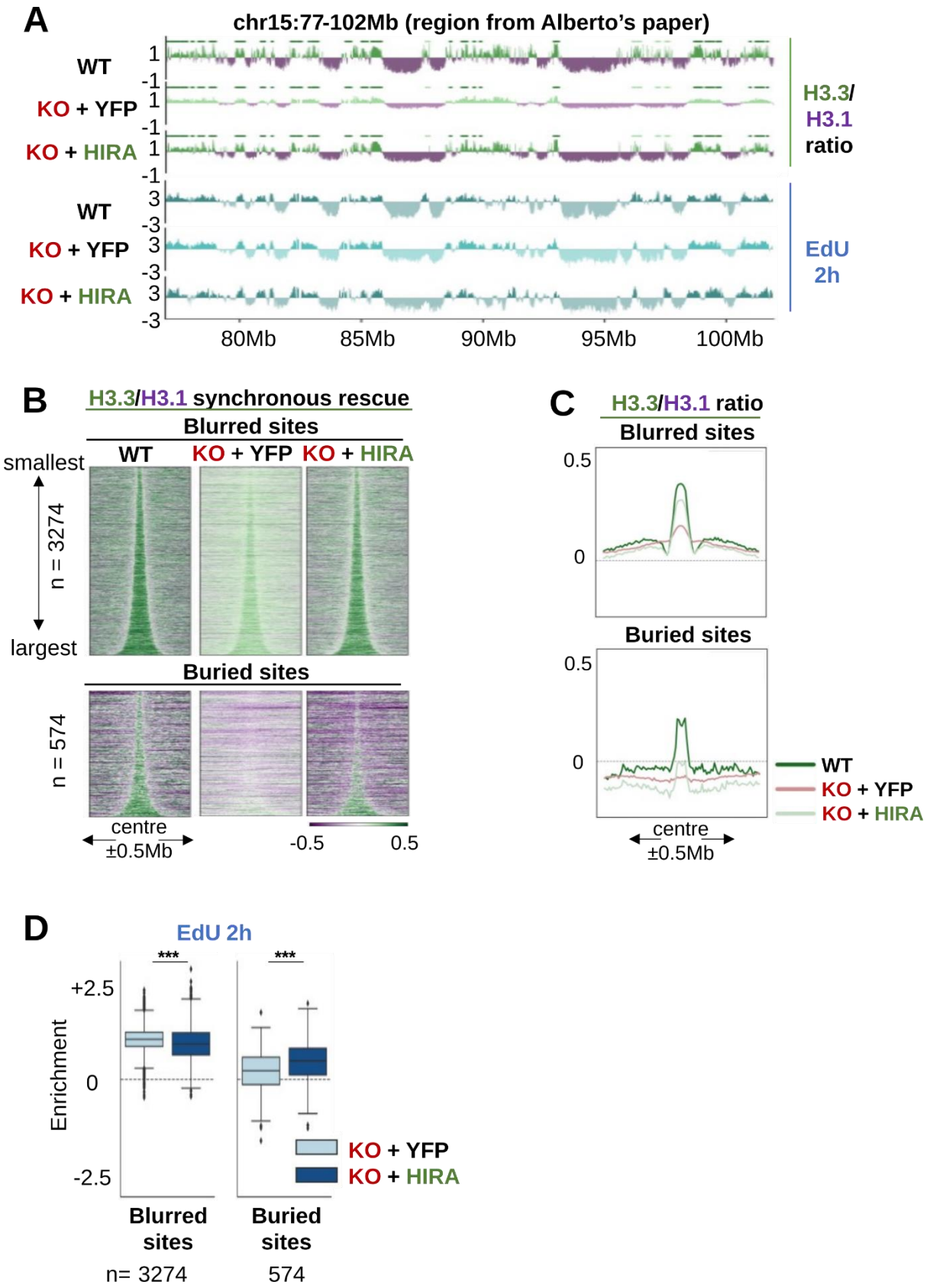

Supplementary Figure 7. HIRA rescue partially restores H3.3/H3.1 ratio at blurred and buried sites

A. H3.3/H3.1 ratio (top) and EdU 2h in S phase enrichment at a representative region (chr15:77-102Mb) from HIRA WT (as reference), and HIRA KO rescue with YFP (control) and HIRA plasmid.

B. H3.3/H3.1 ratio (G1/S-arrest) from HIRA WT (as reference), and HIRA KO rescue with YFP (control) and HIRA plasmid at blurred sites (top) and buried sites (bottom), centred at their middle ±0.5Mb and sorted by size.

C. Mean H3.3/H3.1 ratio (G1/S-arrest) at blurred (top) and buried (bottom) sites between 60-160kb in length, centred in their middle ±0.5Mb, is summarized in the bottom panel.

D. EdU from 2h release in S phase enrichment (z-score $\log_2$ IP/input) from HIRA KO cells transfected with YFP (control) or HIRA plasmid quantified at blurred and buried sites. Two-tailed Mann-Whitney U test adjusted for multiple testing by FDR (5% cut-off) was used to determine significance of differences between HIRA KO + YFP (control) and HIRA KO + HIRA rescue. Significance was noted as: * (p<=0.05), ** (p<=0.01), *** (p<=0.001).

EdU 2h S enrichment relative to input was calculated at 10kb bins as z-score of $\log_2$ IP/input.

Supplementary Figure 8

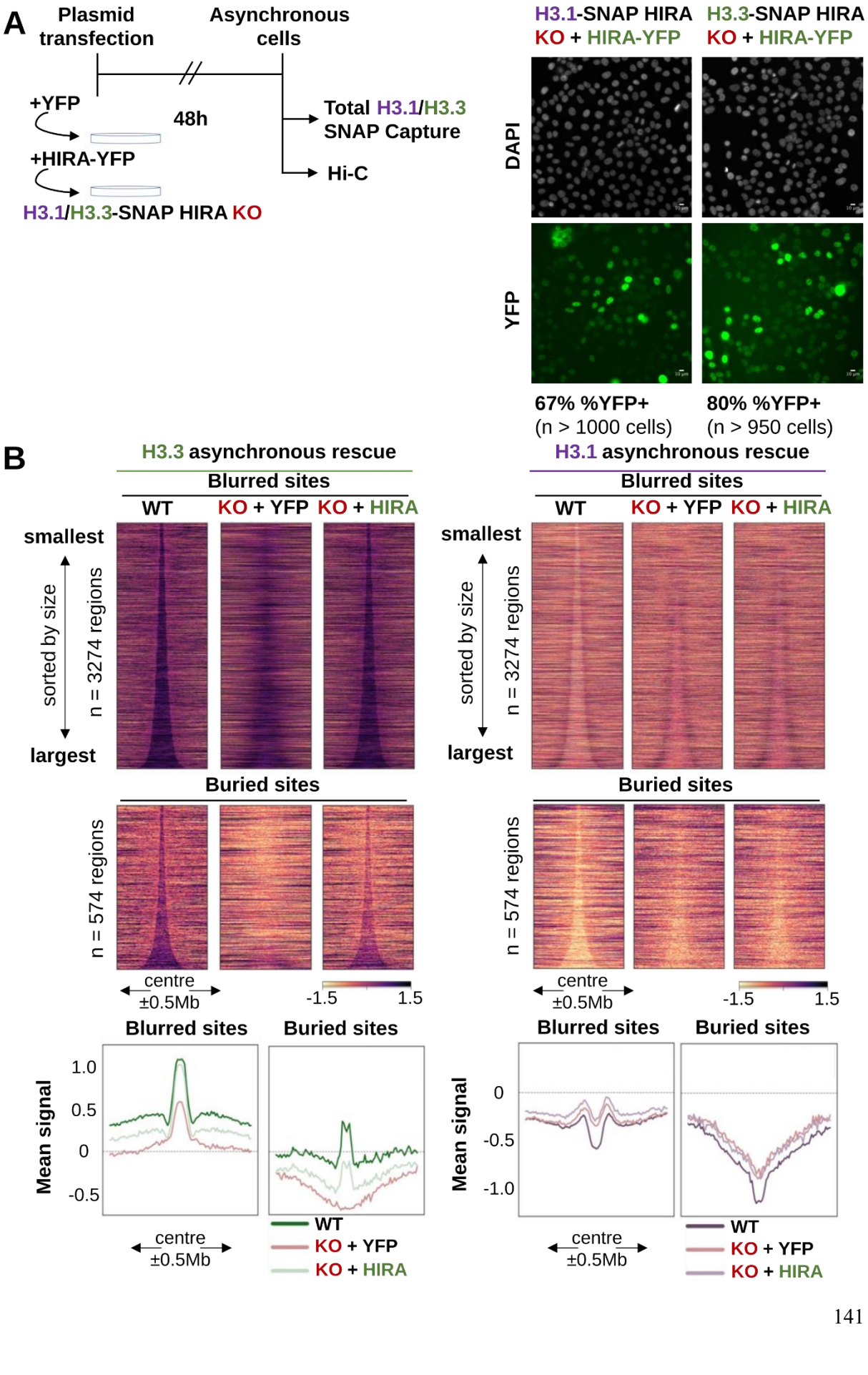

Supplementary Figure 8. HIRA rescue in asynchronous cells recovers H3.3 distribution at blurred and buried sites

A. Left: Scheme of experimental strategy to perform HIRA rescue in asynchronous cells to assay total H3.1/H3.3-SNAP by ChIP-seq and 3D genome organization by Hi-C.

Right: Representative images of DAPI (top) and YFP (HIRA-YFP) signal from asynchronous H3.1-SNAP and H3.3-SNAP cells transfected with HIRA-YFP 48h post-transfection. Transfection efficiency (% YFP+ cells) noted below.

B. H3.3 (left) and H3.1 (right) enrichment profiles from asynchronous HIRA WT (as reference) and HIRA KO cells transfected with YFP (control) or HIRA plasmid at blurred (top) and buried (middle) sites, sorted by size and centred at their middle. The mean signal at blurred and buried sites between 60-160kb in length is summarized in the bottom panel. Enrichment was calculated as z-score of $\log_2$ IP/input.

Supplementary Figure 9

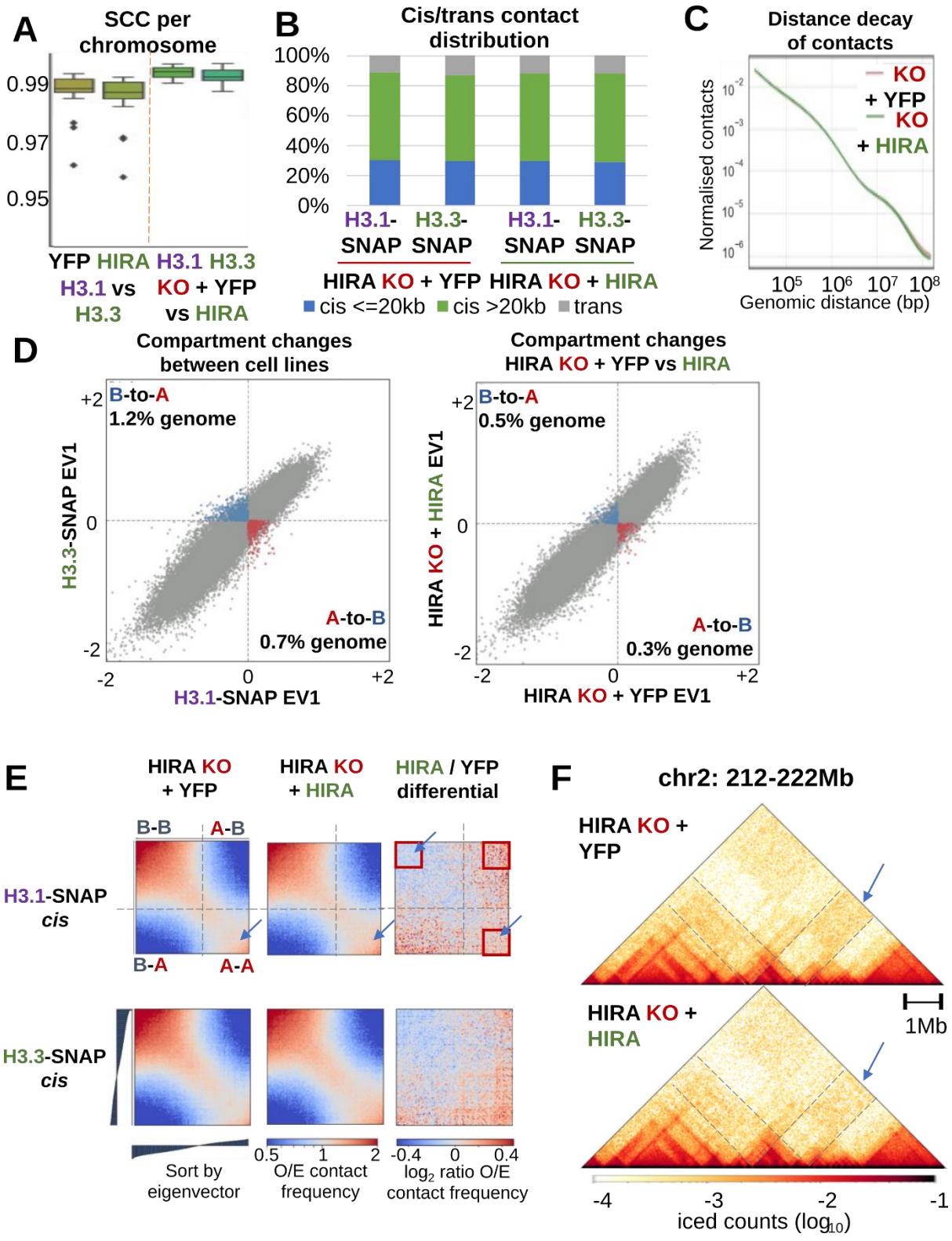

Supplementary Figure 9. HIRA rescue recovers A compartment interaction pattern, but does not reverse compartment switches

A. Matrix similarity between H3.1- and H3.3-SNAP HIRA KO cell lines per rescue (+YFP (control) / +HIRA) status and between HIRA KO + YFP (control) and + HIRA rescue per cell line measured by SCC (stratum-adjusted correlation coefficient) at 1Mb resolution.

B. Proportion of short-range (<=20kb), long-range (>20kb) *cis* and *trans* contacts from Hi-C maps of HIRA KO H3.1- and H3.3-SNAP HeLa cells transfected with YFP (control) or HIRA plasmid.

C. Decay of contact frequency with genomic distance (P(s) curves) from HIRA KO transfected with YFP (control, pink) and HIRA (light green) maps, binned at 10kb after masking of blacklisted regions and ICE normalization.

D. EV1 of 50kb-binned Hi-C matrices from H3.1- vs H3.3-SNAP HIRA KO + YFP cells (left) and from H3.1-SNAP HIRA KO + YFP vs KO + HIRA cells (right). Bins which change from A-to-B (lower right quadrant) or B-to-A (upper left quadrant) in the same direction in both conditions are coloured (red and blue, respectively) and quantified.

E. Saddle plots of observed/expected (O/E) interaction frequency based on EV1 percentiles from HIRA KO + YFP (control) and + HIRA and differential saddle plot (log_2 ratio) of HIRA KO + HIRA / YFP. Shown are H3.1- and H3.3-SNAP saddleplots in *cis*. Red squares denote the regions used for B-B (top left), A-A (bottom right) and A-B (top right) quantifications in Fig. 6D.

F. Hi-C maps at a representative region (chr2: 212-222Mb, cf Suppl. Fig. 4A). Grey vertical lines denote a cluster of buried sites which have regained H3.3 enrichment and increased EdU incorporation at 2h in S phase without switching back from B to A compartment upon rescue with HIRA.

Materials and Methods

Cell culture

We used HeLa cells stably expressing H3.1-SNAP-HA or H3.3-SNAP-HA which were either wild-type (WT, CRISPR/Cas9 GFP KO) or knock-out for HIRA (KO, CRISPR/Cas9 HIRA KO), as described in Ray-Gallet et al. (2018). Cell lines were tested negative for mycoplasma and grown as described in Ray-Gallet et al. (2018). We transfected cells plasmids expressing with YFP (control) or HIRA-YFP as in Ray-Gallet et al. (2018). We synchronized HeLa cells using a double thymidine block as described in Gatto et al. (2022). For synchronization of transfected cells (rescue experiments), we started the first thymidine block 6h after transfection.

Microscopy

To monitor replication, we performed 20 minutes EdU pulse in G1/S-synchronised and 2 hours released cells and detected EdU in cells with the Click-iT EdU Cell Proliferation kit as described in Gatto et al., 2022. We monitored transfection efficiency 48 hours after transfection by detecting YFP in cells after fixation for 15min with 2% PFA. Cells were co-stained with DAPI to label DNA. We imaged using a Zeiss Images Z1 fluorescence microscope with 63x and 40x oil objective lenses, ORCA-Flash4.0 LT camera (Hamamatsu) and MetaMorph software. We used ImageJ (Fiji) software for image visualization and analysis.

SNAP capture-seq, EdU-seq, and histone PTM ChIP-seq

We performed SNAP capture-seq and EdU-seq from native nucleosomes isolation as described in Gatto et al., 2022. For ChIP-seq of histone post-translational modifications (histone PTM ChIP-seq, antibodies in table below) we used the same procedure to prepare native nucleosomes but we used 5 million cells per IP and Dynabeads Protein A-conjugated antibodies against histone PTMs for immunoprecipitation. All steps were performed at 4°C and in the presence of Protease inhibitors (Roche) and 1mM TSA in every buffer to prevent protease and HDAC activity, respectively. For each IP reaction, we prepared 50uL of Ab-conjugated beads by blocking for 4 hours in Bead blocking buffer (2.5% BSA in PBS-T, 1mg/mL tRNA), washing once in 0.02% PBS-T and incubating for 15 minutes with the antibodies (diluted in 0.2mL 0.02% PBS-T) on a rotating wheel. Ab-conjugated beads were then washed twice with 0.02% PBS-T and resuspended in 0.2mL 0.02% PBS-T. Native nucleosomes (80uL per IP) from up to 3 samples were pooled, diluted in 5x volumes of Incubation buffer (50mM Tris-HCl pH 7.5, 100mM NaCl, 0.5% BSA) and pre-cleared by incubating with Dynabeads Protein A (15uL per input pool) for 30 min on a rotating wheel. We kept 20uL (1%) pre-cleared chromatin as input sample. We incubated the remaining (460uL/IP) with the Ab-conjugated beads (washed once in Incubation buffer) overnight on a rotating wheel. Beads were washed and DNA was purified from the IPed material as described for SNAP-seq in Gatto et al. (2022)A. Sequencing libraries were prepared at

the NGS (Next-Generation Sequencing) platform at Institut Curie with the Illumina TruSeq ChIP kit and sequenced on Illumina NovaSeq 6000 (PE100).

Antibodies used for native ChIP-seq			
Ab	**Source**	**Cat no.**	**Amount (ug)**
H3K4me1	Abcam	ab8895	4
H3K4me3	Active Motif	39915	4
H3K9me3	Active Motif	39765	10
H3K27ac	Active Motif	39133	5
H3K7me3	Active Motif	39155	5
rabbit IgG	Abcam	ab46540	5

Hi-C

We performed Hi-C using the Arima Hi-C+ kit following the manufacturer's instructions. Briefly, 5-10 million asynchronous HeLa cells per condition were fixed in 4% formaldehyde for 10min before quenching the reaction with Stop Solution 1. Fixed cells were washed in PBS and snap-frozen in liquid nitrogen at 1million cell aliquots. We performed cell and nuclear lysis, restriction enzyme digestion, end repair, biotinylation, ligation and decrosslinking as per manufacturer's instructions and proximally-ligated DNA was isolated using AMPure XP beads. Arima QC1 was performed and was successful for all samples. We sonicated DNA using Covaris E220 Evolution (100uL sample, 7°C, peak incident power: 105W, duty factor: 5%, cycles/burst: 200 for 100s), and fragmented DNA was size-selected using AMPure XP beads. We verified that the mean size of selected DNA was 400bp using Tapestation. After biotin enrichment, we performed library preparation using the KAPA HyperPrep kit, following the modified protocol described in the Arima Hi-C+ kit instructions. After ligation of Illumina TruSeq sequencing adaptors, we performed Arima QC2 (library quantification) to determine the number of amplification cycles for the library PCR using the KAPA Library Quantification Sample kit following the manufacturer's instructions. Amplified libraries were sequenced as described above.

Total cell extract preparation and Western Blot

Asynchronous HeLa cells were collected and snap-frozen at 1-3million cells per aliquot. We prepared total extracts by lysis of the cell pellet in 100uL RIPA buffer (150mM NaCl, 1% Triton X-100, 0.5% sodium deoxycholate, 0.1% SDS, 50mM Tris pH 8.0). We treated extract samples with universal nuclease (Pierce) immediately prior to reduction with the NuPAGE sample reducing agent and boiling. We performed electrophoresis on 4-12% Bis-Tris gels with MES SDS running buffer (Invitrogen) and blotting on nitrocellulose membranes (BIO-RAD). Primary antibodies were detected using horseradish peroxidase-conjugated secondary antibodies and Pico Chemiluminescent Substrate on a ChemiDoc Imager (Bio-Rad).

Sequencing data processing

Both in-house-generated and publicly available data was processed from raw reads in FASTQ format as described in Gatto et al., 2022. Briefly, for each sample, we mapped reads to the soft-masked human

reference genome (GRCh38) downloaded from ensembl using bowtie2 v2.3.4.2 (Langmead and Salzberg, 2012) with --very-sensitive parameters. We used SAMtools v1.9 to sort, flag duplicates and index bam files (Danecek et al., 2021). We used samtools view (-f 2 -F 3840 parameters to keep reads mapped in pairs and exclude QC fails, non-primary alignments and duplicates) to compute coverage over the genome as a BED file (chromosome, start, end, MAPQ), and then used BEDtools v2.27.1 (Quinlan and Hall, 2010) to calculate number of fragments in consecutive 1kb bins.

Analysis of the data was carried out by custom Python scripts using pandas v1.2.3 (McKinney, 2010), NumPy v1.21.5 (Harris et al., 2020) and scipy v1.7.3 (Virtanen et al., 2020). Visualization was performed using matplotlib v3.4.3 (Hunter, 2007) and seaborn v0.9.0 (Waskom, 2021). For each sample, counts at 1kb resolution were read, aggregated to 10kb bins, normalized to the total number of mapped counts to generate cpm (counts per million) and then normalized to matched input sample by computing a $\log_2$ ratio (IP/input). To enable cross-sample comparison, signal was then scaled and centered by computing a z-score per chromosome. The only exception to input-normalization and z-scoring was RNA-seq data, which was represented as $\log_2(\text{cpm} + 1)$.

Hi-C data processing

We used HiC-Pro (Servant et al., 2015) with default parameters (except MIN_MAPQ = 2) to generate raw count Hi-C matrices at 1Mb, 100kb, 50kb, 25kb, 10kb and 5kb resolution from raw FASTQ files for in-house and publicly available data (Wutz et al., 2017). First, we used MultiQC (Ewels et al., 2016) to perform quality control and extract the number of short-range (<=20kb), long-range (>20kb) *cis* and *trans* interactions for each sample. HiCExplorer (Ramírez et al., 2018; Wolff et al., 2020, 2018) was then used to convert matrices to cool format and to generate a single mcool file per sample, containing matrices at all resolutions listed above.

Matrices were visualized interactively with HiGlass (Kerpedjiev et al., 2018) at 1Mb and 100kb resolutions to be manually inspected for large inter- and intra-chromosomal aberrations (translocations, inversions, duplications, etc.), and the subsequently generated list of regions was merged with the set of blacklisted regions of the human genome (ensembl). This custom set of blacklisted regions was used to mask matrices prior to normalization by iterative correction (ICE, Imakaev et al., 2012) with a single iteration using cooler (Abdennur and Mirny, 2020). Matrix similarity was computed per chromosome at 1Mb, 100kb, 50kb and 10kb resolution with HiCRep (Lin et al., 2021; Yang et al., 2017) before and after masking, showing no substantial changes. Expected interactions per chromosome arm (coordinates downloaded with bioframe (Open2C et al., 2022)) were calculated using cooltools (Open 2C et al., 2022). P(s) curves, representing decay of interaction frequency with increasing genomic distance, were calculated per chromosome arm at 10kb resolution, aggregated and smoothed. Differential maps were plotted as $\log_2$ ratio of observed/expected (O/E) normalized contacts from HIRA KO/WT or HIRA KO

+ HIRA/YFP rescue at 1Mb resolution. Insulation score was computed from 10kb binned matrices with a window size of 100kb using cooltools.

Compartment analysis

Compartment analysis of Hi-C matrices was performed by eigenvector (EV) decomposition (Lieberman-Aiden et al., 2009) at 50kb resolution with cooltools using GC content track to orient the sign of the first eigenvector (EV1). A/B compartment domains were defined for each sample as contiguous segments of the genome with the same EV1 sign. Compartment switching was determined on a per bin basis, where a compartment-switching bin undergoes the same EV1 sign change in H3.1-SNAP and H3.3-SNAP cell lines, either from HIRA WT to KO (WT-to-KO) or HIRA KO + YFP to HIRA KO + HIRA rescue (YFP-to-HIRA). As control, we compared compartment switching between H3.1-SNAP and H3.3-SNAP cells in the same way. Proportion of the genome switching compartment was calculated as the % compartment-switching 50kb bins out of all non-masked 50kb bins.

To assess A/B compartment interactions, we performed saddle-plot analysis using cooltools. For this purpose, we split 50kb-binned EV1 signal into percentiles, re-ordered and averaged O/E-normalised Hi-C maps per chromosome arm from lowest (most strongly B) to highest (most strongly A) EV1 percentile and plotted O/E interaction frequency. To generate differential saddle-plots, we calculated the $\log_2$ ratio of HIRA KO/WT or HIRA KO + HIRA/YFP. To obtain the difference in intra- and inter-compartment interactions, we quantified the top 20 percentile EV1 (A-A), bottom 20 percentile EV1 (B-B), or top/bottom 20 percentile EV1 (A-B) as indicated by the red squares in Figure 2C.

H3.3 site analysis

The list of blurred (n = 3274) and buried (n = 574) site locations was retrieved from Gatto et al., 2022, and all sites were used when analyzing the SNAP capture-seq, EdU-seq, and histone PTM ChIP-seq experiments. After performing the masking required for the Hi-C analysis, we retained 2382 blurred and 439 buried sites that were used in downstream analysis. To assess compartment identity of the sites, we re-binned the EV1 signal to 10kb and we calculated the mean EV1 value from each sample. A/B compartment identity per condition was assigned only to sites where the compartment call from both H3.1- and H3.3-SNAP cells was the same, in order to avoid false positives when assessing compartment switching.

To determine compartment switches of the sites, we compared their compartment assignment between HIRA WT and KO (WT-to-KO) or HIRA KO + YFP to HIRA KO + HIRA rescue (YFP-to-HIRA). When focusing on the compartment switching buried sites from WT-to-KO and back from KO+YFP-to-HIRA rescue, we only analysed sites which had the same compartment assignment in KO and KO + YFP rescue (94% sites). As a control, we generated sets of random and random compartment-matched blurred and buried sites with the same size distribution by randomly sampling the genome. For random

compartment-matched sites, compartment was determined as described above to match the A/B compartment proportion of HIRA WT.

Quantifications and statistical analysis

Statistical analysis was performed in pyhton using statsmodels 0.13.2 (Seabold and Perktold, 2010). p-values were calculated by two-tailed Mann-Whitney U test. Multiple testing correction was performed by controlling the false discovery rate (FDR) using the Benjamini-Hochberg method. Differences with adjusted p-value <0.05 were considered statistically significant.

Author contributions

G.A conceived the overall strategy, supervised the work, and wrote the paper with T.K. T.K performed ChIP-seq, Hi-C and add-back experiments, their analysis, made figures and drafted the manuscript. J.P.Q contributed to the add-back experiments with A.F. A.F. contributed to replicate ChIP-seq experiments. A.G. supported development of initial analysis pipelines. M.M.-R. performed METALoci analysis. A.G. and L.M. provided advice for the analysis. Critical reading and discussion of data involved all authors.

Acknowledgements

We thank Sébastien Lemaire for critical reading of the Methods. We thank the members of UMR3664 and Almouzni team for helpful discussions. We acknowledge the Cell and Tissue Imaging Platform PICT-IBiSA (member of France-Bioimaging ANR-10-INBS-04) of the UMR3664 and ICGex NGS platform of the Institut Curie. This work benefited from fundings of the ERC-2015-ADG694694 ChromADICT to G.A, La Ligue Nationale contre le Cancer (labellisation and Grant No. TDLM23697), Labex DEEP-PSL (ANR-11LABEX-0044_DEEP, ANR-10-IDEX-0001-02). T.K benefited from an individual funding of H2020 MSCA-ITN – ChromDesign (Grant No. 813327).

References

Abdennur, N., Mirny, L.A., 2020. Cooler: scalable storage for Hi-C data and other genomically labeled arrays. Bioinformatics 36, 311–316. https://doi.org/10.1093/bioinformatics/btz540

Akerman, I., Kasaai, B., Bazarova, A., Sang, P.B., Peiffer, I., Artufel, M., Derelle, R., Smith, G., Rodriguez-Martinez, M., Romano, M., Kinet, S., Tino, P., Theillet, C., Taylor, N., Ballester, B., Méchali, M., 2020. A predictable conserved DNA base composition signature defines human core DNA replication origins. Nat. Commun. 11, 4826. https://doi.org/10.1038/s41467-020-18527-0

Armache, A., Yang, S., Martínez de Paz, A., Robbins, L.E., Durmaz, C., Cheong, J.Q., Ravishankar, A., Daman, A.W., Ahimovic, D.J., Klevorn, T., Yue, Y., Arslan, T., Lin, S., Panchenko, T., Hrit, J., Wang, M., Thudium, S., Garcia, B.A., Korb, E., Armache, K.-J., Rothbart, S.B., Hake, S.B., Allis, C.D., Li, H., Josefowicz, S.Z., 2020. Histone H3.3 phosphorylation amplifies stimulation-induced transcription. Nature 583, 852–857. https://doi.org/10.1038/s41586-020-2533-0

Banaszynski, L.A., Wen, D., Dewell, S., Whitcomb, S.J., Lin, M., Diaz, N., Elsässer, S.J., Chapgier, A., Goldberg, A.D., Canaani, E., Rafii, S., Zheng, D., Allis, C.D., 2013. Hira-Dependent Histone H3.3 Deposition Facilitates PRC2 Recruitment at Developmental Loci in ES Cells. Cell 155, 107–120. https://doi.org/10.1016/j.cell.2013.08.061

Barutcu, A.R., Blencowe, B.J., Rinn, J.L., 2019. Differential contribution of steady-state RNA and active transcription in chromatin organization. EMBO Rep. 20, e48068. https://doi.org/10.15252/embr.201948068

Bonev, B., Mendelson Cohen, N., Szabo, Q., Fritsch, L., Papadopoulos, G.L., Lubling, Y., Xu, X., Lv, X., Hugnot, J.-P., Tanay, A., Cavalli, G., 2017. Multiscale 3D Genome Rewiring during Mouse Neural Development. Cell 171, 557-572.e24. https://doi.org/10.1016/j.cell.2017.09.043

Brewer, B.J., Fangman, W.L., 1987. The localization of replication origins on ARS plasmids in S. cerevisiae. Cell 51, 463–471. https://doi.org/10.1016/0092-8674(87)90642-8

Cadoret, J.-C., Meisch, F., Hassan-Zadeh, V., Luyten, I., Guillet, C., Duret, L., Quesneville, H., Prioleau, M.-N., 2008. Genome-wide studies highlight indirect links between human replication origins and gene regulation. Proc. Natl. Acad. Sci. 105, 15837–15842. https://doi.org/10.1073/pnas.0805208105

Cayrou, C., Ballester, B., Peiffer, I., Fenouil, R., Coulombe, P., Andrau, J.-C., van Helden, J., Méchali, M., 2015. The chromatin environment shapes DNA replication origin organization and defines origin classes. Genome Res. 25, 1873–1885. https://doi.org/10.1101/gr.192799.115

Cayrou, C., Coulombe, P., Vigneron, A., Stanojcic, S., Ganier, O., Peiffer, I., Rivals, E., Puy, A., Laurent-Chabalier, S., Desprat, R., Méchali, M., 2011. Genome-scale analysis of metazoan replication origins reveals their organization in specific but flexible sites defined by conserved features. Genome Res. 21, 1438–1449. https://doi.org/10.1101/gr.121830.111

Cheloufi, S., Elling, U., Hopfgartner, B., Jung, Y.L., Murn, J., Ninova, M., Hubmann, M., Badeaux, A.I., Euong Ang, C., Tenen, D., Wesche, D.J., Abazova, N., Hogue, M., Tasdemir, N., Brumbaugh, J., Rathert, P., Jude, J., Ferrari, F., Blanco, A., Fellner, M., Wenzel, D., Zinner, M., Vidal, S.E., Bell, O., Stadtfeld, M., Chang, H.Y., Almouzni, G., Lowe, S.W., Rinn, J., Wernig, M., Aravin, A., Shi, Y., Park, P.J., Penninger, J.M., Zuber, J., Hochedlinger, K., 2015. The histone chaperone CAF-1 safeguards somatic cell identity. Nature 528, 218–224. https://doi.org/10.1038/nature15749

Clément, C., Orsi, G.A., Gatto, A., Boyarchuk, E., Forest, A., Hajj, B., Miné-Hattab, J., Garnier, M., Gurard-Levin, Z.A., Quivy, J.-P., Almouzni, G., 2018. High-resolution visualization of H3 variants during replication reveals their controlled recycling. Nat. Commun. 9, 3181. https://doi.org/10.1038/s41467-018-05697-1

Cornacchia, D., Dileep, V., Quivy, J.-P., Foti, R., Tili, F., Santarella-Mellwig, R., Antony, C., Almouzni, G., Gilbert, D.M., Buonomo, S.B.C., 2012. Mouse Rif1 is a key regulator of the replication-timing programme in mammalian cells: Mouse Rif1 controls replication timing. EMBO J. 31, 3678–3690. https://doi.org/10.1038/emboj.2012.214

Cremer, M., Brandstetter, K., Maiser, A., Rao, S.S.P., Schmid, V.J., Guirao-Ortiz, M., Mitra, N., Mamberti, S., Klein, K.N., Gilbert, D.M., Leonhardt, H., Cardoso, M.C., Aiden, E.L., Harz, H., Cremer, T., 2020. Cohesin depleted cells rebuild functional nuclear compartments after endomitosis. Nat. Commun. 11, 6146. https://doi.org/10.1038/s41467-020-19876-6

Daganzo, S.M., Erzberger, J.P., Lam, W.M., Skordalakes, E., Zhang, R., Franco, A.A., Brill, S.J., Adams, P.D., Berger, J.M., Kaufman, P.D., 2003. Structure and Function of the Conserved Core of Histone Deposition Protein Asf1. Curr. Biol. 13, 2148–2158. https://doi.org/10.1016/j.cub.2003.11.027

Danecek, P., Bonfield, J.K., Liddle, J., Marshall, J., Ohan, V., Pollard, M.O., Whitwham, A., Keane, T., McCarthy, S.A., Davies, R.M., Li, H., 2021. Twelve years of SAMtools and BCFtools. GigaScience 10, giab008. https://doi.org/10.1093/gigascience/giab008

Deaton, A.M., Gómez-Rodríguez, M., Mieczkowski, J., Tolstorukov, M.Y., Kundu, S., Sadreyev, R.I., Jansen, L.E., Kingston, R.E., 2016. Enhancer regions show high histone H3.3 turnover that changes during differentiation. eLife 5, e15316. https://doi.org/10.7554/eLife.15316

Dellino, G.I., Cittaro, D., Piccioni, R., Luzi, L., Banfi, S., Segalla, S., Cesaroni, M., Mendoza-Maldonado, R., Giacca, M., Pelicci, P.G., 2013. Genome-wide mapping of human DNA-replication origins: Levels of transcription at ORC1 sites regulate origin selection and replication timing. Genome Res. 23, 1–11. https://doi.org/10.1101/gr.142331.112
Dileep, V., Wilson, K.A., Marchal, C., Lyu, X., Zhao, P.A., Li, B., Poulet, A., Bartlett, D.A., Rivera-Mulia, J.C., Qin, Z.S., Robins, A.J., Schulz, T.C., Kulik, M.J., McCord, R.P., Dekker, J., Dalton, S., Corces, V.G., Gilbert, D.M., 2019. Rapid Irreversible Transcriptional Reprogramming in Human Stem Cells Accompanied by Discordance between Replication Timing and Chromatin Compartment. Stem Cell Rep. 13, 193–206. https://doi.org/10.1016/j.stemcr.2019.05.021
Drane, P., Ouararhni, K., Depaux, A., Shuaib, M., Hamiche, A., 2010. The death-associated protein DAXX is a novel histone chaperone involved in the replication-independent deposition of H3.3. Genes Dev. 24, 1253–1265. https://doi.org/10.1101/gad.566910
Du, Q., Smith, G.C., Luu, P.L., Ferguson, J.M., Armstrong, N.J., Caldon, C.E., Campbell, E.M., Nair, S.S., Zotenko, E., Gould, C.M., Buckley, M., Chia, K.-M., Portman, N., Lim, E., Kaczorowski, D., Chan, C.-L., Barton, K., Deveson, I.W., Smith, M.A., Powell, J.E., Skvortsova, K., Stirzaker, C., Achinger-Kawecka, J., Clark, S.J., 2021. DNA methylation is required to maintain both DNA replication timing precision and 3D genome organization integrity. Cell Rep. 36, 109722. https://doi.org/10.1016/j.celrep.2021.109722
Du, Z., Zheng, H., Huang, B., Ma, R., Wu, J., Zhang, Xianglin, He, J., Xiang, Y., Wang, Q., Li, Y., Ma, J., Zhang, Xu, Zhang, K., Wang, Y., Zhang, M.Q., Gao, J., Dixon, J.R., Wang, X., Zeng, J., Xie, W., 2017. Allelic reprogramming of 3D chromatin architecture during early mammalian development. Nature 547, 232–235. https://doi.org/10.1038/nature23263
Elsässer, S.J., Noh, K.-M., Diaz, N., Allis, C.D., Banaszynski, L.A., 2015. Histone H3.3 is required for endogenous retroviral element silencing in embryonic stem cells. Nature 522, 240–244. https://doi.org/10.1038/nature14345
Ewels, P., Magnusson, M., Lundin, S., Käller, M., 2016. MultiQC: summarize analysis results for multiple tools and samples in a single report. Bioinformatics 32, 3047–3048. https://doi.org/10.1093/bioinformatics/btw354
Feng, S., Ma, S., Li, K., Gao, S., Ning, S., Shang, J., Guo, Ruiyuan, Chen, Y., Blumenfeld, B., Simon, I., Li, Q., Guo, Rong, Xu, D., 2022. RIF1-ASF1-mediated high-order chromatin structure safeguards genome integrity. Nat. Commun. 13, 957. https://doi.org/10.1038/s41467-022-28588-y
Flyamer, I.M., Gassler, J., Imakaev, M., Brandão, H.B., Ulianov, S.V., Abdennur, N., Razin, S.V., Mirny, L.A., Tachibana-Konwalski, K., 2017. Single-nucleus Hi-C reveals unique chromatin reorganization at oocyte-to-zygote transition. Nature 544, 110–114. https://doi.org/10.1038/nature21711
Foti, R., Gnan, S., Cornacchia, D., Dileep, V., Bulut-Karslioglu, A., Diehl, S., Buness, A., Klein, F.A., Huber, W., Johnstone, E., Loos, R., Bertone, P., Gilbert, D.M., Manke, T., Jenuwein, T., Buonomo, S.C.B., 2016. Nuclear Architecture Organized by Rif1 Underpins the Replication-Timing Program. Mol. Cell 61, 260–273. https://doi.org/10.1016/j.molcel.2015.12.001
Gassler, J., Brandão, H.B., Imakaev, M., Flyamer, I.M., Ladstätter, S., Bickmore, W.A., Peters, J.-M., Mirny, L.A., Tachibana, K., 2017. A mechanism of cohesin-dependent loop extrusion organizes zygotic genome architecture. EMBO J. 36, 3600–3618. https://doi.org/10.15252/embj.201798083
Gatto, A., Forest, A., Quivy, J.-P., Almouzni, G., 2022. HIRA-dependent boundaries between H3 variants shape early replication in mammals. Mol. Cell S1097276522002556. https://doi.org/10.1016/j.molcel.2022.03.017
Giles, K.A., Lamm, N., Taberlay, P.C., Cesare, A.J., 2022. Three-dimensional chromatin organisation shapes origin activation and replication fork directionality (preprint). Bioinformatics. https://doi.org/10.1101/2022.06.24.497492
Goldberg, A.D., Banaszynski, L.A., Noh, K.-M., Lewis, P.W., Elsaesser, S.J., Stadler, S., Dewell, S., Law, M., Guo, X., Li, X., Wen, D., Chapgier, A., DeKelver, R.C., Miller, J.C., Lee, Y.-L., Boydston, E.A., Holmes, M.C., Gregory, P.D., Greally, J.M., Rafii, S., Yang, C., Scambler, P.J., Garrick, D., Gibbons, R.J., Higgs, D.R., Cristea, I.M., Urnov, F.D., Zheng, D., Allis, C.D., 2010. Distinct Factors Control Histone Variant H3.3 Localization at Specific Genomic Regions. Cell 140, 678–691. https://doi.org/10.1016/j.cell.2010.01.003
Hansen, R.S., Thomas, S., Sandstrom, R., Canfield, T.K., Thurman, R.E., Weaver, M., Dorschner, M.O., Gartler, S.M., Stamatoyannopoulos, J.A., 2010. Sequencing newly replicated DNA reveals widespread plasticity in human replication timing. Proc. Natl. Acad. Sci. 107, 139–144. https://doi.org/10.1073/pnas.0912402107
Harris, C.R., Millman, K.J., van der Walt, S.J., Gommers, R., Virtanen, P., Cournapeau, D., Wieser, E., Taylor, J., Berg, S., Smith, N.J., Kern, R., Picus, M., Hoyer, S., van Kerkwijk, M.H., Brett, M., Haldane, A., del Río, J.F., Wiebe, M., Peterson, P., Gérard-Marchant, P., Sheppard, K., Reddy, T., Weckesser, W., Abbasi, H., Gohlke, C., Oliphant, T.E., 2020. Array programming with NumPy. Nature 585, 357–362. https://doi.org/10.1038/s41586-020-2649-2
Hildebrand, E.M., Dekker, J., 2020. Mechanisms and Functions of Chromosome Compartmentalization. Trends Biochem. Sci. 45, 385–396. https://doi.org/10.1016/j.tibs.2020.01.002

Hsieh, T.-H.S., Cattoglio, C., Slobodyanyuk, E., Hansen, A.S., Rando, O.J., Tjian, R., Darzacq, X., 2020. Resolving the 3D Landscape of Transcription-Linked Mammalian Chromatin Folding. Mol. Cell 78, 539-553.e8. https://doi.org/10.1016/j.molcel.2020.03.002
Hu, Y., Stillman, B., 2023. Origins of DNA replication in eukaryotes. Mol. Cell S1097276522012035. https://doi.org/10.1016/j.molcel.2022.12.024
Huberman, J.A., Spotila, L.D., Nawotka, K.A., El-Assouli, S.M., Davis, L.R., 1987. The in vivo replication origin of the yeast 2μm plasmid. Cell 51, 473–481. https://doi.org/10.1016/0092-8674(87)90643-X
Hunter, J.D., 2007. Matplotlib: A 2D Graphics Environment. Comput. Sci. Eng. 9, 90–95. https://doi.org/10.1109/MCSE.2007.55
Imakaev, M., Fudenberg, G., McCord, R.P., Naumova, N., Goloborodko, A., Lajoie, B.R., Dekker, J., Mirny, L.A., 2012. Iterative correction of Hi-C data reveals hallmarks of chromosome organization. Nat. Methods 9, 999–1003. https://doi.org/10.1038/nmeth.2148
Ishiuchi, T., Abe, S., Inoue, K., Yeung, W.K.A., Miki, Y., Ogura, A., Sasaki, H., 2020. Reprogramming of the histone H3.3 landscape in the early mouse embryo. Nat. Struct. Mol. Biol. https://doi.org/10.1038/s41594-020-00521-1
Ishiuchi, T., Enriquez-Gasca, R., Mizutani, E., Bošković, A., Ziegler-Birling, C., Rodriguez-Terrones, D., Wakayama, T., Vaquerizas, J.M., Torres-Padilla, M.-E., 2015. Early embryonic-like cells are induced by downregulating replication-dependent chromatin assembly. Nat. Struct. Mol. Biol. 22, 662–671. https://doi.org/10.1038/nsmb.3066
Jiang, Y., Huang, J., Lun, K., Li, B., Zheng, H., Li, Y., Zhou, R., Duan, W., Wang, C., Feng, Y., Yao, H., Li, C., Ji, X., 2020. Genome-wide analyses of chromatin interactions after the loss of Pol I, Pol II, and Pol III. Genome Biol. 21, 158. https://doi.org/10.1186/s13059-020-02067-3
Jin, C., Zang, C., Wei, G., Cui, K., Peng, W., Zhao, K., Felsenfeld, G., 2009. H3.3/H2A.Z double variant–containing nucleosomes mark "nucleosome-free regions" of active promoters and other regulatory regions. Nat. Genet. 41, 941–945. https://doi.org/10.1038/ng.409
Jodkowska, K., Pancaldi, V., Rigau, M., Almeida, R., Fernández-Justel, J.M., Graña-Castro, O., Rodríguez-Acebes, S., Rubio-Camarillo, M., Carrillo-de Santa Pau, E., Pisano, D., Al-Shahrour, F., Valencia, A., Gómez, M., Méndez, J., 2022. 3D chromatin connectivity underlies replication origin efficiency in mouse embryonic stem cells. Nucleic Acids Res. gkac1111. https://doi.org/10.1093/nar/gkac1111
Kerpedjiev, P., Abdennur, N., Lekschas, F., McCallum, C., Dinkla, K., Strobelt, H., Luber, J.M., Ouellette, S.B., Azhir, A., Kumar, N., Hwang, J., Lee, S., Alver, B.H., Pfister, H., Mirny, L.A., Park, P.J., Gehlenborg, N., 2018. HiGlass: web-based visual exploration and analysis of genome interaction maps. Genome Biol. 19, 125. https://doi.org/10.1186/s13059-018-1486-1
Klein, K.N., Zhao, P.A., Lyu, X., Sasaki, T., Bartlett, D.A., Singh, A.M., Tasan, I., Zhang, M., Watts, L.P., Hiraga, S., Natsume, T., Zhou, X., Baslan, T., Leung, D., Kanemaki, M.T., Donaldson, A.D., Zhao, H., Dalton, S., Corces, V.G., Gilbert, D.M., 2021. Replication timing maintains the global epigenetic state in human cells 9.
Kruse, K., Díaz, N., Enriquez-Gasca, R., Gaume, X., Torres-Padilla, M.-E., Vaquerizas, J.M., 2019. Transposable elements drive reorganisation of 3D chromatin during early embryogenesis (preprint). Genomics. https://doi.org/10.1101/523712
Langmead, B., Salzberg, S.L., 2012. Fast gapped-read alignment with Bowtie 2. Nat. Methods 9, 357–359. https://doi.org/10.1038/nmeth.1923
Lieberman-Aiden, E., van Berkum, N.L., Williams, L., Imakaev, M., Ragoczy, T., Telling, A., Amit, I., Lajoie, B.R., Sabo, P.J., Dorschner, M.O., Sandstrom, R., Bernstein, B., Bender, M.A., Groudine, M., Gnirke, A., Stamatoyannopoulos, J., Mirny, L.A., Lander, E.S., Dekker, J., 2009. Comprehensive Mapping of Long-Range Interactions Reveals Folding Principles of the Human Genome. Science 326, 289–293. https://doi.org/10.1126/science.1181369
Lin, D., Sanders, J., Noble, W.S., 2021. HiCRep.py : Fast comparison of Hi-C contact matrices in Python 3.
Long, H., Zhang, L., Lv, M., Wen, Z., Zhang, W., Chen, X., Zhang, P., Li, T., Chang, L., Jin, C., Wu, G., Wang, X., Yang, F., Pei, J., Chen, P., Margueron, R., Deng, H., Zhu, M., Li, G., 2020. H2A.Z facilitates licensing and activation of early replication origins. Nature 577, 576–581. https://doi.org/10.1038/s41586-019-1877-9
Loyola, A., Bonaldi, T., Roche, D., Imhof, A., Almouzni, G., 2006. PTMs on H3 Variants before Chromatin Assembly Potentiate Their Final Epigenetic State. Mol. Cell 24, 309–316. https://doi.org/10.1016/j.molcel.2006.08.019
MacAlpine, H.K., Gordân, R., Powell, S.K., Hartemink, A.J., MacAlpine, D.M., 2010. *Drosophila* ORC localizes to open chromatin and marks sites of cohesin complex loading. Genome Res. 20, 201–211. https://doi.org/10.1101/gr.097873.109
Martire, S., Gogate, A.A., Whitmill, A., Tafessu, A., Nguyen, J., Teng, Y.-C., Tastemel, M., Banaszynski, L.A., 2019. Phosphorylation of histone H3.3 at serine 31 promotes p300 activity and enhancer acetylation. Nat. Genet. 51, 941–946. https://doi.org/10.1038/s41588-019-0428-5

Maze, I., Wenderski, W., Noh, K.-M., Bagot, R.C., Tzavaras, N., Purushothaman, I., Elsässer, S.J., Guo, Y., Ionete, C., Hurd, Y.L., Tamminga, C.A., Halene, T., Farrelly, L., Soshnev, A.A., Wen, D., Rafii, S., Birtwistle, M.R., Akbarian, S., Buchholz, B.A., Blitzer, R.D., Nestler, E.J., Yuan, Z.-F., Garcia, B.A., Shen, L., Molina, H., Allis, C.D., 2015. Critical Role of Histone Turnover in Neuronal Transcription and Plasticity. Neuron 87, 77–94. https://doi.org/10.1016/j.neuron.2015.06.014
McKinney, W., 2010. Data Structures for Statistical Computing in Python. Presented at the Python in Science Conference, Austin, Texas, pp. 56–61. https://doi.org/10.25080/Majora-92bf1922-00a
Méchali, M., 2010. Eukaryotic DNA replication origins: many choices for appropriate answers. Nat. Rev. Mol. Cell Biol. 11, 728–738. https://doi.org/10.1038/nrm2976
Miotto, B., Ji, Z., Struhl, K., 2016. Selectivity of ORC binding sites and the relation to replication timing, fragile sites, and deletions in cancers. Proc. Natl. Acad. Sci. 113. https://doi.org/10.1073/pnas.1609060113
Mito, Y., Henikoff, J.G., Henikoff, S., 2005. Genome-scale profiling of histone H3.3 replacement patterns. Nat. Genet. 37, 1090–1097. https://doi.org/10.1038/ng1637
Miura, H., Takahashi, S., Poonperm, R., Tanigawa, A., Takebayashi, S., Hiratani, I., 2019. Single-cell DNA replication profiling identifies spatiotemporal developmental dynamics of chromosome organization. Nat. Genet. 51, 1356–1368. https://doi.org/10.1038/s41588-019-0474-z
Morozov, V.M., Riva, A., Sarwar, S., Kim, W., Li, J., Zhou, L., Licht, J.D., Daaka, Y., Ishov, A.M., 2023. HIRA-mediated loading of histone variant H3.3 controls androgen-induced transcription by regulation of AR/BRD4 complex assembly at enhancers (preprint). Molecular Biology. https://doi.org/10.1101/2023.05.08.536256
Mota-Gómez, I., Rodríguez, J.A., Dupont, S., Lao, O., Jedamzick, J., Kuhn, R., Lacadie, S., García-Moreno, S.A., Hurtado, A., Acemel, R.D., Capel, B., Marti-Renom, M.A., Lupiáñez, D.G., 2022. Sex-determining 3D regulatory hubs revealed by genome spatial auto-correlation analysis (preprint). Developmental Biology. https://doi.org/10.1101/2022.11.18.516861
Nakatani, T., Lin, J., Ji, F., Ettinger, A., Pontabry, J., Tokoro, M., Altamirano-Pacheco, L., Fiorentino, J., Mahammadov, E., Hatano, Y., Van Rechem, C., Chakraborty, D., Ruiz-Morales, E.R., Arguello Pascualli, P.Y., Scialdone, A., Yamagata, K., Whetstine, J.R., Sadreyev, R.I., Torres-Padilla, M.-E., 2022. DNA replication fork speed underlies cell fate changes and promotes reprogramming. Nat. Genet. https://doi.org/10.1038/s41588-022-01023-0
Open 2C, Abdennur, N., Abraham, S., Fudenberg, G., Flyamer, I.M., Galitsyna, A.A., Goloborodko, A., Imakaev, M., Oksuz, B.A., Venev, S.V., 2022. Cooltools: enabling high-resolution Hi-C analysis in Python (preprint). Bioinformatics. https://doi.org/10.1101/2022.10.31.514564
Open2C, Abdennur, N., Fudenberg, G., Flyamer, I., Galitsyna, A.A., Goloborodko, A., Imakaev, M., Venev, S.V., 2022. Bioframe: Operations on Genomic Intervals in Pandas Dataframes (preprint). Bioinformatics. https://doi.org/10.1101/2022.02.16.480748
Petryk, N., Kahli, M., d'Aubenton-Carafa, Y., Jaszczyszyn, Y., Shen, Y., Silvain, M., Thermes, C., Chen, C.-L., Hyrien, O., 2016. Replication landscape of the human genome. Nat. Commun. 7, 10208. https://doi.org/10.1038/ncomms10208
Pope, B.D., Ryba, T., Dileep, V., Yue, F., Wu, W., Denas, O., Vera, D.L., Wang, Y., Hansen, R.S., Canfield, T.K., Thurman, R.E., Cheng, Y., Gülsoy, G., Dennis, J.H., Snyder, M.P., Stamatoyannopoulos, J.A., Taylor, J., Hardison, R.C., Kahveci, T., Ren, B., Gilbert, D.M., 2014. Topologically associating domains are stable units of replication-timing regulation. Nature 515, 402–405. https://doi.org/10.1038/nature13986
Quinlan, A.R., Hall, I.M., 2010. BEDTools: a flexible suite of utilities for comparing genomic features. Bioinformatics 26, 841–842. https://doi.org/10.1093/bioinformatics/btq033
Ramírez, F., Bhardwaj, V., Arrigoni, L., Lam, K.C., Grüning, B.A., Villaveces, J., Habermann, B., Akhtar, A., Manke, T., 2018. High-resolution TADs reveal DNA sequences underlying genome organization in flies. Nat. Commun. 9, 189. https://doi.org/10.1038/s41467-017-02525-w
Ray-Gallet, D., Ricketts, M.D., Sato, Y., Gupta, K., Boyarchuk, E., Senda, T., Marmorstein, R., Almouzni, G., 2018. Functional activity of the H3.3 histone chaperone complex HIRA requires trimerization of the HIRA subunit. Nat. Commun. 9, 3103. https://doi.org/10.1038/s41467-018-05581-y
Ray-Gallet, D., Woolfe, A., Vassias, I., Pellentz, C., Lacoste, N., Puri, A., Schultz, D.C., Pchelintsev, N.A., Adams, P.D., Jansen, L.E.T., Almouzni, G., 2011. Dynamics of Histone H3 Deposition In Vivo Reveal a Nucleosome Gap-Filling Mechanism for H3.3 to Maintain Chromatin Integrity. Mol. Cell 44, 928–941. https://doi.org/10.1016/j.molcel.2011.12.006
Rhind, N., Yang, S.C.-H., Bechhoefer, J., 2010. Reconciling stochastic origin firing with defined replication timing. Chromosome Res. 18, 35–43. https://doi.org/10.1007/s10577-009-9093-3
Rivera-Mulia, J.C., Buckley, Q., Sasaki, T., Zimmerman, J., Didier, R.A., Nazor, K., Loring, J.F., Lian, Z., Weissman, S., Robins, A.J., Schulz, T.C., Menendez, L., Kulik, M.J., Dalton, S., Gabr, H., Kahveci, T., Gilbert, D.M., 2015. Dynamic changes in replication timing and gene expression during lineage specification of human pluripotent stem cells. Genome Res. 25, 1091–1103. https://doi.org/10.1101/gr.187989.114

Roberts, C., Sutherland, H.F., Farmer, H., Kimber, W., Halford, S., Carey, A., Brickman, J.M., Wynshaw-Boris, A., Scambler, P.J., 2002. Targeted Mutagenesis of the Hira Gene Results in Gastrulation Defects and Patterning Abnormalities of Mesoendodermal Derivatives Prior to Early Embryonic Lethality. Mol. Cell. Biol. 22, 2318–2328. https://doi.org/10.1128/MCB.22.7.2318-2328.2002
Seabold, S., Perktold, J., 2010. Statsmodels: Econometric and Statistical Modeling with Python. Proc. 9th Python Sci. Conf. 92–96. https://doi.org/10.25080/Majora-92bf1922-011
Servant, N., Varoquaux, N., Lajoie, B.R., Viara, E., Chen, C.-J., Vert, J.-P., Heard, E., Dekker, J., Barillot, E., 2015. HiC-Pro: an optimized and flexible pipeline for Hi-C data processing. Genome Biol. 16, 259. https://doi.org/10.1186/s13059-015-0831-x
Sima, J., Chakraborty, A., Dileep, V., Michalski, M., Klein, K.N., Holcomb, N.P., Turner, J.L., Paulsen, M.T., Rivera-Mulia, J.C., Trevilla-Garcia, C., Bartlett, D.A., Zhao, P.A., Washburn, B.K., Nora, E.P., Kraft, K., Mundlos, S., Bruneau, B.G., Ljungman, M., Fraser, P., Ay, F., Gilbert, D.M., 2019. Identifying cis Elements for Spatiotemporal Control of Mammalian DNA Replication. Cell 176, 816-830.e18. https://doi.org/10.1016/j.cell.2018.11.036
Spracklin, G., Abdennur, N., Imakaev, M., Chowdhury, N., Pradhan, S., Mirny, L.A., Dekker, J., 2022. Diverse silent chromatin states modulate genome compartmentalization and loop extrusion barriers. Nat. Struct. Mol. Biol. https://doi.org/10.1038/s41594-022-00892-7
Sugimoto, N., Maehara, K., Yoshida, K., Ohkawa, Y., Fujita, M., 2018. Genome-wide analysis of the spatiotemporal regulation of firing and dormant replication origins in human cells. Nucleic Acids Res. 46, 6683–6696. https://doi.org/10.1093/nar/gky476
Tafessu, A., O'Hara, R., Martire, S., Dube, A.L., Saha, P., Gant, V.U., Banaszynski, L.A., 2023. H3.3 contributes to chromatin accessibility and transcription factor binding at promoter-proximal regulatory elements in embryonic stem cells. Genome Biol. 24, 25. https://doi.org/10.1186/s13059-023-02867-3
Tagami, H., Ray-Gallet, D., Almouzni, G., Nakatani, Y., 2004. Histone H3.1 and H3.3 Complexes Mediate Nucleosome Assembly Pathways Dependent or Independent of DNA Synthesis. Cell 116, 51–61. https://doi.org/10.1016/S0092-8674(03)01064-X
Tang, M., Chen, Z., Wang, C., Feng, X., Lee, N., Huang, M., Zhang, H., Li, S., Xiong, Y., Chen, J., 2022. Histone chaperone ASF1 acts with RIF1 to promote DNA end joining in BRCA1-deficient cells. J. Biol. Chem. 298, 101979. https://doi.org/10.1016/j.jbc.2022.101979
Torné, J., Ray-Gallet, D., Boyarchuk, E., Garnier, M., Le Baccon, P., Coulon, A., Orsi, G.A., Almouzni, G., 2020. Two HIRA-dependent pathways mediate H3.3 de novo deposition and recycling during transcription. Nat. Struct. Mol. Biol. 27, 1057–1068. https://doi.org/10.1038/s41594-020-0492-7
Udugama, M., Vinod, B., Chan, F.L., Hii, L., Garvie, A., Collas, P., Kalitsis, P., Steer, D., Das, P.P., Tripathi, P., Mann, J.R., Voon, H.P.J., Wong, L.H., 2022. Histone H3.3 phosphorylation promotes heterochromatin formation by inhibiting H3K9/K36 histone demethylase. Nucleic Acids Res. gkac259. https://doi.org/10.1093/nar/gkac259
Van Rechem, C., Ji, F., Chakraborty, D., Black, J.C., Sadreyev, R.I., Whetstine, J.R., 2021. Collective regulation of chromatin modifications predicts replication timing during cell cycle. Cell Rep. 37, 109799. https://doi.org/10.1016/j.celrep.2021.109799
Virtanen, P., Gommers, R., Oliphant, T.E., Haberland, M., Reddy, T., Cournapeau, D., Burovski, E., Peterson, P., Weckesser, W., Bright, J., van der Walt, S.J., Brett, M., Wilson, J., Millman, K.J., Mayorov, N., Nelson, A.R.J., Jones, E., Kern, R., Larson, E., Carey, C.J., Polat, İ., Feng, Y., Moore, E.W., VanderPlas, J., Laxalde, D., Perktold, J., Cimrman, R., Henriksen, I., Quintero, E.A., Harris, C.R., Archibald, A.M., Ribeiro, A.H., Pedregosa, F., van Mulbregt, P., 2020. SciPy 1.0: fundamental algorithms for scientific computing in Python. Nat. Methods 17, 261–272. https://doi.org/10.1038/s41592-019-0686-2
Vouzas, A.E., Gilbert, D.M., 2021. Mammalian DNA Replication Timing. DNA Replication 23.
Wang, X., Wang, L., Dou, J., Yu, T., Cao, P., Fan, N., Borjigin, U., Nashun, B., 2021. Distinct role of histone chaperone Asf1a and Asf1b during fertilization and pre-implantation embryonic development in mice. Epigenetics Chromatin 14, 55. https://doi.org/10.1186/s13072-021-00430-7
Waskom, M.L., 2021. seaborn: statistical data visualization. J. Open Source Softw. 6, 3021. https://doi.org/10.21105/joss.03021
Wen, D., Banaszynski, L.A., Liu, Y., Geng, F., Noh, K.-M., Xiang, J., Elemento, O., Rosenwaks, Z., Allis, C.D., Rafii, S., 2014a. Histone variant H3.3 is an essential maternal factor for oocyte reprogramming. Proc. Natl. Acad. Sci. 111, 7325–7330. https://doi.org/10.1073/pnas.1406389111
Wen, D., Banaszynski, L.A., Rosenwaks, Z., Allis, C.D., Rafii, S., 2014b. H3.3 replacement facilitates epigenetic reprogramming of donor nuclei in somatic cell nuclear transfer embryos. Nucleus 5, 369–375. https://doi.org/10.4161/nucl.36231
Wolff, J., Bhardwaj, V., Nothjunge, S., Richard, G., Renschler, G., Gilsbach, R., Manke, T., Backofen, R., Ramírez, F., Grüning, B.A., 2018. Galaxy HiCExplorer: a web server for reproducible Hi-C data analysis, quality control and visualization. Nucleic Acids Res. 46, W11–W16. https://doi.org/10.1093/nar/gky504

Wolff, J., Rabbani, L., Gilsbach, R., Richard, G., Manke, T., Backofen, R., Grüning, B.A., 2020. Galaxy HiCExplorer 3: a web server for reproducible Hi-C, capture Hi-C and single-cell Hi-C data analysis, quality control and visualization. Nucleic Acids Res. 48, W177–W184. https://doi.org/10.1093/nar/gkaa220
Wutz, G., Várnai, C., Nagasaka, K., Cisneros, D.A., Stocsits, R.R., Tang, W., Schoenfelder, S., Jessberger, G., Muhar, M., Hossain, M.J., Walther, N., Koch, B., Kueblbeck, M., Ellenberg, J., Zuber, J., Fraser, P., Peters, J., 2017. Topologically associating domains and chromatin loops depend on cohesin and are regulated by CTCF, WAPL, and PDS5 proteins. EMBO J. 36, 3573–3599. https://doi.org/10.15252/embj.201798004
Xie, L., Dong, P., Qi, Y., Hsieh, T.-H.S., English, B.P., Jung, S., Chen, X., De Marzio, M., Casellas, R., Chang, H.Y., Zhang, B., Tjian, R., Liu, Z., 2022. BRD2 compartmentalizes the accessible genome. Nat. Genet. 54, 481–491. https://doi.org/10.1038/s41588-022-01044-9
Yamazaki, S., Ishii, A., Kanoh, Y., Oda, M., Nishito, Y., Masai, H., 2012. Rif1 regulates the replication timing domains on the human genome: Rif1 regulates the replication timing domains. EMBO J. 31, 3667–3677. https://doi.org/10.1038/emboj.2012.180
Yang, T., Zhang, F., Yardımcı, G.G., Song, F., Hardison, R.C., Noble, W.S., Yue, F., Li, Q., 2017. HiCRep: assessing the reproducibility of Hi-C data using a stratum-adjusted correlation coefficient. Genome Res. 27, 1939–1949. https://doi.org/10.1101/gr.220640.117
Yang, Y., Zhang, L., Xiong, C., Chen, J., Wang, L., Wen, Z., Yu, J., Chen, P., Xu, Y., Jin, J., Cai, Y., Li, G., 2021. HIRA complex presets transcriptional potential through coordinating depositions of the histone variants H3.3 and H2A.Z on the poised genes in mESCs. Nucleic Acids Res. gkab1221. https://doi.org/10.1093/nar/gkab1221
Zenk, F., Zhan, Y., Kos, P., Löser, E., Atinbayeva, N., Schächtle, M., Tiana, G., Giorgetti, L., Iovino, N., 2021. HP1 drives de novo 3D genome reorganization in early Drosophila embryos. Nature. https://doi.org/10.1038/s41586-021-03460-z
Zhang, R., Poustovoitov, M.V., Ye, X., Santos, H.A., Chen, W., Daganzo, S.M., Erzberger, J.P., Serebriiskii, I.G., Canutescu, A.A., Dunbrack, R.L., Pehrson, J.R., Berger, J.M., Kaufman, P.D., Adams, P.D., 2005. Formation of MacroH2A-Containing Senescence-Associated Heterochromatin Foci and Senescence Driven by ASF1a and HIRA. Dev. Cell 8, 19–30. https://doi.org/10.1016/j.devcel.2004.10.019

Additional results

With the results included in the manuscript, we were able to answer a series of questions concerning the role of the balance of histone H3 variants with respect to higher-order chromatin folding, replication initiation, and the interplay between them. We demonstrated that, on the Mb scale, HIRA-mediated H3.3 enrichment at active regions is important for their organisation in compartments independently of histone marks. We also showed, on the sub-Mb scale, HIRA was required to maintain A compartment identity of early IZs in the absence of transcription in addition to its key role in ensuring their early firing. Finally, we revealed the importance of HIRA in early IZ definition is not dependent on their compartmental organization.

The importance of H3.3 deposition by HIRA for active compartment interactions indicated that the dynamics of histone variants and not just their presence or modifications should be considered when trying to understand the processes underlying chromatin segregation on the Mb scale. However, we could not detect an impact of HIRA on sub-Mb scale organization, suggesting loop extrusion is the dominant process on this scale. To investigate this further, I identified TADs and profiled the enrichment of H3 variants from HIRA WT and KO cells. To better understand the link with early initiation, I also examined the distribution of early origins of replication and nascent synthesis in early S phase. Continuing the investigation of the organization of H3 variants across scales and their link to genome function, I identified peaks of active marks from the ChIP-seq I performed and characterized the changes in modifications and H3.3 in the absence of HIRA. Finally, I wanted to explore how H3 variants behave with respect to 3D chromatin folding in the context of differentiation. To address this question, I carried out the same analysis strategy in mouse ESC and *in vitro* differentiated neural progenitor cells (NPC) using unique H3 variant-specific SNAP-seq generated in the team and publicly available Hi-C data (Bonev et al., 2017). These results bring valuable information for discussion and provide insights for a better understanding of the importance of H3 variants in multi-scale chromatin organization.

H3 variant pattern and early firing are disrupted at TAD borders without impairing their strength or position

To better understand the relationship between H3 variant distribution and sub-Mb scale chromatin organization, we identified TADs from HIRA WT Hi-C maps at 10kb resolution using the insulation score metric (Manuscript, Supplementary Figure 5C) (Crane et al., 2015). TAD border positions aligned well (>90%, +/-20kb) between the H3.1- and H3.3-SNAP cell lines, allowing us to confidently profile the distribution of H3.1 and H3.3. As we had previously shown that the variants had compartment-specific enrichment (Manuscript, Figure 1, Supplementary Figure 1), we focused on TAD borders within A (Figure 26A, top) or B compartments (Figure 26A, bottom) to avoid biases from A/B transitions. This analysis revealed that in compartment A, H3.3 has a specific peak at TAD borders in

addition to its generally high levels (Figure 26A, right). In compartment B, H3.3 was generally depleted and showed a very small increase at TAD borders, whereas H3.1 was specifically depleted there. These H3 variant patters may stem from the binding of proteins like CTCF and RNAPII at TAD borders (Dixon et al., 2012), but it is unclear whether they are important for function. To address this issue, we mapped the enrichment of H3.1 and H3.3 from HIRA KO cells at TAD borders. This revealed the peak of H3.3 at TAD borders was blurred in compartment A and lost in compartment B, accompanied by blurring of the H3.1 depletion at compartment B TAD borders (Figure 26A, right). These results were consistent with the blurring of individual H3.3 peaks within active regions (blurred sites) and loss of individual H3.3 peaks in inactive regions (buried sites) we had previously documented (Gatto et al., 2022).

To examine the impact of H3 variant redistribution at TAD borders, we also called TADs from HIRA KO cells. TAD borders overlap between HIRA WT and KO was as good as between H3.1- and H3.3-SNAP cell lines (>90%, +/-20kb), indicating the absence of HIRA did not impact the sub-Mb folding of the genome into TADs. As the major characteristic of TAD borders is the insulation of contacts between neighbouring domains, we also investigated the insulation score distribution specifically at TAD borders (Figure 26A). This analysis revealed that TAD borders in both A (Figure 26A, top) and B compartments (Figure 26A, bottom) maintained their strength, confirming HIRA did not affect their function. Thus, H3 variant balance does not contribute to sub-Mb scale chromatin organization.

TAD borders have been reported to be enriched in origins of replication (Akerman et al., 2020; Murat et al., 2022; Petryk et al., 2016), but it remains unclear if this may be functionally relevant. We addressed this question in our model by investigating the defect in early firing in the absence of HIRA with respect to TAD borders. First, we confirmed that previously-mapped origins of replication were enriched at the TAD borders we identified in our cells (Figure 27A). We used a set of ‘core’ origins, detected by SNS-seq (Table 4) and showing high (top 20%) efficiency across several human cell lines (Akerman et al., 2020) and ‘constitutive’ origins, identified by ini-seq2 (Table 4), which fire early and overlap well (>72%) with the set of ‘core’ origins (Murat et al., 2022). Both core and constitutive origins were enriched at TAD borders in compartment A (Figure 27A, top) and also at B (Figure 27A, bottom), although more weakly. Examining nascent DNA incorporation in early S in WT cells showed that at 2h in S phase, TAD borders in compartment A have already replicated prior to the TAD interior (weak depletion of EdU 2h at borders relative to interior, which is enriched in EdU 2h signal, Figure 27B, left). In compartment B, initiation was observed only at few TAD borders and domains were not replicating yet. This was consistent with previous work showing A compartments typically replicate in early, whereas B in late S phase (Pope et al., 2014). In the absence of HIRA, early initiation was delayed, reflected by the elevated levels of EdU 2h at compartment A TAD borders and their decrease in compartment B (Figure 27B, right). These data indicate that early initiation at TAD borders is impaired

upon disruption of the H3 variant balance without affecting border strength or position. Thus, sub-Mb scale level of organization is not sufficient to promote early initiation at origins found at TAD borders.

Figure 26

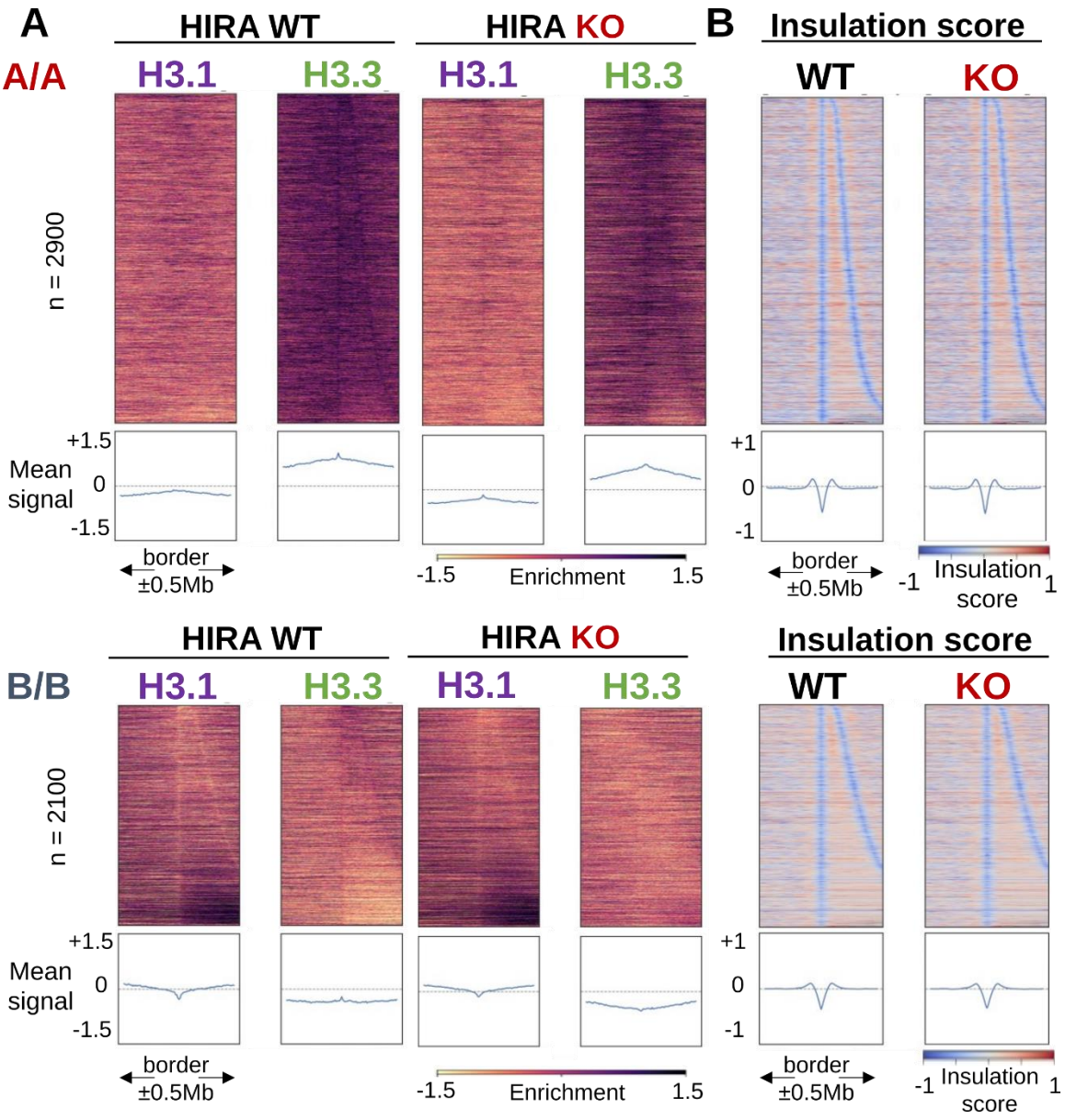

Figure 26. HIRA KO disrupts H3 variant pattern at TAD borders without affecting their strength

A. Total H3.1 and H3.3 enrichment (z-score of $\log_2$ IP/input) at 10kb bins from G1/S-arrested cells at TAD borders between A/A (top) and B/B (bottom) compartments from HIRA WT (left) and KO (right) cells. TADs are sorted by size and centred at their start border ±0.5Mb.

B. Insulation score plotted at the same regions as in **A.**

Figure 27

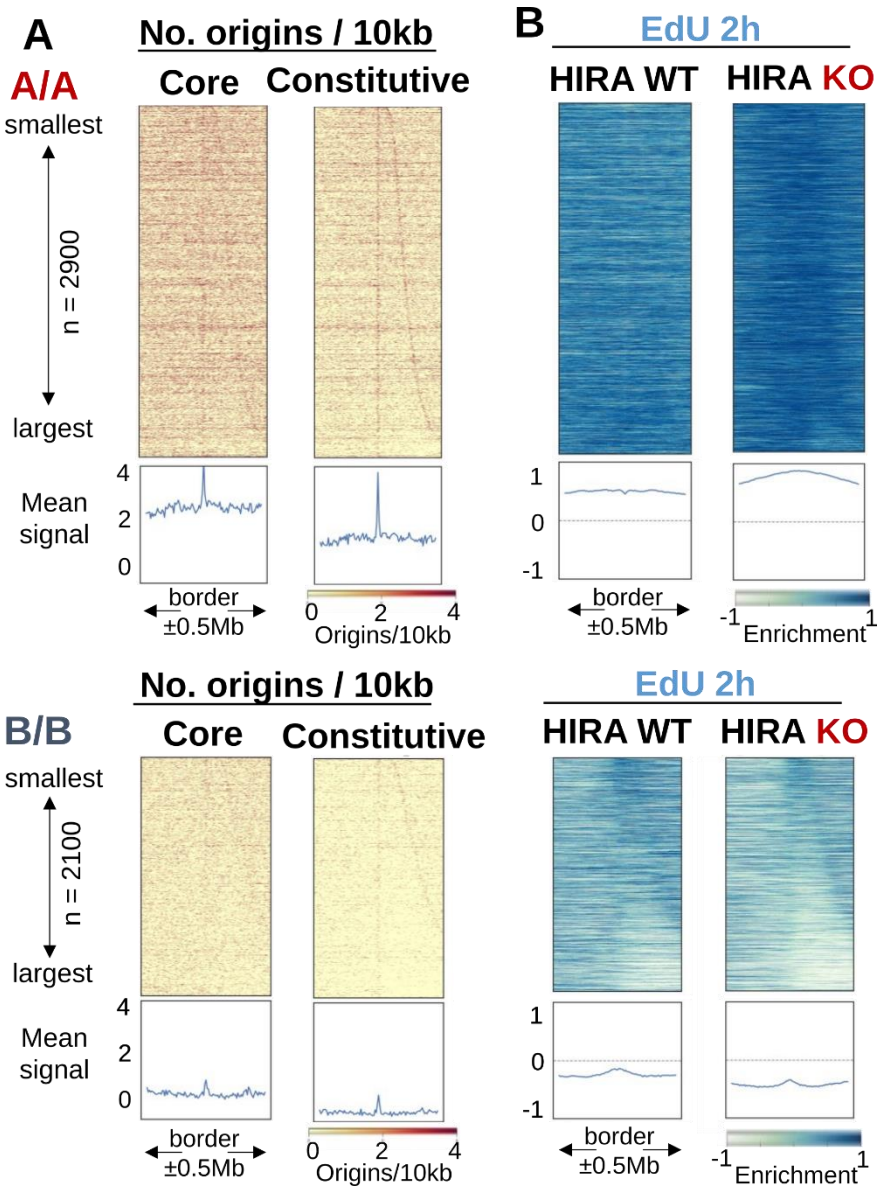

Figure 27. Early origins are enriched at TAD borders and their firing is impaired by HIRA KO

A. Number of core (common origins between cell lines, defined by SNS-seq in Akerman et al., 2020) and constitutive (early-firing origins defined by ini-seq2, Murat et al., 2022) per 10kb at TAD borders between A/A (top) and B/B (bottom) compartments from HIRA WT cells. TADs are sorted by size and centred at their start border ±0.5Mb.

B. EdU at 2h in S (z-score of $\log_2$ IP/input) at 10kb bins plotted at the same regions as in A. from HIRA WT (left) and KO (right) cells.

Enhancer, but not promoter-associated histone marks are decreased in the absence of HIRA on the kb scale

The phosphorylation of the H3.3-specific serine at position 31 has been previously shown to promote H3K27ac at enhancers in mESC (Martire et al., 2019) and human prostate cancer cells (Morozov et al., 2023), which was important for gene expression upon differentiation induction in both systems. H3.3S31phos has also been observed at the TSS and along the bodies of genes induced upon mouse macrophage stimulation, where it promotes H3K36me3 deposition (Armache et al., 2020). Thus, we investigated whether the absence of HIRA in HeLa cells led to site-specific changes in promoter (H3K4me3) and enhancer (H3K4me1, H3K27ac)-associated PTMs on the kb scale even though we did not detect changes at the Mb scale. To address this question, we performed peak-calling at 1kb resolution for the three marks from both HIRA WT and KO cells. H3K4me3-enriched peaks were maintained in the absence of HIRA, while the number of H3K4me1-rich peaks decreased by 50% (Figure 28A). Strikingly, we identified 90% fewer H3K27ac peaks in HIRA KO cells, which was accompanied by 70% increase in their average size (8.5kb to 14.3kb, $p = 0$). To evaluate if active mark and H3.3 levels were affected in the peaks overlapping between HIRA WT and KO cells, we computed their mean enrichment (Figure 28B). This revealed H3K4me3 peaks maintained their trimethylation despite their decrease in H3.3. On the contrary, H3K4me1 and H3K27ac were both reduced at their respective peaks, accompanied by a stronger H3.3 decrease compared to H3K4me3 peaks. Thus, the absence of HIRA impacted the distribution of enhancer-, but not promoter-associated PTMs despite the reduction of H3.3 at both types of elements.

Figure 28

A Number of peaks called from active PTMs

HIRA / Peaks	H3K4me3		H3K4me1		H3K27ac	
	WT	KO	WT	KO	WT	KO
Enriched	12K	12K	8K	4K	7.4K	870
Non-enriched	15K	8K	85K	78K	30K	19K

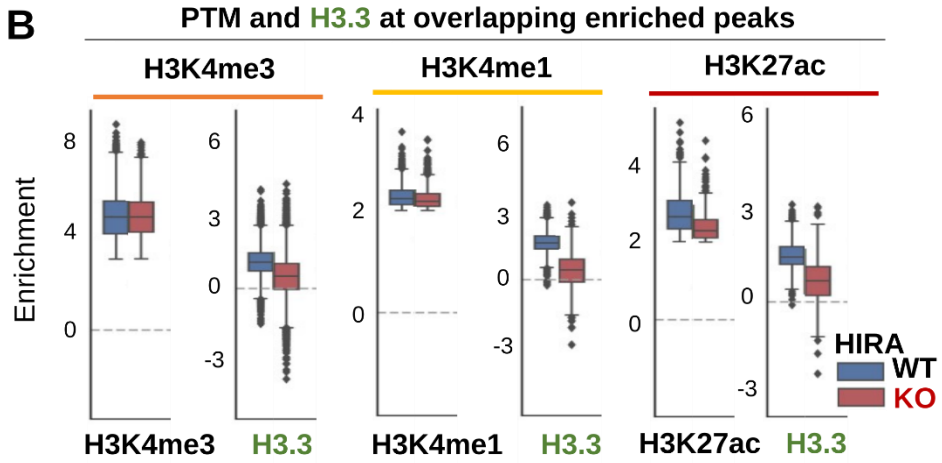

Figure 28. Distribution of enhancer- but not promoter-associated PTMs is affected by HIRA KO

A. Number of peaks for H3K4me3 (promoter), H3K4me1 and H3K27ac (enhancer) PTMs binned at 1kb and called using a 3-state Hidden Markov model. Enrichment was determined as detailed in Methods.

B. Enrichment (z-score of $\log_2$ IP/input) at H3K4me3 (left), H3K4me1 (middle) and H3K27ac (right) peaks (common for WT and KO) of the respective PTM and H3.3 (G1/S arrest) from HIRA WT and KO cells.

H3 variants redistribute along the mouse genome linearly and with respect to 3D genome features across scales during differentiation

To explore how the relationship between histone H3 variants and higher-order chromatin structure may change between cells with different potentials, we applied our analysis approach to compare mESC and *in vitro* differentiated neural progenitor cells (NPC). For this purpose, we used H3.1- and H3.3-SNAP ChIP-seq from mESC and NPC differentiated for 7 days, generated in the team (Arfè et al., in prep) and Hi-C from mESC and NPCs differentiated for 12 days which was publicly available (Bonev et al., 2017). First, we observe the variants exhibit largely reciprocal patterns, with H3.1 enriched in inactive and H3.3 in active regions in mESC (as previously documented, Deaton et al., 2016; Goldberg et al., 2010) and NPC (as shown for H3.3 in Deaton et al. (2016), Figure 29A). Nevertheless, both variants re-distribute upon differentiation with H3.3 showing more distinct peaks within broadly active regions, and H3.1 consolidating in domains and becoming more depleted from large active domains. This occurred without large changes in compartmentalisation and is in line with the idea that pluripotent cells have a generally 'open' chromatin state, which is lost as the cells differentiate and the distinction between active and inactive chromatin is strengthened (Schlesinger and Meshorer, 2019). Indeed, (Bonev et al., 2017) observed a stronger correlation of inactive PTMs (H3K9me3 and H3K27me3) with B compartments in NPC, which was also the case for H3.1 (Pearon's r = -0.38 compared to -0.72 with EV1 at 10kb from ESC vs NPC). They also detected a better correspondence of active marks (H3K4me1, H3K27ac, H3K36me3) with A compartments in ESC, as was the case for H3.3 (Pearon's r = 0.73 compared to 0.56 with EV1 at 10kb from ESC vs NPC).

To characterize better the linear reorganization of H3.1 and H3.3, we identified sites enriched for each variant based on their ratio at 10kb resolution from ESC and NPC, as we previously did in HeLa cells (Gatto et al., 2022). This analysis demonstrated that H3.1 sites more than doubled in number (n = 239 to 538) and decreased by half in size from ESC to NPC, while H3.3 sites had a modest increase in number and size (Figure 29B). Over differentiation, H3.1 became more evenly enriched throughout its sites and more depleted at their boundaries, making them better delineated (Figure 29C, top). On the contrary, H3.1 was present at H3.3 sites in ESCs but became strongly depleted there in NPCs, while a weak peak at H3.3 site boundaries remained, similar to the pattern in HeLa cells (Gatto et al., 2022). H3.3 patterns remained more stable during differentiation: it remained depleted in H3.1 sites and enriched in its own (Figure 29C, bottom). Notably, H3.3 became more depleted at the boundaries of its sites, which was also more similar to its pattern in HeLa (Gatto et al., 2022). Thus, H3 variants become better partitioned over the genome during differentiation from pluripotent stem cells to multipotent progenitors. This repartitioning resulted in a H3.3/H3.1 pattern in NPC which resembles their distribution in HeLa cells.

Finally, we compared H3.1 and H3.3 enrichment to 3D genome architecture features on the Mb (Figure 29D) and sub-Mb scale (Figure 29E). On the Mb scale, H3.3 was enriched throughout A compartments in both ESC and NPC (Figure 29D), as in HeLa cells. Furthermore, H3.1 enrichment was clear only for large B compartments and it was stronger in NPC compared to ESC, in agreement with the idea of heterochromatin consolidation with differentiation. On the sub-Mb scale, H3.3 had a peak only in A compartment TAD borders in both ESC and NPC, whereas H3.1 was clearly depleted at B compartment TAD borders only in NPC (Figure 29E). This analysis reveals that the relationship between H3 variant distribution and 3D genome organization is conserved between mouse and human on the Mb and sub-Mb scales. Furthermore, it highlights that H3.1 and H3.3 become repartitioned along the genome and with respect to its spatial organization.

Figure 29

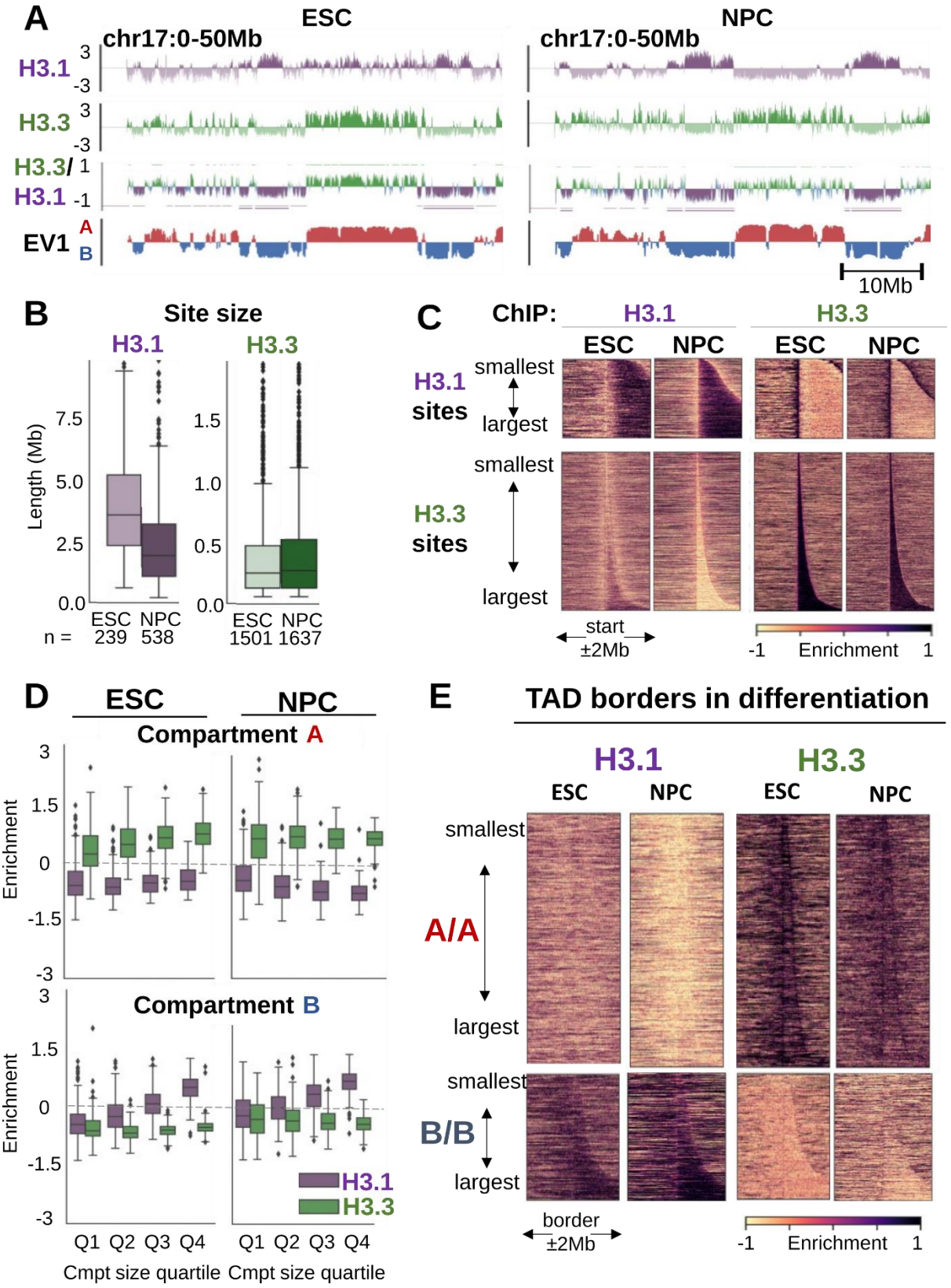
A
ESC
NPC
chr17:0-50Mb
chr17:0-50Mb
H3.1
H3.3
H3.3/ H3.1
EV1
A
B
10Mb
B
Site size
H3.1
H3.3
Length (Mb)
n = ESC 239 NPC 538
ESC 1501 NPC 1637
C
ChIP:
H3.1
H3.3
ESC
NPC
ESC
NPC
H3.1 sites
H3.3 sites
smallest
largest
start ±2Mb
-1 Enrichment 1
D
ESC
NPC
Compartment A
Compartment B
Enrichment
Q1 Q2 Q3 Q4
Cmpt size quartile
H3.1
H3.3
E
TAD borders in differentiation
H3.1
H3.3
A/A
B/B
border ±2Mb
-1 Enrichment 1

Figure 29. H3 variants reorganize along the mouse genome and with respect to 3D chromatin features during differentiation

A. H3.1 and H3.3 enrichment (z-score of $\log_2$ IP/input), H3.3/H3.1 ratio and EV1 (from 150kb-binned matrices) at a large representative region (chr 17:0-50Mb) from mouse ESC (**left**) and NPC (**right**). All signals are plotted at 10kb bins smoothed over 3 non-zero bins. H3.3 and H3.1-enriched sites are indicated as lines above (in green) and below (in purple) of the H3.3/H3.1 track, respectively.

B. Size distribution of H3.1- (**left**) and H3.3-enriched (**right**) sites from ESCs and NPCs. The number of sites is noted below.

C. H3.1 (**left**) and H3.3 (**right**) enrichment from ESC and NPC at H3.1 (**top**) and H3.3 (**bottom**) sites, sorted by size and centred at their start ±2Mb. Enrichment is shown as z-score of $\log_2$ IP/input at 10kb bins.

D. H3.1 and H3.3 enrichment from ESC (**left**) and NPC (**right**) quantified at A (**top**) and B (**bottom**) compartment domains stratified by size quartiles.

E. H3.1 (**left**) and H3.3 (**right**) at at TAD borders between A/A (**top**) and B/B (**bottom**) compartments from ESC and NPC. Enrichment is shown as z-score of $\log_2$ IP/input at 10kb bins. TADs are sorted by size and centred at their start border ±2Mb.

Methods

Publicly available data

Coordinates of core (Akerman et al., 2020, GSE128477) and constitutive (Murat et al., 2022, GSE202799) origins were obtained from GEO. Hi-C data from mouse ESC and NPC (Bonev et al., 2017, PRJNA378980) was downloaded from ENA.

Sequencing data processing

Both in-house-generated and publicly available data was processed from raw reads in FASTQ format as described in the manuscript. Mouse reference genome (GRCm38) was downloaded from ensembl.

Hi-C data processing

Hi-C data was processed as detailed in the manuscript. No custom masking was performed for the mouse Hi-C data.

Compartment analysis

Compartment analysis of Hi-C matrices was performed as described in the manuscript. Mouse data was binned at 150kb and compartment calling was done using TADbit.

TAD analysis

Insulation score was calculated from 10kb binned matrices with a window size of 100kb using cooltools and TAD borders were called based on default parameters for the HeLa data. For mouse data, window size of 300kb was used for insulation score calculation with TADbit and TAD boundary calling was done with delta = 3.

Active PTM peak calling

Identification of regions enriched for active marks was performed using a 3-state hidden Markov model (HMM), adapting the strategy used in Gatto et al. (2022) to identify H3.3 sites with the following adaptations. As regions enriched in active marks, especially H3K4me3, show a narrower enrichment profile compared to H3.3, 1kb binned data was used as input. Furthermore, instead of ratio between the variants, $\log_2$IP/input ratio was binarized, setting all bins > 0 to 1 and the rest to 0. Consecutive bins of the PTM-positive state were merged into peaks. A peak was considered enriched if its mean PTM enrichment (z-score of $\log_2$IP/input) was above 2 (H3K4me1, H3K27ac) or 3 (H3K4me3) standard deviations from the genome-wide mean of the respective mark (z-score of $\log_2$IP/input) binned at 1kb.

H3.1/H3.3 site identification

Sites enriched in H3.1 or H3.3 from mouse ESC and NPC were detected using a 3-state HMM as described for H3.3 sites in Gatto et al. (2022). As G1/S-synchronized data was not available, asynchronous H3.1 and H3.3 SNAP-seq was used as input.

Discussion

During my PhD, I uncovered a new role for the histone variant H3.3 in the higher-order organisation of active chromatin. I demonstrated that H3.3 incorporation in active (A) compartment promotes its interactions independently of histone PTMs, indicating histone dynamics should be considered when trying to understand the principles of genome compartmentalisation at the Mb scale. I also showed HIRA is required to maintain the A compartment identity of non-transcribed early IZs, supporting the idea that active nucleosome turnover can contribute to the segregation of active from inactive chromatin even in the absence of expression. On the contrary, I did not detect an effect of HIRA loss on the local folding of early IZs or genome-wide, indicating the sub-Mb scale of organization is not sufficient to promote early firing of IZs. Finally, I could disentangle the importance of HIRA for replication and chromatin architecture by showing that recovery of early IZ firing is dependent on restoration of their H3 variant balance, but not their compartment identity. These results have several biological implications and open up new avenues to explore the role of H3 variants in replication initiation and genome organisation. In the following section, I will discuss how H3.3 distribution along the genome is ensured by concerted action of its chaperones and what are the effects of changing the balance of this network. I will elaborate on how HIRA and H3 variant balance can define early initiation zones and their link with preserving epigenomic integrity. Additionally, I will consider the relationship between H3 distribution and multi-scale chromatin organisation in cells with different potential in the context of development. Finally, I will discuss the possible implications for disease.

H3 variant organisation across scales: a dynamic balancing act

The enrichment of H3.3 correlates with expression of active promoters and genes (Goldberg et al., 2010, Ray-Gallet et al., 2011) and turnover at regulatory elements (Ha et al., 2014, Deaton et al., 2016, Schlesinger et al., 2017). The deposition of H3.3 at transcriptionally active sites is likely ensured by the interaction of HIRA with RNAPII components (Ray-Gallet et al., 2011) and may also be supported by its gap-filling capacity (Ray-Gallet et al., 2011). However, how HIRA is recruited to non-transcribed regions remains an open question. Its reported interactions with some TFs (Pchelintsev et al., 2013, Soni et al., 2014), CTCF (Pchelintsev et al., 2013, Weth et al., 2014), RPA (Zhang et al., 2017) and chromatin remodellers of the CHD (Konev et al., 2007, Luijstreburg et al., 2016) and SWI/SNF family (Pchelintsev et al., 2013) may provide a partial explanation for this, at least with respect to relatively short regulatory elements. However, the non/low-transcribed HIRA-dependent sites of H3.3 enrichment, defined in Gatto et al. (2022) as ‘buried’, are much larger (median size 160kb) than TF binding sites and TSSs. Furthermore, while they become depleted in H3.3 in the absence of HIRA, our rescue experiments demonstrate they can regain H3.3 enrichment within 48h of HIRA re-expression (Manuscript, Figure 5). This indicates that the mechanism which recruits HIRA there may remain active in its absence. A tempting speculation would be that some histone turnover occurs at these sites, resulting in reduced nucleosome density which can enable HIRA recruitment via its capacity to bind naked DNA (Ray-Gallet et al., 2011). This would result in H3.3 incorporation in WT cells, whereas in

the absence of HIRA it may lead to increased accessibility of these regions. A similar phenomenon was recently documented by Navaro et al. (2020) in mESC at a subset of endogenous retroviral elements (ERVs), which require H3.3 incorporation by DAXX for their H3K9me3 and repression (Elsässer et al., 2015). Navarro et al. (2020) show that the SWI/SNF remodeller SMARCAD1 evicts nucleosomes at these elements, increasing their accessibility, and H3.3 incorporation by DAXX/ATRX (Tafessu et al., 2023) is required to maintain their nucleosome occupancy and heterochromatic state. Experiments depleting HIRA have shown this leads to increased DNaseI sensitivity in HeLa (Ray-Gallet et al., 2011), whereas it has been reported to both increase (mESC, Yang et al., 2021) and decrease accessibility at promoters (mESCs, Tafessu et al., 2023) and enhancers (human prostate cancer cells, Morozov et al., 2023). Thus, to assess the effect of HIRA absence on chromatin accessibility at specific sites, we performed ATAC-seq in HIRA WT and KO cells. Surprisingly, preliminary results suggest that nucleosome density decreases at expressed, but not non-transcribed H3.3-rich sites, suggesting a different mechanism may be employed to recruit HIRA there, although more in-depth analysis is ongoing.

Alternatively, there may be some epigenetic memory that can efficiently target HIRA to non-transcribed sites. Indeed, while we detect compartment changes (Manuscript, Figure 3), their sub-Mb scale organization (Manuscript, Figure 4, Supplementary Figure 5) and PTM profiles are maintained, despite small quantitative changes in the levels of some marks (Manuscript, Supplementary Figure 3). On the sub-Mb scale, the organization of the genome into TADs has been proposed to provide a framework for restricting enhancer-promoter contacts and regulating gene expression, especially in the context of development (Karpinska and Oudelaar, 2023). Furthermore, TADs align to some extent with replication domains (Pope et al., 2014): regions of the genome replicated from synchronously firing IZs and cluster in space, forming replication foci (Nakamura et al., 1986, Jackson and Pombo, 1998). Thus, it is possible that early-firing IZs found at the flanks of both transcribed and non-transcribed H3.3 sites cluster in the same foci during replication and this organization promotes HIRA recruitment to non-expressed sites. To test this idea, it would be interesting to deplete CTCF or cohesin, disrupting TAD formation in a HIRA KO background and then perform HIRA rescue.

Another interesting question to consider is how is H3.3 deposited on chromatin in the absence of HIRA? Previous imaging work from the team has demonstrated that upon HIRA knock-down, new H3.3 incorporation is reduced by ~50% globally (Ray-Gallet et al., 2011). Subsequently, Torné et al. (2020) showed that this *de novo* deposition of H3.3 occurs largely to compensate for histone loss associated with transcription (Torné et al., 2020). This may suggest that upon loss of HIRA, H3.3 would specifically be lost at expressed genes. However, genome-wide profiling of H3.3 in the absence of HIRA indicates this is not the case (Gatto et al., 2022; Goldberg et al., 2010). More specifically, in HIRA KO HeLa cells we observed blurring and decreased enrichment of H3.3 peaks in broadly active regions and loss individual H3.3 peaks where transcription is absent (Gatto et al., 2022). Furthermore, here we show

this is accompanied by H3.3 repartitioning from active only to large inactive compartments (Manuscript, Figure 1). Thus, other chaperones may act in parallel to enable H3.3 deposition in the absence of HIRA but not recapitulate its specific targeting to active domains.

One candidate for this is DAXX, which was reported to promote H3.3 incorporation upon gene activation in neurons (Michod et al., 2012), in addition to its well-established role in mediating H3.3 accumulation at repetitive (Elsässer et al., 2015), pericentric (Drané et al., 2010) and telomeric regions (Goldberg et al., 2010), described in steady state. H3.3-H4 associated with DAXX and HIRA exhibit different pre-deposition marks (H3.3K9me3 (Carraro et al., 2023) vs H3.3K9ac (Elsaesser and Allis, 2010), respectively), which suggests the choice of chaperone may impact the maintenance of chromatin state. While we did not observe a defect on the Mb scale (Manuscript, Figure 1), we detected a decrease of enhancer-associated peaks and mark enrichment on the kb scale (Additional results, Figure 28). Regulatory elements show high turnover of H3.3, which is the predominant variant incorporated there (Deaton et al., 2016, Schlessinger et al., 2017). Hence, its decreased levels at these regions coupled with a potential supply of H3.3K9 trimethylated version by DAXX may present a challenge to preserve their active mark enrichment. Indeed, H3.3 reduction at enhancers, observed in other systems upon HIRA KO (Martire et al., 2019, Morozov et al., 2023) impairs their function. This is due to the capacity of the H3.3-specific Serine 31 to be phosphorylated, which promotes p300 activity and H3K27ac (Martire et al., 2019). The presence of this Serine is also critical in early *X. laevis* development, although this is independent of the mechanism (DNA synthesis-coupled or independent) used for its deposition (Sitbon et al., 2020). Thus, variant identity, mode of incorporation and choice of chaperone may affect chromatin state.

Another reason to consider DAXX as an alternative system for depositing H3.3 in the absence of HIRA is that DAXX has been shown to handle excess histones when the variant-chaperone balance is disrupted. Upon overexpression of CENP-A in HeLa, DAXX promotes its deposition to chromosome arms at H3.3-rich sites, some CTCF binding sites and enhancers, taking it in charge from its dedicated chaperone HJURP (Lacoste et al., 2014). Overexpression of H3.3 has not been tested in similar settings, but it would be interesting to test if it would result increased incorporation or re-distribution and how this may be mediated. In transcriptionally silent *X. laevis* embryos with nuclei transplanted from muscle cells, H3.3 overexpression promotes the memory of an active MyoD (muscle-specific gene) state over 24 cell divisions (Ng and Gurdon, 2008). This occurs through H3.3 incorporation at the MyoD promoter, although it is unclear if it is specifically targeted only there, how this occurs and whether it is mediated by HIRA or another chaperone. Thus, co-depleting DAXX and HIRA or overexpressing H3.3 may provide further insights into how cells balance the variant-chaperone network.

Another potential player is the oncoprotein DEK, which in complex with casein kinase 2 (CK2) proved to be a H3.3-specific chaperone in *D. melanogaster* and human, ensuring deposition at active sites (Sawatsubashi et al., 2010). A later study in human mesenchymal stem cells (hMSCs) showed that DEK

localises to PML bodies and promotes H3.3 accumulation there, restricting its availability to HIRA and ATRX/DAXX and preventing aberrant incorporation into chromatin (Ivanauskiene et al., 2014). However, it would be interesting to investigate if DEK would adapt its function from promoting H3.3 storage to incorporation in the absence of HIRA. Finally, another candidate that can be considered is Spt2, one of the chaperones involved in H3-H4 recycling in transcription first identified in yeast (Nourani et al., 2006). While Spt2 was shown to genetically interact with HIRA in *S. cerevisiae* (Nourani et al., 2006), its function in more complex eukaryotes remains poorly understood. Recent work by Saredi et al. (2023) demonstrated that *C. elegans* Spt2 plays a role in transgenerational silencing and binds highly expressed genes, limiting their accessibility likely due through its activity in histone recycling. Notably, double mutant Spt2/HIRA worms showed more severe phenotypes than single mutants, indicating that they do not act redundantly. However, similar gene de-regulation occurred in the two single mutants, suggesting that they affect the same pathway. Finally, the authors showed that Spt2 depletion in human U2OS cells results in decrease of new H3.3 incorporation into chromatin (Saredi et al., 2023). Thus, another avenue to explore could be whether Spt2 can promote new H3.3 deposition in a manner uncoupled from transcription and if this activity is enhanced in the absence of HIRA.

H3 variant re-distribution in 3D chromatin space: functional implications

The redistribution of H3.3 from active to large repressed compartments that we detect in the absence of HIRA (Manuscript, Figure 1) did not result in changes in PTM distribution at these domains. This is in agreement with the findings from Loyola et al. (2006) demonstrating that the modification of a variant in a set of oligonucleosomes is largely dependent on the chromatin context and not its identity. We also did not detect gain of accessibility (preliminary results), in line with Navarro et al. (2020) who show histone exchange in mESC heterochromatin can take place without increase in chromatin accessibility. Furthermore, as our ChIP-seq measures relative enrichment, and H3.1 makes up the majority of H3 on chromatin in dividing cells, most nucleosomes in repressed regions likely still contain H3.1. This is supported by the absence of large changes in H3.1 distribution (Manuscript, Supplementary Figure 1) and the maintained prevalence of H3.1 over H3.3 based on the variant ratio at inactive compartments in the absence of HIRA (Manuscript, Supplementary Figure 7), suggesting heterochromatin in our system is not perturbed. Indeed, we detect a slight increase in interactions between repressed (B) compartments in HIRA KO, indicating their spatial organization is also largely maintained.

Curiously, pluripotent mESC show weaker H3.1 enrichment at large heterochromatin domains compared to their more differentiated (NPC) counterparts (Supplementary Figure 29D). Thus, it would be interesting to explore the effect of HIRA KO in this system: if H3.3 becomes redistributed to these regions, would that be sufficient to upset the balance between the variants? If so, would this impact their spatial segregation? Could the potential emergence of H3.3-rich sites generate new early IZs? So

far, we could detect H3.3 sites in mESC and NPC (Supplementary Figure 29A-C) with similar characteristics to the ones identified in HeLa (Gatto et al., 2022). The following step in this analysis would be to understand if they also play a role in the definition of early IZs. If this is the case, a HIRA KO mESC model may provide the opportunity to better understand the importance of H3 variants in development and dissect how they impact replication initiation and compartmentalisation in cells of different potential. This would bring valuable insights as, to date, studies using HIRA KO mESCs have focused on the consequences on gene expression changes upon induction of differentiation (Goldberg et al., 2010, Banaszynski et al., 2013, Yang et al., 2021, Tafessu et al., 2023) without considering the possible effects on chromatin organization or replication (discussed below).

On the sub-Mb scale, we did not detect changes of either IZ organisation (Manuscript, Figure 4, Supplementary Figure 5) or insulation and position of TAD borders (Figure 26). This is in line with other studies depleting histone PTM writers (Mas et al., 2018) or readers (Xie et al., 2022) which have also reported no impact on TAD organization. Mammalian TADs are largely generated by loop extrusion by cohesin, whereas their boundaries are defined by convergently oriented CTCF sites which block cohesin movement (Szabo et al., 2019). CTCF has been previously shown to co-localise with H3.3 (Jin et al., 2009), establishing ordered nucleosome arrays of the variant (Lacoste et al., 2014). Furthermore, there is evidence CTCF can interact with HIRA (Pchelintsev et al., 2013) and promote H3.3 deposition (Weth et al., 2014), indicating a potential functional link between the two may exist. Here, we detect an enrichment of H3.3 and depletion of H3.1 at TAD borders, both in HeLa (Figure 26) and mESC/NPC (Figure 29). This H3 variant pattern may be a consequence of CTCF binding, although it may also result from the enrichment of active TSSs at TAD borders (Dixon et al., 2012). Profiling H3.1 and H3.3 in the absence of CTCF and cohesin could provide an answer to this and improve our understanding of what factors can dictate histone chaperone localisation on chromatin. On the other hand, recent work in mESC showed that H3.3 can facilitate TF binding (Tafessu et al., 2023), indicating that H3.3 enrichment at TAD borders may contribute to their CTCF occupancy and function. However, our HIRA KO data indicates that this is not likely, as TAD border strength and positions are maintained despite the blurring of the H3 variant enrichment there (Figure 26).

TAD borders have been reported as enriched in origins of replication (Petryk et al., 2016, Akerman et al., 2020, Giles et al., 2022), as we also show in our data (Figure 27). The impaired early firing at TAD borders without a detectable defect in their insulation or position in the absence of HIRA indicates they are not sufficient to promote early initiation at the origins localised there. Indeed, studies depleting CTCF (Sima et al., 2019) or cohesin (Cremer et al., 2020) have not detected changes in RT by Repli-seq or profiling of S phase nucleotide incorporation patterns. However, the resolution of the Repli-seq analysis (5kb smoothed at 0.5Mb in Sima et al., 2019 and 50kb in Cremer et al., 2020) may not allow the detection of blurring of early initiation we detect on the kb scale upon HIRA KO. Thus, exploring the H3 variant pattern and mapping early replication in the absence of CTCF or cohesin can provide a

better understanding of the relationship between precision of early initiation and kb-scale organisation. With this aim, I established mESC constitutively expressing low levels of H3.1- and H3.3-SNAP in WT and CTCF-AID lines, which enable rapid, complete, and reversible CTCF depletion (kindly provided by Elphège Nora). Overall, the data generated so far indicates that kb-scale organization is neither sufficient nor necessary for early IZ firing.

How does the H3 variant balance define early IZs?

Our previous work demonstrated that HIRA-mediated H3.3 deposition defines early IZs independently of transcription (Gatto et al., 2022) and in my PhD project I could show this role is independent of chromatin organization on the Mb (compartment identity) and kb scale. Thus, the question of how the H3 variant balance established by HIRA contributes to early initiation is yet to be answered. Furthermore, as we have focused on early initiation, it remains unclear if the absence of HIRA leads to later activation of these IZs or prevents their firing altogether. This may have important implications for understanding whether HIRA can impact the definition, licensing or firing of origins within these IZs. Long et al. (2020) showed a role for another histone variant, H2A.Z in promoting origin licensing and firing in HeLa cells. H2A.Z is recognised by SUV420H1, which leads to H4K20me2 and increased ORC1 recruitment (Long et al., 2020). H2A.Z co-localises with H3.3 in active regions (Jin et al., 2009) and was suggested to form less stable double-variant (H2A.Z/H3.3) nucleosomes (Jin and Felsenfeld, 2007). H2A.Z is also found in heterochromatin (Hardy et al., 2009; Rangasamy, 2003), which may lead to formation of more labile nucleosomes upon H3.3 redistribution in the absence of HIRA. Preliminary ATAC-seq results from HIRA WT and KO cells suggest this is not the case, which may reflect that the absolute amount of H3.3 there is not high, or that H2A.Z itself has become redistributed. Indeed, recent work in mESC reported an interaction between HIRA and the H2A.Z chaperone complex SRCAP and demonstrated that HIRA depletion can impact the occupancy pattern of H2A.Z along the genome (Yang et al., 2021). This suggests that HIRA may also impact H2A.Z localisation in human cells and suggests that early initiation may be regulated by particular combinations of histone variants. To understand this relationship better, we are now performing ChIP-seq for H2A.Z and H4K20me2 in our HIRA WT and KO HeLa cells.

In *C. elegans*, Strobino et al. (2020) detected H3.3 enrichment at early, late and dormant origins, suggesting the presence of the variant may be related to their definition. H3.3 is not essential in worms, but its loss leads to a decrease in viable progeny at restrictive temperature (Delaney et al., 2018), indicating its functions in *C. elegans* may differs from mammals. Indeed, early origin firing was not impaired in H3.3-null worms grown at restrictive temperature (Strobino et al., 2020). However, the authors detect an impaired fork restart and potentially progression in the absence of H3.3 at restrictive temperatures (Strobino et al., 2020), which was not detected in human cells in the absence of HIRA (Gatto et al., 2022). The absence of H3.3 also did not affect origin density in avian DT40 cells, but it

resulted in impaired replication fork progression after UV damage. Notably, this was dependent on the mode of deposition of H3.3 but not the presence of its unique S31 (Frey et al., 2014). In human cells HIRA is important for transcription re-start after UV damage repair (Adam et al., 2013) although recent work shows this is independent of its H3.3 chaperone activity (Bouvier et al., 2021). Therefore, another avenue worth exploring further is whether it is the act of HIRA-mediated deposition or the identity of the variant itself which are important for early IZ definition in human. Furthermore, these studies highlight the species-specific roles H3.3 can play and emphasize that translating findings from one organism to another should be done with caution.

H3 variants and chromatin organization in differentiation and development

To examine how H3.1 and H3.3 are distributed along the genome and with respect to its spatial organization in cells with distinct differentiation potential, we used unique H3 variant ChIP-seq generated in the team (Arfé et al., in prep) and publicly available Hi-C data (Bonev et al., 2017) in mESC and neural progenitor cells (NPC) derived from them *in vitro*. To date, mainly H3.3 dynamics have been explored during differentiation or reprogramming, focusing specifically on changes associated with transcription or its regulation (Deaton et al., 2016, Fang et al., 2018). However, one of the major hallmarks of chromatin reorganisation in early development and during differentiation is the proper establishment and increased compaction of heterochromatin, respectively (McCarthy et al., 2023; Rang et al., 2023). H3.1 is the predominant variant in heterochromatin and depletion of its chaperone CAF-1 results in early embryonic lethality in mouse due to failure of heterochromatin formation (Houlard et al., 2006), while facilitating cell state changes in mESC (Ishiuchi et al., 2015, Nakatani et al., 2022), mouse embryonic fibroblasts (Cheloufi et al., 2015) and macrophage progenitors (Franklin et al., 2022). Furthermore, Ishiuchi et al. (2020) demonstrated the importance of CAF-1-mediated H3.1 deposition for establishment of a canonical H3.3 pattern in early (2 cell stage) mouse embryogenesis, showcasing the importance of interplay between the variants (discussed in Manuscript).

Here, we observed that while H3.1 is enriched in large inactive compartments in both ESC and NPC, its levels are higher in more differentiated cells (Figure 29). This is in agreement with our genome-wide analysis showing H3.1 becomes better partitioned over differentiation, becoming organised in more narrow, but better-defined domains. One important limitation of our work is that we profiled H3.1 from asynchronous mESC, which spend the majority of their time in S phase (Palmer and Kaldis, 2016). This may affect the enrichment profiles we detected, resulting in increased detection in active regions, where new H3.1 would be incorporated in early S phase. Nevertheless, our results are in agreement with super-resolution imaging revealing increased chromatin compaction (Ricci et al., 2015), and Hi-C showing stronger compartment B interactions (Bonev et al., 2017) in more differentiated cells. While NPC are still cycling, focusing on post-mitotic cells may offer a unique opportunity to explore the functional relationship between H3 variants and compartmentalization. H3.3 accumulates in terminally

differentiated neurons (Piña and Suau, 1987, Maze et al., 2015) but its genomic distribution has not been systematically compared to cycling cells. Thus, profiling the H3 variant patterns and higher-order genome organization in cells that have exited the cell cycle can provide further insights into their functional relationship.

On the kb scale, we observed similar patterns of H3.1 and H3.3 at TAD borders in ESC and NPC (Figure 29) as for HeLa (Figure 26), although they were more pronounced in NPC. This indicated that alongside changes in compartments and TAD borders during differentiation (Bonev et al., 2017), H3 variants are also re-organised across scales with respect to 3D genome architecture features. Whether these differences stem from the changes in cell cycle length, potential up- or down-regulation of histone chaperones, variants or factors involved in higher-order chromatin folding remains to be determined.

H3 variants, replication and chromatin organization in disease

Mutations and dysregulation of both histone variants and chaperones have been linked to disease, in particular to cancer. For example, work from the team revealed that overexpression of the centromeric variant CENP-A, which is observed in many cancers (Renaud-Pageot et al., 2022), promoted a subpopulation of p53-defective MCF10-2A cells to undergo epithelial-to-mesenchymal transition (EMT) (Jeffery et al., 2021). However, it is yet to be determined whether this is due to CENP-A misincorporation along the arms perturbing gene expression, chromatin organisation or potentially replication, as overexpressed CENP-A in HeLa mislocalises to H3.3-rich regions (Lacoste et al., 2014), which may perturb early IZ function. Metastasis, which includes the process of EMT, is also enhanced upon down-regulation of CAF-1 and increased H3.3 incorporation (Gomes et al., 2019), indicating the importance of H3 variant balance for epigenetic state maintenance and cell fate transitions. In their study, Gomes et al. (2019) show the gap-filling mechanism by HIRA is employed to deposit H3.3 in the absence of CAF-1, but do not assess if H3.3 becomes redistributed along the genome. Thus, exploring the effects on replication and chromatin structure in this model would provide valuable insights intro understanding how disrupting the chaperone-variant balance leads to cell fate transitions and disease.

Mutations in both H3.1 and H3.3 resulting in amino acid substitutions (most commonly on the histone tail), termed oncohistones, have been shown to play a driver role in cancer (Behjati et al., 2013; Schwartzentruber et al, 2012). One of the best studied examples is the K27M mutation, which reduces PRC2 activity when incorporated into chromatin (Lee et al., 2019; Stafford et al., 2018). K27M is found in 80% paediatric diffuse intrinsic pontine gliomas (DIPG), which tend to be poorly differentiated and spread through the tissue (Ghiraldini et al., 2021). Notably, H3.1K27M compared to H3.3K27M leads to a stronger decrease in H3K27me3, likely due to its DSC mode of incorporation which results in deposition along the entire genome (Sarthy et al., 2020). The two are also associated with distinct spectra of secondary mutations, although how this is linked to the mutant variant remains unknown.

While the current view is that the near-complete inhibition of PRC2 activity and concomitant increase in H3K27ac drive epigenetic dysregulation in these tumours, treatment with HDAC inhibitors has shown only partial success (Mitchener and Muir, 2022). Thus, characterizing how these mutations act on the molecular level beyond their effect on PTMs can provide alternative ideas for development of therapeutics. As the H3 variant balance is linked to early IZ firing (Gatto et al., 2022) and ORC1 has shown association with H3K27me3 (Vermeulen et al., 2010), understanding how replication control may be affected or modulated in these cells may be of interest. Indeed, introducing K27M and other oncohistone substitutions in avian DT40 cells led to an increase in UV damage sensitivity, suggesting an impact on DNA repair (Frey et al., 2014). Finally, given the stronger loss of K27me3 in H3.1K27M mutants, interfering with CAF-1 in order to promote H3.3 deposition via HIRA-mediated gap-filling may present a therapeutic avenue. Improving our understanding of how balancing histone variant dynamics impacts replication, repair and organization of chromatin in addition to their role in transcription can provide key insights into their functional importance in development and disease.

Conclusion

My PhD project aimed to understand how H3 variants are organised with respect to 3D chromatin architecture and to disentangle the interplay between chromatin state, function and spatial organization. Few studies have investigated the role of histone variants and the impact of their dynamic incorporation during the cell cycle on these processes. Thus, the goal of my project was to characterize H3 variant enrichment across genomic scales and gain insights in the structure-function relationship of chromatin.

Firstly, I established a custom analysis pipeline in the lab to integrate 1D and 3D chromatin information, combining previously developed scripts and published tools, which allowed me to analyse and compare data generated in the lab to publicly available datasets. It also enabled me to investigate my question in other cell types, opening avenues for future investigation. Finally, by developing this expertise I could also contribute to other projects in the lab and examine H3 variant distribution in various contexts.

Secondly, the results from my work provided several important biological insights about the role of H3 variants in chromatin organization and early replication initiation. I characterised for the first time the distribution of H3 variants with respect to features of 3D genome architecture across scales. This revealed that, on the Mb scale, H3.3 was found in the active (A) compartment, whereas H3.1 was specifically enriched only in large repressed (B) domains, likely reflecting the variants' deposition and eviction dynamics. I could then show that targeting H3.3 to compartment A was important for its interactions independently of histone marks. It is still unclear what drives compartment segregation, but the strong correlation with chromatin states has suggested it may be mediated by phase separation of distinct histone PTMs and/or their readers. My work emphasizes histone turnover should be considered when examining the dynamic organization of chromatin in cycling cells. On the sub-Mb scale, I showed loss of early firing at initiation zones was associated with compartment reorganization only in the absence of transcription. This is in line with the idea that histone exchange may contribute to the spatial segregation of chromatin independently of expression. Furthermore, the absence of HIRA did not affect the local folding of early initiation zones, indicating their sub-Mb organization is not sufficient for their function. Finally, rescue experiments allowed me to disentangle the role of HIRA in early replication and higher-order chromatin folding. Overall, my results indicate that HIRA-mediated H3.3 incorporation is important for the organization of active chromatin, while H3 variant balance defines early initiation zones independently of its role in genome architecture.

This project opens up several avenues for future work aiming to disentangle the impact of H3 variants on chromatin organization and function. Combining rapid depletion or longer re-expression of HIRA with cell synchronization can be used to understand if going through S phase is required for its roles in early initiation zone definition and chromatin organization. A similar strategy can be employed in other models, like embryonic stem cells, where the physiological impact of disrupting replication initiation or compartmentalization can be assessed upon differentiation. This would allow a better understanding of the roles HIRA and targeted H3.3 deposition play in development and disease.

References

Abascal, F., Corpet, A., Gurard-Levin, Z.A., Juan, D., Ochsenbein, F., Rico, D., Valencia, A., Almouzni, G., 2013. Subfunctionalization via Adaptive Evolution Influenced by Genomic Context: The Case of Histone Chaperones ASF1a and ASF1b. Mol. Biol. Evol. 30, 1853–1866. https://doi.org/10.1093/molbev/mst086
Abdulla, A.Z., Salari, H., Tortora, M.M.C., Vaillant, C., Jost, D., 2023. 4D epigenomics: deciphering the coupling between genome folding and epigenomic regulation with biophysical modeling. Curr. Opin. Genet. Dev. 79, 102033. https://doi.org/10.1016/j.gde.2023.102033
Abramo, K., Valton, A.-L., Venev, S.V., Ozadam, H., Fox, A.N., Dekker, J., 2019. A chromosome folding intermediate at the condensin-to-cohesin transition during telophase. Nat. Cell Biol. 21, 1393–1402. https://doi.org/10.1038/s41556-019-0406-2
Adam, S., Dabin, J., Chevallier, O., Leroy, O., Baldeyron, C., Corpet, A., Lomonte, P., Renaud, O., Almouzni, G., Polo, S.E., 2016. Real-Time Tracking of Parental Histones Reveals Their Contribution to Chromatin Integrity Following DNA Damage. Mol. Cell 64, 65–78. https://doi.org/10.1016/j.molcel.2016.08.019
Adam, S., Polo, S.E., Almouzni, G., 2013. Transcription Recovery after DNA Damage Requires Chromatin Priming by the H3.3 Histone Chaperone HIRA. Cell 155, 94–106. https://doi.org/10.1016/j.cell.2013.08.029
Aguilera, P., López-Contreras, A.J., 2023. ATRX, a guardian of chromatin. Trends Genet. 39, 505–519. https://doi.org/10.1016/j.tig.2023.02.009
Ahmad, K., Henikoff, S., 2002. The Histone Variant H3.3 Marks Active Chromatin by Replication-Independent Nucleosome Assembly. Mol. Cell 9, 1191–1200. https://doi.org/10.1016/S1097-2765(02)00542-7
Aho, S., Buisson, M., Pajunen, T., Ryoo, Y.W., Giot, J.-F., Gruffat, H., Sergeant, A., Uitto, J., 2000. Ubinuclein, a Novel Nuclear Protein Interacting with Cellular and Viral Transcription Factors. J. Cell Biol. 148, 1165–1176. https://doi.org/10.1083/jcb.148.6.1165
Akerman, I., Kasaai, B., Bazarova, A., Sang, P.B., Peiffer, I., Artufel, M., Derelle, R., Smith, G., Rodriguez-Martinez, M., Romano, M., Kinet, S., Tino, P., Theillet, C., Taylor, N., Ballester, B., Méchali, M., 2020. A predictable conserved DNA base composition signature defines human core DNA replication origins. Nat. Commun. 11, 4826. https://doi.org/10.1038/s41467-020-18527-0
Akhmanova, A.S., Bindels, P.C.T., Xu, J., Miedema, K., Kremer, H., Hennig, W., Xu, J., Hennig, W., 1995. Structure and expression of histone H3.3 genes in Drosophila melanogaster and Drosophila hydei. Genome 38, 586–600. https://doi.org/10.1139/g95-075
Akiyama, T., Suzuki, O., Matsuda, J., Aoki, F., 2011. Dynamic Replacement of Histone H3 Variants Reprograms Epigenetic Marks in Early Mouse Embryos. PLoS Genet. 7, e1002279. https://doi.org/10.1371/journal.pgen.1002279
Alabert, C., Barth, T.K., Reverón-Gómez, N., Sidoli, S., Schmidt, A., Jensen, O.N., Imhof, A., Groth, A., 2015. Two distinct modes for propagation of histone PTMs across the cell cycle. Genes Dev. 29, 585–590. https://doi.org/10.1101/gad.256354.114
Alavi, S., Ghadiri, H., Dabirmanesh, B., Moriyama, K., Khajeh, K., Masai, H., 2021. G-quadruplex binding protein Rif1, a key regulator of replication timing. J. Biochem. (Tokyo) 169, 1–14. https://doi.org/10.1093/jb/mvaa128
Albig, W., Bramlage, B., Gruber, K., Klobeck, H.-G., Kunz, J., Doenecke, D., 1995. The Human Replacement Histone H3.3B Gene (H3F3B). Genomics 30, 264–272. https://doi.org/10.1006/geno.1995.9878
Alexander, J.M., Guan, J., Li, B., Maliskova, L., Song, M., Shen, Y., Huang, B., Lomvardas, S., Weiner, O.D., 2019. Live-cell imaging reveals enhancer-dependent Sox2 transcription in the absence of enhancer proximity. eLife 8, e41769. https://doi.org/10.7554/eLife.41769
Ali-Ahmad, A., Bilokapić, S., Schäfer, I.B., Halić, M., Sekulić, N., 2019. CENP-C unwraps the human CENP-A nucleosome through the H2A C-terminal tail. EMBO Rep. 20, e48913. https://doi.org/10.15252/embr.201948913
Alipour, E., Marko, J.F., 2012. Self-organization of domain structures by DNA-loop-extruding enzymes. Nucleic Acids Res. 40, 11202–11212. https://doi.org/10.1093/nar/gks925
Allan, J., Hartman, P.G., Crane-Robinson, C., Aviles, F.X., 1980. The structure of histone H1 and its location in chromatin. Nature 288, 675–679. https://doi.org/10.1038/288675a0
Allfrey, V.G., Faulkner, R., Mirsky, A.E., 1964. ACETYLATION AND METHYLATION OF HISTONES AND THEIR POSSIBLE ROLE IN THE REGULATION OF RNA SYNTHESIS. Proc. Natl. Acad. Sci. 51, 786–794. https://doi.org/10.1073/pnas.51.5.786
Allshire, R.C., Madhani, H.D., 2018. Ten principles of heterochromatin formation and function. Nat. Rev. Mol. Cell Biol. 19, 229–244. https://doi.org/10.1038/nrm.2017.119
Almouzni, G., Clark, D.J., Méchali, M., Wolffe, A.P., 1990. Chromatin assembly on replicating DNA in vitro. Nucleic Acids Res. 18, 5767–5774. https://doi.org/10.1093/nar/18.19.5767
Almouzni, G., Méchali, M., 1988a. Xenopus egg extracts: A model system for chromatin replication. Biochim. Biophys. Acta BBA - Gene Struct. Expr., Special Issue: Enzymology of DNA Replication 951, 443–450. https://doi.org/10.1016/0167-4781(88)90118-2
Almouzni, G., Méchali, M., 1988b. Assembly of spaced chromatin promoted by DNA synthesis in extracts from Xenopus eggs. EMBO J. 7, 665–672. https://doi.org/10.1002/j.1460-2075.1988.tb02861.x

Altman, A.L., Fanning, E., 2004. Defined Sequence Modules and an Architectural Element Cooperate To Promote Initiation at an Ectopic Mammalian Chromosomal Replication Origin. Mol. Cell. Biol. 24, 4138–4150. https://doi.org/10.1128/MCB.24.10.4138-4150.2004
Alvarez, F., Muñoz, F., Schilcher, P., Imhof, A., Almouzni, G., Loyola, A., 2011. Sequential Establishment of Marks on Soluble Histones H3 and H4. J. Biol. Chem. 286, 17714–17721. https://doi.org/10.1074/jbc.M111.223453
Alvarez, V., Bandau, S., Jiang, H., Rios-Szwed, D., Hukelmann, J., Garcia-Wilson, E., Wiechens, N., Griesser, E., Ten Have, S., Owen-Hughes, T., Lamond, A., Alabert, C., 2023. Proteomic profiling reveals distinct phases to the restoration of chromatin following DNA replication. Cell Rep. 42, 111996. https://doi.org/10.1016/j.celrep.2023.111996
Alver, R.C., Chadha, G.S., Gillespie, P.J., Blow, J.J., 2017. Reversal of DDK-Mediated MCM Phosphorylation by Rif1-PP1 Regulates Replication Initiation and Replisome Stability Independently of ATR/Chk1. Cell Rep. 18, 2508–2520. https://doi.org/10.1016/j.celrep.2017.02.042
Annunziato, A., 2015. The Fork in the Road: Histone Partitioning During DNA Replication. Genes 6, 353–371. https://doi.org/10.3390/genes6020353
Annunziato, A.T., 2012. Assembling chromatin: The long and winding road. Biochim. Biophys. Acta BBA - Gene Regul. Mech. 1819, 196–210. https://doi.org/10.1016/j.bbagrm.2011.07.005
Aranda, S., Mas, G., Di Croce, L., 2015. Regulation of gene transcription by Polycomb proteins. Sci. Adv. 1, e1500737. https://doi.org/10.1126/sciadv.1500737
Arimura, Y., Tachiwana, H., Takagi, H., Hori, T., Kimura, H., Fukagawa, T., Kurumizaka, H., 2019. The CENP-A centromere targeting domain facilitates H4K20 monomethylation in the nucleosome by structural polymorphism. Nat. Commun. 10, 576. https://doi.org/10.1038/s41467-019-08314-x
Armache, A., Yang, S., Martínez de Paz, A., Robbins, L.E., Durmaz, C., Cheong, J.Q., Ravishankar, A., Daman, A.W., Ahimovic, D.J., Klevorn, T., Yue, Y., Arslan, T., Lin, S., Panchenko, T., Hrit, J., Wang, M., Thudium, S., Garcia, B.A., Korb, E., Armache, K.-J., Rothbart, S.B., Hake, S.B., Allis, C.D., Li, H., Josefowicz, S.Z., 2020. Histone H3.3 phosphorylation amplifies stimulation-induced transcription. Nature 583, 852–857. https://doi.org/10.1038/s41586-020-2533-0
Arnould, C., Rocher, V., Finoux, A.-L., Clouaire, T., Li, K., Zhou, F., Caron, P., Mangeot, P.E., Ricci, E.P., Mourad, R., Haber, J.E., Noordermeer, D., Legube, G., 2021. Loop extrusion as a mechanism for formation of DNA damage repair foci. Nature 590, 660–665. https://doi.org/10.1038/s41586-021-03193-z
Athwal, R.K., Walkiewicz, M.P., Baek, S., Fu, S., Bui, M., Camps, J., Ried, T., Sung, M.-H., Dalal, Y., 2015. CENP-A nucleosomes localize to transcription factor hotspots and subtelomeric sites in human cancer cells. Epigenetics Chromatin 8, 2. https://doi.org/10.1186/1756-8935-8-2
Attali, I., Botchan, M.R., Berger, J.M., 2021. Structural Mechanisms for Replicating DNA in Eukaryotes. Annu. Rev. Biochem. 90, 77–106. https://doi.org/10.1146/annurev-biochem-090120-125407
Avery, O., MacLeod, C., McCarty, M., 1944. Studies on the Chemical Nature of the Substance Inducing Transformation of Pneumococcal Types: Induction of Transformation by a Deoxyribonucleic Acid Fraction Isolated from Pneumococcus Type III. J. Exp. Med. 79, 137–158. https://doi.org/10.1084/jem.79.2.137
Balaji, S., Iyer, L.M., Aravind, L., 2009. HPC2 and ubinuclein define a novel family of histone chaperones conserved throughout eukaryotes. Mol. Biosyst. 5, 269. https://doi.org/10.1039/b816424j
Banaszynski, L.A., Wen, D., Dewell, S., Whitcomb, S.J., Lin, M., Diaz, N., Elsässer, S.J., Chapgier, A., Goldberg, A.D., Canaani, E., Rafii, S., Zheng, D., Allis, C.D., 2013. Hira-Dependent Histone H3.3 Deposition Facilitates PRC2 Recruitment at Developmental Loci in ES Cells. Cell 155, 107–120. https://doi.org/10.1016/j.cell.2013.08.061
Banigan, E.J., Tang, W., van den Berg, A.A., Stocsits, R.R., Wutz, G., Brandão, H.B., Busslinger, G.A., Peters, J.-M., Mirny, L.A., 2023. Transcription shapes 3D chromatin organization by interacting with loop extrusion. Proc. Natl. Acad. Sci. 120, e2210480120. https://doi.org/10.1073/pnas.2210480120
Bantignies, F., Roure, V., Comet, I., Leblanc, B., Schuettengruber, B., Bonnet, J., Tixier, V., Mas, A., Cavalli, G., 2011. Polycomb-Dependent Regulatory Contacts between Distant Hox Loci in Drosophila. Cell 144, 214–226. https://doi.org/10.1016/j.cell.2010.12.026
Banumathy, G., Somaiah, N., Zhang, R., Tang, Y., Hoffmann, J., Andrake, M., Ceulemans, H., Schultz, D., Marmorstein, R., Adams, P.D., 2009. Human UBN1 Is an Ortholog of Yeast Hpc2p and Has an Essential Role in the HIRA/ASF1a Chromatin-Remodeling Pathway in Senescent Cells. Mol. Cell. Biol. 29, 758–770. https://doi.org/10.1128/MCB.01047-08
Barlow, J.H., Faryabi, R.B., Callén, E., Wong, N., Malhowski, A., Chen, H.T., Gutierrez-Cruz, G., Sun, H.-W., McKinnon, P., Wright, G., Casellas, R., Robbiani, D.F., Staudt, L., Fernandez-Capetillo, O., Nussenzweig, A., 2013. Identification of Early Replicating Fragile Sites that Contribute to Genome Instability. Cell 152, 620–632. https://doi.org/10.1016/j.cell.2013.01.006

Barnhart, M.C., Kuich, P.H.J.L., Stellfox, M.E., Ward, J.A., Bassett, E.A., Black, B.E., Foltz, D.R., 2011. HJURP is a CENP-A chromatin assembly factor sufficient to form a functional de novo kinetochore. J. Cell Biol. 194, 229–243. https://doi.org/10.1083/jcb.201012017
Barski, A., Cuddapah, S., Cui, K., Roh, T.-Y., Schones, D.E., Wang, Z., Wei, G., Chepelev, I., Zhao, K., 2007. High-Resolution Profiling of Histone Methylations in the Human Genome. Cell 129, 823–837. https://doi.org/10.1016/j.cell.2007.05.009
Barth, T.K., Imhof, A., 2010. Fast signals and slow marks: the dynamics of histone modifications. Trends Biochem. Sci. 35, 618–626. https://doi.org/10.1016/j.tibs.2010.05.006
Barutcu, A.R., Blencowe, B.J., Rinn, J.L., 2019. Differential contribution of steady-state RNA and active transcription in chromatin organization. EMBO Rep. 20, e48068. https://doi.org/10.15252/embr.201948068
Bassett, E.A., DeNizio, J., Barnhart-Dailey, M.C., Panchenko, T., Sekulic, N., Rogers, D.J., Foltz, D.R., Black, B.E., 2012. HJURP Uses Distinct CENP-A Surfaces to Recognize and to Stabilize CENP-A/Histone H4 for Centromere Assembly. Dev. Cell 22, 749–762. https://doi.org/10.1016/j.devcel.2012.02.001
Batty, P., Gerlich, D.W., 2019. Mitotic Chromosome Mechanics: How Cells Segregate Their Genome. Trends Cell Biol. 29, 717–726. https://doi.org/10.1016/j.tcb.2019.05.007
Batty, P., Langer, C.C., Takács, Z., Tang, W., Blaukopf, C., Peters, J., Gerlich, D.W., 2023. Cohesin-mediated loop extrusion resolves sister chromatids in G2 phase. EMBO J. e113475. https://doi.org/10.15252/embj.2023113475
Bauman, J.G.J., Wiegant, J., Borst, P., van Duijn, P., 1980. A new method for fluorescence microscopical localization of specific DNA sequences by in situ hybridization of fluorochrome-labelled RNA. Exp. Cell Res. 128, 485–490. https://doi.org/10.1016/0014-4827(80)90087-7
Baxevanis, A., Landsman, D., 1998. Histone Sequence Database: new histone fold family members. Nucleic Acids Res. 26, 372–375. https://doi.org/10.1093/nar/26.1.372
Beagan, J.A., Phillips-Cremins, J.E., 2020. On the existence and functionality of topologically associating domains. Nat. Genet. 52, 8–16. https://doi.org/10.1038/s41588-019-0561-1
Beagrie, R.A., Scialdone, A., Schueler, M., Kraemer, D.C.A., Chotalia, M., Xie, S.Q., Barbieri, M., de Santiago, I., Lavitas, L.-M., Branco, M.R., Fraser, J., Dostie, J., Game, L., Dillon, N., Edwards, P.A.W., Nicodemi, M., Pombo, A., 2017. Complex multi-enhancer contacts captured by genome architecture mapping. Nature 543, 519–524. https://doi.org/10.1038/nature21411
Beall, E.L., Manak, J.R., Zhou, S., Bell, M., Lipsick, J.S., Botchan, M.R., 2002. Role for a Drosophila Myb-containing protein complex in site-specific DNA replication. Nature 420, 833–837. https://doi.org/10.1038/nature01228
Beau, M.M.L., Rassool, F.V., Neilly, M.E., Iii, R.E., Glover, T.W., Smith, D.I., McKeithan, T.W., 1998. Replication of a common fragile site, FRA3B, occurs late in S phase and is delayed further upon induction: implications for the mechanism of fragile site induction 7.
Bednar, J., Garcia-Saez, I., Boopathi, R., Cutter, A.R., Papai, G., Reymer, A., Syed, S.H., Lone, I.N., Tonchev, O., Crucifix, C., Menoni, H., Papin, C., Skoufias, D.A., Kurumizaka, H., Lavery, R., Hamiche, A., Hayes, J.J., Schultz, P., Angelov, D., Petosa, C., Dimitrov, S., 2017. Structure and Dynamics of a 197 bp Nucleosome in Complex with Linker Histone H1. Mol. Cell 66, 384-397.e8. https://doi.org/10.1016/j.molcel.2017.04.012
Behjati, S., Tarpey, P.S., Presneau, N., Scheipl, S., Pillay, N., Van Loo, P., Wedge, D.C., Cooke, S.L., Gundem, G., Davies, H., Nik-Zainal, S., Martin, S., McLaren, S., Goody, V., Robinson, B., Butler, A., Teague, J.W., Halai, D., Khatri, B., Myklebost, O., Baumhoer, D., Jundt, G., Hamoudi, R., Tirabosco, R., Amary, M.F., Futreal, P.A., Stratton, M.R., Campbell, P.J., Flanagan, A.M., 2013. Distinct H3F3A and H3F3B driver mutations define chondroblastoma and giant cell tumor of bone. Nat. Genet. 45, 1479–1482. https://doi.org/10.1038/ng.2814
Beliveau, B.J., Boettiger, A.N., Avendaño, M.S., Jungmann, R., McCole, R.B., Joyce, E.F., Kim-Kiselak, C., Bantignies, F., Fonseka, C.Y., Erceg, J., Hannan, M.A., Hoang, H.G., Colognori, D., Lee, J.T., Shih, W.M., Yin, P., Zhuang, X., Wu, C., 2015. Single-molecule super-resolution imaging of chromosomes and in situ haplotype visualization using Oligopaint FISH probes. Nat. Commun. 6, 7147. https://doi.org/10.1038/ncomms8147
Beliveau, B.J., Boettiger, A.N., Nir, G., Bintu, B., Yin, P., Zhuang, X., Wu, C. -ting, 2017. In Situ Super-Resolution Imaging of Genomic DNA with OligoSTORM and OligoDNA-PAINT, in: Erfle, H. (Ed.), Super-Resolution Microscopy. Springer New York, New York, NY, pp. 231–252. https://doi.org/10.1007/978-1-4939-7265-4_19
Beliveau, B.J., Joyce, E.F., Apostolopoulos, N., Yilmaz, F., Fonseka, C.Y., McCole, R.B., Chang, Y., Li, J.B., Senaratne, T.N., Williams, B.R., Rouillard, J.-M., Wu, C. -t., 2012. Versatile design and synthesis platform for visualizing genomes with Oligopaint FISH probes. Proc. Natl. Acad. Sci. 109, 21301–21306. https://doi.org/10.1073/pnas.1213818110
Bell, S.P., Stillman, B., 1992. AlP.dependent recognition of eukaryotic origins of DNA replication by a multiprotein complex 357.
Bellelli, R., Belan, O., Pye, V.E., Clement, C., Maslen, S.L., Skehel, J.M., Cherepanov, P., Almouzni, G., Boulton, S.J., 2018a. POLE3-POLE4 Is a Histone H3-H4 Chaperone that Maintains Chromatin Integrity during DNA Replication. Mol. Cell 72, 112-126.e5. https://doi.org/10.1016/j.molcel.2018.08.043

Bellelli, R., Borel, V., Logan, C., Svendsen, J., Cox, D.E., Nye, E., Metcalfe, K., O'Connell, S.M., Stamp, G., Flynn, H.R., Snijders, A.P., Lassailly, F., Jackson, A., Boulton, S.J., 2018b. Polε Instability Drives Replication Stress, Abnormal Development, and Tumorigenesis. Mol. Cell 70, 707-721.e7. https://doi.org/10.1016/j.molcel.2018.04.008
Belsky, J.A., MacAlpine, H.K., Lubelsky, Y., Hartemink, A.J., MacAlpine, D.M., 2015. Genome-wide chromatin footprinting reveals changes in replication origin architecture induced by pre-RC assembly. Genes Dev. 29, 212–224. https://doi.org/10.1101/gad.247924.114
Benabdallah, N.S., Williamson, I., Illingworth, R.S., Kane, L., Boyle, S., Sengupta, D., Grimes, G.R., Therizols, P., Bickmore, W.A., 2019. Decreased Enhancer-Promoter Proximity Accompanying Enhancer Activation. Mol. Cell 76, 473-484.e7. https://doi.org/10.1016/j.molcel.2019.07.038
Bender, S., Tang, Y., Lindroth, A.M., Hovestadt, V., Jones, D.T.W., Kool, M., Zapatka, M., Northcott, P.A., Sturm, D., Wang, W., Radlwimmer, B., Højfeldt, J.W., Truffaux, N., Castel, D., Schubert, S., Ryzhova, M., Şeker-Cin, H., Gronych, J., Johann, P.D., Stark, S., Meyer, J., Milde, T., Schuhmann, M., Ebinger, M., Monoranu, C.-M., Ponnuswami, A., Chen, S., Jones, C., Witt, O., Collins, V.P., von Deimling, A., Jabado, N., Puget, S., Grill, J., Helin, K., Korshunov, A., Lichter, P., Monje, M., Plass, C., Cho, Y.-J., Pfister, S.M., 2013. Reduced H3K27me3 and DNA Hypomethylation Are Major Drivers of Gene Expression in K27M Mutant Pediatric High-Grade Gliomas. Cancer Cell 24, 660–672. https://doi.org/10.1016/j.ccr.2013.10.006
Bensimon, A., Simon, A., Chiffaudel, A., Croquette, V., Heslot, F., Bensimon, D., 1994. Alignment and Sensitive Detection of DNA by a Moving Interface. Science 265, 2096–2098. https://doi.org/10.1126/science.7522347
Bentley, D.R., Balasubramanian, S., Swerdlow, H.P., Smith, G.P., Milton, J., Brown, C.G., Hall, K.P., Evers, D.J., Barnes, C.L., Bignell, H.R., Boutell, J.M., Bryant, J., Carter, R.J., Keira Cheetham, R., Cox, A.J., Ellis, D.J., Flatbush, M.R., Gormley, N.A., Humphray, S.J., Irving, L.J., Karbelashvili, M.S., Kirk, S.M., Li, H., Liu, X., Maisinger, K.S., Murray, L.J., Obradovic, B., Ost, T., Parkinson, M.L., Pratt, M.R., Rasolonjatovo, I.M.J., Reed, M.T., Rigatti, R., Rodighiero, C., Ross, M.T., Sabot, A., Sankar, S.V., Scally, A., Schroth, G.P., Smith, M.E., Smith, V.P., Spiridou, A., Torrance, P.E., Tzonev, S.S., Vermaas, E.H., Walter, K., Wu, X., Zhang, L., Alam, M.D., Anastasi, C., Aniebo, I.C., Bailey, D.M.D., Bancarz, I.R., Banerjee, S., Barbour, S.G., Baybayan, P.A., Benoit, V.A., Benson, K.F., Bevis, C., Black, P.J., Boodhun, A., Brennan, J.S., Bridgham, J.A., Brown, R.C., Brown, A.A., Buermann, D.H., Bundu, A.A., Burrows, J.C., Carter, N.P., Castillo, N., Chiara E. Catenazzi, M., Chang, S., Neil Cooley, R., Crake, N.R., Dada, O.O., Diakoumakos, K.D., Dominguez-Fernandez, B., Earnshaw, D.J., Egbujor, U.C., Elmore, D.W., Etchin, S.S., Ewan, M.R., Fedurco, M., Fraser, L.J., Fuentes Fajardo, K.V., Scott Furey, W., George, D., Gietzen, K.J., Goddard, C.P., Golda, G.S., Granieri, P.A., Green, D.E., Gustafson, D.L., Hansen, N.F., Harnish, K., Haudenschild, C.D., Heyer, N.I., Hims, M.M., Ho, J.T., Horgan, A.M., Hoschler, K., Hurwitz, S., Ivanov, D.V., Johnson, M.Q., James, T., Huw Jones, T.A., Kang, G.-D., Kerelska, T.H., Kersey, A.D., Khrebtukova, I., Kindwall, A.P., Kingsbury, Z., Kokko-Gonzales, P.I., Kumar, A., Laurent, M.A., Lawley, C.T., Lee, S.E., Lee, X., Liao, A.K., Loch, J.A., Lok, M., Luo, S., Mammen, R.M., Martin, J.W., McCauley, P.G., McNitt, P., Mehta, P., Moon, K.W., Mullens, J.W., Newington, T., Ning, Z., Ling Ng, B., Novo, S.M., O'Neill, M.J., Osborne, M.A., Osnowski, A., Ostadan, O., Paraschos, L.L., Pickering, L., Pike, Andrew C., Pike, Alger C., Chris Pinkard, D., Pliskin, D.P., Podhasky, J., Quijano, V.J., Raczy, C., Rae, V.H., Rawlings, S.R., Chiva Rodriguez, A., Roe, P.M., Rogers, John, Rogert Bacigalupo, M.C., Romanov, N., Romieu, A., Roth, R.K., Rourke, N.J., Ruediger, S.T., Rusman, E., Sanches-Kuiper, R.M., Schenker, M.R., Seoane, J.M., Shaw, R.J., Shiver, M.K., Short, S.W., Sizto, N.L., Sluis, J.P., Smith, M.A., Ernest Sohna Sohna, J., Spence, E.J., Stevens, K., Sutton, N., Szajkowski, L., Tregidgo, C.L., Turcatti, G., vandeVondele, S., Verhovsky, Y., Virk, S.M., Wakelin, S., Walcott, G.C., Wang, J., Worsley, G.J., Yan, J., Yau, L., Zuerlein, M., Rogers, Jane, Mullikin, J.C., Hurles, M.E., McCooke, N.J., West, J.S., Oaks, F.L., Lundberg, P.L., Klenerman, D., Durbin, R., Smith, A.J., 2008. Accurate whole human genome sequencing using reversible terminator chemistry. Nature 456, 53–59. https://doi.org/10.1038/nature07517
Berbenetz, N.M., Nislow, C., Brown, G.W., 2010. Diversity of Eukaryotic DNA Replication Origins Revealed by Genome-Wide Analysis of Chromatin Structure. PLoS Genet. 6, e1001092. https://doi.org/10.1371/journal.pgen.1001092
Berezney, R., Dubey, D.D., Huberman, J.A., 2000. Heterogeneity of eukaryotic replicons, replicon clusters, and replication foci. Chromosoma 108, 471–484. https://doi.org/10.1007/s004120050399
Bernardes, N.E., Fung, H.Y.J., Li, Y., Chen, Z., Chook, Y.M., 2022. Structure of Importin-4 bound to the H3-H4·ASF1 histone·histone chaperone complex (preprint). Molecular Biology. https://doi.org/10.1101/2022.04.08.487665
Bernstein, B.E., Kamal, M., Lindblad-Toh, K., Bekiranov, S., Bailey, D.K., Huebert, D.J., McMahon, S., Karlsson, E.K., Kulbokas, E.J., Gingeras, T.R., Schreiber, S.L., Lander, E.S., 2005. Genomic Maps and Comparative Analysis of Histone Modifications in Human and Mouse. Cell 120, 169–181. https://doi.org/10.1016/j.cell.2005.01.001

Bernstein, E., Duncan, E.M., Masui, O., Gil, J., Heard, E., Allis, C.D., 2006. Mouse Polycomb Proteins Bind Differentially to Methylated Histone H3 and RNA and Are Enriched in Facultative Heterochromatin. Mol. Cell. Biol. 26, 2560–2569. https://doi.org/10.1128/MCB.26.7.2560-2569.2006
Beroukhim, R., Zhang, X., Meyerson, M., 2017. Copy number alterations unmasked as enhancer hijackers. Nat. Genet. 49, 5–6. https://doi.org/10.1038/ng.3754
Bersaglieri, C., Kresoja-Rakic, J., Gupta, S., Bär, D., Kuzyakiv, R., Panatta, M., Santoro, R., 2022. Genome-wide maps of nucleolus interactions reveal distinct layers of repressive chromatin domains. Nat. Commun. 13, 1483. https://doi.org/10.1038/s41467-022-29146-2
Bertero, A., Fields, P.A., Smith, A.S.T., Leonard, A., Beussman, K., Sniadecki, N.J., Kim, D.-H., Tse, H.-F., Pabon, L., Shendure, J., Noble, W.S., Murry, C.E., 2019. Chromatin compartment dynamics in a haploinsufficient model of cardiac laminopathy. J. Cell Biol. 218, 2919–2944. https://doi.org/10.1083/jcb.201902117
Besnard, E., Babled, A., Lapasset, L., Milhavet, O., Parrinello, H., Dantec, C., Marin, J.-M., Lemaitre, J.-M., 2012. Unraveling cell type–specific and reprogrammable human replication origin signatures associated with G-quadruplex consensus motifs. Nat. Struct. Mol. Biol. 19, 837–844. https://doi.org/10.1038/nsmb.2339
Bickmore, W.A., 2013. The Spatial Organization of the Human Genome. Annu. Rev. Genomics Hum. Genet. 14, 67–84. https://doi.org/10.1146/annurev-genom-091212-153515
Bintu, B., Mateo, L.J., Su, J.-H., Sinnott-Armstrong, N.A., Parker, M., Kinrot, S., Yamaya, K., Boettiger, A.N., Zhuang, X., 2018. Super-resolution chromatin tracing reveals domains and cooperative interactions in single cells. Science 362, eaau1783. https://doi.org/10.1126/science.aau1783
Bird, A., 2007. Perceptions of epigenetics. Nature 447, 396–398. https://doi.org/10.1038/nature05913
Bird, A., Taggart, M., Frommer, M., Miller, O.J., Macleod, D., 1985. A fraction of the mouse genome that is derived from islands of nonmethylated, CpG-rich DNA. Cell 40, 91–99. https://doi.org/10.1016/0092-8674(85)90312-5
Bird, A.P., 1978. Use of restriction enzymes to study eukaryotic DNA methylation: II. The symmetry of methylated sites supports semi-conservative copying of the methylation pattern. J. Mol. Biol. 118, 49–60. https://doi.org/10.1016/0022-2836(78)90243-7
Blasiak, J., Szczepańska, J., Sobczuk, A., Fila, M., Pawlowska, E., 2021. RIF1 Links Replication Timing with Fork Reactivation and DNA Double-Strand Break Repair. Int. J. Mol. Sci. 22, 11440. https://doi.org/10.3390/ijms222111440
Blumenfeld, B., Ben-Zimra, M., Simon, I., 2017. Perturbations in the Replication Program Contribute to Genomic Instability in Cancer. Int. J. Mol. Sci. 18, 1138. https://doi.org/10.3390/ijms18061138
Blumenthal, A.B., Kriegstein, H.J., Hogness, D.S., 1974. The Units of DNA Replication in Drosophila melanogaster Chromosomes. Cold Spring Harb. Symp. Quant. Biol. 38, 205–223. https://doi.org/10.1101/SQB.1974.038.01.024
Boehning, M., Dugast-Darzacq, C., Rankovic, M., Hansen, A.S., Yu, T., Marie-Nelly, H., McSwiggen, D.T., Kokic, G., Dailey, G.M., Cramer, P., Darzacq, X., Zweckstetter, M., 2018. RNA polymerase II clustering through carboxy-terminal domain phase separation. Nat. Struct. Mol. Biol. 25, 833–840. https://doi.org/10.1038/s41594-018-0112-y
Boettiger, A., Murphy, S., 2020. Advances in Chromatin Imaging at Kilobase-Scale Resolution. Trends Genet. S0168952519302719. https://doi.org/10.1016/j.tig.2019.12.010
Bolzer, A., Kreth, G., Solovei, I., Koehler, D., Saracoglu, K., Fauth, C., Müller, S., Eils, R., Cremer, C., Speicher, M.R., Cremer, T., 2005. Three-Dimensional Maps of All Chromosomes in Human Male Fibroblast Nuclei and Prometaphase Rosettes. PLoS Biol. 3, e157. https://doi.org/10.1371/journal.pbio.0030157
Bonev, B., Mendelson Cohen, N., Szabo, Q., Fritsch, L., Papadopoulos, G.L., Lubling, Y., Xu, X., Lv, X., Hugnot, J.-P., Tanay, A., Cavalli, G., 2017. Multiscale 3D Genome Rewiring during Mouse Neural Development. Cell 171, 557-572.e24. https://doi.org/10.1016/j.cell.2017.09.043
Bönisch, C., Hake, S.B., 2012. Histone H2A variants in nucleosomes and chromatin: more or less stable? Nucleic Acids Res. 40, 10719–10741. https://doi.org/10.1093/nar/gks865
Borsos, M., Perricone, S.M., Schauer, T., Pontabry, J., De Luca, K.L., De Vries, S.S., Ruiz-Morales, E.R., Torres-Padilla, M.-E., Kind, J., 2019. Genome–lamina interactions are established de novo in the early mouse embryo. Nature 569, 729–733. https://doi.org/10.1038/s41586-019-1233-0
Bortvin, A., Winston, F., 1996. Evidence That Spt6p Controls Chromatin Structure by a Direct Interaction with Histones. Science 272, 1473–1476. https://doi.org/10.1126/science.272.5267.1473
Bosco, G., Du, W., Orr-Weaver, T.L., 2001. DNA replication control through interaction of E2F–RB and the origin recognition complex. Nat. Cell Biol. 3, 289–295. https://doi.org/10.1038/35060086
Bostick, M., Kim, J.K., Estève, P.-O., Clark, A., Pradhan, S., Jacobsen, S.E., 2007. UHRF1 Plays a Role in Maintaining DNA Methylation in Mammalian Cells. Science 317, 1760–1764. https://doi.org/10.1126/science.1147939
Bourc'his, D., Xu, G.-L., Lin, C.-S., Bollman, B., Bestor, T.H., 2001. Dnmt3L and the Establishment of Maternal Genomic Imprints. Science 294, 2536–2539. https://doi.org/10.1126/science.1065848

Bouvier, D., Ferrand, J., Chevallier, O., Paulsen, M.T., Ljungman, M., Polo, S.E., 2021. Dissecting regulatory pathways for transcription recovery following DNA damage reveals a non-canonical function of the histone chaperone HIRA. Nat. Commun. 12, 3835. https://doi.org/10.1038/s41467-021-24153-1
Boveri, T., 1888. Zellen – Studien Heft 2, Die Befruchtung und Teilung des Eles von Ascaris megalocephala II. Verlag von Gustav Fischer, Jena, Germany.
Boveri, T., 1902. Ueber mehrpolige mitosen als mittel zur analyse des zellkerns. Verh Phys-Med Ges Zu Würzbg. 67–90.
Boyarchuk, E., Filipescu, D., Vassias, I., Cantaloube, S., Almouzni, G., 2014. The histone variant composition of centromeres is controlled by the pericentric heterochromatin state during the cell cycle. J. Cell Sci. 127, 3347–3359. https://doi.org/10.1242/jcs.148189
Boyle, S., 2001. The spatial organization of human chromosomes within the nuclei of normal and emerin-mutant cells. Hum. Mol. Genet. 10, 211–219. https://doi.org/10.1093/hmg/10.3.211
Brahma, S., Henikoff, S., 2019. RSC-Associated Subnucleosomes Define MNase-Sensitive Promoters in Yeast. Molecular Cell 73, 238-249.e3. https://doi.org/10.1016/j.molcel.2018.10.046
Branco, M.R., Pombo, A., 2006. Intermingling of Chromosome Territories in Interphase Suggests Role in Translocations and Transcription-Dependent Associations. PLoS Biol. 4, e138. https://doi.org/10.1371/journal.pbio.0040138
Brandão, H.B., Paul, P., Van Den Berg, A.A., Rudner, D.Z., Wang, X., Mirny, L.A., 2019. RNA polymerases as moving barriers to condensin loop extrusion. Proc. Natl. Acad. Sci. 116, 20489–20499. https://doi.org/10.1073/pnas.1907009116
Braunschweig, U., Hogan, G.J., Pagie, L., van Steensel, B., 2009. Histone H1 binding is inhibited by histone variant H3.3. EMBO J. 28, 3635–3645. https://doi.org/10.1038/emboj.2009.301
Brewer, B.J., Fangman, W.L., 1993. Initiation at Closely Spaced Replication Origins in a Yeast Chromosome. Science 262, 1728–1731. https://doi.org/10.1126/science.8259517
Brewer, B.J., Fangman, W.L., 1987. The localization of replication origins on ARS plasmids in S. cerevisiae. Cell 51, 463–471. https://doi.org/10.1016/0092-8674(87)90642-8
Brind'Amour, J., Liu, S., Hudson, M., Chen, C., Karimi, M.M., Lorincz, M.C., 2015. An ultra-low-input native ChIP-seq protocol for genome-wide profiling of rare cell populations. Nat Commun 6, 6033. https://doi.org/10.1038/ncomms7033
Brown, Z.Z., Müller, M.M., Jain, S.U., Allis, C.D., Lewis, P.W., Muir, T.W., 2014. Strategy for "Detoxification" of a Cancer-Derived Histone Mutant Based on Mapping Its Interaction with the Methyltransferase PRC2. J. Am. Chem. Soc. 136, 13498–13501. https://doi.org/10.1021/ja5060934
Brush, D., Dodgson, J.B., Choi, O.-R., Stevens, P.W., Engel, J.D., 1985. Replacement Variant Histone Genes Contain Intervening Sequences. Mol. Cell. Biol. 5, 1307–1317. https://doi.org/10.1128/mcb.5.6.1307-1317.1985
Buitrago, D., Labrador, M., Arcon, J.P., Lema, R., Flores, O., Esteve-Codina, A., Blanc, J., Villegas, N., Bellido, D., Gut, M., Dans, P.D., Heath, S.C., Gut, I.G., Brun Heath, I., Orozco, M., 2021. Impact of DNA methylation on 3D genome structure. Nat. Commun. 12, 3243. https://doi.org/10.1038/s41467-021-23142-8
Buongiorno-Nardelli, M., Micheli, G., Carrĩ, M.T., Marilley, M., 1982. A relationship between replicon size and supercoiled loop domains in the eukaryotic genome. Nature 298, 100–102. https://doi.org/10.1038/298100a0
Buonomo, S.B.C., Wu, Y., Ferguson, D., de Lange, T., 2009. Mammalian Rif1 contributes to replication stress survival and homology-directed repair. J. Cell Biol. 187, 385–398. https://doi.org/10.1083/jcb.200902039
Burgers, P.M.J., Kunkel, T.A., 2017. Eukaryotic DNA Replication Fork. Annu. Rev. Biochem. 86, 417–438. https://doi.org/10.1146/annurev-biochem-061516-044709
Burgess, R.J., Zhang, Z., 2013. Histone chaperones in nucleosome assembly and human disease. Nat. Struct. Mol. Biol. 20, 14–22. https://doi.org/10.1038/nsmb.2461
Burns, J., Chan, V.T., Jonasson, J.A., Fleming, K.A., Taylor, S., McGee, J.O., 1985. Sensitive system for visualising biotinylated DNA probes hybridised in situ: rapid sex determination of intact cells. J. Clin. Pathol. 38, 1085–1092. https://doi.org/10.1136/jcp.38.10.1085
Bush, K.M., Yuen, B.T., Barrilleaux, B.L., Riggs, J.W., O'Geen, H., Cotterman, R.F., Knoepfler, P.S., 2013. Endogenous mammalian histone H3.3 exhibits chromatin-related functions during development. Epigenetics Chromatin 6, 7. https://doi.org/10.1186/1756-8935-6-7
Busslinger, G.A., Stocsits, R.R., van der Lelij, P., Axelsson, E., Tedeschi, A., Galjart, N., Peters, J.-M., 2017. Cohesin is positioned in mammalian genomes by transcription, CTCF and Wapl. Nature 544, 503–507. https://doi.org/10.1038/nature22063
Cadoret, J.-C., Meisch, F., Hassan-Zadeh, V., Luyten, I., Guillet, C., Duret, L., Quesneville, H., Prioleau, M.-N., 2008. Genome-wide studies highlight indirect links between human replication origins and gene regulation. Proc. Natl. Acad. Sci. 105, 15837–15842. https://doi.org/10.1073/pnas.0805208105
Cairns, J., 1966. Autoradiography of HeLa cell DNA. J. Mol. Biol. 15, 372-IN32. https://doi.org/10.1016/S0022-2836(66)80233-4

Cajal, S.R., 1903. Un sencillo método de coloración selectiva del retículo protoplasmático y sus efectos en diversos órganos nerviosos. Trab Lab Invest Biol 129–221.
Callan, H.G., 1974. DNA Replication in the Chromosomes of Eukaryotes. Cold Spring Harb. Symp. Quant. Biol. 38, 195–203. https://doi.org/10.1101/SQB.1974.038.01.023
Campos, E.I., Fillingham, J., Li, G., Zheng, H., Voigt, P., Kuo, W.-H.W., Seepany, H., Gao, Z., Day, L.A., Greenblatt, J.F., Reinberg, D., 2010. The program for processing newly synthesized histones H3.1 and H4. Nat. Struct. Mol. Biol. 17, 1343–1351. https://doi.org/10.1038/nsmb.1911
Cardozo Gizzi, A.M., Cattoni, D.I., Fiche, J.-B., Espinola, S.M., Gurgo, J., Messina, O., Houbron, C., Ogiyama, Y., Papadopoulos, G.L., Cavalli, G., Lagha, M., Nollmann, M., 2019. Microscopy-Based Chromosome Conformation Capture Enables Simultaneous Visualization of Genome Organization and Transcription in Intact Organisms. Mol. Cell 74, 212-222.e5. https://doi.org/10.1016/j.molcel.2019.01.011
Carraro, M., Flury, V., Liu, Y., Luo, M., Chen, L., Groth, A., Huang, H., 2022. NASP maintains histone H3–H4 homeostasis through two distinct H3 binding modes 20.
Carraro, M., Hendriks, I.A., Hammond, C.M., Solis-Mezarino, V., Völker-Albert, M., Elsborg, J.D., Weisser, M.B., Spanos, C., Montoya, G., Rappsilber, J., Imhof, A., Nielsen, M.L., Groth, A., 2023. DAXX adds a de novo H3.3K9me3 deposition pathway to the histone chaperone network. Mol. Cell S1097276523001077. https://doi.org/10.1016/j.molcel.2023.02.009
Caspersson, T., De La Chapelle, A., Schröder, J., Zech, L., 1972. Quinacrine fluorescence of metaphase chromosomes. Exp. Cell Res. 72, 56–59. https://doi.org/10.1016/0014-4827(72)90566-6
Caspersson, T., Zech, L., Johansson, C., Modest, E.J., 1970. Identification of human chromosomes by DNA-binding fluorescent agents. Chromosoma 30, 215–227. https://doi.org/10.1007/BF00282002
Cayrou, C., Ballester, B., Peiffer, I., Fenouil, R., Coulombe, P., Andrau, J.-C., van Helden, J., Méchali, M., 2015. The chromatin environment shapes DNA replication origin organization and defines origin classes. Genome Res. 25, 1873–1885. https://doi.org/10.1101/gr.192799.115
Cayrou, C., Coulombe, P., Vigneron, A., Stanojcic, S., Ganier, O., Peiffer, I., Rivals, E., Puy, A., Laurent-Chabalier, S., Desprat, R., Méchali, M., 2011. Genome-scale analysis of metazoan replication origins reveals their organization in specific but flexible sites defined by conserved features. Genome Res. 21, 1438–1449. https://doi.org/10.1101/gr.121830.111
Cayrou, C., Grégoire, D., Coulombe, P., Danis, E., Méchali, M., 2012. Genome-scale identification of active DNA replication origins. Methods 57, 158–164. https://doi.org/10.1016/j.ymeth.2012.06.015
Chacin, E., Reusswig, K.-U., Furtmeier, J., Bansal, P., Karl, L.A., Pfander, B., Straub, T., Korber, P., Kurat, C.F., 2023. Establishment and function of chromatin organization at replication origins. Nature 616, 836–842. https://doi.org/10.1038/s41586-023-05926-8
Chan, K.-M., Fang, D., Gan, H., Hashizume, R., Yu, C., Schroeder, M., Gupta, N., Mueller, S., James, C.D., Jenkins, R., Sarkaria, J., Zhang, Z., 2013. The histone H3.3K27M mutation in pediatric glioma reprograms H3K27 methylation and gene expression. Genes Dev. 27, 985–990. https://doi.org/10.1101/gad.217778.113
Chandrasekhara, C., Ranjan, R., Urban, J.A., Davis, B.E.M., Ku, W.L., Snedeker, J., Zhao, K., Chen, X., 2023. A single N-terminal amino acid determines the distinct roles of histones H3 and H3.3 in the Drosophila male germline stem cell lineage. PLOS Biol. 21, e3002098. https://doi.org/10.1371/journal.pbio.3002098
Chang, F.T.M., McGhie, J.D., Chan, F.L., Tang, M.C., Anderson, M.A., Mann, J.R., Andy Choo, K.H., Wong, L.H., 2013. PML bodies provide an important platform for the maintenance of telomeric chromatin integrity in embryonic stem cells. Nucleic Acids Res. 41, 4447–4458. https://doi.org/10.1093/nar/gkt114
Chargaff, E., 1950. Chemical specificity of nucleic acids and mechanism of their enzymatic degradation. Experientia 6, 201–209. https://doi.org/10.1007/BF02173653
Cheloufi, S., Elling, U., Hopfgartner, B., Jung, Y.L., Murn, J., Ninova, M., Hubmann, M., Badeaux, A.I., Euong Ang, C., Tenen, D., Wesche, D.J., Abazova, N., Hogue, M., Tasdemir, N., Brumbaugh, J., Rathert, P., Jude, J., Ferrari, F., Blanco, A., Fellner, M., Wenzel, D., Zinner, M., Vidal, S.E., Bell, O., Stadtfeld, M., Chang, H.Y., Almouzni, G., Lowe, S.W., Rinn, J., Wernig, M., Aravin, A., Shi, Y., Park, P.J., Penninger, J.M., Zuber, J., Hochedlinger, K., 2015. The histone chaperone CAF-1 safeguards somatic cell identity. Nature 528, 218–224. https://doi.org/10.1038/nature15749
Chen, B., MacAlpine, H.K., Hartemink, A.J., MacAlpine, D.M., 2023. Spatiotemporal kinetics of CAF-1-dependent chromatin maturation ensures transcription fidelity during S-phase (preprint). Molecular Biology. https://doi.org/10.1101/2023.05.25.541209
Chen, S., Rufiange, A., Huang, H., Rajashankar, K.R., Nourani, A., Patel, D.J., 2015. Structure–function studies of histone H3/H4 tetramer maintenance during transcription by chaperone Spt2. Genes Dev. 29, 1326–1340. https://doi.org/10.1101/gad.261115.115
Chen, H., Levo, M., Barinov, L., Fujioka, M., Jaynes, J.B., Gregor, T., 2018. Dynamic interplay between enhancer–promoter topology and gene activity. Nat. Genet. 50, 1296–1303. https://doi.org/10.1038/s41588-018-0175-z

Chen, X., Ke, Y., Wu, K., Zhao, H., Sun, Y., Gao, L., Liu, Z., Zhang, J., Tao, W., Hou, Z., Liu, H., Liu, J., Chen, Z.-J., 2019. Key role for CTCF in establishing chromatin structure in human embryos. Nature. https://doi.org/10.1038/s41586-019-1812-0
Chen, X., Müller, G.A., Quaas, M., Fischer, M., Han, N., Stutchbury, B., Sharrocks, A.D., Engeland, K., 2013. The Forkhead Transcription Factor FOXM1 Controls Cell Cycle-Dependent Gene Expression through an Atypical Chromatin Binding Mechanism. Mol. Cell. Biol. 33, 227–236. https://doi.org/10.1128/MCB.00881-12
Cheng, L., Zhang, X., Wang, Y., Gan, H., Xu, X., Lv, X., Hua, X., Que, J., Ordog, T., Zhang, Z., 2019. Chromatin Assembly Factor 1 (CAF-1) facilitates the establishment of facultative heterochromatin during pluripotency exit. Nucleic Acids Res. gkz858. https://doi.org/10.1093/nar/gkz858
Choy, J.S., Wei, S., Lee, J.Y., Tan, S., Chu, S., Lee, T.-H., 2010. DNA Methylation Increases Nucleosome Compaction and Rigidity. J. Am. Chem. Soc. 132, 1782–1783. https://doi.org/10.1021/ja910264z
Ciemerych, M.A., Sicinski, P., 2005. Cell cycle in mouse development. Oncogene 24, 2877–2898. https://doi.org/10.1038/sj.onc.1208608
Clapier, C.R., Iwasa, J., Cairns, B.R., Peterson, C.L., 2017. Mechanisms of action and regulation of ATP-dependent chromatin-remodelling complexes. Nat. Rev. Mol. Cell Biol. 18, 407–422. https://doi.org/10.1038/nrm.2017.26
Clark, D.J., 2010. Nucleosome Positioning, Nucleosome Spacing and the Nucleosome Code. J. Biomol. Struct. Dyn. 27, 781–793. https://doi.org/10.1080/073911010010524945
Clément, C., Almouzni, G., 2015. MCM2 binding to histones H3–H4 and ASF1 supports a tetramer-to-dimer model for histone inheritance at the replication fork. Nat. Struct. Mol. Biol. 22, 587–589. https://doi.org/10.1038/nsmb.3067
Clément, C., Orsi, G.A., Gatto, A., Boyarchuk, E., Forest, A., Hajj, B., Miné-Hattab, J., Garnier, M., Gurard-Levin, Z.A., Quivy, J.-P., Almouzni, G., 2018. High-resolution visualization of H3 variants during replication reveals their controlled recycling. Nat. Commun. 9, 3181. https://doi.org/10.1038/s41467-018-05697-1
Cleveland, D.W., Mao, Y., Sullivan, K.F., 2003. Centromeres and Kinetochores: From Epigenetics to Mitotic Checkpoint Signaling. Cell 112, 407–421. https://doi.org/10.1016/S0092-8674(03)00115-6
Clynes, D., Jelinska, C., Xella, B., Ayyub, H., Scott, C., Mitson, M., Taylor, S., Higgs, D.R., Gibbons, R.J., 2015. Suppression of the alternative lengthening of telomere pathway by the chromatin remodelling factor ATRX. Nat. Commun. 6, 7538. https://doi.org/10.1038/ncomms8538
Collart, C., Allen, G.E., Bradshaw, C.R., Smith, J.C., Zegerman, P., 2013. Titration of Four Replication Factors Is Essential for the *Xenopus laevis* Midblastula Transition. Science 341, 893–896. https://doi.org/10.1126/science.1241530
Collombet, S., Ranisavljevic, N., Nagano, T., Varnai, C., Shisode, T., Leung, W., Piolot, T., Galupa, R., Borensztein, M., Servant, N., Fraser, P., Ancelin, K., Heard, E., 2020. Parental-to-embryo switch of chromosome organization in early embryogenesis. Nature 580, 142–146. https://doi.org/10.1038/s41586-020-2125-z
Conti, C., Sacca, B., Herrick, J., Lalou, C., Pommier, Y., Bensimon, A., 2007. Replication Fork Velocities at Adjacent Replication Origins Are Coordinately Modified during DNA Replication in Human Cells□D. Mol. Biol. Cell 18.
Cook, A.J.L., Gurard-Levin, Z.A., Vassias, I., Almouzni, G., 2011. A Specific Function for the Histone Chaperone NASP to Fine-Tune a Reservoir of Soluble H3-H4 in the Histone Supply Chain. Molecular Cell 44, 918–927. https://doi.org/10.1016/j.molcel.2011.11.021
Cornacchia, D., Dileep, V., Quivy, J.-P., Foti, R., Tili, F., Santarella-Mellwig, R., Antony, C., Almouzni, G., Gilbert, D.M., Buonomo, S.B.C., 2012. Mouse Rif1 is a key regulator of the replication-timing programme in mammalian cells: Mouse Rif1 controls replication timing. EMBO J. 31, 3678–3690. https://doi.org/10.1038/emboj.2012.214
Corpet, A., Olbrich, T., Gwerder, M., Fink, D., Stucki, M., 2014. Dynamics of histone H3.3 deposition in proliferating and senescent cells reveals a DAXX-dependent targeting to PML-NBs important for pericentromeric heterochromatin organization. Cell Cycle 13, 249–267. https://doi.org/10.4161/cc.26988
Costa, A., Diffley, J.F.X., 2022. The Initiation of Eukaryotic DNA Replication. Annu. Rev. Biochem. 91, 107–131. https://doi.org/10.1146/annurev-biochem-072321-110228
Costlow, N., Lis, J.T., 1984. High-Resolution Mapping of DNase I-Hypersensitive Sites of *Drosophila* Heat Shock Genes in *Drosophila melanogaster* and *Saccharomyces cerevisiae*. Mol. Cell. Biol. 4, 1853–1863. https://doi.org/10.1128/mcb.4.9.1853-1863.1984
Couldrey, C., Carlton, M.B.L., Nolan, P.M., Colledge, W.H., Evans, M.J., 1999. A retroviral Gene Trap Insertion into the Histone 3.3A Gene Causes Partial Neonatal Lethality, Stunted Growth, Neuromuscular Deficits and Male Sub-fertility in Transgenic Mice. Hum. Mol. Genet. 8, 2489–2495. https://doi.org/10.1093/hmg/8.13.2489
Courbet, S., Gay, S., Arnoult, N., Wronka, G., Anglana, M., Brison, O., Debatisse, M., 2008. Replication fork movement sets chromatin loop size and origin choice in mammalian cells. Nature 455, 557–560. https://doi.org/10.1038/nature07233

Cousens, L.S., Alberts, B.M., 1982. Accessibility of newly synthesized chromatin to histone acetylase. J. Biol. Chem. 257, 3945–3949. https://doi.org/10.1016/S0021-9258(18)34874-9
Crane, E., Bian, Q., McCord, R.P., Lajoie, B.R., Wheeler, B.S., Ralston, E.J., Uzawa, S., Dekker, J., Meyer, B.J., 2015. Condensin-driven remodelling of X chromosome topology during dosage compensation. Nature 523, 240–244. https://doi.org/10.1038/nature14450
Cremer, M., Brandstetter, K., Maiser, A., Rao, S.S.P., Schmid, V.J., Guirao-Ortiz, M., Mitra, N., Mamberti, S., Klein, K.N., Gilbert, D.M., Leonhardt, H., Cardoso, M.C., Aiden, E.L., Harz, H., Cremer, T., 2020. Cohesin depleted cells rebuild functional nuclear compartments after endomitosis. Nat. Commun. 11, 6146. https://doi.org/10.1038/s41467-020-19876-6
Cremer, T., Cremer, C., 2006a. Rise, fall and resurrection of chromosome territories: a historical perspective Part II. Fall and resurrection of chromosome territories during the 1950s to 1980s. Part III. Chromosome territories and the functional nuclear architecture: experiments and m. Eur. J. Histochem. 50, 223–272. https://doi.org/10.4081/995
Cremer, T., Cremer, C., 2006b. Rise, fall and resurrection of chromosome territories: a historical perspective. Part I. The rise of chromosome territories. Eur. J. Histochem. 50, 161–176. https://doi.org/10.4081/989
Creyghton, M.P., Cheng, A.W., Welstead, G.G., Kooistra, T., Carey, B.W., Steine, E.J., Hanna, J., Lodato, M.A., Frampton, G.M., Sharp, P.A., Boyer, L.A., Young, R.A., Jaenisch, R., 2010. Histone H3K27ac separates active from poised enhancers and predicts developmental state. Proc. Natl. Acad. Sci. 107, 21931–21936. https://doi.org/10.1073/pnas.1016071107
Croft, J.A., Bridger, J.M., Boyle, S., Perry, P., Teague, P., Bickmore, W.A., 1999. Differences in the Localization and Morphology of Chromosomes in the Human Nucleus. J. Cell Biol. 145, 1119–1131. https://doi.org/10.1083/jcb.145.6.1119
Cuartero, S., Weiss, F.D., Dharmalingam, G., Guo, Y., Ing-Simmons, E., Masella, S., Robles-Rebollo, I., Xiao, X., Wang, Y.-F., Barozzi, I., Djeghloul, D., Amano, M.T., Niskanen, H., Petretto, E., Dowell, R.D., Tachibana, K., Kaikkonen, M.U., Nasmyth, K.A., Lenhard, B., Natoli, G., Fisher, A.G., Merkenschlager, M., 2018. Control of inducible gene expression links cohesin to hematopoietic progenitor self-renewal and differentiation. Nat. Immunol. 19, 932–941. https://doi.org/10.1038/s41590-018-0184-1
Czajkowsky, D.M., Liu, J., Hamlin, J.L., Shao, Z., 2008. DNA Combing Reveals Intrinsic Temporal Disorder in the Replication of Yeast Chromosome VI. J. Mol. Biol. 375, 12–19. https://doi.org/10.1016/j.jmb.2007.10.046
Dan, J., Liu, Y., Liu, N., Chiourea, M., Okuka, M., Wu, T., Ye, X., Mou, C., Wang, Lei, Wang, Lingling, Yin, Y., Yuan, J., Zuo, B., Wang, F., Li, Z., Pan, X., Yin, Z., Chen, L., Keefe, D.L., Gagos, S., Xiao, A., Liu, L., 2014. Rif1 Maintains Telomere Length Homeostasis of ESCs by Mediating Heterochromatin Silencing. Dev. Cell 29, 7–19. https://doi.org/10.1016/j.devcel.2014.03.004
Dang, D., Zhang, S.-W., Duan, R., Zhang, S., 2023. Defining the separation landscape of topological domains for decoding consensus domain organization of the 3D genome. Genome Res. genome;gr.277187.122v2. https://doi.org/10.1101/gr.277187.122
Danis, E., Brodolin, K., Menut, S., Maiorano, D., Girard-Reydet, C., Méchali, M., 2004. Specification of a DNA replication origin by a transcription complex. Nat. Cell Biol. 6, 721–730. https://doi.org/10.1038/ncb1149
D'Anna, J.A.Jr., Isenberg, I., 1974. Histone cross-complexing pattern. Biochemistry 13, 4992–4997. https://doi.org/10.1021/bi00721a019
Davidson, I.F., Barth, R., Zaczek, M., Van Der Torre, J., Tang, W., Nagasaka, K., Janissen, R., Kerssemakers, J., Wutz, G., Dekker, C., Peters, J.-M., 2023. CTCF is a DNA-tension-dependent barrier to cohesin-mediated loop extrusion. Nature. https://doi.org/10.1038/s41586-023-05961-5
Davidson, I.F., Bauer, B., Goetz, D., Tang, W., Wutz, G., Peters, J.-M., 2019. DNA loop extrusion by human cohesin. Science eaaz3418. https://doi.org/10.1126/science.aaz3418
Davidson, I.F., Goetz, D., Zaczek, M.P., Molodtsov, M.I., Huis in 't Veld, P.J., Weissmann, F., Litos, G., Cisneros, D.A., Ocampo-Hafalla, M., Ladurner, R., Uhlmann, F., Vaziri, A., Peters, J.-M., 2016. Rapid movement and transcriptional re-localization of human cohesin on DNA. EMBO J. 35, 2671–2685. https://doi.org/10.15252/embj.201695402
Davidson, I.F., Peters, J.-M., 2021. Genome folding through loop extrusion by SMC complexes. Nat. Rev. Mol. Cell Biol. https://doi.org/10.1038/s41580-021-00349-7
De Koning, L., Corpet, A., Haber, J.E., Almouzni, G., 2007. Histone chaperones: an escort network regulating histone traffic. Nat. Struct. Mol. Biol. 14, 997–1007. https://doi.org/10.1038/nsmb1318
de Vries, H., 1900a. Sur la loi de disjonction des hybrides. Comptes Rendus Acad. Sci. Paris 845–47.
de Vries, H., 1900b. Das Spaltungsgestetz der Bastarde. Berichte Dtsch. Bot. Ges. 83–90.
Deaton, A.M., Gómez-Rodríguez, M., Mieczkowski, J., Tolstorukov, M.Y., Kundu, S., Sadreyev, R.I., Jansen, L.E., Kingston, R.E., 2016. Enhancer regions show high histone H3.3 turnover that changes during differentiation. eLife 5, e15316. https://doi.org/10.7554/eLife.15316
Debatisse, Mi., Toledo, F., Anglana, M., 2004. Replication Initiation In Mammalian Cells: Changing Preferences. Cell Cycle 3, 18–20. https://doi.org/10.4161/cc.3.1.628

Debaugny, R.E., Skok, J.A., 2020. CTCF and CTCFL in cancer. Curr. Opin. Genet. Dev. 61, 44–52. https://doi.org/10.1016/j.gde.2020.02.021
Dekker, J., Rippe, K., Dekker, M., Kleckner, N., 2002. Capturing Chromosome Conformation 295, 7.
Delaney, K., Mailler, J., Wenda, J.M., Gabus, C., Steiner, F.A., 2018. Differential Expression of Histone H3.3 Genes and Their Role in Modulating Temperature Stress Response in Caenorhabditis elegans. Genetics 209, 551–565. https://doi.org/10.1534/genetics.118.300909
Delbarre, E., Ivanauskiene, K., Kuntziger, T., Collas, P., 2013. DAXX-dependent supply of soluble (H3.3-H4) dimers to PML bodies pending deposition into chromatin. Genome Res. 23, 440–451. https://doi.org/10.1101/gr.142703.112
Dellino, G.I., Cittaro, D., Piccioni, R., Luzi, L., Banfi, S., Segalla, S., Cesaroni, M., Mendoza-Maldonado, R., Giacca, M., Pelicci, P.G., 2013. Genome-wide mapping of human DNA-replication origins: Levels of transcription at ORC1 sites regulate origin selection and replication timing. Genome Res. 23, 1–11. https://doi.org/10.1101/gr.142331.112
Deng, Y., Bartosovic, M., Kukanja, P., Zhang, D., Liu, Y., Su, G., Enninful, A., Bai, Z., Castelo-Branco, G., Fan, R., 2022. Spatial-CUT&Tag: Spatially resolved chromatin modification profiling at the cellular level. Science 375, 681–686. https://doi.org/10.1126/science.abg7216
DePamphilis, M.L., 1999. Replication origins in metazoan chromosomes: fact or fiction? BioEssays 21, 5–16. https://doi.org/10.1002/(SICI)1521-1878(199901)21:1<5::AID-BIES2>3.0.CO;2-6
Dequeker, B.J.H., Scherr, M.J., Brandão, H.B., Gassler, J., Powell, S., Gaspar, I., Flyamer, I.M., Lalic, A., Tang, W., Stocsits, R., Davidson, I.F., Peters, J.-M., Duderstadt, K.E., Mirny, L.A., Tachibana, K., 2022. MCM complexes are barriers that restrict cohesin-mediated loop extrusion. Nature. https://doi.org/10.1038/s41586-022-04730-0
Di Cerbo, V., Mohn, F., Ryan, D.P., Montellier, E., Kacem, S., Tropberger, P., Kallis, E., Holzner, M., Hoerner, L., Feldmann, A., Richter, F.M., Bannister, A.J., Mittler, G., Michaelis, J., Khochbin, S., Feil, R., Schuebeler, D., Owen-Hughes, T., Daujat, S., Schneider, R., 2014. Acetylation of histone H3 at lysine 64 regulates nucleosome dynamics and facilitates transcription. eLife 3, e01632. https://doi.org/10.7554/eLife.01632
Di Pierro, M., Cheng, R.R., Lieberman Aiden, E., Wolynes, P.G., Onuchic, J.N., 2017. De novo prediction of human chromosome structures: Epigenetic marking patterns encode genome architecture. Proc. Natl. Acad. Sci. 114, 12126–12131. https://doi.org/10.1073/pnas.1714980114
Dileep, V., Ay, F., Sima, J., Vera, D.L., Noble, W.S., Gilbert, D.M., 2015a. Topologically associating domains and their long-range contacts are established during early G1 coincident with the establishment of the replication-timing program. Genome Res. 25, 1104–1113. https://doi.org/10.1101/gr.183699.114
Dileep, V., Gilbert, D.M., 2018. Single-cell replication profiling to measure stochastic variation in mammalian replication timing. Nat. Commun. 9, 427. https://doi.org/10.1038/s41467-017-02800-w
Dileep, V., Rivera-Mulia, J.C., Sima, J., Gilbert, D.M., 2015b. Large-Scale Chromatin Structure–Function Relationships during the Cell Cycle and Development: Insights from Replication Timing. Cold Spring Harb. Symp. Quant. Biol. 80, 53–63. https://doi.org/10.1101/sqb.2015.80.027284
Dileep, V., Wilson, K.A., Marchal, C., Lyu, X., Zhao, P.A., Li, B., Poulet, A., Bartlett, D.A., Rivera-Mulia, J.C., Qin, Z.S., Robins, A.J., Schulz, T.C., Kulik, M.J., McCord, R.P., Dekker, J., Dalton, S., Corces, V.G., Gilbert, D.M., 2019. Rapid Irreversible Transcriptional Reprogramming in Human Stem Cells Accompanied by Discordance between Replication Timing and Chromatin Compartment. Stem Cell Rep. 13, 193–206. https://doi.org/10.1016/j.stemcr.2019.05.021
Dilworth, S.M., Black, S.J., Laskey, R.A., 1987. Two complexes that contain histones are required for nucleosome assembly in vitro: Role of nucleoplasmin and N1 in Xenopus egg extracts. Cell 51, 1009–1018. https://doi.org/10.1016/0092-8674(87)90587-3
Dimitrova, D.S., Berezney, R., 2002. The spatio-temporal organization of DNA replication sites is identical in primary, immortalized and transformed mammalian cells. J. Cell Sci. 115, 4037–4051. https://doi.org/10.1242/jcs.00087
Dimitrova, D.S., Gilbert, D.M., 1999. The Spatial Position and Replication Timing of Chromosomal Domains Are Both Established in Early G1 Phase. Mol. Cell 4, 983–993. https://doi.org/10.1016/S1097-2765(00)80227-0
Dixon, J.R., Jung, I., Selvaraj, S., Shen, Y., Antosiewicz-Bourget, J.E., Lee, A.Y., Ye, Z., Kim, A., Rajagopal, N., Xie, W., Diao, Y., Liang, J., Zhao, H., Lobanenkov, V.V., Ecker, J.R., Thomson, J.A., Ren, B., 2015. Chromatin architecture reorganization during stem cell differentiation. Nature 518, 331–336. https://doi.org/10.1038/nature14222
Dixon, J.R., Selvaraj, S., Yue, F., Kim, A., Li, Y., Shen, Y., Hu, M., Liu, J.S., Ren, B., 2012. Topological domains in mammalian genomes identified by analysis of chromatin interactions. Nature 485, 376–380. https://doi.org/10.1038/nature11082
Donato, J.J., Chung, S.C.C., Tye, B.K., 2006. Genome-Wide Hierarchy of Replication Origin Usage in Saccharomyces cerevisiae. PLOS Genet. 2, e141. https://doi.org/10.1371/journal.pgen.0020141

Doskočil, J., Šorm, F., 1962. Distribution of 5-methylcytosine in pyrimidine sequences of deoxyribonucleic acids. Biochim. Biophys. Acta 55, 953–959. https://doi.org/10.1016/0006-3002(62)90909-5
Dostie, J., Richmond, T.A., Arnaout, R.A., Selzer, R.R., Lee, W.L., Honan, T.A., Rubio, E.D., Krumm, A., Lamb, J., Nusbaum, C., Green, R.D., Dekker, J., 2006. Chromosome Conformation Capture Carbon Copy (5C): A massively parallel solution for mapping interactions between genomic elements. Genome Res. 16, 1299–1309. https://doi.org/10.1101/gr.5571506
Dowen, J.M., Fan, Z.P., Hnisz, D., Ren, G., Abraham, B.J., Zhang, L.N., Weintraub, A.S., Schuijers, J., Lee, T.I., Zhao, K., Young, R.A., 2014. Control of Cell Identity Genes Occurs in Insulated Neighborhoods in Mammalian Chromosomes. Cell 159, 374–387. https://doi.org/10.1016/j.cell.2014.09.030
Draker, R., Sarcinella, E., Cheung, P., 2011. USP10 deubiquitylates the histone variant H2A.Z and both are required for androgen receptor-mediated gene activation. Nucleic Acids Res. 39, 3529–3542. https://doi.org/10.1093/nar/gkq1352
Drané, P., Ouararhni, K., Depaux, A., Shuaib, M., Hamiche, A., 2010. The death-associated protein DAXX is a novel histone chaperone involved in the replication-independent deposition of H3.3. Genes Dev. 24, 1253–1265. https://doi.org/10.1101/gad.566910
Du, Q., Smith, G.C., Luu, P.L., Ferguson, J.M., Armstrong, N.J., Caldon, C.E., Campbell, E.M., Nair, S.S., Zotenko, E., Gould, C.M., Buckley, M., Chia, K.-M., Portman, N., Lim, E., Kaczorowski, D., Chan, C.-L., Barton, K., Deveson, I.W., Smith, M.A., Powell, J.E., Skvortsova, K., Stirzaker, C., Achinger-Kawecka, J., Clark, S.J., 2021. DNA methylation is required to maintain both DNA replication timing precision and 3D genome organization integrity. Cell Rep. 36, 109722. https://doi.org/10.1016/j.celrep.2021.109722
Du, Z., Zheng, H., Huang, B., Ma, R., Wu, J., Zhang, Xianglin, He, J., Xiang, Y., Wang, Q., Li, Y., Ma, J., Zhang, Xu, Zhang, K., Wang, Y., Zhang, M.Q., Gao, J., Dixon, J.R., Wang, X., Zeng, J., Xie, W., 2017. Allelic reprogramming of 3D chromatin architecture during early mammalian development. Nature 547, 232–235. https://doi.org/10.1038/nature23263
Du, Z., Zheng, H., Kawamura, Y.K., Zhang, K., Gassler, J., Powell, S., Xu, Q., Lin, Z., Xu, K., Zhou, Q., Ozonov, E.A., Véron, N., Huang, B., Li, L., Yu, G., Liu, L., Au Yeung, W.K., Wang, P., Chang, L., Wang, Q., He, A., Sun, Y., Na, J., Sun, Q., Sasaki, H., Tachibana, K., Peters, A.H.F.M., Xie, W., 2020. Polycomb Group Proteins Regulate Chromatin Architecture in Mouse Oocytes and Early Embryos. Mol. Cell 77, 825-839.e7. https://doi.org/10.1016/j.molcel.2019.11.011
Duan, Z., Andronescu, M., Schutz, K., McIlwain, S., Kim, Y.J., Lee, C., Shendure, J., Fields, S., Blau, C.A., Noble, W.S., 2010. A three-dimensional model of the yeast genome. Nature 465, 363–367. https://doi.org/10.1038/nature08973
Dunleavy, E.M., Almouzni, G., Karpen, G.H., 2011. H3.3 is deposited at centromeres in S phase as a placeholder for newly assembled CENP-A in G $_1$ phase. Nucleus 2, 146–157. https://doi.org/10.4161/nucl.2.2.15211
Dunleavy, E.M., Roche, D., Tagami, H., Lacoste, N., Ray-Gallet, D., Nakamura, Y., Daigo, Y., Nakatani, Y., Almouzni-Pettinotti, G., 2009. HJURP Is a Cell-Cycle-Dependent Maintenance and Deposition Factor of CENP-A at Centromeres. Cell 137, 485–497. https://doi.org/10.1016/j.cell.2009.02.040
Earnshaw, W.C., Rothfield, N., 1985. Identification of a family of human centromere proteins using autoimmune sera from patients with scleroderma. Chromosoma 91, 313–321. https://doi.org/10.1007/BF00328227
Eaton, M.L., Galani, K., Kang, S., Bell, S.P., MacAlpine, D.M., 2010. Conserved nucleosome positioning defines replication origins. Genes Dev. 24, 748–753. https://doi.org/10.1101/gad.1913210
Eaton, M.L., Prinz, J.A., MacAlpine, H.K., Tretyakov, G., Kharchenko, P.V., MacAlpine, D.M., 2011. Chromatin signatures of the Drosophila replication program. Genome Res. 21, 164–174. https://doi.org/10.1101/gr.116038.110
Edenberg, H.J., Huberman, J.A., 1975. EUKARYOTIC CHROMOSOME REPLICATION. Annu. Rev. Genet. 9, 245–284. https://doi.org/10.1146/annurev.ge.09.120175.001333
Edmunds, J.W., Mahadevan, L.C., Clayton, A.L., 2008. Dynamic histone H3 methylation during gene induction: HYPB/Setd2 mediates all H3K36 trimethylation. EMBO J. 27, 406–420. https://doi.org/10.1038/sj.emboj.7601967
Efroni, S., Duttagupta, R., Cheng, J., Dehghani, H., Hoeppner, D.J., Dash, C., Bazett-Jones, D.P., Le Grice, S., McKay, R.D.G., Buetow, K.H., Gingeras, T.R., Misteli, T., Meshorer, E., 2008. Global Transcription in Pluripotent Embryonic Stem Cells. Cell Stem Cell 2, 437–447. https://doi.org/10.1016/j.stem.2008.03.021
Ejlassi-Lassallette, A., Mocquard, E., Arnaud, M.-C., Thiriet, C., 2011. H4 replication-dependent diacetylation and Hat1 promote S-phase chromatin assembly in vivo. Mol. Biol. Cell 22, 245–255. https://doi.org/10.1091/mbc.e10-07-0633
El Khattabi, L., Zhao, H., Kalchschmidt, J., Young, N., Jung, S., Van Blerkom, P., Kieffer-Kwon, P., Kieffer-Kwon, K.-R., Park, S., Wang, X., Krebs, J., Tripathi, S., Sakabe, N., Sobreira, D.R., Huang, S.-C., Rao, S.S.P., Pruett, N., Chauss, D., Sadler, E., Lopez, A., Nóbrega, M.A., Aiden, E.L., Asturias, F.J., Casellas, R., 2019. A Pliable Mediator Acts as a Functional Rather Than an Architectural Bridge between Promoters and Enhancers. Cell 178, 1145-1158.e20. https://doi.org/10.1016/j.cell.2019.07.011

Elsaesser, S.J., Allis, C.D., 2010. HIRA and Daxx Constitute Two Independent Histone H3.3-Containing Predeposition Complexes. Cold Spring Harb. Symp. Quant. Biol. 75, 27–34. https://doi.org/10.1101/sqb.2010.75.008
Elsässer, S.J., Noh, K.-M., Diaz, N., Allis, C.D., Banaszynski, L.A., 2015. Histone H3.3 is required for endogenous retroviral element silencing in embryonic stem cells. Nature 522, 240–244. https://doi.org/10.1038/nature14345
Emelyanov, A.V., Konev, A.Y., Vershilova, E., Fyodorov, D.V., 2010. Protein Complex of Drosophila ATRX/XNP and HP1a Is Required for the Formation of Pericentric Beta-heterochromatin in Vivo. J. Biol. Chem. 285, 15027–15037. https://doi.org/10.1074/jbc.M109.064790
Emerson, D.J., Zhao, P.A., Cook, A.L., Barnett, R.J., Klein, K.N., Saulebekova, D., Ge, C., Zhou, L., Simandi, Z., Minsk, M.K., Titus, K.R., Wang, W., Gong, W., Zhang, D., Yang, L., Venev, S.V., Gibcus, J.H., Yang, H., Sasaki, T., Kanemaki, M.T., Yue, F., Dekker, J., Chen, C.-L., Gilbert, D.M., Phillips-Cremins, J.E., 2022. Cohesin-mediated loop anchors confine the locations of human replication origins. Nature 606, 812–819. https://doi.org/10.1038/s41586-022-04803-0
English, C.M., Adkins, M.W., Carson, J.J., Churchill, M.E.A., Tyler, J.K., 2006. Structural Basis for the Histone Chaperone Activity of Asf1. Cell 127, 495–508. https://doi.org/10.1016/j.cell.2006.08.047
Engreitz, J.M., Agarwala, V., Mirny, L.A., 2012. Three-Dimensional Genome Architecture Influences Partner Selection for Chromosomal Translocations in Human Disease. PLoS ONE 7, e44196. https://doi.org/10.1371/journal.pone.0044196
Erdel, F., 2023. Phase transitions in heterochromatin organization. Curr. Opin. Struct. Biol. 80, 102597. https://doi.org/10.1016/j.sbi.2023.102597
Erdel, F., Rademacher, A., Vlijm, R., Tünnermann, J., Frank, L., Weinmann, R., Schweigert, E., Yserentant, K., Hummert, J., Bauer, C., Schumacher, S., Al Alwash, A., Normand, C., Herten, D.-P., Engelhardt, J., Rippe, K., 2020. Mouse Heterochromatin Adopts Digital Compaction States without Showing Hallmarks of HP1-Driven Liquid-Liquid Phase Separation. Mol. Cell 78, 236-249.e7. https://doi.org/10.1016/j.molcel.2020.02.005
Erdel, F., Rippe, K., 2018. Formation of Chromatin Subcompartments by Phase Separation. Biophys. J. 114, 2262–2270. https://doi.org/10.1016/j.bpj.2018.03.011
Erkek, S., Hisano, M., Liang, C.-Y., Gill, M., Murr, R., Dieker, J., Schübeler, D., Vlag, J. van der, Stadler, M.B., Peters, A.H.F.M., 2013. Molecular determinants of nucleosome retention at CpG-rich sequences in mouse spermatozoa. Nat. Struct. Mol. Biol. 20, 868–875. https://doi.org/10.1038/nsmb.2599
Escobar, T.M., Oksuz, O., Saldaña-Meyer, R., Descostes, N., Bonasio, R., Reinberg, D., 2019. Active and Repressed Chromatin Domains Exhibit Distinct Nucleosome Segregation during DNA Replication. Cell 179, 953-963.e11. https://doi.org/10.1016/j.cell.2019.10.009
Escobar, T.M., Yu, J.-R., Liu, S., Lucero, K., Vasilyev, N., Nudler, E., Reinberg, D., 2021. Inheritance of Repressed Chromatin Domains during S-phase Requires the Histone Chaperone NPM1 (preprint). Molecular Biology. https://doi.org/10.1101/2021.08.31.458436
Esposito, A., Bianco, S., Chiariello, A.M., Abraham, A., Fiorillo, L., Conte, M., Campanile, R., Nicodemi, M., 2022. Polymer physics reveals a combinatorial code linking 3D chromatin architecture to 1D chromatin states. Cell Rep. 38, 110601. https://doi.org/10.1016/j.celrep.2022.110601
Evano, B., Khalilian, S., Le Carrou, G., Almouzni, G., Tajbakhsh, S., 2020. Dynamics of Asymmetric and Symmetric Divisions of Muscle Stem Cells In Vivo and on Artificial Niches. Cell Rep. 30, 3195-3206.e7. https://doi.org/10.1016/j.celrep.2020.01.097
Evrin, C., Clarke, P., Zech, J., Lurz, R., Sun, J., Uhle, S., Li, H., Stillman, B., Speck, C., 2009. A double-hexameric MCM2-7 complex is loaded onto origin DNA during licensing of eukaryotic DNA replication. Proc. Natl. Acad. Sci. 106, 20240–20245. https://doi.org/10.1073/pnas.0911500106
Evrin, C., Maman, J.D., Diamante, A., Pellegrini, L., Labib, K., 2018. Histone H2A-H2B binding by Pol α in the eukaryotic replisome contributes to the maintenance of repressive chromatin. EMBO J. 37, e99021. https://doi.org/10.15252/embj.201899021
Fachinetti, D., Diego Folco, H., Nechemia-Arbely, Y., Valente, L.P., Nguyen, K., Wong, A.J., Zhu, Q., Holland, A.J., Desai, A., Jansen, L.E.T., Cleveland, D.W., 2013. A two-step mechanism for epigenetic specification of centromere identity and function. Nat. Cell Biol. 15, 1056–1066. https://doi.org/10.1038/ncb2805
Falk, M., Feodorova, Y., Naumova, N., Imakaev, M., Lajoie, B.R., Leonhardt, H., Joffe, B., Dekker, J., Fudenberg, G., Solovei, I., Mirny, L.A., 2019. Heterochromatin drives compartmentalization of inverted and conventional nuclei. Nature 570, 395–399. https://doi.org/10.1038/s41586-019-1275-3
Fang, D., Gan, H., Lee, J.-H., Han, J., Wang, Z., Riester, S.M., Jin, L., Chen, J., Zhou, H., Wang, J., Zhang, H., Yang, N., Bradley, E.W., Ho, T.H., Rubin, B.P., Bridge, J.A., Thibodeau, S.N., Ordog, T., Chen, Y., van Wijnen, A.J., Oliveira, A.M., Xu, R.-M., Westendorf, J.J., Zhang, Z., 2016. The histone H3.3K36M mutation reprograms the epigenome of chondroblastomas. Science 352, 1344–1348. https://doi.org/10.1126/science.aae0065

Fang, R., Yu, M., Li, G., Chee, S., Liu, T., Schmitt, A.D., Ren, B., 2016. Mapping of long-range chromatin interactions by proximity ligation-assisted ChIP-seq. Cell Res. 26, 1345–1348. https://doi.org/10.1038/cr.2016.137
Fang, H.-T., EL Farran, C.A., Xing, Q.R., Zhang, L.-F., Li, H., Lim, B., Loh, Y.-H., 2018. Global H3.3 dynamic deposition defines its bimodal role in cell fate transition. Nat. Commun. 9, 1537. https://doi.org/10.1038/s41467-018-03904-7
Feng, F., Yao, Y., Wang, X.Q.D., Zhang, X., Liu, J., 2022. Connecting high-resolution 3D chromatin organization with epigenomics. Nat. Commun. 13, 2054. https://doi.org/10.1038/s41467-022-29695-6
Ferreira, J., Carmo-Fonseca, M., 1997. Genome replication in early mouse embryos follows a defined temporal and spatial order. J. Cell Sci. 110, 889–897. https://doi.org/10.1242/jcs.110.7.889
Figueiredo, M.L.A., Philip, P., Stenberg, P., Larsson, J., 2012. HP1a Recruitment to Promoters Is Independent of H3K9 Methylation in Drosophila melanogaster. PLoS Genet. 8, e1003061. https://doi.org/10.1371/journal.pgen.1003061
Filipescu, D., Naughtin, M., Podsypanina, K., Lejour, V., Wilson, L., Gurard-Levin, Z.A., Orsi, G.A., Simeonova, I., Toufektchan, E., Attardi, L.D., Toledo, F., Almouzni, G., 2017. Essential role for centromeric factors following p53 loss and oncogenic transformation. Genes Dev. 31, 463–480. https://doi.org/10.1101/gad.290924.116
Finch, J.T., Klug, A., 1976. Solenoidal model for superstructure in chromatin. Proc. Natl. Acad. Sci. 73, 1897–1901. https://doi.org/10.1073/pnas.73.6.1897
Finn, E.H., Pegoraro, G., Brandão, H.B., Valton, A.-L., Oomen, M.E., Dekker, J., Mirny, L., Misteli, T., 2019. Extensive Heterogeneity and Intrinsic Variation in Spatial Genome Organization. Cell 176, 1502-1515.e10. https://doi.org/10.1016/j.cell.2019.01.020
Fischer, M., Grossmann, P., Padi, M., DeCaprio, J.A., 2016. Integration of TP53, DREAM, MMB-FOXM1 and RB-E2F target gene analyses identifies cell cycle gene regulatory networks. Nucleic Acids Res. 44, 6070–6086. https://doi.org/10.1093/nar/gkw523
Fischle, W., Tseng, B.S., Dormann, H.L., Ueberheide, B.M., Garcia, B.A., Shabanowitz, J., Hunt, D.F., Funabiki, H., Allis, C.D., 2005. Regulation of HP1–chromatin binding by histone H3 methylation and phosphorylation. Nature 438, 1116–1122. https://doi.org/10.1038/nature04219
Flavahan, W.A., Drier, Y., Liau, B.B., Gillespie, S.M., Venteicher, A.S., Stemmer-Rachamimov, A.O., Suvà, M.L., Bernstein, B.E., 2016. Insulator dysfunction and oncogene activation in IDH mutant gliomas. Nature 529, 110–114. https://doi.org/10.1038/nature16490
Flemming, W., 1882. Zellsubstanz, Kern und Zelltheilung. Vogel.
Flemming, W., 1879. Ueber das Verhalten des Kerns bei der Zelltheilung, und über die Bedeutung mehrkerniger Zellen. Arch. Für Pathol. Anat. Physiol. Für Klin. Med. 77, 1–29.
Flury, V., Reverón-Gómez, N., Alcaraz, N., Stewart-Morgan, K.R., Wenger, A., Klose, R.J., Groth, A., 2023. Recycling of modified H2A-H2B provides short-term memory of chromatin states. Cell S0092867423000077. https://doi.org/10.1016/j.cell.2023.01.007
Flyamer, I.M., Gassler, J., Imakaev, M., Brandão, H.B., Ulianov, S.V., Abdennur, N., Razin, S.V., Mirny, L.A., Tachibana-Konwalski, K., 2017. Single-nucleus Hi-C reveals unique chromatin reorganization at oocyte-to-zygote transition. Nature 544, 110–114. https://doi.org/10.1038/nature21711
Foltman, M., Evrin, C., De Piccoli, G., Jones, R.C., Edmondson, R.D., Katou, Y., Nakato, R., Shirahige, K., Labib, K., 2013. Eukaryotic Replisome Components Cooperate to Process Histones During Chromosome Replication. Cell Rep. 3, 892–904. https://doi.org/10.1016/j.celrep.2013.02.028
Foltz, D.R., Jansen, L.E.T., Bailey, A.O., Yates, J.R., Bassett, E.A., Wood, S., Black, B.E., Cleveland, D.W., 2009. Centromere-Specific Assembly of CENP-A Nucleosomes Is Mediated by HJURP. Cell 137, 472–484. https://doi.org/10.1016/j.cell.2009.02.039
Foltz, D.R., Jansen, L.E.T., Black, B.E., Bailey, A.O., Yates, J.R., Cleveland, D.W., 2006. The human CENP-A centromeric nucleosome-associated complex. Nat. Cell Biol. 8, 458–469. https://doi.org/10.1038/ncb1397
Foss, E.J., Gatbonton-Schwager, T., Thiesen, A.H., Taylor, E., Soriano, R., Lao, U., MacAlpine, D.M., Bedalov, A., 2019. Sir2 suppresses transcription-mediated displacement of Mcm2-7 replicative helicases at the ribosomal DNA repeats. PLOS Genet. 15, e1008138. https://doi.org/10.1371/journal.pgen.1008138
Foti, R., Gnan, S., Cornacchia, D., Dileep, V., Bulut-Karslioglu, A., Diehl, S., Buness, A., Klein, F.A., Huber, W., Johnstone, E., Loos, R., Bertone, P., Gilbert, D.M., Manke, T., Jenuwein, T., Buonomo, S.C.B., 2016. Nuclear Architecture Organized by Rif1 Underpins the Replication-Timing Program. Mol. Cell 61, 260–273. https://doi.org/10.1016/j.molcel.2015.12.001
Fox, M.H., AKNDT-JOVINt, D.J., Jovin, T.M., Baumann, P.H., 1991. Spatial and temporal distribution of DNA replication sites localized by immunofluorescence and confocal microscopy in mouse fibroblasts.
Fragkos, M., Ganier, O., Coulombe, P., Méchali, M., 2015. DNA replication origin activation in space and time. Nat. Rev. Mol. Cell Biol. 16, 360–374. https://doi.org/10.1038/nrm4002
Franke, M., Ibrahim, D.M., Andrey, G., Schwarzer, W., Heinrich, V., Schöpflin, R., Kraft, K., Kempfer, R., Jerković, I., Chan, W.-L., Spielmann, M., Timmermann, B., Wittler, L., Kurth, I., Cambiaso, P., Zuffardi, O.,

Houge, G., Lambie, L., Brancati, F., Pombo, A., Vingron, M., Spitz, F., Mundlos, S., 2016. Formation of new chromatin domains determines pathogenicity of genomic duplications. Nature 538, 265–269. https://doi.org/10.1038/nature19800
Franklin, R., Gosling, R., 1953. Molecular Configuration in Sodium Thymonucleate. Nature 171, 740–741. https://doi.org/10.1038/171740a0
Franklin, R., Guo, Y., He, S., Chen, M., Ji, F., Zhou, X., Frankhouser, D., Do, B.T., Chiem, C., Jang, M., Blanco, M.A., Vander Heiden, M.G., Rockne, R.C., Ninova, M., Sykes, D.B., Hochedlinger, K., Lu, R., Sadreyev, R.I., Murn, J., Volk, A., Cheloufi, S., 2022. Regulation of chromatin accessibility by the histone chaperone CAF-1 sustains lineage fidelity. Nat. Commun. 13, 2350. https://doi.org/10.1038/s41467-022-29730-6
Franklin, S.G., Zweidler, A., 1977. Non-allelic variants of histones 2a, 2b and 3 in mammals. Nature 266, 273–275. https://doi.org/10.1038/266273a0
Frey, A., Listovsky, T., Guilbaud, G., Sarkies, P., Sale, J.E., 2014. Histone H3.3 Is Required to Maintain Replication Fork Progression after UV Damage. Curr. Biol. 24, 2195–2201. https://doi.org/10.1016/j.cub.2014.07.077
Friedman, K.L., Brewer, B.J., Fangman, W.L., 1997. Replication profile of Saccharomyces cerevisiae chromosome VI. Genes Cells 2, 667–678. https://doi.org/10.1046/j.1365-2443.1997.1520350.x
Frottin, F., Schueder, F., Tiwary, S., Gupta, R., Körner, R., Schlichthaerle, T., Cox, J., Jungmann, R., Hartl, F.U., Hipp, M.S., 2019. The nucleolus functions as a phase-separated protein quality control compartment. Science 365, 342–347. https://doi.org/10.1126/science.aaw9157
Fu, Y., Sinha, M., Peterson, C.L., Weng, Z., 2008. The Insulator Binding Protein CTCF Positions 20 Nucleosomes around Its Binding Sites across the Human Genome. PLoS Genet. 4, e1000138. https://doi.org/10.1371/journal.pgen.1000138
Fudenberg, G., Abdennur, N., Imakaev, M., Goloborodko, A., Mirny, L.A., 2017. Emerging Evidence of Chromosome Folding by Loop Extrusion. Cold Spring Harb. Symp. Quant. Biol. 82, 45–55. https://doi.org/10.1101/sqb.2017.82.034710
Fudenberg, G., Imakaev, M., Lu, C., Goloborodko, A., Abdennur, N., Mirny, L.A., 2016. Formation of Chromosomal Domains by Loop Extrusion. Cell Rep. 15, 2038–2049. https://doi.org/10.1016/j.celrep.2016.04.085
Fujita, S., 1965. Chromosomal Organization as a Genetic Basis of Cytodifferentiation in Multicellular Organisms. Nature 206, 742–744. https://doi.org/10.1038/206742a0
Fullwood, M.J., Liu, M.H., Pan, Y.F., Liu, J., Xu, H., Mohamed, Y.B., Orlov, Y.L., Velkov, S., Ho, A., Mei, P.H., Chew, E.G.Y., Huang, P.Y.H., Welboren, W.-J., Han, Y., Ooi, H.S., Ariyaratne, P.N., Vega, V.B., Luo, Y., Tan, P.Y., Choy, P.Y., Wansa, K.D.S.A., Zhao, B., Lim, K.S., Leow, S.C., Yow, J.S., Joseph, R., Li, H., Desai, K.V., Thomsen, J.S., Lee, Y.K., Karuturi, R.K.M., Herve, T., Bourque, G., Stunnenberg, H.G., Ruan, X., Cacheux-Rataboul, V., Sung, W.-K., Liu, E.T., Wei, C.-L., Cheung, E., Ruan, Y., 2009. An oestrogen-receptor-α-bound human chromatin interactome. Nature 462, 58–64. https://doi.org/10.1038/nature08497
Gabriele, M., Brandão, H.B., Grosse-Holz, S., Jha, A., Dailey, G.M., Cattoglio, C., Hsieh, T.-H.S., Mirny, L., Zechner, C., Hansen, A.S., 2022. Dynamics of CTCF- and cohesin-mediated chromatin looping revealed by live-cell imaging 7.
Gaillard, P.-H.L., Martini, E.M.-D., Kaufman, P.D., Stillman, B., Moustacchi, E., Almouzni, G., 1996. Chromatin Assembly Coupled to DNA Repair: A New Role for Chromatin Assembly Factor I. Cell 86, 887–896. https://doi.org/10.1016/S0092-8674(00)80164-6
Gan, H., Serra-Cardona, A., Hua, X., Zhou, H., Labib, K., Yu, C., Zhang, Z., 2018. The Mcm2-Ctf4-Polα Axis Facilitates Parental Histone H3-H4 Transfer to Lagging Strands. Mol. Cell 72, 140-151.e3. https://doi.org/10.1016/j.molcel.2018.09.001
Gandhi, R., Gillespie, P.J., Hirano, T., 2006. Human Wapl Is a Cohesin-Binding Protein that Promotes Sister-Chromatid Resolution in Mitotic Prophase. Curr. Biol. 16, 2406–2417. https://doi.org/10.1016/j.cub.2006.10.061
Ganji, M., Shaltiel, I.A., Bisht, S., Kim, E., Kalichava, A., Haering, C.H., Dekker, C., 2018. Real-time imaging of DNA loop extrusion by condensin. Science 360, 102–105. https://doi.org/10.1126/science.aar7831
García Del Arco, A., Edgar, B.A., Erhardt, S., 2018. In Vivo Analysis of Centromeric Proteins Reveals a Stem Cell-Specific Asymmetry and an Essential Role in Differentiated, Non-proliferating Cells. Cell Rep. 22, 1982–1993. https://doi.org/10.1016/j.celrep.2018.01.079
Garzón, J., Ursich, S., Lopes, M., Hiraga, S., Donaldson, A.D., 2019. Human RIF1-Protein Phosphatase 1 Prevents Degradation and Breakage of Nascent DNA on Replication Stalling. Cell Rep. 27, 2558-2566.e4. https://doi.org/10.1016/j.celrep.2019.05.002
Gascoigne, K.E., Takeuchi, K., Suzuki, A., Hori, T., Fukagawa, T., Cheeseman, I.M., 2011. Induced Ectopic Kinetochore Assembly Bypasses the Requirement for CENP-A Nucleosomes. Cell 145, 410–422. https://doi.org/10.1016/j.cell.2011.03.031

Gassler, J., Brandão, H.B., Imakaev, M., Flyamer, I.M., Ladstätter, S., Bickmore, W.A., Peters, J.-M., Mirny, L.A., Tachibana, K., 2017. A mechanism of cohesin-dependent loop extrusion organizes zygotic genome architecture. EMBO J. 36, 3600–3618. https://doi.org/10.15252/embj.201798083
Gatto, A., Forest, A., Quivy, J.-P., Almouzni, G., 2022. HIRA-dependent boundaries between H3 variants shape early replication in mammals. Mol. Cell S1097276522002556. https://doi.org/10.1016/j.molcel.2022.03.017
Ge, X.Q., Jackson, D.A., Blow, J.J., 2007. Dormant origins licensed by excess Mcm2–7 are required for human cells to survive replicative stress. Genes Dev. 21, 3331–3341. https://doi.org/10.1101/gad.457807
Gehre, M., Bunina, D., Sidoli, S., Lübke, M.J., Diaz, N., Trovato, M., Garcia, B.A., Zaugg, J.B., Noh, K.-M., 2020. Lysine 4 of histone H3.3 is required for embryonic stem cell differentiation, histone enrichment at regulatory regions and transcription accuracy. Nat. Genet. 52, 273–282. https://doi.org/10.1038/s41588-020-0586-5
Ghavi-Helm, Y., Jankowski, A., Meiers, S., Viales, R.R., Korbel, J.O., Furlong, E.E.M., 2019. Highly rearranged chromosomes reveal uncoupling between genome topology and gene expression. Nat. Genet. 51, 1272–1282. https://doi.org/10.1038/s41588-019-0462-3
Ghavi-Helm, Y., Klein, F.A., Pakozdi, T., Ciglar, L., Noordermeer, D., Huber, W., Furlong, E.E.M., 2014. Enhancer loops appear stable during development and are associated with paused polymerase. Nature 512, 96–100. https://doi.org/10.1038/nature13417
Ghiraldini, F.G., Filipescu, D., Bernstein, E., 2021. Solid tumours hijack the histone variant network. Nat. Rev. Cancer. https://doi.org/10.1038/s41568-020-00330-0
Gibbons, R.J., Picketts, D.J., Villard, L., Higgs, D.R., 1995. Mutations in a putative global transcriptional regulator cause X-linked mental retardation with α-thalassemia (ATR-X syndrome). Cell 80, 837–845. https://doi.org/10.1016/0092-8674(95)90287-2
Gibcus, J.H., Samejima, K., Goloborodko, A., Samejima, I., Naumova, N., Nuebler, J., Kanemaki, M.T., Xie, L., Paulson, J.R., Earnshaw, W.C., Mirny, L.A., Dekker, J., 2018. A pathway for mitotic chromosome formation. Science 359, eaao6135. https://doi.org/10.1126/science.aao6135
Gibson, B.A., Doolittle, L.K., Schneider, M.W.G., Jensen, L.E., Gamarra, N., Henry, L., Gerlich, D.W., Redding, S., Rosen, M.K., 2019. Organization of Chromatin by Intrinsic and Regulated Phase Separation. Cell 179, 470-484.e21. https://doi.org/10.1016/j.cell.2019.08.037
Giles, K.A., Lamm, N., Taberlay, P.C., Cesare, A.J., 2022. Three-dimensional chromatin organisation shapes origin activation and replication fork directionality (preprint). Bioinformatics. https://doi.org/10.1101/2022.06.24.497492
Giorgetti, L., Galupa, R., Nora, E.P., Piolot, T., Lam, F., Dekker, J., Tiana, G., Heard, E., 2014. Predictive Polymer Modeling Reveals Coupled Fluctuations in Chromosome Conformation and Transcription. Cell 157, 950–963. https://doi.org/10.1016/j.cell.2014.03.025
Girelli, G., Custodio, J., Kallas, T., Agostini, F., Wernersson, E., Spanjaard, B., Mota, A., Kolbeinsdottir, S., Gelali, E., Crosetto, N., Bienko, M., 2020. GPSeq reveals the radial organization of chromatin in the cell nucleus. Nat. Biotechnol. 38, 1184–1193. https://doi.org/10.1038/s41587-020-0519-y
Goel, V.Y., Huseyin, M.K., Hansen, A.S., 2023. Region Capture Micro-C reveals coalescence of enhancers and promoters into nested microcompartments. Nat. Genet. https://doi.org/10.1038/s41588-023-01391-1
Goldberg, A.D., Banaszynski, L.A., Noh, K.-M., Lewis, P.W., Elsaesser, S.J., Stadler, S., Dewell, S., Law, M., Guo, X., Li, X., Wen, D., Chapgier, A., DeKelver, R.C., Miller, J.C., Lee, Y.-L., Boydston, E.A., Holmes, M.C., Gregory, P.D., Greally, J.M., Rafii, S., Yang, C., Scambler, P.J., Garrick, D., Gibbons, R.J., Higgs, D.R., Cristea, I.M., Urnov, F.D., Zheng, D., Allis, C.D., 2010. Distinct Factors Control Histone Variant H3.3 Localization at Specific Genomic Regions. Cell 140, 678–691. https://doi.org/10.1016/j.cell.2010.01.003
Goloborodko, A., Imakaev, M.V., Marko, J.F., Mirny, L., 2016. Compaction and segregation of sister chromatids via active loop extrusion. eLife 5, e14864. https://doi.org/10.7554/eLife.14864
Gomes, A.P., Ilter, D., Low, V., Rosenzweig, A., Shen, Z.-J., Schild, T., Rivas, M.A., Er, E.E., McNally, D.R., Mutvei, A.P., Han, J., Ou, Y.-H., Cavaliere, P., Mullarky, E., Nagiec, M., Shin, S., Yoon, S.-O., Dephoure, N., Massagué, J., Melnick, A.M., Cantley, L.C., Tyler, J.K., Blenis, J., 2019. Dynamic Incorporation of Histone H3 Variants into Chromatin Is Essential for Acquisition of Aggressive Traits and Metastatic Colonization. Cancer Cell 36, 402-417.e13. https://doi.org/10.1016/j.ccell.2019.08.006
Gómez Acuña, L.I., Flyamer, I., Boyle, S., Friman, E.T., Bickmore, W.A., 2023. Transcription decouples estrogen-dependent changes in enhancer-promoter contact frequencies and physical proximity (preprint). Genomics. https://doi.org/10.1101/2023.03.29.534720
Gómez, M., Brockdorff, N., 2004. Heterochromatin on the inactive X chromosome delays replication timing without affecting origin usage. Proc. Natl. Acad. Sci. 101, 6923–6928. https://doi.org/10.1073/pnas.0401854101
Gonzalez, I., Molliex, A., Navarro, P., 2021. Mitotic memories of gene activity. Curr. Opin. Cell Biol. 69, 41–47. https://doi.org/10.1016/j.ceb.2020.12.009
Gopalan, S., Wang, Y., Harper, N.W., Garber, M., Fazzio, T.G., 2021. Simultaneous profiling of multiple chromatin proteins in the same cells. Molecular Cell 81, 4736-4746.e5. https://doi.org/10.1016/j.molcel.2021.09.019

Graham, C.F., Morgan, R.W., 1966. Changes in the cell cycle during early amphibian development. Dev. Biol. 14, 439–460. https://doi.org/10.1016/0012-1606(66)90024-8
Greaves, I.K., Rangasamy, D., Ridgway, P., Tremethick, D.J., 2007. H2A.Z contributes to the unique 3D structure of the centromere. Proc. Natl. Acad. Sci. 104, 525–530. https://doi.org/10.1073/pnas.0607870104
Greenberg, M.V.C., Bourc'his, D., 2019. The diverse roles of DNA methylation in mammalian development and disease. Nat. Rev. Mol. Cell Biol. 20, 590–607. https://doi.org/10.1038/s41580-019-0159-6
Griffith, F., 1928. The Significance of Pneumococcal Types. J. Hyg. (Lond.) 27, 113–159. https://doi.org/10.1017/S0022172400031879
Gros, J., Kumar, C., Lynch, G., Yadav, T., Whitehouse, I., Remus, D., 2015. Post-licensing Specification of Eukaryotic Replication Origins by Facilitated Mcm2-7 Sliding along DNA. Mol. Cell 60, 797–807. https://doi.org/10.1016/j.molcel.2015.10.022
Gröschel, S., Sanders, M.A., Hoogenboezem, R., de Wit, E., Bouwman, B.A.M., Erpelinck, C., van der Velden, V.H.J., Havermans, M., Avellino, R., van Lom, K., Rombouts, E.J., van Duin, M., Döhner, K., Beverloo, H.B., Bradner, J.E., Döhner, H., Löwenberg, B., Valk, P.J.M., Bindels, E.M.J., de Laat, W., Delwel, R., 2014. A Single Oncogenic Enhancer Rearrangement Causes Concomitant EVI1 and GATA2 Deregulation in Leukemia. Cell 157, 369–381. https://doi.org/10.1016/j.cell.2014.02.019
Grosveld, F., Antoniou, M., Berry, M., Boer, E.D., Dillon, N., Ellis, J., Fraser, P., Hanscombe, O., Hurst, J., Imam, A., Lindenbaum, M., Philipsen, S., Pruzina, S., Strouboulis, J.H.N., Raguz-Bolognesi, S., Talbot, D., 1993. The regulation of human globin gene switching.
Groth, A., Corpet, A., Cook, A.J.L., Roche, D., Bartek, J., Lukas, J., Almouzni, G., 2007. Regulation of Replication Fork Progression Through Histone Supply and Demand. Science 318, 1928–1931. https://doi.org/10.1126/science.1148992
Groth, A., Ray-Gallet, D., Quivy, J.-P., Lukas, J., Bartek, J., Almouzni, G., 2005. Human Asf1 Regulates the Flow of S Phase Histones during Replicational Stress. Mol. Cell 17, 301–311. https://doi.org/10.1016/j.molcel.2004.12.018
Grover, P., Asa, J.S., Campos, E.I., 2018. H3–H4 Histone Chaperone Pathways. Annu. Rev. Genet. 52, 109–130. https://doi.org/10.1146/annurev-genet-120417-031547
Grubert, F., Srivas, R., Spacek, D.V., Kasowski, M., Ruiz-Velasco, M., Sinnott-Armstrong, N., Greenside, P., Narasimha, A., Liu, Q., Geller, B., Sanghi, A., Kulik, M., Sa, S., Rabinovitch, M., Kundaje, A., Dalton, S., Zaugg, J.B., Snyder, M., 2020. Landscape of cohesin-mediated chromatin loops in the human genome. Nature 583, 737–743. https://doi.org/10.1038/s41586-020-2151-x
Grunstein, M., 1997. Histone acetylation in chromatin structure and transcription. Nature 389, 349–352. https://doi.org/10.1038/38664
Gruszka, D.T., Xie, S., Kimura, H., Yardimci, H., 2020. Single-molecule imaging reveals control of parental histone recycling by free histones during DNA replication. Sci. Adv. 6, eabc0330. https://doi.org/10.1126/sciadv.abc0330
Guelen, L., Pagie, L., Brasset, E., Meuleman, W., Faza, M.B., Talhout, W., Eussen, B.H., de Klein, A., Wessels, L., de Laat, W., van Steensel, B., 2008. Domain organization of human chromosomes revealed by mapping of nuclear lamina interactions. Nature 453, 948–951. https://doi.org/10.1038/nature06947
Guilbaud, G., Murat, P., Wilkes, H.S., Lerner, L.K., Sale, J.E., Krude, T., 2022. Determination of human DNA replication origin position and efficiency reveals principles of initiation zone organisation. Nucleic Acids Res. 50, 7436–7450. https://doi.org/10.1093/nar/gkac555
Guillou, E., Ibarra, A., Coulon, V., Casado-Vela, J., Rico, D., Casal, I., Schwob, E., Losada, A., Méndez, J., 2010. Cohesin organizes chromatin loops at DNA replication factories. Genes Dev. 24, 2812–2822. https://doi.org/10.1101/gad.608210
Guo, Y.E., Manteiga, J.C., Henninger, J.E., Sabari, B.R., Dall'Agnese, A., Hannett, N.M., Spille, J.-H., Afeyan, L.K., Zamudio, A.V., Shrinivas, K., Abraham, B.J., Boija, A., Decker, T.-M., Rimel, J.K., Fant, C.B., Lee, T.I., Cisse, I.I., Sharp, P.A., Taatjes, D.J., Young, R.A., 2019. Pol II phosphorylation regulates a switch between transcriptional and splicing condensates. Nature 572, 543–548. https://doi.org/10.1038/s41586-019-1464-0
Gurard-Levin, Z.A., Quivy, J.-P., Almouzni, G., 2014. Histone Chaperones: Assisting Histone Traffic and Nucleosome Dynamics. Annu. Rev. Biochem. 83, 487–517. https://doi.org/10.1146/annurev-biochem-060713-035536
Gutiérrez, M.P., MacAlpine, H.K., MacAlpine, D.M., 2019. Nascent chromatin occupancy profiling reveals locus- and factor-specific chromatin maturation dynamics behind the DNA replication fork. Genome Res. 29, 1123–1133. https://doi.org/10.1101/gr.243386.118
Ha, M., Kraushaar, D.C., Zhao, K., 2014. Genome-wide analysis of H3.3 dissociation reveals high nucleosome turnover at distal regulatory regions of embryonic stem cells. Epigenetics Chromatin 7, 38. https://doi.org/10.1186/1756-8935-7-38

Haarhuis, J.H.I., van der Weide, R.H., Blomen, V.A., Flach, K.D., Teunissen, H., Willems, L., Brummelkamp, T.R., Rowland, B.D., de Wit, E., 2022. A Mediator-cohesin axis controls heterochromatin domain formation. Nat. Commun. 13, 754. https://doi.org/10.1038/s41467-022-28377-7
Haarhuis, J.H.I., van der Weide, R.H., Blomen, V.A., Yáñez-Cuna, J.O., Amendola, M., van Ruiten, M.S., Krijger, P.H.L., Teunissen, H., Medema, R.H., van Steensel, B., Brummelkamp, T.R., de Wit, E., Rowland, B.D., 2017. The Cohesin Release Factor WAPL Restricts Chromatin Loop Extension. Cell 169, 693-707.e14. https://doi.org/10.1016/j.cell.2017.04.013
Haddad, N., Jost, D., Vaillant, C., 2017. Perspectives: using polymer modeling to understand the formation and function of nuclear compartments. Chromosome Res. 25, 35–50. https://doi.org/10.1007/s10577-016-9548-2
Hafner, A., Park, M., Berger, S.E., Murphy, S.E., Nora, E.P., Boettiger, A.N., 2023. Loop stacking organizes genome folding from TADs to chromosomes. Mol. Cell 83, 1377-1392.e6. https://doi.org/10.1016/j.molcel.2023.04.008
Hainer, S.J., Fazzio, T.G., 2019. High-Resolution Chromatin Profiling Using CUT&RUN. Current Protocols in Molecular Biology 126, e85. https://doi.org/10.1002/cpmb.85
Hake, S.B., Allis, C.D., 2006. Histone H3 variants and their potential role in indexing mammalian genomes: The "H3 barcode hypothesis." Proc. Natl. Acad. Sci. 103, 6428–6435. https://doi.org/10.1073/pnas.0600803103
Hake, S.B., Garcia, B.A., Duncan, E.M., Kauer, M., Dellaire, G., Shabanowitz, J., Bazett-Jones, D.P., Allis, C.D., Hunt, D.F., 2006. Expression Patterns and Post-translational Modifications Associated with Mammalian Histone H3 Variants. J. Biol. Chem. 281, 559–568. https://doi.org/10.1074/jbc.M509266200
Hake, S.B., Garcia, B.A., Kauer, M., Baker, S.P., Shabanowitz, J., Hunt, D.F., Allis, C.D., 2005. Serine 31 phosphorylation of histone variant H3.3 is specific to regions bordering centromeres in metaphase chromosomes. Proc. Natl. Acad. Sci. 102, 6344–6349. https://doi.org/10.1073/pnas.0502413102
Hammond, C.M., Strømme, C.B., Huang, H., Patel, D.J., Groth, A., 2017. Histone chaperone networks shaping chromatin function. Nat. Rev. Mol. Cell Biol. 18, 141–158. https://doi.org/10.1038/nrm.2016.159
Hammoud, S.S., Nix, D.A., Zhang, H., Purwar, J., Carrell, D.T., Cairns, B.R., 2009. Distinctive chromatin in human sperm packages genes for embryo development. Nature 460, 473–478. https://doi.org/10.1038/nature08162
Hand, R., 1978. Eucaryotic DNA: Organization of the genome for replication. Cell 15, 317–325. https://doi.org/10.1016/0092-8674(78)90001-6
Hanna, C.W., Taudt, A., Huang, J., Gahurova, L., Kranz, A., Andrews, S., Dean, W., Stewart, A.F., Colomé-Tatché, M., Kelsey, G., 2018. MLL2 conveys transcription-independent H3K4 trimethylation in oocytes. Nat. Struct. Mol. Biol. 25, 73–82. https://doi.org/10.1038/s41594-017-0013-5
Hardy, C.F., Sussel, L., Shore, D., 1992. A RAP1-interacting protein involved in transcriptional silencing and telomere length regulation. Genes Dev. 6, 801–814. https://doi.org/10.1101/gad.6.5.801
Hardy, S., Gaudreau, L., Robert, F., 2009. The Euchromatic and Heterochromatic Landscapes Are Shaped by Antagonizing Effects of Transcription on H2A.Z Deposition. PLoS Genet. 5.
Hargreaves, D.C., Crabtree, G.R., 2011. ATP-dependent chromatin remodeling: genetics, genomics and mechanisms. Cell Res. 21, 396–420. https://doi.org/10.1038/cr.2011.32
Harland, R., Laskey, R.A., 1980. Regulated replication of DNA microinjected into eggs of Xenopus laevis. Cell 21, 761–771. https://doi.org/10.1016/0092-8674(80)90439-0
Harris, H.L., Gu, H., Olshansky, M., Wang, A., Farabella, I., Eliaz, Y., Kalluchi, A., Krishna, A., Jacobs, M., Cauer, G., Pham, M., Rao, S.S.P., Dudchenko, O., Omer, A., Mohajeri, K., Kim, S., Nichols, M.H., Davis, E.S., Gkountaroulis, D., Udupa, D., Aiden, A.P., Corces, V.G., Phanstiel, D.H., Noble, W.S., Nir, G., Di Pierro, M., Seo, J.-S., Talkowski, M.E., Aiden, E.L., Rowley, M.J., 2023. Chromatin alternates between A and B compartments at kilobase scale for subgenic organization. Nat. Commun. 14, 3303. https://doi.org/10.1038/s41467-023-38429-1
Hartwell, L.H., 1976. Sequential function of gene products relative to DNA synthesis in the yeast cell cycle. J. Mol. Biol. 104, 803–817. https://doi.org/10.1016/0022-2836(76)90183-2
Hashimshony, T., Zhang, J., Keshet, I., Bustin, M., Cedar, H., 2003. The role of DNA methylation in setting up chromatin structure during development. Nat. Genet. 34, 187–192. https://doi.org/10.1038/ng1158
Hasson, D., Panchenko, T., Salimian, K.J., Salman, M.U., Sekulic, N., Alonso, A., Warburton, P.E., Black, B.E., 2013. The octamer is the major form of CENP-A nucleosomes at human centromeres. Nat. Struct. Mol. Biol. 20, 687–695. https://doi.org/10.1038/nsmb.2562
Hayano, M., Kanoh, Y., Matsumoto, S., Renard-Guillet, C., Shirahige, K., Masai, H., 2012. Rif1 is a global regulator of timing of replication origin firing in fission yeast. Genes Dev. 26, 137–150. https://doi.org/10.1101/gad.178491.111
Hayashi, M.T., Takahashi, T.S., Nakagawa, T., Nakayama, J., Masukata, H., 2009. The heterochromatin protein Swi6/HP1 activates replication origins at the pericentromeric region and silent mating-type locus. Nat. Cell Biol. 11, 357–362. https://doi.org/10.1038/ncb1845

He, H., Li, Y., Dong, Q., Chang, A.-Y., Gao, F., Chi, Z., Su, M., Zhang, F., Ban, H., Martienssen, R., Chen, Y., Li, F., 2017. Coordinated regulation of heterochromatin inheritance by Dpb3–Dpb4 complex. Proc. Natl. Acad. Sci. 114, 12524–12529. https://doi.org/10.1073/pnas.1712961114
He, Q., Kim, H., Huang, R., Lu, W., Tang, M., Shi, F., Yang, D., Zhang, X., Huang, J., Liu, D., Songyang, Z., 2015. The Daxx/Atrx Complex Protects Tandem Repetitive Elements during DNA Hypomethylation by Promoting H3K9 Trimethylation. Cell Stem Cell 17, 273–286. https://doi.org/10.1016/j.stem.2015.07.022
He, Y.-F., Li, B.-Z., Li, Z., Liu, P., Wang, Y., Tang, Q., Ding, J., Jia, Y., Chen, Z., Li, L., Sun, Y., Li, X., Dai, Q., Song, C.-X., Zhang, K., He, C., Xu, G.-L., 2011. Tet-Mediated Formation of 5-Carboxylcytosine and Its Excision by TDG in Mammalian DNA. Science 333, 1303–1307. https://doi.org/10.1126/science.1210944
Hebbes, T.R., Thorne, A.W., Crane-Robinson, C., 1988. A direct link between core histone acetylation and transcriptionally active chromatin. EMBO J. 7, 1395–1402. https://doi.org/10.1002/j.1460-2075.1988.tb02956.x
Heintzman, N.D., Hon, G.C., Hawkins, R.D., Kheradpour, P., Stark, A., Harp, L.F., Ye, Z., Lee, L.K., Stuart, R.K., Ching, C.W., Ching, K.A., Antosiewicz-Bourget, J.E., Liu, H., Zhang, X., Green, R.D., Lobanenkov, V.V., Stewart, R., Thomson, J.A., Crawford, G.E., Kellis, M., Ren, B., 2009. Histone modifications at human enhancers reflect global cell-type-specific gene expression. Nature 459, 108–112. https://doi.org/10.1038/nature07829
Heitz, E., 1935. Chromosomenstruktur und Gene. Z Indukt Vererb 402–447.
Heitz, E., 1933. Uber totale und partielle somatische Heteropyknose, sowie strukturelle Geschlechtschromosomen bei Drosophilafunebris. Z Zellforsch Mikrosk Anat 720–742.
Heitz, E., 1929. Heterochromatin, Chromocentren, Chromomeren. Ber Bot. Ges 274–284.
Heitz, E., 1928. Das Heterochromatin der Moose. I. Jahrb Wiss Bot 762–818.
Helmrich, A., Ballarino, M., Tora, L., 2011. Collisions between Replication and Transcription Complexes Cause Common Fragile Site Instability at the Longest Human Genes. Mol. Cell 44, 966–977. https://doi.org/10.1016/j.molcel.2011.10.013
Henikoff, S., Shilatifard, A., 2011. Histone modification: cause or cog? Trends Genet. 27, 389–396. https://doi.org/10.1016/j.tig.2011.06.006
Hereford, L.M., Hartwell, L.H., 1974. Sequential gene function in the initiation of Saccharomyces cerevisiae DNA synthesis. J. Mol. Biol. 84, 445–461. https://doi.org/10.1016/0022-2836(74)90451-3
Hildebrand, E.M., Dekker, J., 2020. Mechanisms and Functions of Chromosome Compartmentalization. Trends Biochem. Sci. 45, 385–396. https://doi.org/10.1016/j.tibs.2020.01.002
Hinchcliffe, E.H., Day, C.A., Karanjeet, K.B., Fadness, S., Langfald, A., Vaughan, K.T., Dong, Z., 2016. Chromosome missegregation during anaphase triggers p53 cell cycle arrest through histone H3.3 Ser31 phosphorylation. Nat. Cell Biol. 18, 668–675. https://doi.org/10.1038/ncb3348
Hiraga, S., Ly, T., Garzón, J., Hořejší, Z., Ohkubo, Y., Endo, A., Obuse, C., Boulton, S.J., Lamond, A.I., Donaldson, A.D., 2017. Human RIF1 and protein phosphatase 1 stimulate DNA replication origin licensing but suppress origin activation. EMBO Rep. 18, 403–419. https://doi.org/10.15252/embr.201641983
Hiratani, I., Ryba, T., Itoh, M., Yokochi, T., Schwaiger, M., Chang, C.-W., Lyou, Y., Townes, T.M., Schübeler, D., Gilbert, D.M., 2008. Global Reorganization of Replication Domains During Embryonic Stem Cell Differentiation. PLoS Biol. 6, e245. https://doi.org/10.1371/journal.pbio.0060245
Hirota, T., Lipp, J.J., Toh, B.-H., Peters, J.-M., 2005. Histone H3 serine 10 phosphorylation by Aurora B causes HP1 dissociation from heterochromatin. Nature 438, 1176–1180. https://doi.org/10.1038/nature04254
Hnisz, D., Weintraub, A.S., Day, D.S., Valton, A.-L., Bak, R.O., Li, C.H., Goldmann, J., Lajoie, B.R., Fan, Z.P., Sigova, A.A., Reddy, J., Borges-Rivera, D., Lee, T.I., Jaenisch, R., Porteus, M.H., Dekker, J., Young, R.A., 2016. Activation of proto-oncogenes by disruption of chromosome neighborhoods. Science 351, 1454–1458. https://doi.org/10.1126/science.aad9024
Hödl, M., Basler, K., 2009. Transcription in the Absence of Histone H3.3. Curr. Biol. 19, 1221–1226. https://doi.org/10.1016/j.cub.2009.05.048
Hoek, M., Stillman, B., 2003. Chromatin assembly factor 1 is essential and couples chromatin assembly to DNA replication *in vivo*. Proc. Natl. Acad. Sci. 100, 12183–12188. https://doi.org/10.1073/pnas.1635158100
Hoelper, D., Huang, H., Jain, A.Y., Patel, D.J., Lewis, P.W., 2017. Structural and mechanistic insights into ATRX-dependent and -independent functions of the histone chaperone DAXX. Nat. Commun. 8, 1193. https://doi.org/10.1038/s41467-017-01206-y
Hoencamp, C., Dudchenko, O., Elbatsh, A.M.O., Brahmachari, S., Raaijmakers, J.A., van Schaik, T., Sedeño Cacciatore, Á., Contessoto, V.G., van Heesbeen, R.G.H.P., van den Broek, B., Mhaskar, A.N., Teunissen, H., St Hilaire, B.G., Weisz, D., Omer, A.D., Pham, M., Colaric, Z., Yang, Z., Rao, S.S.P., Mitra, N., Lui, C., Yao, W., Khan, R., Moroz, L.L., Kohn, A., St. Leger, J., Mena, A., Holcroft, K., Gambetta, M.C., Lim, F., Farley, E., Stein, N., Haddad, A., Chauss, D., Mutlu, A.S., Wang, M.C., Young, N.D., Hildebrandt, E., Cheng, H.H., Knight, C.J., Burnham, T.L.U., Hovel, K.A., Beel, A.J., Mattei, P.-J., Kornberg, R.D., Warren, W.C., Cary, G., Gómez-Skarmeta, J.L., Hinman, V., Lindblad-Toh, K., Di Palma, F., Maeshima, K., Multani, A.S., Pathak, S., Nel-Themaat, L., Behringer, R.R., Kaur, P., Medema, R.H., van Steensel, B., de Wit, E., Onuchic, J.N., Di Pierro, M.,

Lieberman Aiden, E., Rowland, B.D., 2021. 3D genomics across the tree of life reveals condensin II as a determinant of architecture type. Science 372, 984–989. https://doi.org/10.1126/science.abe2218
Hou, C., Li, L., Qin, Z.S., Corces, V.G., 2012. Gene Density, Transcription, and Insulators Contribute to the Partition of the Drosophila Genome into Physical Domains. Mol. Cell 48, 471–484. https://doi.org/10.1016/j.molcel.2012.08.031
Houlard, M., Berlivet, S., Probst, A.V., Quivy, J.-P., 2006. CAF-1 Is Essential for Heterochromatin Organization in Pluripotent Embryonic Cells. PLoS Genet. 2, 11.
Howlett, S.K., Bolton, V.N., 1985. Sequence and regulation of morphological and molecular events during the first cell cycle of mouse embryogenesis. Development 87, 175–206. https://doi.org/10.1242/dev.87.1.175
Howman, E.V., Fowler, K.J., Newson, A.J., Redward, S., MacDonald, A.C., Kalitsis, P., Choo, K.H.A., 2000. Early disruption of centromeric chromatin organization in centromere protein A (*Cenpa*) null mice. Proc. Natl. Acad. Sci. 97, 1148–1153. https://doi.org/10.1073/pnas.97.3.1148
Hsieh, T.-H.S., Cattoglio, C., Slobodyanyuk, E., Hansen, A.S., Rando, O.J., Tjian, R., Darzacq, X., 2020. Resolving the 3D Landscape of Transcription-Linked Mammalian Chromatin Folding. Mol. Cell 78, 539-553.e8. https://doi.org/10.1016/j.molcel.2020.03.002
Hsieh, T.-H.S., Fudenberg, G., Goloborodko, A., Rando, O.J., 2016. Micro-C XL: assaying chromosome conformation from the nucleosome to the entire genome. Nat. Methods 13, 1009–1011. https://doi.org/10.1038/nmeth.4025
Hsieh, T.-H.S., Weiner, A., Lajoie, B., Dekker, J., Friedman, N., Rando, O.J., 2015. Mapping Nucleosome Resolution Chromosome Folding in Yeast by Micro-C. Cell 162, 108–119. https://doi.org/10.1016/j.cell.2015.05.048
Hsiung, C.C.-S., Bartman, C.R., Huang, P., Ginart, P., Stonestrom, A.J., Keller, C.A., Face, C., Jahn, K.S., Evans, P., Sankaranarayanan, L., Giardine, B., Hardison, R.C., Raj, A., Blobel, G.A., 2016. A hyperactive transcriptional state marks genome reactivation at the mitosis–G1 transition. Genes Dev. 30, 1423–1439. https://doi.org/10.1101/gad.280859.116
Hu, S., Lv, P., Yan, Z., Wen, B., 2019. Disruption of nuclear speckles reduces chromatin interactions in active compartments. Epigenetics Chromatin 12, 43. https://doi.org/10.1186/s13072-019-0289-2
Hu, Y., Stillman, B., 2023. Origins of DNA replication in eukaryotes. Mol. Cell S1097276522012035. https://doi.org/10.1016/j.molcel.2022.12.024
Huang, H., Strømme, C.B., Saredi, G., Hödl, M., Strandsby, A., González-Aguilera, C., Chen, S., Groth, A., Patel, D.J., 2015. A unique binding mode enables MCM2 to chaperone histones H3–H4 at replication forks. Nat. Struct. Mol. Biol. 22, 618–626. https://doi.org/10.1038/nsmb.3055
Huberman, J.A., Riggs, A.D., 1968. On the mechanism of DNA replication in mammalian chromosomes. J. Mol. Biol. 32, 327–341. https://doi.org/10.1016/0022-2836(68)90013-2
Huberman, J.A., Spotila, L.D., Nawotka, K.A., El-Assouli, S.M., Davis, L.R., 1987. The in vivo replication origin of the yeast 2μm plasmid. Cell 51, 473–481. https://doi.org/10.1016/0092-8674(87)90643-X
Hug, C.B., Grimaldi, A.G., Kruse, K., Vaquerizas, J.M., 2017. Chromatin Architecture Emerges during Zygotic Genome Activation Independent of Transcription. Cell 169, 216-228.e19. https://doi.org/10.1016/j.cell.2017.03.024
Hughes, A.L., Szczurek, A.T., Kelley, J.R., Lastuvkova, A., Turberfield, A.H., Dimitrova, E., Blackledge, N.P., Klose, R.J., 2023. A CpG island-encoded mechanism protects genes from premature transcription termination. Nat. Commun. 14, 726. https://doi.org/10.1038/s41467-023-36236-2
Huppert, J.L., Balasubramanian, S., 2005. Prevalence of quadruplexes in the human genome. Nucleic Acids Res. 33, 2908–2916. https://doi.org/10.1093/nar/gki609
Hyrien, O., Maric, C., Méchali, M., 1995. Transition in Specification of Embryonic Metazoan DNA Replication Origins. Science 270, 994–997. https://doi.org/10.1126/science.270.5238.994
Ibarra, A., Schwob, E., Méndez, J., 2008. Excess MCM proteins protect human cells from replicative stress by licensing backup origins of replication. Proc. Natl. Acad. Sci. 105, 8956–8961. https://doi.org/10.1073/pnas.0803978105
Iida, T., Araki, H., 2004. Noncompetitive Counteractions of DNA Polymerase ε and ISW2/yCHRAC for Epigenetic Inheritance of Telomere Position Effect in *Saccharomyces cerevisiae*. Mol. Cell. Biol. 24, 217–227. https://doi.org/10.1128/MCB.24.1.217-227.2004
Iizuka, M., Stillman, B., 1999. Histone Acetyltransferase HBO1 Interacts with the ORC1 Subunit of the Human Initiator Protein *. J. Biol. Chem. 274, 23027–23034. https://doi.org/10.1074/jbc.274.33.23027
Ishimi, Y., Komamura-Kohno, Y., Arai, K., Masai, H., 2001. Biochemical Activities Associated with Mouse Mcm2 Protein. J. Biol. Chem. 276, 42744–42752. https://doi.org/10.1074/jbc.M106861200
Ishiuchi, T., Abe, S., Inoue, K., Yeung, W.K.A., Miki, Y., Ogura, A., Sasaki, H., 2020. Reprogramming of the histone H3.3 landscape in the early mouse embryo. Nat. Struct. Mol. Biol. https://doi.org/10.1038/s41594-020-00521-1

Ishiuchi, T., Enriquez-Gasca, R., Mizutani, E., Bošković, A., Ziegler-Birling, C., Rodriguez-Terrones, D., Wakayama, T., Vaquerizas, J.M., Torres-Padilla, M.-E., 2015. Early embryonic-like cells are induced by downregulating replication-dependent chromatin assembly. Nat. Struct. Mol. Biol. 22, 662–671. https://doi.org/10.1038/nsmb.3066
Isobe, S.-Y., Hiraga, S., Nagao, K., Sasanuma, H., Donaldson, A.D., Obuse, C., 2021. Protein phosphatase 1 acts as a RIF1 effector to suppress DSB resection prior to Shieldin action. Cell Rep. 36, 109383. https://doi.org/10.1016/j.celrep.2021.109383
Ito, S., D'Alessio, A.C., Taranova, O.V., Hong, K., Sowers, L.C., Zhang, Y., 2010. Role of Tet proteins in 5mC to 5hmC conversion, ES-cell self-renewal and inner cell mass specification. Nature 466, 1129–1133. https://doi.org/10.1038/nature09303
Ito, S., Shen, L., Dai, Q., Wu, S.C., Collins, L.B., Swenberg, J.A., He, C., Zhang, Y., 2011. Tet Proteins Can Convert 5-Methylcytosine to 5-Formylcytosine and 5-Carboxylcytosine. Science 333, 1300–1303. https://doi.org/10.1126/science.1210597
Ivanauskiene, K., Delbarre, E., McGhie, J.D., Küntziger, T., Wong, L.H., Collas, P., 2014. The PML-associated protein DEK regulates the balance of H3.3 loading on chromatin and is important for telomere integrity. Genome Res. 24, 1584–1594. https://doi.org/10.1101/gr.173831.114
Jackson, D.A., Pombo, A., 1998. Replicon Clusters Are Stable Units of Chromosome Structure: Evidence That Nuclear Organization Contributes to the Efficient Activation and Propagation of S Phase in Human Cells. J. Cell Biol. 140, 1285–1295. https://doi.org/10.1083/jcb.140.6.1285
Jackson, V., 1990. In vivo studies on the dynamics of histone-DNA interaction: evidence for nucleosome dissolution during replication and transcription and a low level of dissolution independent of both. Biochemistry 29, 719–731. https://doi.org/10.1021/bi00455a019
Jackson, V., 1988. Deposition of newly synthesized histones: hybrid nucleosomes are not tandemly arranged on daughter DNA strands. Biochemistry 27, 2109–2120. https://doi.org/10.1021/bi00406a044
Jackson, V., Chalkley, R., 1985. Histone segregation of replicating chromatin. Biochemistry 24, 6930–6938. https://doi.org/10.1021/bi00345a027
Jackson, V., Chalkley, R., 1981a. A reevaluation of new histone deposition on replicating chromatin. J. Biol. Chem. 256, 5095–5103. https://doi.org/10.1016/S0021-9258(19)69371-3
Jackson, V., Chalkley, R., 1981b. A new method for the isolation of replicative chromatin: Selective deposition of histone on both new and old DNA. Cell 23, 121–134. https://doi.org/10.1016/0092-8674(81)90277-4
Jackson, V., Shires, A., Tanphaichitr, N., Chalkley, R., 1976. Modifications to histones immediately after synthesis. J. Mol. Biol. 104, 471–483. https://doi.org/10.1016/0022-2836(76)90282-5
Jain, S.U., Do, T.J., Lund, P.J., Rashoff, A.Q., Diehl, K.L., Cieslik, M., Bajic, A., Juretic, N., Deshmukh, S., Venneti, S., Muir, T.W., Garcia, B.A., Jabado, N., Lewis, P.W., 2019. PFA ependymoma-associated protein EZHIP inhibits PRC2 activity through a H3 K27M-like mechanism. Nat. Commun. 10, 2146. https://doi.org/10.1038/s41467-019-09981-6
Jain, S.U., Rashoff, A.Q., Krabbenhoft, S.D., Hoelper, D., Do, T.J., Gibson, T.J., Lundgren, S.M., Bondra, E.R., Deshmukh, S., Harutyunyan, A.S., Juretic, N., Jabado, N., Harrison, M.M., Lewis, P.W., 2020. H3 K27M and EZHIP Impede H3K27-Methylation Spreading by Inhibiting Allosterically Stimulated PRC2. Mol. Cell 80, 726-735.e7. https://doi.org/10.1016/j.molcel.2020.09.028
Jang, C.-W., Shibata, Y., Starmer, J., Yee, D., Magnuson, T., 2015. Histone H3.3 maintains genome integrity during mammalian development. Genes Dev. 29, 1377–1392. https://doi.org/10.1101/gad.264150.115
Jansen, L.E.T., Black, B.E., Foltz, D.R., Cleveland, D.W., 2007. Propagation of centromeric chromatin requires exit from mitosis. J. Cell Biol. 176, 795–805. https://doi.org/10.1083/jcb.200701066
Jasencakova, Z., Scharf, A.N.D., Ask, K., Corpet, A., Imhof, A., Almouzni, G., Groth, A., 2010. Replication Stress Interferes with Histone Recycling and Predeposition Marking of New Histones. Mol. Cell 37, 736–743. https://doi.org/10.1016/j.molcel.2010.01.033
Jeffery, D., Gatto, A., Podsypanina, K., Renaud-Pageot, C., Ponce Landete, R., Bonneville, L., Dumont, M., Fachinetti, D., Almouzni, G., 2021. CENP-A overexpression promotes distinct fates in human cells, depending on p53 status. Commun. Biol. 4, 417. https://doi.org/10.1038/s42003-021-01941-5
Jerkovic, I., Cavalli, G., 2021. Understanding 3D genome organization by multidisciplinary methods 18.
Ji, X., Dadon, D.B., Powell, B.E., Fan, Z.P., Borges-Rivera, D., Shachar, S., Weintraub, A.S., Hnisz, D., Pegoraro, G., Lee, T.I., Misteli, T., Jaenisch, R., Young, R.A., 2016. 3D Chromosome Regulatory Landscape of Human Pluripotent Cells. Cell Stem Cell 18, 262–275. https://doi.org/10.1016/j.stem.2015.11.007
Jiang, C., Pugh, B.F., 2009. Nucleosome positioning and gene regulation: advances through genomics. Nat. Rev. Genet. 10, 161–172. https://doi.org/10.1038/nrg2522
Jiang, Y., Huang, J., Lun, K., Li, B., Zheng, H., Li, Y., Zhou, R., Duan, W., Wang, C., Feng, Y., Yao, H., Li, C., Ji, X., 2020. Genome-wide analyses of chromatin interactions after the loss of Pol I, Pol II, and Pol III. Genome Biol. 21, 158. https://doi.org/10.1186/s13059-020-02067-3

Jiao, L., Liu, X., 2015. Structural basis of histone H3K27 trimethylation by an active polycomb repressive complex 2. Science 350, aac4383. https://doi.org/10.1126/science.aac4383
Jin, C., Felsenfeld, G., 2007. Nucleosome stability mediated by histone variants H3.3 and H2A.Z. Genes Dev. 21, 1519–1529. https://doi.org/10.1101/gad.1547707
Jin, C., Zang, C., Wei, G., Cui, K., Peng, W., Zhao, K., Felsenfeld, G., 2009. H3.3/H2A.Z double variant–containing nucleosomes mark "nucleosome-free regions" of active promoters and other regulatory regions. Nat. Genet. 41, 941–945. https://doi.org/10.1038/ng.409
Jin, F., Li, Y., Dixon, J.R., Selvaraj, S., Ye, Z., Lee, A.Y., Yen, C.-A., Schmitt, A.D., Espinoza, C.A., Ren, B., 2013. A high-resolution map of the three-dimensional chromatin interactome in human cells. Nature 503, 290–294. https://doi.org/10.1038/nature12644
Jodkowska, K., Pancaldi, V., Rigau, M., Almeida, R., Fernández-Justel, J.M., Graña-Castro, O., Rodríguez-Acebes, S., Rubio-Camarillo, M., Carrillo-de Santa Pau, E., Pisano, D., Al-Shahrour, F., Valencia, A., Gómez, M., Méndez, J., 2022. 3D chromatin connectivity underlies replication origin efficiency in mouse embryonic stem cells. Nucleic Acids Res. gkac1111. https://doi.org/10.1093/nar/gkac1111
Johns, E.W., Phillips, D.M.P., Simson, P., Butler, J.A.V., 1960. Improved fractionations of arginine-rich histones from calf thymus. Biochem. J. 77, 631–636. https://doi.org/10.1042/bj0770631
Jost, D., Carrivain, P., Cavalli, G., Vaillant, C., 2014. Modeling epigenome folding: formation and dynamics of topologically associated chromatin domains. Nucleic Acids Res. 42, 9553–9561. https://doi.org/10.1093/nar/gku698
Jullien, J., Astrand, C., Szenker, E., Garrett, N., Almouzni, G., Gurdon, J.B., 2012. HIRA dependent H3.3 deposition is required for transcriptional reprogramming following nuclear transfer to Xenopus oocytes. Epigenetics Chromatin 5, 17. https://doi.org/10.1186/1756-8935-5-17
Justin, N., Zhang, Y., Tarricone, C., Martin, S.R., Chen, S., Underwood, E., De Marco, V., Haire, L.F., Walker, P.A., Reinberg, D., Wilson, J.R., Gamblin, S.J., 2016. Structural basis of oncogenic histone H3K27M inhibition of human polycomb repressive complex 2. Nat. Commun. 7, 11316. https://doi.org/10.1038/ncomms11316
Kagey, M.H., Newman, J.J., Bilodeau, S., Zhan, Y., Orlando, D.A., van Berkum, N.L., Ebmeier, C.C., Goossens, J., Rahl, P.B., Levine, S.S., Taatjes, D.J., Dekker, J., Young, R.A., 2010. Mediator and cohesin connect gene expression and chromatin architecture. Nature 467, 430–435. https://doi.org/10.1038/nature09380
Kahney, E.W., Zion, E.H., Sohn, L., Viets-Layng, K., Johnston, R., Chen, X., 2021. Characterization of histone inheritance patterns in the *Drosophila* female germline. EMBO Rep. 22, e51530. https://doi.org/10.15252/embr.202051530
Kang, B., Pu, M., Hu, G., Wen, W., Dong, Z., Zhao, K., Stillman, B., Zhang, Z., 2011. Phosphorylation of H4 Ser 47 promotes HIRA-mediated nucleosome assembly. Genes Dev. 25, 1359–1364. https://doi.org/10.1101/gad.2055511
Kanoh, J., Ishikawa, F., 2001. spRap1 and spRif1, recruited to telomeres by Taz1, are essential for telomere function in fission yeast. Curr. Biol. 11, 1624–1630. https://doi.org/10.1016/S0960-9822(01)00503-6
Kara, N., Hossain, M., Prasanth, S.G., Stillman, B., 2015. Orc1 Binding to Mitotic Chromosomes Precedes Spatial Patterning during G1 Phase and Assembly of the Origin Recognition Complex in Human Cells. J. Biol. Chem. 290, 12355–12369. https://doi.org/10.1074/jbc.M114.625012
Karpinska, M.A., Oudelaar, A.M., 2023. The role of loop extrusion in enhancer-mediated gene activation. Curr. Opin. Genet. Dev. 79, 102022. https://doi.org/10.1016/j.gde.2023.102022
Katainen, R., Dave, K., Pitkänen, E., Palin, K., Kivioja, T., Välimäki, N., Gylfe, A.E., Ristolainen, H., Hänninen, U.A., Cajuso, T., Kondelin, J., Tanskanen, T., Mecklin, J.-P., Järvinen, H., Renkonen-Sinisalo, L., Lepistö, A., Kaasinen, E., Kilpivaara, O., Tuupanen, S., Enge, M., Taipale, J., Aaltonen, L.A., 2015. CTCF/cohesin-binding sites are frequently mutated in cancer. Nat. Genet. 47, 818–821. https://doi.org/10.1038/ng.3335
Kato, T., Sato, N., Hayama, S., Yamabuki, T., Ito, T., Miyamoto, M., Kondo, S., Nakamura, Y., Daigo, Y., 2007. Activation of Holliday Junction–Recognizing Protein Involved in the Chromosomal Stability and Immortality of Cancer Cells. Cancer Res. 67, 8544–8553. https://doi.org/10.1158/0008-5472.CAN-07-1307
Kaya-Okur, H.S., Wu, S.J., Codomo, C.A., Pledger, E.S., Bryson, T.D., Henikoff, J.G., Ahmad, K., Henikoff, S., 2019. CUT&Tag for efficient epigenomic profiling of small samples and single cells. Nat Commun 10, 1930. https://doi.org/10.1038/s41467-019-09982-5
Ke, Y., Xu, Y., Chen, X., Feng, S., Liu, Z., Sun, Y., Yao, X., Li, F., Zhu, W., Gao, L., Chen, H., Du, Z., Xie, W., Xu, X., Huang, X., Liu, J., 2017. 3D Chromatin Structures of Mature Gametes and Structural Reprogramming during Mammalian Embryogenesis. Cell 170, 367-381.e20. https://doi.org/10.1016/j.cell.2017.06.029
Kempfer, R., Pombo, A., 2019. Methods for mapping 3D chromosome architecture. Nat. Rev. Genet. https://doi.org/10.1038/s41576-019-0195-2
Keppler, A., Gendreizig, S., Gronemeyer, T., Pick, H., Vogel, H., Johnsson, K., 2003. A general method for the covalent labeling of fusion proteins with small molecules in vivo. Nat. Biotechnol. 21, 86–89. https://doi.org/10.1038/nbt765

Kim, E., Gonzalez, A.M., Pradhan, B., Van Der Torre, J., Dekker, C., 2022. Condensin-driven loop extrusion on supercoiled DNA. Nat. Struct. Mol. Biol. 29, 719–727. https://doi.org/10.1038/s41594-022-00802-x
Kim, E., Kerssemakers, J., Shaltiel, I.A., Haering, C.H., Dekker, C., 2020. DNA-loop extruding condensin complexes can traverse one another. Nature 579, 438–442. https://doi.org/10.1038/s41586-020-2067-5
Kim, H., Heo, K., Choi, J., Kim, K., An, W., 2011. Histone variant H3.3 stimulates HSP70 transcription through cooperation with HP1γ. Nucleic Acids Res. 39, 8329–8341. https://doi.org/10.1093/nar/gkr529
Kim, J., Sun, C., Tran, A.D., Chin, P.-J., Ruiz, P.D., Wang, K., Gibbons, R.J., Gamble, M.J., Liu, Y., Oberdoerffer, P., 2019. The macroH2A1.2 histone variant links ATRX loss to alternative telomere lengthening. Nat. Struct. Mol. Biol. 26, 213–219. https://doi.org/10.1038/s41594-019-0192-3
Kimura, H., Cook, P.R., 2001. Kinetics of Core Histones in Living Human Cells: Little Exchange of H3 and H4 and Some Rapid Exchange of H2B. J. Cell Biol. 153.
Kind, J., Pagie, L., Ortabozkoyun, H., Boyle, S., de Vries, S.S., Janssen, H., Amendola, M., Nolen, L.D., Bickmore, W.A., van Steensel, B., 2013. Single-Cell Dynamics of Genome-Nuclear Lamina Interactions. Cell 153, 178–192. https://doi.org/10.1016/j.cell.2013.02.028
Kind, J., Van Steensel, B., 2010. Genome–nuclear lamina interactions and gene regulation. Curr. Opin. Cell Biol. 22, 320–325. https://doi.org/10.1016/j.ceb.2010.04.002
Kinkade, J.M., Cole, R.D., 1966. The Resolution of Four Lysine-rich Histones Derived from Calf Thymus. J. Biol. Chem. 241, 5790–5797. https://doi.org/10.1016/S0021-9258(18)96342-8
Kleijwegt, C., Bressac, F., Seurre, C., Bouchereau, W., Cohen, C., Texier, P., Simonet, T., Schaeffer, L., Lomonte, P., Corpet, A., 2023. Interplay between PML NBs and HIRA for H3.3 dynamics following type I interferon stimulus. eLife 12, e80156. https://doi.org/10.7554/eLife.80156
Klein, D.C., Hainer, S.J., 2020. Chromatin regulation and dynamics in stem cells, in: Current Topics in Developmental Biology. Elsevier, pp. 1–71. https://doi.org/10.1016/bs.ctdb.2019.11.002
Klein, K.N., Zhao, P.A., Lyu, X., Sasaki, T., Bartlett, D.A., Singh, A.M., Tasan, I., Zhang, M., Watts, L.P., Hiraga, S., Natsume, T., Zhou, X., Baslan, T., Leung, D., Kanemaki, M.T., Donaldson, A.D., Zhao, H., Dalton, S., Corces, V.G., Gilbert, D.M., 2021. Replication timing maintains the global epigenetic state in human cells 9.
Köhler, G., Milstein, C., 1975. Continuous cultures of fused cells secreting antibody of predefined specificity. Nature 256, 495–497. https://doi.org/10.1038/256495a0
Konev, A.Y., Tribus, M., Park, S.Y., Podhraski, V., Lim, C.Y., Emelyanov, A.V., Vershilova, E., Pirrotta, V., Kadonaga, J.T., Lusser, A., Fyodorov, D.V., 2007. CHD1 Motor Protein Is Required for Deposition of Histone Variant H3.3 into Chromatin in Vivo. Science 317, 1087–1090. https://doi.org/10.1126/science.1145339
Kong, Q., Banaszynski, L.A., Geng, F., Zhang, X., Zhang, J., Zhang, H., O'Neill, C.L., Yan, P., Liu, Z., Shido, K., Palermo, G.D., Allis, C.D., Rafii, S., Rosenwaks, Z., Wen, D., 2018. Histone variant H3.3–mediated chromatin remodeling is essential for paternal genome activation in mouse preimplantation embryos. J. Biol. Chem. 293, 3829–3838. https://doi.org/10.1074/jbc.RA117.001150
Koren, A., Polak, P., Nemesh, J., Michaelson, J.J., Sebat, J., Sunyaev, S.R., McCarroll, S.A., 2012. Differential Relationship of DNA Replication Timing to Different Forms of Human Mutation and Variation. Am. J. Hum. Genet. 91, 1033–1040. https://doi.org/10.1016/j.ajhg.2012.10.018
Kornberg, R.D., 1974. Chromatin Structure: A Repeating Unit of Histones and DNA. Science 184, 868–871. https://doi.org/10.1126/science.184.4139.868
Kossel, A., 1884. Ueber einen peptonartigen Bestandtheil des Zellkerns. Zschr Physiol Chem 511.
Kragesteen, B.K., Spielmann, M., Paliou, C., Heinrich, V., Schöpflin, R., Esposito, A., Annunziatella, C., Bianco, S., Chiariello, A.M., Jerković, I., Harabula, I., Guckelberger, P., Pechstein, M., Wittler, L., Chan, W.-L., Franke, M., Lupiáñez, D.G., Kraft, K., Timmermann, B., Vingron, M., Visel, A., Nicodemi, M., Mundlos, S., Andrey, G., 2018. Dynamic 3D chromatin architecture contributes to enhancer specificity and limb morphogenesis. Nat. Genet. 50, 1463–1473. https://doi.org/10.1038/s41588-018-0221-x
Krietenstein, N., Abraham, S., Venev, S.V., Abdennur, N., Gibcus, J., Hsieh, T.-H.S., Parsi, K.M., Yang, L., Maehr, R., Mirny, L.A., Dekker, J., Rando, O.J., 2020. Ultrastructural Details of Mammalian Chromosome Architecture. Mol. Cell 78, 554-565.e7. https://doi.org/10.1016/j.molcel.2020.03.003
Kueng, S., Hegemann, B., Peters, B.H., Lipp, J.J., Schleiffer, A., Mechtler, K., Peters, J.-M., 2006. Wapl Controls the Dynamic Association of Cohesin with Chromatin. Cell 127, 955–967. https://doi.org/10.1016/j.cell.2006.09.040
Kujirai, T., Horikoshi, N., Sato, K., Maehara, K., Machida, S., Osakabe, A., Kimura, H., Ohkawa, Y., Kurumizaka, H., 2016. Structure and function of human histone H3.Y nucleosome. Nucleic Acids Res. 44, 6127–6141. https://doi.org/10.1093/nar/gkw202
Kundu, S., Ji, F., Sunwoo, H., Jain, G., Lee, J.T., Sadreyev, R.I., Dekker, J., Kingston, R.E., 2017. Polycomb Repressive Complex 1 Generates Discrete Compacted Domains that Change during Differentiation. Mol. Cell 65, 432-446.e5. https://doi.org/10.1016/j.molcel.2017.01.009

Kuo, A.J., Song, J., Cheung, P., Ishibe-Murakami, S., Yamazoe, S., Chen, J.K., Patel, D.J., Gozani, O., 2012. The BAH domain of ORC1 links H4K20me2 to DNA replication licensing and Meier–Gorlin syndrome. Nature 484, 115–119. https://doi.org/10.1038/nature10956
Lacoste, N., Woolfe, A., Tachiwana, H., Garea, A.V., Barth, T., Cantaloube, S., Kurumizaka, H., Imhof, A., Almouzni, G., 2014. Mislocalization of the Centromeric Histone Variant CenH3/CENP-A in Human Cells Depends on the Chaperone DAXX. Mol. Cell 53, 631–644. https://doi.org/10.1016/j.molcel.2014.01.018
Lafontaine, D.L., Yang, L., Dekker, J., Gibcus, J.H., 2021. Hi-C 3.0: Improved Protocol for Genome-Wide Chromosome Conformation Capture. Curr. Protoc. 1. https://doi.org/10.1002/cpz1.198
Lamour, V., Lécluse, Y., Desmaze, C., Spector, M., Bodescot, M., Aurias, A., Osley, M.A., Lipinski, M., 1995. A human homolog of the S.cerevisiae HIR1 and HIR2 transcriptional repressors cloned from the DiGeorge syndrome critical region. Hum. Mol. Genet. 4, 791–799. https://doi.org/10.1093/hmg/4.5.791
Lander, E.S., Linton, L.M., Birren, B., Nusbaum, C., Zody, M.C., Baldwin, J., Devon, K., Dewar, K., Doyle, M., FitzHugh, W., Funke, R., Gage, D., Harris, K., Heaford, A., Howland, J., Kann, L., Lehoczky, J., LeVine, R., McEwan, P., McKernan, K., Meldrim, J., Mesirov, J.P., Miranda, C., Morris, W., Naylor, J., Raymond, Christina, Rosetti, M., Santos, R., Sheridan, A., Sougnez, C., Stange-Thomann, N., Stojanovic, N., Subramanian, A., Wyman, D., Rogers, J., Sulston, J., Ainscough, R., Beck, S., Bentley, D., Burton, J., Clee, C., Carter, N., Coulson, A., Deadman, R., Deloukas, P., Dunham, A., Dunham, I., Durbin, R., French, L., Grafham, D., Gregory, S., Hubbard, T., Humphray, S., Hunt, A., Jones, M., Lloyd, C., McMurray, A., Matthews, L., Mercer, S., Milne, S., Mullikin, J.C., Mungall, A., Plumb, R., Ross, M., Shownkeen, R., Sims, S., Waterston, R.H., Wilson, R.K., Hillier, L.W., McPherson, J.D., Marra, M.A., Mardis, E.R., Fulton, L.A., Chinwalla, A.T., Pepin, K.H., Gish, W.R., Chissoe, S.L., Wendl, M.C., Delehaunty, K.D., Miner, T.L., Delehaunty, A., Kramer, J.B., Cook, L.L., Fulton, R.S., Johnson, D.L., Minx, P.J., Clifton, S.W., Hawkins, T., Branscomb, E., Predki, P., Richardson, P., Wenning, S., Slezak, T., Doggett, N., Cheng, J.-F., Olsen, A., Lucas, S., Elkin, C., Uberbacher, E., Frazier, M., Gibbs, R.A., Muzny, D.M., Scherer, S.E., Bouck, J.B., Sodergren, E.J., Worley, K.C., Rives, C.M., Gorrell, J.H., Metzker, M.L., Naylor, S.L., Kucherlapati, R.S., Nelson, D.L., Weinstock, G.M., Sakaki, Y., Fujiyama, A., Hattori, M., Yada, T., Toyoda, A., Itoh, T., Kawagoe, C., Watanabe, H., Totoki, Y., Taylor, T., Weissenbach, J., Heilig, R., Saurin, W., Artiguenave, F., Brottier, P., Bruls, T., Pelletier, E., Robert, C., Wincker, P., Rosenthal, A., Platzer, M., Nyakatura, G., Taudien, S., Rump, A., Smith, D.R., Doucette-Stamm, L., Rubenfield, M., Weinstock, K., Lee, H.M., Dubois, J., Yang, H., Yu, J., Wang, J., Huang, G., Gu, J., Hood, L., Rowen, L., Madan, A., Qin, S., Davis, R.W., Federspiel, N.A., Abola, A.P., Proctor, M.J., Roe, B.A., Chen, F., Pan, H., Ramser, J., Lehrach, H., Reinhardt, R., McCombie, W.R., de la Bastide, M., Dedhia, N., Blöcker, H., Hornischer, K., Nordsiek, G., Agarwala, R., Aravind, L., Bailey, J.A., Bateman, A., Batzoglou, S., Birney, E., Bork, P., Brown, D.G., Burge, C.B., Cerutti, L., Chen, H.-C., Church, D., Clamp, M., Copley, R.R., Doerks, T., Eddy, S.R., Eichler, E.E., Furey, T.S., Galagan, J., Gilbert, J.G.R., Harmon, C., Hayashizaki, Y., Haussler, D., Hermjakob, H., Hokamp, K., Jang, W., Johnson, L.S., Jones, T.A., Kasif, S., Kaspryzk, A., Kennedy, S., Kent, W.J., Kitts, P., Koonin, E.V., Korf, I., Kulp, D., Lancet, D., Lowe, T.M., McLysaght, A., Mikkelsen, T., Moran, J.V., Mulder, N., Pollara, V.J., Ponting, C.P., Schuler, G., Schultz, J., Slater, G., Smit, A.F.A., Stupka, E., Szustakowki, J., Thierry-Mieg, D., Thierry-Mieg, J., Wagner, L., Wallis, J., Wheeler, R., Williams, A., Wolf, Y.I., Wolfe, K.H., Yang, S.-P., Yeh, R.-F., Collins, F., Guyer, M.S., Peterson, J., Felsenfeld, A., Wetterstrand, K.A., Myers, R.M., Schmutz, J., Dickson, M., Grimwood, J., Cox, D.R., Olson, M.V., Kaul, R., Raymond, Christopher, Shimizu, N., Kawasaki, K., Minoshima, S., Evans, G.A., Athanasiou, M., Schultz, R., Patrinos, A., Morgan, M.J., International Human Genome Sequencing Consortium, Whitehead Institute for Biomedical Research, C. for G.R., The Sanger Centre:, Washington University Genome Sequencing Center, US DOE Joint Genome Institute:, Baylor College of Medicine Human Genome Sequencing Center:, RIKEN Genomic Sciences Center:, Genoscope and CNRS UMR-8030:, Department of Genome Analysis, I. of M.B., GTC Sequencing Center:, Beijing Genomics Institute/Human Genome Center:, Multimegabase Sequencing Center, T.I. for S.B., Stanford Genome Technology Center:, University of Oklahoma's Advanced Center for Genome Technology:, Max Planck Institute for Molecular Genetics:, Cold Spring Harbor Laboratory, L.A.H.G.C., GBF—German Research Centre for Biotechnology:, *Genome Analysis Group (listed in alphabetical order, also includes individuals listed under other headings):, Scientific management: National Human Genome Research Institute, U.N.I. of H., Stanford Human Genome Center:, University of Washington Genome Center:, Department of Molecular Biology, K.U.S. of M., University of Texas Southwestern Medical Center at Dallas:, Office of Science, U.D. of E., The Wellcome Trust:, 2001. Initial sequencing and analysis of the human genome. Nature 409, 860–921. https://doi.org/10.1038/35057062
Langer, P.R., Waldrop, A.A., Ward, D.C., 1981. Enzymatic synthesis of biotin-labeled polynucleotides: novel nucleic acid affinity probes. Proc. Natl. Acad. Sci. 78, 6633–6637. https://doi.org/10.1073/pnas.78.11.6633
Langley, A.R., Gräf, S., Smith, J.C., Krude, T., 2016. Genome-wide identification and characterisation of human DNA replication origins by initiation site sequencing (ini-seq). Nucleic Acids Res gkw760. https://doi.org/10.1093/nar/gkw760

Larson, A.G., Elnatan, D., Keenen, M.M., Trnka, M.J., Johnston, J.B., Burlingame, A.L., Agard, D.A., Redding, S., Narlikar, G.J., 2017. Liquid droplet formation by HP1α suggests a role for phase separation in heterochromatin. Nature 547, 236–240. https://doi.org/10.1038/nature22822
Laskey, R.A., Honda, B.M., Mills, A.D., Finch, J.T., 1978. Nucleosomes are assembled by an acidic protein which binds histones and transfers them to DNA. Nature 275, 416–420. https://doi.org/10.1038/275416a0
Lau, M.S., Schwartz, M.G., Kundu, S., Savol, A.J., Wang, P.I., Marr, S.K., Grau, D.J., Schorderet, P., Sadreyev, R.I., Tabin, C.J., Kingston, R.E., 2017. Mutation of a nucleosome compaction region disrupts Polycomb-mediated axial patterning. Science 355, 1081–1084. https://doi.org/10.1126/science.aah5403
Lawrence, J.B., Singer, R.H., McNeil, J.A., 1990. Interphase and Metaphase Resolution of Different Distances Within the Human Dystrophin Gene. Science 249, 928–932. https://doi.org/10.1126/science.2203143
Lebofsky, R., Heilig, R., Sonnleitner, M., Weissenbach, J., Bensimon, A., 2006. DNA Replication Origin Interference Increases the Spacing between Initiation Events in Human Cells□D. Mol. Biol. Cell 17.
Lee, C.-H., Yu, J.-R., Granat, J., Saldaña-Meyer, R., Andrade, J., LeRoy, G., Jin, Y., Lund, P., Stafford, J.M., Garcia, B.A., Ueberheide, B., Reinberg, D., 2019. Automethylation of PRC2 promotes H3K27 methylation and is impaired in H3K27M pediatric glioma. Genes Dev. 33, 1428–1440. https://doi.org/10.1101/gad.328773.119
Lee, J.Y., Lee, T.-H., 2012. Effects of DNA Methylation on the Structure of Nucleosomes. J. Am. Chem. Soc. 134, 173–175. https://doi.org/10.1021/ja210273w
Lemaitre, J.-M., Danis, E., Pasero, P., Vassetzky, Y., Méchali, M., 2005. Mitotic Remodeling of the Replicon and Chromosome Structure. Cell 123, 787–801. https://doi.org/10.1016/j.cell.2005.08.045
Lengronne, A., Schwob, E., 2002. The Yeast CDK Inhibitor Sic1 Prevents Genomic Instability by Promoting Replication Origin Licensing in Late G1. Mol. Cell 9, 1067–1078. https://doi.org/10.1016/S1097-2765(02)00513-0
Lewis, P.W., Elsaesser, S.J., Noh, K.-M., Stadler, S.C., Allis, C.D., 2010. Daxx is an H3.3-specific histone chaperone and cooperates with ATRX in replication-independent chromatin assembly at telomeres. Proc. Natl. Acad. Sci. 107, 14075–14080. https://doi.org/10.1073/pnas.1008850107
Lewis, P.W., Müller, M.M., Koletsky, M.S., Cordero, F., Lin, S., Banaszynski, L.A., Garcia, B.A., Muir, T.W., Becher, O.J., Allis, C.D., 2013. Inhibition of PRC2 Activity by a Gain-of-Function H3 Mutation Found in Pediatric Glioblastoma. Science 340, 857–861. https://doi.org/10.1126/science.1232245
Li, E., Zhang, Y., 2014. DNA Methylation in Mammals. Cold Spring Harb. Perspect. Biol. 6, a019133–a019133. https://doi.org/10.1101/cshperspect.a019133
Li, J., Dong, J., Wang, W., Yu, D., Fan, X., Hui, Y.C., Lee, C.S.K., Lam, W.H., Alary, N., Yang, Y., Zhang, Y., Zhao, Q., Chen, C.-L., Tye, B.-K., Dang, S., Zhai, Y., 2023. The human pre-replication complex is an open complex. Cell 186, 98-111.e21. https://doi.org/10.1016/j.cell.2022.12.008
Li, N., Lam, W.H., Zhai, Y., Cheng, J., Cheng, E., Zhao, Y., Gao, N., Tye, B.-K., 2018. Structure of the origin recognition complex bound to DNA replication origin. Nature 559, 217–222. https://doi.org/10.1038/s41586-018-0293-x
Li, Q., Zhou, H., Wurtele, H., Davies, B., Horazdovsky, B., Verreault, A., Zhang, Z., 2008. Acetylation of Histone H3 Lysine 56 Regulates Replication-Coupled Nucleosome Assembly. Cell 134, 244–255. https://doi.org/10.1016/j.cell.2008.06.018
Li, Shuxiang, Peng, Y., Panchenko, A.R., 2022. DNA methylation: Precise modulation of chromatin structure and dynamics. Curr. Opin. Struct. Biol. 75, 102430. https://doi.org/10.1016/j.sbi.2022.102430
Li, Sai, Wasserman, M.R., Yurieva, O., Bai, L., O'Donnell, M.E., Liu, S., 2022. Origin recognition complex harbors an intrinsic nucleosome remodeling activity. Proc. Natl. Acad. Sci. 119, e2211568119. https://doi.org/10.1073/pnas.2211568119
Li, Y., Jiao, J., 2017. Histone chaperone HIRA regulates neural progenitor cell proliferation and neurogenesis via β-catenin. J. Cell Biol. 216, 1975–1992. https://doi.org/10.1083/jcb.201610014
Li, Z., Hua, X., Serra-Cardona, A., Xu, X., Gan, S., Zhou, H., Yang, W.-S., Chen, C., Xu, R.-M., Zhang, Z., 2020. DNA polymerase alpha interacts with H3-H4 and facilitates the transfer of parental histones to lagging strands. Sci. Adv. 6, 1–14. https://doi.org/10.1126/sciadv.abb5820
Lichter, P., Cremer, T., Borden, J., Manuelidis, L., Ward, D.C., 1988. Delineation of individual human chromosomes in metaphase and interphase cells by in situ suppression hybridization using recombinant DNA libraries. Hum. Genet. 80, 224–234. https://doi.org/10.1007/BF01790090
Lieberman-Aiden, E., van Berkum, N.L., Williams, L., Imakaev, M., Ragoczy, T., Telling, A., Amit, I., Lajoie, B.R., Sabo, P.J., Dorschner, M.O., Sandstrom, R., Bernstein, B., Bender, M.A., Groudine, M., Gnirke, A., Stamatoyannopoulos, J., Mirny, L.A., Lander, E.S., Dekker, J., 2009. Comprehensive Mapping of Long-Range Interactions Reveals Folding Principles of the Human Genome. Science 326, 289–293. https://doi.org/10.1126/science.1181369
Lim, P.S.L., Meshorer, E., 2020. Organization of the Pluripotent Genome. Cold Spring Harb. Perspect. Biol. a040204. https://doi.org/10.1101/cshperspect.a040204

Lipford, J.R., Bell, S.P., 2001. Nucleosomes Positioned by ORC Facilitate the Initiation of DNA Replication. Mol. Cell 7, 21–30. https://doi.org/10.1016/S1097-2765(01)00151-4
Liu, C.-P., Xiong, C., Wang, M., Yu, Z., Yang, N., Chen, P., Zhang, Z., Li, G., Xu, R.-M., 2012. Structure of the variant histone H3.3–H4 heterodimer in complex with its chaperone DAXX. Nat. Struct. Mol. Biol. 19, 1287–1292. https://doi.org/10.1038/nsmb.2439
Liu, J.-L., Murphy, C., Buszczak, M., Clatterbuck, S., Goodman, R., Gall, J.G., 2006. The Drosophila melanogaster Cajal body. J. Cell Biol. 172, 875–884. https://doi.org/10.1083/jcb.200511038
Liu, S., Xu, Z., Leng, H., Zheng, P., Yang, J., Chen, K., Feng, J., Li, Q., 2017. RPA binds histone H3-H4 and functions in DNA replication–coupled nucleosome assembly. Science 355, 415–420. https://doi.org/10.1126/science.aah4712
Liu, Y., Nanni, L., Sungalee, S., Zufferey, M., Tavernari, D., Mina, M., Ceri, S., Oricchio, E., Ciriello, G., 2021. Systematic inference and comparison of multi-scale chromatin sub-compartments connects spatial organization to cell phenotypes. Nat. Commun. 12, 2439. https://doi.org/10.1038/s41467-021-22666-3
Liu, Z., Tardat, M., Gill, M.E., Royo, H., Thierry, R., Ozonov, E.A., Peters, A.H., 2020. SUMOylated PRC1 controls histone H3.3 deposition and genome integrity of embryonic heterochromatin. EMBO J. 39. https://doi.org/10.15252/embj.2019103697
Liyanage, V.R.B., Jarmasz, J.S., Murugeshan, N., Del Bigio, M.R., Rastegar, M., Davie, J.R., 2014. DNA Modifications: Function and Applications in Normal and Disease States. Biology 3, 670–723. https://doi.org/10.3390/biology3040670
Long, H., Zhang, L., Lv, M., Wen, Z., Zhang, W., Chen, X., Zhang, P., Li, T., Chang, L., Jin, C., Wu, G., Wang, X., Yang, F., Pei, J., Chen, P., Margueron, R., Deng, H., Zhu, M., Li, G., 2020. H2A.Z facilitates licensing and activation of early replication origins. Nature 577, 576–581. https://doi.org/10.1038/s41586-019-1877-9
Long, M., Sun, X., Shi, W., Yanru, A., Leung, S.T.C., Ding, D., Cheema, M.S., MacPherson, N., Nelson, C.J., Ausio, J., Yan, Y., Ishibashi, T., 2019. A novel histone H4 variant H4G regulates rDNA transcription in breast cancer. Nucleic Acids Res. 47, 8399–8409. https://doi.org/10.1093/nar/gkz547
Loppin, B., Berger, F., 2020. Histone Variants: The Nexus of Developmental Decisions and Epigenetic Memory. Annu. Rev. Genet. 54, annurev-genet-022620-100039. https://doi.org/10.1146/annurev-genet-022620-100039
Loppin, B., Bonnefoy, E., Anselme, C., Laurençon, A., Karr, T.L., Couble, P., 2005. The histone H3.3 chaperone HIRA is essential for chromatin assembly in the male pronucleus. Nature 437, 1386–1390. https://doi.org/10.1038/nature04059
Loyola, A., Almouzni, G., 2007. Marking histone H3 variants: How, when and why? Trends Biochem. Sci. 32, 425–433. https://doi.org/10.1016/j.tibs.2007.08.004
Loyola, A., Almouzni, G., 2004. Histone chaperones, a supporting role in the limelight. Biochim. Biophys. Acta BBA - Gene Struct. Expr., Chromatin structure and function 1677, 3–11. https://doi.org/10.1016/j.bbaexp.2003.09.012
Loyola, A., Bonaldi, T., Roche, D., Imhof, A., Almouzni, G., 2006. PTMs on H3 Variants before Chromatin Assembly Potentiate Their Final Epigenetic State. Mol. Cell 24, 309–316. https://doi.org/10.1016/j.molcel.2006.08.019
Loyola, A., Tagami, H., Bonaldi, T., Roche, D., Quivy, J.P., Imhof, A., Nakatani, Y., Dent, S.Y.R., Almouzni, G., 2009. The HP1α–CAF1–SetDB1-containing complex provides H3K9me1 for Suv39-mediated K9me3 in pericentric heterochromatin. EMBO Rep. 10, 769–775. https://doi.org/10.1038/embor.2009.90
Lu, C., Jain, S.U., Hoelper, D., Bechet, D., Molden, R.C., Ran, L., Murphy, D., Venneti, S., Hameed, M., Pawel, B.R., Wunder, J.S., Dickson, B.C., Lundgren, S.M., Jani, K.S., De Jay, N., Papillon-Cavanagh, S., Andrulis, I.L., Sawyer, S.L., Grynspan, D., Turcotte, R.E., Nadaf, J., Fahiminiyah, S., Muir, T.W., Majewski, J., Thompson, C.B., Chi, P., Garcia, B.A., Allis, C.D., Jabado, N., Lewis, P.W., 2016. Histone H3K36 mutations promote sarcomagenesis through altered histone methylation landscape. Science 352, 844–849. https://doi.org/10.1126/science.aac7272
Lu, J., Li, F., Murphy, C.S., Davidson, M.W., Gilbert, D.M., 2010. G2 phase chromatin lacks determinants of replication timing. J. Cell Biol. 189, 967–980. https://doi.org/10.1083/jcb.201002002
Lucas, I.A., Raghuraman, M.K., 2003. The Dynamics of Chromosome Replication in Yeast, in: Current Topics in Developmental Biology. Academic Press, pp. 1–73. https://doi.org/10.1016/S0070-2153(03)01001-9
Luger, K., Mäder, A.W., Richmond, R.K., Sargent, D.F., Richmond, T.J., 1997. Crystal structure of the nucleosome core particle at 2.8 Å resolution. Nature 389, 251–260. https://doi.org/10.1038/38444
Luijsterburg, M.S., de Krijger, I., Wiegant, W.W., Shah, R.G., Smeenk, G., de Groot, A.J.L., Pines, A., Vertegaal, A.C.O., Jacobs, J.J.L., Shah, G.M., van Attikum, H., 2016. PARP1 Links CHD2-Mediated Chromatin Expansion and H3.3 Deposition to DNA Repair by Non-homologous End-Joining. Mol. Cell 61, 547–562. https://doi.org/10.1016/j.molcel.2016.01.019
Luperchio, T., Sauria, M., Hoskins, V., Wong, X., DeBoy, E., Gaillard, M.-C., Tsang, P., Pekrun, K., Ach, R., Yamada, N., Taylor, J., Reddy, K., 2018. The repressive genome compartment is established early in the cell cycle before forming the lamina associated domains (preprint). Genomics. https://doi.org/10.1101/481598

Lupiáñez, D.G., Kraft, K., Heinrich, V., Krawitz, P., Brancati, F., Klopocki, E., Horn, D., Kayserili, H., Opitz, J.M., Laxova, R., Santos-Simarro, F., Gilbert-Dussardier, B., Wittler, L., Borschiwer, M., Haas, S.A., Osterwalder, M., Franke, M., Timmermann, B., Hecht, J., Spielmann, M., Visel, A., Mundlos, S., 2015. Disruptions of Topological Chromatin Domains Cause Pathogenic Rewiring of Gene-Enhancer Interactions. Cell 161, 1012–1025. https://doi.org/10.1016/j.cell.2015.04.004
Luppino, J.M., Park, D.S., Nguyen, S.C., Lan, Y., Xu, Z., Yunker, R., Joyce, E.F., 2020. Cohesin promotes stochastic domain intermingling to ensure proper regulation of boundary-proximal genes. Nat. Genet. https://doi.org/10.1038/s41588-020-0647-9
Lusser, A., Urwin, D.L., Kadonaga, J.T., 2005. Distinct activities of CHD1 and ACF in ATP-dependent chromatin assembly. Nat. Struct. Mol. Biol. 12, 160–166. https://doi.org/10.1038/nsmb884
Ma, B., Trieu, T.-J., Cheng, J., Zhou, S., Tang, Q., Xie, J., Liu, J.-L., Zhao, K., Habib, S.J., Chen, X., 2020. Differential Histone Distribution Patterns in Induced Asymmetrically Dividing Mouse Embryonic Stem Cells. Cell Rep. 32, 108003. https://doi.org/10.1016/j.celrep.2020.108003
Ma, H., Samarabandu, J., Devdhar, R.S., Acharya, R., Cheng, P., Meng, C., Berezney, R., 1998. Spatial and Temporal Dynamics of DNA Replication Sites in Mammalian Cells. J. Cell Biol. 143, 1415–1425. https://doi.org/10.1083/jcb.143.6.1415
MacAlpine, D.M., Rodríguez, H.K., Bell, S.P., 2004. Coordination of replication and transcription along a *Drosophila* chromosome. Genes Dev. 18, 3094–3105. https://doi.org/10.1101/gad.1246404
MacAlpine, H.K., Gordân, R., Powell, S.K., Hartemink, A.J., MacAlpine, D.M., 2010. Drosophila ORC localizes to open chromatin and marks sites of cohesin complex loading. Genome Res. 20, 201–211. https://doi.org/10.1101/gr.097873.109
Mach, P., Kos, P.I., Zhan, Y., Cramard, J., Gaudin, S., Tünnermann, J., Marchi, E., Eglinger, J., Zuin, J., Kryzhanovska, M., Smallwood, S., Gelman, L., Roth, G., Nora, E.P., Tiana, G., Giorgetti, L., 2022. Cohesin and CTCF control the dynamics of chromosome folding. Nat. Genet. https://doi.org/10.1038/s41588-022-01232-7
Machida, S., Takizawa, Y., Ishimaru, M., Sugita, Y., Sekine, S., Nakayama, J., Wolf, M., Kurumizaka, H., 2018. Structural Basis of Heterochromatin Formation by Human HP1. Mol. Cell 69, 385-397.e8. https://doi.org/10.1016/j.molcel.2017.12.011
Madamba, E.V., Berthet, E.B., Francis, N.J., 2017. Inheritance of Histones H3 and H4 during DNA Replication In Vitro. Cell Rep. 21, 1361–1374. https://doi.org/10.1016/j.celrep.2017.10.033
Maehara, K., Harada, A., Sato, Y., Matsumoto, M., Nakayama, K.I., Kimura, H., Ohkawa, Y., 2015. Tissue-specific expression of histone H3 variants diversified after species separation. Epigenetics Chromatin 8, 35. https://doi.org/10.1186/s13072-015-0027-3
Maehara, K., Takahashi, K., Saitoh, S., 2010. CENP-A Reduction Induces a p53-Dependent Cellular Senescence Response To Protect Cells from Executing Defective Mitoses. Mol. Cell. Biol. 30, 2090–2104. https://doi.org/10.1128/MCB.01318-09
Magaña-Acosta, M., Valadez-Graham, V., 2020. Chromatin Remodelers in the 3D Nuclear Compartment. Front. Genet. 11, 600615. https://doi.org/10.3389/fgene.2020.600615
Maharana, S., Iyer, K.V., Jain, N., Nagarajan, M., Wang, Y., Shivashankar, G.V., 2016. Chromosome intermingling—the physical basis of chromosome organization in differentiated cells. Nucleic Acids Res. 44, 5148–5160. https://doi.org/10.1093/nar/gkw131
Mahy, N.L., Perry, P.E., Bickmore, W.A., 2002. Gene density and transcription influence the localization of chromatin outside of chromosome territories detectable by FISH. J. Cell Biol. 159, 753–763. https://doi.org/10.1083/jcb.200207115
Maine, G.T., Sinha, P., Tye, B.-K., 1984. Mutants of S. cerevisiae defective in the maintenance of minichromosomes.
Maiti, A., Drohat, A.C., 2011. Thymine DNA Glycosylase Can Rapidly Excise 5-Formylcytosine and 5-Carboxylcytosine: POTENTIAL IMPLICATIONS FOR ACTIVE DEMETHYLATION OF CpG SITES *. J. Biol. Chem. 286, 35334–35338. https://doi.org/10.1074/jbc.C111.284620
Malik, H.S., Henikoff, S., 2009. Major Evolutionary Transitions in Centromere Complexity. Cell 138, 1067–1082. https://doi.org/10.1016/j.cell.2009.08.036
Mantiero, D., Mackenzie, A., Donaldson, A., Zegerman, P., 2011. Limiting replication initiation factors execute the temporal programme of origin firing in budding yeast: Limiting replication factors execute temporal programme. EMBO J. 30, 4805–4814. https://doi.org/10.1038/emboj.2011.404
Marahrens, Y., Stillman, B., 1992. A Yeast Chromosomal Origin of DNA Replication Defined by Multiple Functional Elements. Science 255, 817–823. https://doi.org/10.1126/science.1536007
Marchal, C., Sima, J., Gilbert, D.M., 2019. Control of DNA replication timing in the 3D genome. Nat. Rev. Mol. Cell Biol. https://doi.org/10.1038/s41580-019-0162-y
Margulies, M., Egholm, M., Altman, W.E., Attiya, S., Bader, J.S., Bemben, L.A., Berka, J., Braverman, M.S., Chen, Y.-J., Chen, Z., Dewell, S.B., Du, L., Fierro, J.M., Gomes, X.V., Godwin, B.C., He, W., Helgesen, S., Ho, C.H., Irzyk, G.P., Jando, S.C., Alenquer, M.L.I., Jarvie, T.P., Jirage, K.B., Kim, J.-B., Knight, J.R., Lanza, J.R.,

Leamon, J.H., Lefkowitz, S.M., Lei, M., Li, J., Lohman, K.L., Lu, H., Makhijani, V.B., McDade, K.E., McKenna, M.P., Myers, E.W., Nickerson, E., Nobile, J.R., Plant, R., Puc, B.P., Ronan, M.T., Roth, G.T., Sarkis, G.J., Simons, J.F., Simpson, J.W., Srinivasan, M., Tartaro, K.R., Tomasz, A., Vogt, K.A., Volkmer, G.A., Wang, S.H., Wang, Y., Weiner, M.P., Yu, P., Begley, R.F., Rothberg, J.M., 2005. Genome sequencing in microfabricated high-density picolitre reactors. Nature 437, 376–380. https://doi.org/10.1038/nature03959

Marheineke, K., Hyrien, O., 2004. Control of Replication Origin Density and Firing Time in Xenopus Egg Extracts. J. Biol. Chem. 279, 28071–28081. https://doi.org/10.1074/jbc.M401574200

Martin, M.M., Ryan, M., Kim, R., Zakas, A.L., Fu, H., Lin, C.M., Reinhold, W.C., Davis, S.R., Bilke, S., Liu, H., Doroshow, J.H., Reimers, M.A., Valenzuela, M.S., Pommier, Y., Meltzer, P.S., Aladjem, M.I., 2011. Genome-wide depletion of replication initiation events in highly transcribed regions. Genome Res. 21, 1822–1832. https://doi.org/10.1101/gr.124644.111

Martini, E., Roche, D.M.J., Marheineke, K., Verreault, A., Almouzni, G., 1998. Recruitment of Phosphorylated Chromatin Assembly Factor 1 to Chromatin after UV Irradiation of Human Cells. J. Cell Biol. 143, 563–575. https://doi.org/10.1083/jcb.143.3.563

Martire, S., Banaszynski, L.A., 2020. The roles of histone variants in fine-tuning chromatin organization and function. Nat. Rev. Mol. Cell Biol. https://doi.org/10.1038/s41580-020-0262-8

Martire, S., Gogate, A.A., Whitmill, A., Tafessu, A., Nguyen, J., Teng, Y.-C., Tastemel, M., Banaszynski, L.A., 2019. Phosphorylation of histone H3.3 at serine 31 promotes p300 activity and enhancer acetylation. Nat. Genet. 51, 941–946. https://doi.org/10.1038/s41588-019-0428-5

Mas, G., Blanco, E., Ballaré, C., Sansó, M., Spill, Y.G., Hu, D., Aoi, Y., Le Dily, F., Shilatifard, A., Marti-Renom, M.A., Di Croce, L., 2018. Promoter bivalency favors an open chromatin architecture in embryonic stem cells. Nat. Genet. 50, 1452–1462. https://doi.org/10.1038/s41588-018-0218-5

Masai, H., Matsumoto, S., You, Z., Yoshizawa-Sugata, N., Oda, M., 2010. Eukaryotic Chromosome DNA Replication: Where, When, and How? Annu. Rev. Biochem. 79, 89–130. https://doi.org/10.1146/annurev.biochem.052308.103205

Mateo, L.J., Murphy, S.E., Hafner, A., Cinquini, I.S., Walker, C.A., Boettiger, A.N., 2019. Visualizing DNA folding and RNA in embryos at single-cell resolution. Nature 568, 49–54. https://doi.org/10.1038/s41586-019-1035-4

Mattarocci, S., Hafner, L., Lezaja, A., Shyian, M., Shore, D., 2016. Rif1: A Conserved Regulator of DNA Replication and Repair Hijacked by Telomeres in Yeasts. Front. Genet. 7. https://doi.org/10.3389/fgene.2016.00045

Maze, I., Wenderski, W., Noh, K.-M., Bagot, R.C., Tzavaras, N., Purushothaman, I., Elsässer, S.J., Guo, Y., Ionete, C., Hurd, Y.L., Tamminga, C.A., Halene, T., Farrelly, L., Soshnev, A.A., Wen, D., Rafii, S., Birtwistle, M.R., Akbarian, S., Buchholz, B.A., Blitzer, R.D., Nestler, E.J., Yuan, Z.-F., Garcia, B.A., Shen, L., Molina, H., Allis, C.D., 2015. Critical Role of Histone Turnover in Neuronal Transcription and Plasticity. Neuron 87, 77–94. https://doi.org/10.1016/j.neuron.2015.06.014

McCarthy, R.L., Zhang, J., Zaret, K.S., 2023. Diverse heterochromatin states restricting cell identity and reprogramming. Trends Biochem. Sci. 48, 513–526. https://doi.org/10.1016/j.tibs.2023.02.007

McKeon, C., Ohkubo, H., Pastan, I., Crombrugghe, B. de, 1982. Unusual methylation pattern of the α2(I) collagen gene. Cell 29, 203–210. https://doi.org/10.1016/0092-8674(82)90104-0

McSwiggen, Hansen, A.S., Teves, S.S., Marie-Nelly, H., Hao, Y., Heckert, A.B., Umemoto, K.K., Dugast-Darzacq, C., Tjian, R., Darzacq, X., 2019a. Evidence for DNA-mediated nuclear compartmentalization distinct from phase separation. eLife 8, e47098. https://doi.org/10.7554/eLife.47098

McSwiggen, Mir, M., Darzacq, X., Tjian, R., 2019b. Evaluating phase separation in live cells: diagnosis, caveats, and functional consequences. Genes Dev. genesdev;gad.331520.119v1. https://doi.org/10.1101/gad.331520.119

Meers, M.P., Llagas, G., Janssens, D.H., Codomo, C.A., Henikoff, S., 2023. Multifactorial profiling of epigenetic landscapes at single-cell resolution using MulTI-Tag. Nat Biotechnol 41, 708–716. https://doi.org/10.1038/s41587-022-01522-9

Mei, L., Kedziora, K.M., Song, E.-A., Purvis, J.E., Cook, J.G., 2022. The consequences of differential origin licensing dynamics in distinct chromatin environments. Nucleic Acids Res. 50, 9601–9620. https://doi.org/10.1093/nar/gkac003

Mejlvang, J., Feng, Y., Alabert, C., Neelsen, K.J., Jasencakova, Z., Zhao, X., Lees, M., Sandelin, A., Pasero, P., Lopes, M., Groth, A., 2014. New histone supply regulates replication fork speed and PCNA unloading. J. Cell Biol. 204, 29–43. https://doi.org/10.1083/jcb.201305017

Mendiratta, S., Gatto, A., Almouzni, G., 2019. Histone supply: Multitiered regulation ensures chromatin dynamics throughout the cell cycle. J. Cell Biol. 218, 39–54. https://doi.org/10.1083/jcb.201807179

Mendiratta, S., Ray-Gallet, D., Gatto, A., Lemaire, S., Kerlin, M.A., Coulon, A., Almouzni, G., 2022. Regulation of replicative histone RNA metabolism by the histone chaperone ASF1 (preprint). Molecular Biology. https://doi.org/10.1101/2022.11.30.518476

Meshorer, E., Yellajoshula, D., George, E., Scambler, P.J., Brown, D.T., Misteli, T., 2006. Hyperdynamic Plasticity of Chromatin Proteins in Pluripotent Embryonic Stem Cells. Dev. Cell 10, 105–116. https://doi.org/10.1016/j.devcel.2005.10.017
Michalet, X., Ekong, R., Fougerousse, F., Rousseaux, S., Schurra, C., Hornigold, N., Slegtenhorst, M. van, Wolfe, J., Povey, S., Beckmann, J.S., Bensimon, A., 1997. Dynamic Molecular Combing: Stretching the Whole Human Genome for High-Resolution Studies. Science 277, 1518–1523. https://doi.org/10.1126/science.277.5331.1518
Michod, D., Bartesaghi, S., Khelifi, A., Bellodi, C., Berliocchi, L., Nicotera, P., Salomoni, P., 2012. Calcium-Dependent Dephosphorylation of the Histone Chaperone DAXX Regulates H3.3 Loading and Transcription upon Neuronal Activation. Neuron 74, 122–135. https://doi.org/10.1016/j.neuron.2012.02.021
Miescher, F., 1871. Hoppe-Seyler's Med. Chem Unters 502.
Mifsud, B., Tavares-Cadete, F., Young, A.N., Sugar, R., Schoenfelder, S., Ferreira, L., Wingett, S.W., Andrews, S., Grey, W., Ewels, P.A., Herman, B., Happe, S., Higgs, A., LeProust, E., Follows, G.A., Fraser, P., Luscombe, N.M., Osborne, C.S., 2015. Mapping long-range promoter contacts in human cells with high-resolution capture Hi-C. Nat. Genet. 47, 598–606. https://doi.org/10.1038/ng.3286
Mikkelsen, T.S., Ku, M., Jaffe, D.B., Issac, B., Lieberman, E., Giannoukos, G., Alvarez, P., Brockman, W., Kim, T.-K., Koche, R.P., Lee, W., Mendenhall, E., O'Donovan, A., Presser, A., Russ, C., Xie, X., Meissner, A., Wernig, M., Jaenisch, R., Nusbaum, C., Lander, E.S., Bernstein, B.E., 2007. Genome-wide maps of chromatin state in pluripotent and lineage-committed cells. Nature 448, 553–560. https://doi.org/10.1038/nature06008
Millán-Ariño, L., Izquierdo-Bouldstridge, A., Jordan, A., 2016. Specificities and genomic distribution of somatic mammalian histone H1 subtypes. Biochim. Biophys. Acta BBA - Gene Regul. Mech. 1859, 510–519. https://doi.org/10.1016/j.bbagrm.2015.10.013
Millán-Zambrano, G., Burton, A., Bannister, A.J., Schneider, R., 2022. Histone post-translational modifications — cause and consequence of genome function. Nat. Rev. Genet. 23, 563–580. https://doi.org/10.1038/s41576-022-00468-7
Miotto, B., Ji, Z., Struhl, K., 2016. Selectivity of ORC binding sites and the relation to replication timing, fragile sites, and deletions in cancers. Proc. Natl. Acad. Sci. 113. https://doi.org/10.1073/pnas.1609060113
Miotto, B., Struhl, K., 2010. HBO1 Histone Acetylase Activity Is Essential for DNA Replication Licensing and Inhibited by Geminin. Mol. Cell 37, 57–66. https://doi.org/10.1016/j.molcel.2009.12.012
Miotto, B., Struhl, K., 2008. HBO1 histone acetylase is a coactivator of the replication licensing factor Cdt1. Genes Dev. 22, 2633–2638. https://doi.org/10.1101/gad.1674108
Mitchener, M.M., Muir, T.W., 2022. Oncohistones: Exposing the nuances and vulnerabilities of epigenetic regulation. Mol. Cell 82, 2925–2938. https://doi.org/10.1016/j.molcel.2022.07.008
Mito, Y., Henikoff, J.G., Henikoff, S., 2005. Genome-scale profiling of histone H3.3 replacement patterns. Nat. Genet. 37, 1090–1097. https://doi.org/10.1038/ng1637
Mitter, M., Gasser, C., Takacs, Z., Langer, C.C.H., Tang, W., Jessberger, G., Beales, C.T., Neuner, E., Ameres, S.L., Peters, J.-M., Goloborodko, A., Micura, R., Gerlich, D.W., 2020. Conformation of sister chromatids in the replicated human genome. Nature 586, 139–144. https://doi.org/10.1038/s41586-020-2744-4
Miura, H., Takahashi, S., Poonperm, R., Tanigawa, A., Takebayashi, S., Hiratani, I., 2019. Single-cell DNA replication profiling identifies spatiotemporal developmental dynamics of chromosome organization. Nat. Genet. 51, 1356–1368. https://doi.org/10.1038/s41588-019-0474-z
Moggs, J.G., Grandi, P., Quivy, J.-P., Jónsson, Z.O., Hübscher, U., Becker, P.B., Almouzni, G., 2000. A CAF-1–PCNA-Mediated Chromatin Assembly Pathway Triggered by Sensing DNA Damage. Mol. Cell. Biol. 20, 1206–1218. https://doi.org/10.1128/MCB.20.4.1206-1218.2000
Monk, M., Boubelik, M., Lehnert, S., 1987. Temporal and regional changes in DNA methylation in the embryonic, extraembryonic and germ cell lineages during mouse embryo development. Development 99, 371–382. https://doi.org/10.1242/dev.99.3.371
Monneron, A., Bernhard, W., 1969. Fine structural organization of the interphase nucleus in some mammalian cells. J. Ultrastruct. Res. 27, 266–288. https://doi.org/10.1016/S0022-5320(69)80017-1
Montavon, T., Soshnikova, N., Mascrez, B., Joye, E., Thevenet, L., Splinter, E., de Laat, W., Spitz, F., Duboule, D., 2011. A Regulatory Archipelago Controls Hox Genes Transcription in Digits. Cell 147, 1132–1145. https://doi.org/10.1016/j.cell.2011.10.023
Montellier, E., Boussouar, F., Rousseaux, S., Zhang, K., Buchou, T., Fenaille, F., Shiota, H., Debernardi, A., Héry, P., Curtet, S., Jamshidikia, M., Barral, S., Holota, H., Bergon, A., Lopez, F., Guardiola, P., Pernet, K., Imbert, J., Petosa, C., Tan, M., Zhao, Y., Gérard, M., Khochbin, S., 2013. Chromatin-to-nucleoprotamine transition is controlled by the histone H2B variant TH2B. Genes Dev. 27, 1680–1692. https://doi.org/10.1101/gad.220095.113
Morey, C., Da Silva, N.R., Perry, P., Bickmore, W.A., 2007. Nuclear reorganisation and chromatin decondensation are conserved, but distinct, mechanisms linked to Hox gene activation. Development 134, 909–919. https://doi.org/10.1242/dev.02779
Morgan, T.H., 1910. Chromosomes and Heredity. Am. Nat. 44, 449–496.

Morozov, V.M., Riva, A., Sarwar, S., Kim, W., Li, J., Zhou, L., Licht, J.D., Daaka, Y., Ishov, A.M., 2023. HIRA-mediated loading of histone variant H3.3 controls androgen-induced transcription by regulation of AR/BRD4 complex assembly at enhancers (preprint). Molecular Biology. https://doi.org/10.1101/2023.05.08.536256
Mousson, F., Lautrette, A., Thuret, J.-Y., Agez, M., Courbeyrette, R., Amigues, B., Becker, E., Neumann, J.-M., Guerois, R., Mann, C., Ochsenbein, F., 2005. Structural basis for the interaction of Asf1 with histone H3 and its functional implications. Proc. Natl. Acad. Sci. 102, 5975–5980. https://doi.org/10.1073/pnas.0500149102
Mukherjee, C., Tripathi, V., Manolika, E.M., Heijink, A.M., Ricci, G., Merzouk, S., De Boer, H.R., Demmers, J., Van Vugt, M.A.T.M., Ray Chaudhuri, A., 2019. RIF1 promotes replication fork protection and efficient restart to maintain genome stability. Nat. Commun. 10, 3287. https://doi.org/10.1038/s41467-019-11246-1
Müller, S., Almouzni, G., 2017. Chromatin dynamics during the cell cycle at centromeres. Nat. Rev. Genet. 18, 192–208. https://doi.org/10.1038/nrg.2016.157
Müller, S., Montes de Oca, R., Lacoste, N., Dingli, F., Loew, D., Almouzni, G., 2014. Phosphorylation and DNA Binding of HJURP Determine Its Centromeric Recruitment and Function in CenH3CENP-A Loading. Cell Rep. 8, 190–203. https://doi.org/10.1016/j.celrep.2014.06.002
Murat, P., Perez, C., Crisp, A., van Eijk, P., Reed, S.H., Guilbaud, G., Sale, J.E., 2022. DNA replication initiation shapes the mutational landscape and expression of the human genome. Sci. Adv. 8, eadd3686. https://doi.org/10.1126/sciadv.add3686
Nagano, T., Lubling, Y., Stevens, T.J., Schoenfelder, S., Yaffe, E., Dean, W., Laue, E.D., Tanay, A., Fraser, P., 2013. Single-cell Hi-C reveals cell-to-cell variability in chromosome structure. Nature 502, 59–64. https://doi.org/10.1038/nature12593
Nagano, T., Lubling, Y., Várnai, C., Dudley, C., Leung, W., Baran, Y., Mendelson Cohen, N., Wingett, S., Fraser, P., Tanay, A., 2017. Cell-cycle dynamics of chromosomal organization at single-cell resolution. Nature 547, 61–67. https://doi.org/10.1038/nature23001
Nagarajan, P., Ge, Z., Sirbu, B., Doughty, C., Agudelo Garcia, P.A., Schlederer, M., Annunziato, A.T., Cortez, D., Kenner, L., Parthun, M.R., 2013. Histone Acetyl Transferase 1 Is Essential for Mammalian Development, Genome Stability, and the Processing of Newly Synthesized Histones H3 and H4. PLoS Genet. 9, e1003518. https://doi.org/10.1371/journal.pgen.1003518
Nakamura, H., Morita, T., Sato, C., 1986. Structural organizations of replicon domains during DNA synthetic phase in the mammalian nucleus. Exp. Cell Res. 165, 291–297. https://doi.org/10.1016/0014-4827(86)90583-5
Nakamura, K., Saredi, G., Becker, J.R., Foster, B.M., Nguyen, N.V., Beyer, T.E., Cesa, L.C., Faull, P.A., Lukauskas, S., Frimurer, T., Chapman, J.R., Bartke, T., Groth, A., 2019. H4K20me0 recognition by BRCA1–BARD1 directs homologous recombination to sister chromatids. Nat. Cell Biol. 21, 311–318. https://doi.org/10.1038/s41556-019-0282-9
Nakatani, T., Lin, J., Ji, F., Ettinger, A., Pontabry, J., Tokoro, M., Altamirano-Pacheco, L., Fiorentino, J., Mahammadov, E., Hatano, Y., Van Rechem, C., Chakraborty, D., Ruiz-Morales, E.R., Arguello Pascualli, P.Y., Scialdone, A., Yamagata, K., Whetstine, J.R., Sadreyev, R.I., Torres-Padilla, M.-E., 2022. DNA replication fork speed underlies cell fate changes and promotes reprogramming. Nat. Genet. https://doi.org/10.1038/s41588-022-01023-0
Nakayasu, H., Berezney, R., 1989. Mapping replicational sites in the eucaryotic cell nucleus. J. Cell Biol. 108, 1–11. https://doi.org/10.1083/jcb.108.1.1
Nan, X., Hou, J., Maclean, A., Nasir, J., Lafuente, M.J., Shu, X., Kriaucionis, S., Bird, A., 2007. Interaction between chromatin proteins MECP2 and ATRX is disrupted by mutations that cause inherited mental retardation. Proc. Natl. Acad. Sci. 104, 2709–2714. https://doi.org/10.1073/pnas.0608056104
Nashun, B., Akiyama, T., Suzuki, M.G., Aoki, F., 2011. Dramatic replacement of histone variants during genome remodeling in nuclear-transferred embryos. Epigenetics 6, 1489–1497. https://doi.org/10.4161/epi.6.12.18206
Nashun, B., Hill, P.W.S., Smallwood, S.A., Dharmalingam, G., Amouroux, R., Clark, S.J., Sharma, V., Ndjetehe, E., Pelczar, P., Festenstein, R.J., Kelsey, G., Hajkova, P., 2015. Continuous Histone Replacement by Hira Is Essential for Normal Transcriptional Regulation and De Novo DNA Methylation during Mouse Oogenesis. Mol. Cell 60, 611–625. https://doi.org/10.1016/j.molcel.2015.10.010
Nasmyth, K., 2001. Disseminating the Genome: Joining, Resolving, and Separating Sister Chromatids During Mitosis and Meiosis. Annu. Rev. Genet. 35, 673–745. https://doi.org/10.1146/annurev.genet.35.102401.091334
Natsume, R., Eitoku, M., Akai, Y., Sano, N., Horikoshi, M., Senda, T., 2007. Structure and function of the histone chaperone CIA/ASF1 complexed with histones H3 and H4. Nature 446, 338–341. https://doi.org/10.1038/nature05613
Naumova, N., Imakaev, M., Fudenberg, G., Zhan, Y., Lajoie, B.R., Mirny, L.A., Dekker, J., 2013. Organization of the Mitotic Chromosome. Science 342, 948–953. https://doi.org/10.1126/science.1236083
Navarro, C., Lyu, J., Katsori, A.-M., Caridha, R., Elsässer, S.J., 2020. An embryonic stem cell-specific heterochromatin state promotes core histone exchange in the absence of DNA accessibility. Nat. Commun. 11, 5095. https://doi.org/10.1038/s41467-020-18863-1

Nechemia-Arbely, Y., Miga, K.H., Shoshani, O., Aslanian, A., McMahon, M.A., Lee, A.Y., Fachinetti, D., Yates, J.R., Ren, B., Cleveland, D.W., 2019. DNA replication acts as an error correction mechanism to maintain centromere identity by restricting CENP-A to centromeres. Nat. Cell Biol. 21, 743–754. https://doi.org/10.1038/s41556-019-0331-4
Nelson, D.M., Ye, X., Hall, C., Santos, H., Ma, T., Kao, G.D., Yen, T.J., Harper, J.W., Adams, P.D., 2002. Coupling of DNA Synthesis and Histone Synthesis in S Phase Independent of Cyclin/cdk2 Activity. Mol. Cell. Biol. 22, 7459–7472. https://doi.org/10.1128/MCB.22.21.7459-7472.2002
Németh, A., Conesa, A., Santoyo-Lopez, J., Medina, I., Montaner, D., Péterfia, B., Solovei, I., Cremer, T., Dopazo, J., Längst, G., 2010. Initial Genomics of the Human Nucleolus. PLOS Genet. 6, e1000889. https://doi.org/10.1371/journal.pgen.1000889
Ng, R.K., Gurdon, J.B., 2008. Epigenetic memory of an active gene state depends on histone H3.3 incorporation into chromatin in the absence of transcription. Nat. Cell Biol. 10, 102–109. https://doi.org/10.1038/ncb1674
Nguyen, H.Q., Chattoraj, S., Castillo, D., Nguyen, S.C., Nir, G., Lioutas, A., Hershberg, E.A., Martins, N.M.C., Reginato, P.L., Hannan, M., Beliveau, B.J., Church, G.M., Daugharthy, E.R., Marti-Renom, M.A., Wu, C. -ting, 2020. 3D mapping and accelerated super-resolution imaging of the human genome using in situ sequencing. Nat. Methods 17, 822–832. https://doi.org/10.1038/s41592-020-0890-0
Nicetto, D., Zaret, K.S., 2019. Role of H3K9me3 heterochromatin in cell identity establishment and maintenance. Curr. Opin. Genet. Dev. 55, 1–10. https://doi.org/10.1016/j.gde.2019.04.013
Nichols, M.H., Corces, V.G., 2021. Principles of 3D compartmentalization of the human genome. Cell Rep. 35, 109330. https://doi.org/10.1016/j.celrep.2021.109330
Nieduszynski, C.A., 2005. The requirement of yeast replication origins for pre-replication complex proteins is modulated by transcription. Nucleic Acids Res. 33, 2410–2420. https://doi.org/10.1093/nar/gki539
Nieduszynski, C.A., Knox, Y., Donaldson, A.D., 2006. Genome-wide identification of replication origins in yeast by comparative genomics. Genes Dev. 20, 1874–1879. https://doi.org/10.1101/gad.385306
Nir, G., Farabella, I., Pérez Estrada, C., Ebeling, C.G., Beliveau, B.J., Sasaki, H.M., Lee, S.D., Nguyen, S.C., McCole, R.B., Chattoraj, S., Erceg, J., AlHaj Abed, J., Martins, N.M.C., Nguyen, H.Q., Hannan, M.A., Russell, S., Durand, N.C., Rao, S.S.P., Kishi, J.Y., Soler-Vila, P., Di Pierro, M., Onuchic, J.N., Callahan, S.P., Schreiner, J.M., Stuckey, J.A., Yin, P., Aiden, E.L., Marti-Renom, M.A., Wu, C. -ting, 2018. Walking along chromosomes with super-resolution imaging, contact maps, and integrative modeling. PLOS Genet. 14, e1007872. https://doi.org/10.1371/journal.pgen.1007872
Nishiyama, A., Yamaguchi, L., Sharif, J., Johmura, Y., Kawamura, T., Nakanishi, K., Shimamura, S., Arita, K., Kodama, T., Ishikawa, F., Koseki, H., Nakanishi, M., 2013. Uhrf1-dependent H3K23 ubiquitylation couples maintenance DNA methylation and replication. Nature 502, 249–253. https://doi.org/10.1038/nature12488
Noll, M., Kornberg, R.D., 1977. Action of micrococcal nuclease on chromatin and the location of histone H1. J. Mol. Biol. 109, 393–404. https://doi.org/10.1016/S0022-2836(77)80019-3
Noordermeer, D., Branco, M.R., Splinter, E., Klous, P., IJcken, W. van, Swagemakers, S., Koutsourakis, M., Spek, P. van der, Pombo, A., Laat, W. de, 2008. Transcription and Chromatin Organization of a Housekeeping Gene Cluster Containing an Integrated β-Globin Locus Control Region. PLOS Genet. 4, e1000016. https://doi.org/10.1371/journal.pgen.1000016
Noordermeer, D., Leleu, M., Splinter, E., Rougemont, J., De Laat, W., Duboule, D., 2011. The Dynamic Architecture of Hox Gene Clusters. Science 334, 222–225. https://doi.org/10.1126/science.1207194
Nora, E.P., Goloborodko, A., Valton, A.-L., Gibcus, J.H., Uebersohn, A., Abdennur, N., Dekker, J., Mirny, L.A., Bruneau, B.G., 2017. Targeted Degradation of CTCF Decouples Local Insulation of Chromosome Domains from Genomic Compartmentalization. Cell 169, 930-944.e22. https://doi.org/10.1016/j.cell.2017.05.004
Nora, E.P., Lajoie, B.R., Schulz, E.G., Giorgetti, L., Okamoto, I., Servant, N., Piolot, T., van Berkum, N.L., Meisig, J., Sedat, J., Gribnau, J., Barillot, E., Blüthgen, N., Dekker, J., Heard, E., 2012. Spatial partitioning of the regulatory landscape of the X-inactivation centre. Nature 485, 381–385. https://doi.org/10.1038/nature11049
Nourani, A., Robert, F., Winston, F., 2006. Evidence that Spt2/Sin1, an HMG-Like Factor, Plays Roles in Transcription Elongation, Chromatin Structure, and Genome Stability in *Saccharomyces cerevisiae*. Mol. Cell. Biol. 26, 1496–1509. https://doi.org/10.1128/MCB.26.4.1496-1509.2006
Nuebler, J., Fudenberg, G., Imakaev, M., Abdennur, N., Mirny, L.A., 2018. Chromatin organization by an interplay of loop extrusion and compartmental segregation. Proc. Natl. Acad. Sci. 115, E6697–E6706. https://doi.org/10.1073/pnas.1717730115
Nye, J., Sturgill, D., Athwal, R., Dalal, Y., 2018. HJURP antagonizes CENP-A mislocalization driven by the H3.3 chaperones HIRA and DAXX. PLOS ONE 13, e0205948. https://doi.org/10.1371/journal.pone.0205948
Oegema, K., Desai, A., Rybina, S., Kirkham, M., Hyman, A.A., 2001. Functional Analysis of Kinetochore Assembly in Caenorhabditis elegans. J. Cell Biol. 153, 1209–1226. https://doi.org/10.1083/jcb.153.6.1209
Ogiyama, Y., Schuettengruber, B., Papadopoulos, G.L., Chang, J.-M., Cavalli, G., 2018. Polycomb-Dependent Chromatin Looping Contributes to Gene Silencing during Drosophila Development. Mol. Cell 71, 73-88.e5. https://doi.org/10.1016/j.molcel.2018.05.032

Okano, M., Bell, D.W., Haber, D.A., Li, E., 1999. DNA Methyltransferases Dnmt3a and Dnmt3b Are Essential for De Novo Methylation and Mammalian Development. Cell 99, 247–257. https://doi.org/10.1016/S0092-8674(00)81656-6
Okano, M., Xie, S., Li, E., 1998. Cloning and characterization of a family of novel mammalian DNA (cytosine-5) methyltransferases. Nat. Genet. 19, 219–220. https://doi.org/10.1038/890
Okuno, Y., 2001. Stability, chromatin association and functional activity of mammalian pre-replication complex proteins during the cell cycle. EMBO J. 20, 4263–4277. https://doi.org/10.1093/emboj/20.15.4263
Olins, A.L., Olins, D.E., 1974. Spheroid Chromatin Units (ν Bodies). Science 183, 330–332. https://doi.org/10.1126/science.183.4122.330
Olins, D.E., Olins, A.L., 2003. Chromatin history: our view from the bridge. Nat. Rev. Mol. Cell Biol. 4, 809–814. https://doi.org/10.1038/nrm1225
O'Neill, L., Turner, B., 2003. Immunoprecipitation of native chromatin: NChIP. Methods 31, 76–82. https://doi.org/10.1016/S1046-2023(03)00090-2
Ooi, S.K.T., Qiu, C., Bernstein, E., Li, K., Jia, D., Yang, Z., Erdjument-Bromage, H., Tempst, P., Lin, S.-P., Allis, C.D., Cheng, X., Bestor, T.H., 2007. DNMT3L connects unmethylated lysine 4 of histone H3 to de novo methylation of DNA. Nature 448, 714–717. https://doi.org/10.1038/nature05987
Oomen, M.E., Hansen, A.S., Liu, Y., Darzacq, X., Dekker, J., 2019. CTCF sites display cell cycle–dependent dynamics in factor binding and nucleosome positioning. Genome Res. 29, 236–249. https://doi.org/10.1101/gr.241547.118
Open 2C, Abdennur, N., Abraham, S., Fudenberg, G., Flyamer, I.M., Galitsyna, A.A., Goloborodko, A., Imakaev, M., Oksuz, B.A., Venev, S.V., 2022. Cooltools: enabling high-resolution Hi-C analysis in Python (preprint). Bioinformatics. https://doi.org/10.1101/2022.10.31.514564
Osakabe, A., Tachiwana, H., Takaku, M., Hori, T., Obuse, C., Kimura, H., Fukagawa, T., Kurumizaka, H., 2013. Vertebrate Spt2 is a novel nucleolar histone chaperone that assists in ribosomal DNA transcription. Journal of Cell Science 126, 1323–1332. https://doi.org/10.1242/jcs.112623
Osborne, C.S., Chakalova, L., Brown, K.E., Carter, D., Horton, A., Debrand, E., Goyenechea, B., Mitchell, J.A., Lopes, S., Reik, W., Fraser, P., 2004. Active genes dynamically colocalize to shared sites of ongoing transcription. Nat. Genet. 36, 1065–1071. https://doi.org/10.1038/ng1423
Ouasti, F., Audin, M., Freon, K., Quivy, J.-P., Tachekort, M., Cesard, E., Thureau, A., Ropars, V., Varela, P.F., Moal, G., Soumana-Amadou, I., Uryga, A., Legrand, P., Andreani, J., Guerois, R., Almouzni, G., Lambert, sarah A., Ochsenbein, F., 2023. Disordered regions and folded modules in CAF-1 promote histone deposition in S. pombe. https://doi.org/10.1101/2023.06.02.543505
Oudet, P., Gross-Bellard, M., Chambon, P., 1975. Electron microscopic and biochemical evidence that chromatin structure is a repeating unit. Cell 4, 281–300. https://doi.org/10.1016/0092-8674(75)90149-X
Owens, N., Papadopoulou, T., Festuccia, N., Tachtsidi, A., Gonzalez, I., Dubois, A., Vandormael-Pournin, S., Nora, E.P., Bruneau, B.G., Cohen-Tannoudji, M., Navarro, P., 2019. CTCF confers local nucleosome resiliency after DNA replication and during mitosis. eLife 8, e47898. https://doi.org/10.7554/eLife.47898
Ozeri-Galai, E., Tur-Sinai, M., Bester, A.C., Kerem, B., 2014. Interplay between genetic and epigenetic factors governs common fragile site instability in cancer. Cell. Mol. Life Sci. 71, 4495–4506. https://doi.org/10.1007/s00018-014-1719-8
Paixão, S., Colaluca, I.N., Cubells, M., Peverali, F.A., Destro, A., Giadrossi, S., Giacca, M., Falaschi, A., Riva, S., Biamonti, G., 2004. Modular Structure of the Human Lamin B2 Replicator. Mol. Cell. Biol. 24, 2958–2967. https://doi.org/10.1128/MCB.24.7.2958-2967.2004
Pak, D.T.S., Pflumm, M., Chesnokov, I., Huang, D.W., Kellum, R., Marr, J., Romanowski, P., Botchan, M.R., 1997. Association of the Origin Recognition Complex with Heterochromatin and HP1 in Higher Eukaryotes. Cell 91, 311–323. https://doi.org/10.1016/S0092-8674(00)80415-8
Paliou, C., Guckelberger, P., Schöpflin, R., Heinrich, V., Esposito, A., Chiariello, A.M., Bianco, S., Annunziatella, C., Helmuth, J., Haas, S., Jerković, I., Brieske, N., Wittler, L., Timmermann, B., Nicodemi, M., Vingron, M., Mundlos, S., Andrey, G., 2019. Preformed chromatin topology assists transcriptional robustness of Shh during limb development. Proc. Natl. Acad. Sci. 116, 12390–12399. https://doi.org/10.1073/pnas.1900672116
Palmer, D., O'Day, K., Wener, M., Andrews, B., Margolis, R., 1987. A 17-kD centromere protein (CENP-A) copurifies with nucleosome core particles and with histones. J. Cell Biol. 104, 805–815. https://doi.org/10.1083/jcb.104.4.805
Palmer, D.K., O'Day, K., Trong, H.L., Charbonneau, H., Margolis, R.L., 1991. Purification of the centromere-specific protein CENP-A and demonstration that it is a distinctive histone. Proc. Natl. Acad. Sci. 88, 3734–3738. https://doi.org/10.1073/pnas.88.9.3734
Palmer, N., Kaldis, P., 2016. Chapter One - Regulation of the Embryonic Cell Cycle During Mammalian Preimplantation Development, in: DePamphilis, M.L. (Ed.), Current Topics in Developmental Biology, Mammalian Preimplantation Development. Academic Press, pp. 1–53. https://doi.org/10.1016/bs.ctdb.2016.05.001

Palzkill, T.G., Newlon, C.S., 1988. A yeast replication origin consists of multiple copies of a small conserved sequence. Cell 53, 441–450. https://doi.org/10.1016/0092-8674(88)90164-X
Panchenko, T., Sorensen, T.C., Woodcock, C.L., Kan, Z., Wood, S., Resch, M.G., Luger, K., Englander, S.W., Hansen, J.C., Black, B.E., 2011. Replacement of histone H3 with CENP-A directs global nucleosome array condensation and loosening of nucleosome superhelical termini. Proc. Natl. Acad. Sci. 108, 16588–16593. https://doi.org/10.1073/pnas.1113621108
Pang, M.Y.H., Sun, X., Ausió, J., Ishibashi, T., 2020. Histone H4 variant, H4G, drives ribosomal RNA transcription and breast cancer cell proliferation by loosening nucleolar chromatin structure. J. Cell. Physiol. 235, 9601–9608. https://doi.org/10.1002/jcp.29770
Pardue, M.L., Gall, J.G., 1969. Molecular hybridization of radioactive dna to the dna of cytological preparations. Proc. Natl. Acad. Sci. 64, 600–604. https://doi.org/10.1073/pnas.64.2.600
Pasero, P., Bensimon, A., Schwob, E., 2002. Single-molecule analysis reveals clustering and epigenetic regulation of replication origins at the yeast rDNA locus. Genes Dev. 16, 2479–2484. https://doi.org/10.1101/gad.232902
Passarge, E., 1979. Emil Heitz and the Concept of Heterochromatin: Longitudinal Chromosome Differentiation was Recognized Fifty Years Ago.
Pchelintsev, N.A., McBryan, T., Rai, T.S., van Tuyn, J., Ray-Gallet, D., Almouzni, G., Adams, P.D., 2013. Placing the HIRA Histone Chaperone Complex in the Chromatin Landscape. Cell Rep. 3, 1012–1019. https://doi.org/10.1016/j.celrep.2013.03.026
Pease, A.C., Solas, D., Sullivan, E.J., Cronin, M.T., Holmes, C.P., Fodor, S.P., 1994. Light-generated oligonucleotide arrays for rapid DNA sequence analysis. Proc. Natl. Acad. Sci. 91, 5022–5026. https://doi.org/10.1073/pnas.91.11.5022
Pelc, S.R., Howard, A., 1956. Metabolic activity of salivary gland chromosomes in Diptera. Exp. Cell Res. 10, 549–552. https://doi.org/10.1016/0014-4827(56)90029-5
Pelham-Webb, B., Polyzos, A., Wojenski, L., Kloetgen, A., Li, J., Di Giammartino, D.C., Sakellaropoulos, T., Tsirigos, A., Core, L., Apostolou, E., 2021. H3K27ac bookmarking promotes rapid post-mitotic activation of the pluripotent stem cell program without impacting 3D chromatin reorganization. Mol. Cell 81, 1732-1748.e8. https://doi.org/10.1016/j.molcel.2021.02.032
Pellegrino, S., Michelena, J., Teloni, F., Imhof, R., Altmeyer, M., 2017. Replication-Coupled Dilution of H4K20me2 Guides 53BP1 to Pre-replicative Chromatin. Cell Rep. 19, 1819–1831. https://doi.org/10.1016/j.celrep.2017.05.016
Pelling, C., 1964. Ribonukleinsäure-Synthese der Riesenchromosomen. Chromosoma 15, 71–122. https://doi.org/10.1007/BF00326915
Pérez-Montero, S., Carbonell, A., Azorín, F., 2016. Germline-specific H1 variants: the “sexy” linker histones. Chromosoma 125, 1–13. https://doi.org/10.1007/s00412-015-0517-x
Peters, A.H.F.M., Kubicek, S., Mechtler, K., O’Sullivan, R.J., Derijck, A.A.H.A., Perez-Burgos, L., Kohlmaier, A., Opravil, S., Tachibana, M., Shinkai, Y., Martens, J.H.A., Jenuwein, T., 2003. Partitioning and Plasticity of Repressive Histone Methylation States in Mammalian Chromatin. Mol. Cell 12, 1577–1589. https://doi.org/10.1016/S1097-2765(03)00477-5
Peters, A.H.F.M., O’Carroll, D., Scherthan, H., Mechtler, K., Sauer, S., Schöfer, C., Weipoltshammer, K., Pagani, M., Lachner, M., Kohlmaier, A., Opravil, S., Doyle, M., Sibilia, M., Jenuwein, T., 2001. Loss of the Suv39h Histone Methyltransferases Impairs Mammalian Heterochromatin and Genome Stability. Cell 107, 323–337. https://doi.org/10.1016/S0092-8674(01)00542-6
Peters, J.-M., Nishiyama, T., 2012. Sister Chromatid Cohesion. Cold Spring Harb. Perspect. Biol. 4, a011130–a011130. https://doi.org/10.1101/cshperspect.a011130
Petryk, N., Dalby, M., Wenger, A., Stromme, C.B., Strandsby, A., Andersson, R., Groth, A., 2018. MCM2 promotes symmetric inheritance of modified histones during DNA replication. Science 361, 1389–1392. https://doi.org/10.1126/science.aau0294
Petryk, N., Kahli, M., d’Aubenton-Carafa, Y., Jaszczyszyn, Y., Shen, Y., Silvain, M., Thermes, C., Chen, C.-L., Hyrien, O., 2016. Replication landscape of the human genome. Nat. Commun. 7, 10208. https://doi.org/10.1038/ncomms10208
Peycheva, M., Neumann, T., Malzl, D., Nazarova, M., Schoeberl, U., Pavri, R., 2021. DNA replication timing directly regulates the frequency of oncogenic chromosomal translocations (preprint). Molecular Biology. https://doi.org/10.1101/2021.05.29.446276
Phillips-Cremins, J.E., Sauria, M.E.G., Sanyal, A., Gerasimova, T.I., Lajoie, B.R., Bell, J.S.K., Ong, C.-T., Hookway, T.A., Guo, C., Sun, Y., Bland, M.J., Wagstaff, W., Dalton, S., McDevitt, T.C., Sen, R., Dekker, J., Taylor, J., Corces, V.G., 2013. Architectural Protein Subclasses Shape 3D Organization of Genomes during Lineage Commitment. Cell 153, 1281–1295. https://doi.org/10.1016/j.cell.2013.04.053
Picard, F., Cadoret, J.-C., Audit, B., Arneodo, A., Alberti, A., Battail, C., Duret, L., Prioleau, M.-N., 2014. The Spatiotemporal Program of DNA Replication Is Associated with Specific Combinations of Chromatin Marks in Human Cells. PLOS Genetics 10, e1004282. https://doi.org/10.1371/journal.pgen.1004282

Piña, B., Suau, P., 1987. Changes in histones H2A and H3 variant composition in differentiating and mature rat brain cortical neurons. Dev. Biol. 123, 51–58. https://doi.org/10.1016/0012-1606(87)90426-X
Piquet, S., Le Parc, F., Bai, S.-K., Chevallier, O., Adam, S., Polo, S.E., 2018. The Histone Chaperone FACT Coordinates H2A.X-Dependent Signaling and Repair of DNA Damage. Mol. Cell 72, 888-901.e7. https://doi.org/10.1016/j.molcel.2018.09.010
Plys, A.J., Davis, C.P., Kim, J., Rizki, G., Keenen, M.M., Marr, S.K., Kingston, R.E., 2019. Phase separation of Polycomb-repressive complex 1 is governed by a charged disordered region of CBX2. Genes Dev. 33, 799–813. https://doi.org/10.1101/gad.326488.119
Pokholok, D.K., Harbison, C.T., Levine, S., Cole, M., Hannett, N.M., Lee, T.I., Bell, G.W., Walker, K., Rolfe, P.A., Herbolsheimer, E., Zeitlinger, J., Lewitter, F., Gifford, D.K., Young, R.A., 2005. Genome-wide Map of Nucleosome Acetylation and Methylation in Yeast. Cell 122, 517–527. https://doi.org/10.1016/j.cell.2005.06.026
Poleshko, A., Smith, C.L., Nguyen, S.C., Sivaramakrishnan, P., Wong, K.G., Murray, J.I., Lakadamyali, M., Joyce, E.F., Jain, R., Epstein, J.A., 2019. H3K9me2 orchestrates inheritance of spatial positioning of peripheral heterochromatin through mitosis. eLife 8, e49278. https://doi.org/10.7554/eLife.49278
Polo, S.E., Roche, D., Almouzni, G., 2006. New Histone Incorporation Marks Sites of UV Repair in Human Cells. Cell 127, 481–493. https://doi.org/10.1016/j.cell.2006.08.049
Pope, B.D., Ryba, T., Dileep, V., Yue, F., Wu, W., Denas, O., Vera, D.L., Wang, Y., Hansen, R.S., Canfield, T.K., Thurman, R.E., Cheng, Y., Gülsoy, G., Dennis, J.H., Snyder, M.P., Stamatoyannopoulos, J.A., Taylor, J., Hardison, R.C., Kahveci, T., Ren, B., Gilbert, D.M., 2014. Topologically associating domains are stable units of replication-timing regulation. Nature 515, 402–405. https://doi.org/10.1038/nature13986
Pourkarimi, E., Bellush, J.M., Whitehouse, I., 2016. Spatiotemporal coupling and decoupling of gene transcription with DNA replication origins during embryogenesis in C. elegans. eLife 5, e21728. https://doi.org/10.7554/eLife.21728
Pradhan, B., Barth, R., Kim, E., Davidson, I.F., Bauer, B., van Laar, T., Yang, W., Ryu, J.-K., van der Torre, J., Peters, J.-M., Dekker, C., 2022a. SMC complexes can traverse physical roadblocks bigger than their ring size. Cell Rep. 41, 111491. https://doi.org/10.1016/j.celrep.2022.111491
Pradhan, B., Kanno, T., Igarashi, M.U., Baaske, M.D., Kei Wong, J.S., Jeppsson, K., Björkegren, C., Kim, E., 2022b. The Smc5/6 complex is a DNA loop extruding motor (preprint). Biophysics. https://doi.org/10.1101/2022.05.13.491800
Pradhan, S.K., Su, T., Yen, L., Jacquet, K., Huang, C., Côté, J., Kurdistani, S.K., Carey, M.F., 2016. EP400 Deposits H3.3 into Promoters and Enhancers during Gene Activation. Mol. Cell 61, 27–38. https://doi.org/10.1016/j.molcel.2015.10.039
Prendergast, L., Reinberg, D., 2021. The missing linker : emerging trends for H1 variant-specific functions. Genes Dev. 35, 40–58. https://doi.org/10.1101/gad.344531.120
Prioleau, M.-N., MacAlpine, D.M., 2016. DNA replication origins—where do we begin? Genes Dev. 30, 1683–1697. https://doi.org/10.1101/gad.285114.116
Probst, A.V., Dunleavy, E., Almouzni, G., 2009. Epigenetic inheritance during the cell cycle. Nat. Rev. Mol. Cell Biol. 10, 192–206. https://doi.org/10.1038/nrm2640
Prorok, P., Artufel, M., Aze, A., Coulombe, P., Peiffer, I., Lacroix, L., Guédin, A., Mergny, J.-L., Damaschke, J., Schepers, A., Cayrou, C., Teulade-Fichou, M.-P., Ballester, B., Méchali, M., 2019. Involvement of G-quadruplex regions in mammalian replication origin activity. Nat. Commun. 10, 3274. https://doi.org/10.1038/s41467-019-11104-0
Protacio, R.U., Li, G., Lowary, P.T., Widom, J., 2000. Effects of Histone Tail Domains on the Rate of Transcriptional Elongation through a Nucleosome. Mol. Cell. Biol. 20, 8866–8878. https://doi.org/10.1128/MCB.20.23.8866-8878.2000
Pueschel, R., Coraggio, F., Meister, P., 2016. From single genes to entire genomes: the search for a function of nuclear organization.
Quinodoz, S.A., Ollikainen, N., Tabak, B., Palla, A., Schmidt, J.M., Detmar, E., Lai, M.M., Shishkin, A.A., Bhat, P., Takei, Y., Trinh, V., Aznauryan, E., Russell, P., Cheng, C., Jovanovic, M., Chow, A., Cai, L., McDonel, P., Garber, M., Guttman, M., 2018. Higher-Order Inter-chromosomal Hubs Shape 3D Genome Organization in the Nucleus. Cell 174, 744-757.e24. https://doi.org/10.1016/j.cell.2018.05.024
Quivy, J.-P., 2001. Dimerization of the largest subunit of chromatin assembly factor 1: importance in vitro and during Xenopus early development. EMBO J. 20, 2015–2027. https://doi.org/10.1093/emboj/20.8.2015
Quivy, J.-P., Roche, D., Kirschner, D., Tagami, H., Nakatani, Y., Almouzni, G., 2004. A CAF-1 dependent pool of HP1 during heterochromatin duplication. EMBO J. 23, 3516–3526. https://doi.org/10.1038/sj.emboj.7600362
Rabl, C., 1885. Uber zellthilung 214–330.
Rada-Iglesias, A., Bajpai, R., Swigut, T., Brugmann, S.A., Flynn, R.A., Wysocka, J., 2011. A unique chromatin signature uncovers early developmental enhancers in humans. Nature 470, 279–283. https://doi.org/10.1038/nature09692

Radman-Livaja, M., Verzijlbergen, K.F., Weiner, A., Van Welsem, T., Friedman, N., Rando, O.J., Van Leeuwen, F., 2011. Patterns and Mechanisms of Ancestral Histone Protein Inheritance in Budding Yeast. PLoS Biol. 9, e1001075. https://doi.org/10.1371/journal.pbio.1001075
Ragazzini, R., Pérez-Palacios, R., Baymaz, I.H., Diop, S., Ancelin, K., Zielinski, D., Michaud, A., Givelet, M., Borsos, M., Aflaki, S., Legoix, P., Jansen, P.W.T.C., Servant, N., Torres-Padilla, M.-E., Bourc'his, D., Fouchet, P., Vermeulen, M., Margueron, R., 2019. EZHIP constrains Polycomb Repressive Complex 2 activity in germ cells. Nat. Commun. 10, 3858. https://doi.org/10.1038/s41467-019-11800-x
Rai, T.S., Puri, A., McBryan, T., Hoffman, J., Tang, Y., Pchelintsev, N.A., van Tuyn, J., Marmorstein, R., Schultz, D.C., Adams, P.D., 2011. Human CABIN1 Is a Functional Member of the Human HIRA/UBN1/ASF1a Histone H3.3 Chaperone Complex. Mol. Cell. Biol. 31, 4107–4118. https://doi.org/10.1128/MCB.05546-11
Ramachandran, S., Henikoff, S., 2016. Transcriptional Regulators Compete with Nucleosomes Post-replication. Cell 165, 580–592. https://doi.org/10.1016/j.cell.2016.02.062
Ramakrishnan, V., Finch, J.T., Graziano, V., Lee, P.L., Sweet, R.M., 1993. Crystal structure of globular domain of histone H5 and its implications for nucleosome binding. Nature 362, 219–223. https://doi.org/10.1038/362219a0
Raman, P., Rominger, M.C., Young, J.M., Molaro, A., Tsukiyama, T., Malik, H.S., 2022. Novel Classes and Evolutionary Turnover of Histone H2B Variants in the Mammalian Germline. Mol. Biol. Evol. 39, msac019. https://doi.org/10.1093/molbev/msac019
Ramírez, F., Bhardwaj, V., Arrigoni, L., Lam, K.C., Grüning, B.A., Villaveces, J., Habermann, B., Akhtar, A., Manke, T., 2018. High-resolution TADs reveal DNA sequences underlying genome organization in flies. Nat. Commun. 9, 189. https://doi.org/10.1038/s41467-017-02525-w
Rang, F.J., Kind, J., Guerreiro, I., 2023. The role of heterochromatin in 3D genome organization during preimplantation development. Cell Rep. 112248. https://doi.org/10.1016/j.celrep.2023.112248
Rangasamy, D., 2003. Pericentric heterochromatin becomes enriched with H2A.Z during early mammalian development. EMBO J. 22, 1599–1607. https://doi.org/10.1093/emboj/cdg160
Rangasamy, D., Greaves, I., Tremethick, D.J., 2004. RNA interference demonstrates a novel role for H2A.Z in chromosome segregation. Nat. Struct. Mol. Biol. 11, 650–655. https://doi.org/10.1038/nsmb786
Rao, S.S.P., Huang, S.-C., Glenn St Hilaire, B., Engreitz, J.M., Perez, E.M., Kieffer-Kwon, K.-R., Sanborn, A.L., Johnstone, S.E., Bascom, G.D., Bochkov, I.D., Huang, X., Shamim, M.S., Shin, J., Turner, D., Ye, Z., Omer, A.D., Robinson, J.T., Schlick, T., Bernstein, B.E., Casellas, R., Lander, E.S., Aiden, E.L., 2017. Cohesin Loss Eliminates All Loop Domains. Cell 171, 305-320.e24. https://doi.org/10.1016/j.cell.2017.09.026
Rao, S.S.P., Huntley, M.H., Durand, N.C., Stamenova, E.K., Bochkov, I.D., Robinson, J.T., Sanborn, A.L., Machol, I., Omer, A.D., Lander, E.S., Aiden, E.L., 2014. A 3D Map of the Human Genome at Kilobase Resolution Reveals Principles of Chromatin Looping. Cell 159, 1665–1680. https://doi.org/10.1016/j.cell.2014.11.021
Ratnakumar, K., Duarte, L.F., LeRoy, G., Hasson, D., Smeets, D., Vardabasso, C., Bönisch, C., Zeng, T., Xiang, B., Zhang, D.Y., Li, H., Wang, X., Hake, S.B., Schermelleh, L., Garcia, B.A., Bernstein, E., 2012. ATRX-mediated chromatin association of histone variant macroH2A1 regulates α-globin expression. Genes Dev. 26, 433–438. https://doi.org/10.1101/gad.179416.111
Rattner, J.B., Hamkalo, B.A., 1979. Nucleosome packing in interphase chromatin. J. Cell Biol. 81, 453–457. https://doi.org/10.1083/jcb.81.2.453
Ray-Gallet, D., Almouzni, G., 2021. The Histone H3 Family and Its Deposition Pathways, in: Fang, D., Han, J. (Eds.), Histone Mutations and Cancer, Advances in Experimental Medicine and Biology. Springer, Singapore, pp. 17–42. https://doi.org/10.1007/978-981-15-8104-5_2
Ray-Gallet, D., Quivy, J.-P., Scamps, C., Martini, E.M.-D., Lipinski, M., Almouzni, G., 2002. HIRA Is Critical for a Nucleosome Assembly Pathway Independent of DNA Synthesis. Mol. Cell 9, 1091–1100. https://doi.org/10.1016/S1097-2765(02)00526-9
Ray-Gallet, D., Ricketts, M.D., Sato, Y., Gupta, K., Boyarchuk, E., Senda, T., Marmorstein, R., Almouzni, G., 2018. Functional activity of the H3.3 histone chaperone complex HIRA requires trimerization of the HIRA subunit. Nat. Commun. 9, 3103. https://doi.org/10.1038/s41467-018-05581-y
Ray-Gallet, D., Woolfe, A., Vassias, I., Pellentz, C., Lacoste, N., Puri, A., Schultz, D.C., Pchelintsev, N.A., Adams, P.D., Jansen, L.E.T., Almouzni, G., 2011. Dynamics of Histone H3 Deposition In Vivo Reveal a Nucleosome Gap-Filling Mechanism for H3.3 to Maintain Chromatin Integrity. Mol. Cell 44, 928–941. https://doi.org/10.1016/j.molcel.2011.12.006
Razin, A., 1998. CpG methylation, chromatin structure and gene silencing—a three-way connection. EMBO J. 17, 4905–4908. https://doi.org/10.1093/emboj/17.17.4905
Razin, A., Cedar, H., 1977. Distribution of 5-methylcytosine in chromatin. Proc. Natl. Acad. Sci. 74, 2725–2728. https://doi.org/10.1073/pnas.74.7.2725
Régnier, V., Novelli, J., Fukagawa, T., Vagnarelli, P., Brown, W., 2003. Characterization of chicken CENP-A and comparative sequence analysis of vertebrate centromere-specific histone H3-like proteins. Gene 316, 39–46. https://doi.org/10.1016/S0378-1119(03)00768-6

Remus, D., Beall, E.L., Botchan, M.R., 2004. DNA topology, not DNA sequence, is a critical determinant for Drosophila ORC–DNA binding. EMBO J. 23, 897–907. https://doi.org/10.1038/sj.emboj.7600077
Renaud-Pageot, C., Quivy, J.-P., Lochhead, M., Almouzni, G., 2022. CENP-A Regulation and Cancer. Front. Cell Dev. Biol. 10, 13.
Resnick, R., Wong, C.-J., Hamm, D.C., Bennett, S.R., Skene, P.J., Hake, S.B., Henikoff, S., van der Maarel, S.M., Tapscott, S.J., 2019. DUX4-Induced Histone Variants H3.X and H3.Y Mark DUX4 Target Genes for Expression. Cell Rep. 29, 1812-1820.e5. https://doi.org/10.1016/j.celrep.2019.10.025
Reverón-Gómez, N., González-Aguilera, C., Stewart-Morgan, K.R., Petryk, N., Flury, V., Graziano, S., Johansen, J.V., Jakobsen, J.S., Alabert, C., Groth, A., 2018. Accurate Recycling of Parental Histones Reproduces the Histone Modification Landscape during DNA Replication. Mol. Cell 72, 239-249.e5. https://doi.org/10.1016/j.molcel.2018.08.010
Rhind, N., 2006. DNA replication timing: random thoughts about origin firing. Nat. Cell Biol. 8, 1313–1316. https://doi.org/10.1038/ncb1206-1313
Rhind, N., Yang, S.C.-H., Bechhoefer, J., 2010. Reconciling stochastic origin firing with defined replication timing. Chromosome Res. 18, 35–43. https://doi.org/10.1007/s10577-009-9093-3
Ricci, M.A., Manzo, C., García-Parajo, M.F., Lakadamyali, M., Cosma, M.P., 2015. Chromatin Fibers Are Formed by Heterogeneous Groups of Nucleosomes In Vivo. Cell 160, 1145–1158. https://doi.org/10.1016/j.cell.2015.01.054
Richet, N., Liu, D., Legrand, P., Velours, C., Corpet, A., Gaubert, A., Bakail, M., Moal-Raisin, G., Guerois, R., Compper, C., Besle, A., Guichard, B., Almouzni, G., Ochsenbein, F., 2015. Structural insight into how the human helicase subunit MCM2 may act as a histone chaperone together with ASF1 at the replication fork. Nucleic Acids Res. 43, 1905–1917. https://doi.org/10.1093/nar/gkv021
Ricketts, M.D., Frederick, B., Hoff, H., Tang, Y., Schultz, D.C., Singh Rai, T., Grazia Vizioli, M., Adams, P.D., Marmorstein, R., 2015. Ubinuclein-1 confers histone H3.3-specific-binding by the HIRA histone chaperone complex. Nat. Commun. 6, 7711. https://doi.org/10.1038/ncomms8711
Rivera-Mulia, J.C., Buckley, Q., Sasaki, T., Zimmerman, J., Didier, R.A., Nazor, K., Loring, J.F., Lian, Z., Weissman, S., Robins, A.J., Schulz, T.C., Menendez, L., Kulik, M.J., Dalton, S., Gabr, H., Kahveci, T., Gilbert, D.M., 2015. Dynamic changes in replication timing and gene expression during lineage specification of human pluripotent stem cells. Genome Res. 25, 1091–1103. https://doi.org/10.1101/gr.187989.114
Roark, D.E., Geoghegan, T.E., Keller, G.H., 1974. A two-subunit histone complex from calf thymus. Biochem. Biophys. Res. Commun. 59, 542–547. https://doi.org/10.1016/S0006-291X(74)80014-8
Roberts, C., Sutherland, H.F., Farmer, H., Kimber, W., Halford, S., Carey, A., Brickman, J.M., Wynshaw-Boris, A., Scambler, P.J., 2002. Targeted Mutagenesis of the Hira Gene Results in Gastrulation Defects and Patterning Abnormalities of Mesoendodermal Derivatives Prior to Early Embryonic Lethality. Mol. Cell. Biol. 22, 2318–2328. https://doi.org/10.1128/MCB.22.7.2318-2328.2002
Roix, J.J., McQueen, P.G., Munson, P.J., Parada, L.A., Misteli, T., 2003. Spatial proximity of translocation-prone gene loci in human lymphomas. Nat. Genet. 34, 287–291. https://doi.org/10.1038/ng1177
Rosin, L.F., Crocker, O., Isenhart, R.L., Nguyen, S.C., Xu, Z., Joyce, E.F., 2019. Chromosome territory formation attenuates the translocation potential of cells. eLife 8, e49553. https://doi.org/10.7554/eLife.49553
Rothberg, J.M., Hinz, W., Rearick, T.M., Schultz, J., Mileski, W., Davey, M., Leamon, J.H., Johnson, K., Milgrew, M.J., Edwards, M., Hoon, J., Simons, J.F., Marran, D., Myers, J.W., Davidson, J.F., Branting, A., Nobile, J.R., Puc, B.P., Light, D., Clark, T.A., Huber, M., Branciforte, J.T., Stoner, I.B., Cawley, S.E., Lyons, M., Fu, Y., Homer, N., Sedova, M., Miao, X., Reed, B., Sabina, J., Feierstein, E., Schorn, M., Alanjary, M., Dimalanta, E., Dressman, D., Kasinskas, R., Sokolsky, T., Fidanza, J.A., Namsaraev, E., McKernan, K.J., Williams, A., Roth, G.T., Bustillo, J., 2011. An integrated semiconductor device enabling non-optical genome sequencing. Nature 475, 348–352. https://doi.org/10.1038/nature10242
Rotondo, J.C., Bosi, S., Bassi, C., Ferracin, M., Lanza, G., Gafà, R., Magri, E., Selvatici, R., Torresani, S., Marci, R., Garutti, P., Negrini, M., Tognon, M., Martini, F., 2015. Gene Expression Changes in Progression of Cervical Neoplasia Revealed by Microarray Analysis of Cervical Neoplastic Keratinocytes. J. Cell. Physiol. 230, 806–812. https://doi.org/10.1002/jcp.24808
Rouillon, C., Eckhardt, B.V., Kollenstart, L., Gruss, F., Verkennis, A.E.E., Rondeel, I., Krijger, P.H.L., Ricci, G., Biran, A., van Laar, T., Delvaux de Fenffe, C.M., Luppens, G., Albanese, P., Sato, K., Scheltema, R.A., de Laat, W., Knipscheer, P., Dekker, N.H., Groth, A., Mattiroli, F., 2023. CAF-1 deposits newly synthesized histones during DNA replication using distinct mechanisms on the leading and lagging strands. Nucleic Acids Res. 51, 3770–3792. https://doi.org/10.1093/nar/gkad171
Rowley, M.J., Corces, V.G., 2018. Organizational principles of 3D genome architecture. Nat. Rev. Genet. 19, 789–800. https://doi.org/10.1038/s41576-018-0060-8
Rowley, M.J., Nichols, M.H., Lyu, X., Ando-Kuri, M., Rivera, I.S.M., Hermetz, K., Wang, P., Ruan, Y., Corces, V.G., 2017. Evolutionarily Conserved Principles Predict 3D Chromatin Organization. Mol. Cell 67, 837-852.e7. https://doi.org/10.1016/j.molcel.2017.07.022

Ruiz-Carrillo, A., Wangh, L.J., Allfrey, V.G., 1975. Processing of Newly Synthesized Histone Molecules: Nascent histone H4 chains are reversibly phosphorylated and acetylated. Science 190, 117–128. https://doi.org/10.1126/science.1166303
Russev, G., Hancock, R., 1982. Assembly of new histones into nucleosomes and their distribution in replicating chromatin. Proc. Natl. Acad. Sci. 79, 3143–3147. https://doi.org/10.1073/pnas.79.10.3143
Russo, V., Martienssen, R., Riggs, A.D., 1996. Epigenetic mechanisms of gene regulation. Plainview, N.Y. : Cold Spring Harbor Laboratory Press.
Rust, M.J., Bates, M., Zhuang, X., 2006. Sub-diffraction-limit imaging by stochastic optical reconstruction microscopy (STORM). Nat. Methods 3, 793–796. https://doi.org/10.1038/nmeth929
Ryba, T., Hiratani, I., Lu, J., Itoh, M., Kulik, M., Zhang, J., Schulz, T.C., Robins, A.J., Dalton, S., Gilbert, D.M., 2010. Evolutionarily conserved replication timing profiles predict long-range chromatin interactions and distinguish closely related cell types. Genome Res. 20, 761–770. https://doi.org/10.1101/gr.099655.109
Sabari, B.R., Dall'Agnese, A., Boija, A., Klein, I.A., Coffey, E.L., Shrinivas, K., Abraham, B.J., Hannett, N.M., Zamudio, A.V., Manteiga, J.C., Li, C.H., Guo, Y.E., Day, D.S., Schuijers, J., Vasile, E., Malik, S., Hnisz, D., Lee, T.I., Cisse, I.I., Roeder, R.G., Sharp, P.A., Chakraborty, A.K., Young, R.A., 2018. Coactivator condensation at super-enhancers links phase separation and gene control. Science 361, eaar3958. https://doi.org/10.1126/science.aar3958
Sadic, D., Schmidt, K., Groh, S., Kondofersky, I., Ellwart, J., Fuchs, C., Theis, F.J., Schotta, G., 2015. Atrx promotes heterochromatin formation at retrotransposons. EMBO Rep. 16, 836–850. https://doi.org/10.15252/embr.201439937
Saha, A.K., Contreras-Galindo, R., Niknafs, Y.S., Iyer, M., Qin, T., Padmanabhan, K., Siddiqui, J., Palande, M., Wang, C., Qian, B., Ward, E., Tang, T., Tomlins, S.A., Gitlin, S.D., Sartor, M.A., Omenn, G.S., Chinnaiyan, A.M., Markovitz, D.M., 2020. The role of the histone H3 variant CENPA in prostate cancer. J. Biol. Chem. 295, 8537–8549. https://doi.org/10.1074/jbc.RA119.010080
Sahasrabuddhe, C.G., Van Holde, K.E., 1974. The Effect of Trypsin on Nuclease-resistant Chromatin Fragments. J. Biol. Chem. 249, 152–156. https://doi.org/10.1016/S0021-9258(19)43104-9
Sakai, A., Schwartz, B.E., Goldstein, S., Ahmad, K., 2009. Transcriptional and Developmental Functions of the H3.3 Histone Variant in Drosophila. Curr. Biol. 19, 1816–1820. https://doi.org/10.1016/j.cub.2009.09.021
Sanford, J.P., Clark, H.J., Chapman, V.M., Rossant, J., 1987. Differences in DNA methylation during oogenesis and spermatogenesis and their persistence during early embryogenesis in the mouse. Genes Dev. 1, 1039–1046. https://doi.org/10.1101/gad.1.10.1039
Sankar, A., Mohammad, F., Sundaramurthy, A.K., Wang, H., Lerdrup, M., Tatar, T., Helin, K., 2022. Histone editing elucidates the functional roles of H3K27 methylation and acetylation in mammals. Nat. Genet. https://doi.org/10.1038/s41588-022-01091-2
Sansam, C.G., Pietrzak, K., Majchrzycka, B., Kerlin, M.A., Chen, J., Rankin, S., Sansam, C.L., 2018. A mechanism for epigenetic control of DNA replication. Genes Dev. 32, 224–229. https://doi.org/10.1101/gad.306464.117
Santenard, A., Ziegler-Birling, C., Koch, M., Tora, L., Bannister, A.J., Torres-Padilla, M.-E., 2010. Heterochromatin formation in the mouse embryo requires critical residues of the histone variant H3.3. Nat. Cell Biol. 12, 853–862. https://doi.org/10.1038/ncb2089
Santoro, S.W., Dulac, C., 2012. The activity-dependent histone variant H2BE modulates the life span of olfactory neurons. eLife 1, e00070. https://doi.org/10.7554/eLife.00070
Sarcinella, E., Zuzarte, P.C., Lau, P.N.I., Draker, R., Cheung, P., 2007. Monoubiquitylation of H2A.Z Distinguishes Its Association with Euchromatin or Facultative Heterochromatin. Mol. Cell. Biol. 27, 6457–6468. https://doi.org/10.1128/MCB.00241-07
Saredi, G., Carelli, F.N., Furlan, G., Rolland, S., Piquet, S., Appert, A., Sanchez-Pulido, L., Price, J.L., Alcon, P., Lampersberger, L., Declais, A.-C., Ramakrishna, N.B., Toth, R., Ponting, C.P., Polo, S.E., Miska, E.A., Ahringer, J., Gartner, A., Rouse, J., 2023. The histone chaperone activity of SPT2 controls chromatin structure and function in Metazoa (preprint). Molecular Biology. https://doi.org/10.1101/2023.02.16.528451
Saredi, G., Huang, H., Hammond, C.M., Alabert, C., Bekker-Jensen, S., Forne, I., Reverón-Gómez, N., Foster, B.M., Mlejnkova, L., Bartke, T., Cejka, P., Mailand, N., Imhof, A., Patel, D.J., Groth, A., 2016. H4K20me0 marks post-replicative chromatin and recruits the TONSL–MMS22L DNA repair complex. Nature 534, 714–718. https://doi.org/10.1038/nature18312
Sarthy, J.F., Meers, M.P., Janssens, D.H., Henikoff, J.G., Feldman, H., Paddison, P.J., Lockwood, C.M., Vitanza, N.A., Olson, J.M., Ahmad, K., Henikoff, S., 2020. Histone deposition pathways determine the chromatin landscapes of H3.1 and H3.3 K27M oncohistones. eLife 9, e61090. https://doi.org/10.7554/eLife.61090
Sawatsubashi, S., Murata, T., Lim, J., Fujiki, R., Ito, S., Suzuki, E., Tanabe, M., Zhao, Y., Kimura, S., Fujiyama, S., Ueda, T., Umetsu, D., Ito, T., Takeyama, K., Kato, S., 2010. A histone chaperone, DEK, transcriptionally coactivates a nuclear receptor. Genes Dev. 24, 159–170. https://doi.org/10.1101/gad.1857410
Saxton, D.S., Rine, J., 2019. Epigenetic memory independent of symmetric histone inheritance 21.

Schaarschmidt, D., Baltin, J., Stehle, I.M., Lipps, H.J., Knippers, R., 2004. An episomal mammalian replicon: sequence-independent binding of the origin recognition complex. EMBO J. 23, 191–201. https://doi.org/10.1038/sj.emboj.7600029
Scharf, A.N.D., Barth, T.K., Imhof, A., 2009. Establishment of Histone Modifications after Chromatin Assembly. Nucleic Acids Res. 37, 5032–5040. https://doi.org/10.1093/nar/gkp518
Schena, M., Shalon, D., Davis, R.W., Brown, P.O., 1995. Quantitative Monitoring of Gene Expression Patterns with a Complementary DNA Microarray. Science 270, 467–470. https://doi.org/10.1126/science.270.5235.467
Schenk, R., Jenke, A., Zilbauer, M., Wirth, S., Postberg, J., 2011. H3.5 is a novel hominid-specific histone H3 variant that is specifically expressed in the seminiferous tubules of human testes. Chromosoma 120, 275–285. https://doi.org/10.1007/s00412-011-0310-4
Schermelleh, L., Carlton, P.M., Haase, S., Shao, L., Winoto, L., Kner, P., Burke, B., Cardoso, M.C., Agard, D.A., Gustafsson, M.G.L., Leonhardt, H., Sedat, J.W., 2008. Subdiffraction Multicolor Imaging of the Nuclear Periphery with 3D Structured Illumination Microscopy. Science 320, 1332–1336. https://doi.org/10.1126/science.1156947
Scherr, M.J., Wahab, S.A., Remus, D., Duderstadt, K.E., 2022. Mobile origin-licensing factors confer resistance to conflicts with RNA polymerase. Cell Rep. 38, 110531. https://doi.org/10.1016/j.celrep.2022.110531
Schlesinger, S., Kaffe, B., Melcer, S., Aguilera, J.D., Sivaraman, D.M., Kaplan, T., Meshorer, E., 2017. A hyperdynamic H3.3 nucleosome marks promoter regions in pluripotent embryonic stem cells. Nucleic Acids Res. 45, 12181–12194. https://doi.org/10.1093/nar/gkx817
Schlesinger, S., Meshorer, E., 2019. Open Chromatin, Epigenetic Plasticity, and Nuclear Organization in Pluripotency. Dev. Cell 48, 135–150. https://doi.org/10.1016/j.devcel.2019.01.003
Schlissel, G., Rine, J., 2019. The nucleosome core particle remembers its position through DNA replication and RNA transcription. Proc. Natl. Acad. Sci. 116, 20605–20611. https://doi.org/10.1073/pnas.1911943116
Schmidt, T.L., Beliveau, B.J., Uca, Y.O., Theilmann, M., Da Cruz, F., Wu, C.-T., Shih, W.M., 2015. Scalable amplification of strand subsets from chip-synthesized oligonucleotide libraries. Nat. Commun. 6, 8634. https://doi.org/10.1038/ncomms9634
Schmitz, M.L., Higgins, J.M.G., Seibert, M., 2020. Priming chromatin for segregation: functional roles of mitotic histone modifications. Cell Cycle 19, 625–641. https://doi.org/10.1080/15384101.2020.1719585
Schoberleitner, I., Bauer, I., Huang, A., Andreyeva, E.N., Sebald, J., Pascher, K., Rieder, D., Brunner, M., Podhraski, V., Oemer, G., Cázarez-García, D., Rieder, L., Keller, M.A., Winkler, R., Fyodorov, D.V., Lusser, A., 2021. CHD1 controls H3.3 incorporation in adult brain chromatin to maintain metabolic homeostasis and normal lifespan. Cell Rep. 37, 109769. https://doi.org/10.1016/j.celrep.2021.109769
Schoenfelder, S., Sexton, T., Chakalova, L., Cope, N.F., Horton, A., Andrews, S., Kurukuti, S., Mitchell, J.A., Umlauf, D., Dimitrova, D.S., Eskiw, C.H., Luo, Y., Wei, C.-L., Ruan, Y., Bieker, J.J., Fraser, P., 2010. Preferential associations between co-regulated genes reveal a transcriptional interactome in erythroid cells. Nat. Genet. 42, 53–61. https://doi.org/10.1038/ng.496
Schoenfelder, S., Furlan-Magaril, M., Mifsud, B., Tavares-Cadete, F., Sugar, R., Javierre, B.-M., Nagano, T., Katsman, Y., Sakthidevi, M., Wingett, S.W., Dimitrova, E., Dimond, A., Edelman, L.B., Elderkin, S., Tabbada, K., Darbo, E., Andrews, S., Herman, B., Higgs, A., LeProust, E., Osborne, C.S., Mitchell, J.A., Luscombe, N.M., Fraser, P., 2015a. The pluripotent regulatory circuitry connecting promoters to their long-range interacting elements. Genome Res. 25, 582–597. https://doi.org/10.1101/gr.185272.114
Schoenfelder, S., Sugar, R., Dimond, A., Javierre, B.-M., Armstrong, H., Mifsud, B., Dimitrova, E., Matheson, L., Tavares-Cadete, F., Furlan-Magaril, M., Segonds-Pichon, A., Jurkowski, W., Wingett, S.W., Tabbada, K., Andrews, S., Herman, B., LeProust, E., Osborne, C.S., Koseki, H., Fraser, P., Luscombe, N.M., Elderkin, S., 2015. Polycomb repressive complex PRC1 spatially constrains the mouse embryonic stem cell genome. Nat. Genet. 47, 1179–1186. https://doi.org/10.1038/ng.3393
Schones, D.E., Cui, K., Cuddapah, S., Roh, T.-Y., Barski, A., Wang, Z., Wei, G., Zhao, K., 2008. Dynamic Regulation of Nucleosome Positioning in the Human Genome. Cell 132, 887–898. https://doi.org/10.1016/j.cell.2008.02.022
Schübeler, D., Scalzo, D., Kooperberg, C., Van Steensel, B., Delrow, J., Groudine, M., 2002. Genome-wide DNA replication profile for Drosophila melanogaster: a link between transcription and replication timing. Nat. Genet. 32, 438–442. https://doi.org/10.1038/ng1005
Schuettengruber, B., Bourbon, H.-M., Di Croce, L., Cavalli, G., 2017. Genome Regulation by Polycomb and Trithorax: 70 Years and Counting. Cell 171, 34–57. https://doi.org/10.1016/j.cell.2017.08.002
Schwaiger, M., Kohler, H., Oakeley, E.J., Stadler, M.B., Schübeler, D., 2010. Heterochromatin protein 1 (HP1) modulates replication timing of the *Drosophila* genome. Genome Res. 20, 771–780. https://doi.org/10.1101/gr.101790.109
Schwartzentruber, J., Korshunov, A., Liu, X.-Y., Jones, D.T.W., Pfaff, E., Jacob, K., Sturm, D., Fontebasso, A.M., Quang, D.-A.K., Tönjes, M., Hovestadt, V., Albrecht, S., Kool, M., Nantel, A., Konermann, C., Lindroth, A., Jäger, N., Rausch, T., Ryzhova, M., Korbel, J.O., Hielscher, T., Hauser, P., Garami, M., Klekner, A., Bognar, L., Ebinger, M., Schuhmann, M.U., Scheurlen, W., Pekrun, A., Frühwald, M.C., Roggendorf, W., Kramm, C., Dürken, M.,

Atkinson, J., Lepage, P., Montpetit, A., Zakrzewska, M., Zakrzewski, K., Liberski, P.P., Dong, Z., Siegel, P., Kulozik, A.E., Zapatka, M., Guha, A., Malkin, D., Felsberg, J., Reifenberger, G., von Deimling, A., Ichimura, K., Collins, V.P., Witt, H., Milde, T., Witt, O., Zhang, C., Castelo-Branco, P., Lichter, P., Faury, D., Tabori, U., Plass, C., Majewski, J., Pfister, S.M., Jabado, N., 2012. Driver mutations in histone H3.3 and chromatin remodelling genes in paediatric glioblastoma. Nature 482, 226–231. https://doi.org/10.1038/nature10833
Schwarzer, W., Abdennur, N., Goloborodko, A., Pekowska, A., Fudenberg, G., Loe-Mie, Y., Fonseca, N.A., Huber, W., Haering, C.H., Mirny, L., Spitz, F., 2017. Two independent modes of chromatin organization revealed by cohesin removal. Nature 551, 51–56. https://doi.org/10.1038/nature24281
See, K., Kiseleva, A.A., Smith, C.L., Liu, F., Li, J., Poleshko, A., Epstein, J.A., 2020. Histone methyltransferase activity programs nuclear peripheral genome positioning. Dev. Biol. 466, 90–98. https://doi.org/10.1016/j.ydbio.2020.07.010
Sekulic, N., Bassett, E.A., Rogers, D.J., Black, B.E., 2010. The structure of (CENP-A–H4)2 reveals physical features that mark centromeres. Nature 467, 347–351. https://doi.org/10.1038/nature09323
Sexton, T., Yaffe, E., Kenigsberg, E., Bantignies, F., Leblanc, B., Hoichman, M., Parrinello, H., Tanay, A., Cavalli, G., 2012. Three-Dimensional Folding and Functional Organization Principles of the Drosophila Genome. Cell 148, 458–472. https://doi.org/10.1016/j.cell.2012.01.010
Shahbazian, M.D., Grunstein, M., 2007. Functions of Site-Specific Histone Acetylation and Deacetylation. Annu. Rev. Biochem. 76, 75–100. https://doi.org/10.1146/annurev.biochem.76.052705.162114
Shelby, R.D., Vafa, O., Sullivan, K.F., 1997. Assembly of CENP-A into Centromeric Chromatin Requires a Cooperative Array of Nucleosomal DNA Contact Sites. J. Cell Biol. 136, 501–513. https://doi.org/10.1083/jcb.136.3.501
Shen, Y., Yue, F., McCleary, D.F., Ye, Z., Edsall, L., Kuan, S., Wagner, U., Dixon, J., Lee, L., Lobanenkov, V.V., Ren, B., 2012. A map of the cis-regulatory sequences in the mouse genome. Nature 488, 116–120. https://doi.org/10.1038/nature11243
Shen, Z., Sathyan, K.M., Geng, Y., Zheng, R., Chakraborty, A., Freeman, B., Wang, F., Prasanth, K.V., Prasanth, S.G., 2010. A WD-Repeat Protein Stabilizes ORC Binding to Chromatin. Mol. Cell 40, 99–111. https://doi.org/10.1016/j.molcel.2010.09.021
Shibahara, K., Stillman, B., 1999. Replication-Dependent Marking of DNA by PCNA Facilitates CAF-1-Coupled Inheritance of Chromatin. Cell 96, 575–585. https://doi.org/10.1016/S0092-8674(00)80661-3
Shreeram, S., Sparks, A., Lane, D.P., Blow, J.J., 2002. Cell type-specific responses of human cells to inhibition of replication licensing. Oncogene 21, 6624–6632. https://doi.org/10.1038/sj.onc.1205910
Shrestha, R.L., Ahn, G.S., Staples, M.I., Sathyan, K.M., Karpova, T.S., Foltz, D.R., Basrai, M.A., 2017. Mislocalization of centromeric histone H3 variant CENP-A contributes to chromosomal instability (CIN) in human cells. Oncotarget 8, 46781–46800. https://doi.org/10.18632/oncotarget.18108
Shrestha, R.L., Rossi, A., Wangsa, D., Hogan, A.K., Zaldana, K.S., Suva, E., Chung, Y.J., Sanders, C.L., Difilippantonio, S., Karpova, T.S., Karim, B., Foltz, D.R., Fachinetti, D., Aplan, P.D., Ried, T., Basrai, M.A., 2021. CENP-A overexpression promotes aneuploidy with karyotypic heterogeneity. J. Cell Biol. 220, e202007195. https://doi.org/10.1083/jcb.202007195
Siddiqui, K., On, K.F., Diffley, J.F.X., 2013. Regulating DNA Replication in Eukarya. Cold Spring Harb. Perspect. Biol. 5, a012930–a012930. https://doi.org/10.1101/cshperspect.a012930
Silverman, J., Takai, H., Buonomo, S.B.C., Eisenhaber, F., De Lange, T., 2004. Human Rif1, ortholog of a yeast telomeric protein, is regulated by ATM and 53BP1 and functions in the S-phase checkpoint. Genes Dev. 18, 2108–2119. https://doi.org/10.1101/gad.1216004
Sima, J., Chakraborty, A., Dileep, V., Michalski, M., Klein, K.N., Holcomb, N.P., Turner, J.L., Paulsen, M.T., Rivera-Mulia, J.C., Trevilla-Garcia, C., Bartlett, D.A., Zhao, P.A., Washburn, B.K., Nora, E.P., Kraft, K., Mundlos, S., Bruneau, B.G., Ljungman, M., Fraser, P., Ay, F., Gilbert, D.M., 2019. Identifying cis Elements for Spatiotemporal Control of Mammalian DNA Replication. Cell 176, 816-830.e18. https://doi.org/10.1016/j.cell.2018.11.036
Simonis, M., Klous, P., Splinter, E., Moshkin, Y., Willemsen, R., de Wit, E., van Steensel, B., de Laat, W., 2006. Nuclear organization of active and inactive chromatin domains uncovered by chromosome conformation capture–on-chip (4C). Nat. Genet. 38, 1348–1354. https://doi.org/10.1038/ng1896
Simpson, R.T., 1999. In vivo methods to analyze chromatin structure. Curr. Opin. Genet. Dev. 9, 225–229. https://doi.org/10.1016/S0959-437X(99)80033-1
Simpson, R.T., 1978. Structure of the chromatosome, a chromatin particle containing 160 base pairs of DNA and all the histones. Biochemistry 17, 5524–5531. https://doi.org/10.1021/bi00618a030
Sitbon, D., Boyarchuk, E., Dingli, F., Loew, D., Almouzni, G., 2020. Histone variant H3.3 residue S31 is essential for Xenopus gastrulation regardless of the deposition pathway. Nat. Commun. 11, 1256. https://doi.org/10.1038/s41467-020-15084-4
Skene, P.J., Henikoff, S., 2017. An efficient targeted nuclease strategy for high-resolution mapping of DNA binding sites. eLife 6, e21856. https://doi.org/10.7554/eLife.21856

Smith, R., Pickering, S.J., Kopakaki, A., Thong, K.J., Anderson, R.A., Lin, C.-J., 2021. HIRA contributes to zygote formation in mice and is implicated in human 1PN zygote phenotype. Reproduction 161, 697–707. https://doi.org/10.1530/REP-20-0636
Smith, S., Stillman, B., 1989. Purification and characterization of CAF-I, a human cell factor required for chromatin assembly during DNA replication in vitro. Cell 58, 15–25. https://doi.org/10.1016/0092-8674(89)90398-X
Solomon, M.J., Larsen, P.L., Varshavsky, A., 1988. Mapping proteinDNA interactions in vivo with formaldehyde: Evidence that histone H4 is retained on a highly transcribed gene. Cell 53, 937–947. https://doi.org/10.1016/S0092-8674(88)90469-2
Solovei, I., Kreysing, M., Lanctôt, C., Kösem, S., Peichl, L., Cremer, T., Guck, J., Joffe, B., 2009. Nuclear Architecture of Rod Photoreceptor Cells Adapts to Vision in Mammalian Evolution. Cell 137, 356–368. https://doi.org/10.1016/j.cell.2009.01.052
Solovei, I., Wang, A.S., Thanisch, K., Schmidt, C.S., Krebs, S., Zwerger, M., Cohen, T.V., Devys, D., Foisner, R., Peichl, L., Herrmann, H., Blum, H., Engelkamp, D., Stewart, C.L., Leonhardt, H., Joffe, B., 2013. LBR and Lamin A/C Sequentially Tether Peripheral Heterochromatin and Inversely Regulate Differentiation. Cell 152, 584–598. https://doi.org/10.1016/j.cell.2013.01.009
Soni, S., Pchelintsev, N., Adams, P.D., Bieker, J.J., 2014. Transcription factor EKLF (KLF1) recruitment of the histone chaperone HIRA is essential for β-globin gene expression. Proc. Natl. Acad. Sci. 111, 13337–13342. https://doi.org/10.1073/pnas.1405422111
Spielmann, M., Lupiáñez, D.G., Mundlos, S., 2018. Structural variation in the 3D genome. Nat. Rev. Genet. 19, 453–467. https://doi.org/10.1038/s41576-018-0007-0
Spracklin, G., Abdennur, N., Imakaev, M., Chowdhury, N., Pradhan, S., Mirny, L.A., Dekker, J., 2022. Diverse silent chromatin states modulate genome compartmentalization and loop extrusion barriers. Nat. Struct. Mol. Biol. https://doi.org/10.1038/s41594-022-00892-7
Sreesankar, E., Senthilkumar, R., Bharathi, V., Mishra, R.K., Mishra, K., 2012. Functional diversification of yeast telomere associated protein, Rif1, in higher eukaryotes. BMC Genomics 13, 255. https://doi.org/10.1186/1471-2164-13-255
Stadhouders, R., Vidal, E., Serra, F., Di Stefano, B., Le Dily, F., Quilez, J., Gomez, A., Collombet, S., Berenguer, C., Cuartero, Y., Hecht, J., Filion, G.J., Beato, M., Marti-Renom, M.A., Graf, T., 2018. Transcription factors orchestrate dynamic interplay between genome topology and gene regulation during cell reprogramming. Nat. Genet. 50, 238–249. https://doi.org/10.1038/s41588-017-0030-7
Stafford, J.M., Lee, C.-H., Voigt, P., Descostes, N., Saldaña-Meyer, R., Yu, J.-R., Leroy, G., Oksuz, O., Chapman, J.R., Suarez, F., Modrek, A.S., Bayin, N.S., Placantonakis, D.G., Karajannis, M.A., Snuderl, M., Ueberheide, B., Reinberg, D., 2018. Multiple modes of PRC2 inhibition elicit global chromatin alterations in H3K27M pediatric glioma. Sci. Adv. 4, eaau5935. https://doi.org/10.1126/sciadv.aau5935
Steensel, B. van, Henikoff, S., 2000. Identification of in vivo DNA targets of chromatin proteins using tethered Dam methyltransferase. Nat. Biotechnol. 18, 424–428. https://doi.org/10.1038/74487
Stevens, T.J., Lando, D., Basu, S., Atkinson, L.P., Cao, Y., Lee, S.F., Leeb, M., Wohlfahrt, K.J., Boucher, W., O'Shaughnessy-Kirwan, A., Cramard, J., Faure, A.J., Ralser, M., Blanco, E., Morey, L., Sansó, M., Palayret, M.G.S., Lehner, B., Di Croce, L., Wutz, A., Hendrich, B., Klenerman, D., Laue, E.D., 2017. 3D structures of individual mammalian genomes studied by single-cell Hi-C. Nature 544, 59–64. https://doi.org/10.1038/nature21429
Stewart-Morgan, K.R., Petryk, N., Groth, A., 2020. Chromatin replication and epigenetic cell memory. Nat. Cell Biol. 22, 361–371. https://doi.org/10.1038/s41556-020-0487-y
Stewart-Morgan, K.R., Reverón-Gómez, N., Groth, A., 2019. Transcription Restart Establishes Chromatin Accessibility after DNA Replication. Mol. Cell 75, 284-297.e6. https://doi.org/10.1016/j.molcel.2019.04.033
Stinchcomb, D.T., Struhl, K., Davis, R.W., 1979. Isolation and characterisation of a yeast chromosomal replicator. Nature 282, 39–43. https://doi.org/10.1038/282039a0
Strobino, M., Wenda, J.M., Padayachy, L., Steiner, F.A., 2020. Loss of histone H3.3 results in DNA replication defects and altered origin dynamics in C. elegans 13.
Strom, A.R., Emelyanov, A.V., Mir, M., Fyodorov, D.V., Darzacq, X., Karpen, G.H., 2017. Phase separation drives heterochromatin domain formation. Nature 547, 241–245. https://doi.org/10.1038/nature22989
Sugimoto, N., Maehara, K., Yoshida, K., Ohkawa, Y., Fujita, M., 2018. Genome-wide analysis of the spatiotemporal regulation of firing and dormant replication origins in human cells. Nucleic Acids Res. 46, 6683–6696. https://doi.org/10.1093/nar/gky476
Sullivan, K.F., Hechenberger, M., Masri, K., 1994. Human CENP-A contains a histone H3 related histone fold domain that is required for targeting to the centromere. J. Cell Biol. 127, 581–592. https://doi.org/10.1083/jcb.127.3.581
Supek, F., Lehner, B., 2015. Differential DNA mismatch repair underlies mutation rate variation across the human genome. Nature 521, 81–84. https://doi.org/10.1038/nature14173

Sutton, W., 1900. The spermatogonial divisions of Brachystola magna. Kans Univ Q 135–160.
Symmons, O., Uslu, V.V., Tsujimura, T., Ruf, S., Nassari, S., Schwarzer, W., Ettwiller, L., Spitz, F., 2014. Functional and topological characteristics of mammalian regulatory domains. Genome Res. 24, 390–400. https://doi.org/10.1101/gr.163519.113
Szabo, Q., Bantignies, F., Cavalli, G., 2019. Principles of genome folding into topologically associating domains. Sci. Adv. 5, eaaw1668. https://doi.org/10.1126/sciadv.aaw1668
Szabo, Q., Donjon, A., Jerković, I., Papadopoulos, G.L., Cheutin, T., Bonev, B., Nora, E.P., Bruneau, B.G., Bantignies, F., Cavalli, G., 2020. Regulation of single-cell genome organization into TADs and chromatin nanodomains. Nat. Genet. 1–7. https://doi.org/10.1038/s41588-020-00716-8
Szabo, Q., Jost, D., Chang, J.-M., Cattoni, D.I., Papadopoulos, G.L., Bonev, B., Sexton, T., Gurgo, J., Jacquier, C., Nollmann, M., Bantignies, F., Cavalli, G., 2018. TADs are 3D structural units of higher-order chromosome organization in Drosophila. Sci. Adv. 4, eaar8082. https://doi.org/10.1126/sciadv.aar8082
Szenker, E., Lacoste, N., Almouzni, G., 2012. A Developmental Requirement for HIRA-Dependent H3.3 Deposition Revealed at Gastrulation in Xenopus. Cell Rep. 1, 730–740. https://doi.org/10.1016/j.celrep.2012.05.006
Tachiwana, H., Kagawa, W., Osakabe, A., Kawaguchi, K., Shiga, T., Hayashi-Takanaka, Y., Kimura, H., Kurumizaka, H., 2010. Structural basis of instability of the nucleosome containing a testis-specific histone variant, human H3T. Proc. Natl. Acad. Sci. 107, 10454–10459. https://doi.org/10.1073/pnas.1003064107
Tachiwana, H., Kagawa, W., Shiga, T., Osakabe, A., Miya, Y., Saito, K., Hayashi-Takanaka, Y., Oda, T., Sato, M., Park, S.-Y., Kimura, H., Kurumizaka, H., 2011a. Crystal structure of the human centromeric nucleosome containing CENP-A. Nature 476, 232–235. https://doi.org/10.1038/nature10258
Tachiwana, H., Osakabe, A., Shiga, T., Miya, Y., Kimura, H., Kagawa, W., Kurumizaka, H., 2011b. Structures of human nucleosomes containing major histone H3 variants. Acta Crystallogr. D Biol. Crystallogr. 67, 578–583. https://doi.org/10.1107/S0907444911014818
Tafessu, A., O'Hara, R., Martire, S., Dube, A.L., Saha, P., Gant, V.U., Banaszynski, L.A., 2023. H3.3 contributes to chromatin accessibility and transcription factor binding at promoter-proximal regulatory elements in embryonic stem cells. Genome Biol. 24, 25. https://doi.org/10.1186/s13059-023-02867-3
Tagami, H., Ray-Gallet, D., Almouzni, G., Nakatani, Y., 2004. Histone H3.1 and H3.3 Complexes Mediate Nucleosome Assembly Pathways Dependent or Independent of DNA Synthesis. Cell 116, 51–61. https://doi.org/10.1016/S0092-8674(03)01064-X
Tahiliani, M., Koh, K.P., Shen, Y., Pastor, W.A., Bandukwala, H., Brudno, Y., Agarwal, S., Iyer, L.M., Liu, D.R., Aravind, L., Rao, A., 2009. Conversion of 5-Methylcytosine to 5-Hydroxymethylcytosine in Mammalian DNA by MLL Partner TET1. Science 324, 930–935. https://doi.org/10.1126/science.1170116
Takahashi, S., Miura, H., Shibata, T., Nagao, K., Okumura, K., Ogata, M., Obuse, C., Takebayashi, S., Hiratani, I., 2019. Genome-wide stability of the DNA replication program in single mammalian cells. Nat. Genet. 51, 529–540. https://doi.org/10.1038/s41588-019-0347-5
Takisawa, H., Mimura, S., Kubota, Y., 2000. Eukaryotic DNA replication: from pre-replication complex to initiation complex. Curr. Opin. Cell Biol. 12, 690–696. https://doi.org/10.1016/S0955-0674(00)00153-8
Takizawa, T., Gudla, P.R., Guo, L., Lockett, S., Misteli, T., 2008. Allele-specific nuclear positioning of the monoallelically expressed astrocyte marker GFAP. Genes Dev. 22, 489–498. https://doi.org/10.1101/gad.1634608
Talbert, P.B., Henikoff, S., 2014. Environmental responses mediated by histone variants. Trends Cell Biol. 24, 642–650. https://doi.org/10.1016/j.tcb.2014.07.006
Tamura, T., Smith, M., Kanno, T., Dasenbrock, H., Nishiyama, A., Ozato, K., 2009. Inducible Deposition of the Histone Variant H3.3 in Interferon-stimulated Genes. J. Biol. Chem. 284, 12217–12225. https://doi.org/10.1074/jbc.M805651200
Tan, B.C.-M., Chien, C.-T., Hirose, S., Lee, S.-C., 2006. Functional cooperation between FACT and MCM helicase facilitates initiation of chromatin DNA replication. EMBO J. 25, 3975–3985. https://doi.org/10.1038/sj.emboj.7601271
Tanaka, S., Diffley, J.F.X., 2002. Deregulated G1-cyclin expression induces genomic instability by preventing efficient pre-RC formation. Genes Dev. 16, 2639–2649. https://doi.org/10.1101/gad.1011002
Tanaka, S., Nakato, R., Katou, Y., Shirahige, K., Araki, H., 2011. Origin Association of Sld3, Sld7, and Cdc45 Proteins Is a Key Step for Determination of Origin-Firing Timing. Curr. Biol. 21, 2055–2063. https://doi.org/10.1016/j.cub.2011.11.038
Tang, J., Wu, S., Liu, H., Stratt, R., Barak, O.G., Shiekhattar, R., Picketts, D.J., Yang, X., 2004. A Novel Transcription Regulatory Complex Containing Death Domain-associated Protein and the ATR-X Syndrome Protein *. J. Biol. Chem. 279, 20369–20377. https://doi.org/10.1074/jbc.M401321200
Tang, M., Chen, Z., Wang, C., Feng, X., Lee, N., Huang, M., Zhang, H., Li, S., Xiong, Y., Chen, J., 2022. Histone chaperone ASF1 acts with RIF1 to promote DNA end joining in BRCA1-deficient cells. J. Biol. Chem. 298, 101979. https://doi.org/10.1016/j.jbc.2022.101979

Tang, M.C.W., Jacobs, S.A., Mattiske, D.M., Soh, Y.M., Graham, A.N., Tran, A., Lim, S.L., Hudson, D.F., Kalitsis, P., O'Bryan, M.K., Wong, L.H., Mann, J.R., 2015. Contribution of the Two Genes Encoding Histone Variant H3.3 to Viability and Fertility in Mice. PLOS Genet. 11, e1004964. https://doi.org/10.1371/journal.pgen.1004964
Tang, M.C.W., Jacobs, S.A., Wong, L.H., Mann, J.R., 2013. Conditional allelic replacement applied to genes encoding the histone variant H3.3 in the mouse. genesis 51, 142–146. https://doi.org/10.1002/dvg.22366
Tang, Y., Poustovoitov, M.V., Zhao, K., Garfinkel, M., Canutescu, A., Dunbrack, R., Adams, P.D., Marmorstein, R., 2006. Structure of a human ASF1a–HIRA complex and insights into specificity of histone chaperone complex assembly. Nat Struct Mol Biol 13, 921–929. https://doi.org/10.1038/nsmb1147
Tardat, M., Brustel, J., Kirsh, O., Lefevbre, C., Callanan, M., Sardet, C., Julien, E., 2010. The histone H4 Lys 20 methyltransferase PR-Set7 regulates replication origins in mammalian cells. Nat. Cell Biol. 12, 1086–1093. https://doi.org/10.1038/ncb2113
Tatavosian, R., Kent, S., Brown, K., Yao, T., Duc, H.N., Huynh, T.N., Zhen, C.Y., Ma, B., Wang, H., Ren, X., 2019. Nuclear condensates of the Polycomb protein chromobox 2 (CBX2) assemble through phase separation. J. Biol. Chem. 294, 1451–1463. https://doi.org/10.1074/jbc.RA118.006620
Tavares-Cadete, F., Norouzi, D., Dekker, B., Liu, Y., Dekker, J., 2020. Multi-contact 3C reveals that the human genome during interphase is largely not entangled. Nat. Struct. Mol. Biol. https://doi.org/10.1038/s41594-020-0506-5
Taylor, J.H., 1977. Increase in DNA replication sites in cells held at the beginning of S phase. Chromosoma 62, 291–300. https://doi.org/10.1007/BF00327029
Teng, Y.-C., Sundaresan, A., O'Hara, R., Gant, V.U., Li, M., Martire, S., Warshaw, J.N., Basu, A., Banaszynski, L.A., 2021. ATRX promotes heterochromatin formation to protect cells from G-quadruplex DNA-mediated stress. Nat. Commun. 12, 3887. https://doi.org/10.1038/s41467-021-24206-5
Thakar, A., Gupta, P., Ishibashi, T., Finn, R., Silva-Moreno, B., Uchiyama, S., Fukui, K., Tomschik, M., Ausio, J., Zlatanova, J., 2009. H2A.Z and H3.3 Histone Variants Affect Nucleosome Structure: Biochemical and Biophysical Studies. Biochemistry 48, 10852–10857. https://doi.org/10.1021/bi901129e
Thiecke, M.J., Wutz, G., Muhar, M., Tang, W., Bevan, S., Malysheva, V., Stocsits, R., Neumann, T., Zuber, J., Fraser, P., Schoenfelder, S., Peters, J.-M., Spivakov, M., 2020. Cohesin-Dependent and -Independent Mechanisms Mediate Chromosomal Contacts between Promoters and Enhancers. Cell Rep. 32, 107929. https://doi.org/10.1016/j.celrep.2020.107929
Tolhuis, B., Palstra, R.-J., Splinter, E., Grosveld, F., de Laat, W., 2002. Looping and Interaction between Hypersensitive Sites in the Active ℵ-globin Locus. Mol. Cell.
Torigoe, S.E., Urwin, D.L., Ishii, H., Smith, D.E., Kadonaga, J.T., 2011. Identification of a Rapidly Formed Nonnucleosomal Histone-DNA Intermediate that Is Converted into Chromatin by ACF. Mol. Cell 43, 638–648. https://doi.org/10.1016/j.molcel.2011.07.017
Torné, J., Orsi, G.A., Ray-Gallet, D., Almouzni, G., 2018. Imaging Newly Synthesized and Old Histone Variant Dynamics Dependent on Chaperones Using the SNAP-Tag System, in: Orsi, G.A., Almouzni, G. (Eds.), Histone Variants. Springer New York, New York, NY, pp. 207–221. https://doi.org/10.1007/978-1-4939-8663-7_11
Torné, J., Ray-Gallet, D., Boyarchuk, E., Garnier, M., Le Baccon, P., Coulon, A., Orsi, G.A., Almouzni, G., 2020. Two HIRA-dependent pathways mediate H3.3 de novo deposition and recycling during transcription. Nat. Struct. Mol. Biol. 27, 1057–1068. https://doi.org/10.1038/s41594-020-0492-7
Torres-Padilla, M.-E., Bannister, A.J., Hurd, P.J., Kouzarides, T., Zernicka-Goetz, M., 2006. Dynamic distribution of the replacement histone variant H3.3 in the mouse oocyte and preimplantation embryos. Int. J. Dev. Biol. 50. https://doi.org/10.1387/ijdb.052073mt
Tran, V., Lim, C., Xie, J., Chen, X., 2012. Asymmetric Division of Drosophila Male Germline Stem Cell Shows Asymmetric Histone Distribution. Science 338, 679–682. https://doi.org/10.1126/science.1226028
Tropberger, P., Pott, S., Keller, C., Kamieniarz-Gdula, K., Caron, M., Richter, F., Li, G., Mittler, G., Liu, E.T., Bühler, M., Margueron, R., Schneider, R., 2013. Regulation of Transcription through Acetylation of H3K122 on the Lateral Surface of the Histone Octamer. Cell 152, 859–872. https://doi.org/10.1016/j.cell.2013.01.032
Tsunaka, Y., Fujiwara, Y., Oyama, T., Hirose, S., Morikawa, K., 2016. Integrated molecular mechanism directing nucleosome reorganization by human FACT. Genes Dev. 30, 673–686. https://doi.org/10.1101/gad.274183.115
Tyler, J.K., Adams, C.R., Chen, S.-R., Kobayashi, R., Kamakaka, R.T., Kadonaga, J.T., 1999. The RCAF complex mediates chromatin assembly during DNA replication and repair. Nature 402, 555–560. https://doi.org/10.1038/990147
Udugama, M., M. Chang, F.T., Chan, F.L., Tang, M.C., Pickett, H.A., R. McGhie, J.D., Mayne, L., Collas, P., Mann, J.R., Wong, L.H., 2015. Histone variant H3.3 provides the heterochromatic H3 lysine 9 tri-methylation mark at telomeres. Nucleic Acids Res. 43, 10227–10237. https://doi.org/10.1093/nar/gkv847
Udugama, M., Vinod, B., Chan, F.L., Hii, L., Garvie, A., Collas, P., Kalitsis, P., Steer, D., Das, P.P., Tripathi, P., Mann, J.R., Voon, H.P.J., Wong, L.H., 2022. Histone H3.3 phosphorylation promotes heterochromatin formation by inhibiting H3K9/K36 histone demethylase. Nucleic Acids Res. gkac259. https://doi.org/10.1093/nar/gkac259

Ueda, J., Harada, A., Urahama, T., Machida, S., Maehara, K., Hada, M., Makino, Y., Nogami, J., Horikoshi, N., Osakabe, A., Taguchi, H., Tanaka, H., Tachiwana, H., Yao, T., Yamada, M., Iwamoto, T., Isotani, A., Ikawa, M., Tachibana, T., Okada, Y., Kimura, H., Ohkawa, Y., Kurumizaka, H., Yamagata, K., 2017. Testis-Specific Histone Variant H3t Gene Is Essential for Entry into Spermatogenesis. Cell Rep. 18, 593–600. https://doi.org/10.1016/j.celrep.2016.12.065
Ulianov, S.V., Khrameeva, E.E., Gavrilov, A.A., Flyamer, I.M., Kos, P., Mikhaleva, E.A., Penin, A.A., Logacheva, M.D., Imakaev, M.V., Chertovich, A., Gelfand, M.S., Shevelyov, Y.Y., Razin, S.V., 2016. Active chromatin and transcription play a key role in chromosome partitioning into topologically associating domains. Genome Res. 26, 70–84. https://doi.org/10.1101/gr.196006.115
Urahama, T., Harada, A., Maehara, K., Horikoshi, N., Sato, K., Sato, Y., Shiraishi, K., Sugino, N., Osakabe, A., Tachiwana, H., Kagawa, W., Kimura, H., Ohkawa, Y., Kurumizaka, H., 2016. Histone H3.5 forms an unstable nucleosome and accumulates around transcription start sites in human testis. Epigenetics Chromatin 9, 2. https://doi.org/10.1186/s13072-016-0051-y
Urban, J.A., Ranjan, R., Chen, X., 2022. Asymmetric Histone Inheritance: Establishment, Recognition, and Execution. Annu. Rev. Genet. 56, 113–143. https://doi.org/10.1146/annurev-genet-072920-125226
Valton, A.-L., Hassan-Zadeh, V., Lema, I., Boggetto, N., Alberti, P., Saintome, C., Riou, J.-F., Prioleau, M.-N., 2014. G4 motifs affect origin positioning and efficiency in two vertebrate replicators. EMBO J. 33, 732–746. https://doi.org/10.1002/embj.201387506
Valton, A.-L., Venev, S.V., Mair, B., Khokhar, E.S., Tong, A.H.Y., Usaj, M., Chan, K., Pai, A.A., Moffat, J., Dekker, J., 2022. A cohesin traffic pattern genetically linked to gene regulation. Nat. Struct. Mol. Biol. https://doi.org/10.1038/s41594-022-00890-9
van der Ploeg, M., 2000. Cytochemical nucleic acid research during the twentieth century. Eur. J. Histochem. EJH 44, 7–42.
Van Holde, K.E., 1989. Chromatin, Springer Series in Molecular Biology. Springer, New York, NY. https://doi.org/10.1007/978-1-4612-3490-6
Van Hooser, A.A., Ouspenski, I.I., Gregson, H.C., Starr, D.A., Yen, T.J., Goldberg, M.L., Yokomori, K., Earnshaw, W.C., Sullivan, K.F., Brinkley, B.R., 2001. Specification of kinetochore-forming chromatin by the histone H3 variant CENP-A. J. Cell Sci. 114, 3529–3542. https://doi.org/10.1242/jcs.114.19.3529
van Koningsbruggen, S., Gierliński, M., Schofield, P., Martin, D., Barton, G.J., Ariyurek, Y., den Dunnen, J.T., Lamond, A.I., 2010. High-Resolution Whole-Genome Sequencing Reveals That Specific Chromatin Domains from Most Human Chromosomes Associate with Nucleoli. Mol. Biol. Cell 21, 3735–3748. https://doi.org/10.1091/mbc.e10-06-0508
Varshavsky, A.J., Sundin, O.H., Bohn, M.J., 1978. SV40 viral minichromosome: preferential exposure of the origin of replication as probed by restriction endonucleases. Nucleic Acids Res. 5, 3469–3478. https://doi.org/10.1093/nar/5.10.3469
Vashee, S., Cvetic, C., Lu, W., Simancek, P., Kelly, T.J., Walter, J.C., 2003. Sequence-independent DNA binding and replication initiation by the human origin recognition complex. Genes Dev. 17, 1894–1908. https://doi.org/10.1101/gad.1084203
Vashee, S., Simancek, P., Challberg, M.D., Kelly, T.J., 2001. Assembly of the Human Origin Recognition Complex. J. Biol. Chem. 276, 26666–26673. https://doi.org/10.1074/jbc.M102493200
Vasseur, P., Tonazzini, S., Ziane, R., Camasses, A., Rando, O.J., Radman-Livaja, M., 2016. Dynamics of Nucleosome Positioning Maturation following Genomic Replication. Cell Rep. 16, 2651–2665. https://doi.org/10.1016/j.celrep.2016.07.083
Vastenhouw, N.L., Schier, A.F., 2012. Bivalent histone modifications in early embryogenesis. Curr. Opin. Cell Biol. 24, 374–386. https://doi.org/10.1016/j.ceb.2012.03.009
Venneti, S., Garimella, M.T., Sullivan, L.M., Martinez, D., Huse, J.T., Heguy, A., Santi, M., Thompson, C.B., Judkins, A.R., 2013. Evaluation of Histone 3 Lysine 27 Trimethylation (H3K27me3) and Enhancer of Zest 2 (EZH2) in Pediatric Glial and Glioneuronal Tumors Shows Decreased H3K27me3 in H3F3A K27M Mutant Glioblastomas. Brain Pathol. 23, 558–564. https://doi.org/10.1111/bpa.12042
Venter, J.C., Adams, M.D., Myers, E.W., Li, P.W., Mural, R.J., Sutton, G.G., Smith, H.O., Yandell, M., Evans, C.A., Holt, R.A., Gocayne, J.D., Amanatides, P., Ballew, R.M., Huson, D.H., Wortman, J.R., Zhang, Q., Kodira, C.D., Zheng, X.H., Chen, L., Skupski, M., Subramanian, G., Thomas, P.D., Zhang, J., Gabor Miklos, G.L., Nelson, C., Broder, S., Clark, A.G., Nadeau, J., McKusick, V.A., Zinder, N., Levine, A.J., Roberts, R.J., Simon, M., Slayman, C., Hunkapiller, M., Bolanos, R., Delcher, A., Dew, I., Fasulo, D., Flanigan, M., Florea, L., Halpern, A., Hannenhalli, S., Kravitz, S., Levy, S., Mobarry, C., Reinert, K., Remington, K., Abu-Threideh, J., Beasley, E., Biddick, K., Bonazzi, V., Brandon, R., Cargill, M., Chandramouliswaran, I., Charlab, R., Chaturvedi, K., Deng, Z., Francesco, V.D., Dunn, P., Eilbeck, K., Evangelista, C., Gabrielian, A.E., Gan, W., Ge, W., Gong, F., Gu, Z., Guan, P., Heiman, T.J., Higgins, M.E., Ji, R.-R., Ke, Z., Ketchum, K.A., Lai, Z., Lei, Y., Li, Z., Li, J., Liang, Y., Lin, X., Lu, F., Merkulov, G.V., Milshina, N., Moore, H.M., Naik, A.K., Narayan, V.A., Neelam, B., Nusskern, D., Rusch, D.B., Salzberg, S., Shao, W., Shue, B., Sun, J., Wang, Z.Y., Wang, A., Wang, X., Wang, J., Wei, M.-H.,

Wides, R., Xiao, C., Yan, C., Yao, A., Ye, J., Zhan, M., Zhang, W., Zhang, H., Zhao, Q., Zheng, L., Zhong, F., Zhong, W., Zhu, S.C., Zhao, S., Gilbert, D., Baumhueter, S., Spier, G., Carter, C., Cravchik, A., Woodage, T., Ali, F., An, H., Awe, A., Baldwin, D., Baden, H., Barnstead, M., Barrow, I., Beeson, K., Busam, D., Carver, A., Center, A., Cheng, M.L., Curry, L., Danaher, S., Davenport, L., Desilets, R., Dietz, S., Dodson, K., Doup, L., Ferriera, S., Garg, N., Gluecksmann, A., Hart, B., Haynes, J., Haynes, C., Heiner, C., Hladun, S., Hostin, D., Houck, J., Howland, T., Ibegwam, C., Johnson, J., Kalush, F., Kline, L., Koduru, S., Love, A., Mann, F., May, D., McCawley, S., McIntosh, T., McMullen, I., Moy, M., Moy, L., Murphy, B., Nelson, K., Pfannkoch, C., Pratts, E., Puri, V., Qureshi, H., Reardon, M., Rodriguez, R., Rogers, Y.-H., Romblad, D., Ruhfel, B., Scott, R., Sitter, C., Smallwood, M., Stewart, E., Strong, R., Suh, E., Thomas, R., Tint, N.N., Tse, S., Vech, C., Wang, G., Wetter, J., Williams, S., Williams, M., Windsor, S., Winn-Deen, E., Wolfe, K., Zaveri, J., Zaveri, K., Abril, J.F., Guigó, R., Campbell, M.J., Sjolander, K.V., Karlak, B., Kejariwal, A., Mi, H., Lazareva, B., Hatton, T., Narechania, A., Diemer, K., Muruganujan, A., Guo, N., Sato, S., Bafna, V., Istrail, S., Lippert, R., Schwartz, R., Walenz, B., Yooseph, S., Allen, D., Basu, A., Baxendale, J., Blick, L., Caminha, M., Carnes-Stine, J., Caulk, P., Chiang, Y.-H., Coyne, M., Dahlke, C., Mays, A.D., Dombroski, M., Donnelly, M., Ely, D., Esparham, S., Fosler, C., Gire, H., Glanowski, S., Glasser, K., Glodek, A., Gorokhov, M., Graham, K., Gropman, B., Harris, M., Heil, J., Henderson, S., Hoover, J., Jennings, D., Jordan, C., Jordan, J., Kasha, J., Kagan, L., Kraft, C., Levitsky, A., Lewis, M., Liu, X., Lopez, J., Ma, D., Majoros, W., McDaniel, J., Murphy, S., Newman, M., Nguyen, T., Nguyen, N., Nodell, M., Pan, S., Peck, J., Peterson, M., Rowe, W., Sanders, R., Scott, J., Simpson, M., Smith, T., Sprague, A., Stockwell, T., Turner, R., Venter, E., Wang, M., Wen, M., Wu, D., Wu, M., Xia, A., Zandieh, A., Zhu, X., 2001. The Sequence of the Human Genome. Science 291, 1304–1351. https://doi.org/10.1126/science.1058040

Vermeulen, M., Eberl, H.C., Matarese, F., Marks, H., Denissov, S., Butter, F., Lee, K.K., Olsen, J.V., Hyman, A.A., Stunnenberg, H.G., Mann, M., 2010. Quantitative Interaction Proteomics and Genome-wide Profiling of Epigenetic Histone Marks and Their Readers. Cell 142, 967–980. https://doi.org/10.1016/j.cell.2010.08.020

Vertii, A., Ou, J., Yu, J., Yan, A., Pagès, H., Liu, H., Zhu, L.J., Kaufman, P.D., 2019. Two contrasting classes of nucleolus-associated domains in mouse fibroblast heterochromatin. Genome Res. 29, 1235–1249. https://doi.org/10.1101/gr.247072.118

Vogelauer, M., Rubbi, L., Lucas, I., Brewer, B.J., Grunstein, M., 2002. Histone Acetylation Regulates the Time of Replication Origin Firing. Mol. Cell 10, 1223–1233. https://doi.org/10.1016/S1097-2765(02)00702-5

Volpi, E.V., Chevret, E., Jones, T., Vatcheva, R., Williamson, J., Beck, S., Campbell, R.D., Goldsworthy, M., Powis, S.H., Ragoussis, J., Trowsdale, J., Sheer, D., 2000. Large-scale chromatin organization of the major histocompatibility complex and other regions of human chromosome 6 and its response to interferon in interphase nuclei. J. Cell Sci. 113, 1565–1576. https://doi.org/10.1242/jcs.113.9.1565

Voong, L.N., Xi, L., Sebeson, A.C., Xiong, B., Wang, J.-P., Wang, X., 2016. Insights into Nucleosome Organization in Mouse Embryonic Stem Cells through Chemical Mapping. Cell 167, 1555-1570.e15. https://doi.org/10.1016/j.cell.2016.10.049

Voong, L.N., Xi, L., Wang, J.-P., Wang, X., 2017. Genome-wide Mapping of the Nucleosome Landscape by Micrococcal Nuclease and Chemical Mapping. Trends Genet. 33, 495–507. https://doi.org/10.1016/j.tig.2017.05.007

Vouzas, A.E., Gilbert, D.M., 2021. Mammalian DNA Replication Timing. DNA Replication 23.

Waddington, C.H., 1957. The Strategy of the Genes: A Discussion of Some Aspects of Theoretical Biology. George Allen and Unwin, London.

Waddington, C.H., 1942. Canalization of Development and the Inheritance of Acquired Characters. Nature 150, 563–565. https://doi.org/10.1038/150563a0

Waldeyer, W., 1888. Ueber Karyokinese und ihre Beziehungen zu den Befruchtungsvorgängen. Arch. Für Mikrosk. Anat. 32, 1–122. https://doi.org/10.1007/BF02956988

Wang, C., Liu, X., Gao, Y., Yang, L., Li, C., Liu, W., Chen, C., Kou, X., Zhao, Y., Chen, J., Wang, Y., Le, R., Wang, H., Duan, T., Zhang, Y., Gao, S., 2018. Reprogramming of H3K9me3-dependent heterochromatin during mammalian embryo development. Nat. Cell Biol. 20, 620–631. https://doi.org/10.1038/s41556-018-0093-4

Wang, H., Fan, Z., Shliaha, P.V., Miele, M., Hendrickson, R.C., Jiang, X., Helin, K., 2023. H3K4me3 regulates RNA polymerase II promoter-proximal pause-release. Nature 615, 339–348. https://doi.org/10.1038/s41586-023-05780-8

Wang, I.-C., Chen, Y.-J., Hughes, D., Petrovic, V., Major, M.L., Park, H.J., Tan, Y., Ackerson, T., Costa, R.H., 2005. Forkhead Box M1 Regulates the Transcriptional Network of Genes Essential for Mitotic Progression and Genes Encoding the SCF (Skp2-Cks1) Ubiquitin Ligase. Mol. Cell. Biol. 25, 10875–10894. https://doi.org/10.1128/MCB.25.24.10875-10894.2005

Wang, J., Liu, X., Dou, Z., Chen, L., Jiang, H., Fu, C., Fu, G., Liu, D., Zhang, J., Zhu, T., Fang, J., Zang, J., Cheng, J., Teng, M., Ding, X., Yao, X., 2014. Mitotic Regulator Mis18β Interacts with and Specifies the Centromeric Assembly of Molecular Chaperone Holliday Junction Recognition Protein (HJURP) *. J. Biol. Chem. 289, 8326–8336. https://doi.org/10.1074/jbc.M113.529958

Wang, L., Lin, C.-M., Brooks, S., Cimbora, D., Groudine, M., Aladjem, M.I., 2004. The Human β-Globin Replication Initiation Region Consists of Two Modular Independent Replicators. Mol. Cell. Biol. 24, 3373–3386. https://doi.org/10.1128/MCB.24.8.3373-3386.2004
Wang, P., Yang, W., Zhao, S., Nashun, B., 2021. Regulation of chromatin structure and function: insights into the histone chaperone FACT. Cell Cycle 20, 465–479. https://doi.org/10.1080/15384101.2021.1881726
Wang, Q., Sun, Q., Czajkowsky, D.M., Shao, Z., 2018. Sub-kb Hi-C in D. melanogaster reveals conserved characteristics of TADs between insect and mammalian cells. Nat. Commun. 9, 188. https://doi.org/10.1038/s41467-017-02526-9
Wang, S., Su, J.-H., Beliveau, B.J., Bintu, B., Moffitt, J.R., Wu, C., Zhuang, X., 2016. Spatial organization of chromatin domains and compartments in single chromosomes 6.
Wang, W., Klein, K.N., Proesmans, K., Yang, H., Marchal, C., Zhu, X., Borrman, T., Hastie, A., Weng, Z., Bechhoefer, J., Chen, C.-L., Gilbert, D.M., Rhind, N., 2021. Genome-wide mapping of human DNA replication by optical replication mapping supports a stochastic model of eukaryotic replication. Mol. Cell 81, 2975-2988.e6. https://doi.org/10.1016/j.molcel.2021.05.024
Wang, X., Wang, L., Dou, J., Yu, T., Cao, P., Fan, N., Borjigin, U., Nashun, B., 2021. Distinct role of histone chaperone Asf1a and Asf1b during fertilization and pre-implantation embryonic development in mice. Epigenetics & Chromatin 14, 55. https://doi.org/10.1186/s13072-021-00430-7
Wang, Y., Khan, A., Marks, A.B., Smith, O.K., Giri, S., Lin, Y.-C., Creager, R., MacAlpine, D.M., Prasanth, K.V., Aladjem, M.I., Prasanth, S.G., 2017. Temporal association of ORCA/LRWD1 to late-firing origins during G1 dictates heterochromatin replication and organization. Nucleic Acids Res. 45, 2490–2502. https://doi.org/10.1093/nar/gkw1211
Wang, Z., Zang, C., Rosenfeld, J.A., Schones, D.E., Barski, A., Cuddapah, S., Cui, K., Roh, T.-Y., Peng, W., Zhang, M.Q., Zhao, K., 2008. Combinatorial patterns of histone acetylations and methylations in the human genome. Nat. Genet. 40, 897–903. https://doi.org/10.1038/ng.154
Wani, A.H., Boettiger, A.N., Schorderet, P., Ergun, A., Münger, C., Sadreyev, R.I., Zhuang, X., Kingston, R.E., Francis, N.J., 2016. Chromatin topology is coupled to Polycomb group protein subnuclear organization. Nat. Commun. 7, 10291. https://doi.org/10.1038/ncomms10291
Watson, D., Crick, F.H.C., 1953. Molecular Structure of Nucleic Acids: A Structure for Deoxyribose Nucleic Acid. Nature 171, 737–738. https://doi.org/10.1038/171737a0
Weber, A.R., Krawczyk, C., Robertson, A.B., Kuśnierczyk, A., Vågbø, C.B., Schuermann, D., Klungland, A., Schär, P., 2016. Biochemical reconstitution of TET1–TDG–BER-dependent active DNA demethylation reveals a highly coordinated mechanism. Nat. Commun. 7, 10806. https://doi.org/10.1038/ncomms10806
Wen, B., Wu, H., Shinkai, Y., Irizarry, R.A., Feinberg, A.P., 2009. Large histone H3 lysine 9 dimethylated chromatin blocks distinguish differentiated from embryonic stem cells. Nat. Genet. 41, 246–250. https://doi.org/10.1038/ng.297
Wen, H., Li, Y., Xi, Y., Jiang, S., Stratton, S., Peng, D., Tanaka, K., Ren, Y., Xia, Z., Wu, J., Li, B., Barton, M.C., Li, W., Li, H., Shi, X., 2014. ZMYND11 links histone H3.3K36me3 to transcription elongation and tumour suppression. Nature 508, 263–268. https://doi.org/10.1038/nature13045
Wen, Z., Zhang, L., Ruan, H., Li, G., 2020. Histone variant H2A.Z regulates nucleosome unwrapping and CTCF binding in mouse ES cells. Nucleic Acids Res. gkaa360. https://doi.org/10.1093/nar/gkaa360
Westhorpe, F.G., Fuller, C.J., Straight, A.F., 2015. A cell-free CENP-A assembly system defines the chromatin requirements for centromere maintenance. J. Cell Biol. 209, 789–801. https://doi.org/10.1083/jcb.201503132
Weth, O., Paprotka, C., Günther, K., Schulte, A., Baierl, M., Leers, J., Galjart, N., Renkawitz, R., 2014. CTCF induces histone variant incorporation, erases the H3K27me3 histone mark and opens chromatin. Nucleic Acids Res. 42, 11941–11951. https://doi.org/10.1093/nar/gku937
White, E.J., Emanuelsson, O., Scalzo, D., Royce, T., Kosak, S., Oakeley, E.J., Weissman, S., Gerstein, M., Groudine, M., Snyder, M., Schübeler, D., 2004. DNA replication-timing analysis of human chromosome 22 at high resolution and different developmental states. Proc. Natl. Acad. Sci. 101, 17771–17776. https://doi.org/10.1073/pnas.0408170101
Wiedemann, S.M., Mildner, S.N., Bönisch, C., Israel, L., Maiser, A., Matheisl, S., Straub, T., Merkl, R., Leonhardt, H., Kremmer, E., Schermelleh, L., Hake, S.B., 2010. Identification and characterization of two novel primate-specific histone H3 variants, H3.X and H3.Y. J. Cell Biol. 190, 777–791. https://doi.org/10.1083/jcb.201002043
Wijchers, P.J., Krijger, P.H.L., Geeven, G., Zhu, Y., Denker, A., Verstegen, M.J.A.M., Valdes-Quezada, C., Vermeulen, C., Janssen, M., Teunissen, H., Anink-Groenen, L.C.M., Verschure, P.J., De Laat, W., 2016. Cause and Consequence of Tethering a SubTAD to Different Nuclear Compartments. Mol. Cell 61, 461–473. https://doi.org/10.1016/j.molcel.2016.01.001
Wilkins, B.J., Rall, N.A., Ostwal, Y., Kruitwagen, T., Hiragami-Hamada, K., Winkler, M., Barral, Y., Fischle, W., Neumann, H., 2014. A Cascade of Histone Modifications Induces Chromatin Condensation in Mitosis. Science 343, 77–80. https://doi.org/10.1126/science.1244508

Wilkins, M.H.F., Stokes, A.R., Wilson, H.R., 1953. Molecular Structure of Nucleic Acids: Molecular Structure of Deoxypentose Nucleic Acids. Nature 171, 738–740. https://doi.org/10.1038/171738a0
Williams, R.R.E., Broad, S., Sheer, D., Ragoussis, J., 2002. Subchromosomal Positioning of the Epidermal Differentiation Complex (EDC) in Keratinocyte and Lymphoblast Interphase Nuclei. Exp. Cell Res. 272, 163–175. https://doi.org/10.1006/excr.2001.5400
Witt, O., Albig, W., Doenecke, D., 1996. Testis-Specific Expression of a Novel Human H3 Histone Gene. Exp. Cell Res. 229, 301–306. https://doi.org/10.1006/excr.1996.0375
Wong, L.H., McGhie, J.D., Sim, M., Anderson, M.A., Ahn, S., Hannan, R.D., George, A.J., Morgan, K.A., Mann, J.R., Choo, K.H.A., 2010. ATRX interacts with H3.3 in maintaining telomere structural integrity in pluripotent embryonic stem cells. Genome Res. 20, 351–360. https://doi.org/10.1101/gr.101477.109
Wong, L.H., Ren, H., Williams, E., McGhie, J., Ahn, S., Sim, M., Tam, A., Earle, E., Anderson, M.A., Mann, J., Choo, K.H.A., 2009. Histone H3.3 incorporation provides a unique and functionally essential telomeric chromatin in embryonic stem cells. Genome Res. 19, 404–414. https://doi.org/10.1101/gr.084947.108
Wong, P.G., Winter, S.L., Zaika, E., Cao, T.V., Oguz, U., Koomen, J.M., Hamlin, J.L., Alexandrow, M.G., 2011. Cdc45 Limits Replicon Usage from a Low Density of preRCs in Mammalian Cells. PLOS ONE 6, e17533. https://doi.org/10.1371/journal.pone.0017533
Woodcock, C.L.F., Safer, J.P., Stanchfield, J.E., 1976. Structural repeating units in chromatin: I. Evidence for their general occurrence. Exp. Cell Res. 97, 101–110. https://doi.org/10.1016/0014-4827(76)90659-5
Woodward, A.M., Göhler, T., Luciani, M.G., Oehlmann, M., Ge, X., Gartner, A., Jackson, D.A., Blow, J.J., 2006. Excess Mcm2–7 license dormant origins of replication that can be used under conditions of replicative stress. J. Cell Biol. 173, 673–683. https://doi.org/10.1083/jcb.200602108
Wooten, M., Snedeker, J., Nizami, Z.F., Yang, X., Ranjan, R., Urban, E., Kim, J.M., Gall, J., Xiao, J., Chen, X., 2019. Asymmetric histone inheritance via strand-specific incorporation and biased replication fork movement. Nat. Struct. Mol. Biol. 26, 732–743. https://doi.org/10.1038/s41594-019-0269-z
Worcel, A., Han, S., Wong, M.L., 1978. Assembly of newly replicated chromatin. Cell 15, 969–977. https://doi.org/10.1016/0092-8674(78)90280-5
Wu, C., 1984. Two protein-binding sites in chromatin implicated in the activation of heat-shock genes. Nature 309, 229–234. https://doi.org/10.1038/309229a0
Wu, C., 1980. The 5′ ends of Drosophila heat shock genes in chromatin are hypersensitive to DNase I. Nature 286, 854–860. https://doi.org/10.1038/286854a0
Wu, J.-R., Gilbert, D.M., 1996. A Distinct G1 Step Required to Specify the Chinese Hamster DHFR Replication Origin. Science 271, 1270–1272. https://doi.org/10.1126/science.271.5253.1270
Wu, P.-Y.J., Nurse, P., 2009. Establishing the Program of Origin Firing during S Phase in Fission Yeast. Cell 136, 852–864. https://doi.org/10.1016/j.cell.2009.01.017
Wu, R.S., Bonner, M., 1982. Patterns of Histone Variant Synthesis Can Distinguish GO from Gl Cells 8.
Wu, R.S., Bonner, W.M., 1981. Separation of basal histone synthesis from S-phase histone synthesis in dividing cells. Cell 27, 321–330. https://doi.org/10.1016/0092-8674(81)90415-3
Wu, R.S., Tsai, S., Bonner, W.M., 1983. Changes in histone H3 composition and synthesis pattern during lymphocyte activation. Biochemistry 22, 3868–3873. https://doi.org/10.1021/bi00285a023
Wutz, G., Várnai, C., Nagasaka, K., Cisneros, D.A., Stocsits, R.R., Tang, W., Schoenfelder, S., Jessberger, G., Muhar, M., Hossain, M.J., Walther, N., Koch, B., Kueblbeck, M., Ellenberg, J., Zuber, J., Fraser, P., Peters, J., 2017. Topologically associating domains and chromatin loops depend on cohesin and are regulated by CTCF, WAPL, and PDS5 proteins. EMBO J. 36, 3573–3599. https://doi.org/10.15252/embj.201798004
Xia, W., Jiao, J., 2017. Histone variant H3.3 orchestrates neural stem cell differentiation in the developing brain. Cell Death Differ. 24, 1548–1563. https://doi.org/10.1038/cdd.2017.77
Xiang, W., Roberti, M.J., Hériché, J.-K., Huet, S., Alexander, S., Ellenberg, J., 2018. Correlative live and super-resolution imaging reveals the dynamic structure of replication domains. J. Cell Biol. 217, 1973–1984. https://doi.org/10.1083/jcb.201709074
Xie, L., Dong, P., Qi, Y., Hsieh, T.-H.S., English, B.P., Jung, S., Chen, X., De Marzio, M., Casellas, R., Chang, H.Y., Zhang, B., Tjian, R., Liu, Z., 2022. BRD2 compartmentalizes the accessible genome. Nat. Genet. 54, 481–491. https://doi.org/10.1038/s41588-022-01044-9
Xiong, C., Wen, Z., Yu, J., Chen, J., Liu, C.-P., Zhang, X., Chen, P., Xu, R.-M., Li, G., 2018. UBN1/2 of HIRA complex is responsible for recognition and deposition of H3.3 at cis-regulatory elements of genes in mouse ES cells. BMC Biol. 16, 110. https://doi.org/10.1186/s12915-018-0573-9
Xu, D., Muniandy, P., Leo, E., Yin, J., Thangavel, S., Shen, X., Ii, M., Agama, K., Guo, R., Fox III, D., Meetei, A.R., Wilson, L., Nguyen, H., Weng, N., Brill, S.J., Li, L., Vindigni, A., Pommier, Y., Seidman, M., Wang, W., 2010. Rif1 provides a new DNA-binding interface for the Bloom syndrome complex to maintain normal replication. EMBO J. 29, 3140–3155. https://doi.org/10.1038/emboj.2010.186

Xu, J., Ma, H., Jin, J., Uttam, S., Fu, R., Huang, Y., Liu, Y., 2018. Super-Resolution Imaging of Higher-Order Chromatin Structures at Different Epigenomic States in Single Mammalian Cells. Cell Rep. 24, 873–882. https://doi.org/10.1016/j.celrep.2018.06.085
Xu, L., Blackburn, E.H., 2004. Human Rif1 protein binds aberrant telomeres and aligns along anaphase midzone microtubules. J. Cell Biol. 167, 819–830. https://doi.org/10.1083/jcb.200408181
Xu, M., Long, C., Chen, X., Huang, C., Chen, S., Zhu, B., 2010. Partitioning of Histone H3-H4 Tetramers During DNA Replication-Dependent Chromatin Assembly. Science 328, 94–98. https://doi.org/10.1126/science.1178994
Xu, M., Wang, W., Chen, S., Zhu, B., 2012. A model for mitotic inheritance of histone lysine methylation. EMBO Rep. 13, 60–67. https://doi.org/10.1038/embor.2011.206
Xu, X., Duan, S., Hua, X., Li, Z., He, R., Zhaang, Z., 2022. Stable inheritance of H3.3-containing nucleosomes during mitotic cell divisions. Nat. Commun. 13, 2514. https://doi.org/10.1038/s41467-022-30298-4
Xue, Y., Gibbons, R., Yan, Z., Yang, D., McDowell, T.L., Sechi, S., Qin, J., Zhou, S., Higgs, D., Wang, W., 2003. The ATRX syndrome protein forms a chromatin-remodeling complex with Daxx and localizes in promyelocytic leukemia nuclear bodies. Proc. Natl. Acad. Sci. 100, 10635–10640. https://doi.org/10.1073/pnas.1937626100
Yadav, T., Quivy, J.-P., Almouzni, G., 2018. Chromatin plasticity: A versatile landscape that underlies cell fate and identity. Science 361, 1332–1336. https://doi.org/10.1126/science.aat8950
Yamasu, R., Senshu, T., 1990. Conservative Segregation of Tetrameric Units of H3 and H4 Histones during Nucleosome Replication. J Biochem 107.
Yamazaki, S., Ishii, A., Kanoh, Y., Oda, M., Nishito, Y., Masai, H., 2012. Rif1 regulates the replication timing domains on the human genome: Rif1 regulates the replication timing domains. EMBO J. 31, 3667–3677. https://doi.org/10.1038/emboj.2012.180
Yang, X., Khosravi-Far, R., Chang, H.Y., Baltimore, D., 1997. Daxx, a Novel Fas-Binding Protein That Activates JNK and Apoptosis. Cell 89, 1067–1076. https://doi.org/10.1016/S0092-8674(00)80294-9
Yang, Y., Zhang, L., Xiong, C., Chen, J., Wang, L., Wen, Z., Yu, J., Chen, P., Xu, Y., Jin, J., Cai, Y., Li, G., 2021. HIRA complex presets transcriptional potential through coordinating depositions of the histone variants H3.3 and H2A.Z on the poised genes in mESCs. Nucleic Acids Res. gkab1221. https://doi.org/10.1093/nar/gkab1221
Ye, Q., Callebaut, I., Pezhman, A., Courvalin, J.-C., Worman, H.J., 1997. Domain-specific Interactions of Human HP1-type Chromodomain Proteins and Inner Nuclear Membrane Protein LBR. J. Biol. Chem. 272, 14983–14989. https://doi.org/10.1074/jbc.272.23.14983
Ye, X., Franco, A.A., Santos, H., Nelson, D.M., Kaufman, P.D., Adams, P.D., 2003. Defective S Phase Chromatin Assembly Causes DNA Damage, Activation of the S Phase Checkpoint, and S Phase Arrest. Mol. Cell 11, 341–351. https://doi.org/10.1016/S1097-2765(03)00037-6
Yeeles, J.T.P., Deegan, T.D., Janska, A., Early, A., Diffley, J.F.X., 2015. Regulated eukaryotic DNA replication origin firing with purified proteins. Nature 519, 431–435. https://doi.org/10.1038/nature14285
Yoh, S.M., Lucas, J.S., Jones, K.A., 2008. The Iws1:Spt6:CTD complex controls cotranscriptional mRNA biosynthesis and HYPB/Setd2-mediated histone H3K36 methylation. Genes Dev. 22, 3422–3434. https://doi.org/10.1101/gad.1720008
Yu, C., Gan, H., Serra-Cardona, A., Zhang, L., Gan, S., Sharma, S., Johansson, E., Chabes, A., Xu, R.-M., Zhang, Z., 2018. A mechanism for preventing asymmetric histone segregation onto replicating DNA strands. Science 361, 1386–1389. https://doi.org/10.1126/science.aat8849
Yuan, Z., Riera, A., Bai, L., Sun, J., Nandi, S., Spanos, C., Chen, Z.A., Barbon, M., Rappsilber, J., Stillman, B., Speck, C., Li, H., 2017. Structural basis of Mcm2–7 replicative helicase loading by ORC–Cdc6 and Cdt1. Nat. Struct. Mol. Biol. 24, 316–324. https://doi.org/10.1038/nsmb.3372
Yuen, B.T.K., Knoepfler, P.S., 2013. Histone H3.3 Mutations: A Variant Path to Cancer. Cancer Cell 24, 567–574. https://doi.org/10.1016/j.ccr.2013.09.015
Yukawa, M., Akiyama, T., Franke, V., Mise, N., Isagawa, T., Suzuki, Y., Suzuki, M.G., Vlahovicek, K., Abe, K., Aburatani, H., Aoki, F., 2014. Genome-Wide Analysis of the Chromatin Composition of Histone H2A and H3 Variants in Mouse Embryonic Stem Cells. PLoS ONE 9, e92689. https://doi.org/10.1371/journal.pone.0092689
Zasadzińska, E., Barnhart-Dailey, M.C., Kuich, P.H.J.L., Foltz, D.R., 2013. Dimerization of the CENP-A assembly factor HJURP is required for centromeric nucleosome deposition. EMBO J. 32, 2113–2124. https://doi.org/10.1038/emboj.2013.142
Zasadzińska, E., Huang, J., Bailey, A.O., Guo, L.Y., Lee, N.S., Srivastava, S., Wong, K.A., French, B.T., Black, B.E., Foltz, D.R., 2018. Inheritance of CENP-A Nucleosomes during DNA Replication Requires HJURP. Dev. Cell 47, 348-362.e7. https://doi.org/10.1016/j.devcel.2018.09.003
Zenk, F., Zhan, Y., Kos, P., Löser, E., Atinbayeva, N., Schächtle, M., Tiana, G., Giorgetti, L., Iovino, N., 2021. HP1 drives de novo 3D genome reorganization in early Drosophila embryos. Nature. https://doi.org/10.1038/s41586-021-03460-z
Zhang, B., Zheng, H., Huang, B., Li, W., Xiang, Y., Peng, X., Ming, J., Wu, X., Zhang, Y., Xu, Q., Liu, W., Kou, X., Zhao, Y., He, W., Li, C., Chen, B., Li, Y., Wang, Q., Ma, J., Yin, Q., Kee, K., Meng, A., Gao, S., Xu, F., Na,

J., Xie, W., 2016. Allelic reprogramming of the histone modification H3K4me3 in early mammalian development. Nature 537, 553–557. https://doi.org/10.1038/nature19361
Zhang, H., Blobel, G.A., 2023. Genome folding dynamics during the M-to-G1-phase transition. Curr. Opin. Genet. Dev. 80, 102036. https://doi.org/10.1016/j.gde.2023.102036
Zhang, H., Emerson, D.J., Gilgenast, T.G., Titus, K.R., Lan, Y., Huang, P., Zhang, D., Wang, H., Keller, C.A., Giardine, B., Hardison, R.C., Phillips-Cremins, J.E., Blobel, G.A., 2019. Chromatin structure dynamics during the mitosis-to-G1 phase transition. Nature. https://doi.org/10.1038/s41586-019-1778-y
Zhang, H., Gan, H., Wang, Z., Lee, J.-H., Zhou, H., Ordog, T., Wold, M.S., Ljungman, M., Zhang, Z., 2017. RPA Interacts with HIRA and Regulates H3.3 Deposition at Gene Regulatory Elements in Mammalian Cells. Mol. Cell 65, 272–284. https://doi.org/10.1016/j.molcel.2016.11.030
Zhang, H., Lam, J., Zhang, D., Lan, Y., Vermunt, M.W., Keller, C.A., Giardine, B., Hardison, R.C., Blobel, G.A., 2021. CTCF and transcription influence chromatin structure re-configuration after mitosis. Nat. Commun. 12, 5157. https://doi.org/10.1038/s41467-021-25418-5
Zhang, M., Zhao, Xin, Feng, X., Hu, X., Zhao, Xuan, Lu, W., Lu, X., 2022. Histone chaperone HIRA complex regulates retrotransposons in embryonic stem cells. Stem Cell Res. Ther. 13, 137. https://doi.org/10.1186/s13287-022-02814-2
Zhang, S., Übelmesser, N., Barbieri, M., Papantonis, A., 2023. Enhancer–promoter contact formation requires RNAPII and antagonizes loop extrusion. Nat. Genet. 55, 832–840. https://doi.org/10.1038/s41588-023-01364-4
Zhang, S., Übelmesser, N., Josipovic, N., Forte, G., Slotman, J., Chiang, M., Gothe, H.J., Gade Gusmao, E., Becker, C., Altmüller, J., Houtsmuller, A., Roukos, V., Wendt, K., Marenduzzo, D., Papantonis, A., 2021. RNA polymerase II is required for spatial chromatin reorganization following exit from mitosis. Sci. Adv. 7.
Zhao, P.A., Sasaki, T., Gilbert, D.M., 2020. High-resolution Repli-Seq defines the temporal choreography of initiation, elongation and termination of replication in mammalian cells. Genome Biol. 21, 76. https://doi.org/10.1186/s13059-020-01983-8
Zhao, Z., Tavoosidana, G., Sjölinder, M., Göndör, A., Mariano, P., Wang, S., Kanduri, C., Lezcano, M., Singh Sandhu, K., Singh, U., Pant, V., Tiwari, V., Kurukuti, S., Ohlsson, R., 2006. Circular chromosome conformation capture (4C) uncovers extensive networks of epigenetically regulated intra- and interchromosomal interactions. Nat. Genet. 38, 1341–1347. https://doi.org/10.1038/ng1891
Zhiteneva, A., Bonfiglio, J.J., Makarov, A., Colby, T., Vagnarelli, P., Schirmer, E.C., Matic, I., Earnshaw, W.C., 2017. Mitotic post-translational modifications of histones promote chromatin compaction *in vitro*. Open Biol. 7, 170076. https://doi.org/10.1098/rsob.170076
Zink, D., 2006. The temporal program of DNA replication: new insights into old questions. Chromosoma 115, 273–287. https://doi.org/10.1007/s00412-006-0062-8
Zink, L.-M., Delbarre, E., Eberl, H.C., Keilhauer, E.C., Bönisch, C., Pünzeler, S., Bartkuhn, M., Collas, P., Mann, M., Hake, S.B., 2017. H3.Y discriminates between HIRA and DAXX chaperone complexes and reveals unexpected insights into human DAXX-H3.3-H4 binding and deposition requirements. Nucleic Acids Res. 45, 5691–5706. https://doi.org/10.1093/nar/gkx131
Zion, E.H., Chandrasekhara, C., Chen, X., 2020. Asymmetric inheritance of epigenetic states in asymmetrically dividing stem cells. Curr. Opin. Cell Biol. 67, 27–36. https://doi.org/10.1016/j.ceb.2020.08.003
Zuin, J., Roth, G., Zhan, Y., Cramard, J., Redolfi, J., Piskadlo, E., Mach, P., Kryzhanovska, M., Tihanyi, G., Kohler, H., Eder, M., Leemans, C., van Steensel, B., Meister, P., Smallwood, S., Giorgetti, L., 2022. Nonlinear control of transcription through enhancer–promoter interactions. Nature 604, 571–577. https://doi.org/10.1038/s41586-022-04570-y

RÉSUMÉ

Les multiples échelles d'organisation de la chromatine dans le noyau, de l'empaquetage en nucléosomes distincts à la formation de structures à l'échelle du kilo (kb) ou de la mégabase (Mb), contribuent à la régulation de la fonction du génome tout au long du cycle cellulaire et pendant les changements de destin cellulaire. Les travaux de notre équipe ont notamment démontré que le dépôt de variants H3 distincts dans la chromatine contribue à la définition des régions de réplication précoce. Cependant, la manière dont la distribution des variants H3 est liée au repliement du génome à un niveau supérieur, et ses implications pour l'initiation de la réplication précoce, restent des questions ouvertes. Au cours de mon projet de doctorat, j'ai étudié comment les nucléosomes, avec des variants H3 distincts, sont liés au repliement du génome en structures d'ordre supérieur, et quelles sont les implications pour l'initiation précoce de la réplication. Pour ce faire, j'ai d'abord intégré des données de ChIP-seq spécifiques à certains variants H3, provenant de cellules dans lesquelles le chaperon HIRA spécifique à H3.3 était présent (WT) ou knockout (KO), avec des données Hi-C publiques pour établir le profil de distribution des variants H3 dans les compartiments. Par la suite, j'ai généré des données Hi-C appariées pour évaluer l'effet de la perte d'HIRA sur l'organisation du génome en 3D. Enfin, j'ai réalisé des expériences de sauvetage pour vérifier si le fait de restaurer HIRA permet de rétablir les schémas de variants H3 et, à son tour, restaurer l'initiation précoce de la réplication et/ou l'organisation 3D du génome, simultanément ou séparément. J'ai montré que HIRA est nécessaire au dépôt ciblé de H3.3 dans les régions du compartiment A et au maintien de leurs contacts avec le reste du génome d'une manière indépendante des PTM H3. En outre, l'incorporation de H3.3 médiée par HIRA était essentielle pour maintenir l'identité du compartiment A et les niveaux de PTM dans les ZI précoces non transcrites, sans affecter leur conformation 3D locale. La restauration de HIRA a suffi à rétablir l'enrichissement en H3.3 à l'échelle du génome entier dans les compartiments A, ainsi que leur modèle d'interaction, et à l'échelle locale dans les sites H3.3 préexistants, quelle que soit leur activité transcriptionnelle. Cela s'est accompagné d'un sauvetage partiel de l'initiation précoce de la réplication au niveau de ces sites, mais pas d'une inversion de compartiment à cette échelle de temps. Mes résultats suggèrent que HIRA est important pour l'organisation 3D de la chromatine à l'échelle des compartiments, d'une manière indépendante des PTM d'histones et distincte de son rôle dans la définition des ZI de réplication précoce.

MOTS CLÉS

chromatine, variants d'histone, chaperons d'histone, organisation du génome, structure 3D

ABSTRACT

The multiple scales of chromatin organization in the nucleus: from packaging into distinct nucleosomes up to forming structures on the scale of kilo- (kb) to megabases (Mb), contribute to the regulation of genome function throughout the cell cycle and during cell fate transitions. Notably, work from our team demonstrated that deposition of distinct H3 variants on chromatin contributes to the definition of early-replicating regions. However, how the distribution of H3 variants relates to higher-order genome folding and its implications for early replication initiation remain open questions. During my PhD project, I explored how nucleosomes with distinct H3 variants relate to higher-order genome folding and what their implications for early replication initiation are. To achieve this, I integrated unique H3 variant-specific ChIP-seq data from cells in which the H3.3-specific chaperone HIRA was present (WT) or knocked-out (KO) with publicly available Hi-C data to profile H3 variant distribution with respect to compartments. Secondly, I generated matched Hi-C data to assess the effect of HIRA loss on 3D genome organization. Finally, I performed rescue experiments to test whether supplying back HIRA can re-establish H3 variant patterns, and in turn restore either early replication initiation and/or 3D genome organization simultaneously or separately. I showed that HIRA is required for targeted H3.3 deposition in compartment A regions and maintenance of their contacts with the rest of the genome in a manner independent of H3 PTMs. Furthermore, HIRA-mediated H3.3 incorporation was essential for maintaining A compartment identity and PTM levels at non-transcribing early IZs without affecting their local 3D conformation. Strikingly, re-supplying HIRA was sufficient to restore H3.3 enrichment globally in A compartments along with their interaction pattern, as well as locally at H3.3 pre-existing sites regardless of their transcriptional activity. This was accompanied by a partial rescue of the impaired early replication initiation at these sites, but not by reversal of compartment on this timescale. My results suggest that HIRA is important for 3D chromatin organization on the scale of compartments in a manner that is independent of histone PTMs and separate from its role in defining early replication IZs.

KEYWORDS

chromatin, histone variants, histone chaperones, genome organisation, 3D structure